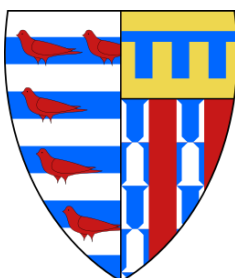




**Design and Synthesis of Chiral
Triazolium and Thiazolium Salts
Incorporating Hydrogen-Bonding
Motifs as Organocatalysts**



Emma Catherine Radoux

Department of Chemistry
University of Cambridge

This dissertation is submitted for the degree of
Doctor of Philosophy

Pembroke College

June 2019

Declaration

This dissertation is the result of my own work and includes nothing which is the outcome of work done in collaboration except as declared in the Preface and specified in the text.

It is not substantially the same as any that I have submitted, or, is being concurrently submitted for a degree or diploma or other qualification at the University of Cambridge or any other University or similar institution except as declared in the Preface and specified in the text. I further state that no substantial part of my dissertation has already been submitted, or, is being concurrently submitted for any such degree, diploma or other qualification at the University of Cambridge or any other University or similar institution except as declared in the Preface and specified in the text.

It does not exceed the prescribed word limit of 60,000 words.

Emma Catherine Radoux

June 2019

Acknowledgements

First and foremost, I would like to thank my supervisor, Dr Finian J. Leeper, for his assistance and support throughout the project. His knowledge on the area and helpful discussions have been invaluable to the project, and having expertise across such a range of areas has provided unique insight and approaches to problems. This project would not have been possible without the generous financial support of the EPSRC.

I would like to thank the Leeper group for their help, friendship and company in the lab, in particular Flaviu Bulat, Dr Annabel Murphy, and Maxime Couturier. I would like to thank David Lawrence for his contributions to this project.

A big thank you to the technical support staff, in particular Nic Davies and Naomi Hobbs. Thanks to Dr Peter Grice, Duncan Howe, Paul Skelton, Asha Boodhun and Alan Dickerson for all their help with characterisation and analysis of compounds.

Thanks to Dr Deborah Longbottom for her support and kindness, and for letting me be part of the Graduate Social and Networking Committee, especially alongside Bianca Provost and Talia Pettigrew, whose friendship made my PhD experience brighter.

To my closest friends Jade Burns, Cat Colquhoun, Steph Edwards and Dani Mehta, who have been there for me every day, thank you for both laughter and support, despite being nearly 200 miles away.

My husband, Dr Chris Radoux, has helped me throughout my PhD not only scientifically but also as my biggest supporter, and I would not be where I am without him. PhDs are not easy at the best of times, but I cannot express my gratitude to him. Finally, I would like to thank my mother Karen, my sister Hannah, and Scrambles and Maya my cats!

Abstract

The benzoin condensation is the first reported example of organocatalysis, and has been studied and used in organic synthesis for over 200 years. Originally catalysed by the cyanide anion, the reaction can also proceed with thiamine as a catalyst. Since then, many N-heterocyclic carbene (NHC) catalysts have been developed for use in umpolung reactions between aldehydes and a range of coupling partners. However, stereoselectivity of the new chiral centre is difficult to control: current existing methods employ steric hindrance of catalysts to influence this, potentially at the cost of slower reaction times. To date, there are very few examples of NHC catalysts incorporating hydrogen-bonding motifs to exploit attractive forces in influencing stereochemistry in these reactions.

An overview of asymmetric organocatalysis and their different modes of action have been detailed. The structures of NHC catalysts and their mechanisms are discussed, and the reactions which are catalysed by these salts reviewed. Current shortcomings are addressed, and both the project and new catalyst designs are proposed. Synthetic routes to new triazolium and thiazolium salt catalysts with unreported chiral backbones are discussed. These involve 1,2-diamine derived salts, 1,4-diamine derived salts, amino acid-derived triazolium salts, and a bicyclic triazolium salt with a piperidine backbone. Representative catalysts from each of these categories were synthesised and the catalytic ability of the NHC salts in umpolung reactions investigated. All of the catalysts are demonstrated to be effective at obtaining yield and ee in the Stetter reaction. These catalysts are critically analysed, future work proposed.

Table of contents

1	Introduction	1
1.1	Introduction to Chirality	1
1.1.1	The Importance of Chiral Centres	1
1.2	Overview of Organocatalysis	4
1.3	Modes of Activation	4
1.3.1	Covalent Organocatalysis	5
1.3.2	Non-covalent Organocatalysis	10
1.3.3	(Thio)urea Organocatalysis	13
1.4	The Benzoin Condensation	21
1.4.1	Mechanism	22
1.4.2	The Breslow Intermediate	25
1.4.3	Beyond N-Heterocyclic Carbenes	26
1.4.4	Asymmetric Thiazolium Salt Catalysts	26
1.4.5	Bicyclic Thiazolium Salts	29
1.4.6	Triazolium Salt Catalysts	30
1.4.7	Current Hydrogen-Bonding Catalysts for the Benzoin Condensation	33
1.5	Other Applications of NHCs	35
1.5.1	Achiral Cross Benzoin Condensations	36
1.5.2	Chiral Cross Benzoin Condensations	38
1.5.3	Reactions with Different Acceptors	41

1.5.4	NHC-Catalysed Cyclisations, Annulations and Complex Domino Cascades	49
1.5.5	Conclusions	57
2	Design of New Catalysts and Reaction Condition Optimisation	59
2.1	Aims of the Project	59
2.1.1	New Catalyst Design	59
2.1.2	Computational Design of Organocatalysts	64
2.2	Analysis of Chiral Compounds	70
2.2.1	Determination of ee	70
2.2.2	Determination of Configuration	73
2.3	Optimisation of Benzoin Condensation Conditions	75
2.3.1	Determination of Conversion to Benzoin	76
2.4	Catalyst Testing Conditions	79
2.4.1	The Benzoin Condensation	79
2.4.2	The Intramolecular Stetter Reaction	79
2.5	Conclusions	82
3	1,2-Diamine-Derived Catalysts	85
3.1	Introduction	85
3.1.1	Synthetic Routes	85
3.1.2	Chiral Resolution of (<i>1R,2R</i>)-Cyclohexane-1,2-diamine	87
3.2	Synthesis of the Catalysts	91
3.2.1	Synthesis of Thiourea	91
3.2.2	Synthesis of Urea	94
3.2.3	Synthesis of the Triazolium Salt	96
3.2.4	Synthesis of the Thiazolium Salt	102
3.2.5	Synthesis of Squaramides	107

3.3	Catalyst Testing	114
3.3.1	The Stetter Reaction	114
3.3.2	The Benzoin Condensation	114
3.4	Conclusions	117
4	1,4-Diamine-Derived Catalysts	121
4.1	Introduction	121
4.2	Synthesis of the Catalysts	123
4.2.1	Synthesis of ((<i>1R,2R</i>)-Cyclohexane-1,2-diyl)dimethanamine	123
4.2.2	Chiral Resolution of the Dicarboxylic Acid	125
4.2.3	Synthesis of the Final Catalyst	127
4.3	Catalyst Testing	130
4.3.1	The Stetter Reaction	130
4.3.2	The Benzoin Condensation	131
4.4	Conclusions	132
5	Phenylalanine-Derived Catalysts	135
5.1	Introduction	135
5.2	Synthesis of the Catalysts	136
5.2.1	Phenylalanine-Derived Synthesis	136
5.3	Catalyst Testing	138
5.4	Alternative Scaffold Investigation	142
5.5	Conclusions	143
6	Bicyclic Piperidine-Derived Catalysts	145
6.1	Introduction	145
6.1.1	Diazotransfer Reagent	150
6.1.2	Synthesis of the Pyrrolidine-Derived Triazolium Salt	156
6.1.3	Proposed Synthesis of the Opposite Enantiomer	156

6.2	Catalyst Testing	159
6.2.1	The Stetter Reaction	159
6.2.2	The Benzoin Condensation	161
6.3	Conclusions	161
7	Conclusions	165
7.1	Synthesis and Testing Conclusions	166
7.1.1	1,2-Diamine-Derived Catalysts	166
7.1.2	1,4-Diamine-Derived Catalysts	170
7.1.3	Phenylalanine-Derived Catalyst	172
7.1.4	Piperidine-Derived Catalyst	173
7.2	Future Work	174
8	Experimental	177
8.1	Computational Experimental	177
8.2	General Experimental	177
8.2.1	Chapter 2: Design and Testing of New Catalysts	178
8.2.2	Chapter 3: 1,2-Diamine-Derived Catalysts	182
8.2.3	Chapter 4: 1,4-Diamine-Derived Catalysts	209
8.2.4	Chapter 5: Phenylalanine-Derived Catalysts	217
8.2.5	Chapter 6: Piperidine-Derived Catalyst	223
	References	237
	Appendix A Supporting Information	253
A.1	New Compound Data	253
A.1.1	Chapter 3 Compounds	253
A.1.2	Chapter 4 Compounds	284
A.1.3	Chapter 5 Compounds	292

A.1.4	Chapter 6 Compounds	300
A.2	HPLC Traces from the Stetter Reaction and Benzoin Condensation	320
A.2.1	Stetter Reaction	320
A.2.2	Benzoin Condensation	330

Acronyms

aza-MBH Aza Morita-Baylis-Hillman. 44

BEMP 2-*tert*-butylimino-2-diethylamino-1,3-dimethylperhydro-1,3,2-diazaphosphorine. 42

BINOL 1,1'-bi-2-naphthol. 10

Boc *tert*-butyloxycarbonyl. 45

BPA binol-derived phosphoric acid diester. 12

CPME cyclopentyl methyl ether. 42

CSP chiral stationary phase. 71

DCC dicyclohexylcarbodiimide. 136

DIPEA N,N-diisopropylethylamine. 49

DMAP 4-dimethylaminopyridine. 124

DMF N,N-dimethylformamide. 5

DMPC tris(3,5-dimethylphenylcarbamate). 71

dr diastereomeric ratio. 50

ee enantiomeric excess. 65

EWG electron-withdrawing group. 46

FTIR Fourier-transform Infrared Spectroscopy. 180

HRMS high-resolution mass spectrometry. 179

JINGLE 1,1-binaphthyl-2,2-bis(sulfuryl)imide. 12

KHDMS potassium bis(trimethylsilyl)amide. 49

LUMO lowest unoccupied molecular orbital. 10

NHC N-heterocyclic carbene. 4

NMR Nuclear Magnetic Resonance. 25

NTPA *N*-triflylphosphoramidate. 12

QM quantum mechanical. 64

rt room temperature. 17

SSRI selective serotonin reuptake inhibitor. 1

TFA trifluoroacetic acid. 136

TLC thin-layer chromatography. 76

UV ultra-violet. 71

Chapter 1

Introduction

1.1 Introduction to Chirality

1.1.1 The Importance of Chiral Centres

Louis Pasteur first discovered the concept of molecular chirality in 1848 through the crystallization of racemic tartaric acid into its enantiomers [1], although the term chirality was not officially used until 1894 by Lord Kelvin [2]. Since then, chiral compounds have been widely exploited across organic chemistry, particularly in biologically important industries such as pharmaceuticals and agrochemicals. Recently compiled data by Njardarson shows that of the top 200 brand-name pharmaceuticals in 2016 by prescription, 43% contained either a chiral centre or important stereochemistry [3]. The importance of chiral centres can be illustrated by escitalopram ((*S*)-**1**) and its racemate citalopram ((\pm)-**1**) (Fig. 1.1), the 26th and 27th most prescribed pharmaceuticals respectively. While both are selective serotonin reuptake inhibitors (SSRIs) prescribed in the treatment of depression, the (*S*)-enantiomer is also prescribed in the treatment of generalised anxiety disorder. This indicates that the two enantiomers interact differently in the human body, giving rise to varied pharmacokinetic properties. The doses are reflected by the proportion of the (*S*)-enantiomer; the dosage of

(S)-1

(±)-1

Fig. 1.1 Chemical structures of escitalopram (**1a**) and citalopram (**1b**).

However, when it comes to the synthesis of new drug-like compounds, the ability to synthesise only one enantiomer is highly attractive. In the pharmaceutical industry, one of the biggest challenges arises when the undesired enantiomer is toxic. Whilst it is possible to synthesise enantiomerically pure compounds, there have been cases where the enantiomer can be converted *in vivo* into the toxic enantiomer; the most well-known example of this is thalidomide (Fig. 1.2).

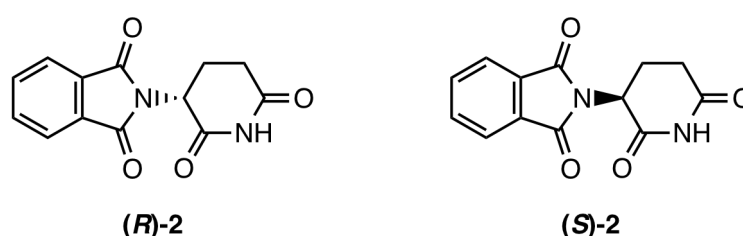


Fig. 1.2 The anti-sickness (*R*)-enantiomer (left), and the teratogenic (*S*)-enantiomer of thalidomide.

In 1954, thalidomide was developed as a sedative by German company Chemie Grunenthal. By 1957, the drug was being prescribed over the counter as an antiemetic for morning sickness in pregnant women. Thalidomide was given as a racemic mixture, but only the (*R*)-enantiomer (***R***-**2**) was beneficial in the treatment of morning sickness, and the (*S*)-enantiomer (***S***-**2**) was ultimately discovered to be a teratogen. This caused malformation of the limbs

in unborn children, and up to 6000 cases were reported by 1961 [4]. The drug was promptly withdrawn from this use, but is still used to this day in treatments of other ailments such as leprosy.

Due to the instability of the desired (*R*)-enantiomer in the human body, attempts to minimise amounts of the teratogenic (*S*)-enantiomer are futile, and the drug is no longer prescribed for treatment of morning sickness in pregnant women. The proton attached to the chiral carbon is acidic, and therefore deprotonation is facile in basic conditions. Studies by Testa [5] determined that human serum albumin, which contains many ϵ -amino groups of lysine residues, is able to catalyse the racemisation of thalidomide. The racemisation also happens in phosphate buffer solutions at pH 7.4 due to the presence of phosphate ions, hydroxyl ions and water. A water-catalysed mechanism has been proposed by Tian *et al.* [6], and was further re-evaluated by Rzepa in 2015 [7]. The calculations were performed in vacuum, using only two water molecules as solvent (Fig. 1.3).

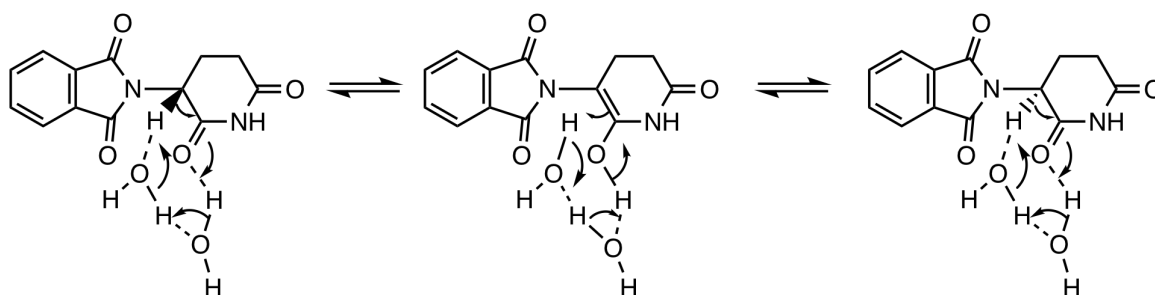


Fig. 1.3 The proposed mechanism for the water-assisted racemisation of thalidomide [6].

In cases where only one enantiomer can be safely administered, it is crucial to be able to develop reliable enantioselective syntheses of new compounds. Whilst enantiomeric separation procedures do exist, these are often done on a small scale, as the cost means that they are not economically feasible to do in mass production of new drugs. Therefore, new methods of enantioselective synthesis are constantly being developed, with the most ground-breaking advances being in the field of asymmetric catalysis.

1.2 Overview of Organocatalysis

Catalysis has played an important role in organic synthesis for centuries. Although this term covers a broad range of reaction modes, including protonation (acid catalysis), conversion of functional groups (*e.g.* enamine catalysis) and reversal of reactivity (umpolung), the main principal of catalysis is an increased rate of chemical reaction by lowering of the activation energy. This allows for a whole range of seemingly impossible reactions to be performed, including formation of C-C bonds.

Traditionally, transition metal catalysts have been used for C-C coupling [8], including palladium catalysts such as those in the Heck [9], Negishi [10] and Suzuki couplings [11]. However, there are limitations with these reactions, such as difficulties in completely purifying the products so no trace metals remain, the sensitivity of metal catalysts to water and air, and the expense of precious metals.

Due to these disadvantages, organocatalysis has grown in popularity over the past few decades, with more and more organic molecules acting as catalysts in reactions. As well as being less toxic than transition metal catalysts, organocatalysts are often less sensitive to air and moisture, work in mild conditions, and are easy to separate from reaction mixtures [12]. With many organocatalysts being inspired by naturally occurring enzymes [13], the formation of C-C bonds can be catalysed in more gentle conditions compared to the transition metal alternatives [14]. The benzoin condensation is an example of a C-C bond forming reaction, where two molecules of benzaldehyde, **3**, are self condensed to form the benzoin product **4**. This is made possible by use of an N-heterocyclic carbene (NHC) as the catalyst (Fig. 1.4).

1.3 Modes of Activation

There are many complex ways that catalysts work, and often *via* several methods at once, but covalent and noncovalent interactions are the most effective way to classify these systems.

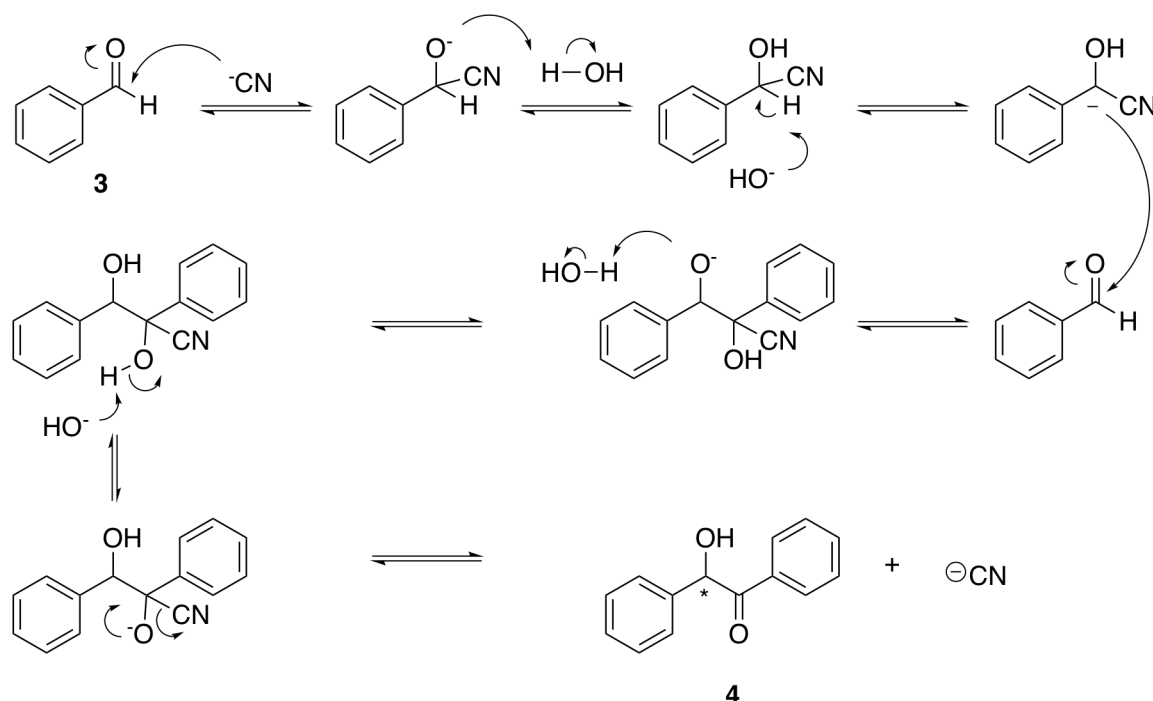


Fig. 1.4 The cyanide ion-catalysed benzoin condensation.

Although more extensive reviews can be found on these methods [15], a brief overview of the main modes in the field are given.

1.3.1 Covalent Organocatalysis

Amino catalysts are the most well-reported area in covalent organocatalysis, with the first use of proline as an enantioselective catalyst being reported by Wiechert and coworkers in 1971 in its use towards steroid synthesis [16]. Inspired by this, Hajos and Parrish described the use of (*S*)-proline **7** as an organocatalyst for the asymmetric synthesis of natural product derivatives [17]. By using aprotic solvents such as *N,N*-dimethylformamide (DMF), products could be achieved in up to 93.4% ee. The amino catalysts work through a combination of covalent and non-covalent interactions; once an enamine is formed, non-covalent interactions between the carboxylic acid and ketone or aldehyde control the stereochemistry in subsequent steps, forming the enantioenriched product *via* a six-membered chair-like transition state **TS-1** or **TS-2** (Fig. 1.5) [18].

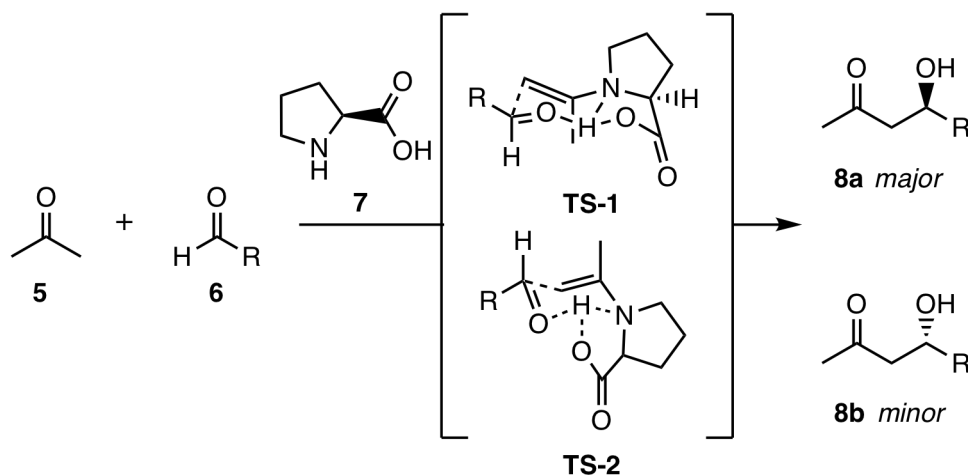


Fig. 1.5 The six-membered chair-like transition states leading to the introduction of stereochemistry in the asymmetric intermolecular aldol reaction, as predicted by Houk, List and co-workers [18].

Many successful catalytic reactions have been reported using (*S*)-proline as a catalyst since its first application, demonstrating not only α -functionalisation of aldehydes, but also β -, and γ -functionalisation. Proceeding *via* iminiums, enamines and dienamine intermediates, a diverse range of products can be obtained using a range of related aminocatalysts, for example **7-7c** (Fig. 1.6) [19].

Beyond aminocatalysis, another well-established class of organocatalysts are NHCs. N-heterocyclic carbenes are a class of organocatalyst which can catalyse a range of transformations, which will be discussed later in this chapter. Three common classes of N-heterocycles which are used for organocatalysis are thiazolium salts, triazolium salts and imidazolium salts (Fig. 1.7). [20].

These three types of cation have extremely interesting electronic configurations which make them such effective catalyst precursors. Firstly, the pre-carbenic proton is relatively acidic, which allows facile deprotonation to give the active carbene species (Fig. 1.8 (i) and (ii)). Although the pK_a varies greatly depending on functional group and solvent, pK_as in DMSO have been reported from 12.1-15.5 for triazoliums, around 16.5 for thiazoliums, and 19.7-23.4 for imidazoliums [21]. The lone pair generated here is stabilised due to the

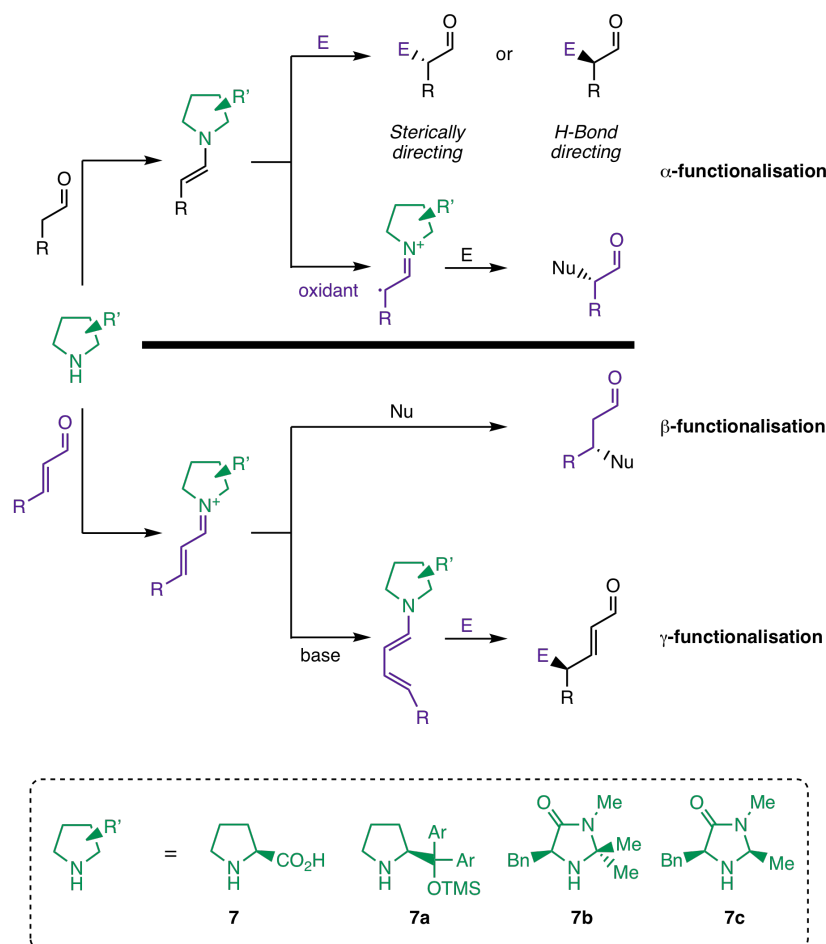


Fig. 1.6 The main pathways of aminocatalysis for formation of a range of products using catalysts **7-7c**, reported by Jørgensen and coworkers [19].

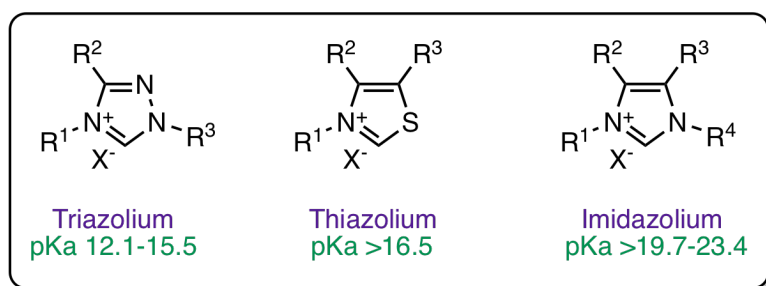


Fig. 1.7 Different common NHC cores used in organocatalysis, adapted from Glorius and coworkers [20]. $\text{X}^- = \text{Br}^-, \text{Cl}^-, \text{I}^-, \text{ClO}_4^-, \text{BF}_4^-$. pK_a s of the C2 proton for a range of pre-catalysts were reported in DMSO by Li and Cheng [21].

aromaticity of the molecule. By having an adjacent electron-rich heteroatom such as nitrogen, its lone pair can donate into the empty P_z orbital of the carbene (Fig. 1.8 (iii)), stabilising this centre and therefore promoting its use as a catalyst.

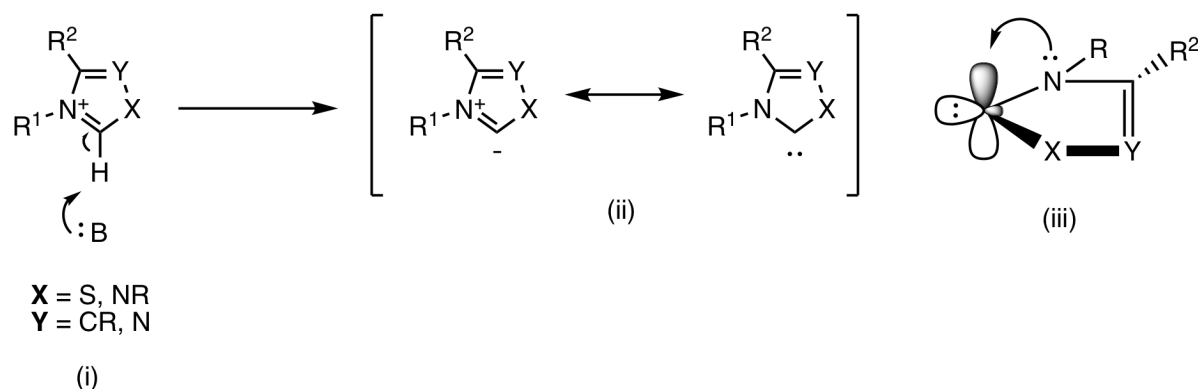


Fig. 1.8 (i) Deprotonation of the general pre-catalyst to form the carbene. (ii) Stabilisation of the carbene by resonance. (iii) The electron-rich NHC has heteroatom lone pair donation into the p orbital [20].

Much research has moved away from using these substrates as organocatalysts, and instead have demonstrated their use as effective ligands for metal catalysis. In particular unsaturated imidazoliums, which do not demonstrate efficacy in the condensation reactions covered in this work, are used as ligands in Grubb's generation II ruthenium catalysts for metathesis reactions [22]. However, there is still a lot to be discovered from the use of these molecules as organocatalysts: much is to be said for the stability of these pre-catalysts both in air and moisture. Organocatalysts can also be relatively cheap if syntheses are kept simple from chiral commercially available starting materials such as proline, as no precious heavy metals are involved. The catalysts can also be easily removed by column chromatography, which is extremely useful in environments where trace metal contamination can have disastrous effects, such as in pharmaceutical or agrochemical industries.

The flexibility and reactivity of NHCs allow them to act *via* a range of activation modes. The reactions described herein all begin with deprotonation of the N-heterocyclic salt to form the NHC, acting as a nucleophile and adding in to an electron-deficient centre (usually an aldehyde). The ability to generate a carbene leads to very interesting reactivity, and different

modes of action have been succinctly summarised in a review by Glorius and coworkers [23] (Fig. 1.9).

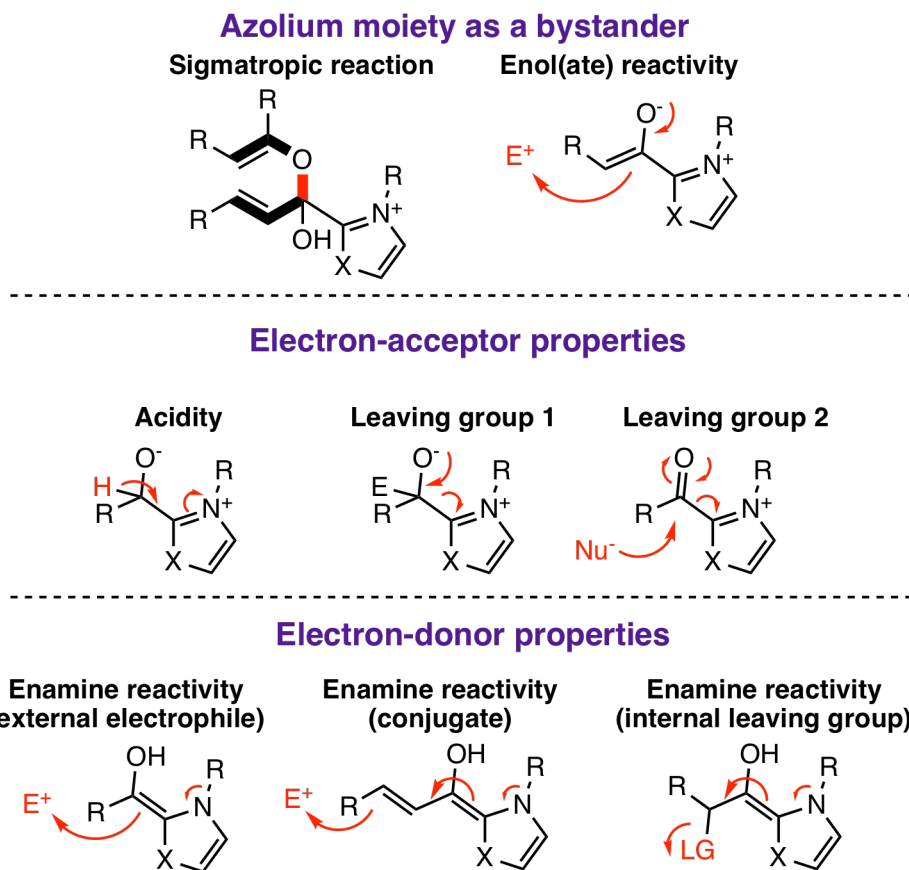


Fig. 1.9 Modes of action involved with NHCs, adapted from Glorius and coworkers [23].

Once the initial adduct has been formed between the carbene and the aldehyde, differing methods of reactivity can influence which product is formed. Adjusting the reagents can modify the adduct, and as such, the catalyst can form a range of scaffolds and products based on whether it acts as an enolate or enamine. Dual activation by the catalyst has also been demonstrated, and exploiting this mechanism can allow access to many cyclised products through cascade reactions. The simplest product formed from an aromatic aldehyde using a carbene is benzoin, which proceeds *via* a¹ to d¹ umpolung of benzaldehyde.

1.3.2 Non-covalent Organocatalysis

Moving from using steric repulsion as a means of introducing stereoselectivity towards the use of attractive forces, many new catalyst classes have been designed and reported. Coordination of catalysts to reagents help lower the energy of the lowest unoccupied molecular orbital (LUMO), giving more reactive intermediates. Consideration of the functional groups of the reagents allows for the most effective catalyst to be used, based on whether the reagent is Brønsted acid or basic, or Lewis acid or basic, as classified by Seayad and List [24]. However, in reality, most organocatalysts use a combination of these modes. The mechanisms for how these catalysts work are mostly proposed based on hydrogen-bonding, but the extent of dissociation of the proton from the organocatalyst dictates the exact terminology; catalysts which completely transfer the proton from the catalyst to the substrate are known as Brønsted acids [15]. Hydrogen-bonding organocatalysts, where the protons do not dissociate from the catalyst, are well developed, but the most notable example of these are (thio)ureas pioneered by Jacobsen and coworkers [25]. These are discussed in more detail in the next section.

Brønsted Acid Organocatalysis

Since the first reported use of phosphoric acid organocatalysts in the asymmetric Mannich-type reaction by Akiyama *et al.* in 2004 [26], 1,1'-bi-2-naphthol (BINOL)-phosphoric acids and their derivatives have been widely established as effective asymmetric organocatalysts. The initial reaction between aldimines **9** and ketene silyl acetals **10** achieved ee's up to 96%, with 100% selectivity of the *syn* diastereomer (*syn*)-**11** and 100% yields (Table 1.1) when catalysed by **BIN-1** [26]. Similarly, the same year Terada and coworkers reported a chiral phosphoric acid-catalysed Mannich reaction of acetoacetone **12** and Boc-imine **13** to form the chiral Boc-amine **14**, shown in Fig. 1.10, with up to 98% ee and 99% yield for 6 examples [27].

The introduction of stereoselectivity initially comes from the axial chirality of the BINOL's C₂-symmetric backbone. The organocatalysts promote the reaction due to the phos-

Table 1.1 The first reported use of BINOL as an organocatalyst by Akiyama in 2004 for the diastereoselective Mannich-type reaction [26].

The reaction scheme shows aldimine **9** (with an ortho-hydroxyphenyl group) reacting with ketene silyl acetal **10** in the presence of the BINOL-derived catalyst **BIN-1** (a bisphosphoric acid derivative). The reaction yields two diastereomeric products: the *syn*-isomer **11** and the *anti*-isomer **11**. The *syn*-isomer has both the hydroxyl group and the amine group on the same side of the molecule, while the *anti*-isomer has them on opposite sides.

Entry	R ¹	R ²	R ³	Yield (%)	<i>syn/anti</i>	ee (%) ^b
1	Ph	Me ^c	Et	100	87:13	96
2	p-MeOC ₆ H ₄	Me ^c	Et	100	92:8	88
3	p-FC ₆ H ₄	Me ^c	Et	100	91:9	84
4	p-ClC ₆ H ₄	Me ^c	Et	100	86:14	83
5	p-MeC ₆ H ₄	Me ^c	Et	100	94:6	81
6	2-Thienyl	Me ^c	Et	81	94:6	88
7	PhCH=CH	Me ^c	Et	91	95:5	90
8	Ph	PhCH ₂ ^d	Et	100	93:7	91
9	p-MeOC ₆ H ₄	PhCH ₂ ^d	Et	92	93:7	87
10	PhCH=CH	PhCH ₂ ^d	Et	65	95:5	90
11	Ph	Ph ₃ SiO ^e	Me	79	100:0	91

^aReaction conditions: Aldimine **9** (1 eq), ketene silyl acetal **10** (1.5 eq), **BIN-1**, toluene, -78 °C, 24 h. ^bee value of *syn* isomer. ^c*E/Z* = 87:13. ^d*E/Z* = 87:13. ^e*E/Z* = 91:9.

phoric acid moiety, which features a Brønsted acidic site offering proton donation. The oxygen of the P=O also acts as a Lewis basic site due to its lone pairs, adding further interactions with the substrate. The catalysts can be extremely complex and the nature of the mechanism depends on the exact catalyst, the substrates and reaction conditions. For example, with Akiyama and coworker's reaction an intramolecular Lewis acid/Brønsted acid mechanism was proposed to activate the aldimine ready for attack [26], whereas for Terada and coworkers's reaction it was proposed that hydrogen bonds were formed with both of the reagents, holding them in position to react [28]; this is illustrated in Fig. 1.11. More information on these mechanisms can be found in the review by Rueping and coworkers [29].

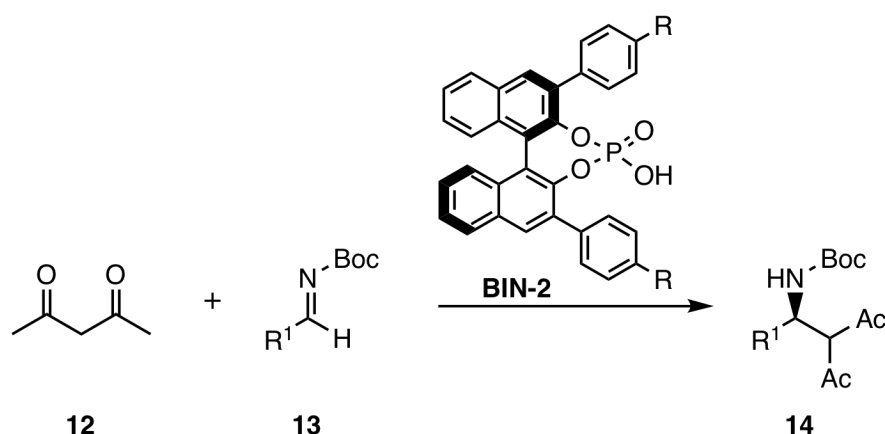


Fig. 1.10 The chiral Brønsted acid-catalysed direct Mannich reaction reported by Terada [27]. R = naphthyl. Reaction conditions: Boc-imine **13** (1 eq), acetoacetone **12** (1.1 eq), phosphoric acid **BIN-2** (2 mol%), CH₂Cl₂, rt, 1h.

These organocatalysts also have the advantages of steric and electronic fine-tuning, as varying the substituents either on the phosphoric acid moiety or the aromatic rings can greatly influence the acidity. A study by Rueping, Leito and co-workers [30] established an order of acidity for the different derivatives of the Brønsted acidic catalysts, including binol-derived phosphoric acid diesters (BPAs) **BIN-3**, *N*-triflylphosphoramides (NTPAs) **BIN-4**, and 1,1-binaphthyl-2,2-bis(sulfuryl)imides (JINGLES) **BIN-5** [31] in acetonitrile (Fig. 1.12). Further studies demonstrated that the catalytic ability of these is directly correlated with their Brønsted acidity [30]. Further notable developments in asymmetric Brønsted organocatalysts

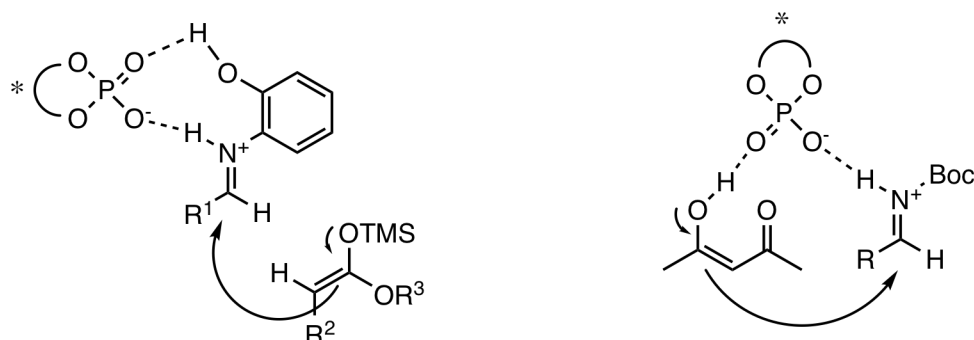


Fig. 1.11 The proposed modes of hydrogen bonding to activate reagents in the diastereoselective Mannich-type reaction [26] (left) and the enantioselective Mannich reaction [27] (right).

include the use of TADDOL derivatives [32] and ammonium salts [33, 34], which can be found in more detailed reviews [35–37].

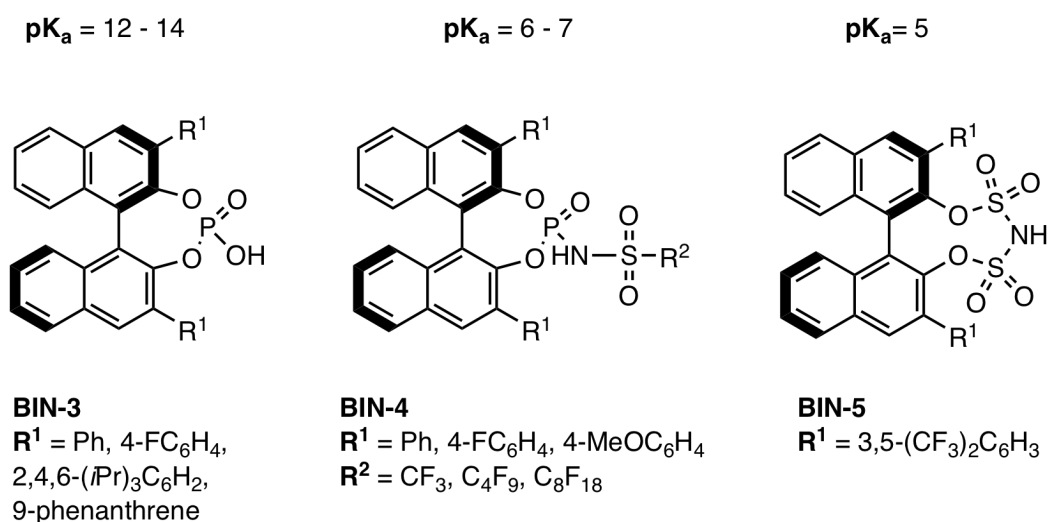


Fig. 1.12 Different structures of BINOL-derived BPAs, NTPAs and JINGLEs organocatalysts, showing the relative pK_a s in acetonitrile as determined by Rueping, Leito and co-workers [30].

1.3.3 (Thio)urea Organocatalysis

A Lewis acid is a chemical species which can accept an electron pair from a donor compound to form an adduct. Although the concept of double hydrogen bonding was first reported in 1984, the power of these bonds were not exploited as a tool for organocatalysis until the late

90s. Hine first reported in 1984 that the two hydroxyl groups of 1,8-biphenylenediol were sufficiently positioned to be able to form hydrogen bonds with several molecules containing a carbonyl [38]. An Oak Ridge Thermal-Ellipsoid Plot (ORTEP) drawing of the crystal structure of the diol with 1,2,6-trimethyl-4-pyridone demonstrated the almost coplanarity of the two molecules (Fig. 1.13).

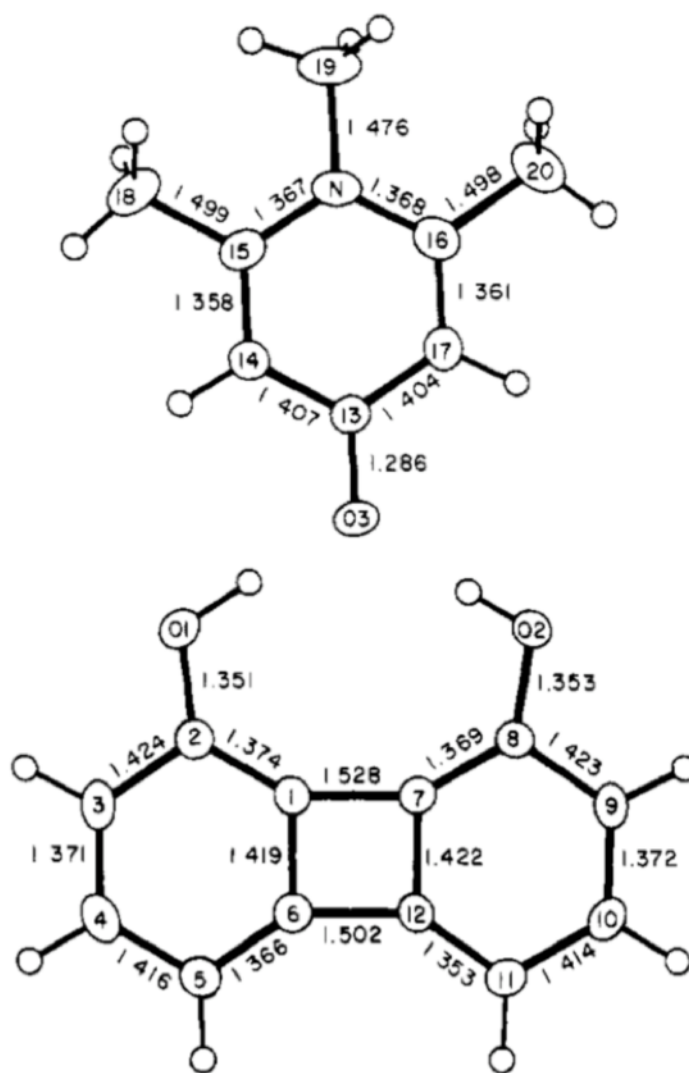


Fig. 1.13 The 1,8-biphenylenediol-1,2,6-trimethyl-4-pyridone complex, reported by Hine [38].

Further studies emphasising the hydrogen bonding interactions of ureas were reported in 1990, when Etter co-crystallised *N,N'*-diphenylureas with Lewis basic compounds such as

triphenylphosphine oxide and dimethylsulfoxide (DMSO) [39]. Further studies gave some important structural insights into these molecules; more stable complexes could be formed by using more electron-deficient ureas, such as 1,3-bis(3-nitrophenyl)urea (Fig. 1.14). This is due to the enhancement of the H-bond donor ability of the urea, a principle which has since become key in the design of new (thio)urea catalysts since Etter's contributions to the field [40, 41]. Interactions between the carbonyl lone pairs and the *ortho*-protons on the electron-deficient rings were demonstrated, which again gave a new direction to catalyst design.

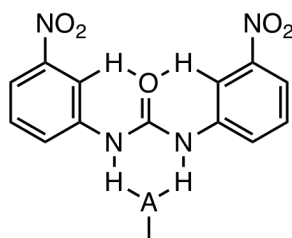


Fig. 1.14 Hydrogen bonding interactions between 1,3-bis(3-nitrophenyl)urea and the hydrogen bond acceptor (A). In the case of this urea, it also acts as a Lewis base. Intramolecular hydrogen bonds are formed between the *ortho*-protons and the carbonyl of the urea.

However, it was not until 1998 that Jacobsen and coworkers first reported the use of (thio)ureas as organocatalysts for the asymmetric Strecker reaction [25]. Initial studies investigated the effects of different metal ions as catalysts in the reaction of **15** and HCN (Fig. 1.15), but it was soon noted that the Schiff bases such as **THIO-1** were more effective when uncoordinated. Effective both in solid phase and solution, yields up to 92% in the formation of **16**, and the highest ee of 91% being obtained for **16a**. Although Jacobsen noted an increase in ee from 45% to 55% when substituting the urea for thiourea, no particular focus was placed on the importance of this particular moiety in catalysing the reaction.

The idea of bifunctional catalysts incorporating both a hydrogen bond donor and hydrogen bond acceptors were not reported until 2003 by Takemoto, for the Michael addition of malonate esters to nitroolefins to form **17** [42]. The catalysts incorporate both thiourea and a tertiary amine. The Lewis acidic thiourea co-ordinates to the electrophilic nitroolefin,

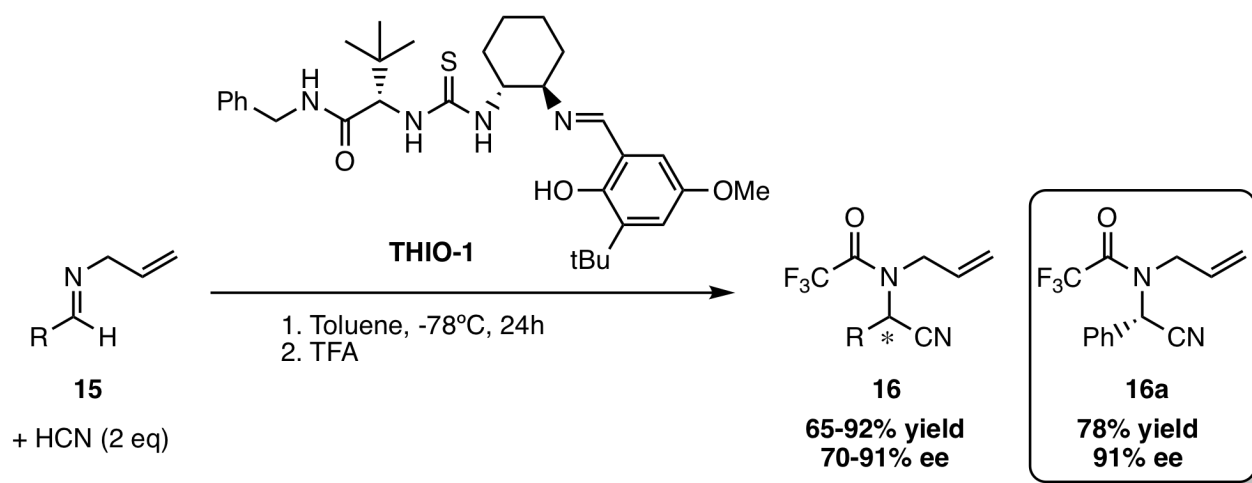


Fig. 1.15 The first reported use of (thio)urea as a catalyst for the asymmetric Strecker reaction [25]. R= Ph, *p*-OCH₃C₆H₄, *p*-BrC₆H₄, 2-naphthyl, *t*Bu, Cy.

whereas the Lewis basic amine co-ordinates and activates the malonate ester (Fig. 1.16). This not only activates both of these reagents but holds them in a position to allow the reaction to proceed in an enantioselective manner due to the chiral backbone. Additives of a Lewis base, trimethylamine, and a thiourea were individually investigated, but it was not until the pair were combined into the same catalyst that high yields and ee's were achieved, as demonstrated by Takemoto (Table 1.2) [42].

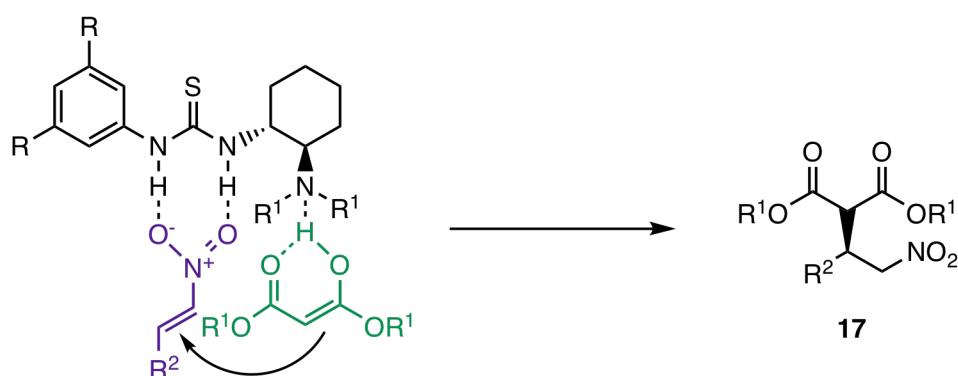
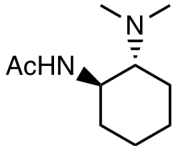
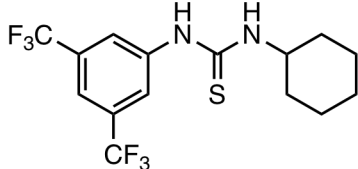
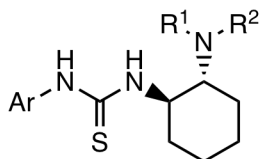


Fig. 1.16 The first bifunctional organocatalyst reported by Takemoto in 2003 [42]. The Lewis acid interaction with the nitroolefin, and the Lewis basic interaction with the malonate tautomer are proposed.

Investigation into the effects of different functional groups determined that more electron-withdrawing groups on the aromatic ring gave higher enantioselectivity, as previously dis-

Table 1.2 Takemoto's investigation into the effect of functional group substitution on the enantioselective Michael addition between trans- β -nitrostyrene and diethyl malonate [42].

				
TAK-1		TAK-2		
		TAK-3: Ar = 3,5-(CF ₃) ₂ C ₆ H ₃ , R ¹ = R ² = <i>o</i> -(CH ₂) ₂ C ₆ H ₄ TAK-4: Ar = 3,5-(CF ₃) ₂ C ₆ H ₃ , R ¹ = Me, R ² = <i>i</i> Pr TAK-5: Ar = Ph, R ¹ = R ² = Me TAK-6: Ar = 2-(MeO)C ₆ H ₄ , R ¹ = R ² = Me		
Entry ^a	Additive	Time (h)	Yield ^b (%)	ee ^c (%)
1	TEA	24	17	-
2	TAK-1	24	14	35
3	TEA + TAK-2	24	57	-
4	TAK-3	48	29	91
5	TAK-4	48	76	87
6	TAK-5	48	58	80
7	TAK-6	48	40	52

^aReaction conditions: Diethyl malonate (2 eq), additive (0.1 eq), PhMe, room temperature (rt). ^bIsolated yield. ^cee determined by HPLC analysis. Absolute configuration determined by comparison with literature.

cussed. This experimental investigation further supports the work of Etter, showing stronger hydrogen bonds are formed when the thioureas have more electron-withdrawing groups on the aromatic ring.

Further work by Takemoto and coworkers investigated a range of bifunctional organocatalysts and applied these to the diastereoselective Michael reaction with unsymmetrical 1,3-dicarbonyls [43]. In-depth optimisation of the reaction conditions led to a range of complex products being accessible, including sterically hindered quaternary centres. The catalyst also offers a simplified route to optically pure (*R*)-baclofen, a γ -amino butyric acid (GABA) agonist used in the treatment of spastic movement disorders. Since then, the Takemoto

group have reported many more uses of bifunctional thiourea catalysts, which can be used to encourage both enantioselective and diastereoselective reactions [44].

Squaramides

Since the widespread use of (thio)ureas as catalysts, varying substituents on the aromatic ring has been the most systematic approach to fine-tuning the electronics of the catalyst to improve Lewis base acidity. However, a new approach in 2008 by Rawal and coworkers introduced squaramides as a hydrogen bond donating scaffold in organocatalysis. The squaramides have an increased distance between the N-Hs, with the *N,N'*-dimethylthiourea distance calculated at 2.13 Å and the *N,N'*-dimethylsquaramide calculated at 2.72 Å. There is also a difference in the rigidity of the structures and their pKa. The increased conjugation of squaramide gives more delocalisation across the system, weakening the N-H bonds and increasing acidity compared to the (thio)urea. This improves the strength of the interaction with the hydrogen bond accepting substrate.

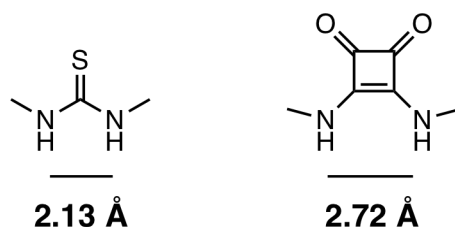


Fig. 1.17 The distance between the two N-H hydrogens, as measured for *N,N'*-dimethylthiourea by Takemoto (left) and *N,N'*-dimethylsquaramide by Rawal (right).

Squaramide derivatives have been used in various asymmetric reactions including Michael and Sulfa-Michael additions [45, 46], aza-Henry reactions [47], Strecker reactions [48] and Mannich reactions [49]. More recently, a range of asymmetric cascade reactions catalysed by bifunctional squaramides have been reported [50].

Croconamides and Deltamides

Croconamides are a newly reported moiety in hydrogen bonding Lewis acids. Inclusion of an extra carbonyl compared to squaramide not only changes the structure but also changes the acidity. As a comparison to the literature values of the related structures in Fig. 1.17, a minimised 3D structure to estimate the distance between the two N-H hydrogens of *N,N'*-dimethylcroconamide was obtained using MMFF94 Force Field with the steepest descent algorithm. This distance was measured to be 2.2 Å, which was in between the analogous thiourea and squaramide (Fig. 1.17).

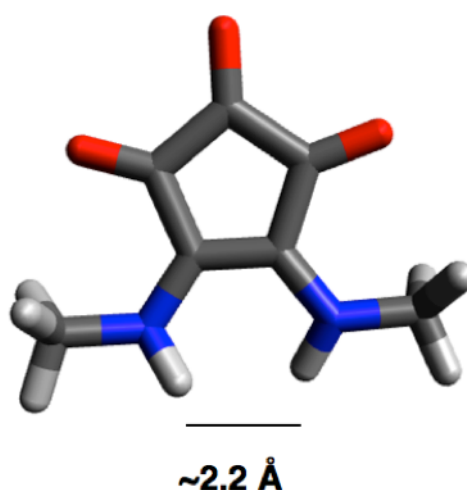


Fig. 1.18 A 3D structure with the energy minimised to estimate the distance between the two N-H hydrogens of *N,N'*-dimethylcroconamide, measured at 2.2 Å.

Croconamides were introduced by Pittelkow and co-workers, with their investigations being in anion recognition and organocatalysis [51]. X-ray studies showed shorter than expected C-N bonds, indicating there may be some tautomerisation. Initial organocatalytic studies investigated the rates of the tetrahydropyranylation of phenols, and these showed that the molecules did indeed catalyse the reaction. However, unexpectedly, this modification of the acidity did not work as expected. By having bis(trifluoromethyl)groups on the aromatic rings to try and increase the acidity, the croconamide **18** was instead susceptible to the

formation of the hydrate **19** (Fig. 1.19). Further functionalisation and expansion of the reaction scope are in progress, with the aim to develop enantioselective catalysts.

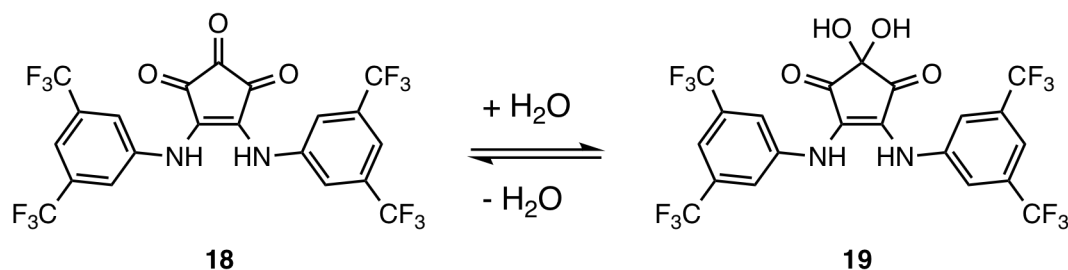


Fig. 1.19 Reversible hydration of *N,N'*-3,5-bis(trifluoromethyl)phenylcroconamide.



Fig. 1.20 The crystal structure of the bis(4- $\text{CF}_3\text{-C}_6\text{H}_4$)deltamide with the benzoate anion obtained by Jolliffe and coworkers [52].

A further report by Jolliffe and coworkers proposed the application of deltamides [52] as a dual hydrogen bond donor for selective ion recognition. Although these are relatively new moieties, their potential to interact as dual hydrogen bond donors has been demonstrated through ion binding studies. A range of symmetrical achiral deltamides were synthesised and investigated, and the H-H bond distance calculated through optimised molecular structure studies varied depending on substituents. A range of distances between 3.11 - 3.56 Å was

predicted, which is around 1 Å higher than those of the other dual hydrogen-bonding motifs. The hydrogen bonding capability has been demonstrated by crystal structures of deltamides with the benzoate anion (Fig. 1.20). Whilst no chiral organocatalysis reactions have been reported with deltamides to date, this unique scaffold could provide interesting opportunities for catalyst development in the future.

1.4 The Benzoin Condensation

The benzoin condensation was first reported by Justus von Liebig and Friedrich Woehler in 1832, using cyanide as a catalyst [53]. Addition of the cyanide anion into benzaldehyde allowed for reversal of the reactivity of the carbonyl centre, known as an umpolung reaction. This adduct could then react with another molecule of benzaldehyde to form an α -hydroxy ketone (Fig. 1.21). The cyanide anion serves three roles in the reaction: it acts as a nucleophile adding to the carbonyl, it facilitates proton abstraction reversing the reactivity of the carbonyl, and it acts as a leaving group in the final stage to allow formation of the product.

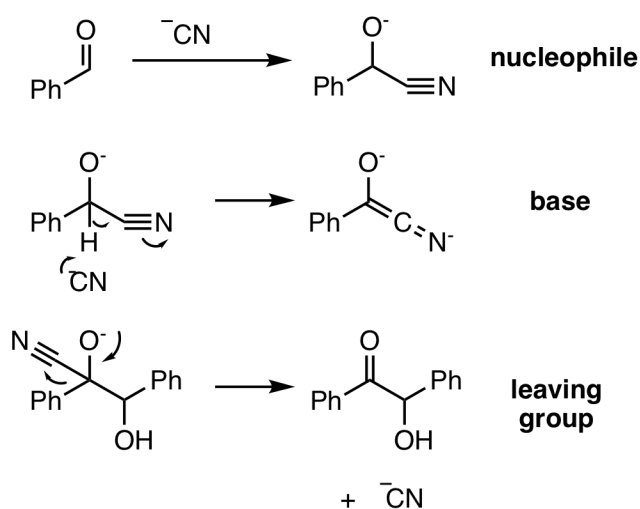


Fig. 1.21 The roles of ^-CN in the benzoin condensation.

Since this initial discovery, a wide range of catalysts have been developed for the benzoin reaction (Fig. 1.22). The first NHC-catalysed benzoin condensation was reported by Ukai and coworkers in 1943 using vitamin B1, thiamine [54]. Thiamine is active in the condensation due to the thiazolium salt ring; the proton in this ring is acidic, and can be deprotonated using a mild base to form the active ylide species. In the case of thiamine, delocalisation of the adjacent heteroatom lone pair into the ring stabilises the active species. This is true even when varying the NHC, *e.g.* triazolium rings are commonly used in the benzoin condensation. In comparison to the initial cyanide anion catalysis, these organocatalysts have the advantage of potential structural modifications to promote stereoselectivity in the benzoin product through sterics and electronics [55].

1.4.1 Mechanism

The mechanism for the benzoin condensation has proved problematic to elucidate since the reaction was first discovered. The most widely accepted mechanism is as demonstrated with thiamine (Fig. 1.23). The first step in the thiamine-catalysed benzoin reaction is deprotonation of **NHC-1** using a mild base to generate the active catalytic species. This attacks the carbonyl π^* orbital of benzaldehyde **3**, and the acidic proton is removed by base to form the so-called Breslow intermediate. This gives the umpolung reactivity of the benzaldehyde centre, allowing the carbonyl to add into another molecule of benzaldehyde. The active catalytic species is regenerated when the α -hydroxy ketone product benzoin **4** is formed, breaking the bond between the product and catalyst by reforming the carbonyl. This has been determined spectroscopically by NMR spectroscopy [56].

All of the steps in this reaction are reversible and an equilibrium is reached between benzaldehyde and benzoin. This often leads to one of the biggest problems of these reactions, which is obtaining a high yield.

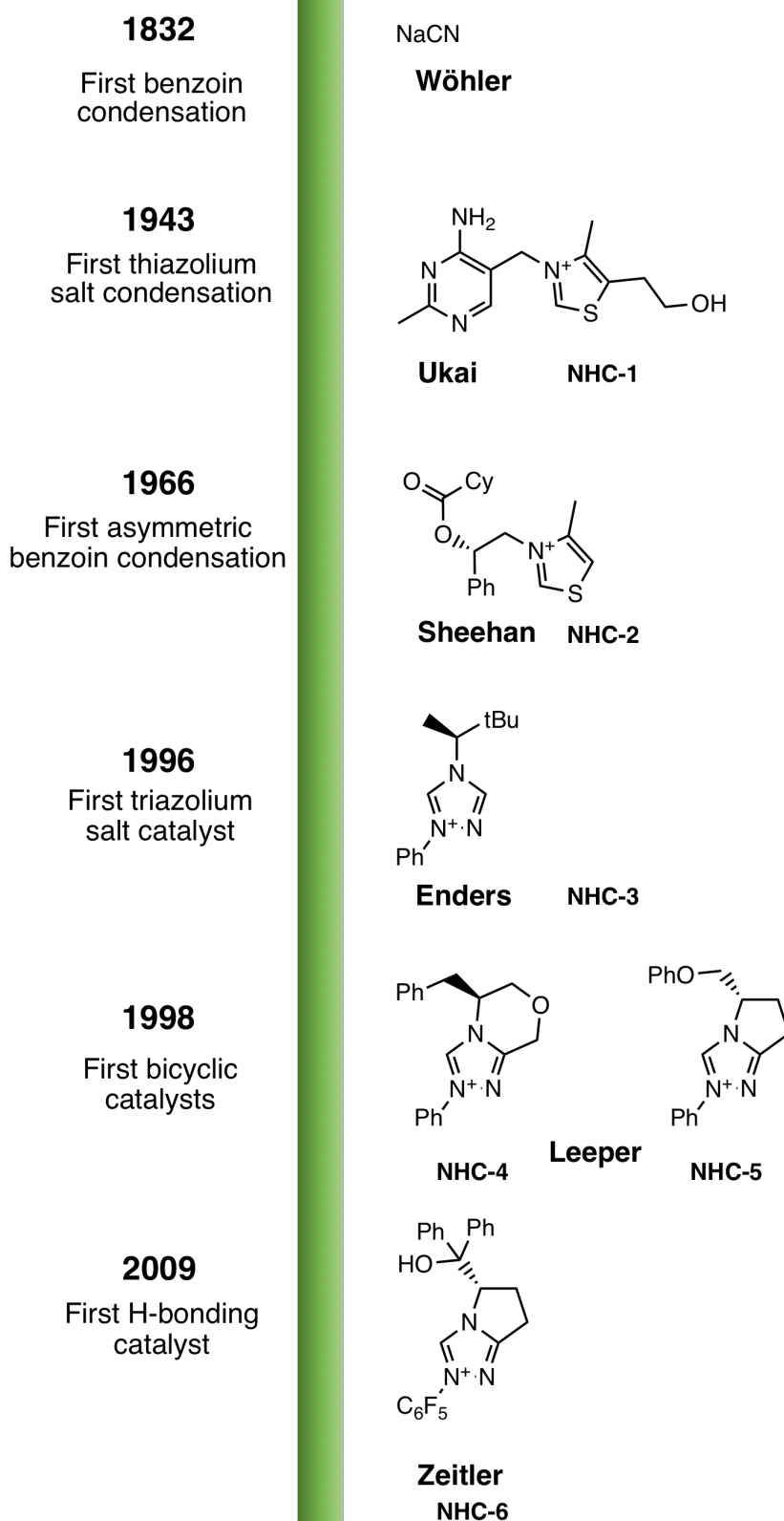


Fig. 1.22 A timeline showing the notable developments in the asymmetric NHC-catalysed benzoin condensation.

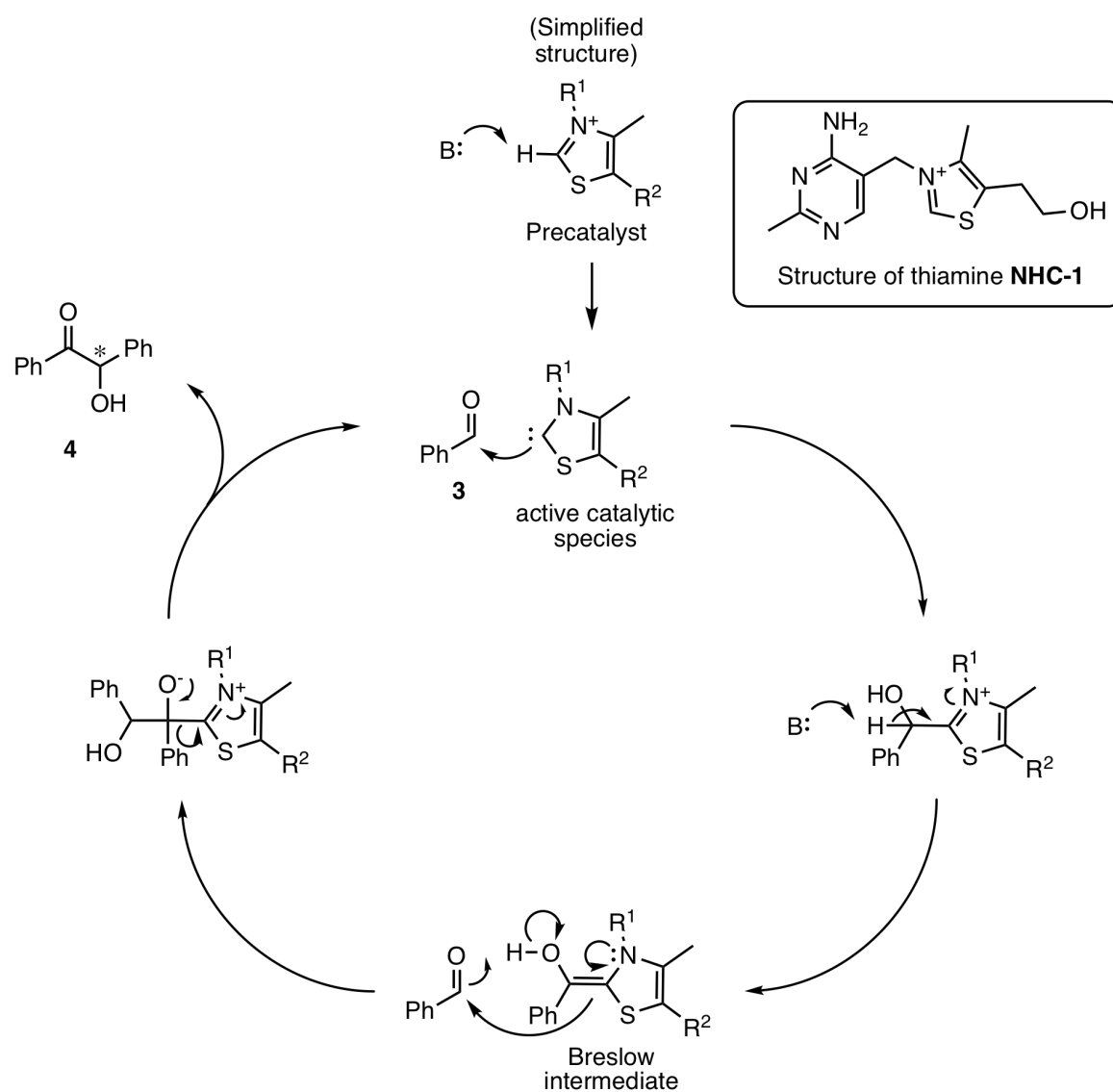


Fig. 1.23 The mechanism for the thiamine-catalysed benzoin condensation, first proposed by Breslow [57].

1.4.2 The Breslow Intermediate

The Breslow intermediate was first proposed by Ronald Breslow in 1958 [57]. The Breslow intermediate has yet to be isolated and fully characterised, although many attempts have been made over the decades. The closest report was in 2014, when Berkessel and coworkers successfully managed to synthesise and characterise 2,2-diamino enols **20a-25b** [58], indicating that these similar structures are plausible intermediates on the pathway to the α -hydroxy ketones catalysed by NHCs. Two peaks for atoms C2 and C6 were detected for the first time by ^{13}C NMR, and the method was demonstrated with a range of starting aldehydes. Although these were specifically generated in non-standard benzoin condensation conditions using imidazoline NHCs, which are not good catalysts for this reaction, these azolium-derived structures give arguably the closest insight to this reaction yet.

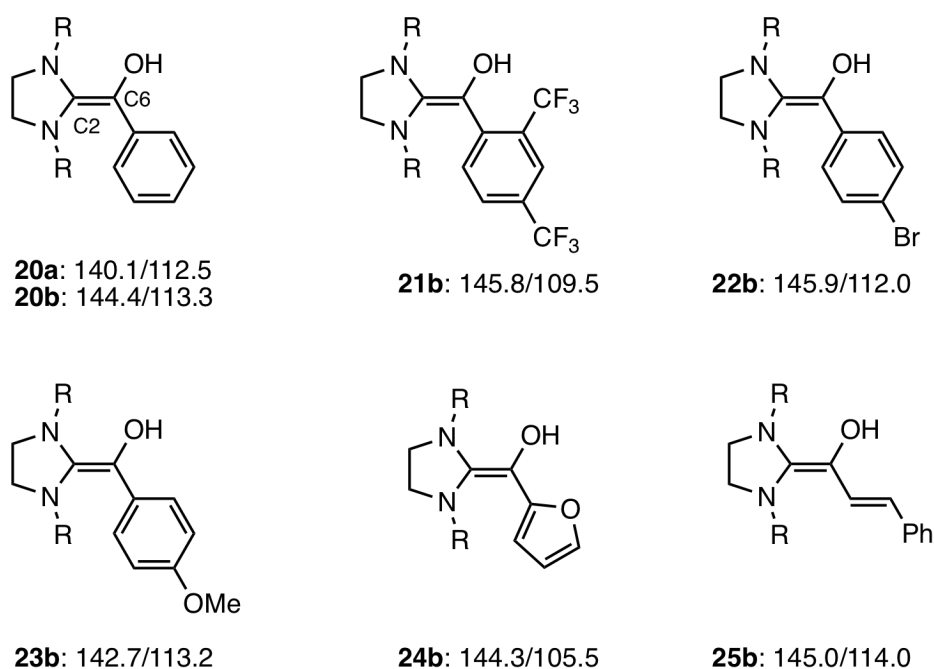


Fig. 1.24 ^{13}C Nuclear Magnetic Resonance (NMR) shifts [ppm] of a range of 2,2-diamino enols generated. **20a** R = 2,4,6-trimethylphenyl, **20b-25b** R = 2,6-bis(2-propyl)phenyl. The labels show C2/C6 carbon shifts respectively.

1.4.3 Beyond N-Heterocyclic Carbenes

More recently, Gehrke and Hollóczki proposed that free carbenes may not even be generated [59]. Energy profiles were calculated for the dissociative and associative mechanisms of benzaldehyde to azolium catalysts. The associative mechanism (Fig. 1.25) demonstrates the reaction between the N-heterocycle and the aldehyde occurring in a single elementary step. This work showed that the associative mechanism pathway **TS_{2→IV}** was favoured by 19-29 kcal mol⁻¹ compared to **TS_{II-III}**. This mechanism further supports reactions which occur with a large pK_a difference between the N-heterocycle and the base, and further studies into this will help clarify these results.

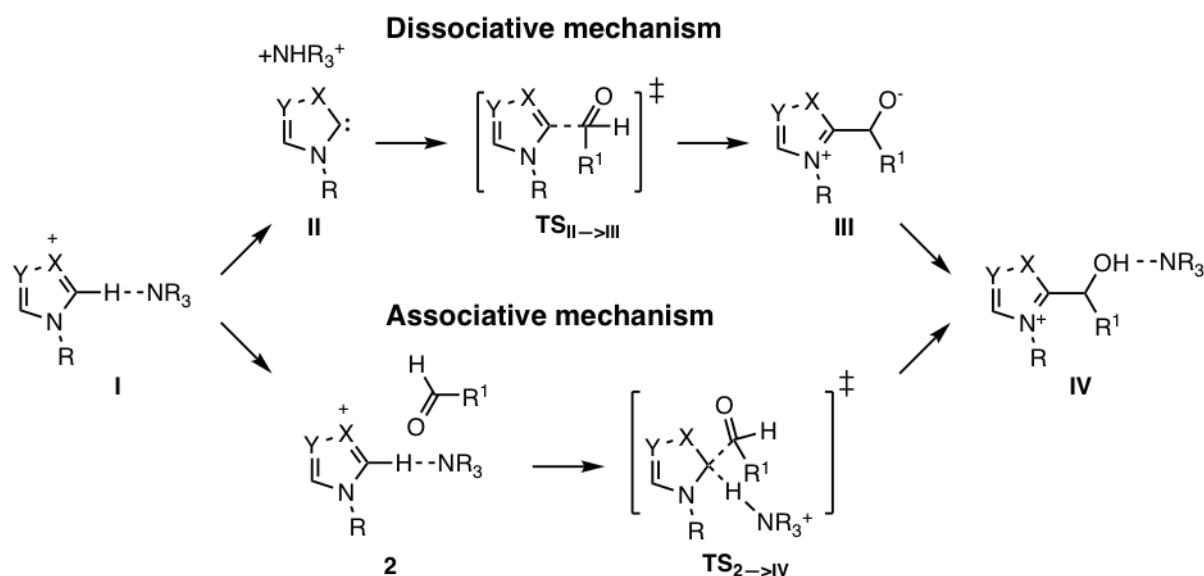


Fig. 1.25 The dissociative and associative mechanisms of benzaldehyde to azolium catalysts, as calculated by Gehrke and Hollóczki [59].

1.4.4 Asymmetric Thiazolium Salt Catalysts

After the thiazolium ring of thiamine had been identified as the active catalytic moiety, other thiazolium salts were tested for their use in the asymmetric benzoin condensation. Sheehan and coworkers reported the first example of a chiral thiazolium pre-catalyst **NHC-2** in 1966 [60] (Table 1.3). Initial efforts yielded an ee of 4.2%. They later reported a 1-naphthyl

group modification to give **NHC-7**, which gave ee's up to 51.5% after recrystallisation [61]. However, as ee increased, the yield of product decreased dramatically, with the most optically pure product being obtained in 6.1% yield. Most of the catalysts discussed in this section have worked for a range of aromatic aldehydes containing electron-donating and electron-withdrawing groups, but only benzaldehyde has been discussed to allow for easier comparison between catalysts.

Several other thiazolium structures have also been reported, but with little improvement in stereoselectivity. Chiral thiazolium salt **NHC-8** based on menthol derivatives [62] achieved ee's up to 35.3%, but again furnished lower yields as ee increased. In this case, micellar two-phase media was used as the solvent, at pH 8.

Table 1.3 Thiazolium catalysts in the benzoin condensation.

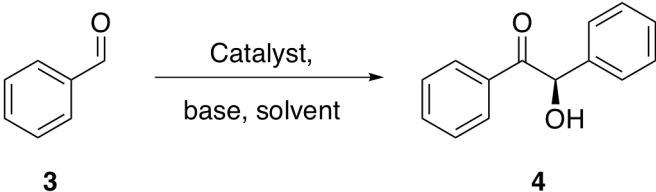
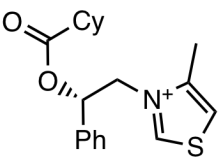
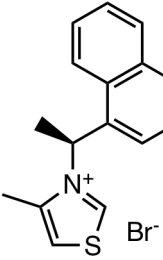
 <div style="display: flex; justify-content: space-around; width: 100%;"> 3 4 </div>				
Catalyst	Yield (%)	R/S config. of product	ee (%)	Conditions
 <p>NHC-2</p>	59	S	4.2	NEt ₃ , MeOH, rt [60]
 <p>NHC-7</p>	6.1	S	51.5	NHC-7 (10 mol%), NEt ₃ , MeOH, 30°C, 6h [61]

Table continues

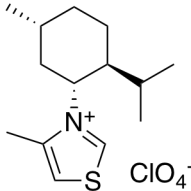
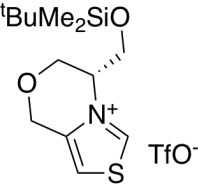
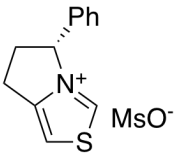
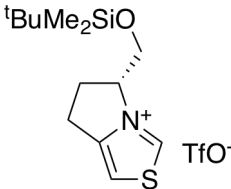
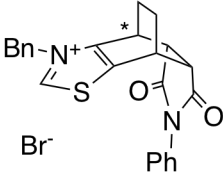
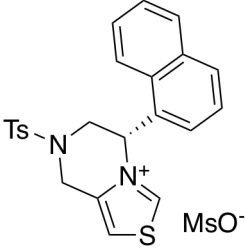
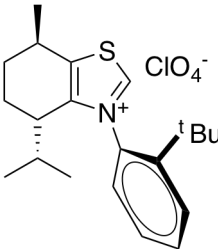
Catalyst	Yield (%)	R/S config. of product	ee (%)	Conditions
 NHC-8	20	<i>R</i>	35.3	NHC-8 (5 mol%), H ₂ O, phosphate buffer (pH 8), N ₂ , rt, 41h [62]
 NHC-9	34	<i>R</i>	19.5	NHC-9 (10 mol%), NEt ₃ , MeOH, 20°C [63]
 NHC-10	20	<i>R</i>	10.5	NHC-10 (10 mol%), NEt ₃ , MeOH, 20°C [63]
 NHC-11	50	<i>R</i>	20.5	NHC-11 (10 mol%), NEt ₃ , MeOH, 20°C [63]
 NHC-12 * = (<i>R</i>)	100	<i>S</i>	26	NHC-12 (5 mol%), NEt ₃ (neat) 20°C, 18h [64]

Table continues

Catalyst	Yield (%)	R/S config. of product	ee (%)	Conditions
 <p>NHC-13</p>	18	<i>R</i>	30	NHC-13 (10 mol%), NEt ₃ , MeOH:H ₂ O (1:2.5), rt, 8h [65]
 <p>NHC-14</p>	85	<i>R</i>	40	NHC-14 (20 mol%), NEt ₃ , THF, rt, 18h [66]

1.4.5 Bicyclic Thiazolium Salts

More rigid structures were proposed by Leeper and coworkers, who reasoned that low yields might be obtained due to free rotation around the chiral moiety, therefore hindering approach of both benzaldehyde molecules [63]. Using 3 different bicyclic catalysts (**NHC-9-11**), yields of up to 50% were reported, but only ees up to 20.5% were achieved (Table 1.3). Leeper and coworkers proposed further rigid catalysts in the form of polycyclic thiazolium salt **NHC-12** [64]. Although these catalysts were less effective and only led to a maximum ee of 26%, the catalysts could be synthesised in only 5 steps. These studies also demonstrated that blocking one face of the thiazolium ring was not enough to encourage enantioselectivity, and so further structural investigations were needed.

The following year, Rawal and coworkers demonstrated the use of bicyclic thiazolium catalyst **NHC-13** in the benzoin condensation [65]. Using MeOH:H₂O as the solvent yielded the product with an ee of 30%. Using Sheehan's naphthyl catalyst **NHC-7** with

these optimised conditions, an ee of 48% was achieved, with a 52% yield. Bach and coworkers proposed axially chiral catalyst **NHC-14** as a different method of introducing enantioselectivity [66]. Benzoin was formed in 85% yield, but with 40% ee. Although the importance of axial chirality was demonstrated in the asymmetric benzoin condensation, the atropisomers used were not configurationally stable and interconverted during the reaction, meaning the enantioselectivity was not as high as hoped.

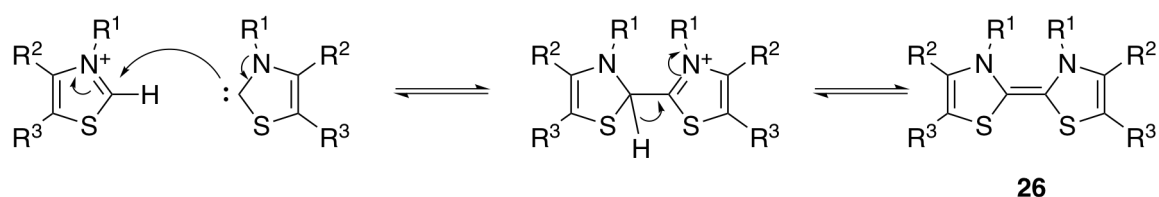


Fig. 1.26 Proposed dimer intermediate **26**.

Several attempts have been made to use thiazolium dimers as catalysts for the benzoin condensation, but these have achieved only modest enantioselectivities [67, 68]. Rationale behind these precatalysts comes from a potential dimer intermediate **26** being the active catalytic species (Fig. 1.26). However, Breslow ruled this route out as unlikely due to his provided kinetic evidence for the Breslow intermediate, which is widely accepted [56]. No further improvements in ee of the thiazolium salt catalysed benzoin condensation have yet been reported.

1.4.6 Triazolium Salt Catalysts

Miyashita and coworkers first reported triazolium salt precatalysts capable of catalysing the benzoin condensation in 1996 [69]. Although achiral, the use of a triazolium catalyst for this reaction of benzaldehyde had not been reported previously. However, Enders and coworkers had shown that formaldehyde could react in a similar fashion to benzaldehyde using a triazolium carbene catalyst to form the formoin product [70]. Motivated by this, Enders and coworkers demonstrated the first successful use of a triazolium salt as a precatalyst in the asymmetric benzoin condensation [71]. Using benzaldehyde, an ee of 75% was determined,

and unlike the thiazolium-catalysed reactions, the product was isolated in 66% yield using only 5 mol% of **NHC-15** (Table 1.4).

To directly compare triazolium and thiazolium salts, Leeper and coworkers trialled both of these in the benzoin condensation [72]. Using identical reaction conditions, the bicyclic triazolium precatalysts including **NHC-16** gave ee's of benzoin up to 80%, around four times higher than the bicyclic thiazolium salts. The catalysts were synthesised in a simple three-step procedure, giving an overall yield of 65% (Fig. 1.27). This facile synthesis starting from chiral amino acid derivatives has inspired the synthesis of many other bicyclic triazolium salt precatalysts.

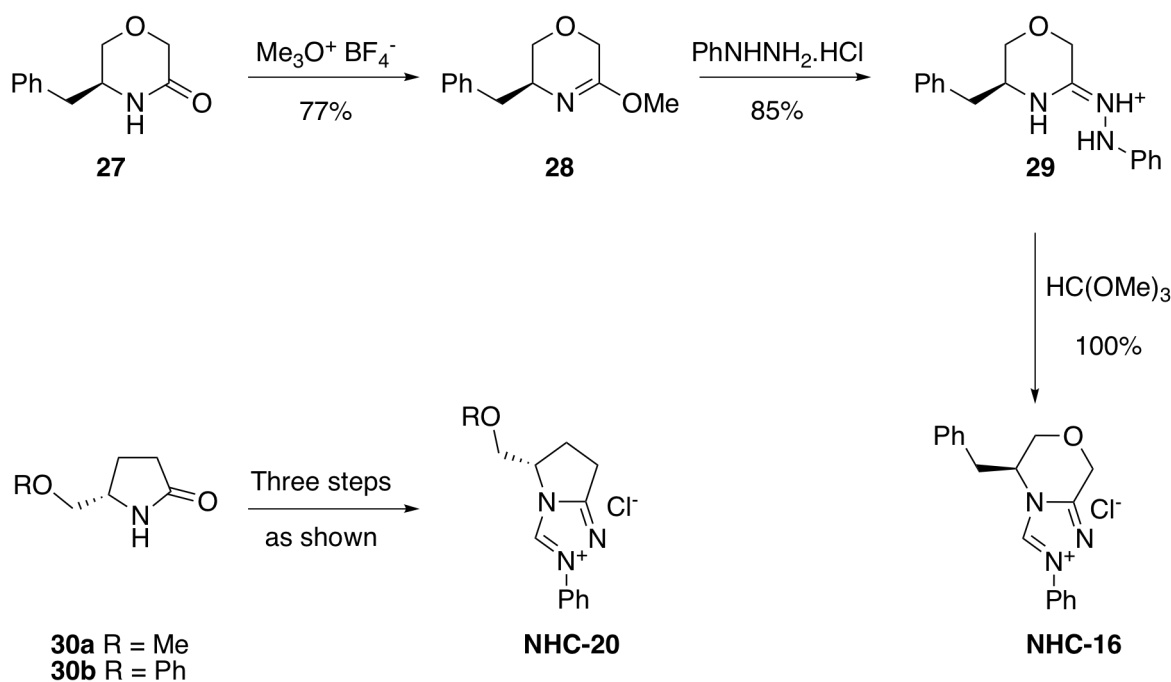


Fig. 1.27 Synthesis of bicyclic triazolium catalysts by Leeper and Knight.

Using a modification of Leeper's synthesis, Enders and coworkers synthesised a bicyclic triazolium salt catalyst **NHC-17** employing a chiral *tert*-butyl group [73]. Variation of the catalyst and base loading demonstrated that higher loading led to higher yield, with 10 mol% loading giving a yield of 83%. However, this led to a lower ee compared to the lower catalyst loadings. A modified bicyclic catalyst by Enders featuring a much bulkier chiral side group,

Table 1.4 Triazolium catalysts in the benzoin condensation.

<p style="text-align: center;">3 4</p>				
Catalyst	Yield (%)	R/S config. of product	ee (%)	Conditions
<p style="text-align: center;">NHC-15</p>	66	<i>R</i>	75	K ₂ CO ₃ , THF, rt, 60h [71]
<p style="text-align: center;">NHC-16</p>	45	<i>S</i>	80	NEt ₃ , MeOH, rt, 18h [72]
<p style="text-align: center;">NHC-17</p>	83	<i>S</i>	90	KOtBu, THF, rt, 16h [73]
<p style="text-align: center;">NHC-18</p>	66	<i>R</i>	95	KHDMS, toluene, rt, 16h [74]
<p style="text-align: center;">NHC-19</p>	95	<i>S</i>	95	KOtBu, THF, rt [75]

NHC-18, led to an increased ee of 95%, but a significantly lower yield than the previous catalyst [74].

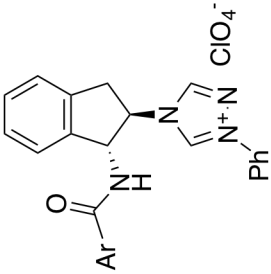
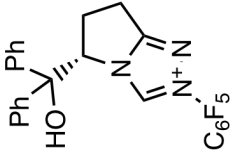
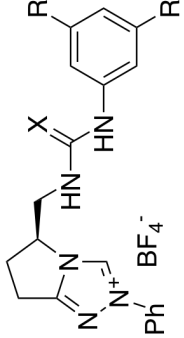
In 2008, You and coworkers investigated C₂-symmetric bis-triazolium salt precatalyst **NHC-19** in the benzoin condensation [75]. It was thought that the higher level of conjugation compared to other catalysts would lead to a higher activity, and the number of active catalytic sites would be increased. An advantage of this method was the low catalyst loading, which was only 1%, compared to other effective triazolium salt catalysts. Both high yield and enantioselectivity were achieved.

1.4.7 Current Hydrogen-Bonding Catalysts for the Benzoin Condensation

There are currently very few examples where H-bonding NHCs have been used for the benzoin condensation. In 2009, Connon and O'Toole reported use of rigid triazolium catalyst **NHC-20** incorporating an amide as a hydrogen-bond donating moiety [76] (Table 1.5). Up to 62% ee was reported, but yields did not exceed 63%. Direct comparison of this catalyst to the methyl-protected amine analogue gave an increased ee of 41%, but with a yield of 25%. Interestingly, H-bonding catalyst **NHC-21** only gave an ee of 16%. This shows that other factors also have an effect on enantioselectivity, such as the electron-withdrawing capabilities of the substituents.

Connon and coworkers reported a rigid bicyclic triazolium catalyst in 2009, **NHC-6**, employing a hydroxyl group as the H-bonding moiety [77]. Containing only one chiral centre, the catalyst obtained ee's of > 99%, with yields up to 100%. Replacing the *N*-phenyl group with an electron withdrawing pentafluorophenyl group obtained much higher yields. An analogue with a methoxy group was synthesised to remove the H-bonding, and the ee dropped to 53% showing not only that H-bonding had a significant effect, but also the structure of the catalyst could reasonably influence stereoselectivity regardless. Both of these catalysts were effective at as low as 4 mol%, and worked at room temperature or lower.

Table 1.5 H-bonding triazolium salt catalysts in the benzoin condensation.

Catalyst	Yield (%)	R/S config. of product	ee (%)	Conditions
 <p>NHC-20 Ar = Ph NHC-21 Ar = 3,5-bis(CF₃)₂C₆H₃</p>	<p>NHC-20 12 NHC-21 11</p>	S	<p>NHC-20 62 NHC-21 16</p>	Toluene, KHDMS, rt [76]
 <p>NHC-6</p>	90	R	80	Rb ₂ CO ₃ , THF, 24h [77]
 <p>NHC-22a X = O, R = H NHC-22b X = S, R = H NHC-22c X = O, R = CF₃ NHC-22d X = S, R = CF₃</p>	<p>NHC-22a 47 NHC-22b 81 NHC-22c 85 NHC-22d 17</p>	R	<p>NHC-22a 64 NHC-22b 60 NHC-22c 42 NHC-22d 90</p>	K ₂ CO ₃ , THF, rt, 15h [78]

Only one example of a triazolium salt incorporating a (thio)urea group has been published to date, by Waser and coworkers who incorporated a (thio)urea moiety onto a bicyclic core [78] (**NHC-22a-d**). The bis-trifluoromethyl phenyl ring catalyst **NHC-22d** gave a much higher ee when in conjunction with the thiourea moiety, achieving 90% ee at room temperature. Both urea and thiourea analogues were synthesised, and it was observed that there was a decrease in yield as enantioselectivity increased. The catalysts themselves were easily synthesised in 7 steps with yields up to 30%, based on Leeper and coworkers' route [72]. There have been no further reports since their initial publication in 2010.

From the original thiazolium salt design to the newer triazolium salts with superior catalytic efficiency, many catalysts have demonstrated nearly 100% ee and equally high yields. However, as discussed previously by Leeper [64], simply blocking the face of the triazolium salt is not enough. Although Connon's catalyst has demonstrated the highest ee and yield of benzoin for any of the hydrogen-bonding catalysts, the bulky phenyl groups attached add a large degree of steric repulsion, leading to reaction times of 24 hours. The thiourea catalyst has shown promise in regard to both yield and enantioselectivity, and due to no other studies in this area being reported, there is great interest to try and improve on these initial results.

1.5 Other Applications of NHCs

Aside from the homobenzoin condensation, NHCs can also catalyse a range of reactions including cross-benzoin and intramolecular benzoin condensations, Stetter reactions, and many cyclisation reactions. More exhaustive reviews for these catalysts can be found elsewhere [23, 79, 80] and only a selection are to be discussed here.

1.5.1 Achiral Cross Benzoin Condensations

The benzoin condensation discussed earlier can also occur between two different aldehydes, known as the cross benzoin (or heterobenzoin) condensation. This is synthetically useful as it widens the scope of the benzoin condensation, accessing many new asymmetric α -hydroxyketones. However, chemoselectivity issues arise as there are now four possible compounds that can be made, and it is difficult to control which of these is favoured (Fig. 1.28).

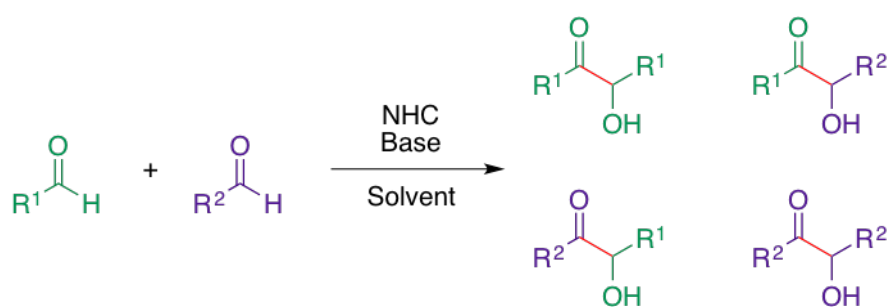
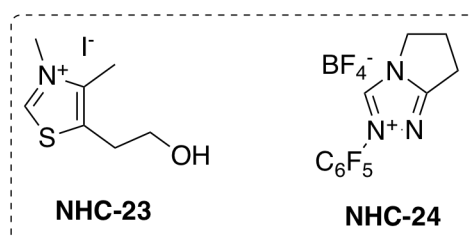
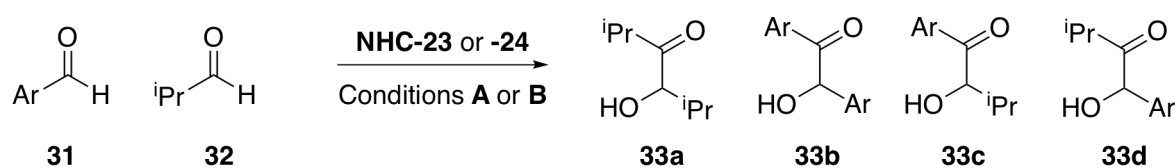


Fig. 1.28 Chemoselectivity issues with the cross-benzoin condensation.

Stetter reported the first attempted cross benzoin condensations using achiral thiazolium salt carbene catalysts as early as 1977 [81, 82], but chemoselectivity was poor. However, this demonstrated the ability of NHC catalysts in reactions other than the homobenzoin condensation.

Cannon and coworkers took major steps forward in the cross-benzoin condensation from 2010 onwards, using triazolium pre-catalysts (Fig. 1.30). These allowed for the cross-coupling of aliphatic aldehydes with electron-rich aromatic aldehydes [83], something which had not been previously reported. Direct comparison of Stetter's catalyst with triazolium salts showed that the triazolium salt **NHC-24** gave a better yield with benzaldehyde derivatives than thiazolium salt **NHC-23** did (Table 1.6). However, the thiazolium salt showed better tolerance to heterocyclic aldehydes. The triazolium salt worked for a wide range of reagents. Again, an achiral catalyst was used here so there was no enantioselectivity.

Table 1.6 Comparing thiazolium and triazolium salt pre-catalysts in the cross benzoin condensation.



Catalyst and Conditions	Ar	Yield (%)			
		a	b	c	d
A	Phenyl	<2	20	27	27
B		<2	13	<2	61
A	2-ClC ₆ H ₄	<2	8	<2	64
B		<2	<2	<2	68
A	4-ClC ₆ H ₄	5	12	27	26
B		0	7	12	63
A	2-furyl	5	<2	78	7
B		<2	13	33	28
A	2-thienyl	<2	9	44	<2
B		<2	14	31	0

Conditions: (A^b) **NHC-23** (10 mol%), Et₃N (60 mol%), EtOH, reflux, 16 h [81]. (B)

NHC-24 (10 mol%), Rb₂CO₃ (10 mol%), THF, 60 °C, 20 h [82].

^a Yield determined by ¹H NMR spectroscopy using (*E*)-stilbene as an internal standard.

^b Data is from the average of a minimum of two experiments.

The chemoselectivity of this cross benzoin condensation using thiazolium NHCs is thought to come from the formation of the more thermodynamically stable aromatic Breslow intermediate **36a** (Fig. 1.29). The increased stability is due to the improved delocalisation through the π -system. However, using bulky triazolium salt catalysts favour the formation of the alkyl-Breslow intermediate **36c** to avoid steric repulsion.

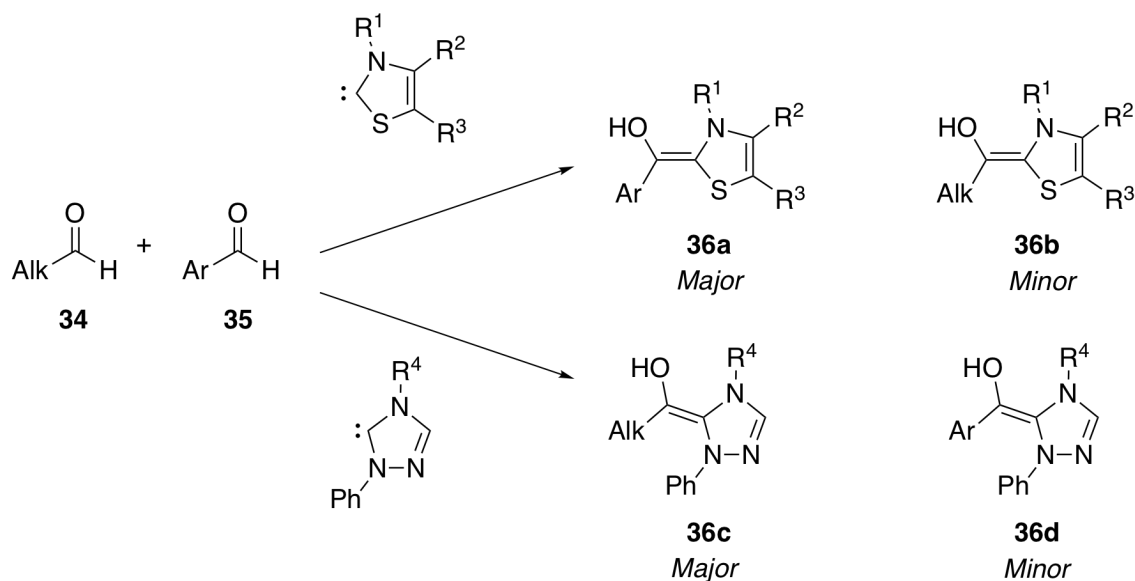


Fig. 1.29 Explanation of chemoselectivity in the cross benzoin condensation.

Using catalyst **NHC-24**, Connon and coworkers demonstrated a wider range of cross-benzoin condensations, between aldehydes and α -keto-esters [84]. Both aliphatic and aromatic aldehydes were tolerated, achieving yields up to 95%. Glorius and coworkers have demonstrated the applicability of effective thiazolium salts in the chemoselective cross benzoin condensation [85], but again with no enantioselectivity due to the achiral catalyst.

1.5.2 Chiral Cross Benzoin Condensations

Building on their work on the benzoin condensation between α -keto-esters **37** and acetaldehyde **38**, Connon and coworkers reported the cross-benzoin reaction using chiral NHC catalysts [86]. **NHC-6** described earlier, **NHC-25** and **NHC-26**, all formed the product **39a-c** with ee up to 76%, whilst still obtaining moderate yields (Fig. 1.30).

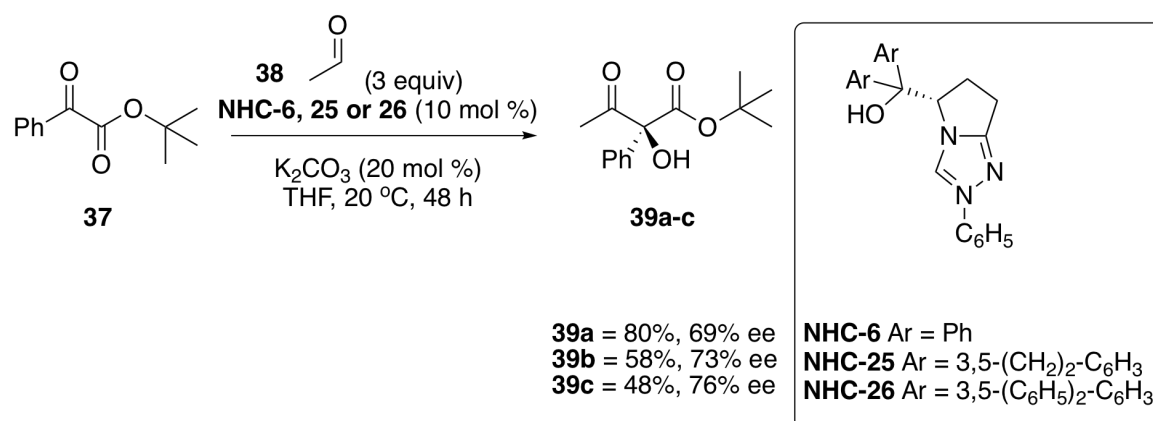


Fig. 1.30 Chemoselectivity and stereoselectivity in the cross benzoin condensation.

The intramolecular benzoin condensation is important in the synthesis of many organic and natural scaffolds. It is important to note that these are normally cross-benzoin reactions. Erhardt and coworkers demonstrated how a polycyclic triazolium salt catalyst, **NHC-27**, could be used for the cyclisation of compound **40** to **41** at room temperature (Fig. 1.31) [87]. Due to the nature of the substrate, a competing intramolecular Aldol reaction led to formation of **42** and dehydration product **43** when screening a range of catalysts. However, catalyst **NHC-27** gave only the desired product. Although employing a chiral catalyst, a racemic product was obtained at the end.

Using a similar polycyclic catalyst, Ema *et al.* showed the asymmetric intramolecular cross-benzoin condensation could be catalysed by **NHC-28** or (*R,S*)-**NHC-27** to form a range of bicyclic diketones [88] (Fig. 1.32). The synthesis of quaternary carbon centres is often difficult due to steric constraints, but employing a range of conditions gave the desired products in yields of up to 90% and ee's up to 99%.

Jia and You demonstrated the use of camphor-based triazolium salt catalyst **NHC-29** in the intramolecular benzoin condensation of **46** to give dihydroquinoline derivatives **47** [89] (Fig. 1.33). Using (*R,S*)-**NHC-27** gave the product in poor ee, but **NHC-29** gave the product in up to 92% ee. Although the reaction required 15 mol% catalyst loading, the reaction gave 17 products in up to 96% yield with mild conditions.

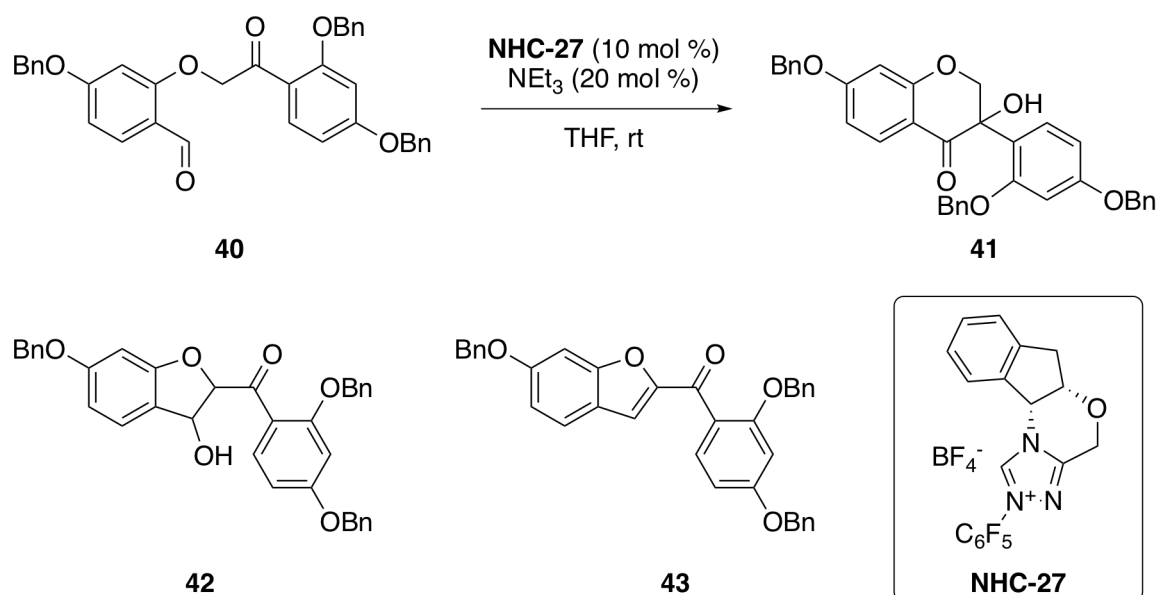


Fig. 1.31 Intramolecular benzoin condensation and associated Aldol side-products [87].

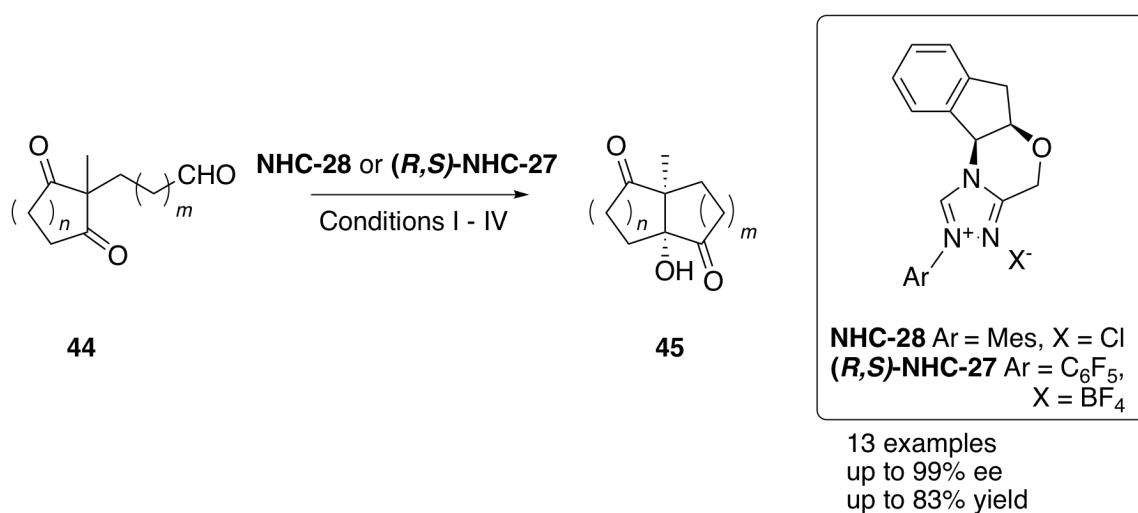


Fig. 1.32 Intramolecular cross benzoin condensation to form quaternary carbon centres, reported by Ema *et al.* [88]. Reaction conditions (I): **NHC-28** or **(R,S)-NHC-27** (30 mol%), Cs_2CO_3 (30 mol%), CH_2Cl_2 , rt, 24 h. (II): identical to (I) except at 40 °C. (III): **NHC-28** or **(R,S)-NHC-27** (20 mol%), Et_3N (20 mol%), THF, 23 °C, 24 h. (IV): Identical to (I), but **45** was added at 23 °C after the active catalyst had been generated at 40 °C.

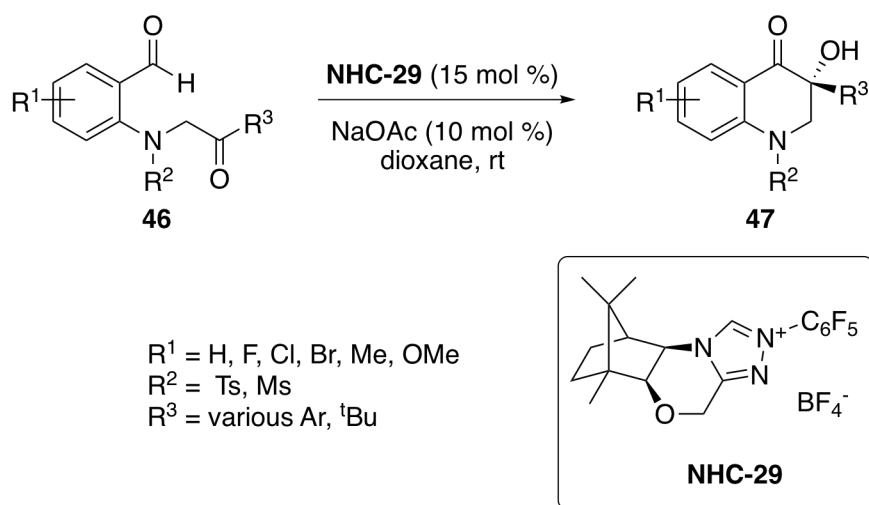


Fig. 1.33 Intramolecular benzoin condensation to form dihydroquinoline derivatives [89].

1.5.3 Reactions with Different Acceptors

Goodman and coworkers demonstrated the coupling of aldehydes with (\pm)- β -bromo- α -keto-esters **49** to form the corresponding esters **50** [90] (Fig. 1.34). Tolerating a range of aromatic aldehydes, the NHC selectively added into the ketone rather than the ester, with over >20:1 diastereomeric ratio (dr) and 96% ee obtained with **NHC-30**.

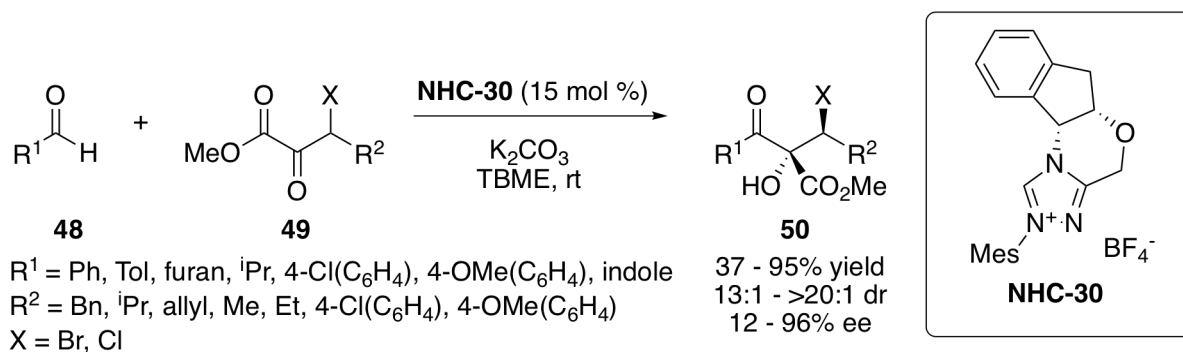


Fig. 1.34 Cross benzoin condensation to form β -bromo α -keto esters [90].

Other benzo-fused heterocycles such as chromanones have been successfully synthesised from reagents such as **51** using NHCs as catalysts. Enders applied three different catalysts **NHC-31**, **-32** and **-17** to the intramolecular benzoin condensation, achieving yields of up to 93% and ee's of up to 99% [91] (Fig. 1.35). **NHC-31** was the most successful, tolerating a

wide range of alkyl chains attached to the ketone. The aryl groups tested were unsubstituted, 2-nitro-, 2,3-methylenedioxy-, 2,4-dibromo- and 2,4-di-*tert*-butyl-phenyl, which all were tolerated, but sterically demanding groups led to low conversions even at elevated temperatures. Increasing reaction temperature led to higher yields of **52**, but lower ee. A further camphor-based organocatalyst **NHC-33** has since been applied to these reactions using 2-*tert*-butylimino-2-diethylamino-1,3-dimethylperhydro-1,3,2-diazaphosphorine (BEMP) as a base and cyclopentyl methyl ether (CPME) solvent, giving yields up to 99% and 96% ee [92].

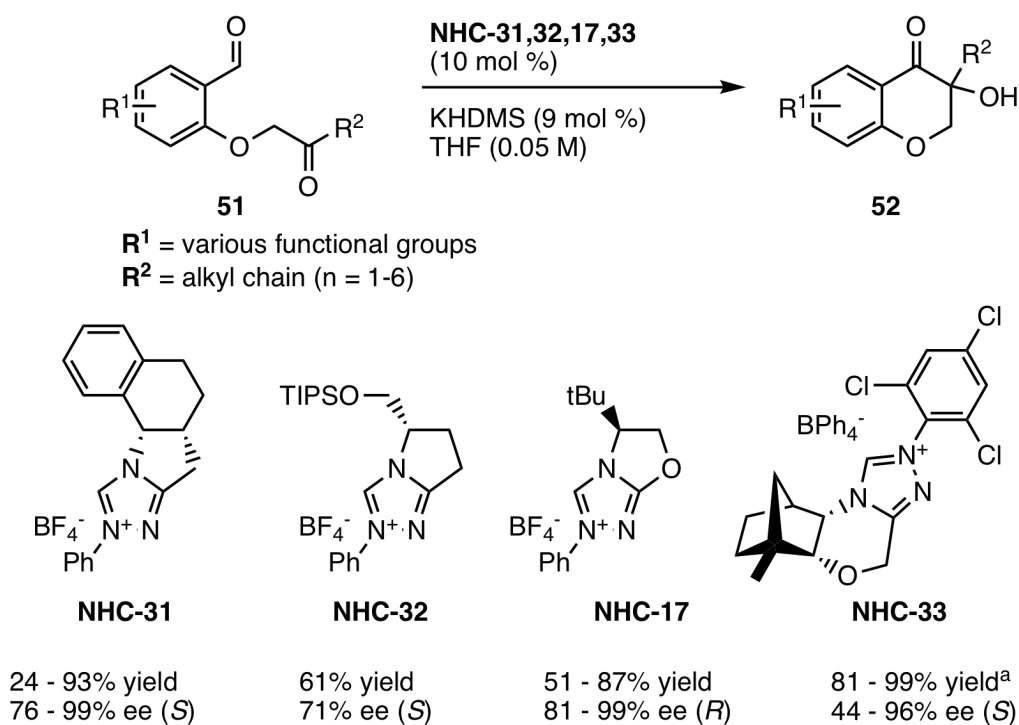


Fig. 1.35 Formation of chromanones *via* an intramolecular benzoin condensation [91, 92].
^a**NHC-33** (15 mol%), BEMP (15 mol%), CPME (0.1 M), rt, 1h.

The triazolium-catalysed intramolecular benzoin condensation to form chromanones has been applied to the synthesis of natural product (+)-sappanone B (Fig. 1.36) [93] 2-hydroxy-4-methoxybenzaldehyde **53** is first converted to the pre-cursor **54** over 5 steps, with an overall yield of 83%. The reaction is then catalysed by **NHC-34**, achieving 95% ee. Finally, subsequent hydrolyses afford the final product **56**.

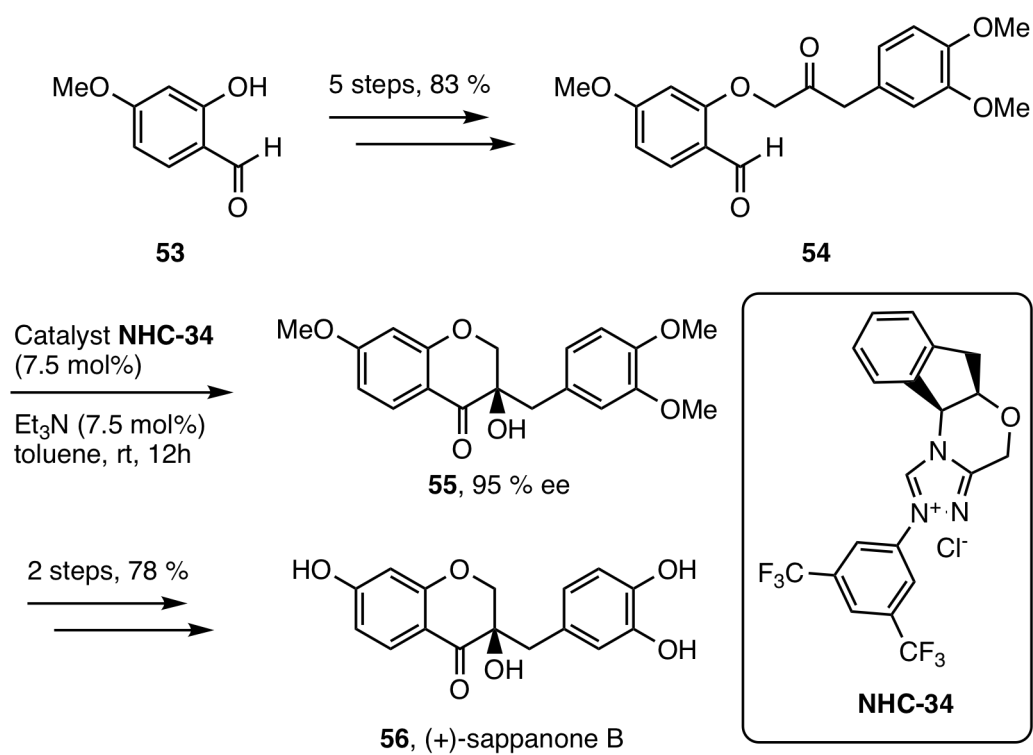


Fig. 1.36 Synthetic route to (+)-sappanone-B using an NHC-organocatalysed intramolecular benzoin condensation [93].

Aldehyde-ketone benzoin condensations are also possible with NHC catalysts. Using thiamine derivative **NHC-35**, Suzuki and coworkers performed an intramolecular benzoin condensation from **57a-c** to form polycyclic preanthraquinones **58a-c** [94] (Fig. 1.37). Cyclohexene rings with chiral groups attached achieved a de of >20:1, in yields up to 95%.

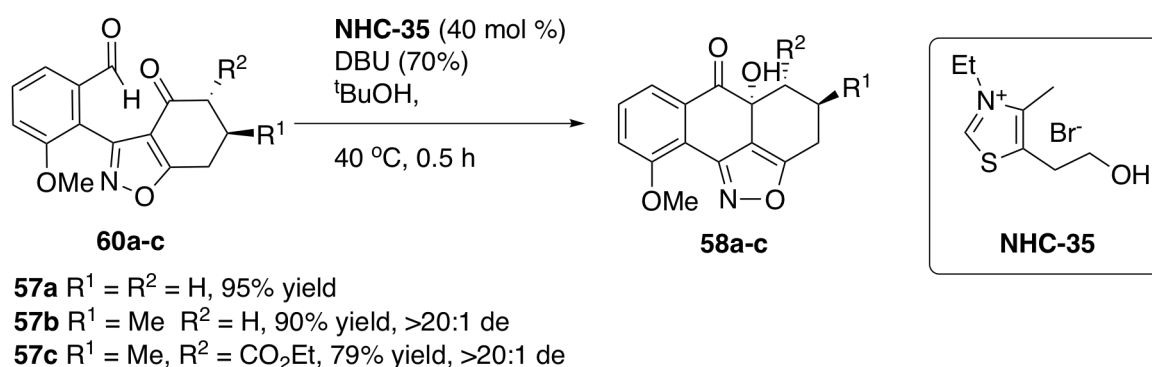


Fig. 1.37 Intramolecular benzoin condensation using a thiazolium salt pre-catalyst [94].

Reactions With Imines

NHCs can also facilitate the reaction of carbonyls with imines in several ways, such as the Aza Morita-Baylis-Hillman (aza-MBH) reaction, and the Staudinger synthesis. Using bifunctional catalyst **NHC-36**, which is capable of H-bonding to the reagents, a new chiral amine centre in product **61** was formed upon addition to the ketone **59** in the aza-MBH reaction as shown by Ye and coworkers [95] (Fig. 1.38). Several catalysts were screened for this reaction, and catalyst **NHC-36** gave the highest enantioselectivity of 44%, with a moderate yield of 54%. Although the enantioselectivity needs improving, it shows how bifunctional catalysts can influence the selectivity in a range of reactions beyond the traditional benzoin condensation.

Using catalyst **NHC-37**, Ye demonstrated the Staudinger synthesis of β -lactams **64** from ketenes **62** and Boc-imines **63** [96] (Fig. 1.39), but included a tert-butyl dimethylsilyl (TBS) protecting group, removing any hydrogen bonding. The catalyst worked extremely well, giving yields from 91 to 99%, and up to 99:1 *cis:trans*. The reaction also worked when the

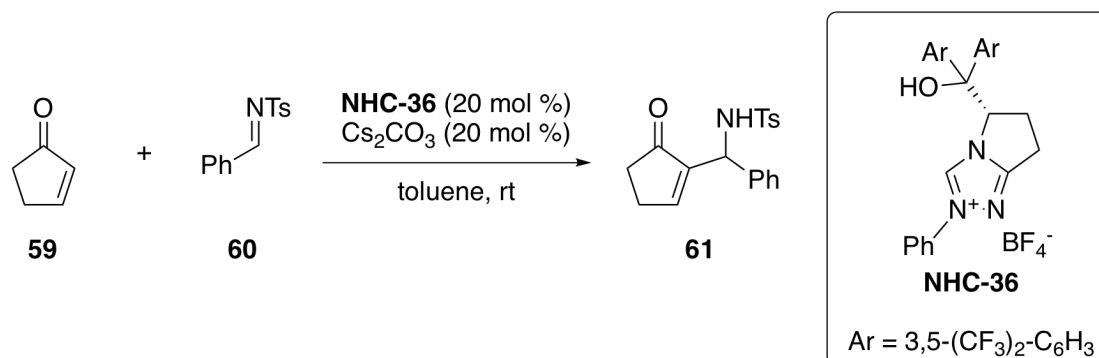


Fig. 1.38 NHC-catalysed reaction [95].

imine had a tosyl (Ts) protecting group instead of a *tert*-butoxycarbonyl (Boc)-protecting group, giving a yield of 88%. Up to 99% ee was obtained.

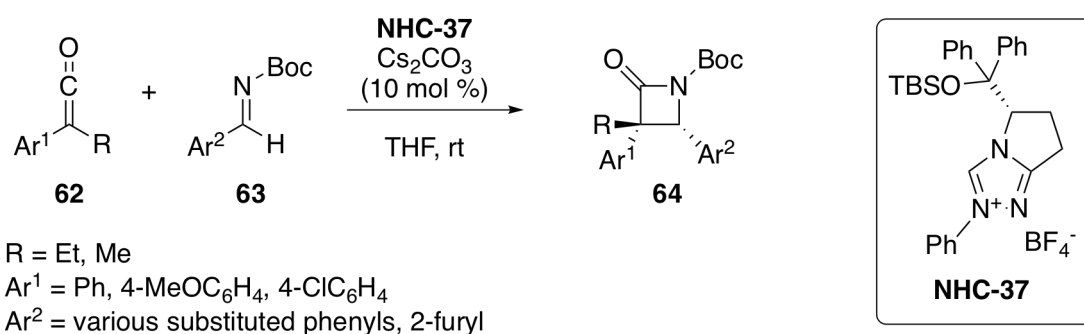


Fig. 1.39 Staudinger reaction using a triazolium salt catalyst [96].

A reaction similar to the Staudinger reaction was discovered by You and coworkers between aldehydes and imines **66**, leading to secondary amine product **67** [97] (Fig. 1.40). Using thiamine-derived catalyst **NHC-38**, yields of 66-95% were achieved, tolerating a range of aryl rings and heterocycles on both of the substituents. Due to the achiral catalyst, no enantioselectivity was observed.

Ye has further applications of NHC catalysts, including the [2+3] cyclocondensation of α -chloroaldehydes with azomethine imines [98].

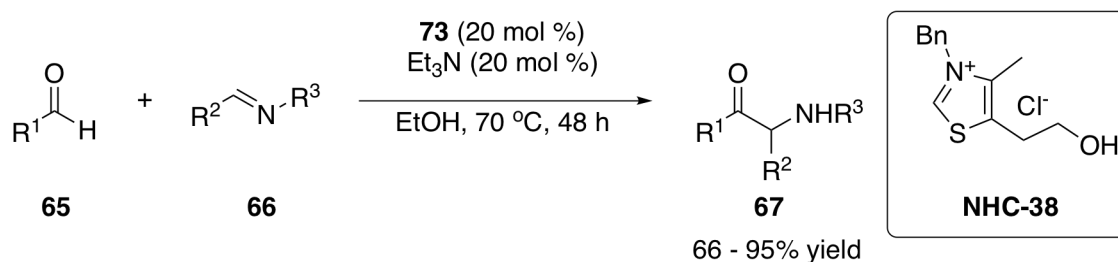


Fig. 1.40 NHC-catalysed coupling of aldehydes with un-activated imines [97].

The Stetter Reaction

Beyond the benzoin condensation, arguably the most successful application of NHC catalysts is in the Stetter reaction. In this reaction, an aldehyde is added into a Michael acceptor, and a wide range of functional groups and therefore products can be synthesised. The Stetter reaction can be catalysed successfully by both thiazolium and triazolium salts. This is only briefly covered here as an application of NHC catalysts; more comprehensive reviews can be found elsewhere [99, 100].

Stetter first reported this reaction in 1973, hence lending his name to the reaction [101]. Aromatic aldehydes such as **68** were added to 1,4-Michael acceptors **69** featuring electron-withdrawing groups (EWGs) such as nitriles and ketones in yields of **70** up to 90%, using a cyanide anion catalyst (Fig. 1.41). One advantage to the Stetter reaction is the lack of reversibility; the final product is stable, and so there is no racemisation of the chiral centre.

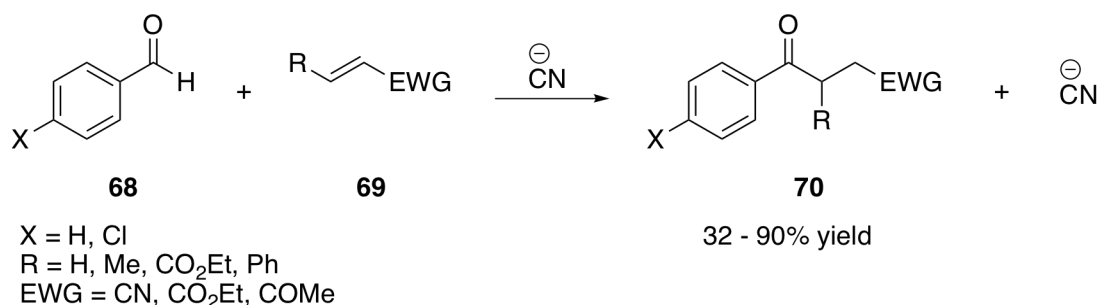


Fig. 1.41 Cyanide-catalysed Stetter reaction [101].

Only in the past few decades have chiral catalysts been used to make the Stetter reaction stereoselective. The Stetter reaction can also be used to form chromanone derivatives (Table

1.7), as with the benzoin condensation discussed earlier. The first reported asymmetric intramolecular Stetter reaction was by Enders and coworkers using catalyst **NHC-15**, which they reported in the asymmetric benzoin condensation. Variation in both EWGs on the aromatic ring and the alkyl chain on the ester [102] were tolerated, and yields up to 73% were obtained, and good enantioselectivity from 41-71% (Entries 1a-h).

Several years later, Rovis applied catalyst **NHC-39** in the formation of chromanones via the Stetter reaction [103]. Again, variation on the ester and aromatic ring were tolerated, but Rovis also varied the heteroatom substituent with protected N-groups and CH₂. Compared to Ender's catalyst, both yields and enantioselectivities were significantly higher, ranging from 82 to 96% ee (Entries 2a-h). Rovis also applied this reaction to the synthesis of cyclopentanone and benzofuranone in equally high yields, but with <5% ee for the latter.

Table 1.7 Asymmetric intramolecular Stetter reaction to form chiral chromanones.

Reaction scheme: **71** (starting material) $\xrightarrow[\text{Base, solvent}]{\text{Catalyst}}$ **72** (product). Structure **71** is a 2-alkoxy-2-aryl-3-oxoprop-1-en-1-yl ester. Structure **72** is a 2-alkoxy-2-aryl-3-oxoprop-1-en-1-yl ester with a new stereocenter marked with an asterisk.

NHC-15^a

NHC-39^b

NHC-40^c

NHC-41^d

Entry	Catalyst	X	R	R ¹	Yield (%)	ee (%) ^e
1a	NHC-15	O	H	Me	73	60

Table continues

Entry	Catalyst	X	R	R ¹	Yield (%)	ee (%) ^c
1b	NHC-15	O	H	Et	69	56
1c	NHC-15	O	8-MeO	Me	44	68
1d	NHC-15	O	8-MeO	Et	69	62
1e	NHC-15	O	7-MeO	Me	22	71
1f	NHC-15	O	6-MeO	Me	56	61
1g	NHC-15	O	6-Cl	Me	50	41
1h	NHC-15	O	5,6-Ph	Me	51	65
2a	NHC-39	O	H	Et	94	94
2b	NHC-39	O	6-Me	Et	80	97
2c	NHC-39	O	8-Me	Et	90	84
2d	NHC-39	O	8-MeO	Et	95	87
2e	NHC-39	S	H	Me	63	96
2f	NHC-39	NMe	H	Me	64	82
2g	NHC-39	NCH ₂ =CHCO ₂ Me	H	Me	72	84
2h	NHC-39	CH ₂	H	Et	35	94 ^f
3a	NHC-40	O	H	Et	94	96
3b	NHC-40	O	8-MeO	Et	95	96
3c	NHC-40	O	7-MeO	Et	89	97
3d	NHC-40	O	6-MeO	Et	97	96
3e	NHC-40	O	8-Me	Et	95	95
3f	NHC-40	O	6-Me	Et	95	97
3g	NHC-40	O	6-Cl	Et	94	93
3h	NHC-40	O	6-Br	Et	94	94
3i	NHC-40	O	6-NO ₂	Et	86	68
3j	NHC-40	O	7-Et ₂ N	Et	90	97

Table continues

Entry	Catalyst	X	R	R ¹	Yield (%)	ee (%) ^e
3k	NHC-40	S	H	Et	26	88
3l	NHC-40	N-Ms	H	Et	77	56
4a	NHC-41	O	H	Et	99	99

Table 1.7 ^aConditions: Cat (20 mol%), K₂CO₃, THF, reported by Enders and coworkers [102]. ^bConditions: Cat (20 mol%), KHDMS (20 mol%), xylenes, rt, 24h, as reported by De Alaniz and Rovis [103]. ^cConditions: Cat (20 mol%), DIPEA (10 mol%), *o*-xylene, rt, reported by You and coworkers [104]. ^dConditions: Cat (8 mol%), DIPEA (8 mol%), cyclohexane, rt, 20h, 99 : 1 er, reported by Ráfiniski [105]. ^e *R* configuration unless stated. ^f *S* configuration.

As the camphor-based catalyst **NHC-40** had been successfully used in the intramolecular benzoin condensation, You and coworkers applied it to reagent **71**, demonstrating the versatility of substrates with this catalyst [104] (Entries 3a-l). Yields were again high for the chromanones, and also showed tolerance for sulfur (Entry 3k) and N-mesyl (Entry 3l), although in lower yield and enantioselectivity. More recently, novel (-)- β -pinene-derived catalyst **NHC-41** was developed and used in this reaction, with up to 99% ee and 99% yield (4a) tolerating various substitutions on the reagents [106].

1.5.4 NHC-Catalysed Cyclisations, Annulations and Complex Domino Cascades

Cross condensation reactions are also found in more complex reactions, such as domino-cascades developed by Ma *et al.* forming acyclic ε -keto esters **76** [107] (Fig. 1.42). A potential mechanism involving a cascade crossed-benzoin/oxy-Cope rearrangement/esterification catalysed by **NHC-42** was proposed for formation of the final product.

Exploiting the reactivity and mechanism of NHC-catalysed reactions has recently led to the development of annulation reactions. Tailoring the starting materials allows for [3+3], [4+2] and [3+2] cycloannulations, giving a range of cyclised products including spirocyclic

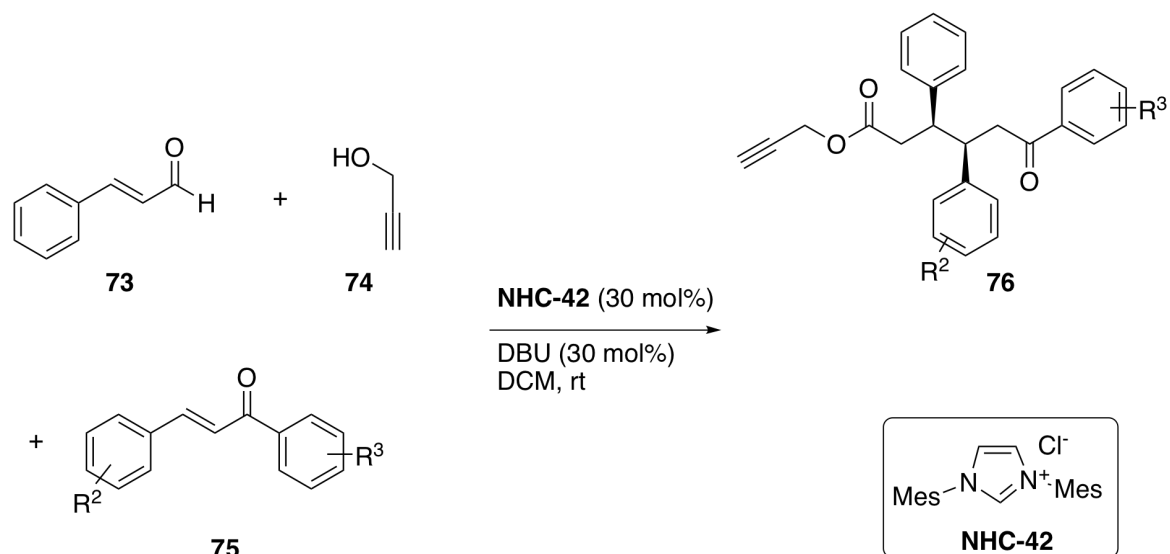


Fig. 1.42 Formation of acyclic ϵ -keto esters using an NHC catalyst [107].

compounds which are notoriously difficult to synthesise due to steric constraints. Further modifications, including addition of leaving groups, allow for greater flexibility in product synthesis. Much progress has been made in these reactions in terms of enantioselectivity, and further functionalisation of the cyclic products gives great value to these reactions in drug discovery programmes. More detailed reviews exist on this topic [108], including computational investigations [109], and the enantioselective reactions are discussed in more detail.

[3+2] Annulations

Spirocyclic centres can be formed by the annulation of enals and unsaturated pyrazolones [110]. Spiropyrazolones have demonstrated potential as therapeutic agents, including in anti-cancer treatments [111]. The reaction proceeds *via* NHC insertion into the initial aldehyde **78** to form the Breslow intermediate, which then undergoes a homoenolate Michael addition with **77** followed by subsequent spiro cyclisation to form final product **79**. Over 17 different spiropyrazolones were catalysed by (*R,S*)-NHC-30 in yields up to 86%, and up to 95% ee (Fig. 1.43). Diastereomeric ratios (dr) were also >20:1 diastereomeric ratio (dr) in some cases.

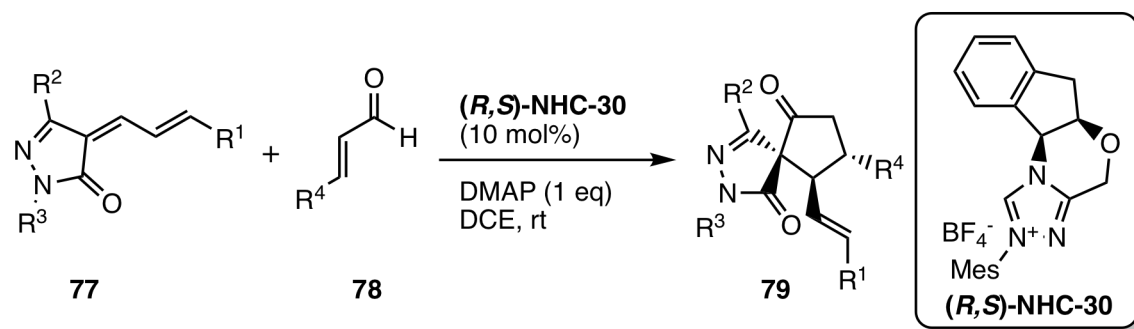


Fig. 1.43 Synthesis of NHC-catalysed spiropyrazolones *via* a [3+2] annulation.

[3+3] Cyclisations

Enders reported that dihydropyranones can be accessed from 1,3-dicarbonyl compounds **80** and *N*-cinnamyltriazole derivatives **81** [112]. **NHC-43** initially displaces the triazole of the *N*-cinnamyltriazole to generate the active species. Tautomerisation of the 1,3-dicarbonyl allows reaction with the intermediate to promote cyclisation and generation of the final dihydropyranone **82**. The reaction tolerates aliphatic and aromatic 1,3-diketones, and both electron rich and deficient groups on the α - β -unsaturated *N*-acyltriazole (Fig. 1.44). Yields of up to 96% were obtained, and up to 86% ee.

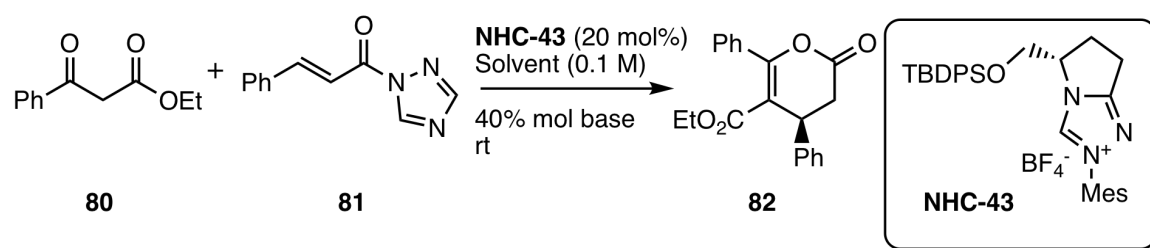


Fig. 1.44 Synthesis of NHC-catalysed dihydropyranones *via* a [3+3] cyclisation [112].

Another way of synthesising dihydropyranones was reported by Zeitler and Fuchs from nitrostyrene, which uses both a chiral and an achiral NHC catalyst, **(R,S)-NHC-30-Cl** and **NHC-24** respectively, in combination with a thiourea catalyst **THIO-2** to generate the final product **86** [113]. Although requiring a number of different catalysts, the three step reaction can be performed in one pot from very simple starting materials **83-85**. The products were

synthesised in yields up to 76% with 99% ee, tolerating aliphatic and aromatic substituents (Fig. 1.45).

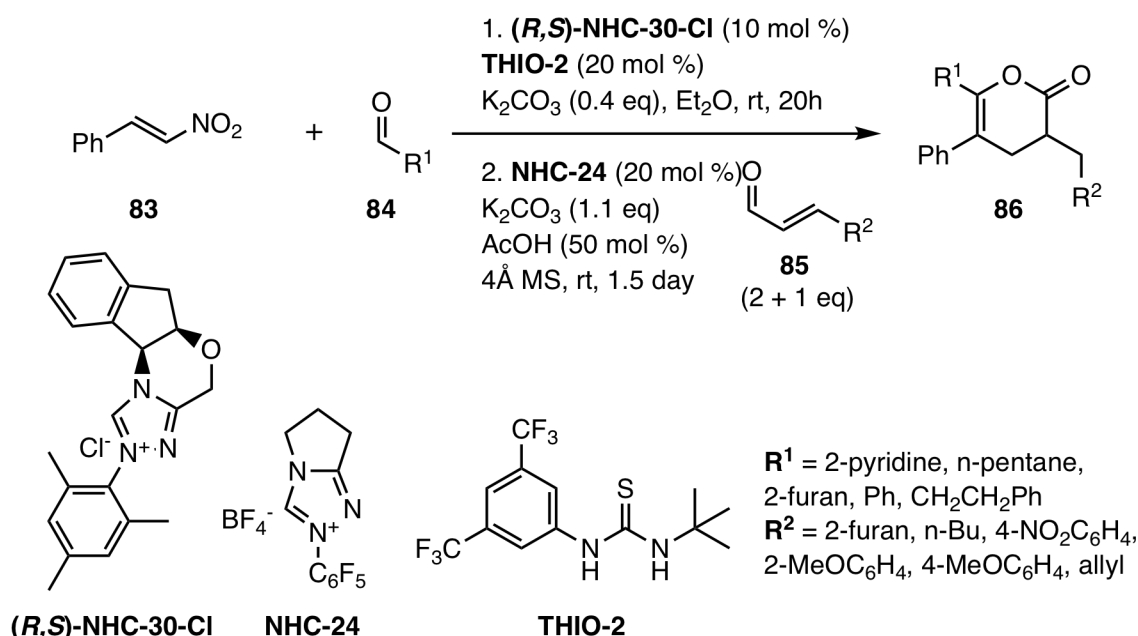


Fig. 1.45 Synthesis of dihydropyranones formed in a one-pot procedure using a combination of three different catalysts, reported by Zeitler and Fuchs [113].

[3+4] Annulations

Incorporating leaving groups into the starting materials has allowed formation of new molecules with bioactive scaffolds, and in 2018 Fang and coworkers reported a new method to access 1,5-benzodiazepin-2-ones **89** using **(*R,S*)-NHC-30** [114]. These compounds and their derivatives have been used as treatments in nervous system disorders, yet little work has been reported in the development of these cores. Optimisation of the reaction between benzene-1,2-diamine derivatives and α -bromoaldehydes led to a wide range of functionalised 1,5-benzodiazepin-2-ones **89a-e**. The reaction proceeded with both symmetric and unsymmetric benzene-1,2-diamine derivatives in up to 99% ee, showing good regioselectivity in the reaction (Fig. 1.46). Scaling up the reaction also worked well, and the products could be N-functionalised to further increase the diversity of the scaffolds. In one case,

N-functionalisation of **89e** by reaction with ethyl chloroformate gave compound **90**, which has been used in treatment of disorders caused by Shiga toxins [115].

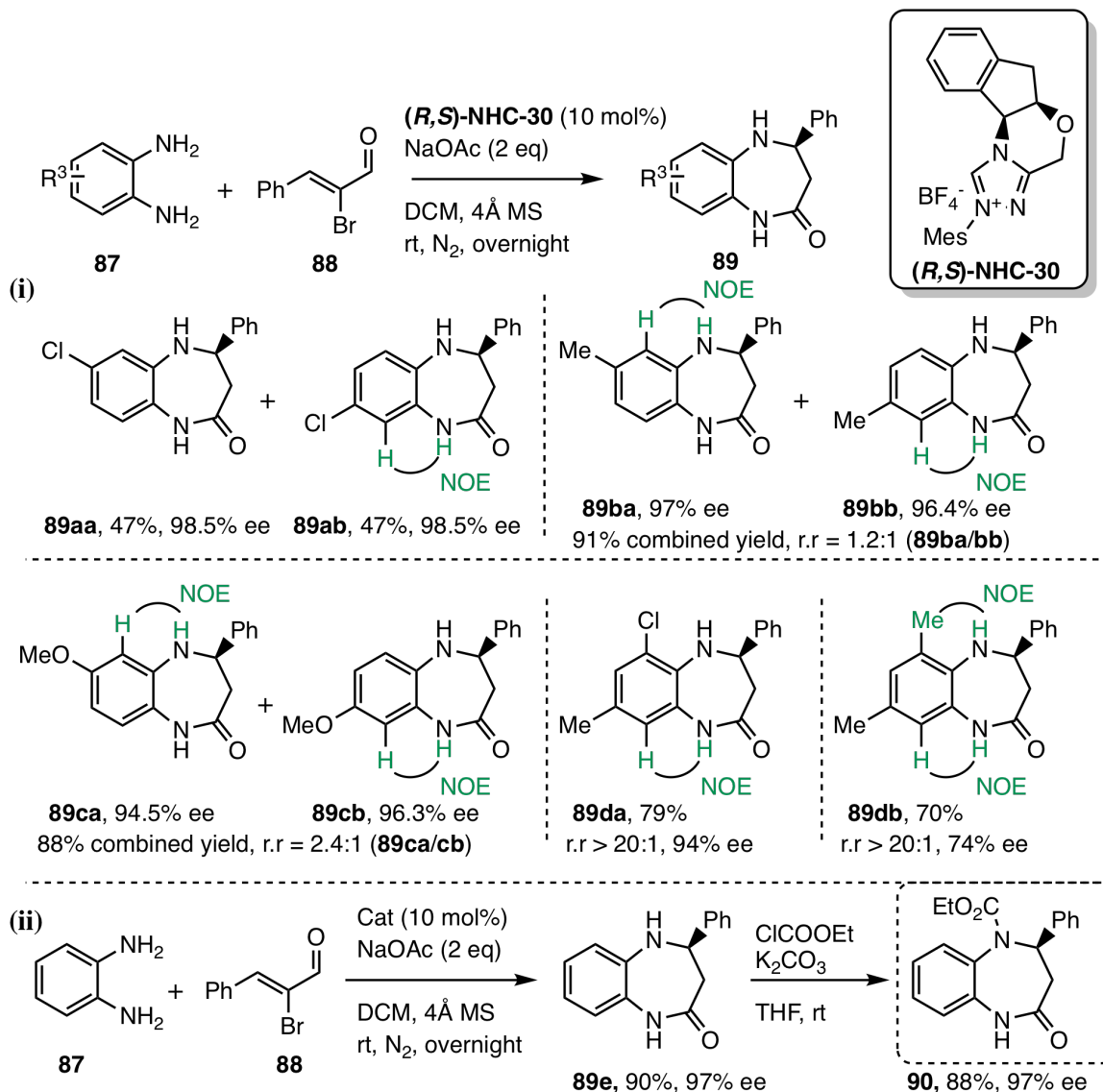


Fig. 1.46 (i) The scope of the unsymmetric NHC-catalysed synthesis of 1,5-benzodiazepin-2-ones *via* a [3+4] annulation. (ii) Further functionalisation of 1,5-benzodiazepin-2-one to generate bioactive molecule **90** used in Shiga toxin disorder treatment [114].

[4+2] Cyclisations

[4+2] cyclisations are common cycloaddition reactions, with one of the most notable being the Diels-Alder reaction between conjugated dienes and substituted alkenes. Using an NHC

catalyst, a range of transformations can be catalysed to give new cyclic scaffolds [116]. An all-carbon cyclisation between 2-acyloxy-3-butenones **91** and α -bromoaldehydes **92** gave highly functionalised cyclohexene scaffolds **93**. Interestingly, the proposed mechanism proceeds *via* a β -lactone intermediate, which is hydrolysed by methanol to give the corresponding methyl ester and alcohol. This method generated over 26 diverse cyclohexenes using **NHC-44**, in yields up to 84% and 99% ee (Fig. 1.47). High dr's (>20:1) were also obtained. The cyclohexene product **93** can then undergo further transformations, demonstrating the scope and attraction of this reaction.

[4+2] Annulations

Zhong and coworkers demonstrated the synthesis of 3'-spirocyclic oxindoles **96** [117]. This core is an important scaffold for biologically active molecules, including Gelsemine 1 and (+)-Welwitindolinone A. These complex compounds are synthesised from γ -fluoroaldehydes **94** and isatin **95**. Initial addition of (*R,S*)-**NHC-30-Cl** to the γ -fluoroaldehyde generates the Breslow intermediate, but C-F cleavage then occurs. The proposed mechanism by Zhong follows with tautomerisation, enolene rearrangement and a deprotonation to generate the reactive vinyl enolate, which then reacts with the carbonyl at the 3-position of isatin to give the 3'-spirocyclic oxindole **96**. The reaction tolerates variation of functionality on both the aromatic rings of the γ -fluoroaldehyde and isatin, and also tolerates N-substitution (Fig. 1.48). 15 examples were demonstrated, giving up to 91% yield and >99% ee.

[4+2] annulations can also occur between α -haloaldehydes and 5-alkenylthiazolones using **NHC-45**, as demonstrated by Enders (Fig. 1.49) [118]. Similar to previous annulations, initial addition of the carbene into the α -haloaldehyde **98** generates the Breslow intermediate, upon which the enolate is generated by loss of the chloride group. Reaction with the Michael acceptor of the 5-alkenylthiazolone **97** occurs, and lactonisation drives the product **99** formation and regeneration of the active catalytic species. Not only did the reaction occur in good ee (99%) and yield (96%), but also in excellent diastereoselectivity (>20:1 de).

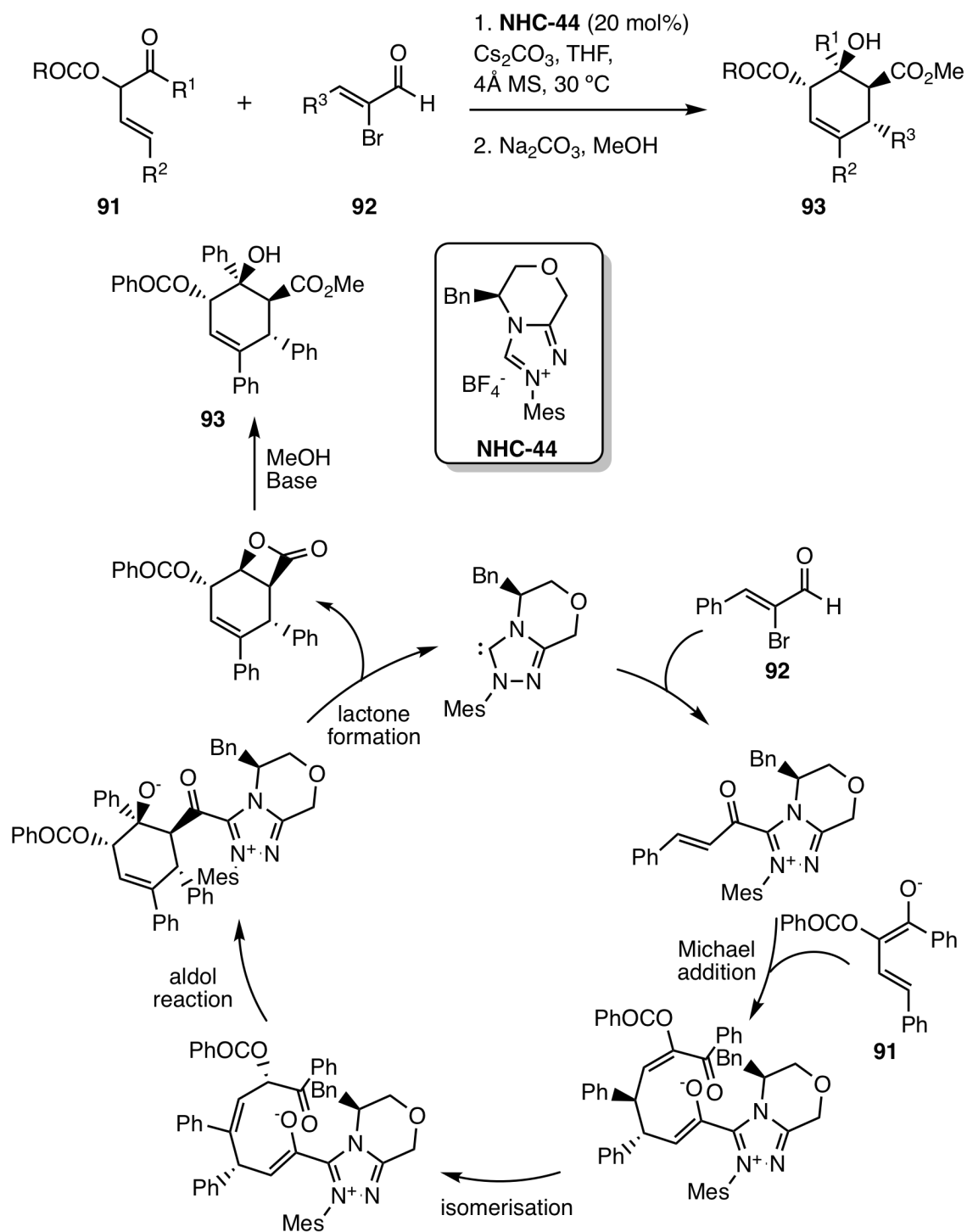


Fig. 1.47 Synthesis of highly substituted cyclohexenes *via* a [4+2] annulation, with mechanism proposed by Fang *et al.* [114].

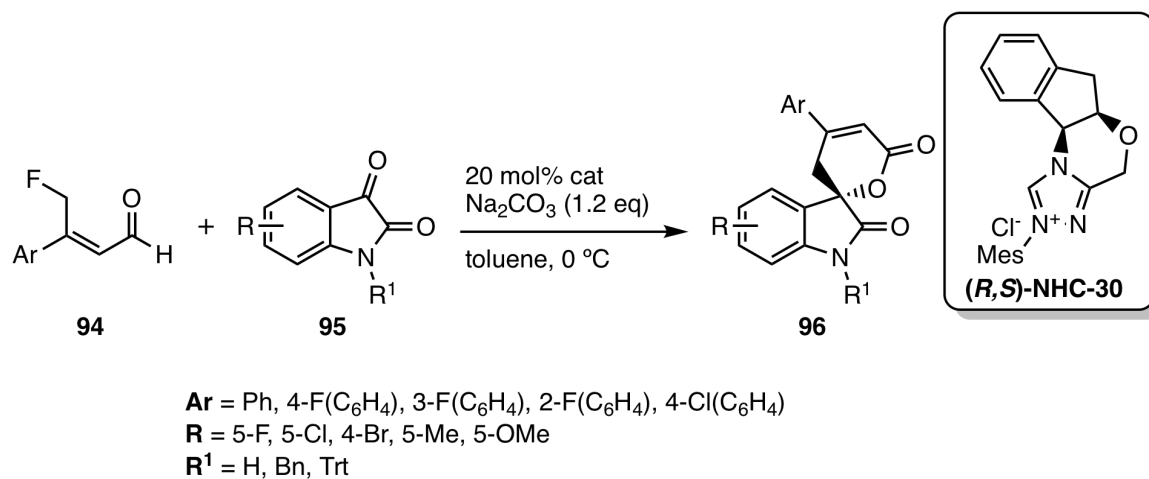


Fig. 1.48 Synthesis of NHC-catalysed 3'-spirocyclic oxindoles *via* a [4+2] annulation [117].

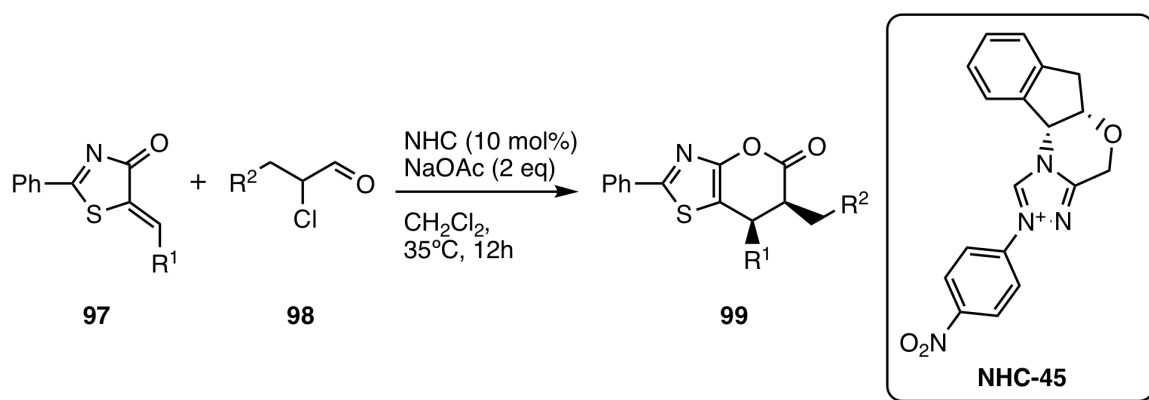


Fig. 1.49 Synthesis of NHC-catalysed dihydropyranthiazoles *via* a [4+2] annulation [118].

Ye and coworkers reported the use of polycyclic catalyst **(R,S)-NHC-30**, incorporating an N-mesityl group and a BF_4^- counter-ion, in an intermolecular cyclisation reaction between α -chloroaldehydes **100** and Michael acceptors **101** to form indenopyrones **102** (Fig. 1.50). This also worked with aliphatic α -chloroaldehydes, in ee's ranging from 91 to 99% [119].

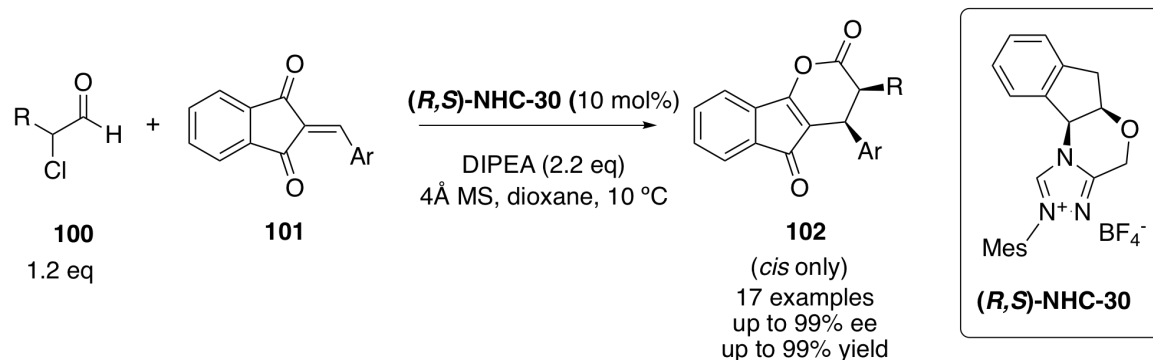


Fig. 1.50 NHC-catalysed formation of indenopyrones from α -chloroaldehydes and Michael acceptors [119].

1.5.5 Conclusions

A broad range of thiazolium and triazolium salt pre-catalysts have been trialled in the benzoin condensation. Initial studies showed that thiazolium salt pre-catalysts could catalyse this reaction, and later developments showed that the triazolium salts gave a better enantioselectivity. Often, increasing the enantioselectivity of a compound would correspond with a decrease in yield. Several bifunctional H-bonding catalysts have been developed, and it was demonstrated that a thiourea or hydroxyl moiety could increase the stereoselectivity, but more improvements in this area are needed.

Thiazolium and triazolium salts have also been demonstrated as effective catalysts over a much wider scope, including cross-benzoin condensations, intramolecular cyclisations and even domino cascade reactions. H-bonding catalysis has been briefly explored in these applications, and has showed high ee's in the cross-benzoin condensation between aldehydes and α -keto-esters.

NHC catalysis using triazolium salts based on the benzoin condensation has allowed for synthesis of natural products, such as (\pm)-sappanone (B), a chromanone derivative. The versatility of these catalysts allow for a range of C-C bond forming reactions. The catalysts work with imines in Staudinger synthesis type reactions, although current reports have often used achiral catalysts.

Based on these findings, triazolium salt pre-catalysts will be further investigated in the asymmetric benzoin condensation, incorporating hydrogen bonding moieties to try and improve enantioselectivity in mild conditions over short reaction times. Thiazolium salt analogues will be investigated and directly compared to the triazolium salts, to ensure consistency with previous studies.

Chapter 2

Design of New Catalysts and Reaction Condition Optimisation

2.1 Aims of the Project

2.1.1 New Catalyst Design

In 2015, Rovis and coworkers compiled all of the currently reported chiral NHC precursors used as catalysts in the literature [108], grouping them according to their scaffold (Fig. 2.1). Most of these are variations on the bicyclic catalyst design originally pioneered by Leeper and coworkers (morpholine and pyrrolidine-based) [63]. However, there are also several notable acyclic triazolium salts (Fig. 2.2), and even polycyclic rings reported. The figure shows that no new developments have been made with thiazolium salts since 2005 due to the relative success of their triazolium salt counterparts (Fig. 2.3). However, new catalysts have been synthesised as recently as 2014 with pyrrolidine and morpholine based scaffolds.

All of the catalysts reported have similar based scaffolds containing important key moieties; the N-heterocyclic ring which acts as the catalytic centre of the molecule, the chiral backbone, and areas for modification allowing fine tuning of electronic properties. This was the basis for the design for new catalysts investigated here, but modifications included

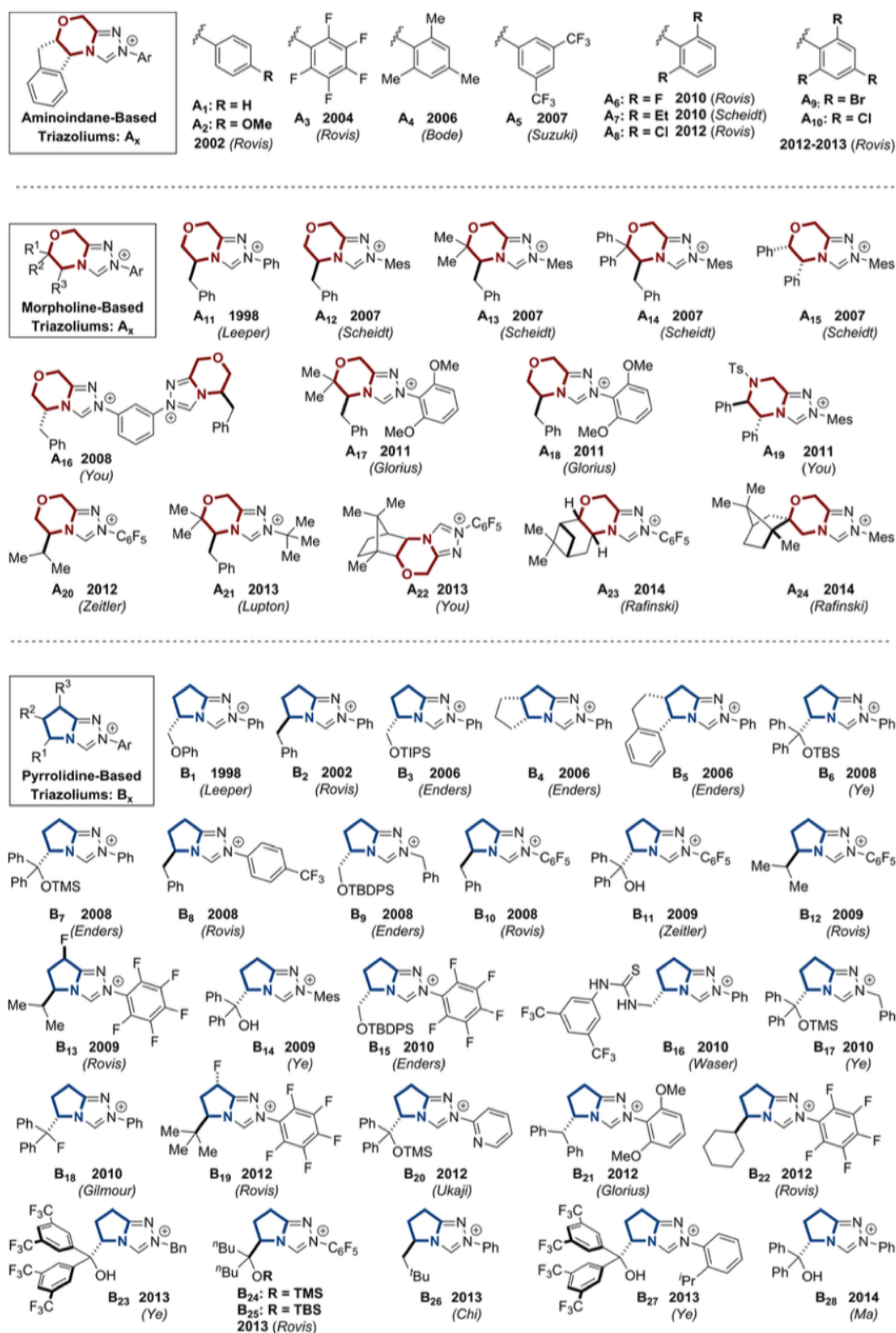


Fig. 2.1 Chiral triazolium salt catalysts based on aminoindane, morpholine and pyrrolidine, collated by Rovis and coworkers [108].

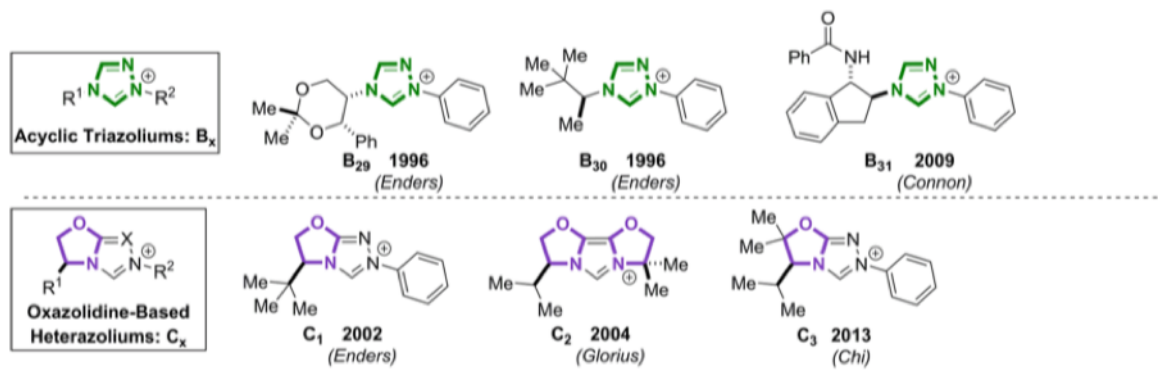


Fig. 2.2 Acyclic and oxazolidine-based chiral triazolium salt catalysts, collated by Rovis and coworkers [108].

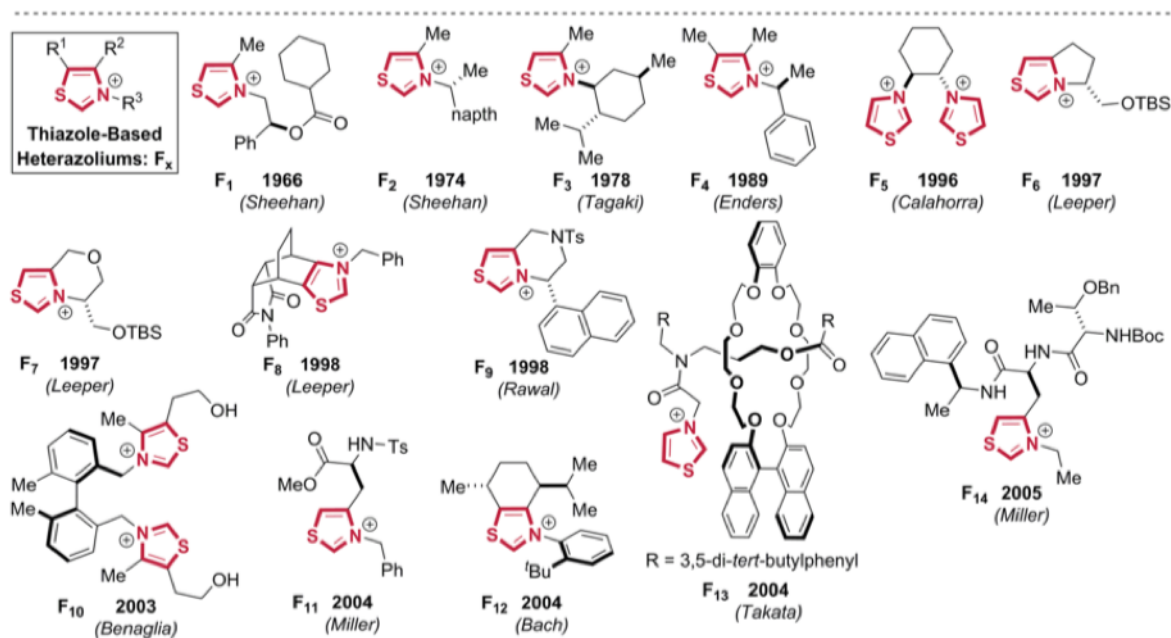


Fig. 2.3 Thiazole-based heterazolium salt catalysts, collated by Rovis and coworkers [108].

an H-bonding moiety to allow stereoselective synthesis (Fig. 2.4). For an organocatalyst to become widely used and accessible, it is important that the catalyst can be made from commercially available starting materials, has relatively straightforward synthesis, and is relatively cheap to synthesise. It is also desirable to allow for late stage functionalisation on each of the chiral scaffolds [120], so a range of catalysts can be synthesised. This will allow investigation of how different properties affect the catalytic ability of these molecules. The aromatic moiety of the triazolium salt can also be varied, *e.g.* electron-poor groups such as the pentafluorophenyl group, or sterically bulky groups such as mesityl or the newly reported carborane group [121] (although its use is only reported in achiral organocatalysts to date).

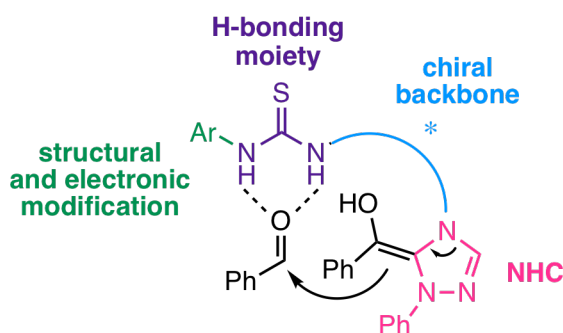


Fig. 2.4 General scaffold for new triazolium salt catalysts, showing the Breslow intermediate and proposed interaction with the second molecule of benzaldehyde. The catalysts include a chiral scaffold to allow stereoselectivity in the formation of the product.

It was envisioned that several new scaffolds could be created from commercial starting materials, including diamines (Fig. 2.5). Takemoto's reported bifunctional H-bonding catalysts based on a 1,2-diamine scaffold [42] were to be investigated as a potential chiral backbone first, due to commercial availability of the chiral starting material, and also the well established synthetic routes to (thio)urea backbones. Modification of the aromatic moiety attached to the (thio)urea will allow for modification of the acidity, a key factor which is important in H-bonding interactions [39]. Another commercially available class of chiral starting materials incorporating various functional groups for synthetic modification are amino acids, as many of the existing bicyclic catalysts come from amino acids and their derivatives [122].

The position of the (thio)urea in relation to the heterocyclic ring is an important consideration in new catalyst design, so a 1,4-diamine-derived catalyst was designed. This will have increased flexibility compared to the 1,2-diamine-derived backbone, which may influence interactions with the incoming benzaldehyde molecule. Although chiral 1,4-diamines are not commercially available, (\pm)-*trans*-cyclohexane-1,2-dicarboxylic acid can be obtained, which will be a good starting point once chirally resolved into its enantiomers.

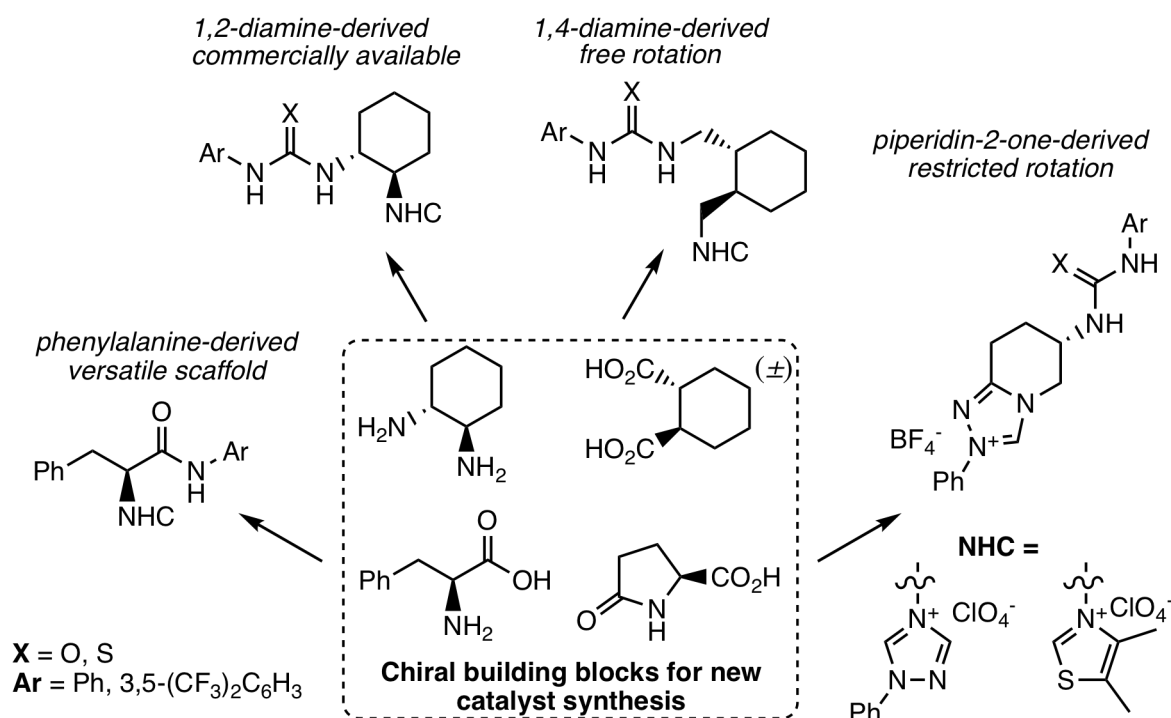


Fig. 2.5 New catalyst scaffold designs, based on syntheses from commercially available chiral starting materials.

Although these new catalyst scaffolds will help to provide insight into how structure influences catalytic ability, the most extensively investigated catalysts incorporate the bicyclic core (Fig. 2.1) [63]. A bicyclic catalyst incorporating (thio)urea has already been designed [78], but allows free rotation of the H-bonding group. To understand the importance of this rotation, a catalyst designed from a δ -valerolactam-derived backbone was designed. Having a similar structure to Waser's catalyst and the same molecular mass, the methylene is

incorporated into the bicyclic ring, meaning the (thio)urea is firmly attached in place on the aromatic ring. Comparing these catalysts may lead to insights into new catalyst design.

2.1.2 Computational Design of Organocatalysts

Classically, when designing new catalysts, a "trial and error" type approach has always been used. By synthesising and testing a catalyst, making a structural modification, and seeing how the results change, reasonably accurate pictures can be built up of what features are important in building new catalysts, especially in terms of asymmetric organocatalysis and introducing stereoselectivity. While this is effective, the synthesis of new catalysts can be time consuming and costly. Since the development of computational methods, new catalysts can now be designed and analysed using quantum mechanical (QM) methods, saving time and precious materials for synthesis.

Houk highlighted the importance of using computational methods in the design of new asymmetric organocatalysts [123], also known as *de novo* design. His research into proline organocatalysts helped to understand the hydrogen bonding in the transition-state of aldol reactions, disproving previous theories [18]. Further work gave an explanation of why (*S*)-pipecolic acid gave *syn*-products in the Mannich reaction, whilst proline-catalysed gave the *anti*-product [124]. These studies were important as it not only showed how QM methods can help rationalise results obtained experimentally, but also highlighted how relatively accurate predictions of ee could be made.

Analysis of transition states is a key indicator of how well a chiral catalyst performs in the formation of the new stereocenter based on bonding interactions and steric bulk. A template needs to be developed by using simplified molecules to gain understanding into the reaction, before applying these conclusions to larger, more relevant catalysts. However, catalytic systems are often huge and complex, and balancing precision against computational time is key. This can be overcome by using different methods for various parts of the system. If the key interactions are known, this can be calculated using a more detailed method on a

select number of atoms. Different methods can then be layered on top for the surrounding atoms of the molecules, of which accuracy is less important. For example, with the benzoin condensation, the interaction around the carbene and the carbonyl is more important to be accurate than that of the functional groups. A general process for using computational design in organocatalysis is given:

- Create a template
- Determine the structure of the transition state
- Minimise the energy of the transition state
- Perform a single-point calculation to determine the ΔG of the transition state
- Take the difference in ΔG_{rel} to calculate the Boltzmann distribution
- Convert the Boltzmann distribution to determine the ee of the reaction.

For the benzoin condensation, Houk calculated the transition state for the formation of the C-C bond between formaldehyde and N-methyl thiazolium [125]. This determined that the intramolecular proton transfer is important in these systems, in determining the rigidity of the transition state therefore the stereochemistry. Other key features in this system is the π -aromatic iminium interactions, which has been determined as 3.4 Å. This corresponds with experimentally determined values in other biological and chemical systems, with an extensive review by Castellano and Diederich [126].

Dudding and Houk proceeded to analyse four currently existing thiazolium and triazolium salt catalysts in the benzoin condensation, to rationalise the stereoselectivity and the ee of each catalyst. The catalysts had been tested experimentally with quantitative data, providing slight to moderate enantiomeric excess (ee) [125]. The catalysts can only interact with the substrates in a set number of ways: the Breslow intermediate can have an *E* or *Z* double bond and the *re* or *si* face of the Breslow intermediate can interact with the *re* or *si* face of

benzaldehyde, meaning there are only 8 combinations and therefore a relatively low number of calculations to be completed for each system. *Re* and *si* are terms used to describe prochiral faces of planar atoms in molecules, such as ketones and aldehydes [127]. Benzaldehyde is prochiral, as it can be desymmetrized in one step, and nomenclature is dependent on the face of attack. Similar to *R* and *S*, these terms are denoted based on the Cahn-Ingold-Prelog priority, where *re* indicates decreasing priority of substituents in a clockwise order when looking at a particular face, and *si* refers to the anti-clockwise decrease in priority (Fig. 2.6); more detailed information on the nomenclature is summarised by Helmchen [128]. It is important to note that these terms do not correspond directly to *R* or *S* in the product of attack at that face, as these are determined by the priority of the incoming reactant.

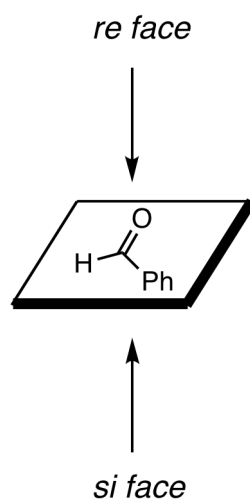


Fig. 2.6 The *re* and *si* face of benzaldehyde as determined by the Cahn-Ingold-Prelog rules of priority.

The calculations are useful in giving some indication of the likely success of an asymmetric catalyst in influencing stereoselectivity. Energies of different possible transition states of catalytic reactions can be determined, the difference in the free energy can be used to calculate the Boltzmann distribution using equation 2.1, using the Curtin-Hammett principle.

$$k_{rel} = e^{\Delta\Delta G^\ddagger/RT} \quad (2.1)$$

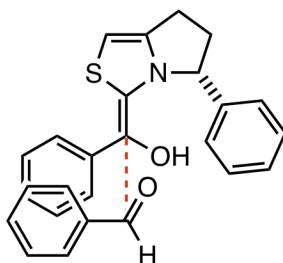
From this, a relatively reliable indication of the ee of a reaction can be given. Using calculated data and comparing to literature values, Houk and Dudding managed to effectively rationalise the ee of the reactions; low ee's occur where there is little energy difference between two transition states leading to opposite enantiomers, as it is relatively easy to form both of these (Fig. 2.1). The chiral thiazolium salt synthesised by Knight and Leeper only gave 10.5% ee [63] when tested in the benzoin condensation. The calculated values by Houk and Dudding demonstrated a relatively low energy barrier between the two enantiomers ($\Delta G_{\text{rel}} = 0.7$ kcal/mol), and the calculated Boltzmann distribution of transition states within 4.0 kcal/mol of the lowest energy structure predicted an ee of 9.5% (Fig. 2.1).

This method often led to overestimation of values in these systems, but still provided a reliable indicator as to whether a catalyst would perform poorly or relatively well, and also to the stereochemistry of the product. Another factor to note is that the calculations give an upper limit which is never usually experimentally obtained. This is due to the racemisation of benzoin by the catalysts in the reaction mixture [129], although Mennen *et al.* reported that using a hindered base such as pentamethylpiperidine can suppress this racemisation [130].

Since Dudding and Houk's studies, computational methods have cemented themselves in the chemist's toolbox for design of new catalysts and explanation of mechanisms. In 2016, Cheong and coworkers reported a range of methods which can be used in nonbonding interactions in covalent organocatalysis [131], and discussed how computational methods can be used to elucidate the mechanism of NHC-catalysed kinetic dynamic resolution of β -lactone formation [132].

There are some limitations to this method, and indeed computational methods in general. In such systems, the method has to be simplified to ensure adequate calculation time. For example, Dudding and Houk performed calculations on the catalysts and transition states in vacuum. Solvents will have a significant effect, as they may provide stabilisation of intermediates, or in this particular case may have an influence on mechanism of the proton transfer. If such calculations were to be performed on the catalysts proposed in this chapter,

Table 2.1 Calculations of ΔG_{rel} by Dudding and Houk for the *re* and *si* combinations of Knight and Leeper's chiral thiazolium salt catalyst with benzaldehyde [125].



(*S*)-Catalyst-(*E*)-Enolamine-(*re*),(*si*)
Transition state geometry

Catalyst	Enolamine	Enolamine face	Aldehyde face	Product configuration	ΔG^{rel} , kcal/mol ^a
<i>S</i>	<i>E</i>	<i>re</i>	<i>si</i>	<i>R</i>	0
<i>S</i>	<i>E</i>	<i>si</i>	<i>re</i>	<i>S</i>	0.7
<i>S</i>	<i>Z</i>	<i>si</i>	<i>re</i>	<i>S</i>	0.8
<i>S</i>	<i>Z</i>	<i>re</i>	<i>re</i>	<i>S</i>	0.8
<i>S</i>	<i>E</i>	<i>si</i>	<i>si</i>	<i>R</i>	1.6
<i>S</i>	<i>E</i>	<i>re</i>	<i>re</i>	<i>S</i>	1.7
<i>S</i>	<i>Z</i>	<i>si</i>	<i>si</i>	<i>R</i>	5.9
<i>S</i>	<i>Z</i>	<i>re</i>	<i>si</i>	<i>R</i>	9.8

^a Relative energies obtained by single-point B3LYP/6–31G(d) calculations

there may be unpredictable solvent effects unaccounted for, for example hydrogen-bonding solvents such as methanol interacting with the (thio)urea moiety and providing competition for the carbonyl of the benzaldehyde. However, these considerations lead into more detailed computational analysis and would require expertise in the area to draw detailed conclusions. Finally, computational conclusions do not take into account synthetic challenges. A computational study by Goldfuss reported that balancing of the electrophilic and nucleophilic properties of NHCs would indicate that oxazol-2-ylidene has the lowest activation energy to the transition state, and therefore would be the best of their investigated catalysts [133], but experimentally these have been demonstrated as ineffective catalysts in the benzoin reaction due to instability and ring opening [134].

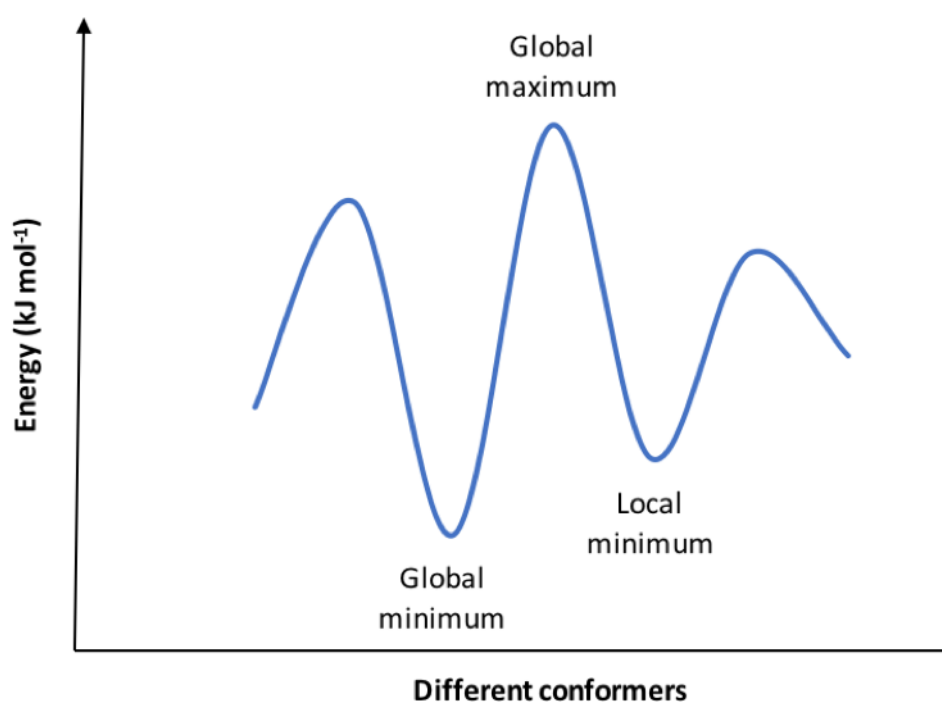


Fig. 2.7 Schematic showing a simplified relationship between global and local energy minima.

In this work, computational methods will be used as a tool to help rationalise findings from the experimental work. Due to limited access to software and expertise, no extensive computational studies will be undertaken here, but will be used more to illustrate conclusions. Using computational methods to obtain global minima would be extremely intensive due to

the size of these catalysts. Therefore, a random selection of conformers will be generated where necessary, and these conformers will undergo energy minimisation. This method is slightly more effective than generating a single structure, as it generates a range of local minima (illustrated in Fig. 2.7), making results more accurate than from a single conformer, but is in no way a comprehensive study representing the absolute global minima of any of the structures presented. The output will be used qualitatively, to rationalise experimental findings rather than to make predictions.

2.2 Analysis of Chiral Compounds

Most physical properties of enantiomers are identical. Due to being mirror images of each other, the main difference between them is the way they interact with other chiral molecules. Therefore, standard methods used in determining compound purity and structure, such as melting point and NMR, will show no differences between two enantiomers, but a range of other techniques can be employed to qualitatively and quantitatively determine stereochemical configuration and ee.

2.2.1 Determination of ee

Optical Rotation

One of the oldest measures of the ee of compounds is the optical rotation of polarised light using a polarimeter. There are, however, several drawbacks to this method. The optical rotations have to be compared to known values, so this method is only beneficial if the specific rotations of the compounds are already known. The direction of rotation of polarised light also has no bearing on the configuration of the compound, so no structural observations can be made using this method. This method is highly sensitive, and while this may seem advantageous, it means that slight variations such as temperature, concentration, and minor contamination by impurities can lead to large errors in measurement.

Chiral HPLC

Chiral HPLC is probably the most effective way of not only determining ee, but also of separating different enantiomers. A column is employed with a chiral stationary phase (CSP), most commonly a polysaccharide derivative, affixed onto an achiral support such as silica.

Modification of the chiral selectors mean that most types of chiral compounds can be successfully separated [135]. The chiral compound is introduced onto the column using solvent, and forced through the column at high pressure. The CSP interacts differently with each enantiomer, and as a result the two enantiomers are eluted at different times.

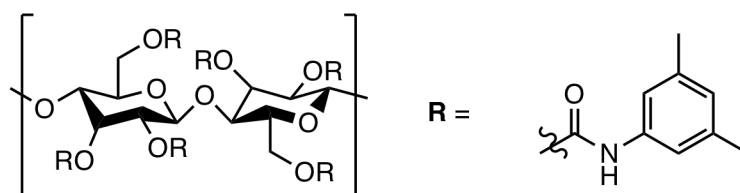


Fig. 2.8 The structure of the CSP of Astec Cellulose.

On an analytical scale, this method works well for molecules with chromophores, as the material is passed through a ultra-violet (UV) detector. This gives a quantitative peak for each enantiomer separated by time, and separation can be improved by optimising the conditions. This may involve changes in the pressure or polarity of the solvents, or in more extreme cases employing a different CSP. This method can also be expanded to allow for separation of the different enantiomers, when preparative columns are used. The separation of benzoin using an Astec tris(3,5-dimethylphenylcarbamate) (DMPC) chiral column is given in Fig. 2.9.

However, this method has its own drawbacks. The equipment is extremely expensive, limiting its wide scale accessibility. As the quantitative measures of ee are determined by elution time and absorbance at a particular wavelength, it is possible that impurities may co-elute, or indeed that an impurity may be mistaken for an enantiomer. However, these problems can be overcome by ensuring the samples are clean, comparing them to literature values, and by cross-comparing several wavelengths to ensure the absorbances correspond

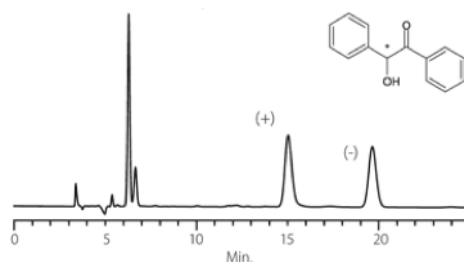


Fig. 2.9 Chiral separation of benzoin using an Astec Cellulose chiral column. Conditions: 10:90:0.1 of *isopropanol*:heptane:TFA at 0.5 mL/min. Chromatogram taken from Sigma-Aldrich.

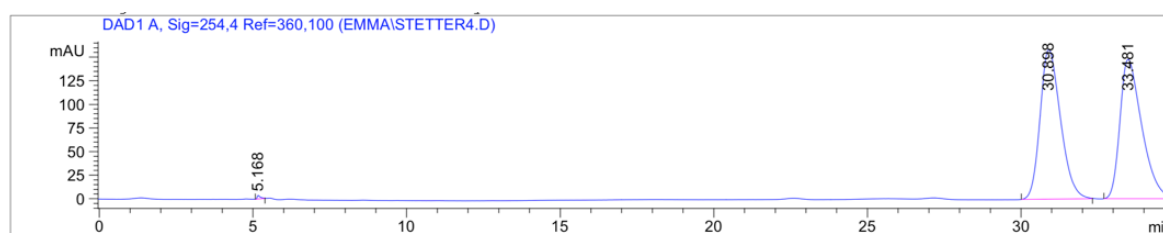


Fig. 2.10 Chiral separation of ethyl 2-(4-oxochroman-3-yl)acetate using an Astec Cellulose DMP chiral column. Conditions: 10:90 of *isopropanol*:hexane at 0.5 mL/min.

with the desired material. In the case of compounds which do not have chromophores, additional reactions can be undertaken to make the compound UV active, which can be time-consuming and also detrimental to potentially precious enantiomerically enriched materials. These can be synthesised using a derivatizing agent such as *m*-toluoyl chloride, which is reactive to common functional groups such as amines (Fig. 2.11).

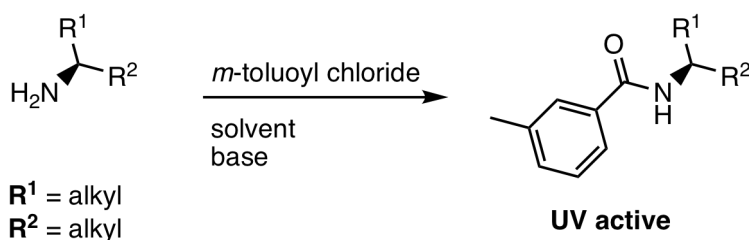


Fig. 2.11 Introduction of a UV-active derivatising agent into non-UV active compounds to allow detection by HPLC.

Similar to optical rotation, there is no stereochemical analysis of the compounds when using HPLC, so the exact enantiomer is not known from this method alone. Whilst the retention times of known compounds can be compared to literature values using the same stationary

phase (as with benzoin above), complementary methods such as X-ray crystallography can be employed to validate this method.

2.2.2 Determination of Configuration

Chiral derivatisation

Whilst enantiomers have identical physical properties, diastereomers can be a lot easier to determine. Due to the presence of two or more chiral centres, diastereomers have different conformations to each other. This leads to different physical properties, for example diastereomers will have different boiling and melting points. Their conformers will allow for different intra-molecular interactions, leading to differences in spectral properties.

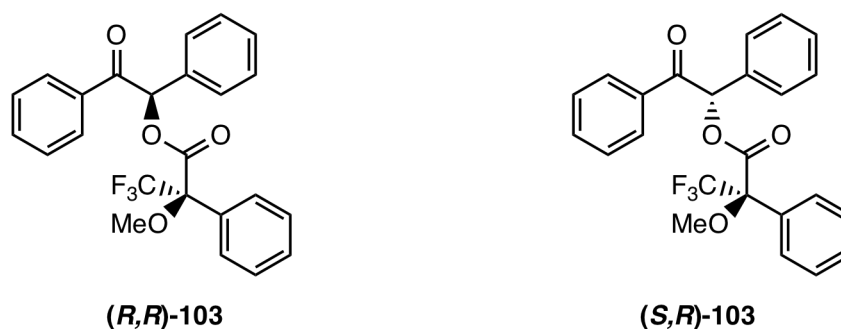


Fig. 2.12 The diastereomers **(R,R)-103** and **(S,R)-103** formed by reaction of (*R*)- and (*S*)-benzoin with the acid chloride of (*R*)-(+)- α -Methoxy- α -trifluoromethylphenylacetic acid (MPTA), known as (+)-Mosher's acid.

This can be useful where it is possible to convert enantiomers to diastereomers with chiral derivatizing agents (CDAs). If the enantiomer contains a functional group such as an alcohol or amine, reaction with a chiral compound of known configuration, such as Mosher's acid, generates diastereomers. This method is very effective for determining the configuration of the major product of unknown compounds, if no standard is available in the literature.

Once the diastereomers have been synthesised, comparative analysis of the ¹H NMR of the two esters can allow for deduction of the absolute configuration accurately. Hoyer *et al.* have reported an efficient protocol for the synthesis and analysis of Mosher ester derivatives

[136]. The alcohol is reacted with the acid chlorides of both the (*R*) and the (*S*)-MTPA, to give two diastereomers. By considering the Fischer projections of the newly formed esters for each diastereomer, the dominant conformer can be predicted. By factoring in shielding effects in the diastereomers, the protons attached to the more shielded group will appear more upfield in the NMR spectrum (Fig. 2.13). Calculation of $\Delta\delta^{\text{SR}}$ values ($\delta_{\text{S}} - \delta_{\text{R}}$) indicates absolute configuration determined on whether the value is positive or negative; Hoyer *et al.* demonstrated a worked example with (-)-menthol [136].

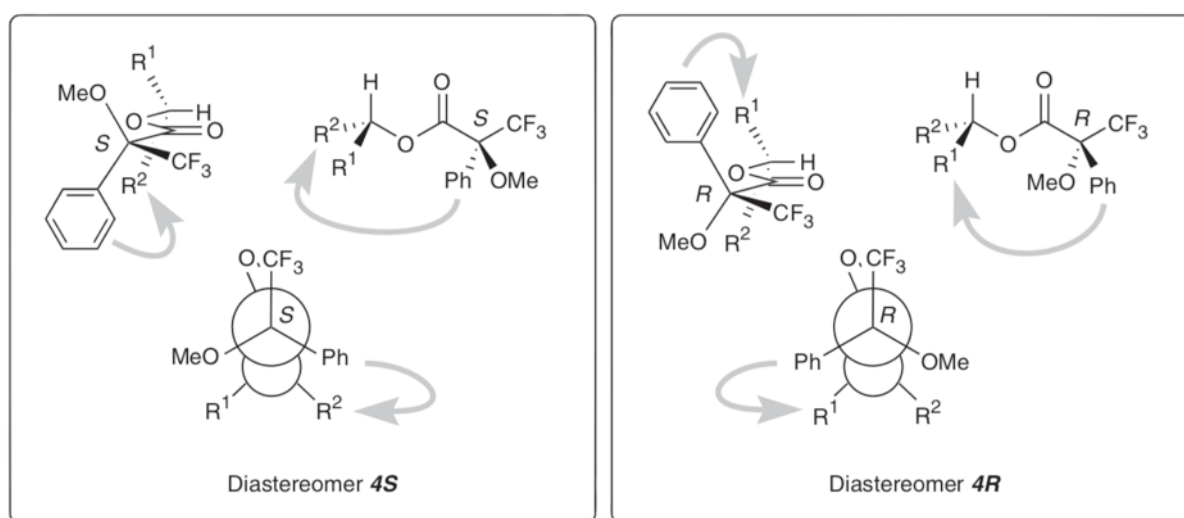


Fig. 2.13 Fischer projections of a chiral secondary alcohol reacted with (*S*)-MPTA (left) and (*R*)-MPTA (right) to give two diastereomers, taken from Hoyer [136]. The grey arrow represents the increase in shielding; in 4S (assuming R^2 is lower priority than R^1), R^2 will have higher shielding, *i.e.* will have more upfield protons in the ^1H NMR spectrum. The same is true for the protons of R^1 in 4R.

While this method is good for determination of configuration, measurement of ee falls short compared to other methods. Firstly, an added step is required to obtain the diastereomer, which can be time-consuming. Secondly, the sample may not have any available functionality to react with the CDA. Finally, the reaction of the sample with the CDA may not reach completion. This leads to problems as one enantiomer may react more readily than the other with the agent, meaning that the quantitative values obtained by NMR will not be an accurate representation of the correct ee.

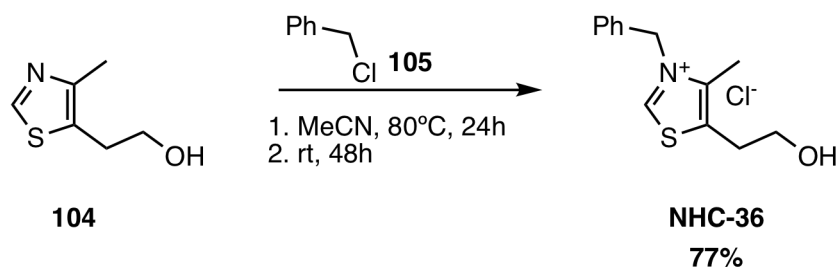


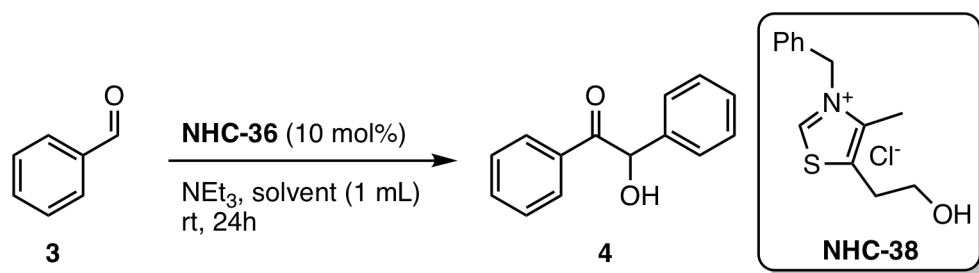
Fig. 2.14 Synthesis of the achiral thiazolium salt pre-catalyst **NHC-35**.

2.3 Optimisation of Benzoin Condensation Conditions

To optimise the conditions for the benzoin condensation, several achiral pre-catalysts were tested to investigate the conditions. 3-Benzyl-5-(2-hydroxyethyl)-4-methylthiazol-3-ium chloride **NHC-35** has been previously used by Stetter in umpolung reactions [137], so was used as a standard. Initially, these reactions were done on a 1 mmol scale to obtain enough product for quantitative analysis on the HPLC, using standard conditions of NEt_3 as base and MeOH as a solvent, due to their robustness in this reaction. The catalyst itself was synthesised in one step from benzyl chloride **105** and 4-methyl-5-thiazole ethanol **104** in acetonitrile, obtained in 77% yield (Fig. 2.14).

NHC-35 was tested both under inert atmosphere and under air, with varying levels of base (Table 2.2). Several useful pieces of information were gathered, in particular the instability of benzaldehyde in air. When exposed to air, benzaldehyde rapidly converts to benzoic acid. This affected the study in two ways: firstly how to measure conversion, and secondly the atmosphere in which it is run. Initially, the conversion of benzaldehyde to benzoin was to be measured by comparison of the key peaks in the ^1H NMR spectrum of CDCl_3 ; measuring loss of the aldehyde proton (10.0 ppm) against appearance of the proton attached to the newly-formed secondary alcohol (5.96 ppm). However, due to the degradation of benzaldehyde to benzoic acid in air, the reaction does not proceed linearly and an accurate value cannot be obtained, especially as benzoic acid often precipitates out in CDCl_3 . Due to this, it is important to use a standard to obtain precise results, especially when smaller scale reactions are used and obtaining an accurate yield by isolation may be more difficult. It is

Table 2.2 Initial investigation of base loading and atmosphere in the benzoin condensation.



Entry	NEt_3 (mol%)	Solvent	Atmosphere	Yield ^a
1	10	MeOH	N_2	33
2	100	MeOH	N_2	N/A ^b
3	10	None	Air	0

^aIsolated yield. ^bStarting material converted to benzoic acid and precipitated out.

also important that all the reactions are run under N_2 as oxidation of the Breslow intermediate can form by-products such as **106** [138]. Going forward, the benzaldehyde would be distilled prior to use and used within 1 hour to minimise conversion to benzoic acid (Fig. 2.15).

2.3.1 Determination of Conversion to Benzoin

After 24 h, the reactions were monitored by thin-layer chromatography (TLC) to detect if any benzoin had been formed. Running the TLC in 1:4 EtOAc-petroleum ether gave a clear spot for benzoin at 0.31, which was compared against (\pm)-benzoin. If any material could be detected, the solvent was removed from the crude reaction mixture, and taken up in deuterated solvent for ^1H NMR analysis. The alcohol's α -proton gives a clear peak around 6 ppm (solvent dependent). The aim then was to compare the integration of this peak with a suitable standard.

Selection of an NMR Standard and Solvent

An ideal NMR standard has a low number of non-equivalent types of proton which have peaks in uncluttered areas of the spectra, and solubility in a range of deuterated solvents. Initially, 1,3,5-trimethoxybenzene was selected, due to its aromatic proton peak being outstanding.

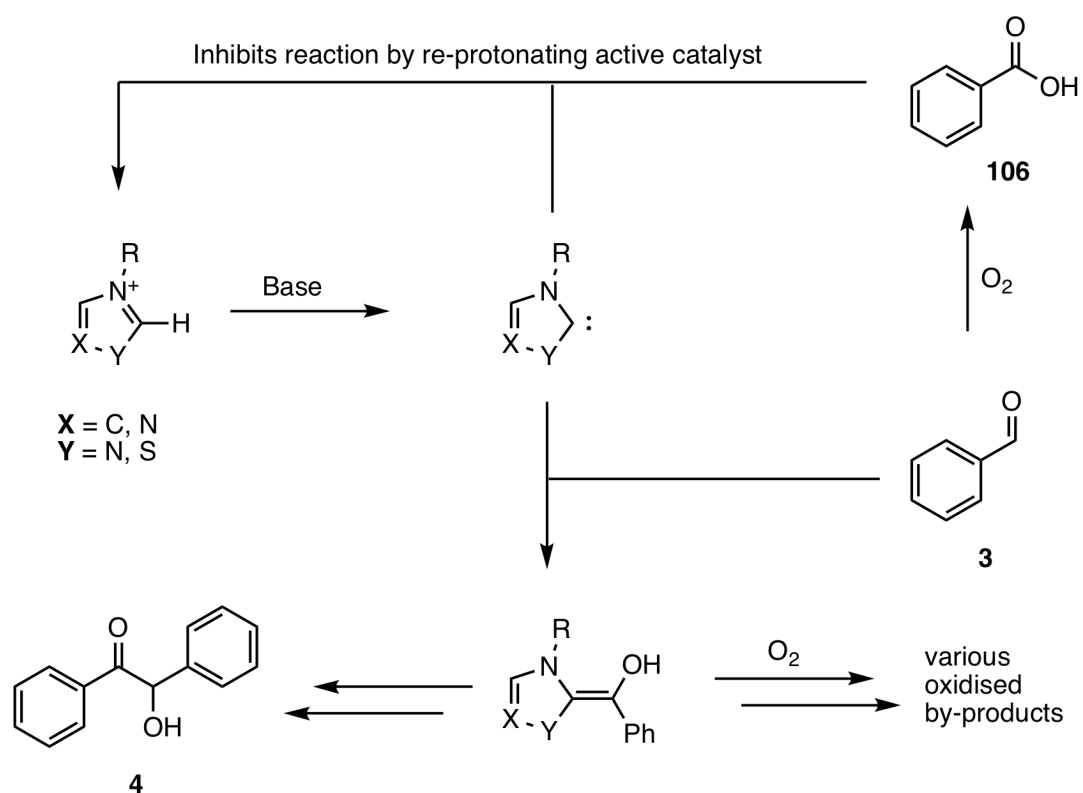


Fig. 2.15 Summary of problems encountered by having oxygen in the system for the benzoin condensation.

A sample of this was run in CDCl_3 with benzoin. However, the proximity of this peak to the key benzoin peak around 6 ppm meant that this was an unsuitable standard. Ethylene carbonate was then investigated, as there was one environment, with the peak around 4.5 ppm (solvent dependent). Initially, the NMR solvent and standard were made to 0.25 M, meaning that a sample run in 0.5 mL would give 0.125 mmol of the material (1:1 ethylene carbonate: theoretical yield benzoin). However, due to the 4:1 ratio of relevant protons, the standard swamped the NMR spectra, and so this was reduced to 3.13×10^{-2} mmol, thereby giving 1:1 of the relevant protons.

The samples initially were made up by dissolving the crude reaction material in CDCl_3 , and filtering out the solid inorganic bases before running the NMR spectrum. However, even when benzoin peaks could be detected by TLC, no benzoin peak was found in the ^1H NMR spectrum, raising questions of solubility. The reactions were re-dried and taken up in CH_3OD due to the increased polarity, but the same problem arose. Due to this, it was decided that the reactions were to be repeated, and the reaction mixtures worked up before quantitative NMR analysis.

Working up the Reactions

The volatile solvents were removed under a flow of N_2 . The crude material was taken up in H_2O (5 mL), and the product extracted with Et_2O (2 x 5 mL). The organic layer was washed with brine (5 mL), dried (MgSO_4) and the volatile solvent removed under a stream of N_2 . This material was taken up in CD_3OD + ethylene carbonate (0.5 mL) and the ^1H NMR spectrum was acquired.

2.4 Catalyst Testing Conditions

2.4.1 The Benzoin Condensation

To test the catalytic ability of the novel catalysts described in this work, the salts would be subjected to different conditions to attempt the benzoin condensation. As most catalysts would only be obtained in small quantities due to multiple step syntheses, an achiral triazolium salt was selected to initially optimise the conditions. Previously synthesised by Connon and coworkers, the cyclohexyl triazolium salt **NHC-46** was used for initial studies. This is due to the similarity of the backbone to catalysts in this work. The starting point chosen was the conditions used by Waser in testing his H-bonding catalyst, as this had been proven to work and gave reasonable yields [78]. However, the scale was decreased to 0.25 mmol of starting material, so the amount of catalyst used each time would be between 4 and 8 mg, thereby increasing the number of tests which could be performed. As well as the cyclohexyl catalyst **NHC-46**, several catalysts synthesised in Chapter 3 were used for optimisation here. The results are shown in Table 2.3.

Interestingly, the cyclohexyl catalyst did not fare well in these conditions, and only traces of the desired product were obtained. However, (\pm)-**NHC-47** achieved product with both bases in THF (Entry 7–8), and the bis(trifluoromethyl) analogue (**IR,2R**)-**NHC-48** achieved 3% of product using Rb_2CO_3 . Based on these results, and in accordance with Waser's study, the conditions in Entry 7 were chosen to use for future catalyst testing in this work.

2.4.2 The Intramolecular Stetter Reaction

As discussed in Chapter 1, the intramolecular Stetter reaction is another reaction which is successfully catalysed by triazolium and thiazolium salts. After the initial discovery by Sheehan [60], further advances in the field were made by Rovis and coworkers [103]. Stetter reactions are considerably easier to perform than the benzoin condensation, as the final product is stable in the reaction conditions, meaning the reaction is irreversible. In this

Table 2.3 Triazolium catalysts in the benzoin condensation.

<div style="display: flex; align-items: center; justify-content: center;"> <div style="text-align: center;"> 3 0.25 mmol </div> <div style="margin: 0 20px;"> $\xrightarrow[\text{Solvent (1 mL), 24h, rt}]{\text{Cat. (5 mol\%), Base (5 mol\%)}}$ </div> <div style="text-align: center;"> 4 </div> </div>				
<div style="display: flex; justify-content: space-around; align-items: flex-end;"> <div style="text-align: center;"> NHC-46 </div> <div style="text-align: center;"> (±)-NHC-47 </div> <div style="text-align: center;"> (1R,2R)-NHC-48 </div> </div>				
Entry ^a	Catalyst	Base	Solvent	Conversion ^b (%)
1	NHC-46	NEt ₃	THF	trace
2	NHC-46	K ₂ CO ₃	THF	trace
3	NHC-46	Rb ₂ CO ₃	THF	0
4	NHC-46	Rb ₂ CO ₃	CH ₂ Cl ₂	0
5	NHC-46	Rb ₂ CO ₃	MeCN	trace
6	NHC-46	Rb ₂ CO ₃	PhMe	0
7	(±)-NHC-47	K ₂ CO ₃	THF	13
8	(±)-NHC-47	Rb ₂ CO ₃	THF	10
9	(1R,2R)-NHC-48	K ₂ CO ₃	THF	trace
10	(1R,2R)-NHC-48	Rb ₂ CO ₃	THF	3

^aConditions: benzaldehyde (0.25 mmol), solvent (0.25 mL), base (5 mol%, 0.013 mmol), cat. (5 mol%, 0.013 mmol) under N₂ at 25 °C, 24 h. ^bMeasured by ¹H NMR in CD₃OD using ethylene carbonate as an internal standard.

case, the product is also easier to form than that of the benzoin condensation, due to the intramolecular nature.

Due to these advantages, the catalysts synthesised in this work were tested in the intramolecular Stetter reaction. There are many complicating factors in the benzoin condensation discussed above, and the Stetter reaction can act as a test to ensure that these triazolium and thiazolium salts actually work as catalysts. By testing these catalysts in the Stetter reaction, their effectiveness can be investigated without taking reversibility into account, meaning enough product may be made to accurately obtain ee and ensure there are no intrinsic problems with their catalytic activity which may otherwise be hidden by other factors such as product decomposition.

Although the ee and yields will be obtained to determine the activity and selectivity of the catalyst, as no existing HPLC separation of ethyl 2-(4-oxochroman-3-yl)acetate has been reported using the Astec Cellulose chiral column in the literature, there is no immediate way of being able to tell which enantiomer is the major product. Therefore the absolute configuration of the major product will not be assigned in this work.

The conditions selected for this reaction were optimised by Rovis and coworkers, using the ethyl ester shown in Fig. 2.16. Studies on the reaction conditions determined that it was vital to keep the reaction under inert and anhydrous conditions to achieve high ee and yield. When the reaction was exposed to air, there was significantly reduced conversion, presumably due to degradation of the catalyst. Importantly, there was also reduction of yield and ee when water was present in the mixture; Rovis discovered saturating toluene with water led to 0% yield. Use of ACS grade toluene led to formation of the aldol product in 30% yield, alongside the desired product. Addition of water scavengers could increase the yield again, with MgSO_4 giving identical yields to dry toluene. However, this was accompanied by a decrease in ee from 90% to 87% [139]. Due the information from this study, it was decided to perform the reactions using toluene dried in a still, and exclude air using a vacuum before backfilling with nitrogen.

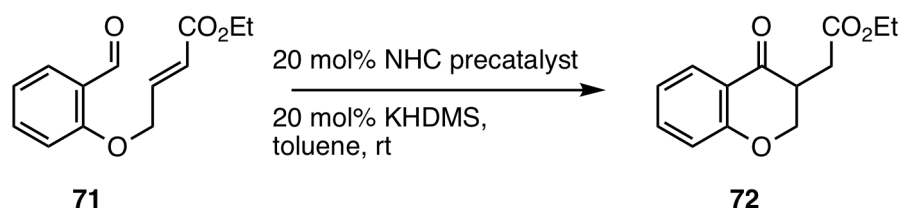


Fig. 2.16 The intramolecular Stetter reaction with conditions optimised by Rovis and coworkers [139].

2.5 Conclusions

Hydrogen-bonding is a useful tool in stereoselective synthesis, and has been successfully incorporated into many different organocatalysts, including proline in the Hajos-Parrish reaction [17], and in Jacobsen's (thio)urea catalyst for the Strecker reaction [25]. Whilst this has been used previously in conjunction with NHC catalysts [78], no further research has been reported, despite the good enantioselectivity demonstrated with these catalysts. To incorporate hydrogen-bonding moieties, commercially available starting materials involving amines have been chosen, so 1,2-diamine-derived (as per Takemoto [42]), and phenylalanine-derived structures have been planned for synthesis and investigation.

The most common structural modification to catalysts reported for inducing enantioselectivity is by having more rigid catalyst [72], so a new bicyclic catalyst incorporating (thio)urea has been designed. Conversely, a more flexible catalyst designed using a 1,4-diamine backbone has been designed, to understand how the position of the (thio)urea in relation to the NHC is important.

Computational methods have been successfully used for helping influence organocatalytic design and analysis of efficiency. Whilst there is limited software available to this particular research project, the importance of QM methods in organocatalysis need to be highlighted. By analysis of Breslow intermediates of these catalysts, approximations can be gathered of important interactions within the reaction, and lowest energy conformers can be useful indicators of whether the hydrogen-bonding is likely to be feasible. This can allow for new design and insights, and therefore pave the way for new catalyst design.

Initial conditions for the benzoin condensation were optimised, including selection of an NMR solvent and standard to accurately compare the reactions. Due to available reaction conditions and comparisons in the literature, the conditions that Waser used (K_2CO_3 and THF) were chosen for initial tests of the catalysts. A reliable standard substrate **71** for the intramolecular Stetter reaction, and corresponding conditions, were chosen for initial catalytic studies based on existing work by Rovis and coworkers [103].

Chapter 3

1,2-Diamine-Derived Catalysts

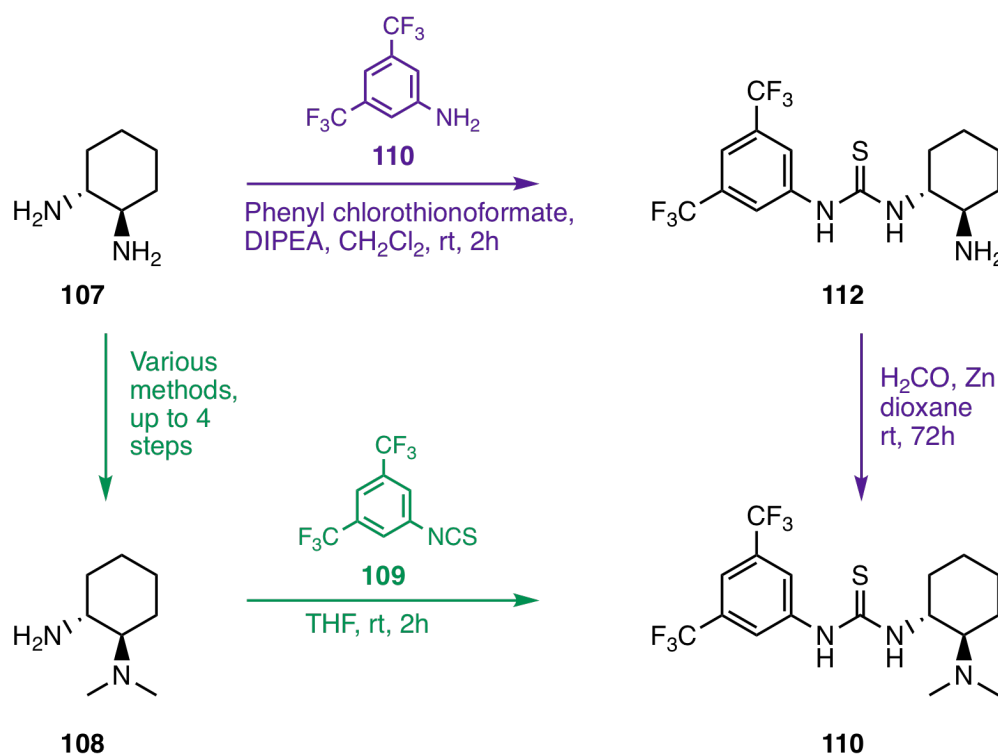
3.1 Introduction

(Thio)ureas have demonstrated their extensive use in asymmetric organocatalysis, especially after the inclusion of a second bifunctional moiety introduced by Takemoto expanded their catalytic capability [42]. Previous studies helped to influence this design of new bifunctional triazolium and thiazolium salt catalysts. The 3,5-bis(trifluoro)methylphenyl ring was selected to optimise studies, as in other catalytic systems this was shown to enhance the hydrogen bond donating ability to external carbonyls. (\pm)-*trans*-1,2-Diaminocyclohexane was selected as the scaffold, due to the commercial availability of the material, and accessibility to the optically pure enantiomers either by their purchase or chiral separation, allowing for enantioselective synthesis.

3.1.1 Synthetic Routes

One of the main advantages of the Takemoto-style backbone is the short synthesis route. The initial synthesis of Takemoto's catalyst **110** occurred in several steps [43], with the main formation of the (thio)urea such as **110** from the corresponding iso(thio)cyanate **109**. However, this requires the use of pre-formed (*R,R*)-N,N-dimethyl-*trans*-cyclohexane-1,2-

Fig. 3.1 Various routes to synthesising Takemoto's catalyst. Green route: original synthesis reported by Takemoto [43]. Purple route: New route reported by Berkessell involving late stage dimethylation [143].



Using a similar method, it was envisioned that the (thio)urea scaffold could be installed in a first as above, followed by construction of the thiazolium or triazolium salt on the remaining free amine (Fig. 3.2), as synthesis of NHC salts from primary amines has been previously reported [85, 144, 145]. As the final catalysts **NHC-48** and **NHC-50** are salts, the last step should be to incorporate the NHC functionality. This is due to the likely difficulty of working with salts, including solubility and purification. Therefore, the (thio)urea moiety will need to be installed initially. Although this means there is no opportunity for late stage modification, for example on the aromatic ring, the synthesis of the backbone should be relatively straightforward in one step, meaning that the modification can be made in the first step. Both the thiourea and the urea are to be synthesised; for the triazolium **NHC-48** and thiazolium salt **NHC-50** respectively. Whilst the thiourea catalysts have generally been reported to be more effective, and so will be the initial starting point for the triazolium salts here, the oxidation step of the thiazolium salt formation may also oxidise the sulfur of the thiourea, forming **NHC-49**. To circumvent this, the urea analogue will be investigated.

3.1.2 Chiral Resolution of (*1R,2R*)-Cyclohexane-1,2-diamine

Although (*1R,2R*)-cyclohexane-1,2-diamine **107** is commercially available, due to the optical purity it is relatively expensive, whereas (\pm)-*trans*-1,2-diaminocyclohexane is much cheaper. Therefore, initial routes to the catalysts were investigated using the racemic *trans*-diamine before repeating with the chiral analogue. However, it is possible to obtain the chiral diamine *via* chiral resolution, using (*L*)-tartaric acid **116** as the chiral resolving agent [146] (Fig. 3.3). The reaction was successfully performed on a 0.2 mole scale, giving 83% of the chiral salt (*1R,2R*)-**117**. Washing with aqueous NaOH gave the free base [147]. However, due to the polarity of the amine **107**, extraction from water proved extremely difficult, and so the maximum yield of the pure diamine obtained after washing was only 31% of the overall theoretical yield of the chiral product (26% over the two steps).

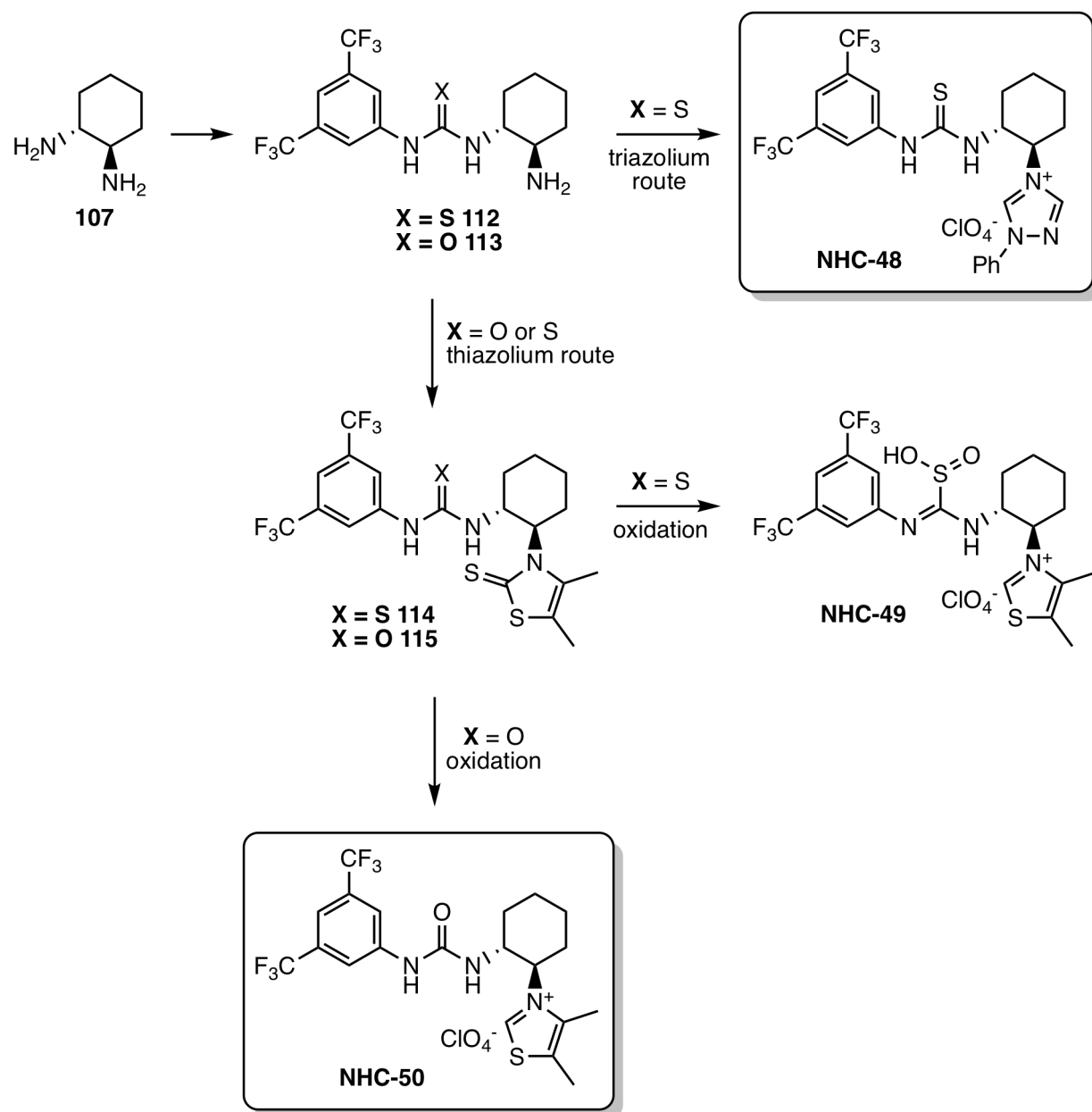


Fig. 3.2 Proposed synthetic routes to the triazolium and thiazolium salts from the primary amine.

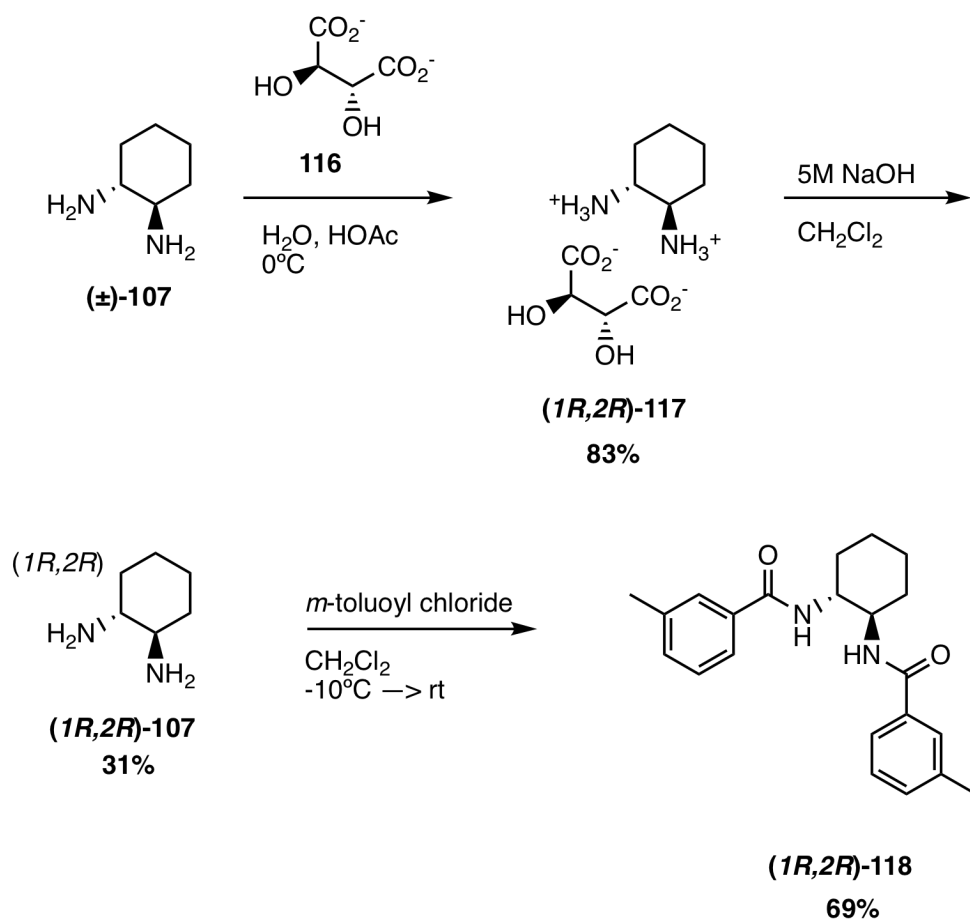


Fig. 3.3 Synthetic route to obtain the (*1R*,*2R*)-diamine, and subsequent synthesis of *N,N'*-((*1R*,*2R*)-cyclohexane-1,2-diyl)bis(3-methylbenzamide). Yield of (***1R*,*2R***)-117 is 83% of the theoretical yield.

To investigate how successful this method was in obtaining the optically pure diamine, a chromophore was added so the ee could be determined by HPLC. The *trans*-1,2-diamine was reacted with *m*-toluoyl chloride to afford the bis-substituted product (\pm)-**118** in 69% yield [148]. Successful separation was achieved *via* chiral HPLC (Fig. 3.4). This was repeated with the commercially bought (*1R,2R*)-diamine to identify the correct peaks. Finally, synthesising the analogue from the chirally resolved diamine derived from (*L*)-tartaric acid demonstrated that the (*1R,2R*)-enantiomer was obtained in 99% ee. Although effective, due to time constraints and material waste the commercially available (*1R,2R*)-diamine was used in future syntheses.

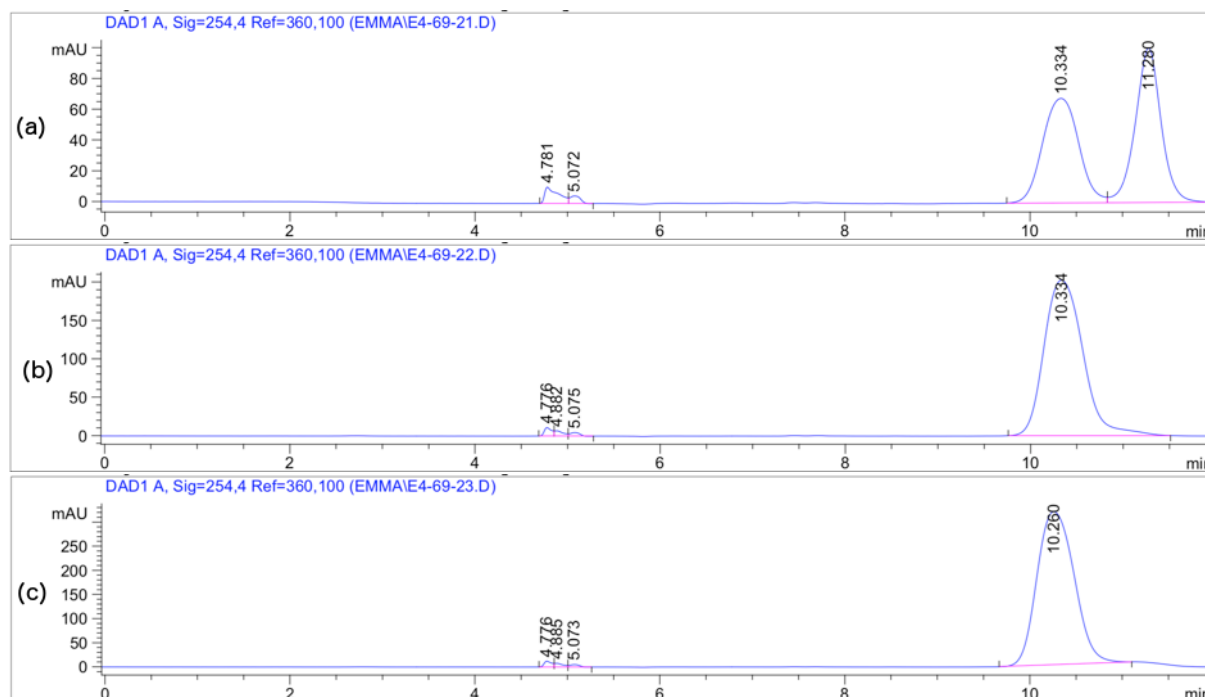


Fig. 3.4 Chiral HPLC separation of the bis(*m*-toluoyl) derivative of (a) (\pm)-*trans*-cyclohexane-1,2-diamine, (b) commercially available (*1R,2R*)-cyclohexane-1,2-diamine, and (c) (*1R,2R*)-cyclohexane-1,2-diamine obtained from chiral resolution with (*L*)-tartaric acid. Conditions: flow rate 0.6 mL/ min, mobile 5% IPA / hexane at 40 °C. CSP is Astec Cellulose DMPC. Measured at 254 nm.

3.2 Synthesis of the Catalysts

3.2.1 Synthesis of Thiourea

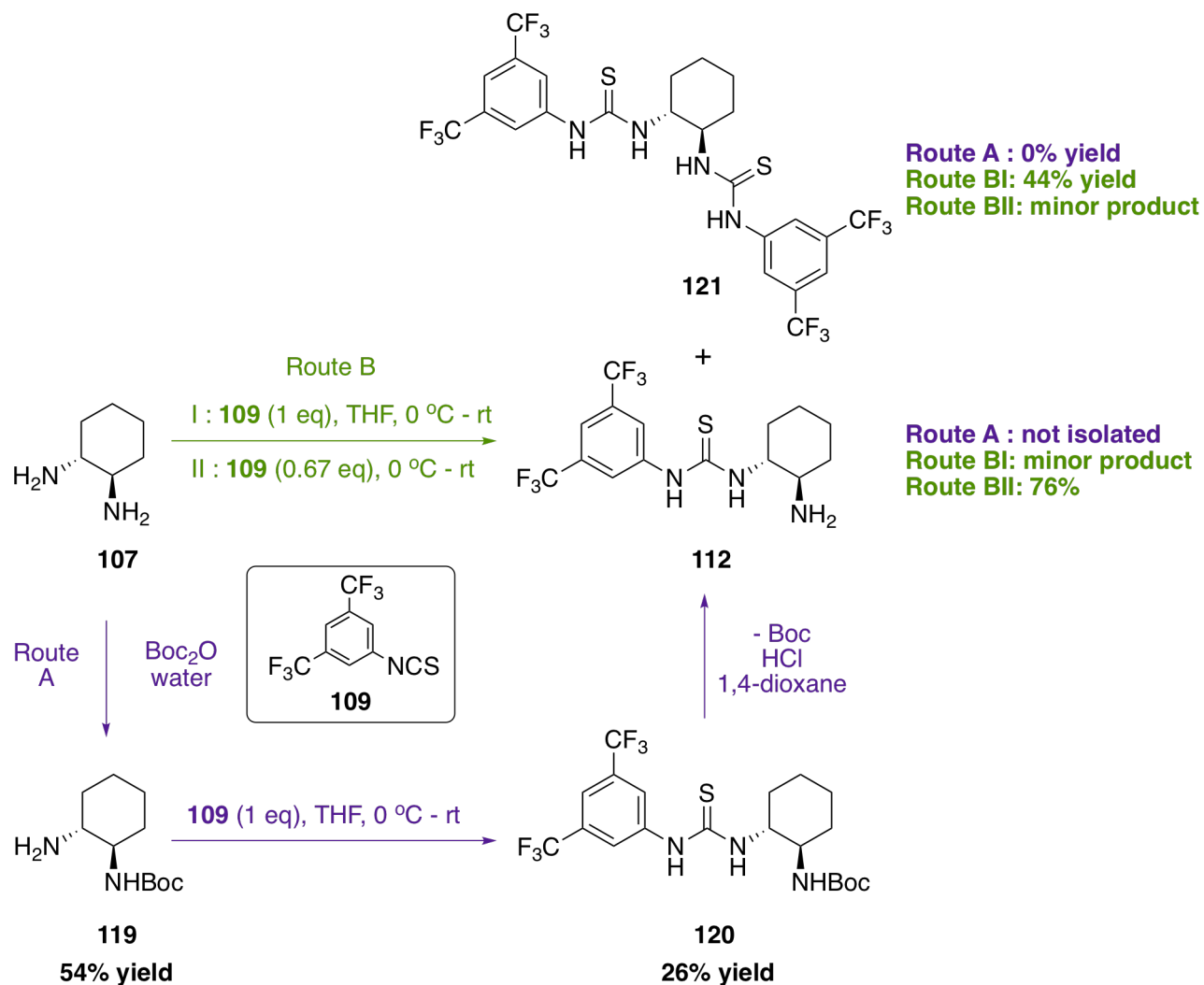


Fig. 3.5 Routes to synthesising thiourea from **107**.

Berkessell reported their new synthesis of Takemoto's catalyst by generating the thiourea thionyl from phenyl chlorothionoformate [143]. Although Takemoto's method used 3,5-bis(trifluoromethyl)phenylisothiocyanate to generate the thiourea [43], the dimethyl protection meant the reaction could only occur once, whereas Berkessell reported the reaction of the isocyanate with the free diamine leading to formation of the bis-thiourea product. Several

syntheses were therefore considered for the formation of amine **112**, to avoid formation of the bis-thiourea product due to the reactivity of the second free amine. An existing method demonstrated that **112** could be synthesised directly from (\pm)-*trans*-1,2-diaminocyclohexane **107** in high yield, using THF as a solvent [149] (Fig. 3.5 Route B, Method I). However, when attempted in this work, only the bis-thiourea product **121** was obtained (Fig. 3.6). The reaction was repeated using a micro-syringe for addition of the isothiocyanate **109**, to decrease drop size and speed to ensure the diamine **107** was always in high excess. However, the bis-thiourea **121** was still obtained as the main product.

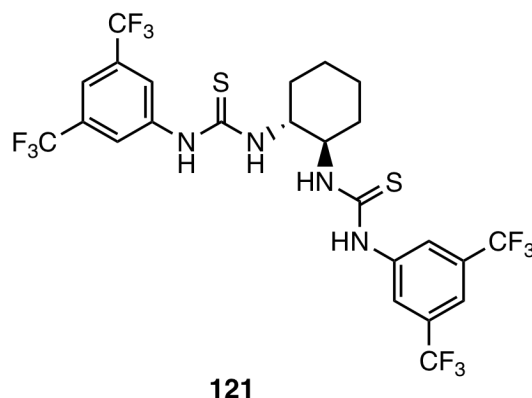


Fig. 3.6 Bis-thiourea by-product.

It was envisioned that *mono*-protection of the starting diamine **107** could lead to the desired *mono*-product **112**, and an easily cleaved protecting group like Boc would allow liberation of the desired primary amine afterwards (Fig. 3.5, route A). (\pm)-*trans*-1,2-Diaminocyclohexane **107** required initial protection of one of the amino groups; due to the C_2 symmetry, regioselectivity did not matter, but selectively mono-protecting the diamine was important. A Boc group was chosen as the procedure is synthetically simple. An initial Boc-protection method was chosen, reported by Chakraborti and coworkers, due to the use of water as a reaction solvent, a 1:1 stoichiometry of diamine and the Boc_2O , easy purification and mild conditions [150]. However, both amines ended up with a Boc protecting group instead. This may be caused by the biphasic layers, as the mono-Boc-protected product is less soluble in water than the diamine starting material. This leaves it more susceptible to

reaction with the insoluble Boc-anhydride and therefore leading to double Boc-protection. Beer and coworkers reported a method using CH_2Cl_2 as a solvent [151]. The reaction was not as economically viable, as it required an 8-fold excess of the diamine, which is more expensive due to the optical purity. However, this reaction was successful and led to the desired mono-Boc protected product **119** in 54% yield.

Reaction of the Boc-protected amine **119** with the isothiocyanate **109** (Fig. 3.5 Route B) led to compound **120** but only in 26% yield. However, NMR analysis also determined an impurity. Initially, NMR was run at room temperature, but due to the bulkiness of the Boc-group and thiourea, rotamers were observed. Wide peaks obscured the spectra making identification of the by-product difficult, but running the spectra at high temperature led to decomposition of the desired product. The by-product was later determined to be bis-thiourea **121** by HRMS. This was thought to be formed due to some remaining diamine starting material **107** in with the Boc-protected amine **118**, which had not been identified due to similar ^1H NMR spectra. Both products co-eluted due to similar polarities, meaning separation at this stage was highly difficult. The deprotection step using HCl was progressed; a polar amine would have a very different R_f value compared to the bis-thiourea **121**. The reaction looked successful by TLC with ninhydrin analysis due to appearance of a spot on the baseline, but isolation of the product proved difficult and was not progressed at this stage.

An alternative method to synthesise **112** by direct reaction of isothiocyanate **109** with diaminocyclohexane **107**, without any Boc protection was described by Kwiatkowski *et al.* [152]. It involved addition of 0.67 equivalents of the isothiocyanate to the amine dissolved in a large volume of dry CH_2Cl_2 at 0°C . The basicity of the primary amine was exploited, meaning that the product could be extracted using acid and base modification, rather than having to purify with extremely polar column chromatography. The reaction mixture was acidified to pH 3, upon which the hydrochloride salt was formed. This was then filtered out, basified to pH 12, and extracted using CH_2Cl_2 to afford the pure product **112**. This reaction also worked well with bench CH_2Cl_2 rather than using anhydrous solvents. The reaction was

repeatable, giving yields up to 77%, and also worked with the optically pure diamine, so this method was used going forward.

This reaction also worked with phenyl isothiocyanate **122**, in much higher yield, giving 93% of the desired (*1R,2R*)-thiourea **123** (Fig. 3.7).

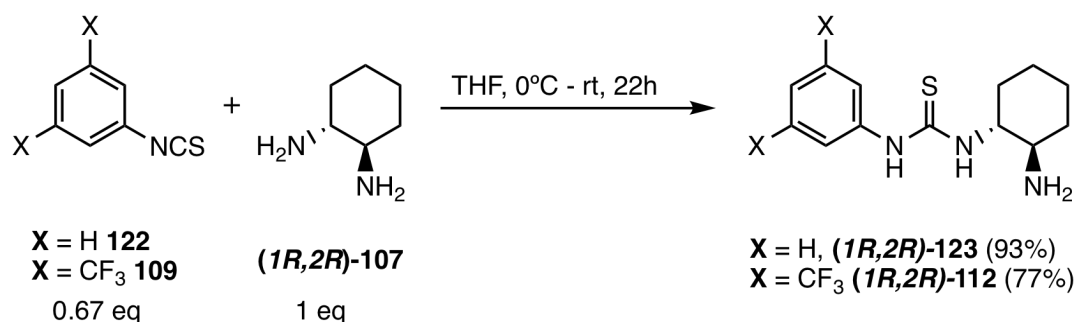


Fig. 3.7 Final reaction conditions to synthesise chiral thioureas.

3.2.2 Synthesis of Urea

The same synthesis was applied to form urea using the isocyanate analogue **124**. However, a greater ratio of the bis-product was obtained (90:10 by LCMS), hinting that the reactivity of the isocyanate was much greater than that of the isothiocyanate, and several repeats of the reaction only gave a maximum yield of 41% of the urea **113**. Alternative methods of synthesis from the *trans*-diamine **107** were investigated to try and improve this yield.

As with the isothiocyanate method earlier, mono-Boc-protection of the diamine was attempted [153]. However, similar issues occur with the reactivity of the diamine – only 54% yield was obtained, as a large amount of the bis-Boc protected product was formed. Reaction of the mono-Boc protected diamine (\pm)-**118** with the isocyanate **124** gave the product (\pm)-**125** in 82% yield, and subsequent deprotection gave 76% yield. However, not only did this have the added disadvantage of being a three-step process, the overall yield of (\pm)-**113** was 34%, which is lower than that of the direct method.

An alternative method using 4-nitrophenylchloroformate as the urea source was attempted [154]. The chloride is initially displaced by the 3,5-bis(trifluoromethyl)phenylaniline to

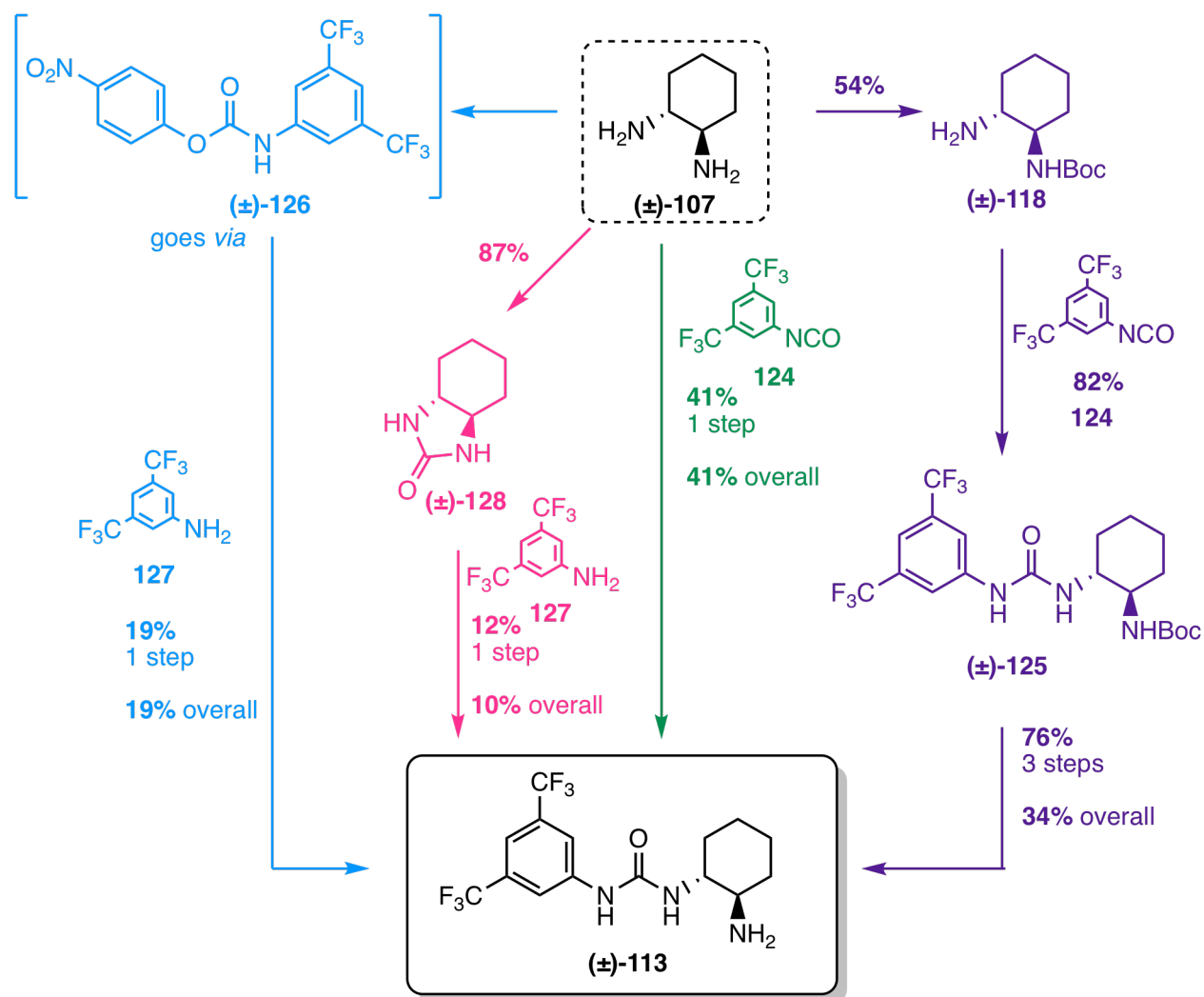


Fig. 3.8 Different synthetic routes attempted to maximise the yield of the urea product.

form (\pm)-**126**. The 4-nitroaniline is a good leaving group due to the electron withdrawing group, which is then displaced by the amine. However, the final product (\pm)-**113** did not form cleanly, only giving a 19% yield.

The final method investigated involved formation of a symmetrical cyclised urea (\pm)-**128** [155]. Reaction of the diamine with diphenylcarbonate means that both amines react to form the cyclised intermediate, and ring opening with 3,5-bis(trifluoromethyl)phenylaniline can only form the mono-urea product (\pm)-**113**. The first step occurs cleanly in 87% yield, but due to poor nucleophilicity of the aniline only 12% of the product was formed, giving an overall 10% yield over two steps.

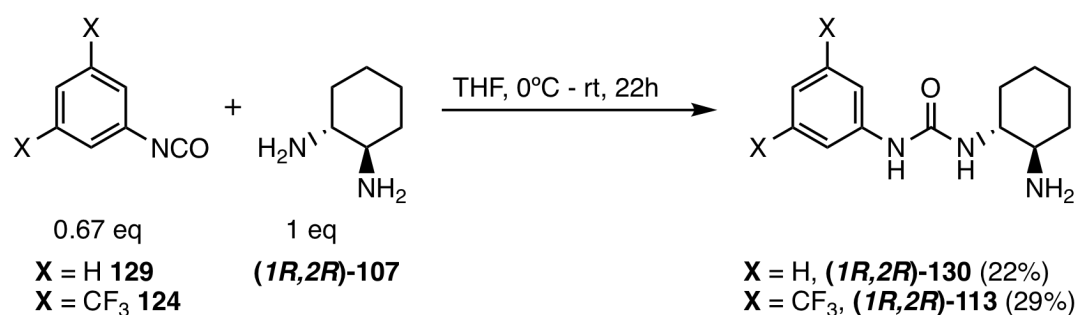


Fig. 3.9 Final reaction conditions to synthesise chiral ureas.

After exploring all these options, the urea synthesised from the initial 1-step synthesis using the isocyanate giving 41% yield was chosen for synthesis of the optically pure (1*R*,2*R*) product. The reaction was repeated with phenylisocyanate **129** to generate the phenyl analogue **130**, and this reaction occurred in a similarly low yield of 22% (Fig. 3.9).

3.2.3 Synthesis of the Triazolium Salt

1,2,4-Triazolium salts can be synthesised from primary amines in high yield with the method described by Connon and coworkers [76]. They synthesised a catalyst using cyclohexylamine (Fig. 3.10), and so this procedure was to be adapted using the thiourea cyclohexylamine derivative **112** as the primary amine. The two secondary amines of the thiourea moiety

should have lower nucleophilicity due to delocalisation of the lone pair into the π -framework, meaning there should be minimal interference forming side-products in subsequent reactions.

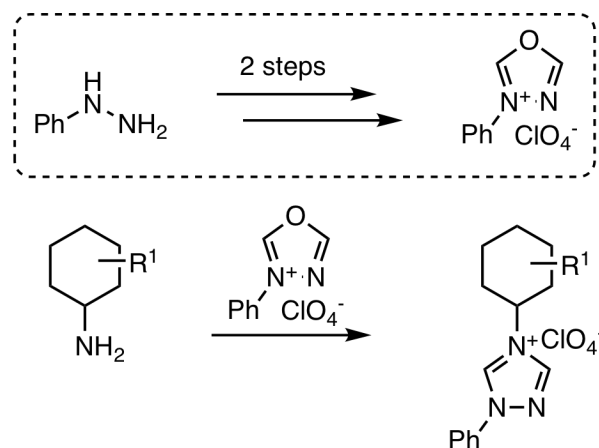


Fig. 3.10 General scheme to show the synthesis of triazolium salt catalysts from primary amines and oxadiazolium salts, reported by Connon and coworkers [76].

Oxadiazolium salt **132** could be made from commercially available phenylhydrazine in a two-step process as shown [145] (Fig. 3.11). *N,N'*-Diformylated phenylhydrazine **131** was synthesised in 30%, starting from a 50 mmol scale. The mono-formylated product was also formed, but could be removed by recrystallisation of the desired product from hot ethanol. **131** was stable in air for long periods of time, and could be used after storage for several months. The cyclisation step was attempted several times, as due to the water sensitivity of the product, dry solvents and dry glassware had to be used, the product kept under nitrogen, and used as quickly as possible in the next stage. The product **132** was eventually isolated in yields up to 83% after washing with dry Et_2O , and its structure confirmed by IR spectroscopy, as instability in NMR solvents meant that it decomposed before it could be characterised.

The 1,2,4-triazolium ring could be synthesised by the same method as Connon and coworkers, using acetonitrile as the solvent [76]. An achiral catalyst was desired as a standard to determine whether the thiourea group had any effect on the enantioselectivity. Connon had already synthesised the cyclohexyl triazolium salt, and so this methodology was used here to form **NHC-51**. Interestingly, the iminium intermediate **NHC-51-int** was not

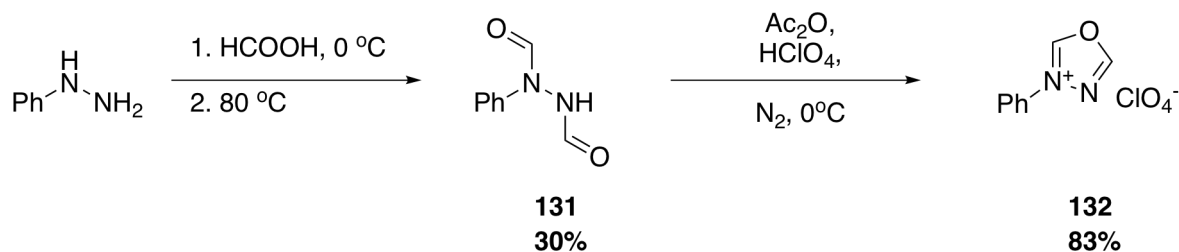


Fig. 3.11 Scheme to show the synthetic route to 3-phenyl-1,3,4-oxadiazol-3-ium **132** from phenylhydrazine.

isolated as reported in the paper, and the cyclisation occurred at room temperature in 70h to obtain **NHC-51** directly in 35% yield (Fig. 3.12). As the methodology had worked for cyclohexylamine, the procedure was repeated using **112** as the primary amine. This time, the iminium intermediate **NHC-48-int** was detected by LCMS (Fig. 3.12), with a small amount of the cyclised product **NHC-48** detected. TLC analysis showed a large number of by-products, which all very closely eluted. Prolonged heating of the mixture did not lead to any more of the cyclised compound, nor did further addition of intermediate **132** to the mixture.

An alternative method using AcOH as a solvent was investigated, as reported by Strand *et al.* [145]. The reaction, as reported, did not require molecular sieves, and the product could be obtained after heating to 110°C. Upon trying with thiourea **112**, the material decomposed at high temperatures. The procedure was repeated but with a lower temperature of 90°C. Careful measurement by LCMS showed that the by-product was still formed over time. However, by stopping the reaction after 1 hour, the amount of product was maximised. The by-product was characterised and determined to be *N*-[3,5-bis(trifluoromethyl)phenyl]formamide **NHC-48-byproduct** (Fig. 3.13). At this moment, it is unknown how this by-product is formed, and this was not investigated further. Isotope labelling of the various starting materials could potentially help identify where the C=O of the newly formed amide comes from; it is likely this will be either from the oxadiazolium directly or one of the corresponding intermediates. This initial synthesis gave the desired (\pm)-**NHC-48** in 3% yield.

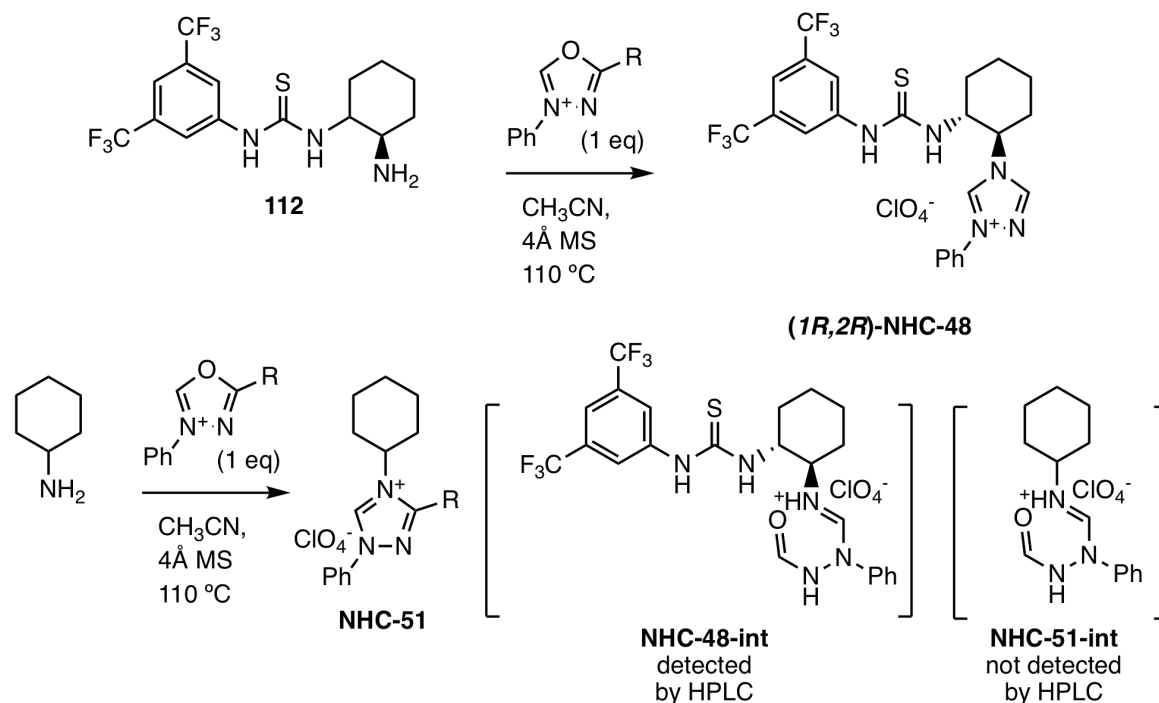


Fig. 3.12 Scheme to show the synthetic route to the final catalysts (\pm)-**NHC-48** and **NHC-51** from amine **112** and cyclohexylamine respectively, as per Connon and coworker's method [76]. **NHC-51-int** was not detected by LCMS as reported (m/z 246), but **NHC-48-int** was (m/z 532).

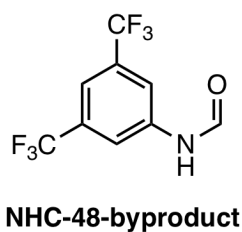


Fig. 3.13 By-product **NHC-48-byproduct** obtained from the reaction to try and obtain the triazolium salt.

Optimisation of the triazolium salt formation

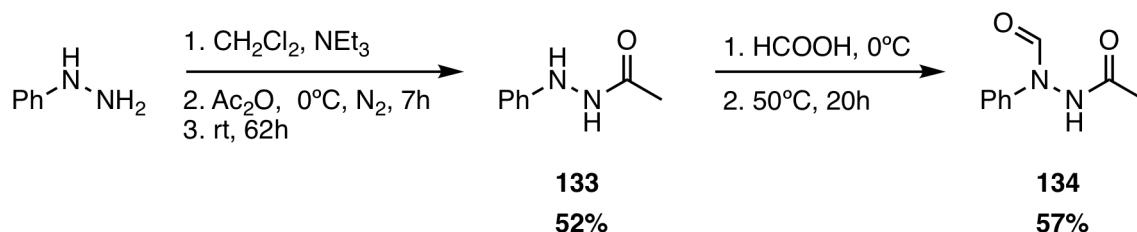


Fig. 3.14 Synthetic route to *N'*-acetyl-*N*-formylphenylhydrazine.

Due to low yield of the the final catalyst (\pm)-**NHC-48**, the reaction conditions were optimised using cyclohexylamine, to try and improve the yield (Table 3.1). Cannon and coworkers had reported the synthesis of the 5-methyl analogue **NHC-52**, which they synthesised in an attempt to improve stability [76], so it was investigated in this work. To form intermediate **133**, phenylhydrazine was stirred in CH_2Cl_2 with dropwise addition of acetic anhydride to generate the *N'*-acetylated product in 52% (Fig. 3.14). Similar to the generation of the unmethylated analogue **131**, the precursor **133** was refluxed in formic acid to synthesise *N'*-acetyl-*N*-formylphenylhydrazine **134** in 57% yield. Finally, cyclisation led to formation of the unstable methylated oxadiazolium salt **135** in quantitative yield. Again, similar to **132**, this could not be analysed by ^1H NMR due to its instability.

Cyclohexylamine was used as a model primary amine for the formation of the triazolium salt. After 2h under the conditions shown in Table 3.1, the formed triazolium salt **NHC-51** was purified by addition of Et_2O to promote crystallisation, and the pure triazolium salt filtered off. It was discovered that the factor which made the most significant difference in yield was lowering the equivalent of the primary amine to 1 equivalent. This was beneficial as this would lead to a lower waste of the chiral starting amine (Table 3.1, Entry 2). Addition of a methyl group led to the lowest amount of catalyst being made, and due to the extra step involved in synthesis, was therefore no longer investigated.

The reaction was repeated using the cyclohexylamine thiourea amine **112**, still at 90°C , but with a 1:1 ratio of the starting materials (Fig. 3.15). Careful monitoring of the reaction

Table 3.1 Optimisation of the 1,3,4-triazolium salt formation.

1 - 3.3 eq
R = H 132
R = Me 135

NHC-51 R = H
NHC-52 R = Me

Entry	Cy-NH ₂ (eq)	R	T (°C)	Yield (%)
1	3.3	H	90	53
2	1	H	110	62
3	3.3	H	110	45
4	3.3	Me	110	32

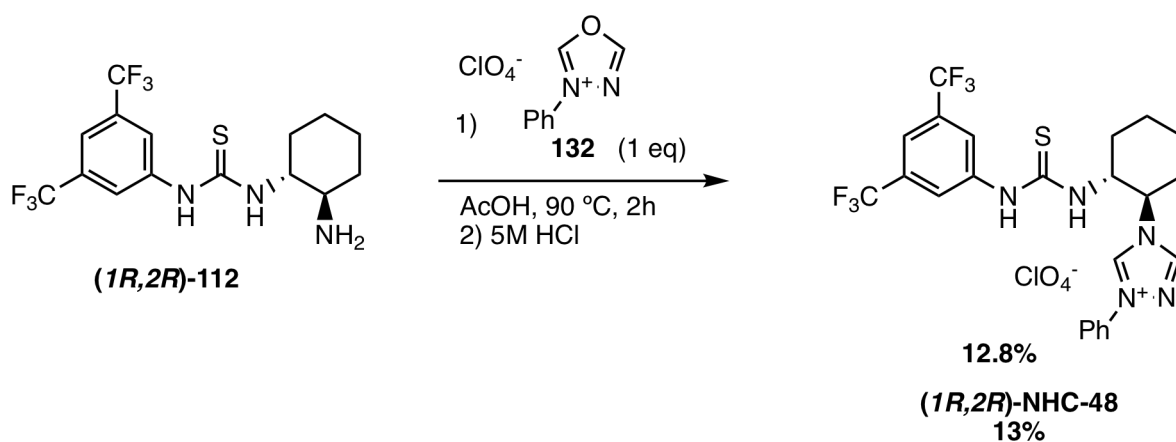


Fig. 3.15 Synthetic route to the final catalyst using the optimised conditions obtained in Table 3.1.

by LC/MS to optimise the reaction conditions also occurred, to monitor at what point degradation of the triazolium salt occurred and generation of the by-product above increased. After two hours, the reaction was turned off. The reaction mixture was concentrated *in vacuo* (although removal of all the acetic acid was not achieved due to the high boiling point). The crude product was taken up in CH₂Cl₂, and this was washed with 5M HCl to remove the acetic acid and starting amine. Elution of the product from silica using 10% MeOH / CH₂Cl₂ led to isolation of the product (***IR,2R***)-NHC-48 in 13%. Although still low, enough material was obtained for testing.

Synthesis of triazolium salt analogues

Similar to the method above, the urea analogue (***IR,2R***)-NHC-53 was synthesised. This reaction also formed the decomposition product, and the final product was only obtained in 5% yield. The phenyl analogues of the cyclohexyl(thio)urea **112** had been synthesised (**123** and **130** for the thiourea and the urea respectively), and were both taken through to their corresponding final triazolium salt catalyst (Fig. 3.16). The reactions did not appear to have any by-product forming, as measured by HPLC. This meant the reactions could be left on for a longer period of time to encourage synthesis of the final product. However, extended heating did not increase the product any further. Work up varied slightly on these reactions; the two catalysts appear to be more water soluble, and so washing with 5M HCl left the product being spread between the aqueous and organic layers. To obtain the final pure products, the catalysts were purified using column chromatography, eluting with 10% MeOH/CH₂Cl₂ to afford the final products (***IR,2R***)-NHC-54 and (***IR,2R***)-NHC-55 in yields of 21% and 15% respectively.

3.2.4 Synthesis of the Thiazolium Salt

The thiazolium salt analogue NHC-50 may also be synthesised from the urea scaffold **113** (Fig. 3.18). By using a method reported by Glorius [156], the primary amine is reacted

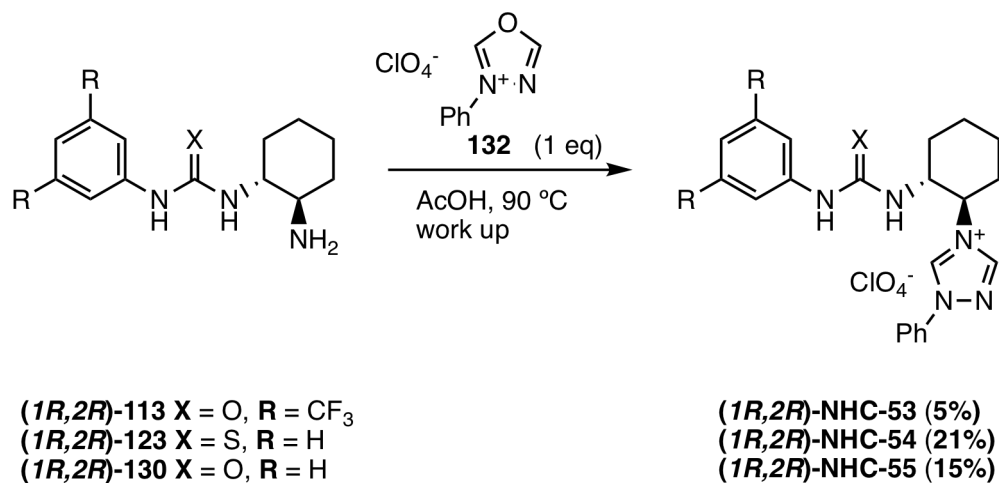


Fig. 3.16 Final synthesis of the triazolium salt catalysts.

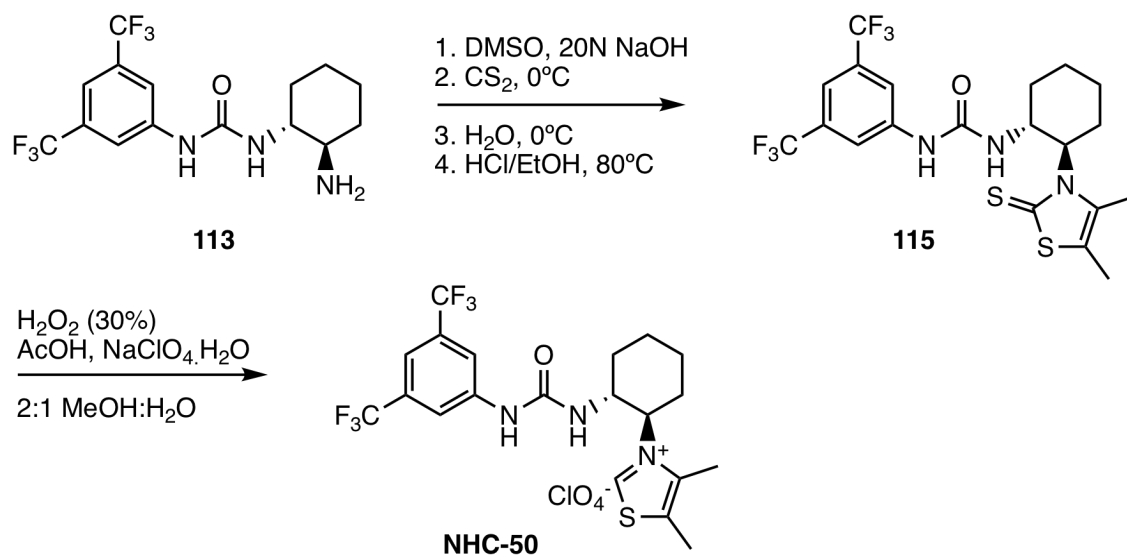


Fig. 3.17 Proposed synthetic route to the thiazolium catalyst, based on Glorius' method [85]

with CS₂ in DMSO using NaOH as a base, before addition of 3-chloro-2-butanone. Once the ring is formed, refluxing in EtOH and HCl will hopefully give dehydration to form thiazolin-2-thione **115**. Oxidation of the thione using hydrogen peroxide followed by loss of SO₂ is hoped to give the thiazolium ylid, which is protonated to generate the final thiazolium salt.

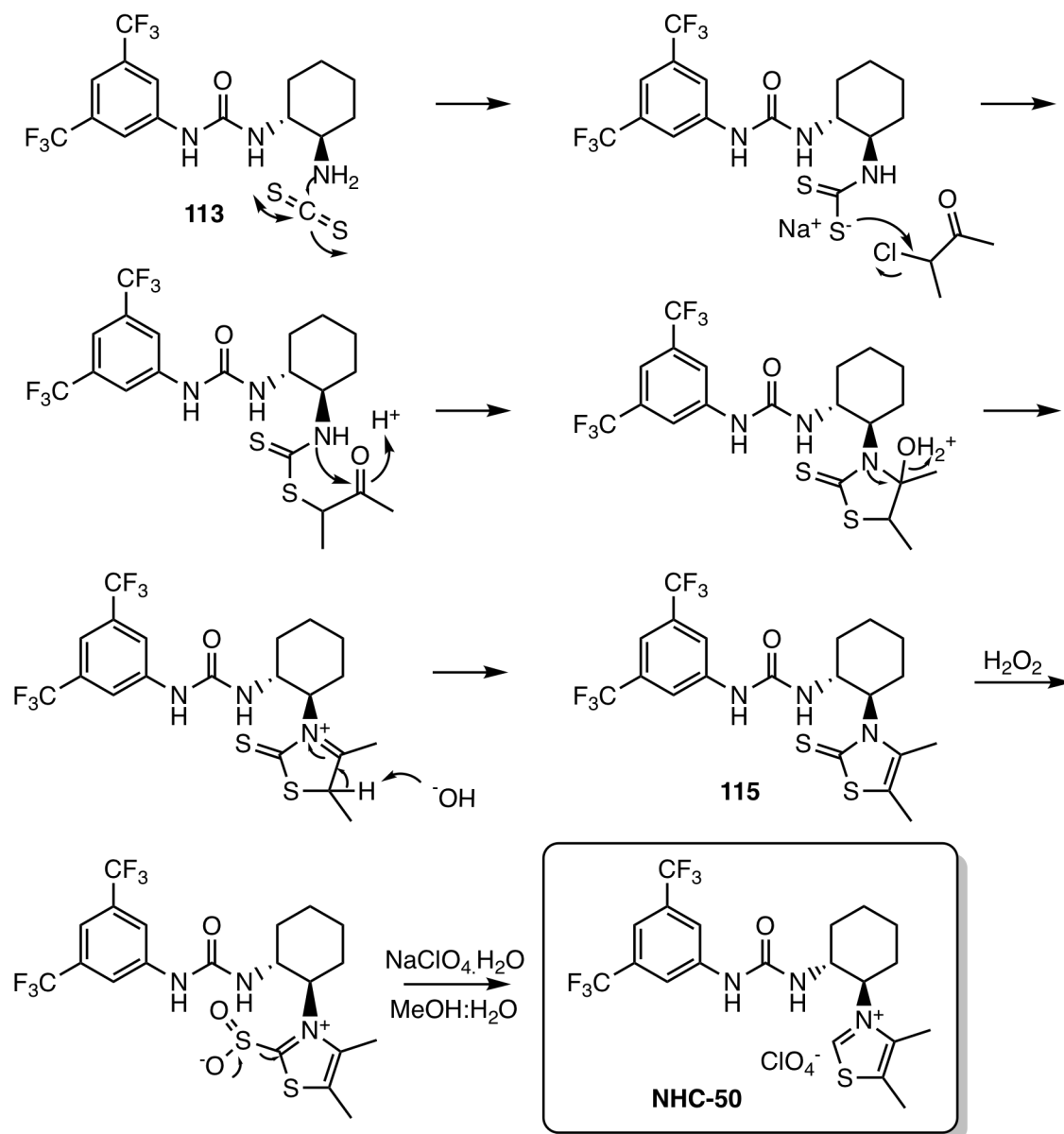


Fig. 3.18 Mechanism to form the final thiazolium salt from the starting primary amine.

Initial attempts led to by-product **136** being formed (Fig. 3.19). This is due to the 1,2-diamine system being in a favourable position to form a stable 5-membered ring. After some investigation, this appeared to be due to leaving the CS₂ to react with the amine for only 10 minutes. Allowing the reaction to warm up to ambient temperature and stirring for an hour, the reaction was successful, and gave the product in 25% yield. However, this did not precipitate out as suggested, perhaps due to traces of DMSO aiding solubility, or the H-bonding urea forming favourable interactions with the solvent. The crude material was taken directly through to the oxidation step, and gave the final product **NHC-50** in 10% yield. However, CHN analysis showed a large amount of inorganic impurity, presumed to be excess NaClO₄.

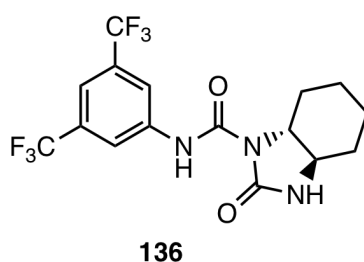


Fig. 3.19 Main by-product obtained in the initial cyclisation reaction.

The reaction was repeated to try and form the optically pure (*1R,2R*) thiazolin-2-thione **115**. However, analysis showed that the final thiazolium salt product (*1R,2R*)-**NHC-50-Cl** (where Cl refers to the counterion being Cl⁻ instead of ClO₄⁻) had been formed. ¹H NMR gave a peak at 8.26 ppm which would correspond to the C-2 proton. Full HMBC showed that the final product had indeed been formed, without the use of hydrogen peroxide. Curious to see if the results were reproducible, and to understand where the oxidation was occurring, the reaction was repeated using cyclohexylamine as the primary amine. However, the thiazolin-2-thione product precipitated out. Due to this, no further reaction occurred.

As previously discussed, the thiourea analogue of this thiazolium salt should be difficult to make, as the thiourea may also be oxidised during the oxidation step. Therefore, some of the starting thiourea **112** was taken through using this method to try and form the final

thiazolium salt (Fig. 3.20). Interestingly, LCMS showed an m/z which corresponded to the thiazol-2-thione **136** as the thiourea appeared to have converted into a urea.

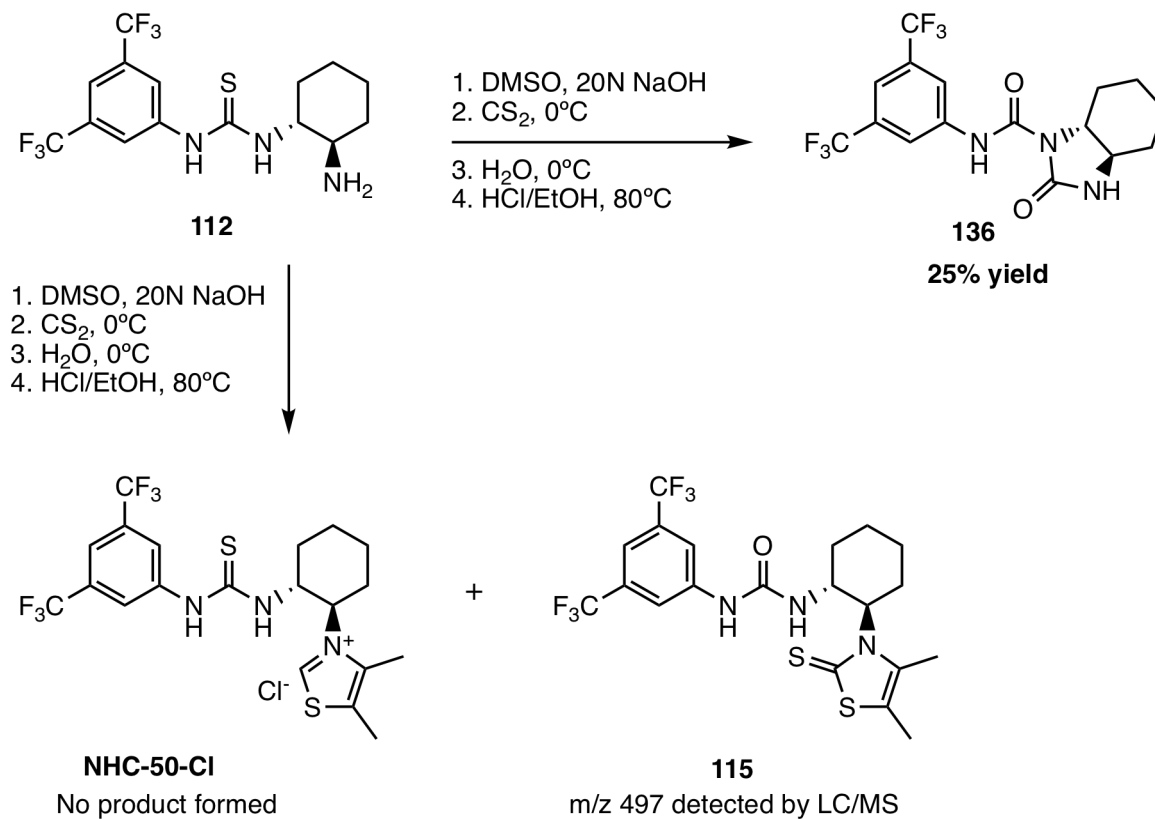


Fig. 3.20 Attempt to product the thiazolium chloride salt in one step from **112**. The initial urea product **115** formed with NaOH, and the cyclised product **136** formed with K₂CO₃.

Disheartened by the result, it was thought that the sodium hydroxide could be acting as a nucleophile and converting the thiourea to a urea. To investigate this, the conditions were kept identical, except substituting NaOH for K₂CO₃. Problems occurred due to the insolubility of the base, meaning slightly more water had to be added. During the reaction, the base precipitated out. After the final step of refluxing in acidic EtOH, the products were purified by column chromatography. This time, the final product appeared to result from attack of the thiourea by the second amine of the diamine, to form the cyclised product. Due to these shortcomings, the idea of forming a thiazolium salt from the starting urea was abandoned. However, enough of the final catalyst (*1R,2R*)-**NHC-50-Cl** had been formed to undertake initial testing with.

3.2.5 Synthesis of Squaramides

Catalysts incorporating squaramide in place of the (thio)urea were designed to further investigate the effects of the hydrogen bonding moiety. The primary amine scaffold can be synthesised in two steps from dimethyl squarate, a commercially available reagent (Fig. 3.21).

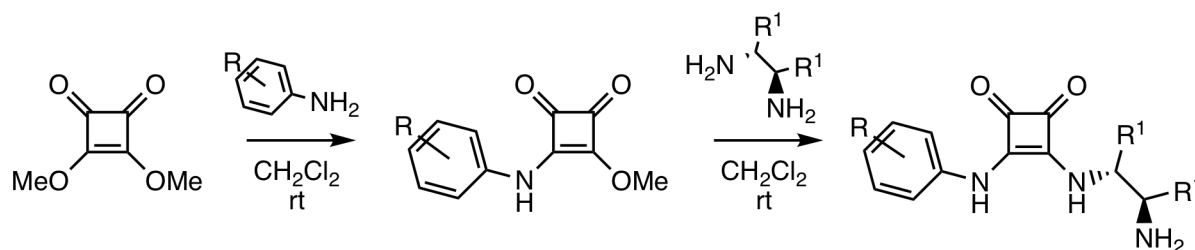


Fig. 3.21 Generic synthetic route to squaramide catalysts, ready for conversion to the triazolium or thiazolium salts. R = 4-CF₃, 3,5-bis(CF₃). R¹ = Ph, (C₂H₄)₄

Triazolium Salt Synthesis

The 4-CF₃ analogue was initially synthesised, as a catalyst incorporating this functionality had given marginally higher ee's compared to the 3,5-bis(CF₃) analogue with organocatalysts in Michael addition reactions [157]. The half-squaramide **139** was formed from stirring dimethyl squarate **137** and 4-trifluoromethylaniline **138** in methanol (Fig.3.22). Work-up involved a simple filtration, giving the product in 67% yield. As previous syntheses were reported with the diamine having groups on the second amine, *e.g.* with the dimethyl catalyst [42], initially the reaction was performed with (±)-Boc-1,2-diaminocyclohexane(±)-**118**. This reaction proceeded well, with 71% of the product (±)-**140** formed, and Boc deprotection gave the free amine (±)-**141** in 77% yield. However, upon reaction with the oxadiazolium **132** to try and form the final triazolium salt, no product was detected by LCMS. Even upon heating to 110°C in acetic acid, the initial squaramide (±)-**141** was unable to dissolve. Increasing the amount of solvent, and addition of DMSO as a co-solvent, did not yield any product.

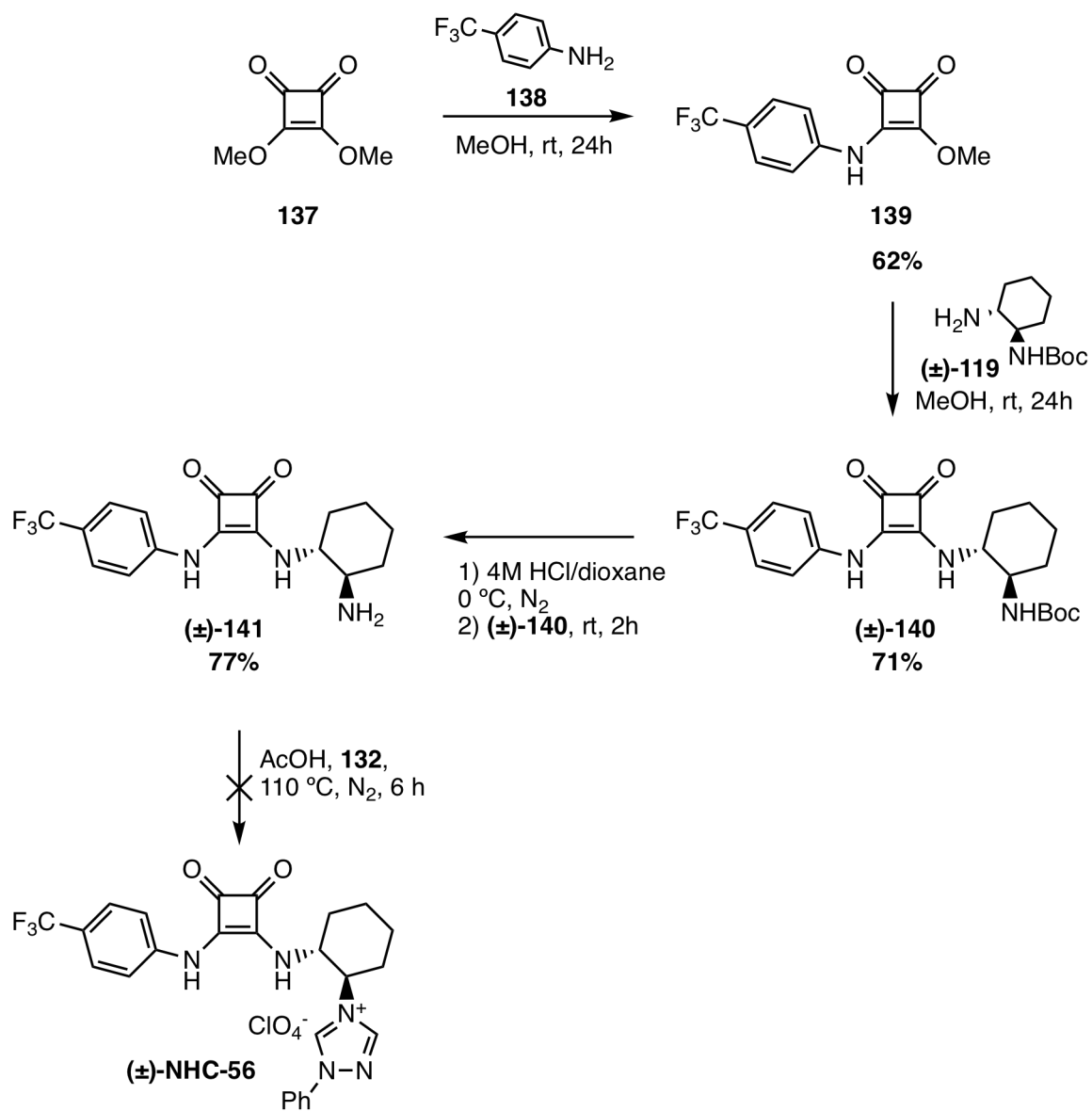


Fig. 3.22 Synthetic route to form the triazolium salt with a chiral cyclohexyl backbone and squaramide moiety.

An alternative method was proposed, investigating the reaction of the Boc-protected diamine (\pm)-**119** with the oxadiazolium salt **132** first (Fig. 3.23). It was hypothesised that once **NHC-57** was formed, an acid-catalysed Boc removal followed by S_N2 reaction of the free amine with the half-squaramide would generate the final product **NHC-56**. With the bulky triazolium group protecting the amine, it was hoped this would be enough to interrupt intermolecular H-bonding, allowing the final catalysts to be soluble. There was no reaction between the oxadiazolium salt and the diamine when attempted, meaning this synthetic route was unviable.

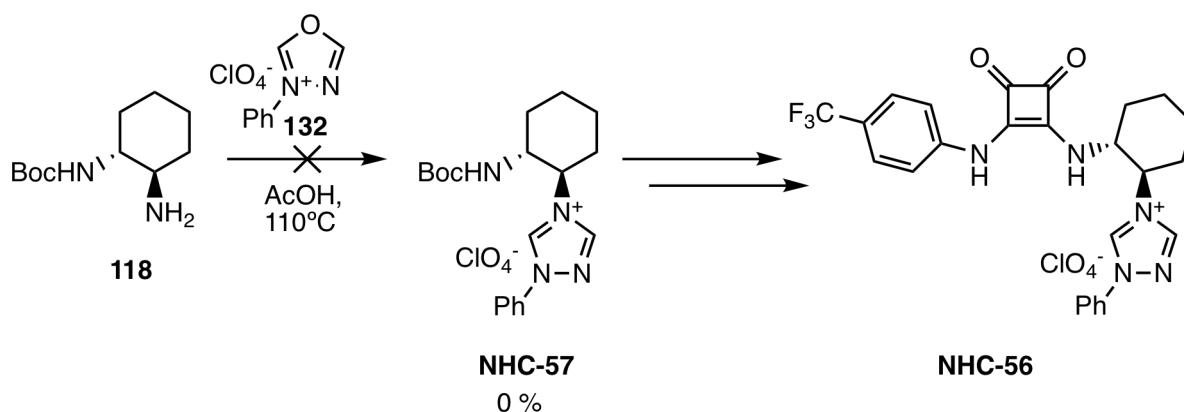


Fig. 3.23 Attempted synthesis of the triazolium salt from the mono-Boc-protected diamine.

Thiazolium Salt Synthesis

As the squaramide (**141**) was sparingly soluble in DMSO, enough to obtain NMR spectra, the route to the thiazolium salt was investigated as this used DMSO as a solvent. The squaramide was re-synthesised as a single enantiomer, but a method published by Yang and Du demonstrated that the reaction could occur directly from the (*1R,2R*)-cyclohexane-1,2-diamine without prior Boc protection of the free amine **107** [45]. This reaction occurred in CH_2Cl_2 , and gave the unprotected product (*1R,2R*)-**141** directly in 77%. However, the attempted synthesis of the corresponding thiazolone-2-thione (*1R,2R*)-**142** did not give the desired product. A large amount of the starting material was obtained back due to insolubility, and a crude mixture of various products. The DMSO was difficult to remove, meaning

column chromatography was ineffective as the by-products were eluted at the same time as the DMSO. Therefore, no clear analysis could be done to identify the main product, but a peak was detected by LC/MS giving $[M^+] = 396$. As with the previous syntheses involving urea, this would correspond with the putative cyclised impurity **(1*R*,2*R*)-143** (Fig. 3.24), although no formal characterisation was undertaken to confirm this.

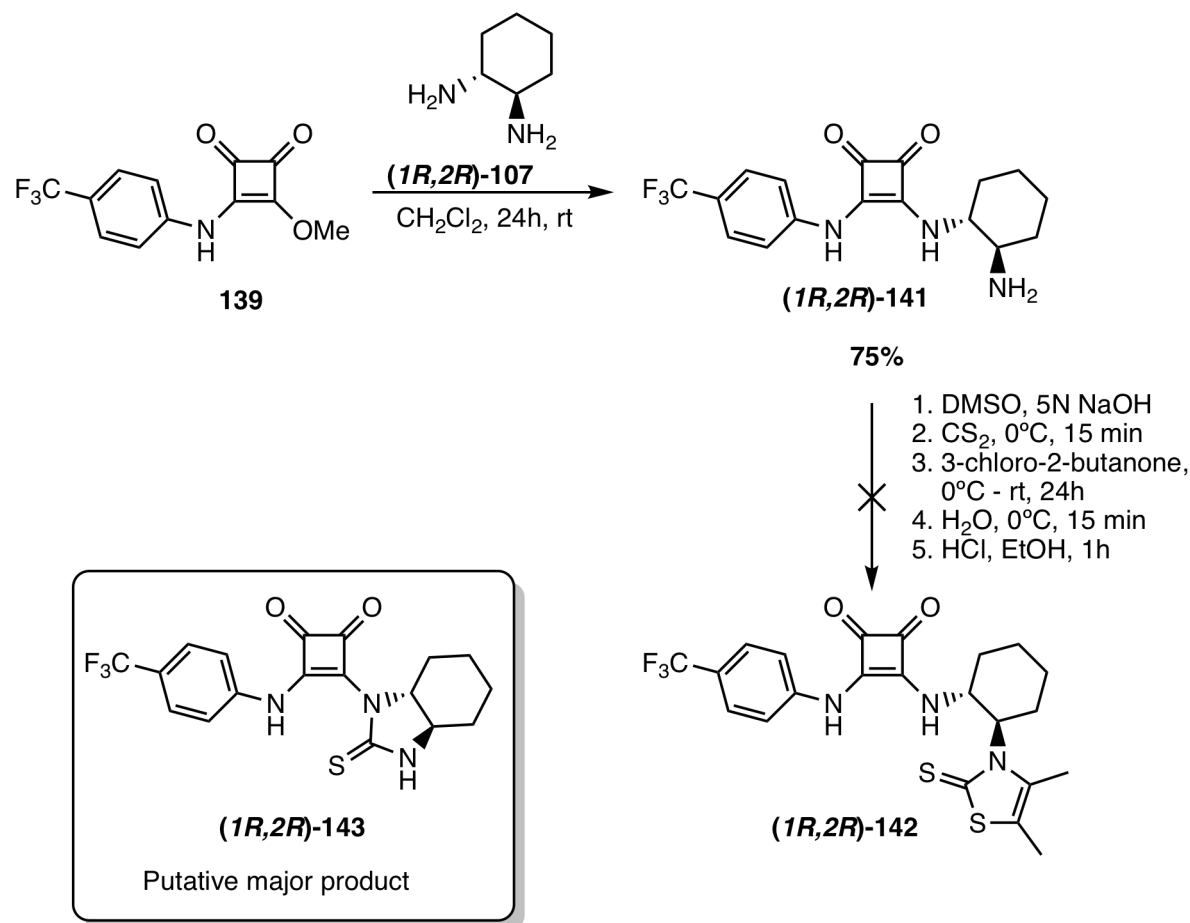


Fig. 3.24 Generic synthetic route to squaramide catalysts, ready for conversion to the triazolium or thiazolium salts. $\text{R} = 4\text{-CF}_3$, 3,5-bis(CF_3). $\text{R}^1 = \text{Ph}$, $(\text{C}_2\text{H}_4)_4$

Investigating Solubility of the Squaramide

An investigation was undertaken to determine why the squaramide **141** was only very sparingly soluble in most solvents, so the desired catalysts could be synthesised by adapting the methods. Due to the positioning of the amine and the two carbonyls, it was hypothesised

that the insolubility may come from intermolecular hydrogen bonding. Searching the Cambridge Structural Database (CSD) for similar structures, several compounds had been submitted which incorporated squaramides. Although none were identical to the structure of the synthesised squaramide **141**, Gale and coworkers reported the crystal structure of 3,4-bis((4-(trifluoromethyl)phenyl)amino)cyclobut-3-ene-1,2-dione. As can be seen, the carbonyls are positioned in such a way that intermolecular hydrogen bonds occur between these and the N-Hs, at a distance of 1.9 Å (Fig. 3.25). As the squaramide incorporates the same N-H pendants, and a further NH₂, it is possible that this bonding is leading to the insolubility of the compound.

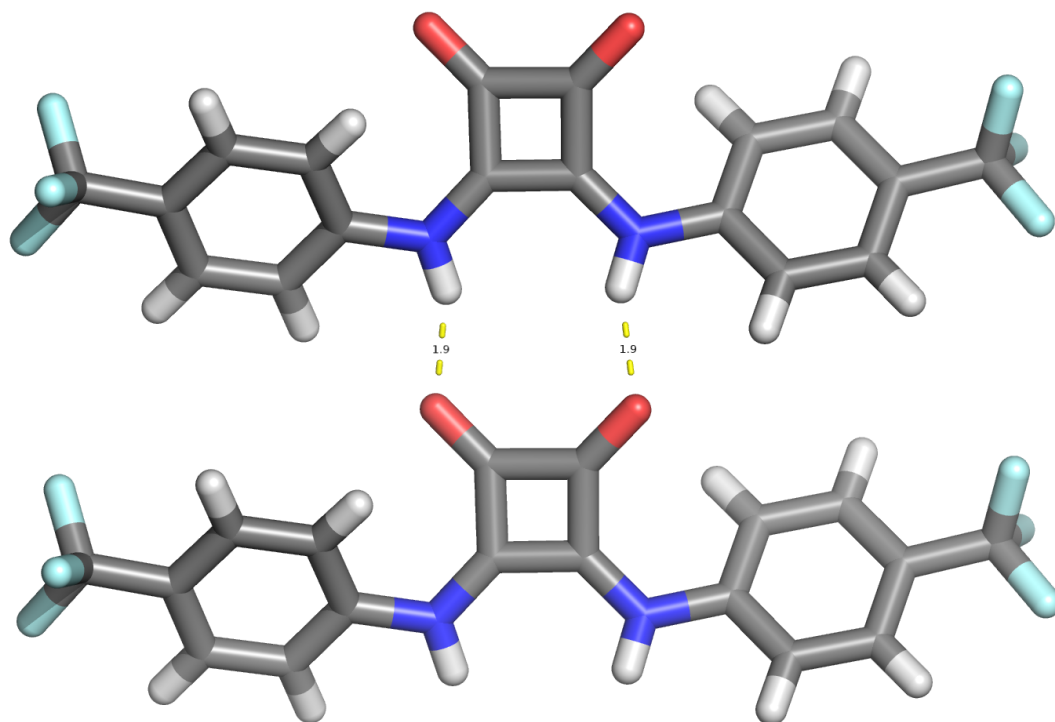


Fig. 3.25 The crystal structure of 3,4-bis((4-(trifluoromethyl)phenyl)amino)cyclobut-3-ene-1,2-dione, obtained by Gale [158]. Obtained through the CSD, reference FAXBEN.

To obtain crystal structures, the crystals have to be dissolved in a solvent before recrystallisation, meaning they must be soluble in some solvents. The reaction conditions for similar compounds were examined to see how the crystals were grown, for further

insight into potential solvents. An investigation by Gale and coworkers of 3,4-bis((3,5-bis(trifluoromethyl)phenyl)amino)cyclobut-3-ene-1,2-dithione gave crystal formation from concentrated DMSO, but it was shown that the thiosquaramide co-crystallised with the solvent due to its carbonyl [159]. This led to abandonment of the thiazolium salt incorporating squaramide, as any co-crystallisation with DMSO would blocking the squaramide's use as a hydrogen-bonding catalyst.

Although the aromatic ring is important in being able to influence the hydrogen bond strength, and is incorporated in most catalytic examples, variation of this to improve solubility was briefly investigated. *n*-Butylamine was used in place of the 4-trifluoromethylaniline in generation of the half squaramide. However, as this amine is more nucleophilic than the aniline, the reaction occurred very quickly and led to the di-*n*-butyl squaramide as the major product, even when reactions were cooled to below 0°C.

Variation of the Chiral Scaffold

Variation of the chiral moiety of the squaramide catalyst may lead to a more soluble product. By using (*1R,2R*)-(+)-1,2-diphenyl-1,2-ethanediamine (DPEN) for the backbone, the added steric bulk may be enough to discourage intermolecular hydrogen bonding by providing more hindrance in between the molecules. Reaction of DPEN (***1R,2R***)-144 with the half-squaramide **139** gave the desired compound (***1R,2R***)-145 in 69% yield (Fig. 3.26). However, this again was insoluble in AcOH for triazolium salt formation, and DMSO for thiazolium salt formation. As variations of the solvents, chiral scaffold, synthetic routes and soluble groups had all been investigated to no avail, efforts were focused elsewhere and squaramides were no longer investigated as hydrogen bonding groups for these organocatalysts at this time.

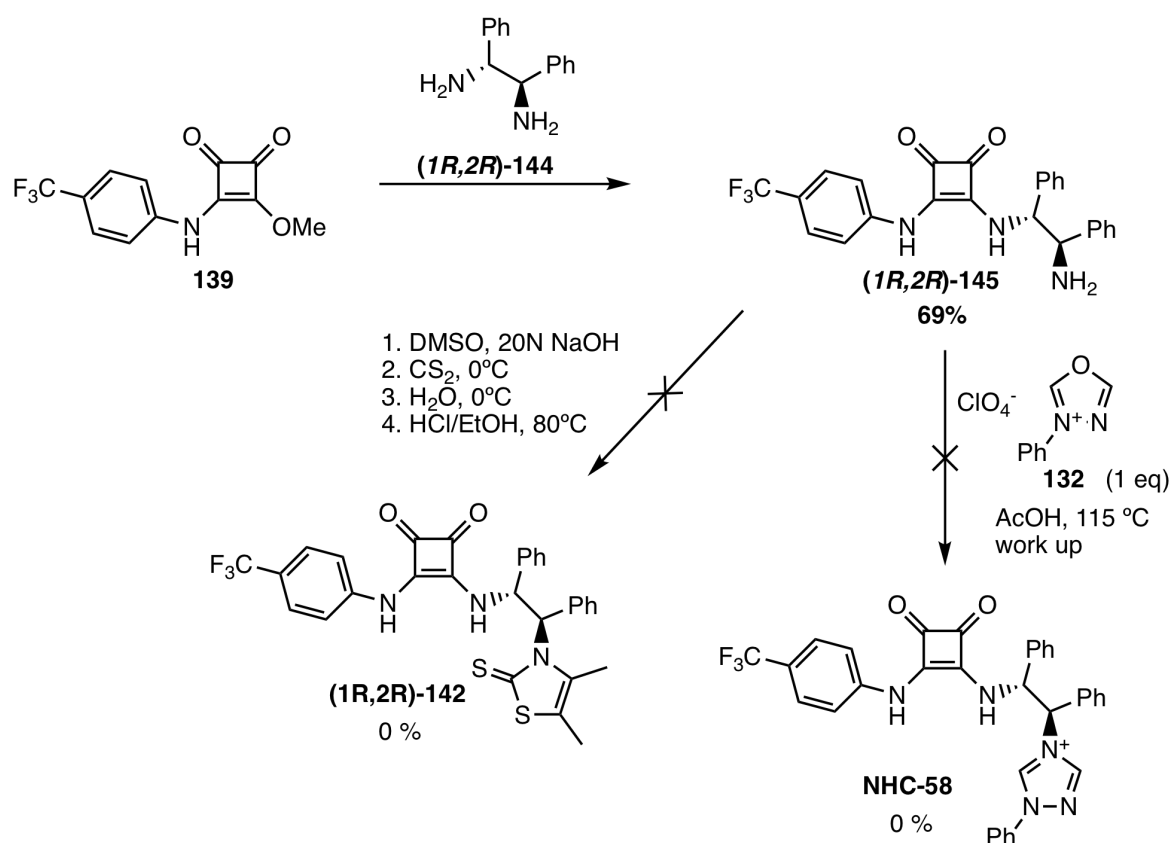


Fig. 3.26 Attempted synthesis of triazolium and thiazolium catalysts incorporating the (1*R*,2*R*)-DPEN backbone.

3.3 Catalyst Testing

3.3.1 The Stetter Reaction

As discussed in Chapter 2, the irreversibility of the Stetter reaction provides a good starting point for initial investigation of the catalytic ability. Although triazolium and thiazolium salts are already known as effective catalysts in the Stetter reaction, it is unknown whether the inclusion of hydrogen bonding moieties will have a detrimental effect on the catalyst, for example inhibiting the base. All of the synthesised catalysts in this chapter were subjected to the Stetter reaction conditions and the results are shown in Table 3.2.

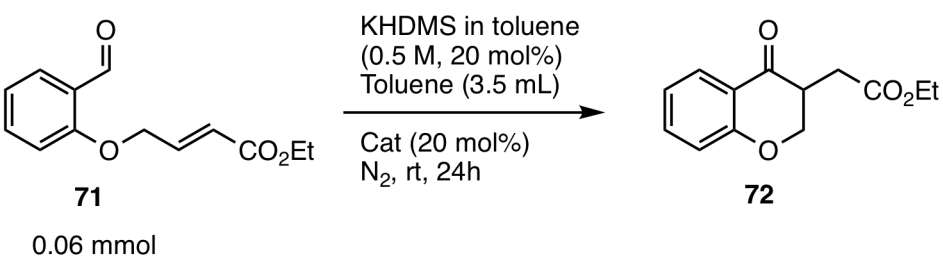
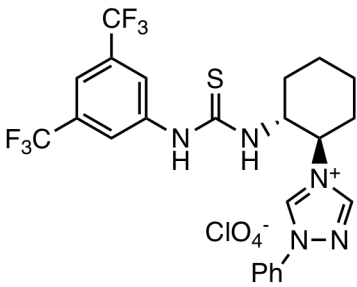
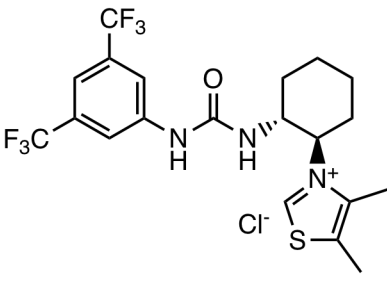
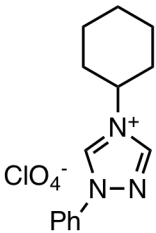
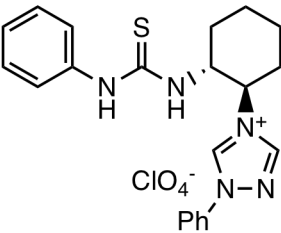
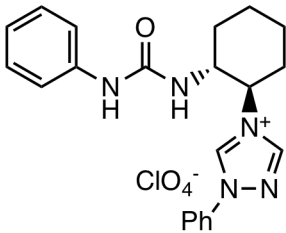
All of the catalysts tested were effective in the Stetter reaction. **NHC-51** (Entry 3) has been used in previous studies [76]. As can be seen, **(1*R*,2*R*)-NHC-48** (Entry 1) performed the best under these conditions. None of the catalysts performed extremely well, although some product was synthesised with every catalyst, showing that the (thio)ureas do not cause enough unfavourable interactions to completely inhibit the reaction. There was also reasonable amounts of enantioselectivity induced in these cases, with the thiazolium salt **(1*R*,2*R*)-NHC-50-Cl** showing the highest enantioselectivity (54%). As discussed in Chapter 2, it is unlikely that this would be due to attractive hydrogen bonding forces, so it seems the catalysts have a reasonable amount of steric bulk to allow for influence of stereoselectivity. Encouraged by these results, all of the catalysts were tested in the benzoin reaction using the previously optimised conditions.

3.3.2 The Benzoin Condensation

All of the catalysts were subjected to the same conditions optimised in Chapter 2. The results are collected in Table 3.3.

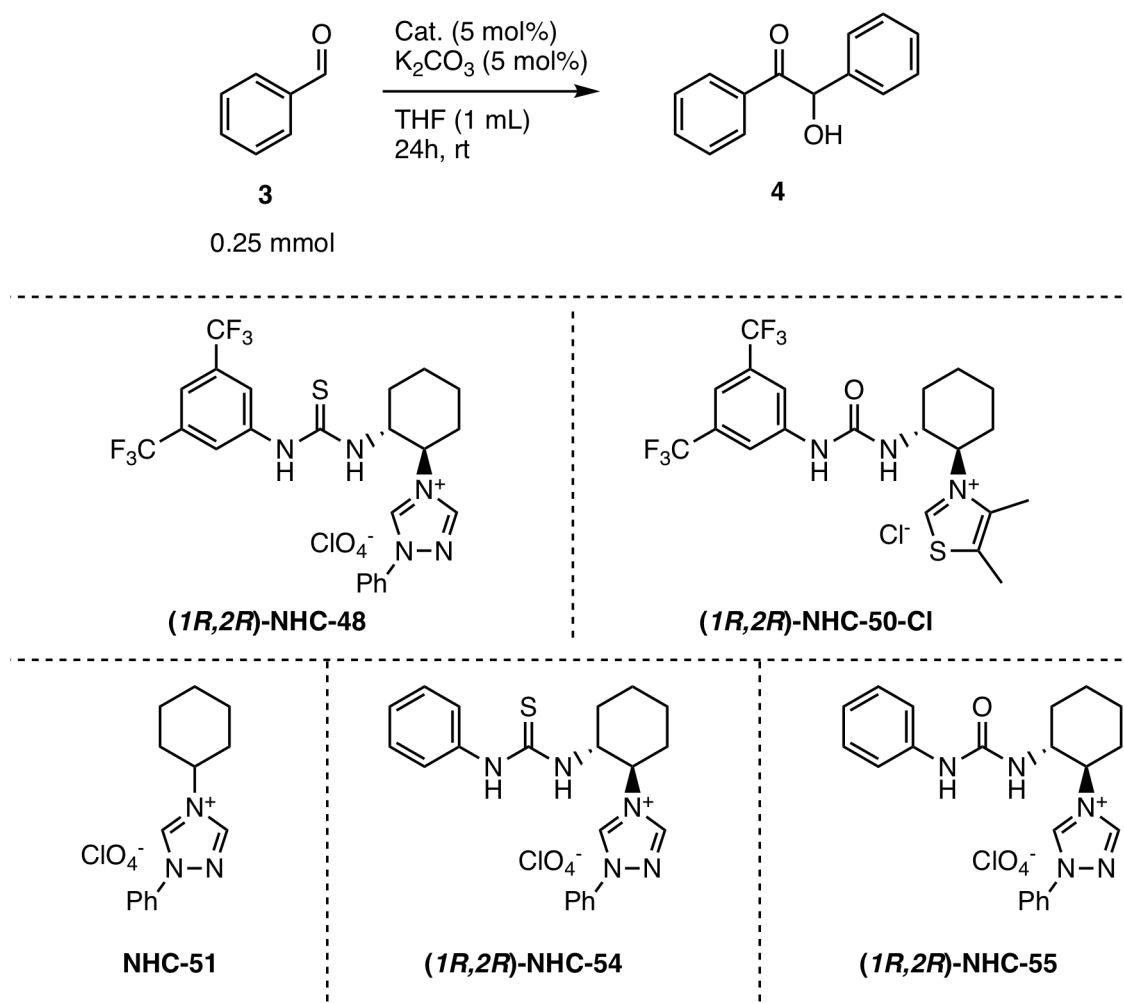
None of the catalysts achieved high yields in this reaction. Although **(1*R*,2*R*)-NHC-54** did demonstrate some enantioselectivity in this reaction with 37% ee (Entry 4), this does not come particularly close to any of the existing literature values reported in Chapter 1

Table 3.2 Triazolium catalysts in the intramolecular Stetter reaction.

 <p>71</p> <p>0.06 mmol</p> <p>72</p>			
 <p>(1<i>R</i>,2<i>R</i>)-NHC-48</p>		 <p>(1<i>R</i>,2<i>R</i>)-NHC-50-Cl</p>	
 <p>NHC-51</p>		 <p>(1<i>R</i>,2<i>R</i>)-NHC-54</p>	
		 <p>(1<i>R</i>,2<i>R</i>)-NHC-55</p>	
Entry	Catalyst	Yield ^a (%)	ee ^b (%)
1	(1<i>R</i>,2<i>R</i>)-NHC-48	42.1	49
2	(1<i>R</i>,2<i>R</i>)-NHC-50-Cl	27	54 ^c
3	NHC-51	16	0
4	(1<i>R</i>,2<i>R</i>)-NHC-54	11	37
5	(1<i>R</i>,2<i>R</i>)-NHC-55	5	-

^aMeasured by NMR. ^bMeasured by chiral HPLC. ^cOpposite enantiomer.

Table 3.3 Triazolium catalysts in the benzoin condensation.



Entry	Catalyst	Yield ^a (%)	ee ^b (%)
1	(1<i>R</i>,2<i>R</i>)-NHC-48	0	-
2	(1<i>R</i>,2<i>R</i>)-NHC-50-Cl	trace	-
3	NHC-51	trace	-
4	(1<i>R</i>,2<i>R</i>)-NHC-54	5	43.6
5	(1<i>R</i>,2<i>R</i>)-NHC-55	1	-

^aMeasured by NMR. ^bMeasured by chiral HPLC.

for this reaction. Upon examining the ^1H NMR spectrum of the crude reaction mixture of **(1*R*,2*R*)-NHC-54**, it was noted that a small amount of a doublet had appeared in the aromatic region at 6.60ppm. Studies on the reaction mechanism kinetics by White and Leeper had indicated this may be explained by the presence of an intermediate [160]. This occurs from the *ortho*-protons of the benzaldehyde ring after the initial adduct has been formed between the carbene and benzaldehyde (before the Breslow intermediate has been formed). However, this was not formally characterised or confirmed. With this in mind, this structure was investigated using the computational methods described in Chapter 2. After randomly sampling conformers, 200 were generated, and all of these underwent energy minimisation. The lowest energy conformer out of these can be seen in Figure 3.27. Interestingly, one of the N-H bonds is in close proximity to the O⁻, at a measured distance of 2.49 Å. It is conceivable that this interaction is playing a part in the reaction; if this intermediate is being stabilised, it may be energetically unfavourable to deprotonate the intermediate to form the Breslow intermediate, therefore stalling the reaction. Further investigation of this would be interesting and may provide some more insight into the system, but is beyond the scope of available resources.

3.4 Conclusions

Four new triazolium salt catalysts, and one new thiazolium salt catalyst, were synthesised. Although the final step to form the triazolium salts do not proceed with high yield, the chiral starting material is commercially available, and can be obtained from the *trans*-diamine-mixture *via* chiral resolution to reduce the costs further. The synthetic routes are simple and proceed in three steps overall, meaning that these are time efficient to make. Customisation of the catalysts in earlier steps is tolerated, meaning different analogues can be synthesised quickly and easily.

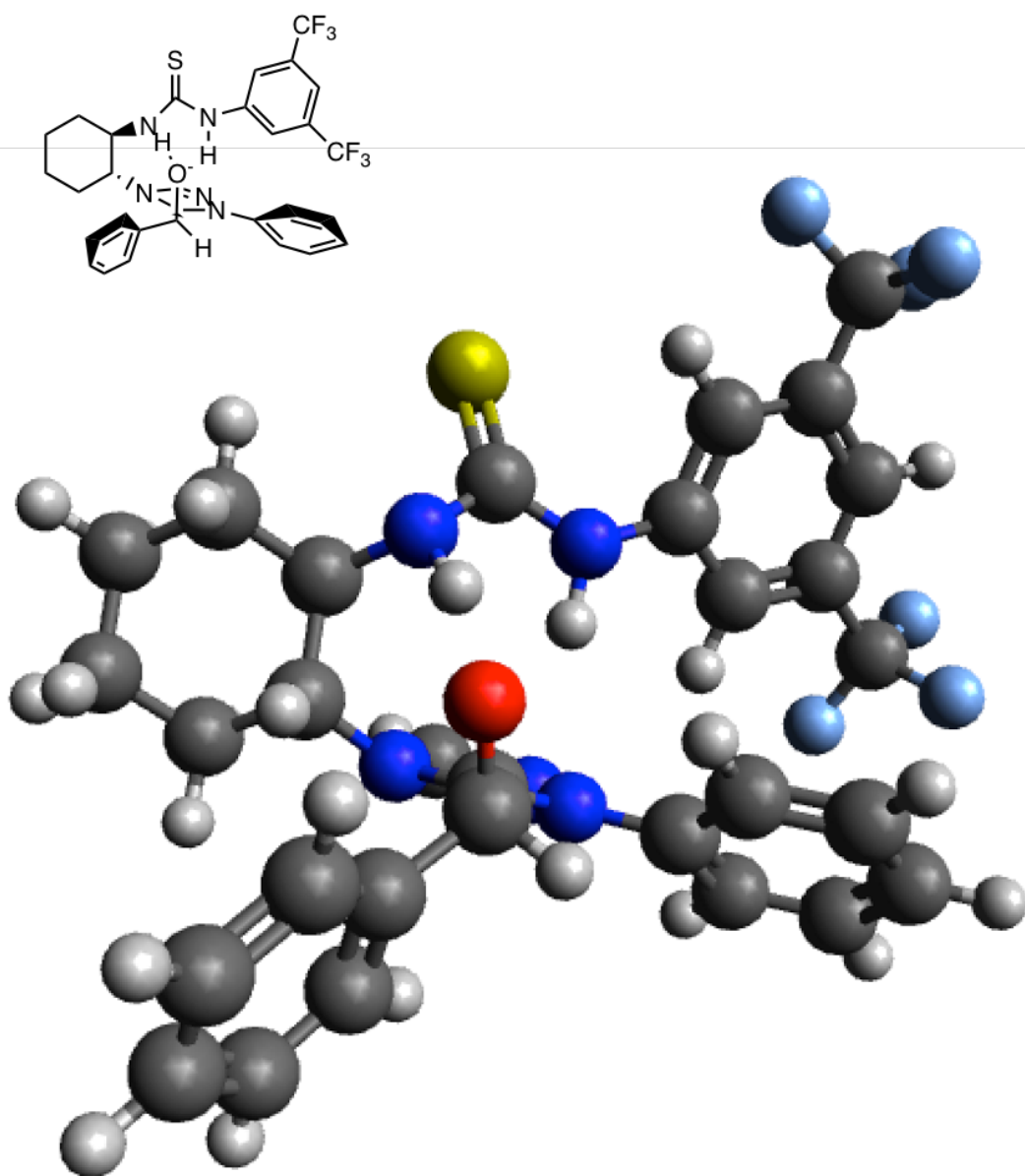


Fig. 3.27 Local minima of the 1,2-diamine-derived thiourea triazolium salt catalyst after initial addition into benzaldehyde. Calculated energy = 566.5 kJ mol⁻¹. Measured bond distance between the H of N-H and O⁻ = 2.49 Å.

Investigation of a squaramide scaffold demonstrated that the intermediates are highly insoluble due to intermolecular H-bonding. Various routes to overcome this were unsuccessful, and while squaramides remain an interesting, under-utilised moiety in hydrogen bonding directed organocatalysis, the difficulty in synthesis of the final desired catalysts meant that efforts were instead focused on the (thio)urea scaffold.

None of the synthesised catalysts performed as highly as previous reports for the benzoin condensation or the Stetter reaction. One plausible explanation for this is due to intramolecular hydrogen bonding once the initial addition of the carbene into the carbonyl has occurred. Further studies including NMR investigations may help to confirm this. There are other factors which can influence a reaction and have an effect on rate, yield and ee, *e.g.* solvents and bases. Therefore it is possible that further optimisation of the reaction conditions may improve the ability of these triazolium salt catalysts, but their inherent structural problems due to the proximity of the (thio)urea to the active carbene centre mean that other strategies will need to be investigated to develop a highly successful enantioselective triazolium salt organocatalyst.

Chapter 4

1,4-Diamine-Derived Catalysts

4.1 Introduction

Due to their relative steric bulk and versatility, organocatalysts incorporating cyclohexyl scaffolds have been employed in many areas of asymmetric synthesis, some of which (such as Takemoto and coworkers [42]) are discussed in Chapter 1. However, with the 1,2-diaminocyclohexyl (thio)urea salts designed in Chapter 3, the 1,2-positioning of the two amino groups meant that their synthesis was challenging, with the most common side product being either double-substitution of functional groups such as (thio)urea and Boc, or intra-molecular reactions forming bicyclic molecules. Modification of this scaffold could alleviate some of these problems, for example by adding an extra methylene linker between the cyclohexyl core and the amines. 1,4-Diamines of this type have been used as ligands in platinum complexes for cytotoxic studies [161], but have had no reported application in organocatalysis to date.

The extra distance between the (thio)urea and active carbene centre, in combination with increased free rotation, may reduce the possibility of any intra-molecular H-bonding as thought with the 1,2-diamine-derived catalysts. If this is the case, the reaction may proceed further and obtain an increased yield than those catalysts. In addition, if the (thio)urea is

not bonding in an intramolecular manner in the initial adduct, it is available to potentially hydrogen bond to a second molecule of benzaldehyde, increasing the ee.

((1*R*,2*R*)-cyclohexane-1,2-diyl)dimethanamine **151** is not commercially available, but has been previously synthesised by Gay *et al.* using (1*R*,2*R*)-cyclohexane-1,2-dicarboxylic acid **146** as the starting material [161] (Fig. 4.1). The material is only available as a racemic mixture of the *trans*-enantiomers, and so chiral resolution must be performed first to obtain the optically pure (1*R*,2*R*) enantiomer. However, the racemic material was used whilst optimising the synthetic route.

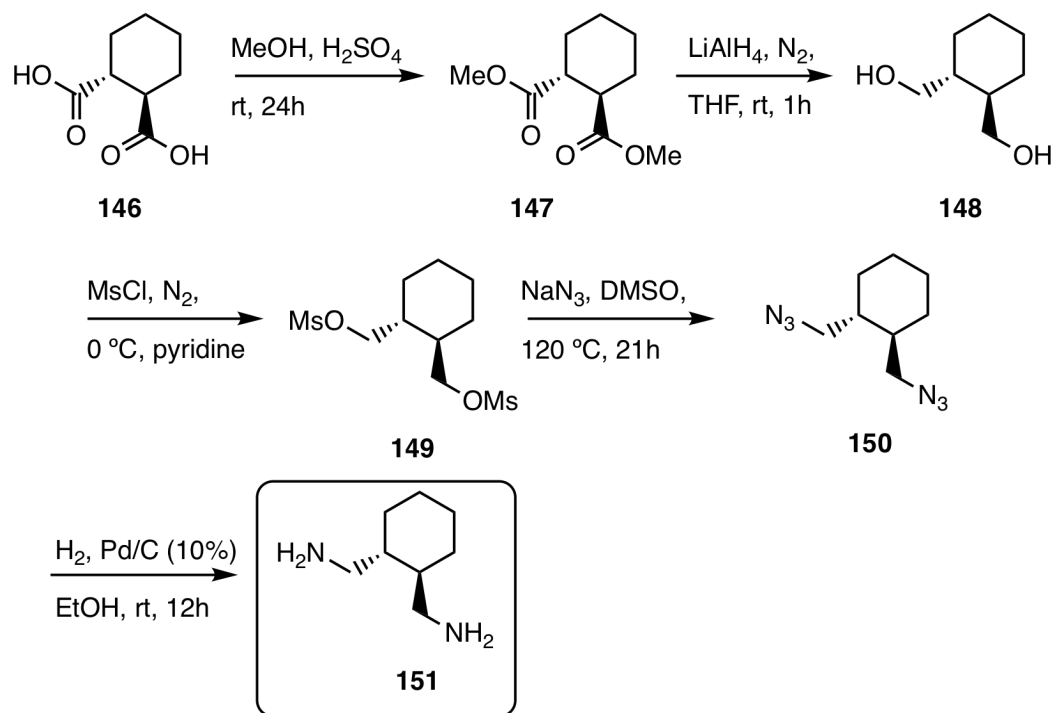


Fig. 4.1 The original route devised by Gay *et al.* to synthesise the diamine [161].

4.2 Synthesis of the Catalysts

4.2.1 Synthesis of ((*1R,2R*)-Cyclohexane-1,2-diyl)dimethanamine

In the route devised by Gay *et al.*, the dicarboxylic acid (\pm)-**146** was converted to the diamine using a series of functional group transformations, beginning with esterification, allowing reduction to the diol. This was turned into a good leaving group to allow nucleophilic substitution by sodium azide. The diazide was then converted into the diamine in one step.

Using this synthetic route as a starting point, several modifications were made here for ease of synthesis. The initial ester was synthesised by converting the di-carboxylic acid into the di-acid chloride. Stirring the acid (\pm)-**146** in methanol at room temperature with dropwise addition of thionyl chloride gave the dimethyl ester product (\pm)-**147** in 100% yield. However, reduction of the ester to the alcohol (\pm)-**148** using LiAlH_4 only gave the diol product in 24%, due to the coagulation of the aluminium salts hindering the purification process.

An alternative method of synthesising alcohols from carboxylic acids is by the use of borane. The method is gentle and one-step, using $\text{BH}_3\cdot\text{Me}_2\text{S}$ as the reagent. A mechanism for this reduction was proposed by Rzepa [162] is shown below (Fig. 4.2). Addition of the carboxylic acid to the borane forms an adduct from insertion into the borane empty p-orbital, giving irreversible evolution of H_2 gas. The process is repeated to give the borane ether product, and quenching by dropwise addition of H_2O releases the desired diol (\pm)-**148**. The reaction has fairly reproducible results, giving yields up to 67%. ^{11}B NMR was run on the product to ensure there was no remaining co-ordination of the borane on the alcohol.

Initially, a methanesulfonyl (mesyl) protecting group was used to protect the diol, as per the route proposed by Gay *et al.* previously. Here, the product (\pm)-**149** was synthesised by stirring the diol (\pm)-**148** in CH_2Cl_2 with NEt_3 . Addition of mesyl chloride at -10°C led to the product (\pm)-**149** in only 28% yield. Furthermore, none of the desired diazide product (\pm)-**150** was obtained when reacted with sodium azide. This may be due to the sensitivity of the mesyl activating group; traces of water can destroy the group, forming

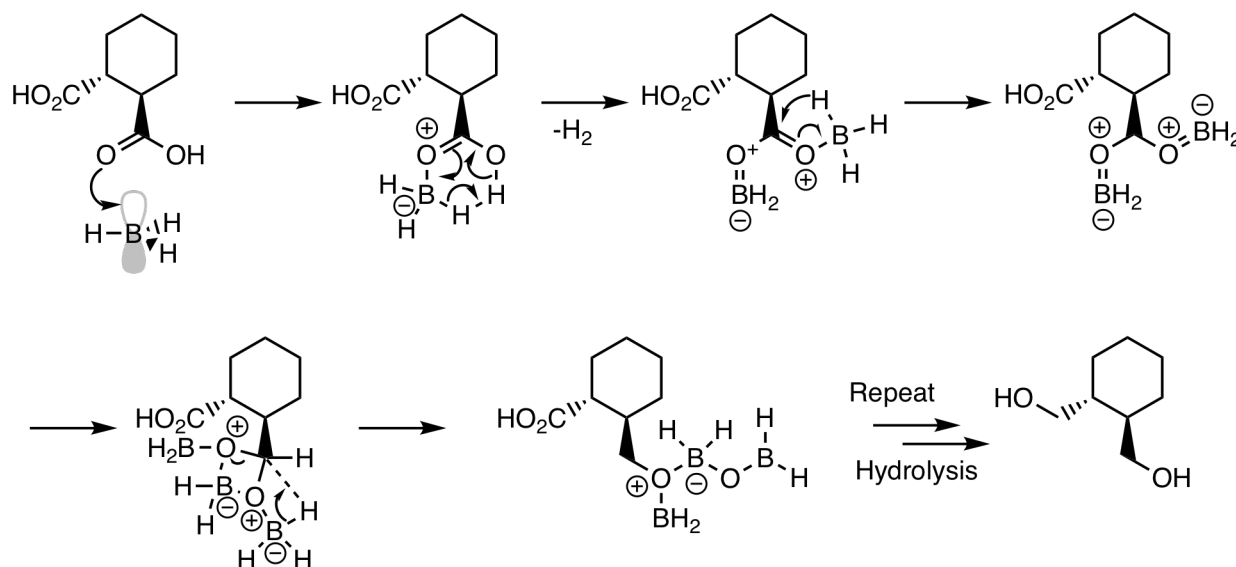


Fig. 4.2 Reduction of carboxylic acid to alcohol using BH_3 , the mechanism proposed by Rzepa [162].

by-products unreactive to the diazide. The tosylate protecting group was investigated as an alternative, as it is tolerant to moisture. The diol (\pm)-**148** was stirred in CH_2Cl_2 with tosyl chloride, 4-dimethylaminopyridine (DMAP) and NEt_3 with yields of (\pm)-**152** up to 87% being obtained. Heating this product with sodium azide in DMF at 55°C afforded the diazide (\pm)-**150** up to 69% yield, and was repeated successfully over 5 times on a similar scale. (Note that in Chapter 8, the route to (*1R,2R*)-**150** is reported, which has yields varying slightly from these.)

For reduction of the diazide to the diamine (\pm)-**151**, Gay opted for hydrogenation using 10% Pd/C [161]. However, attempting the method in this work was not straightforward. The reaction was attempted twice, and each time led to a mixture of products. The conversion of the diazide to the diamine product was monitored by ^1H NMR, by comparing the protons attached to the methylene carbons in these two compounds (both in CDCl_3 : 4H, 3.34 ppm for diazide **150** compared to 2H, 2.80 2H, 2.58 ppm for diamine (\pm)-**151**). One of the products formed in the mixture was the desired diamine (\pm)-**151**, but separation was difficult due to the basicity of the product. The lack of chromophore and low molecular weight meant that LC/MS was not useful to characterise the by-product, and IR spectroscopy did not offer any

insight, so reduction using LiAlH_4 was attempted. Again this led to a crude mix of products which could not be separated.

The hydrogenation was attempted for a final time using a reduced quantity of 10% Pd/C (10% w/w). This reaction worked much more cleanly, giving the product (\pm)-**151** in 79% yield, and about 90% purity. As previously discussed, purification of the diamine is difficult by silica gel chromatography, so the material was used crude at this stage. The full optimised synthesis of the diamine synthesised in this work is summarised below, giving the final diamine backbone in a 32% yield over 4 steps (Fig. 4.3).

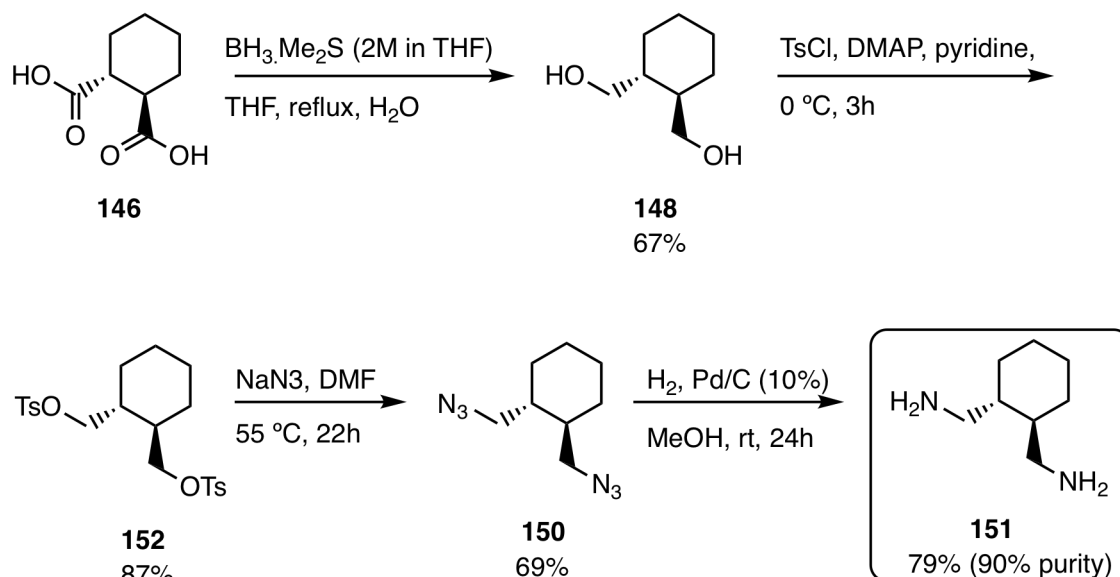


Fig. 4.3 The final optimised synthetic route to ((\pm)-cyclohexane-*trans*-1,2-diyl) dimethanamine synthesised in this work.

4.2.2 Chiral Resolution of the Dicarboxylic Acid

As only the racemic mixture of the (*1R,2R*) and (*1S,2S*)-dicarboxylic acid (\pm)-**146** is commercially available, chirally resolution of the two enantiomers to obtain an enantiomerically pure product is necessary. ((*1R,2R*)-cyclohexane-1,2-diyl)dimethanamine (*1R,2R*)-**151** was chosen over the opposite enantiomer, for direct comparison with the (*1R,2R*)-1,2-diamine catalysts prepared in Chapter 3. The two enantiomers can easily be separated by forming a

salt of the desired enantiomer with (*R*)-methylbenzylamine [163], and recrystallisation from hot EtOH to improve the diastomeric excess (Fig. 4.4). After stirring with 1M HCl and extraction, the desired (*1R,2R*)-enantiomer (**(1*R,2R*)-146**) was obtained in 61% yield.

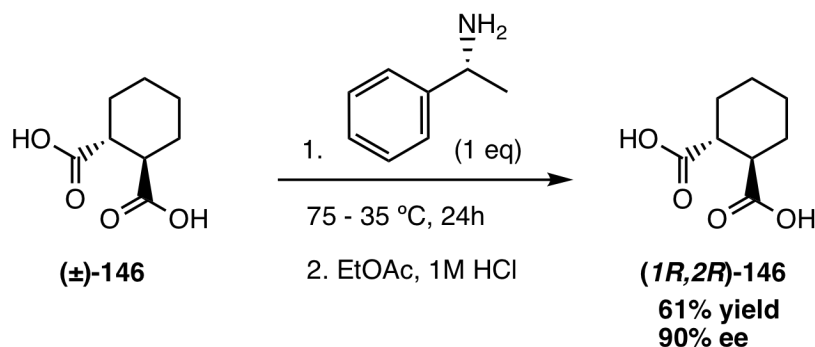


Fig. 4.4 Chiral resolution of (\pm)-*trans*-cyclohexyl-1,2-dicarboxylic acid (**(\pm)-146**) to obtain ((*1R,2R*)-cyclohexane-1,2-diyl)dimethanamine (**(1*R,2R*)-151**) [163].

Determination of the Optical Purity

The chiral purity of the resolved dicarboxylic acid (**(1*R,2R*)-146**) could be determined by chiral HPLC. However, due to the acidic functional group, tailing of the peaks was observed (detection at 210 nm), leading to overlap of the enantiomers. Although modifiers can be added to the solvent to assist with acidic or basic compounds, installation of a chromophore would be beneficial as this would allow determination of the purity at 254 nm. As this wavelength is useful for compounds which exhibit $\pi \rightarrow \pi^*$ transition (aromatic compounds), any remaining traces of starting material or (non-aromatic) impurity will not affect the peaks, leading to a more reliable result. The di-tosylate product (**(\pm)-152**) was synthesised a few steps after the chiral resolution, and would appear to solve both chromophore and acidity issues. This was investigated, and after optimisation satisfactory separation of enantiomers was obtained using chiral HPLC. Comparing the racemic sample with the chirally resolved product, it was determined that the dicarboxylic was obtained in 90% ee (Fig 4.5). After optimising the synthesis above using the racemic dicarboxylic acid, the steps were repeated

using the enantio-enriched dicarboxylic acid. These gave comparable yields and finally ((*1R,2R*)-cyclohexane-1,2-diyl)dimethanamine (**(*1R,2R*)-151**) was obtained.

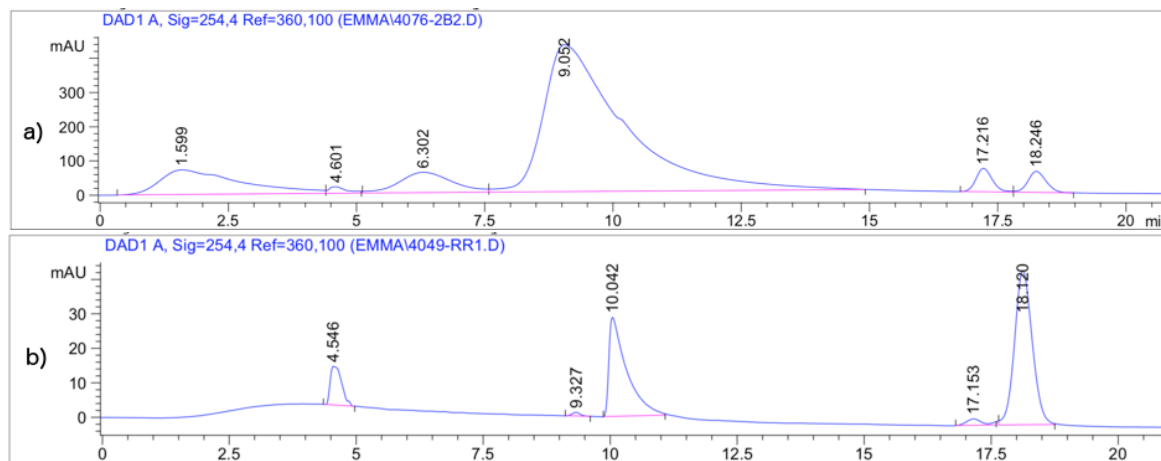


Fig. 4.5 HPLC data confirming both the optical purity of the chirally resolved cyclohexane-1,2-diylbis(methylene) bis(4-methylbenzenesulfonate). Conditions: flow rate 0.6 mL/min, mobile 1% IPA / hexane at 40°C. CSP is Astec Cellulose DMP. Measured at 254nm. (a) Chiral HPLC separation of (±)-*trans*-cyclohexane-1,2-diylbis(methylene) bis(4-methylbenzenesulfonate) showing two enantiomers, at 17.2 min and 18.1 min. (b) Chiral HPLC separation of chirally resolved (*1R,2R*)-cyclohexane-1,2-diylbis(methylene) bis(4-methylbenzenesulfonate), showing formation of the (*1R,2R*)-product in 90% ee as reported in the literature.

4.2.3 Synthesis of the Final Catalyst

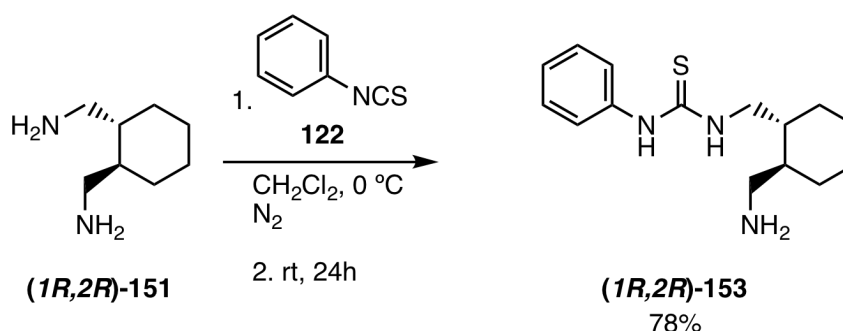


Fig. 4.6 Synthesis of (*1R,2R*)-154.

As discussed previously, (*1R,2R*)-cyclohexane-1,2-diamine (**(*1R,2R*)-107**) was optimised to form (thio)ureas in a reasonable yield. This method was taken as a starting point to form the

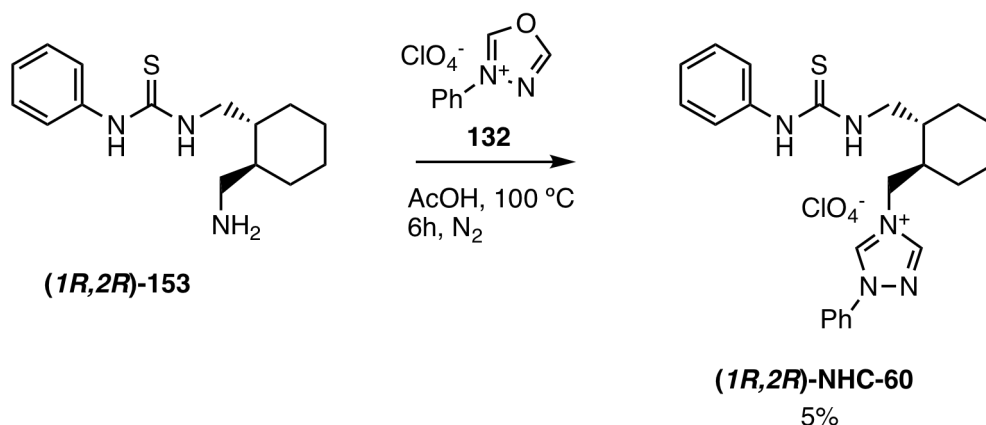


Fig. 4.7 Synthesis of the final catalyst, (1*R*,2*R*)-NHC-60.

(thio)urea using ((±)-cyclohexane-*trans*-1,2-diyl)dimethanamine (1*R*,2*R*)-151. As the phenyl thiourea analogue gave a higher yield of the 1,2-diamine catalyst, this was used in place of the 3,5-bis(trifluoromethyl)phenyl analogue (Fig. 4.6). A crude synthesis was attempted on a small scale using the mixture of the *trans*-enantiomers with phenyl isothiocyanate 122, and analysed by LC/MS; peaks at *m/z* 412 and 277 were detected, which were thought to correspond to the *bis*- and *mono*- thiourea products respectively. Spurred on by this, the reaction was repeated using the enantioenriched (ee = 90%) diamine, and purified to obtain the product (1*R*,2*R*)-153. The *bis*- by-product was not isolated and purified, but the desired *mono*- thiourea was obtained in 78% yield.

The oxadiazolium salt 132 was synthesised in the same manner as previously, and reacted with 1-(((1*R*,2*R*)-2-(aminomethyl)cyclohexyl)methyl)-3-phenylthiourea (1*R*,2*R*)-154 (Fig. 4.6). Unlike the 1,2-diamine thiourea, the reaction to form the 1,2,4-triazolium salt (1*R*,2*R*)-NHC-60 did not give any degradation into a by-product, meaning this final step was more efficient, and the reaction could be left on for extended periods of time. Once the reaction had stalled and no further product was being formed, the reaction was worked up. However, when the reaction mixture was washed with 5M HCl to remove excess primary amine as per the synthesis of the triazolium salts in Chapter 3, the final catalyst was detected by TLC in both the organic layer and the aqueous layer. Due to this, the material was purified by column chromatography instead (10% MeOH/CH₂Cl₂). The product co-eluted with one of

the impurities, which could not be separated, despite optimisation with different solvents. Eventually, the material was purified by column chromatography three times sequentially to get the final product clean enough for use. However, due to the low quantity (18 mg, 5% yield), no clean ^{13}C NMR could be obtained and the catalyst was characterised using other methods (see Chapter 8 and Appendix 1).

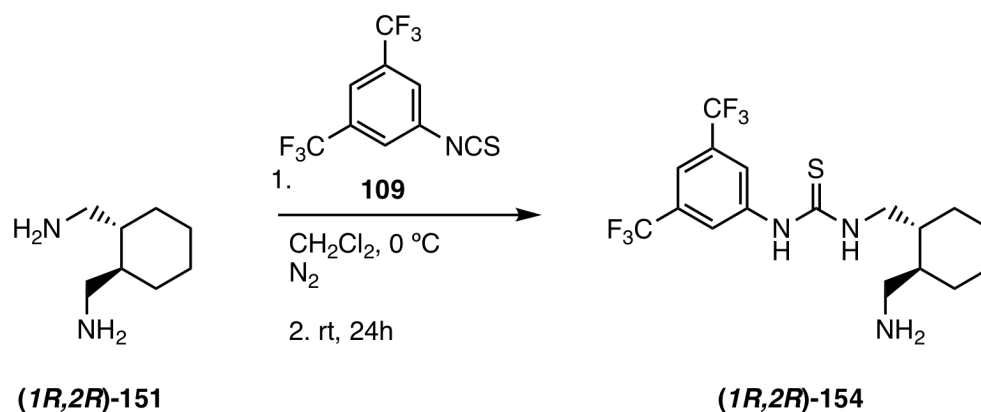


Fig. 4.8 Synthesis of (1R,2R)-154.

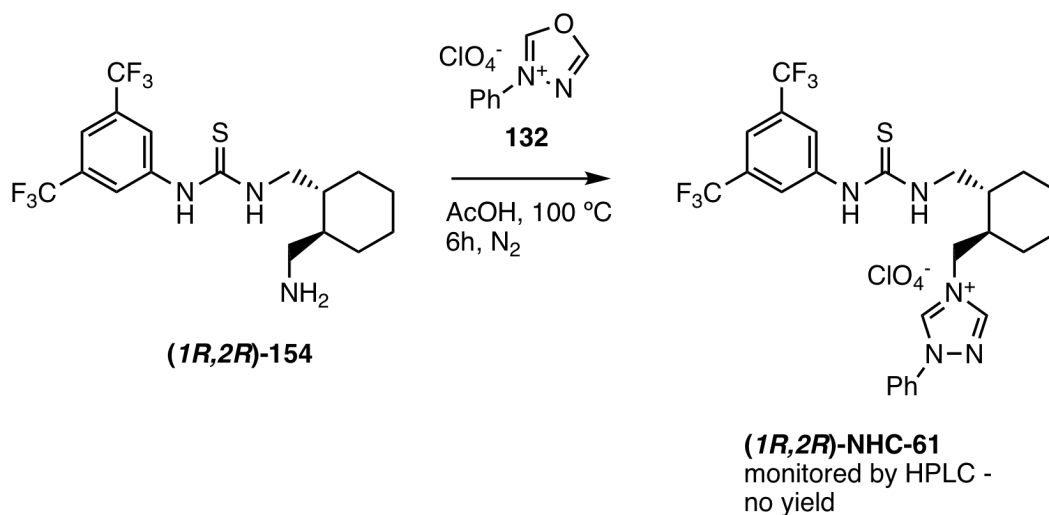


Fig. 4.9 Synthesis of the final catalyst, (1R,2R)-NHC-61. This was performed on a small scale and only monitored by LCMS, rather than isolating and characterising the product.

As a small amount of the 1,4-diamine remained, the reaction using 3,5-bis(trifluoromethyl)phenyl isothiocyanate **109** was attempted (Fig. 4.8). Not enough of (1R,2R)-154 was obtained to get a full characterisation, but a material which matched by exact mass and ^1H

NMR was obtained. was taken through to the final catalyst as per the route above, and monitored by LC/MS (Fig. 4.7). Interestingly, a mass for an unknown intermediate was initially formed and could be detected by LC/MS. The progress of the reaction could be monitored by loss of this peak, and formation of a new peak corresponding to the product mass; after the initial peak was lost, no more product was formed, despite both starting materials remaining. Although the intermediate was not isolated, previous reactions to form the triazolium salt from primary amines gave an uncyclised intermediate, and so structure (*1R,2R*)-**155** was proposed (Fig 4.10).

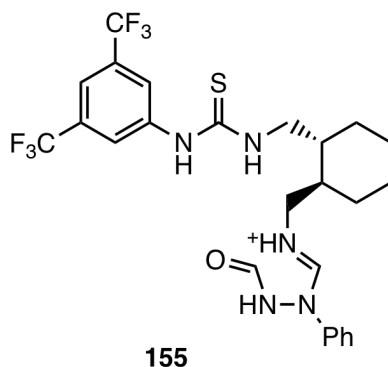


Fig. 4.10 Proposed intermediate formed before the cyclisation to final product. $m/z = 560$.

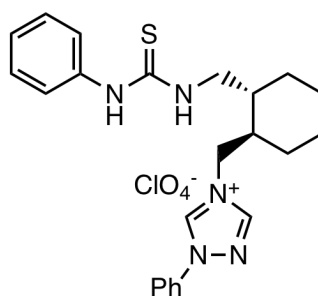
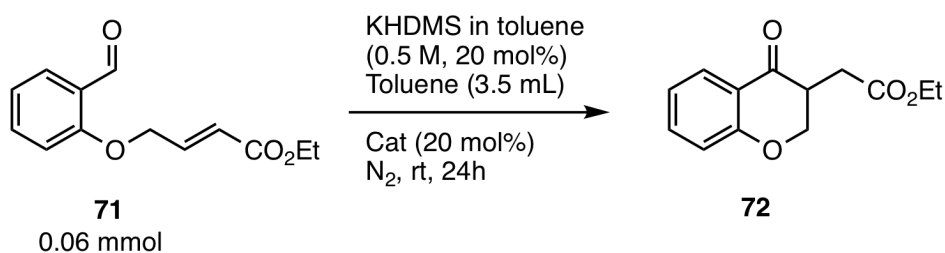
Although not enough of catalyst (*1R,2R*)-NHC-**61** was made for a full characterisation or for testing, this test demonstrates the possibility of different analogues being formed if the phenyl-substituted catalyst proves to be effective enough to warrant continued investigations.

4.3 Catalyst Testing

4.3.1 The Stetter Reaction

The catalyst (*1R,2R*)-NHC-**60** was tested in the conditions for the Stetter reaction discussed in Chapter 2 (Table 4.1). After 24h, the yield as determined by ^1H NMR as only 4%. Due to this, the ee could not be determined, as the small amount of product would not be detected accurately on the HPLC. Although unsuccessful for the Stetter reaction, the catalyst was

Table 4.1 Triazolium catalysts in the intramolecular Stetter reaction.

**(1*R*,2*R*)-NHC-60**

Entry	Catalyst	Yield ^a (%)	ee ^b (%)
1	(1<i>R</i>,2<i>R</i>)-NHC-60	4	-

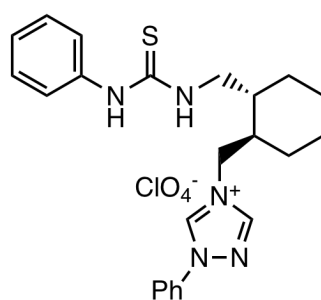
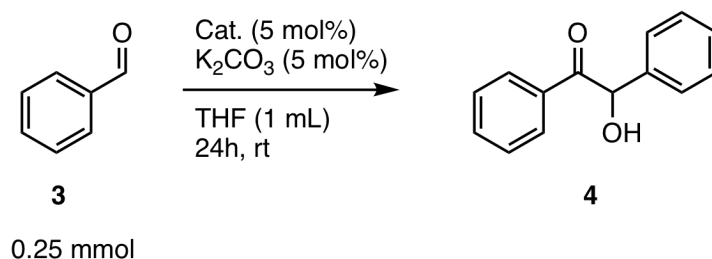
^aMeasured by NMR. ^bMeasured by chiral HPLC. ^cOpposite enantiomer.

trialled in the benzoin condensation regardless, as other factors may have influenced this low yield. For example, the Breslow intermediate formed from initial addition into the aldehyde may be too sterically bulky to allow the cyclisation reaction to occur, in comparison with the smaller benzaldehyde.

4.3.2 The Benzoin Condensation

As per Chapter 2, the catalyst **(1*R*,2*R*)-NHC-60** was tested using K_2CO_3 . The catalyst only achieved 5% yield (Table 4.2). Due to the low yield, the ee could not be accurately determined using HPLC, so how well this performs as a chiral catalyst is still unknown. There are several factors which could be attributed to the low yield here. Firstly, because the

Table 4.2 Triazolium catalysts in the benzoin condensation.

**(1R,2R)-NHC-60**

Entry	Catalyst	Yield ^a (%)	ee ^b (%)
1	(1R,2R)-NHC-60	5	-

^aMeasured by NMR. ^bMeasured by chiral HPLC.

catalyst isn't completely pure, and the by-product was not characterised, it is possible that this could be inhibiting the reaction. Even a tiny trace of an acidic product could be enough to partially deactivate the catalysts, leading to a low yield. Secondly, although the catalyst has increased flexibility, it is plausible that the two extra methylenes may cause unwanted steric hindrance, blocking the active carbene centre.

4.4 Conclusions

A route was devised for a ((1R,2R)-cyclohexane-1,2-diyl)diamine -derived triazolium salt catalyst **(1R,2R)-NHC-60**, starting with chiral resolution of (±)-*trans*-cyclohexane-1,2-dicarboxylic acid which was obtained in 90% ee. The catalyst was synthesised in 6 steps,

going *via* the C₂ symmetric ((*1R,2R*)-cyclohexane-1,2-diyl)dimethanamine. The phenylthiourea analogue was successfully synthesised in sufficient quantity for catalyst testing, and a trial run of the 3,5-*bis*(trifluoromethyl)phenyl analogue attempted to investigate the tolerance of this catalyst formation. This route also allows for late-stage modification, allowing a range of analogues to potentially be synthesised. The final step led to co-elution of an aromatic impurity, and the purification of this will require optimisation. Testing of this catalyst did not achieve high yields in either the intramolecular Stetter reaction or the benzoin condensation, and due to this no ee could be achieved. Computational studies may help elucidate why this catalyst has given such a low yield, and further modifications similar to those in Chapter 3 can be undertaken to influence the acidity of the (thio)urea in future, such as different aryl groups.

Chapter 5

Phenylalanine-Derived Catalysts

5.1 Introduction

Although much of the discussion in Chapters 1-4 has focused on (thio)urea as the hydrogen-bonding moiety, amides are also viable alternatives, as reported by Connon and coworkers in 2009 [76]. Still featuring an N-H pendant as the hydrogen bonding moiety, there are many methods of forming amides, and so this could be a possible synthetically accessible variation in hydrogen bonding NHC catalysts. Amino acids have been used as organocatalysts in their own right [164, 165], or as building blocks for more complex ligands [166]. Proline is an exceptional organocatalyst, as discussed in Chapter 1, and its derivative L-pyroglutamic acid has also been used for synthesis of NHCs [78]. Therefore, amino acids could be a good starting point for new catalyst synthesis, allowing incorporation of an amide H-bonding moiety. This potential backbone was made the subject of investigation to determine whether these would be a suitable monocyclic scaffold for NHC catalysts.

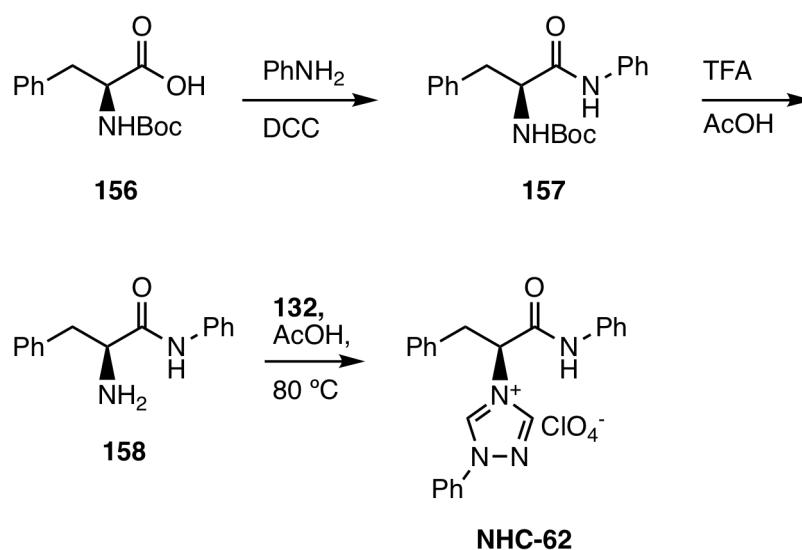


Fig. 5.1 Proposed synthetic route to phenylalanine-derived triazolium salt **NHC-62**. Abbreviations: dicyclohexylcarbodiimide (DCC) trifluoroacetic acid (TFA).

5.2 Synthesis of the Catalysts

5.2.1 Phenylalanine-Derived Synthesis

L-Boc-phenylalanine **156** was chosen as the model amino acid for this catalyst series due to the bulky phenyl group, and there was a large quantity of the starting material available in the lab. The proposed route to the final product **NHC-62** (Fig. 5.1) is synthetically viable in 4 steps from Boc-protected phenylalanine using precedented steps. Initial coupling of the carboxylic acid with an amine such as aniline gives the amide **157**, which after Boc deprotection gives a primary amine **158** which can be reacted with oxadiazolium salt **132** in a similar way to the previous catalysts as per Connon and coworkers' method to give the triazolium salt product **NHC-62** [167]. DCC was used as the coupling agent for formation of the amide **157**, and this step worked well with a yield of 63%. Boc deprotection using TFA afforded quantitative yield of **158**, but slight impurities were detected in the double bond region. These impurities could not be removed by column chromatography, and so the material was taken through crude to the final step. A report by Enyong *et al.* states that (*S*)-2-amino-*N*,3-diphenylpropanamide is unstable in ambient conditions, and therefore

recommends storage either as the CF_3COO^- salt, or in the freezer [168]. The material was used crude in the attempted synthesis of the triazolium salt **NHC-62**. However the reaction was not straightforward and analysis showed a large quantity of by-products which decomposed on silica, and the final catalyst was not obtained.

The route to the corresponding thiazolium salt **NHC-63** was attempted using the material, as per Glorius and coworkers method [156]. However, by-product **159** was the major product obtained (Fig. 5.2). This is most likely due to the 1-2-diamine system allowing for optimal geometry to form a 5-membered ring. Oxidation of the double bond is driven by acidity of the α -proton and stability of conjugation in the ring. The enolate is easily formed on initial cyclisation, and oxidation by air allows for the final by-product formation.

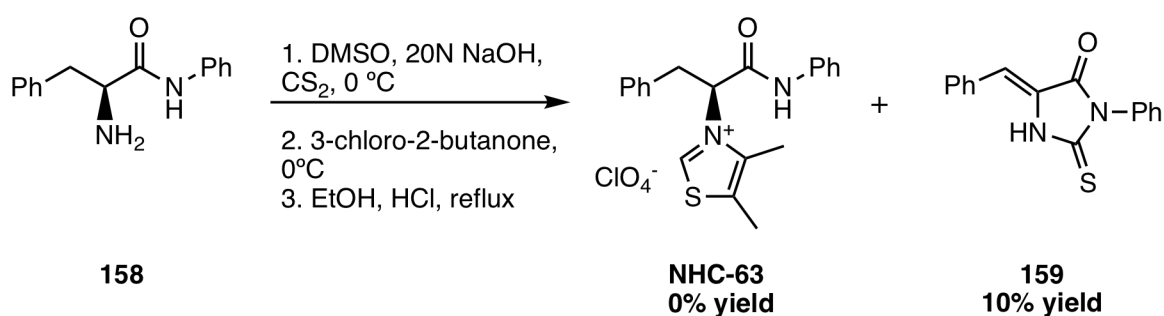


Fig. 5.2 Formation of cyclised, achiral by-product **159** which was obtained instead of **NHC-63**.

Due to these problems, an alternative method to catalyst **NHC-62** was devised (Fig. 5.3). By late stage incorporation of the amide group, the 1,2-diamine would not be formed until after the cyclisation of the triazolium ring, therefore avoiding the problem. The methyl ester **161** would be synthesised to protect the carboxylic acid before cyclisation, with would then be converted to the amide at a later stage.

Esterification of **160** did not go to full conversion. Even after optimisation of the reaction conditions, the maximum yield of **161** obtained was 56%. Reaction with 3-phenyl-1,3,4-oxadiazol-3-ium perchlorate **132** in the usual manner afforded the product **NHC-64**, and due to the anhydrous conditions there was no hydrolysis of the methyl ester, even after being

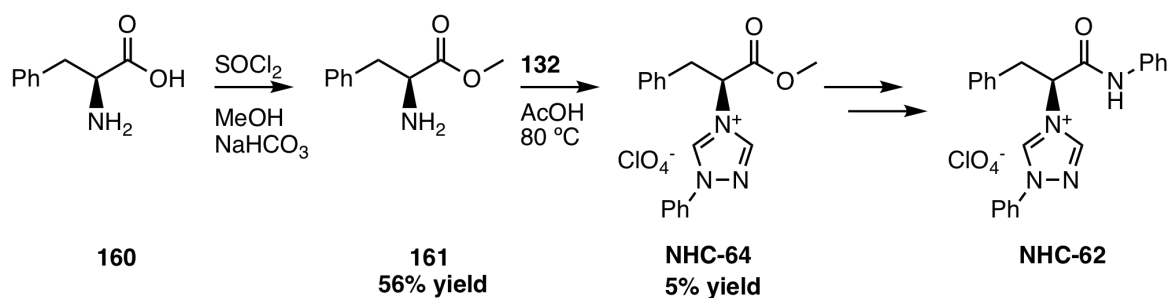


Fig. 5.3 Synthetic route to formation of phenylalanine-derived catalyst **NHC-64** performed in this work.

heated in acetic acid. Although only 2% yield was achieved by precipitation, this was pure and in sufficient quantity to optimise the later step.

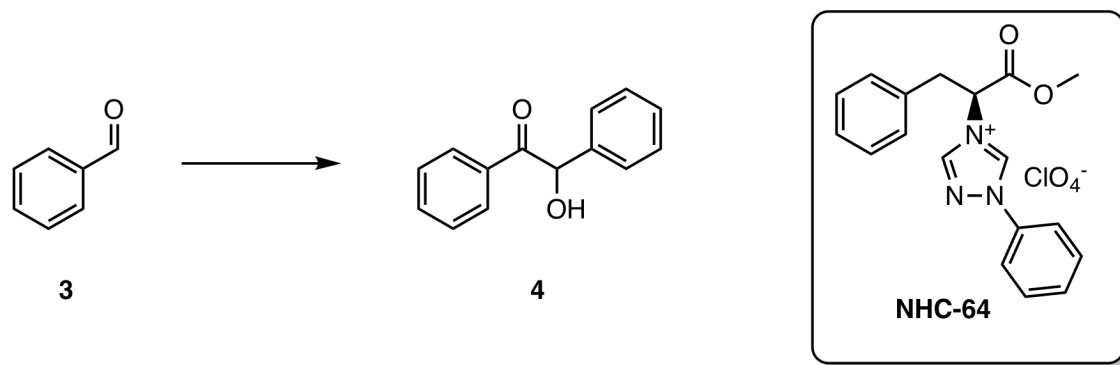
5.3 Catalyst Testing

Although the phenylalanine-derived methyl ester catalyst **NHC-64** does not contain a hydrogen-bonding motif, initial testing of this triazolium salt stage could help to determine how efficient the chiral material is at encouraging ee from sterics alone. However, the conditions tested did not afford any benzoin product **4** (Table 5.1).

^1H NMR analysis showed that there appeared to be several impurities in the reaction mixture. An NMR study was undertaken to determine whether the α -proton was being deprotonated, destroying the chiral centre, as the adjacent ester and triazolium groups in **NHC-64** are electron withdrawing and may stabilise any resulting negative charge formed. The conditions used in Entry 3 were chosen, due to the solubility of the base, and the availability of deuterated methanol to run the reaction in. The solvent was increased to 0.5 mL so it could be measured by ^1H NMR, with 0.1 mL DMSO-d_6 added to aid solubility of the catalyst.

An initial ^1H NMR was run of the catalyst **NHC-64** in this solvent system to have an accurate comparison to later time periods once base had been added. However, there was loss of integration of the α -proton at 5.88 ppm even before adding any base (5.4, (b)), indicating

Table 5.1 Initial substrate testing of the methyl ester phenylalanine-derived catalyst in the benzoin condensation.



Entry ^a	NHC-64 (mol%)	Solvent	Base	Conversion (%) ^b
1	10	CH ₂ Cl ₂	NEt ₃	Trace
2	10	THF	tBuOK	0
3	10	MeOH	NEt ₃	0
4	10	THF	K ₂ CO ₃	0

^aNHC-64 (10 mol%), solvent (0.25 mL), base (100 mol%), N₂, 15 min. PhCHO (0.1 mmol), rt, 24h. ^bMeasured by ¹H NMR.

that there had been deuterium exchange with the solvent. There was still coupling to the adjacent protons as shown by the doublet of doublets in ($J = 6.8, 8.8$ Hz). There was also slight loss of integration of the methyl group, thought to be due to nucleophilic substitution of the deuterated methanol into the ester.

Furthermore the protons at 3.74 ppm and 3.58 ppm (Fig. 5.4 (c)), which should couple to this α -proton, now appear as doublets due to only splitting of each other ($J = 13.9$ Hz), rather than doublet of doublets as expected.

For comparison, the catalyst NHC-64 was run solely in DMSO-d₆ (Fig. 5.5). There was no loss of integration of the crucial proton at 5.86 ppm (b), due to the lack of exchangeable deuterium in the solvent. An overlapping doublet of doublets can be seen ($J = 7.2$ Hz, 8.7 Hz). Finally, the two doublet of doublets expected for the adjacent protons at 3.76 ppm and 3.54 ppm are observed (c), with splittings matching the coupling to the α -proton, and to each other ($J = 14.0$ Hz).

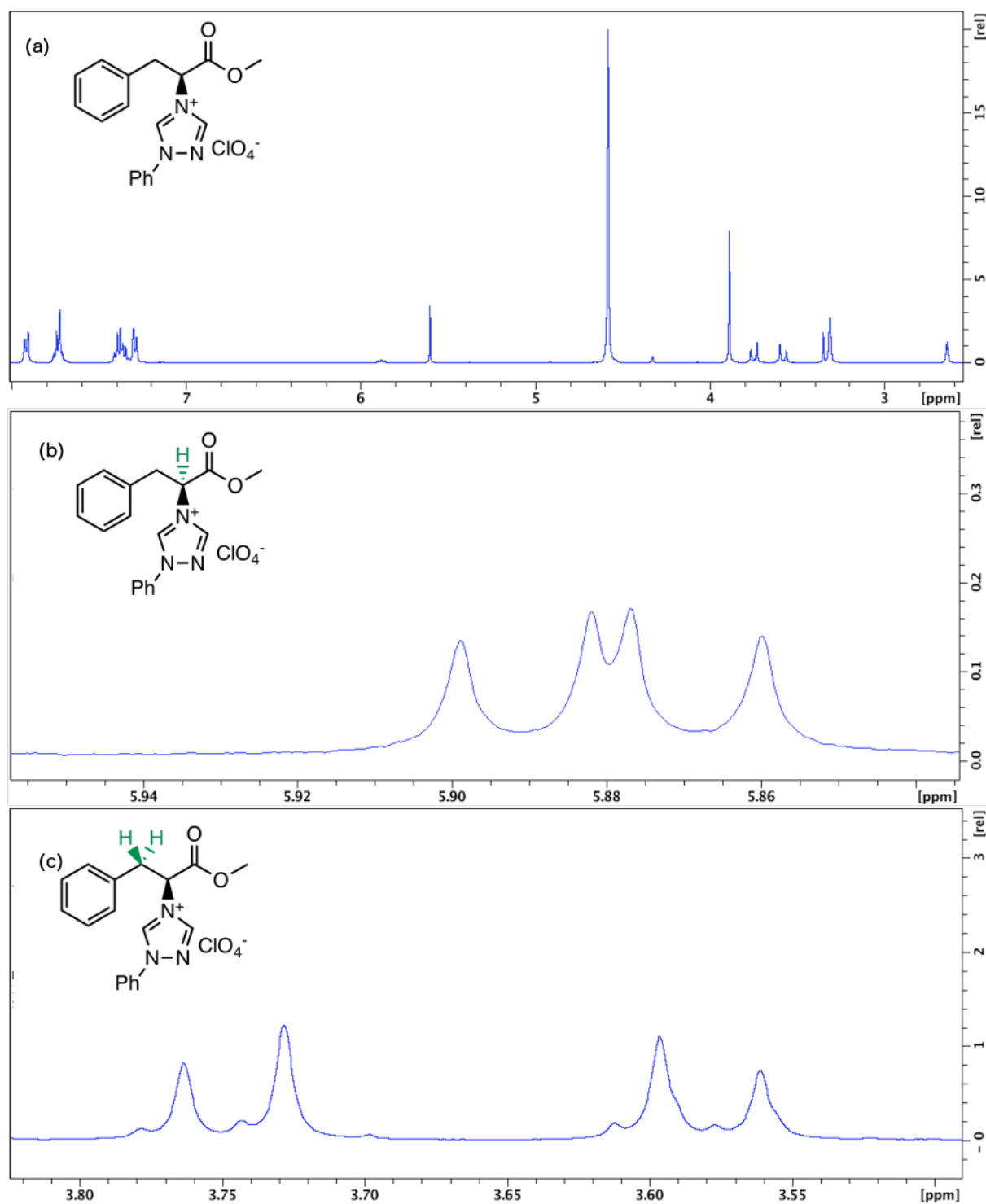


Fig. 5.4 ^1H NMR spectra of the phenylalanine-derived methyl ester catalyst **NHC-64**, with zoom in on the key identifying protons. (a) Full ^1H NMR spectra of the catalyst in $\text{MeOD}/\text{DMSO-d}_6$ (5/1). (b) Close-up of the α -proton. (c) Close-up of the protons adjacent to the α -proton.

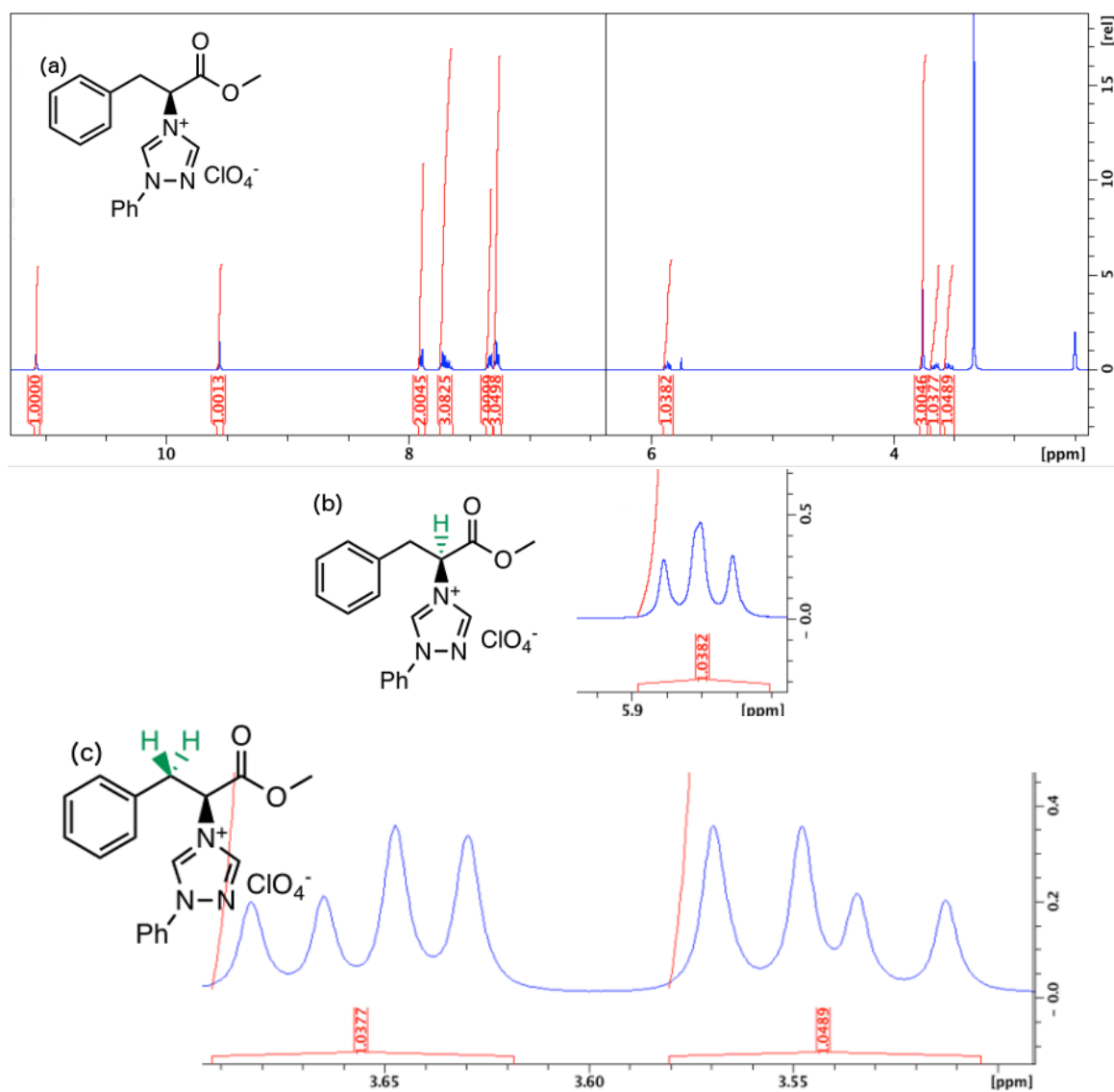


Fig. 5.5 ^1H NMR spectra of the phenylalanine-derived methyl ester catalyst **NHC-64**, with zoom in on the key identifying protons. (a) Full ^1H NMR spectra of the catalyst in DMSO-d_6 . (b) Close-up of the protons adjacent to the α -proton. (c) Close-up of the protons adjacent to the α -proton.

5.4 Alternative Scaffold Investigation

As the problem with catalyst **NHC-64** occurred from having an acidic proton α -to the triazolium ring, an alternative catalyst structure was devised (Fig. 5.6). The bifunctionality of phenylalanine allows for flexible synthetic routes, and utilising the amide instead to form the cyclised triazolium salt, the primary amine can be turned into a hydrogen-bond donor in the form of thiourea. By reversing the functional groups in this way compared to the previous synthesis, and removing the adjacent carbonyl to the α -proton, it is hoped that the proton's acidity will be sufficiently modified to avoid deprotonation. The route proposed is based on steps in catalyst syntheses in Chapter 3, 4 and 6.

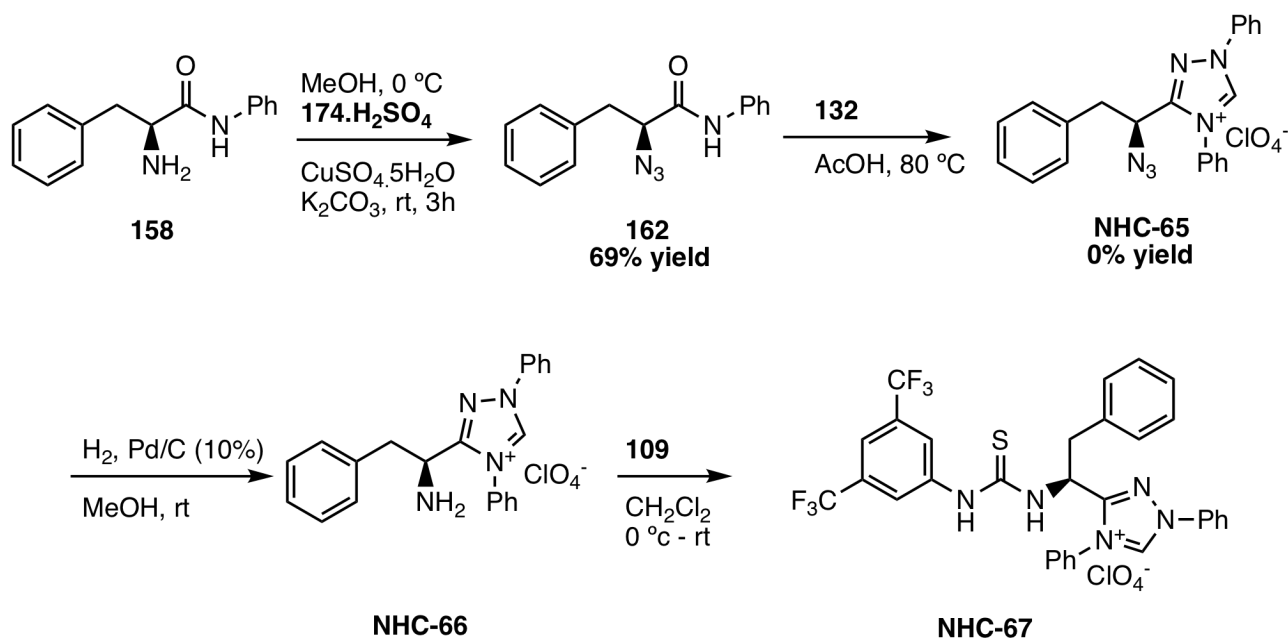


Fig. 5.6 Proposed route to an alternative catalyst, **NHC-67**, starting from phenylalanine. Only the first two steps were attempted.

The starting material **158** had already been synthesised for **NHC-62**. Conversion of the primary amine into the azide **162** worked extremely well, in 69% yield. However, synthesis of the triazolium salt **NHC-65** was unsuccessful, and only starting material was isolated from the reaction. Despite repeating the reaction with a fresh bottle of Me_3OBF_4 , no product could be obtained. A possible reason for this is due to the the proximity of the adjacent

phenyl group. This may promote delocalisation across the amide, meaning that the carbonyl is not nucleophilic enough to be methylated. Due to this, the final product **NHC-66** was no longer pursued. Although this may be fixed by varying the phenyl ring on the amide to an aliphatic group, the previous failures and time constraints led to efforts being focused on alternative catalytic scaffolds.

5.5 Conclusions

Starting from a common phenylalanine core, the synthesis of two new triazolium salt catalysts were attempted. The methyl ester triazolium salt **NHC-64** was shown to be unstable in methanol and basic conditions. Although the problems associated with intra-molecular reactions of the 1,2-diamines can be overcome, the acidity of the α -proton when the triazolium ring is α - to a carbonyl group and therefore loss of chiral centre once the NHC has been installed mean the molecules are not useful as chiral catalysts. The cyclised products are encouraged by the stability of double bond formation due to resonance with the phenyl group, which means it may be plausible to replace phenylalanine with another amino acid, for example leucine. However, by having the NHC adjacent to the ester or amide, the proton will still be too acidic to avoid proton exchange in the fundamental basic conditions of the benzoin condensation. The second triazolium catalyst synthesis that was attempted, involving triazolium salt formation around the amide, was unsuccessful. Again, this was due to unfavourable electronics around the amide, meaning that the crucial methylation step could not take place. Due to these shortcomings, amino acid scaffolds were no longer considered to be viable building blocks for H-bonding NHC precatalysts.

Chapter 6

Bicyclic Piperidine-Derived Catalysts

6.1 Introduction

Bicyclic triazolium and thiazolium salts have demonstrated superior enantioselectivity over their less-rigid analogues, and were first reported by Knight and Leeper in 1998 [72]. Since then, in excess of 40 different bicyclic catalysts have been synthesised, incorporating pyrrolidine, oxazolidine and morpholine derived backbones, as discussed in Chapter 2. Whilst Connon and coworkers have reported several hydrogen-bonding bicyclic triazolium salt catalysts and their use in the benzoin condensation [77], only Waser and coworkers, to date, have incorporated (thio)urea as the hydrogen-bonding moiety in these catalysts [78]. To make the bicyclic triazolium salt catalysts, a simple synthetic route derived from *L*-pyroglutamic acid catalysts offers a relatively straightforward route, with a chiral centre pre-installed in a commercially available starting material. This method also offers late-stage functionalisation of the bicyclic core, meaning that the group on the (thio)urea can be easily modified and investigated.

The synthetic route to Waser and coworkers' bicyclic (thio)urea triazolium salt catalysts is outlined in Fig 6.1. Initial reduction of the enantiomerically pure *L*-pyroglutamic acid gave the alcohol, which was converted to the azide following mesylation of the alcohol

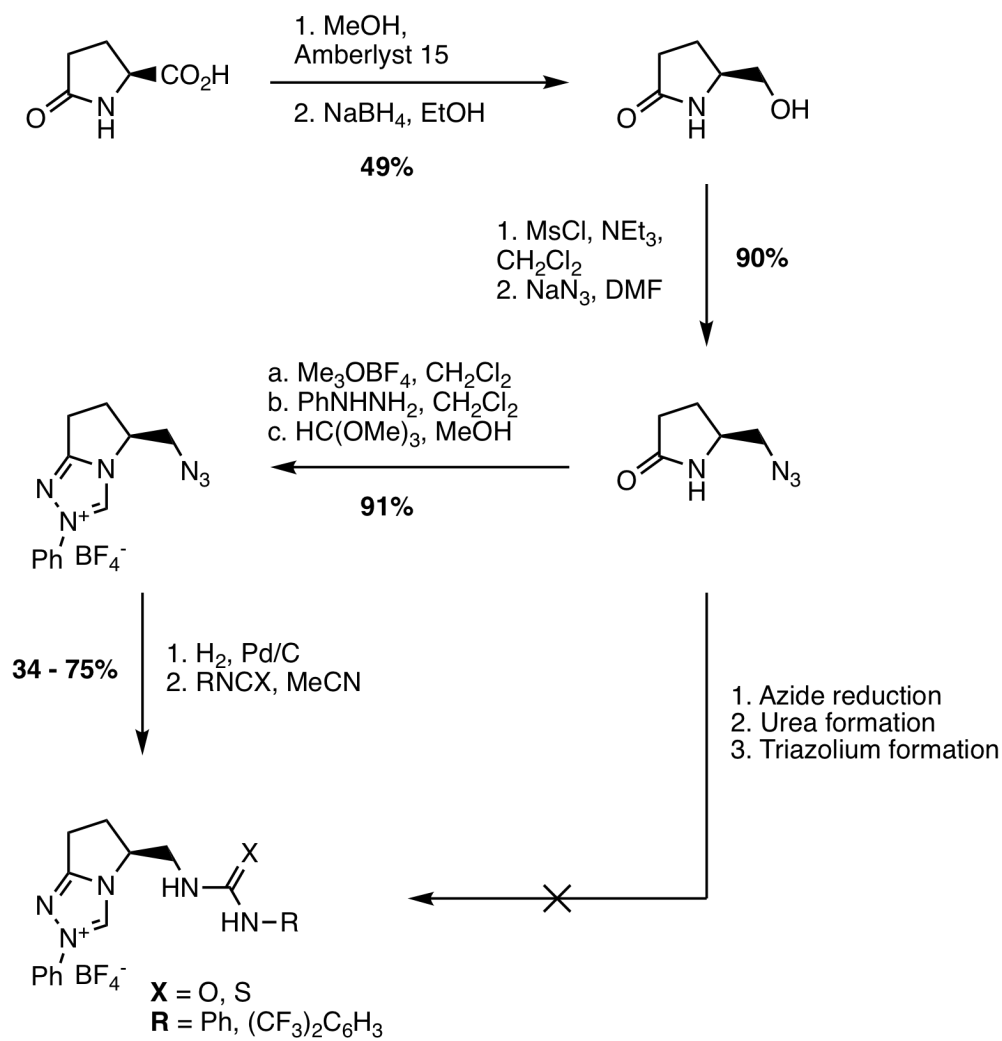


Fig. 6.1 Waser and coworkers' synthetic route to bicyclic catalysts incorporating a (thio)urea functionality. Yields are as reported in the literature [78]

and S_N2 substitution with azide. The bicyclic core was then constructed as per Knight and Leeper's method [72]. Hydrogenation of the azide formed the primary amine, which then reacted with the iso(thio)cyanate to form the (thio)urea, completing the catalysts. Whilst these catalysts did show promising ee and yields, discussed in Chapter 1, the catalysts had no further optimisation or applications reported.

Considering other bicyclic cores which could incorporate (thio)urea, there have been no published NHC precatalysts reported based upon a piperidine scaffold. This is likely due to synthetic difficulty, as there are few synthetic approaches to optically pure functionalised piperidines which could be taken through to the bicyclic catalyst. One advantage this catalyst could offer is further rigidity; the pyrrolidine-derived catalyst by Waser and coworkers has an extra methylene between the bicyclic backbone and the (thio)urea, meaning there is an extra degree of rotation. At this stage, it is unknown whether this rotation enhances the catalytic ability by allowing more flexibility for bonding with the incoming benzaldehyde molecule, or allows too much flexibility that a loss of ee is observed. By investigating the piperidine-based core, the free rotation is minimised, and may act as a useful tool for future design of bicyclic catalysts.

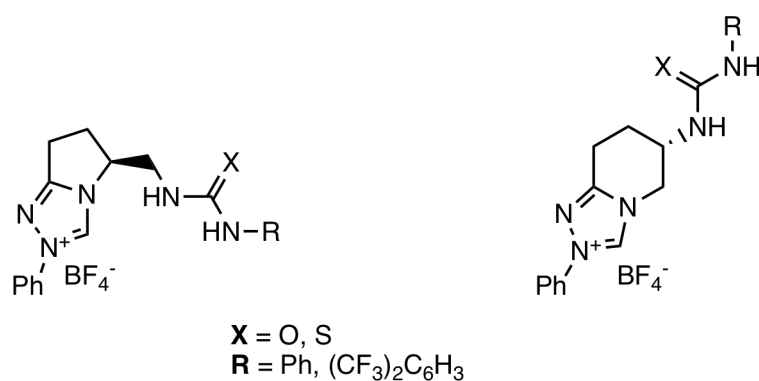


Fig. 6.2 Structural comparison between the piperidine and pyrrolidine incorporated into the bicyclic backbone.

Synthesis of the Catalyst

Attempts to synthesise triazolium salt precatalyst **NHC-70** were originally performed by David Lawrence for his Master's project. ([169]). (*S*)-5-Aminopiperidin-2-one **170** was formed *via* the hydrochloride salt from optically pure, commercially available *L*-pyroglutamic acid **163**, which was converted to the azide **171** using a diazotransfer reagent. The rest of the proposed catalyst synthetic route was as reported by Waser and coworkers [78], which involves cyclisation onto the amide, deprotection of the azide group and formation of the (thio)urea.

The route to final catalyst **NHC-70** was initially developed by Lawrence and is discussed in his report (Fig. 6.3). All of the work up until the bicyclic azide **NHC-68** had been initially synthesised by Lawrence. However, there was too little material left to be taken through to the final product, and insufficient characterisation of the material had been performed, so the material was resynthesised as part of this project. A brief synthesis undertaken in this work is outlined below, with any optimisation clearly stated. All of the yields obtained by Lawrence were at least comparable [169].

In this work, the esterification and reduction of *L*-pyroglutamic acid **163** to the alcohol **164** gave the product in 87%. Rather than trituration using CH₂Cl₂ to afford a solid as per Lawrence's method, here the product was dried under high vacuum. The alcohol was then converted to the tosylate **165** in 75%. Boc-protection of the amide afforded the pure product **166** in 91% yield. The azide **167** formation occurred cleanly in 87%, and was used without further purification. The azide was reduced using Pd/C to give the corresponding amine **168**.

When the transamidation step to form the piperidine **169** was initially performed here, the cyclisation conditions afforded a product lacking the Boc group (Fig. 6.4), which was not reported by Lawrence. Careful analysis of its HMBC spectrum showed that the Boc group had simply been cleaved to give 5-aminomethylpyrrolidin-2-one **172**, without any rearrangement of the ring to give *tert*-butyl-(*S*)-(6-oxopiperidin-3-yl)carbamate **169**. This may have been due to overheating, or traces of Pd/C remaining. The reaction was repeated,

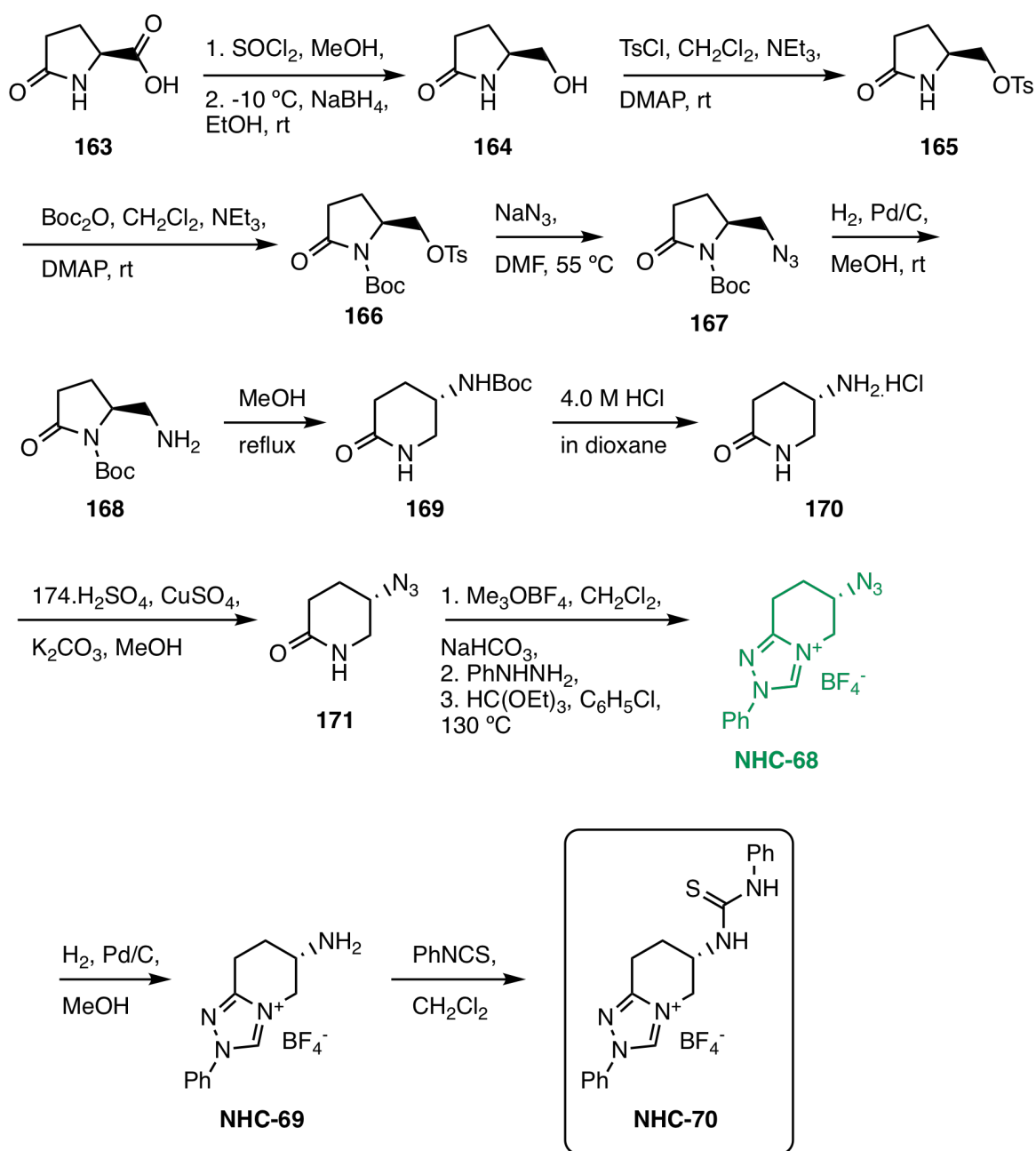


Fig. 6.3 Synthetic route reported by Lawrence to the final catalyst [169]. No further synthetic work was performed by Lawrence past the formation of **NHC-68**.

and the amine was purified using a silica column and characterised by ^1H and ^{13}C NMR to determine the Boc group remained at this stage, giving 42% yield of **168**. Satisfied that the product was correct, the material was taken up in MeOH and heated to give the rearranged product **169** as a yellow crystalline solid in 82% yield.

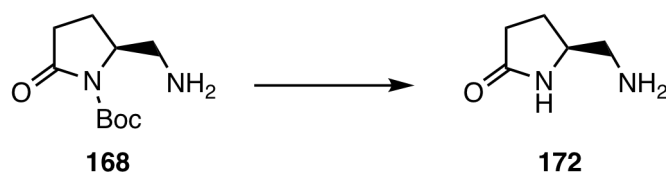


Fig. 6.4 Removal of the Boc group upon heating.

6.1.1 Diazotransfer Reagent

Background

When the deprotection of *tert*-butyl-(*S*)-(6-oxopiperidin-3-yl)carbamate **169** to form the hydrochloride salt **170** was performed here, the product was achieved in quantitative yield, but problems occurred at the following diazotransfer step. This method of azide synthesis from an amine was originally chosen as the azide would need to be attached to a chiral centre. Use of a diazotransfer reagent could build the azide onto a pre-existing chiral amine, retaining the stereochemistry, without any inversion which would occur with nucleophilic attack by azide.

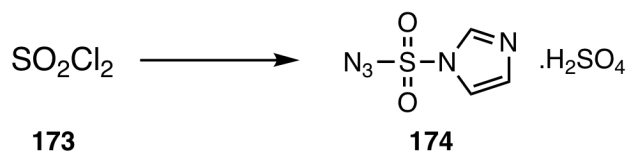


Fig. 6.5 Scheme to show formation of the diazotransfer reagent **174.H₂SO₄**.

The diazotransfer reagent acts as a mild transfer reagent for N_2 onto a primary amine. TfN_3 has been used as a diazotransfer reagent since its discovery in 1972 [170]. However, it suffers from stability problems and is explosive when concentrated, requiring preparations

of solutions to improve safety and reproducibility [171]. Developments in this area led to preparation of the new diazotransfer reagent imidazole-1-sulfonyl azide **174** reported in 72% yield, but this could have problems with being explosive when neat [172]. By preparation of the HCl salt, the diazo transfer reagent **174.HCl** became a solid which was easy to work with and weigh, and was reported in a relatively good yield of 63%. However, further reports state that this salt can be explosive, and explosive sulfonyl diazide or hydrazoic acid can be formed as a by-product (Fig 6.6). Further disadvantages of this method include the generation of *in situ* HCl by use of highly corrosive acetyl chloride, and the material must be purified by column chromatography. Gardiner reported that formation of the H₂SO₄ salt **174.H₂SO₄** gave a much more desirable product [173]. This did not explode in their tests, was stable for periods of over 6 months, and did not form the explosive by-products. However, it must be noted that **174.H₂SO₄** violently decomposes at temperatures above 150°C. The product can be safely stored in the fridge under N₂ for over six months, with no discolouration or loss of activity.

Use of both the **174** HCl salt and the **174** H₂SO₄ salt as a diazotransfer reagent has been reported to work effectively in the diazotransfer reaction, demonstrating utility across a range of primary amines including sugars, amino acids, and both aliphatic and aromatic amines in yields up to 92% [172, 173].

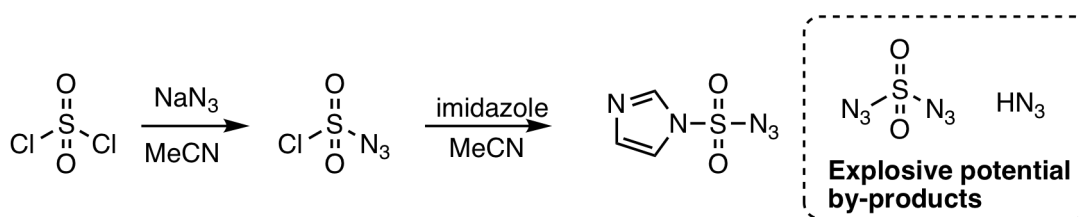


Fig. 6.6 Synthesis of the neat diazotransfer reagent and its associated by-products [172].

Synthesis

Although diazotransfer reagent **174.H₂SO₄** is stable and safer than the alternatives, the synthesis requires the use of several highly corrosive or explosive materials; sulfonyl chloride,

imidazole, sodium azide and sulfuric acid. Two methods to synthesise the diazotransfer reagent were attempted here based on previous reports; these included using dry EtOAc as a co-solvent in combination with MeCN, or just EtOAc alone [172]. Using a combination of 2:1 EtOAc:MeCN gave 29% yield, but EtOAc alone only gave 36% yield. These yields obtained here of **174.H₂SO₄** were much lower than those reported previously, despite following the procedures to scale. However, the material made here was then combined with pure material previously synthesised by Lawrence to have enough for later use.

Currently Reported Diazotransfer Mechanism Studies

The main advantage of synthesising an azide from a primary amine is the retention of stereochemistry. Most reported diazotransfer reactions require a Cu^{II} salt catalyst, but use of Zn^{II} catalysts [171] and even metal-free reactions have been reported [174]. Isotope labelling studies by Samuelson and coworkers were undertaken to try to gain a better understanding of the mechanism [175]. ¹⁵N and ¹³C labelled L-valine and L-isoleucine were reacted with the diazotransfer reagent to give the corresponding azide (Fig 6.7). Analysis of the splitting pattern of the ¹³C NMR indicated that the ¹⁵N remained in the same position, therefore there was no cleavage of the C-N bond, which would occur with S_N2 substitution.

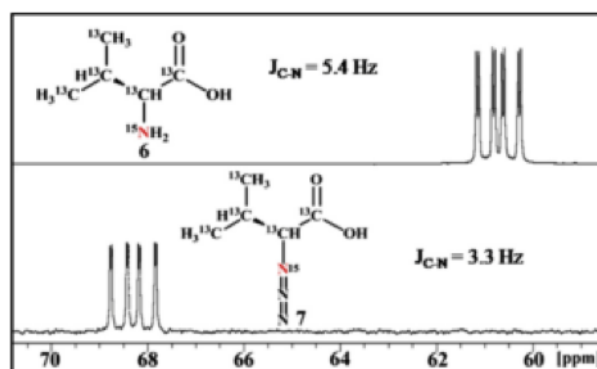


Fig. 6.7 ¹³C NMR comparing the radiolabelled L-valine (top) and the azide protected L-valine (bottom). The similar splitting pattern helps to confirm the ¹⁵N has remained in position. Formation of the azide was confirmed using IR spectroscopy. Spectra taken from Samuelson [175].

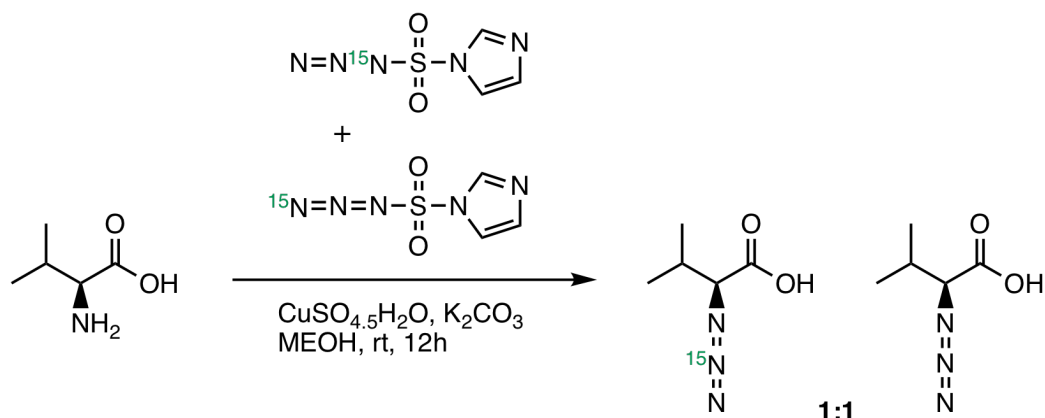


Fig. 6.8 Reaction of L-valine with ^{15}N labelled NaN_3 to give a 1:1 ratio of products consistent with the diazotransfer mechanism.

Further confirmation came from the use of labelled NaN_3 that was ^{15}N labelled on one of the two terminal atoms; two L-valine azide isotopomers were obtained in a 1:1 ratio, which is consistent with a diazotransfer mechanism (Fig. 6.8). This is consistent with the mechanism previously proposed by Wong and coworkers using TfN_3 and a Zn^{II} catalyst, occurring *via* a cyclic tetrazene intermediate [171]. The Cu^{II} -catalysed mechanism was therefore proposed after the NMR studies (Fig. 6.9).

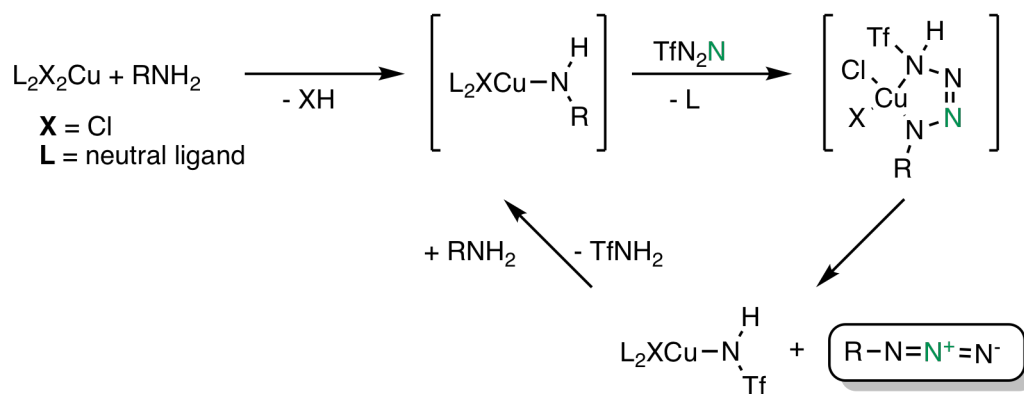


Fig. 6.9 The Cu^{II} -catalysed mechanism for the diazotransfer reaction using TFN_3 proposed by Samuelson *et al.* based on their NMR studies [175] and previous reports by Wong and coworkers. N = labelled ^{15}N .

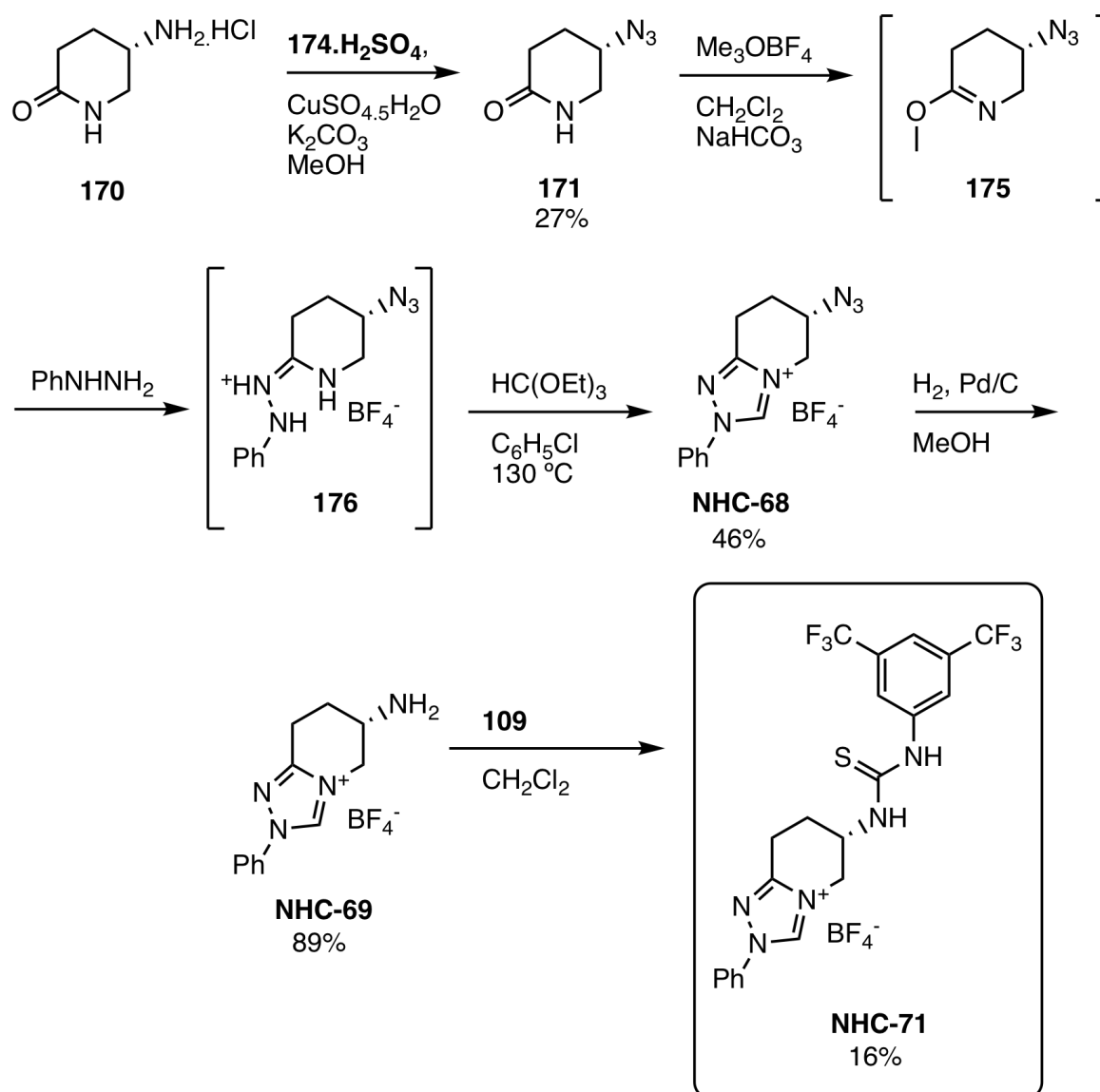


Fig. 6.10 Steps to synthesise the final catalyst **NHC-71** from *(S)*-5-aminopiperidin-2-one hydrochloride **170** as obtained in this work.

Final Catalyst Synthesis

Although Lawrence had previously been working towards synthesis of the phenyl analogue **NHC-70**, due to the highest ee for the benzoin condensation in this work so far being obtained with the 3,5-bis(trifluoromethyl)phenyl analogue (*1R,2R*)-**NHC-48** in Chapter 3, this analogue would be synthesised in this work to give **NHC-71** (Fig. 6.10).

To reach the final catalyst **NHC-71** here, (*S*)-5-aminopiperidin-2-one hydrochloride **170** was reacted with the diazotransfer reagent **174.H₂SO₄**. However, when the diazotransfer reaction was performed here, it did not proceed in high yield, giving only 27% of the product **171**. Due to the late stage of this reaction in the synthesis towards the product, it would be quite difficult to optimise as there was only little material left. Therefore, no optimisation was investigated here.

Nevertheless, the azide **171** was taken through to the cyclisation step. The initial step of methylation of the amide with Me₃OBf₄ to form **175** was left to stir overnight to allow a higher conversion. Used crude without isolation, this was then reacted with phenylhydrazine to form **176**, which was again not isolated, followed by Me₃OBf₄ to form **NHC-68**. Rather than precipitating the product **NHC-68** using acetonitrile and diethyl ether, the crude material was passed through through a column, giving pure product **NHC-68** in 46% yield.

This step was the furthest point Lawrence reached in his synthesis due to a low yield and time constraints, and so all the further work reported herein is novel. Here, full characterisation of the cyclised material was performed (¹H and ¹³C NMR, IR, and accurate mass, available in Chapter 8 and the Appendix). These confirmed the correct desired compound.

The following steps were performed analogous to Waser and coworkers' synthesis [78]. The azide group of **NHC-68** was easily hydrogenated here to give the primary amine **NHC-69** in 89% yield, which was then reacted with the isothiocyanate **120**. Monitoring the reaction using LCMS showed that the reaction did not go to full completion (only around 30%). Although addition of further isothiocyanate **120** did slowly increase the amount of product formed, purification was difficult due to co-elution of the product with the starting

material, and eventually only 14 mg (16%) of the final product **NHC-71** was obtained after purification on a silica column with 10% MeOH/CH₂Cl₂. This low yield may also be due to reactivity or steric issues; when Waser and co-workers synthesised their pyrrolidine analogue from the same isothiocyanate, they achieved a similarly low yield of 7% [78].

6.1.2 Synthesis of the Pyrrolidine-Derived Triazolium Salt

As a comparison, Waser and coworkers' catalyst **NHC-74** was also synthesised here following their procedure (Fig. 6.11) [78]. The (*R*)-4-(azidomethyl)pyrrolidin-2-one **177** was synthesised by Boc-deprotection of *tert*-butyl-(*R*)-4-(azidomethyl)-2-oxopyrrolidine-1-carboxylate **167** in 90% yield. From this, the bicyclic triazolium salt **NHC-72** was formed in 22% yield *via* intermediates **178** and **179**, which were again not isolated. Hydrogenation gave the primary amine **NHC-73** in 49%, and reaction with 3,5-bis(trifluoromethyl)phenyl isothiocyanate **109** gave the pure product **NHC-74** in 21% yield after washing with chloroform.

6.1.3 Proposed Synthesis of the Opposite Enantiomer

One of the main synthetic challenges of the above route to the novel bicyclic catalyst **NHC-71** was the loss of product at the diazotransfer step. A new route, avoiding the need for the diazotransfer step, was proposed (Fig 6.12). All steps up to formation of tosyl-protected (*S*)-5-hydroxypiperidin-2-one **186** are reported in literature. By starting with commercially available L-glutamic acid **180**, diazotisation and cyclisation gives the γ -lactone scaffold **181** [176]. Similar to the previous synthesis using L-pyroglutamic acid, reduction to the alcohol **182** [177] and conversion to the tosylate **183** [178] provides a good leaving group to allow formation of the azide **184** [179]. A reported one-pot procedure shows the azide can undergo hydrogenation to the primary amine [180], and simply stirring the reaction at room temperature is enough to drive the formation of (*S*)-5-hydroxypiperidin-2-one **185**. This has shown to be successfully tosylated to form **186** [181]. It is hoped that reaction of **186** with NaN₃ will provide the azido-product (*R*)-**171**. However, this could lead to complications with

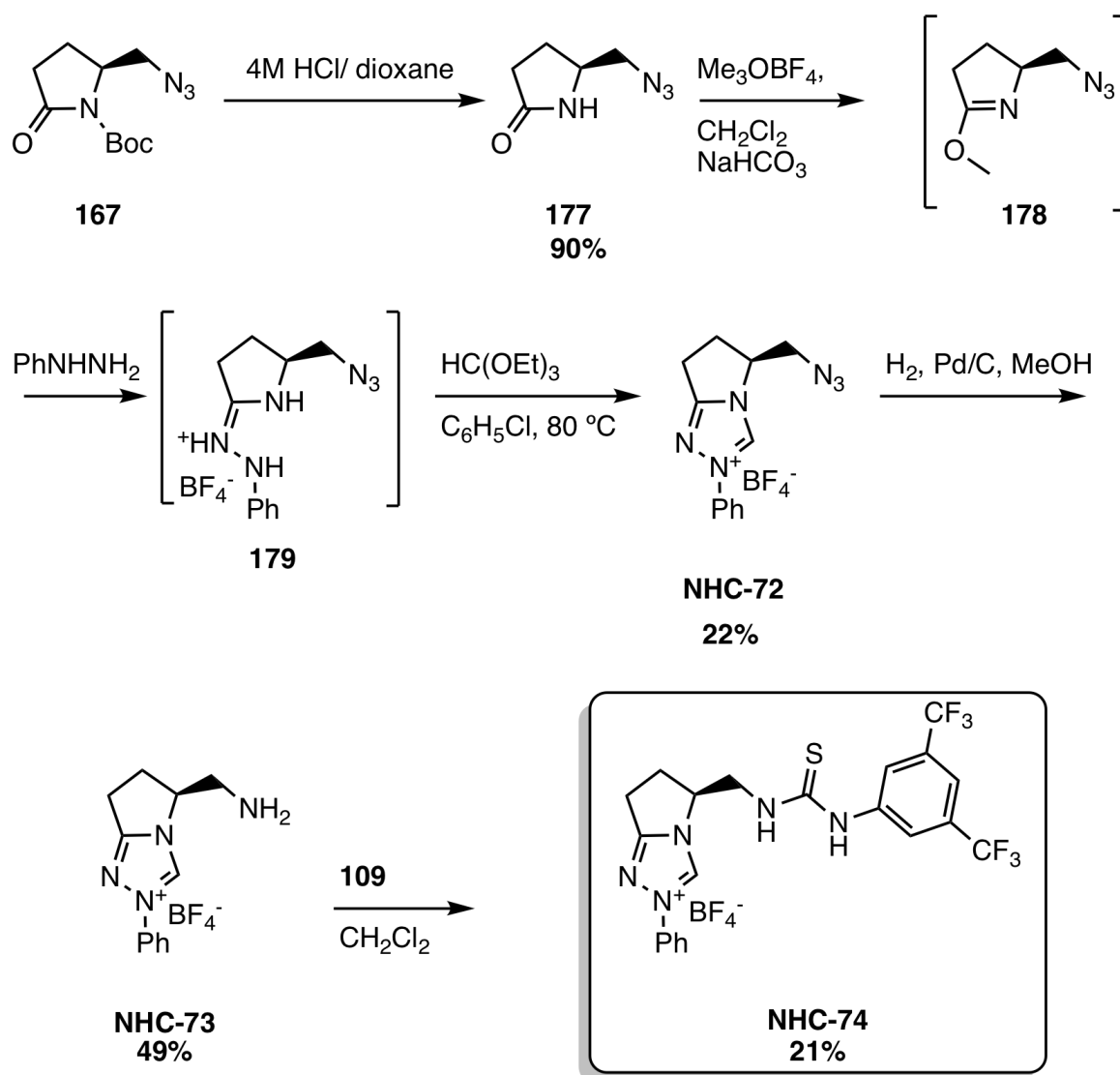


Fig. 6.11 Synthesis of the pyrrolidine-derived triazolium salt as originally reported by Waser and coworkers. Yields shown were obtained in this work.

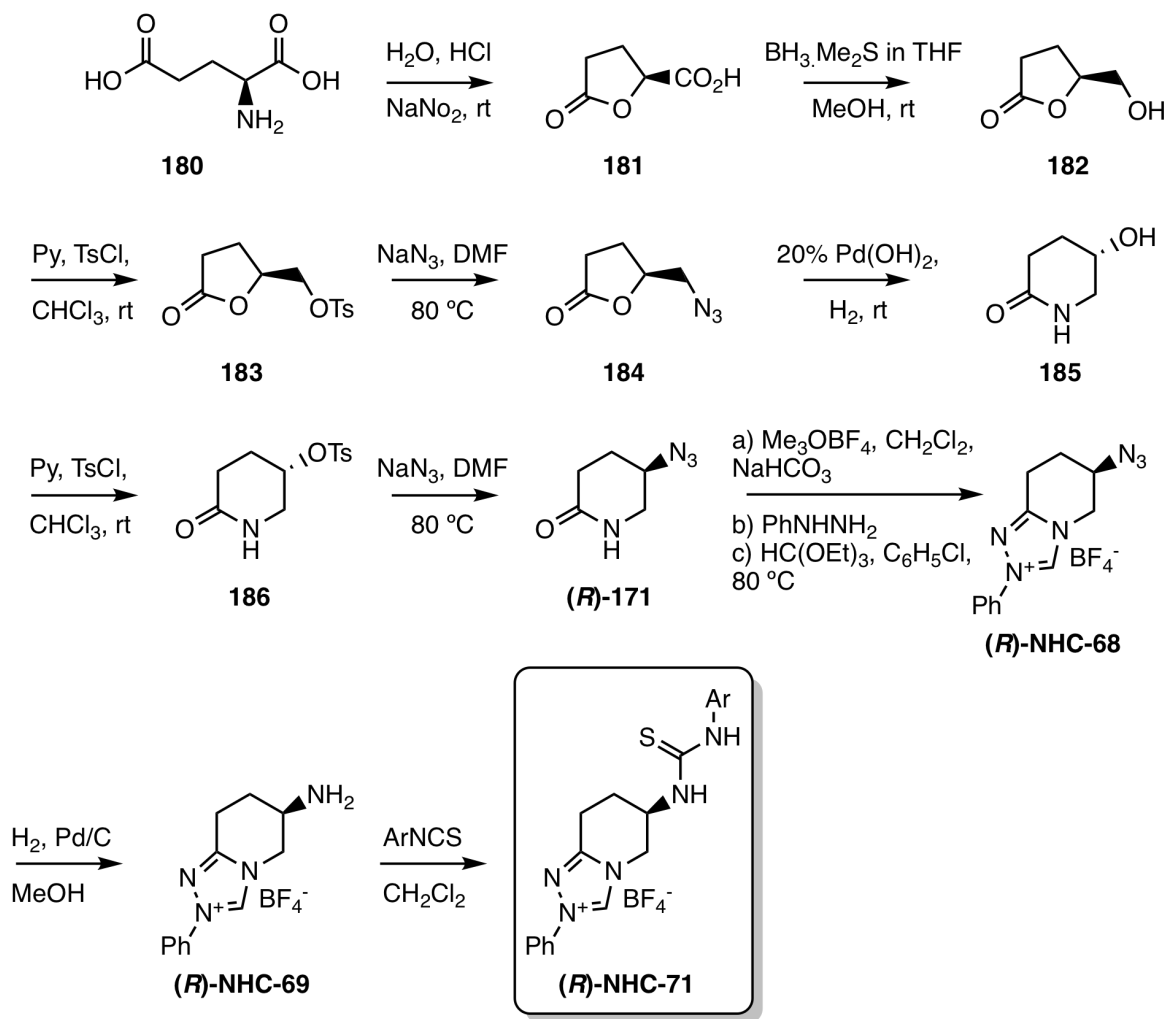


Fig. 6.12 Proposed synthesis of the triazolium salt catalyst opposite enantiomer from L-glutamic acid.

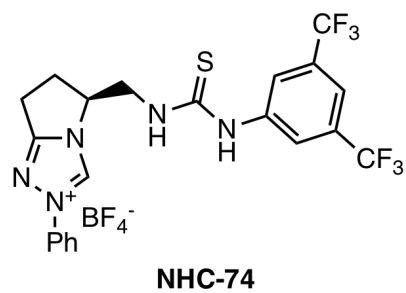
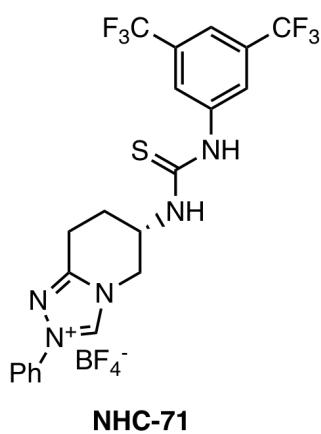
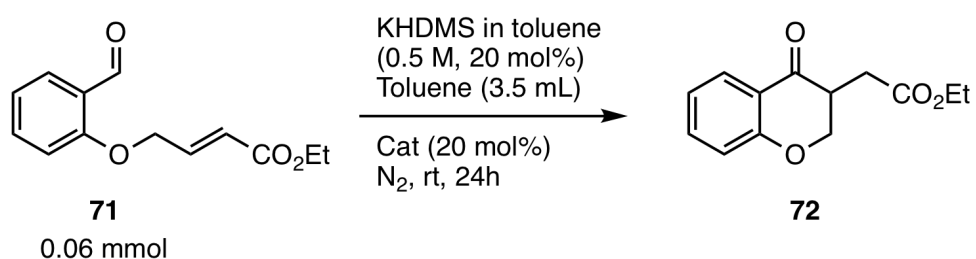
the stereoselectivity. The reaction to form the azide on different materials is well-established, and has been successfully performed in this work, but this has always been on achiral carbons. By having the reaction on the chiral centre, it is important that the reaction proceeds *via* an S_N2 mechanism, leading to inversion of the stereocentre rather than the mixture that occurs with S_N1. S_N2 seems more favourable due to the polar aprotic DMF solvent, the relatively strong nucleophile and a lack of stabilisation of the intermediate carbocation other than it being a secondary centre [182]. However, studies will need to be undertaken to confirm this; one possibility would be comparison with the opposite enantiomer synthesised previously on chiral HPLC. Kinetic studies would also help to confirm the mechanism, as for an S_N2 reaction, the reaction rate is sensitive to both the concentration of the nucleophile and the reagent, i.e. rate = $k [\text{R-OTs}] [\text{N}_3^-]$. If the azido step is successful in maintaining high ee, the material can be taken through to the triazolium salt (**R**)-NHC-68, the azide group hydrogenated to the primary amine to form (**R**)-NHC-69, and this reacted with the iso(thio)cyanate as with the opposite enantiomer to give the final desired catalyst (**R**)-NHC-71, where Ar = Ph or 3,5-bis(trifluoromethyl)phenyl. It is unknown whether this route will obtain higher yields, especially at the azido step, but this route may be a good starting point for an alternative method to the low-yielding diazotransfer step in the previous method.

6.2 Catalyst Testing

6.2.1 The Stetter Reaction

Both of these catalysts managed to form product in the Stetter reaction (Table 6.1). However, Waser and coworkers' catalyst NHC-74 gave a much higher ee of 80% compared to 17% ee obtained with NHC-71. Comparison of NHC-71 and NHC-74 indicates that whilst the bicyclic backbone is effective in influencing the stereocentre, it is possible that the free rotation of the thiourea pendant has contributed to an increase in ee. This indicates that perhaps the steric bulk of the piperidine is in the wrong place for the Stetter reaction, allowing

Table 6.1 Triazolium catalysts in the intramolecular Stetter reaction.



Entry	Catalyst	Yield ^a (%)	ee ^b (%)
1	NHC-71	26	17
2	NHC-74	11	80

^aMeasured by NMR. ^bMeasured by chiral HPLC.

for a higher yield but at the expense of lowered stereoselectivity. However, this is a promising start, and so both catalysts were investigated in the benzoin condensation.

6.2.2 The Benzoin Condensation

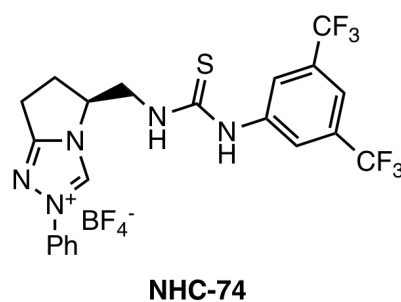
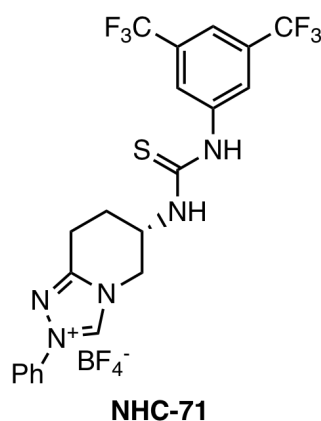
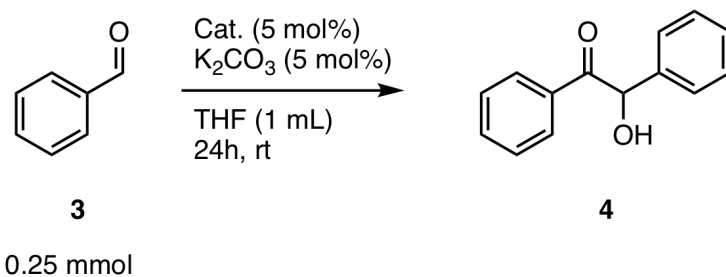
Catalysts **NHC-71** and **NHC-74** were subjected to the same conditions optimised in Chapter 2 (Table 6.2). Surprisingly, the catalyst **NHC-71** obtained the highest yield out of all the catalysts reported in Chapters 3 and 4. However, this came at a cost of ee, and only 5% ee was obtained. When **NHC-74** was used as a comparison, the yields were lower than those reported by Waser and coworkers with the same catalyst [78], despite the reaction conditions being kept the same. This may be due to the scale; any trace impurities in atmosphere or solvent is much more likely to have an effect here, as the scale had been reduced to 25% of what was previously reported. Regardless, **NHC-71** did not perform as effectively as **NHC-74**.

To investigate this further, as per Chapter 3 a random sample of conformers of the Breslow intermediate were generated, and the energies minimised. These computational studies of the catalyst show that both the steric bulk and the hydrogen-bonding moiety of the thiourea in **NHC-71** are orientated away from the active centre of the calculated local minima of the Breslow intermediate. This seems reasonable in line with the results, as the centre is free and open to react with a second molecule of benzaldehyde, giving a higher yield whilst explaining the low ee.

6.3 Conclusions

A new bicyclic catalyst derived from piperidine incorporating thiourea was synthesised. After initial optimisation of earlier steps by Lawrence, the final catalyst was synthesised in sufficient yield for initial tests. The corresponding pyrrolidine-derived catalyst, reported by Waser and coworkers [78], was also synthesised for comparison. Although the piperidine-

Table 6.2 Triazolium catalysts in the benzoin condensation.



Entry	Catalyst	Yield ^a (%)	ee ^b (%)
1	NHC-71	40	5
2	NHC-74^c	trace (17)	- (90)

^aMeasured by NMR. ^bMeasured by chiral HPLC.

^cPreviously tested in literature by Waser and coworkers [78] on a 1 mmol scale, with the reported values given in parentheses.

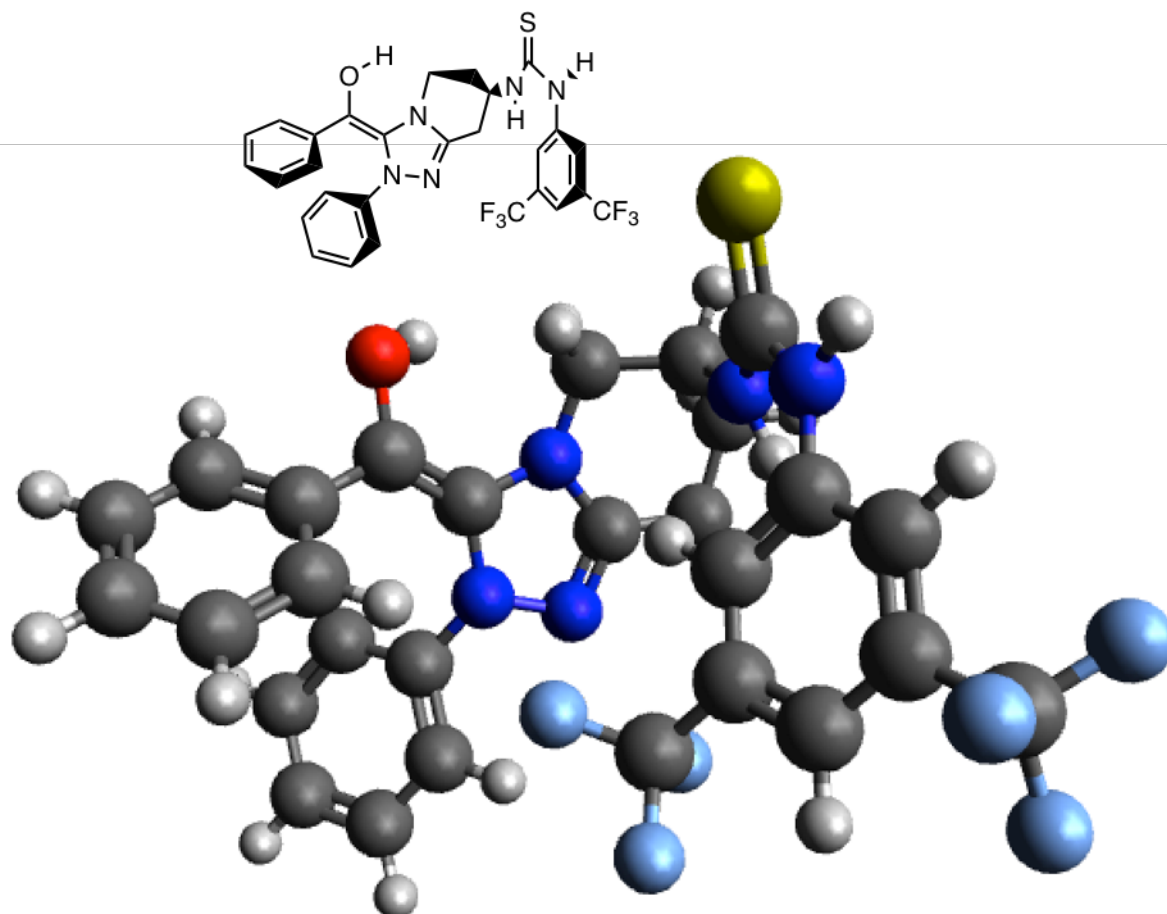


Fig. 6.13 Lowest energy conformation found for the Breslow intermediate from the bicyclic catalyst **NHC-71**. Although there was no intramolecular hydrogen bonding detected, the catalyst may be hindered by the lack of free rotation. Lowest energy conformer points the active centre in wrong direction from H-bonding. Calculated energy = 284.3 kJ mol⁻¹.

derived catalyst gave the highest yield of any catalyst tested in this work for the benzoin condensation at 40%, the ee was barely above that of a racemic catalyst. This shows that although bicyclic triazolium salts are effective as catalysts, the rigidity and angle of the (thio)urea needs to be precisely controlled to allow for improvement in ee. The lowest energy conformer reported above illustrates this. It is unlikely that the (thio)urea group could be moved into the 2- position on the piperidine ring, as this may then suffer with deprotonation issues at the chiral centre, like the phenylalanine-derived catalyst **NHC-64** reported in Chapter 4. However, further modifications to the scaffold may help increase the ee in the future.

Chapter 7

Conclusions

The benzoin condensation and related umpolung reactions have been fundamental in organic synthesis for nearly two centuries. Since the initial discovery in 1832 of the self-condensation of the simplest aromatic aldehyde [53], the reaction has evolved and expanded in many directions. From addition of the carbonyl into different functional groups, to heterocycle formation and cascade reactions, the versatility of this methodology has greatly advanced synthetic routes in many areas, including agrochemical and pharmaceutical industries. Although the reaction does have reasonable stereoselective success, there is still room for development of new catalysts to find quicker and more effective ways of achieving chiral products. To develop all of these umpolung reactions, there needs to be understanding of the Breslow intermediate, which has evidence to back up its existence yet has never been unambiguously identified and characterised. Understanding can come from computational work, but the Breslow intermediate and the initial adduct are fundamental to the rational design of new catalysts. In previous catalyst design, hydrogen-bonding moieties have improved enantioselectivity of reactions, as evidenced by Jacobsen and coworkers [25]. Even in the benzoin condensation, hydrogen bonding catalysts induced stereoselectivity [78], but were not further investigated after the initial report. This work aimed to further investigate hydrogen bonding catalysts in the benzoin condensation, and provide rationale and understanding into new catalyst design.

To this extent, four new variations of NHC catalyst were synthesised incorporating hydrogen bonding, with initial testing in the benzoin condensation and Stetter reaction for investigation as suitable chiral organocatalysts.

7.1 Synthesis and Testing Conclusions

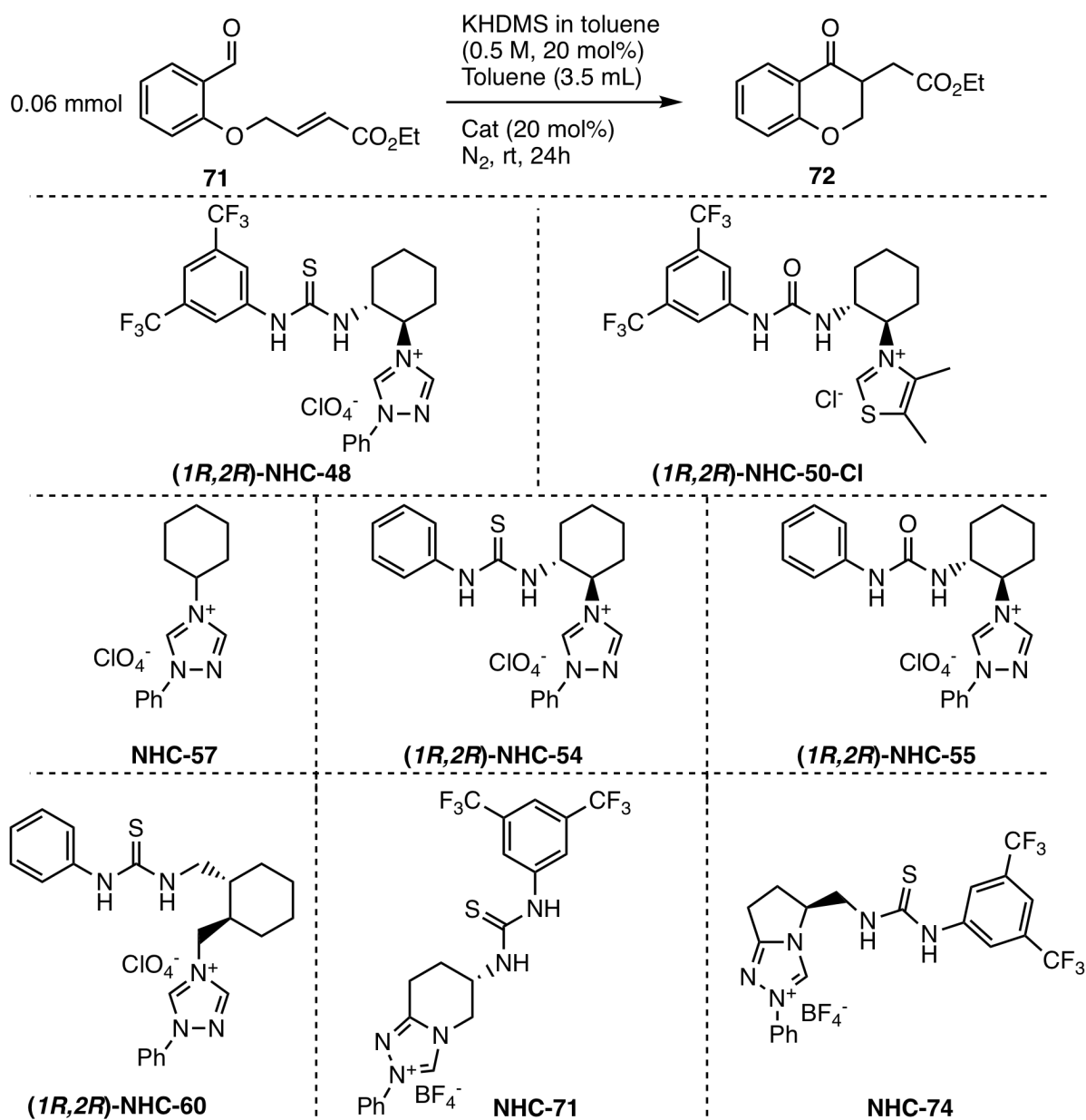
A summary of all of the tested catalysts for the Stetter reaction and the benzoin condensation are shown in Tables 7.1 and 7.2 respectively. All of the catalysts were successful in obtaining quantities of **72** (Table 7.1), with (*1R,2R*)-**NHC-48** performing the best in terms of yield with the third highest ee (Entry 1). (*1R,2R*)-**NHC-50-Cl** interestingly gave the second highest ee (Entry 2) and favoured formation of the opposite enantiomer compared to the other catalysts. However, Waser's original catalyst **NHC-74** gave the overall highest ee of 80% (Entry 8).

When comparing the catalysts for the benzoin condensation in Table 7.2, **NHC-71** fared the best in terms of yield (Entry 7), but only at 5% ee. None of the catalysts managed to synthesise benzoin **4** with an ee comparable to the given literature value of **NHC-74** (Entry 7 in parentheses) [78]. Of the new catalysts reported in this work, (*1R,2R*)-**NHC-54** gave the highest ee of 44%, but only in 5% yield.

7.1.1 1,2-Diamine-Derived Catalysts

Based on initial bifunctional catalysts by Takemoto [42] incorporating a chiral *trans*-1,2-cyclohexane-diamine backbone, four new triazolium salt catalysts and one new thiazolium salt incorporating (thio)urea moieties were synthesised for use in the benzoin condensation (Fig. 7.1). The catalysts, due to the C₂ symmetry of the 1,2-diamine backbone, needed significant optimisation of reaction conditions and routes to form the final product. Bis-functionalisation of the initial 1,2-diamine was a major problem, which was not easily overcome by mono-protection with groups such as Boc due to the same problem. Optimisation of the synthesis with the urea formation showed that it was possible to increase the mono-protection of the

Table 7.1 Triazolium and thiazolium catalysts tested in the intramolecular Stetter reaction.



Entry	Catalyst	Yield ^a (%)	ee ^b (%)
1	(1<i>R</i>,2<i>R</i>)-NHC-48	42	49
2	(1<i>R</i>,2<i>R</i>)-NHC-50-Cl	27	54 ^c
3	NHC-51	16	0
4	(1<i>R</i>,2<i>R</i>)-NHC-54	11	37
5	(1<i>R</i>,2<i>R</i>)-NHC-55	5	-
6	(1<i>R</i>,2<i>R</i>)-NHC-60	4	-
7	NHC-71	26	17
8	NHC-74	11	80

^aMeasured by NMR. ^bMeasured by chiral HPLC. ^cOpposite enantiomer.

Table 7.2 Triazolium and thiazolium catalysts tested in the benzoin condensation.

<div> <div>0.25 mmol</div> <div> </div> <div> <div>3</div> <div>4</div> </div> </div>			
<div> <div> </div> <div>(1<i>R</i>,2<i>R</i>)-NHC-48</div> </div>			
<div> <div> </div> <div>(1<i>R</i>,2<i>R</i>)-NHC-50-Cl</div> </div>			
<div> <div> </div> <div>NHC-57</div> </div>			
<div> <div> </div> <div>(1<i>R</i>,2<i>R</i>)-NHC-54</div> </div>			
<div> <div> </div> <div>(1<i>R</i>,2<i>R</i>)-NHC-55</div> </div>			
<div> <div> </div> <div>(1<i>R</i>,2<i>R</i>)-NHC-60</div> </div>			
<div> <div> </div> <div>NHC-71</div> </div>			
<div> <div> </div> <div>NHC-74</div> </div>			
Entry	Catalyst	Yield ^a (%)	ee ^b (%)
1	(1 <i>R</i> ,2 <i>R</i>)-NHC-48	0	-
2	(1 <i>R</i> ,2 <i>R</i>)-NHC-50-Cl	trace	-
3	NHC-51	trace	-
4	(1 <i>R</i> ,2 <i>R</i>)-NHC-54	5	44
5	(1 <i>R</i> ,2 <i>R</i>)-NHC-55	1	-
6	(1 <i>R</i> ,2 <i>R</i>)-NHC-60	5	-
7	NHC-71	40	5
8	NHC-74 ^c	trace (17)	- (90)

^aMeasured by NMR. ^bMeasured by chiral HPLC.

^cPreviously tested in literature by Waser and coworkers [78] on a 1 mmol scale, with the reported values given in parentheses.

Chemical structures of five NHC ligands (NHC-48, NHC-53, NHC-54, NHC-55, and NHC-50) are shown. Each ligand consists of a 1-phenyl-1H-imidazol-3-ylidene group attached to a cyclohexane ring, which is further substituted with a 2,4,6-trifluorophenyl group. The counterion is ClO_4^- .

- NHC-48**: 1-(2,4,6-trifluorophenyl)-1H-imidazol-3-ylidene-1-cyclohexylmethanimine.
- NHC-53**: 1-(2,4,6-trifluorophenyl)-1H-imidazol-3-ylidene-1-cyclohexylmethanimine.
- NHC-54**: 1-phenyl-1H-imidazol-3-ylidene-1-cyclohexylmethanimine.
- NHC-55**: 1-phenyl-1H-imidazol-3-ylidene-1-cyclohexylmethanimine.
- NHC-50**: 1-(2,4,6-trifluorophenyl)-1H-imidazol-3-ylidene-1-cyclohexylmethanimine.

The triazolium salt synthesis, already known in the literature [77], has its own set of problems. After some optimisation, the oxadiazolium intermediate could be effectively synthesised, although it decomposed quickly and had to be identified by infrared spectroscopy. However, the product was relatively easy to identify by eye due to colour and crystal change. The oxadiazolium salt could be used in acetic acid to form the triazolium salt with a range of different primary amines. Again, due to the positioning of the substituents, degradation with the 1,2-diamine-derived backbone led to a low yield. Careful control of temperature, and reaction monitoring with LC/MS allowed for maximum yields of product to be obtained. Variation of the backbone could remedy these problems, and higher conversions

were obtained with the phenylalanine-derived catalyst, and the ((1*R*,2*R*)-cyclohexane-1,2-diyl)dimethamine backbone described below.

Optimisation of the thiazolium salt synthesis procedure reported by Glorius [85] allowed for synthesis of a new salt incorporating a urea moiety. Initial reactions going *via* the thiazol-2-thione had several difficulties with purification. Initially, similar problems to above occurred with the *trans*-diamine-1,2-cyclohexylamine urea backbone, as an intramolecular cyclisation could occur, forming a bicyclic (3*aR*,7*aR*)-octahydro-2*H*-benzo[*d*]imidazole-2-thione as the major product. Once the 4,5-dimethylthiazole-2(3*H*)-thione heterocycle had been constructed, purification was extremely difficult, meaning the intermediate could not be fully characterised. Interestingly, the final thiazolium salt could also be synthesised directly, but replication of these conditions did not manage to achieve the same results. Mechanistic studies on this reaction may provide further insight, but were beyond the scope of the project.

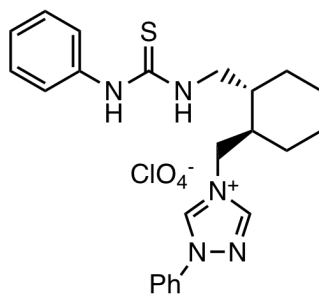
Initial testing of the 1,2-diamine-derived catalysts gave a maximum ee of 54% in the Stetter reaction, and 44% in the benzoin condensation. Unfortunately, none of the catalysts gave a yield over 5% in the benzoin condensation, compared to a maximum yield of 42% in the Stetter reaction. This could be attributed to two factors. Firstly, the reversibility of the benzoin condensation may have led to attrition of the final product. Finally, preliminary computational investigations indicated that it was plausible that there was hydrogen bonding in the intermediate after addition into the initial benzaldehyde, and this stabilisation may have inhibited the reaction. As discussed in Chapter 2, there are shortcomings with the computational method as only a number of local minima are found, which may not include the global minimum, so this would need further confirmation.

7.1.2 1,4-Diamine-Derived Catalysts

After the limited success of the 1,2-diamine system, the relative position of the hydrogen bonding moiety was investigated using two distinct strategies; extension of the system to a 1,4-diamine scaffold, and restriction of the (thio)urea's position by use of a fused bicyclic

backbone, which has had previous success in enantioselective benzoin condensation. Increasing the distance between the active carbene centre and the (thio)urea could be beneficial in two separate ways. Firstly, it was hoped that synthetically there would be no intramolecular reactions, as 7-membered ring formation is less favourable than 5-membered rings. In terms of catalyst testing, a further away (thio)urea may lead to less stabilisation of the initial adduct and its precursor *via* hydrogen-bonding, as proposed in Chapter 3.

The 1,4-diamine, however, suffered with its own synthetic challenges. One of the initial problems comes from isolating the optically pure material. Following the literature procedure, it is difficult to obtain an accurate ee of the dicarboxylic acid after recrystallisation, due to problems with tailing on the HPLC and lack of chromophore. The ee can be determined at the following stage after ditosylation, but by this point it is difficult to correct if washing at the previous step was not thorough enough. It is challenging to find the balance between washing enough for optical purity, and not over-washing leading to mass product attrition. Therefore, the catalyst taken forward in Chapter 4 only had 90% ee, which leads to problems in determining how effective this is as a catalyst.



NHC-60

Fig. 7.2 The catalyst synthesised, optimised and tested in Chapter 4.

After optimisation, the synthesis of this catalyst did eliminate some of the problems with the previous catalysts, most notably with an improvement in the final step with the triazolium salt formation. However, a new set of problems opened up here regarding purification of the final catalyst, which proved extremely difficult, leading to testing of a slightly impure catalyst. The catalyst was also not efficient in the benzoin condensation or the Stetter reaction,

meaning an ee could not be obtained due to the small quantity of product. At this stage, it is unknown why the catalyst was unsuccessful in this reaction. As previously discussed, there was some impurity in the final catalyst, which may inhibit the reaction. In addition, the extra methylene groups may either cause unwanted steric hindrance, or excess rotation which could lead to unfavourable conformations. Further optimisation of the final catalyst synthesis is needed to obtain a purer product, and future work would involve performing the reaction on a larger scale to obtain an ee and further conclude the efficacy of these catalysts.

7.1.3 Phenylalanine-Derived Catalyst

In trying to find synthetically accessible triazolium salt catalysts, a phenylalanine-derived scaffold was investigated. However, this scaffold suffered many problems of its own. Synthesis of the amide from the carboxylic acid precursor led to a decomposition product which could not be purified from the desired product. Despite the (*S*)-2-amino-N,3-diphenylpropanamide having an amide instead of the 1,2-diamine functionality, this material also suffered from the same intramolecular cyclisations, which were further stabilised by the conjugated system formed after oxidation. The combination of these factors led to an alternate synthetic route being devised, first proceeding by triazolium salt construction followed by introduction of the amide functionality.

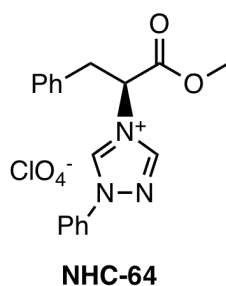


Fig. 7.3 Phenylalanine-derived catalyst **NHC-64** synthesised in Chapter 5.

Once the methyl ester catalyst **NHC-64**, precursor to the final triazolium salt, had been synthesised (Fig. 7.3), initial testing was undertaken to investigate the suitability of this

scaffold as an asymmetric catalyst *via* steric hindrance. However, acidity of the α -proton of the triazolium salt meant that racemisation of the chiral centre could occur, preventing the use of these catalysts in enantioselective synthesis. Although variation of the scaffold may help these catalysts (for example, using leucine may forbid stability by conjugation), the α -proton will still likely be acidic, and so it is probably not feasible to use these linear amino acids as a scaffold.

7.1.4 Piperidine-Derived Catalyst

Previous catalysts reported in Chapters 1 and 2 show how the bicyclic scaffold has been arguably the most important synthetic advance in improving the asymmetric reactions of triazolium salt catalysts. The catalyst designed and synthesised in Chapter 6 was important to investigate, as it would offer insight into how positioning and rotation of the hydrogen-bonding moiety is important in the benzoin condensation. After optimisation of the initial steps by Lawrence [169], the catalyst **NHC-71** was synthesised in 11 steps (Fig. 7.4).

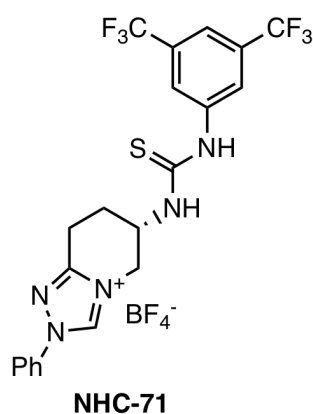


Fig. 7.4 The catalyst synthesised and tested in Chapter 6.

This catalyst suffered with many problems throughout the synthesis; most notably due to major loss of product at the diazotransfer stage, and difficulty in scale up. There are further ways to investigate this catalyst, including variation of the aryl group on the (thio)urea, and the (thio)urea itself. In comparison to Waser's catalyst, this catalyst did not perform

anywhere as effectively in the same conditions. Due to this, it appears that the free rotation is important for this. However, it may be that the hydrogen bonding moiety is just held in the wrong position, as indicated by the conformer presented in Chapter 6. Although this was a preliminary investigation into this catalyst, it is important to weigh up the benefits; the 11 step synthesis is extremely time-consuming, and is difficult to scale larger than 50 mmol, which leads to only traces of final product. This limits the application later on in areas such as industry, although may still be useful to investigate. This is a catalyst where it is particularly important to spend time extending computational studies, to truly understand the effects of flexibility and rotation in these catalysts.

7.2 Future Work

Although the catalysts reported in this work did show some asymmetric induction into the final products, the yields and ee's were not comparable to those currently from catalysts with hydrogen bonding moieties that have been previously reported [77, 78]. However, their initial findings in conjunction with this reported work show the importance of the intricate mechanism of this complex system. As discussed in Chapter 2, computational methods have proven to be a valuable tool in the design of new catalysts, based on steric configurations, unexpected interactions, and elucidation of lowest energy pathways. While the preliminary computational work reported here has been useful with steric configurations and potential detection of intramolecular bonding, comprehensive computational studies could be useful in providing insight into new catalysts. The study by Dudding and Houk [183] provided valuable insight into methods for predicting ee in the benzoin condensation; it would be useful to extend this method to include hydrogen bonding NHC catalysts. A major drawback of this work is the trial-and-error method, as successfully synthesising final catalysts is time-intensive, with no guarantee the catalyst will be effective. In particular, the bicyclic catalyst

took 11 synthetic steps in Chapter 6, and scale-up was ineffective in obtaining significant amounts of final product, meaning testing was limited.

As well as added insight from computational work, X-ray crystal structures of the catalysts could provide valuable structural information. It is possible for the hydrogen bonding group to hydrogen bond to the anion of the catalyst, particularly ClO_4^- , and this may have an effect on hydrogen bonding to the final catalyst. Initial crystallisation of **NHC-48** discussed in Chapter 3 was attempted, but due to surprisingly high solubility of the catalyst in even very apolar solvents, no crystals could be obtained. Due to the low quantities of the other catalysts synthesised in this work, no attempts were made on these. However, this could provide useful steric and bonding information in the future once higher quantities of these catalysts are obtained.

(Thio)ureas, and briefly amides, were used in this work as the hydrogen bonding moieties for these catalysts. The squaramides did not seem synthetically viable during this project. Due to their upsurge in popularity as bifunctional organocatalysts [184], lack of rotation and increased stability due to resonance, successful incorporation of these into chiral NHC catalysts still seems like an attractive option. As seen in Chapter 3, the squaramides suffer from insolubility due to intermolecular bonds between the N-H pendants and the C=O moieties of the squaramide. However, the synthesis of those catalysts required construction of the hydrogen-bonding scaffold first before formation of the triazolium salt. Taking a known successful catalyst, for example Waser's bicyclic backbone [78], and making the final step the reaction with the half squaramide/methyl squarate intermediate may increase the solubility due to lack of intermolecular hydrogen bonding as caused by steric hindrance and lack of 1,2-diamine stabilisation. This would also allow direct comparison to the existing backbone with known asymmetric induction, therefore allowing the direct comparison of the hydrogen bonding moiety.

Although some modifications of the catalysts have been investigated here, one moiety which did not undergo variation was the *N*-phenyl on the triazolium ring. As reported in

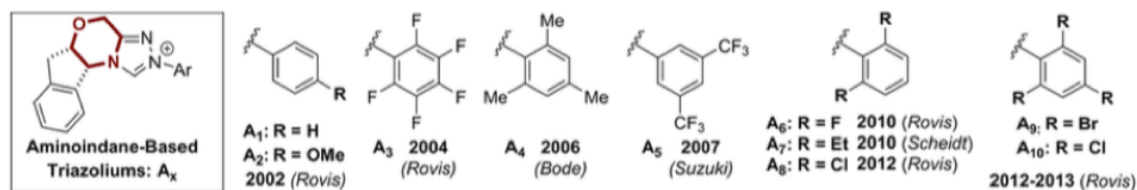


Fig. 7.5 Variations of the Ph groups, represented in the aminoindane-based triazolium catalysts collated by Rovis and coworkers [108]. The modifications were reported by: Rovis and coworkers at the *para*- position [185]; *N*-mesityl by Bode and coworkers [186]; 3,5-bis(trifluoromethyl) substitution by Suzuki and coworkers [187]; *ortho*- substitution by Rovis and coworkers [188], and Scheidt and coworkers [189]; and 2,4,6-trihalo substitution by Rovis and coworkers [190].

Chapter 2, common variations include using the *N*-mesityl or *N*-pentafluorophenyl groups, amongst others collated by Rovis and coworkers [108] (Fig. 7.5). These different aryl groups have demonstrated a large effect on the ee and yield of the materials. By varying the sterics and electronics of this ring, more insight into these systems can be gained, and a picture of how to better design these catalysts in the future. This is a simple modification which could have a significant effect, and now that optimised routes have been developed for the catalysts reported here, it could now be easily incorporated into the final catalysts due to the commercial availability of many phenylhydrazine derivatives.

Finally, the effects of reaction conditions need to be more thoroughly investigated. The catalysts synthesised and investigated here currently do not achieve high yield or ee in the conditions investigated. However, with exception of the cyclohexane-1,2-diamine-derived catalysts, these catalysts have only had a preliminary test in the benzoin condensation and Stetter reactions. As discussed in Chapter 1, the catalysts synthesised and tested by Waser and coworkers managed to achieve a maximum ee of 90% and a yield of 85% [78]. However, investigation of different bases and solvents with the catalysts here could completely change their effectiveness. Further factors such as temperature could also be investigated. With the optimised synthesis routes to the final catalysts presented in this work, these catalysts can be made in a much shorter period of time, and further investigation may lead to highly effective catalysts yet.

Chapter 8

Experimental

8.1 Computational Experimental

All 3D structures of the catalysts and their intermediates were generated from 2D structures in ChemDraw, using either Avogadro [191] or Frog2 [192]. Conformers were generated using Mercury [193] conformer generation, with 200 conformers generated, with 20 maximum unusual torsions and input molecule minimised. The conformers were then loaded back into Avogadro, and the energy minimised using MMFF94 Force Field, and a steepest descent algorithm. Relative energies were recorded in kJ mol^{-1} .

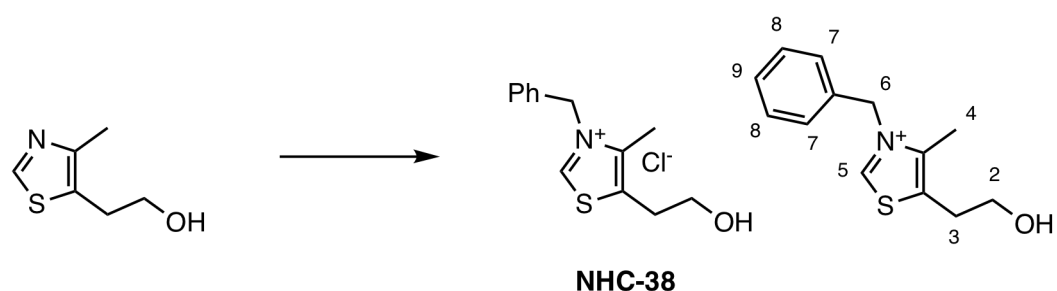
8.2 General Experimental

Commercial reagents were obtained from local suppliers Sigma-Aldrich and Alfa Aesar unless otherwise stated, and used without any further purification. All solvents used were obtained from dry solvent stills, with the exception of 1,4-dioxane, which was supplied in a dry SureSeal bottle by Sigma-Aldrich. Any glassware which was oven-dried has been specified in the experimental. Unless otherwise specified, all ^1H NMR samples were run at room temperature (25 °C) on a Bruker Avance NMR spectrometer at 400 MHz, and ^{13}C NMRs ran at 100 MHz, using Wilmad 528PP tubes. All signals reported are in ppm,

compared to standardised internal solvent peaks, as described by Gottlieb *et al.* in 1997 [194]. Internal solvent peaks are as follows in ppm: (^1H), ^{13}C : CDCl_3 (7.26) 77.2; DMSO-d_6 (2.50) 39.5; acetone- d_6 (2.05) 29.8; acetonitrile- d_3 (1.94) 1.32; methanol- d_4 (3.31) 49.0; D_2O (4.79). Melting points were obtained using a thermal melting point apparatus, Reichert Austria, with samples contained on glass coverslips. CHN analysis was performed by the Analytical Services, Dept. of Chemistry, University of Cambridge. TLC analysis was performed on Merck Kieselgel 60 (230-400 mesh) glass-backed plates. UV active spots were visualised using ultra-violet UV light at 254 nm, and then visualised using potassium permanganate dip, iodine or ninhydrin spray reagent as appropriate. LC/MS analysis was performed on a Waters 2795 system, with UV detection at 254 nm, using a Supelco ABZ + plus column, 3.3 cm x 4.6 mm, with particle size 3 μm . ee was obtained based on separation by HPLC using an Astec Cellulose DMP chiral column, 5 μm particle size, L x I.D. 25 cm x 4.6 mm, with isopropanol:hexane as the mobile phase. Individual conditions (times, flow rates) are reported with the spectra.

8.2.1 Chapter 2: Design and Testing of New Catalysts

Synthesis of Stetter's Achiral Thiazolium Salt NHC-38 [137]



4-Methyl-5-thiazole ethanol (1 eq, 10 mmol, 1.43 g), benzyl chloride (1 eq, 10 mmol, 1.27 g, 1.15 mL) and MeCN (5 mL) were stirred in a round-bottomed flask. A reflux condenser was fitted, and the reaction was heated to reflux for 24h. The mixture was allowed to cool to ambient temperature whilst stirring for a further 48h, in which time the product precipitated

out. The solid was collected under vacuum filtration, washed using MeCN, and further dried under reduced pressure to afford the product **NHC-38** (2.068 g, 77%, 7.67 mmol) as a pale peach solid.

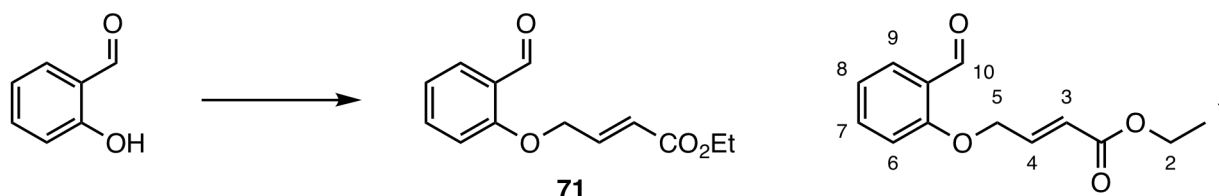
^1H NMR (DMSO- d_6 , 400 MHz, δ) 10.19 (s, 1H, **H₅**), 7.48 - 7.39 (m, 3H, **H₇** or **H₈**, **H₉**), 7.34 - 7.30 (m, 2H, **H₇** or **H₈**), 5.79 (s, 2H, **H₆**), 3.63 (t, 2H, $J = 5.6$ Hz, **H₂**), 3.01 (t, 2H, $J = 5.6$ Hz, **H₃**), 2.35 (s, 3H, **H₄**).

^{13}C NMR (DMSO- d_6 , 100 MHz, δ) 157.1, 136.3, 133.1, 129.3, 129.0, 128.1, 59.7, 55.8, 29.6, 11.6.

high-resolution mass spectrometry (HRMS) for $[\text{M}+\text{H}]^+$ Predicted = 234.0953, Obtained = 234.092.

CHN Calculated C 57.88 H 5.98 N 5.19 Obtained C 57.89 H 5.95 N 5.30. Data matches literature values [137].

Synthesis of Ethyl (*E*)-4-(2-formylphenoxy)but-2-enoate **71** [195]



Salicylaldehyde (1 eq, 10 mmol, 1.22 g) was suspended in DMF (25 mL) and K_2CO_3 (1.5 eq, 15 mmol, 2.07 g) added. To this was added a dropwise solution of ethyl-4-bromocrotonate (75%, 1 eq, 13.3 mmol, 1.63 g) in DMF (5 mL) with stirring. This was stirred for a further 24h. The mixture was poured onto 100 g of ice with stirring. The product was extracted with Et_2O (x3), dried (MgSO_4), and the volatile solvent removed. The crude product was dry-loaded (silica) and purified by column chromatography (20% EtOAc/hexane) to give the product **71** (744 mg, 3.18 mmol, 32%) as a yellow solid.

^1H NMR (CDCl_3 , 400 MHz, δ) 10.55 (s, 1H, **H**₁₀), 7.86 (dd, 1H, $J = 1.8, 7.7$ Hz, **H**₉), 7.57 - 7.52 (m, 1H, **H**₃), 7.14 - 7.04 (m, 2H, **H**_{7/8}), 6.94 (d, 1H, $J = 8.4$ Hz, **H**₆), 6.21 (dt, 1H, $J = 2.0, 15.7$ Hz, **H**₄), 4.83 (dd, 2H, $J = 2.0$ Hz, **H**₅), 4.23 (q, 2H, $J = 7.1$ Hz, **H**₂), 1.31 (t, 3H, $J = 7.1$ Hz, **H**₁).

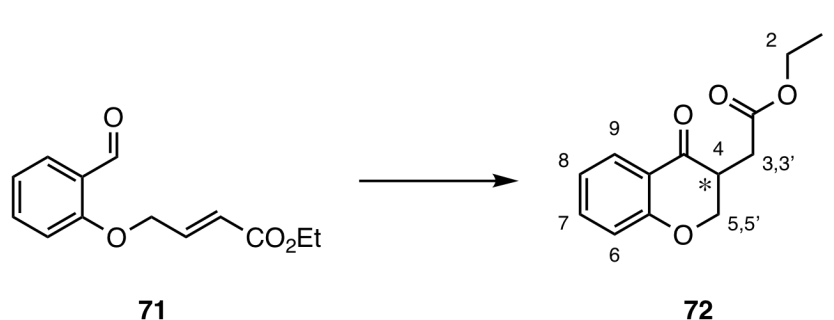
^{13}C NMR (CDCl_3 , 100 MHz, δ) 189.4, 165.9, 160.3, 141.3, 136.0, 128.9, 125.2, 122.7, 121.6, 112.7, 67.0, 60.9, 13.3.

Fourier-transform Infrared Spectroscopy (FTIR) (ν_{max} cm^{-1}) 2979 (C-H), 2866 (C-H aldehyde), 1712 (C=O ester), 1684 (C=O aldehyde), 1665 (C=C), 1597 (C=C arom).

$[\text{M}+\text{Na}]^+$ Obtained 257.0775, Calculated 257.0790.

R_f 0.38 (20% EtOAc/hexane).

General Conditions for the Stetter Reaction [139]



To a 5cm³ round bottomed flask was added the pre-catalyst (20 mol%), and the flask evacuated/flushed with N₂ (x3). Toluene (2.5 mL) was added, and the mixture stirred. KHDMS in toluene (20 mol%, 50 μ L) was added, and stirred for 15 minutes. Ethyl (*E*)-4-(2-formylphenoxy)but-2-enoate **71** (1 eq, 0.06 mmol, 14 mg) in toluene (1 mL) was added to the mixture dropwise and stirred at room temperature under N₂ for a further 24h. The volatile solvents were removed under a stream of N₂ and passed through a silica plugged pipette (20% EtOAc/hexane) to give the product ethyl 2-(4-oxochroman-3-yl)acetate **72**.

^1H NMR (CDCl_3 , 400 MHz, δ) 7.89 (dd, 1H, $J = 1.6, 7.9$ Hz, **H**₉), 7.51 - 7.46 (m, 1H, **H**₇), 7.03 (t, 1H, $J = 7.5$ Hz, **H**₈), 6.97 (d, 1H, $J = 8.6$ Hz, **H**₆), 4.60 (dd, 1H, $J = 5.3, 11.1$

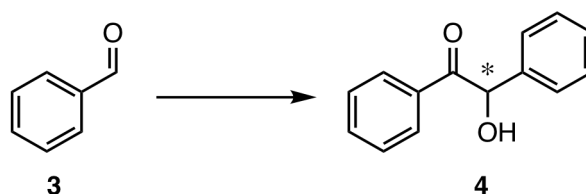
Hz, **H**_{5/5'}), 4.30 (t, 1H, $J = 11.1$ Hz, **H**₄), 4.19 (qd, 2H, $J = 2.0, 7.1$ Hz, **H**₂), 3.38 - 3.29 (m, 1H, **H**_{5/5'}), 2.94 (dd, 1H, $J = 4.8, 16.9$ Hz, **H**_{3/3'}), 2.42 (dd, 1H, $J = 8.1, 16.8$ Hz, **H**_{3/3'}), 1.29 (t, 3H, $J = 7.1$ Hz, **H**₁).

[**M**+**Na**]⁺ Obtained 257.0793, calculated 257.0790.

R_f = 0.42 (20% EtOAc/hexane). Data matches the literature [139].

HPLC analysis: Astec Cellulose DMP chiral column; 40°C; 0-40 min; 0.5mL/min; solvent system: 10/90 isopropanol/hexane; peak 1: 30.9 min, peak 2: 33.5 min.

General Conditions for the Benzoin Condensation [78]



A 1 mM solution of benzaldehyde **3** in solvent was made up. Benzaldehyde (1 mL) was taken up in CH₂Cl₂ (50 mL) and washed with NaHCO₃ (3x50 mL). The organic layer was dried (MgSO₄) and the volatile solvents removed under reduced pressure. The benzaldehyde was distilled off using vacuum distillation (T 130-140 °C, p 23 mbar) to afford the pure product. This was stored under N₂, weighed, and made up into a 1 mM solution with various solvents.

The catalyst (5 mol%) was added to a 1 dram vial with a screw top with the base (5 mol%) and dried in a dessicator overnight. This was removed and put under N₂. To this was added the benzaldehyde solution (0.25 mL, 0.25 mmol benzaldehyde), the vial sealed and stirred at room temperature for 24 h. In the cases where benzoin was isolated, the solution was purified on a pipette silica column (elution 20% EtOAc / pet ether) to afford the product benzoin **4**. Data matches a pure sample of commercially available benzoin.

¹H NMR (CDCl₃, 400 MHz δ) 7.94 – 7.89 (m, 2H, **Ar**), 7.52 (tt, 1H, $J = 1.3, 7.4$ Hz, **Ar**), 7.39 (app t, 2H, $J = 7.7$ Hz, **Ar**), 7.36 – 7.24 (m, 5H, **Ar**), 5.96 (s, 1H, -CH(OH)-), 4.56 (s, 1H, O-H).

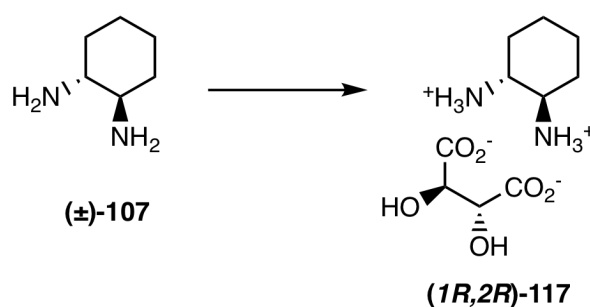
^{13}C NMR (CDCl_3 , 100 MHz, δ) 199.3, 139.1, 134.0, 133.6, 129.3, 129.2, 128.8, 128.7, 127.9, 76.3.

FTIR ν_{max} (cm^{-1}) 3377, 1677, 1594, 1577, 1490.

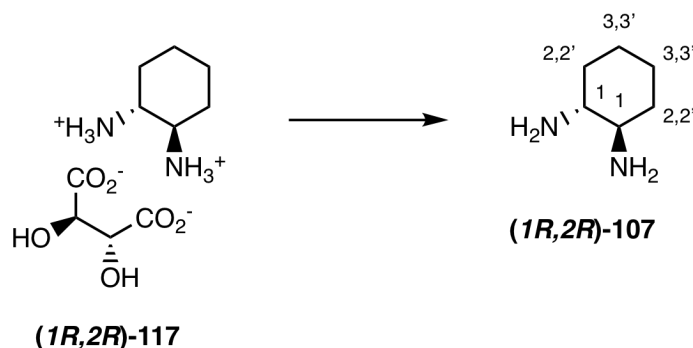
HPLC analysis: Astec Cellulose DMP chiral column; 40°C; 0-40 min; 0.5mL/min; solvent system: 10/90 isopropanol/hexane; peak 1: 14.5 min, peak 2: 19.7 min.

8.2.2 Chapter 3: 1,2-Diamine-Derived Catalysts

Chiral resolution of (\pm)-*Trans*-1,2-diaminocyclohexane **107**



Distilled water (50 mL) was added to a 250 mL Erlenmeyer flask and stirred. *L*-(+)-Tartartic acid (0.1 mol, 15 g) was added in one portion. (\pm)-*Trans*-1,2-diaminocyclohexane (\pm)-**107** (0.2 mol, 23 g, 24 mL, 1 eq) was added carefully in one portion. A slurry was formed. Glacial acetic acid (10 mL) was added in one portion and stirred for 3h, giving an exotherm. The product precipitated, and the reaction was cooled from 60°C to 0°C with stirring in an ice bath for 1 h. This was filtered, and the crude product washed with ice cold water and MeOH. The product was dried both under reduced pressure on a rotary evaporator followed by a dessicator, to give the product (*1R,2R*)-**117** (21.45 g, 83%, 0.08 mol) as a white powder. No data was taken as this will be converted to the free diamine before use. [146].

Liberation of (1*R*,2*R*)-diaminocyclohexane 107 from the chiral tartaric acid salt

The diamine tartaric acid salt **(1*R*,2*R*)-117** (6.40 g, 24.2 mmol) was dissolved in a mixture of 5M NaOH (4 eq, 19 mL) and CH₂Cl₂ (19 mL). This was stirred for 1h. The organic layer was separated, the aqueous layer washed with further CH₂Cl₂, and the organic layers combined. This was dried (MgSO₄), filtered, and the volatile solvent removed under reduced pressure to afford (1*R*,2*R*)-diaminocyclohexane **(1*R*,2*R*)-107** (842 mg, 7.50 mmol, 31%). [146]. Data matches the commercially obtained material. See Chapter 3 for chiral HPLC analysis.

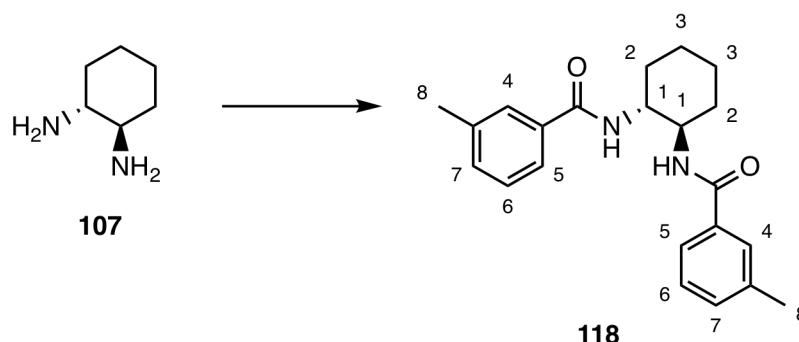
¹H NMR (400 MHz, CDCl₃, δ) 2.27 - 2.17 (m, 2H, **H**₁), 1.87 - 1.77 (m, 2H, **H**_{2/2'}), 1.72 - 1.61 (m, 2H, **H**_{2/2'}), 1.30 - 1.22 (m, 2H, **H**_{3/3'}), 1.14 - 1.02 (m, 2H, **H**_{3/3'}).

¹³C NMR (100 MHz, CDCl₃, δ) 57.9, 35.7, 25.6.

FTIR ν_{max} (cm⁻¹) 2919 (N-H), 2853 (C-H), 1585 (N-H scissoring), 1447 (CH₂ deformation).

HRMS for [M+H]⁺ Obtained 235.0759, required 235.0735.

Synthesis of *N,N'*-((1*R*,2*R*)-cyclohexane-1,2-diyl)bis(3-methylbenzamide) **118**



(±)-*Trans*-1,2-diaminocyclohexane (1 eq, 114 mg, 1.0 mmol, 0.12 mL) was stirred in CH₂Cl₂ (10 mL) and NEt₃ (6 eq, 6 mmol, 607 mg, 0.84 mL) added. This was cooled to -10°C, and *m*-toluoyl chloride (2.1 eq, 155 mg, 0.13 mL) added dropwise. The reaction was warmed to ambient temperature and stirred for 24h. The reaction was quenched with brine, and the product extracted with CH₂Cl₂. The organic layer was dried (MgSO₄) and pre-loaded onto silica before purifying by column chromatography (elution 50% EtOAc/hexane) to afford the product **118** (242 mg, 0.69 mmol, 69%) as a white powder [146].

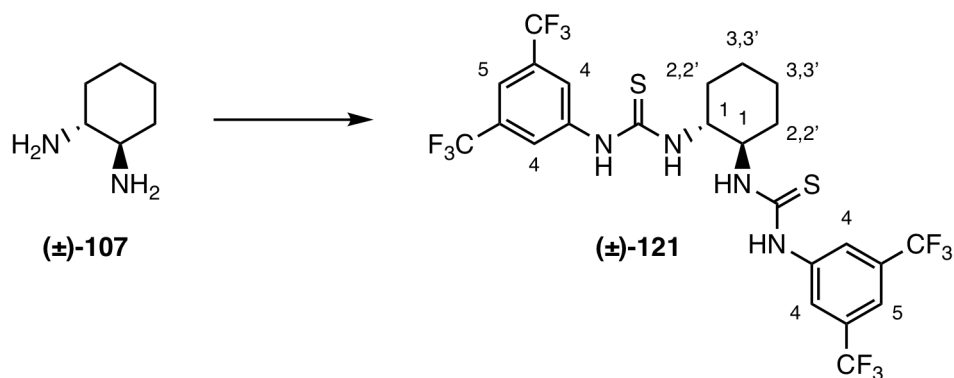
¹H NMR (CDCl₃, 400 MHz, δ) 7.58 (s, 2H, **H**₄), 7.56 - 7.52 (m, 2H, **H**₅), 7.28 - 7.23 (m, 4H, **H**₆₊₇), 6.97 (br s, 2H, N-H), 3.99 - 3.93 (m, 2H, **H**₁), 2.34 (s, 6H, **H**₈), 2.21 - 2.15 (m, 2H, **H**_{2/2'}), 1.79 - 1.73 (m, 2H, **H**_{2/2'}), 1.42 - 1.31 (m, 4H, **H**_{3,3'}).

¹³C NMR (100 MHz, CDCl₃, δ) 168.6, 138.4, 134.4, 132.3, 128.6, 127.9, 124.2, 54.7, 32.5, 25.0, 21.5.

HRMS for [M+H]⁺ Obtained 351.2060, required 351.2073.

FTIR ν_{max} (cm⁻¹) 3290 (N-H), 2924 (C-H), 1631 (Amide C=O), 1584, 1533 (amide II band).

Synthesis of 1,1'-((\pm)-*trans*-cyclohexane-1,2-diyl)bis(3-(3,5-bis(trifluoromethyl)phenyl)thiourea) **121 using THF**

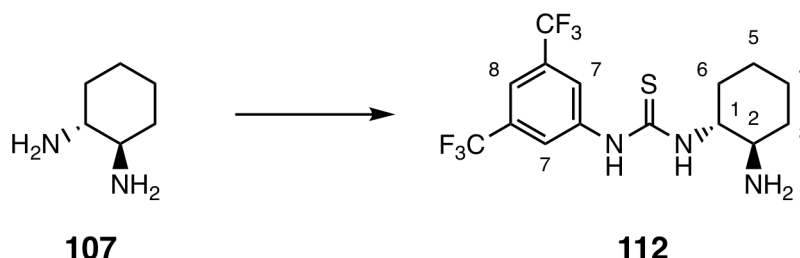


1-Isothiocyanato-3,5-bis(trifluoromethyl)benzene **109** (0.37 mL, 2 mmol) was added to a stirred solution of (\pm)-*trans*-cyclohexane-1,2-diamine (\pm)-**107** (0.24 mL, 2 mmol) in dry THF (6 mL) dropwise at 0 °C. After the reaction mixture was cooled to ambient temperature, and the resulting solution was stirred for 22h. The solvent was removed and the residue was purified by a silica gel plug. The major product was 1,1'-((\pm)-*trans*-cyclohexane-1,2-diyl)bis(3-(3,5-bis(trifluoromethyl)phenyl)thiourea) **121** (576 mg, 0.88 mmol, 44%). NMR is in accordance with the literature [155].

^1H NMR (400 MHz, DMSO- d_6 , δ) 10.12 (s, 2H, N-H), 8.17 (br s, 6H, **H**₄ + N-H overlapped), 7.70 (s, 2H, **H**₅), 4.34 (br s, 2H, **H**₁), 2.18 (br s, 2H, **H**_{2/2'}), 1.72 (br s, 2H, **H**_{2/2'}), 1.30 (br s, 4H, **H**_{3,3'}). **^{13}C NMR** (100 MHz, DMSO- d_6 , δ) 180.1, 141.6, 130.2 (q, J = 33 Hz), 122.2, 123.2 (q, J = 271 Hz), 116.2, 56.8, 31.2, 24.2.

R_f 0.40 (20% EtOAc/hex)

Synthesis of 1-((1*R*,2*R*)-2-aminocyclohexyl)-3-(3,5-bis(trifluoromethyl)phenyl)thiourea **112 using CH₂Cl₂**



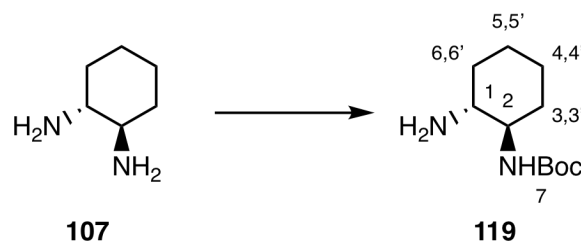
(1*R*,2*R*)-1,2-Diaminocyclohexane (\pm)-**107** (1 eq, 842 mg, 7.50 mmol) was stirred in dry CH₂Cl₂ (100 mL) at 0 °C. To this was added a solution of 1-isothiocyanato-3,5- bis(trifluoromethyl) benzene **109** (0.67 eq, 1.36 g, 5.00 mmol, 0.92 mL) in dry CH₂Cl₂ (30 mL) dropwise over an hour. This was stirred for 2h at 0 °C, the ice bath removed, and stirred at ambient temperature for a further 24 h. The CH₂Cl₂ was removed under reduced pressure to give a yellow oil. The crude material was purified (silica) using 10% MeOH / CH₂Cl₂. A pure fraction of 1-((1*R*,2*R*)-2-aminocyclohexyl)-3-(3,5- bis(trifluoromethyl)phenyl) thiourea **112** (1.49 g, 3.85 mmol, 76%) was obtained as a clear crystalline solid. NMR is in accordance with the literature [196].

¹H NMR (400 MHz, CD₃OD, δ) 8.13 (s, 2H, **H**₇), 7.54 (s, 1H, **H**₈), 4.25-4.19 (m, 1H, **H**₁), 2.62-2.59 (m, 1H, **H**₂), 2.04-1.92 (m, 2H, **H**_{3/3'/6/6'}), 1.70-1.66 (m, 2H, **H**_{3/3'/6/6'}), 1.35-1.10 (m, 4H, **H**_{4,4',5,5'}).

¹³C NMR (100 MHz, CD₃OD, δ) 179.2, 140.6, 129.7, 129.3, 123.4, 121.1, 120.6, 108.8, 60.3, 53.8, 31.7, 29.6, 24.0, 23.9.

HRMS for [**M+H**]⁺ Obtained 386.1122, required 386.1126.

FTIR ν_{max} (cm⁻¹) 2925 (sm), 1534 (sm) 1471 (sm) 1380 (m)

Synthesis of *tert*-butyl-((\pm)-*trans*-2-aminocyclohexyl)carbamate **119**

(\pm)-*Trans*-1,2-diaminocyclohexane (\pm)-**107** (1.142 g, 1.20 mL, 18 mmol) was stirred in distilled water (8.5 mL) at room temperature. Di-*tert*-butyl-dicarbonate (436 mg, 2 mmol) was dissolved in 1,4-dioxane (3.2 mL) and the solution added dropwise to the diamine. This was stirred at room temperature for 22 h. The volatile solvents were removed under reduced pressure, the crude product dissolved in distilled water (6 mL), and the insoluble bis-substituted product removed by filtration. The product was extracted from water using CH_2Cl_2 , and the organic layer washed with distilled water. The organic layer was dried using MgSO_4 , the solids filtered, and the volatile solvents removed under reduced pressure to afford *tert*-butyl-((*trans*)-2-aminocyclohexyl)carbonate **119** (230 mg, 1.07 mmol, 54%) as a yellow powder. NMR is in accordance with the literature [197].

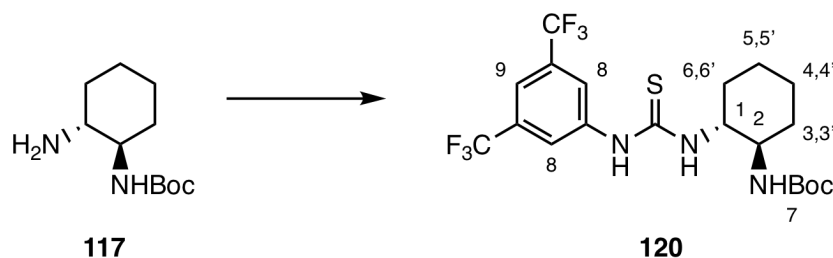
^1H NMR (400 MHz, CDCl_3 , δ) 4.43 (br s, 1H, **H₂**), 3.13 (br s, 1H, **H₁**), 2.27 (m, 1H, **H_{3/3'}**), 1.97 (m, 2H, N-H), 1.84 (m, 1H, **H_{3/3'}**), 1.70 (m, 2H **H_{6,6'}**), 1.42 (s, 9H, **H₇**), 1.33 - 1.00 (m, 4H, **H_{4,4',5,5'}**).

^{13}C NMR (100 MHz, CDCl_3 , δ) 156.3, 67.03, 57.9, 55.9, 35.7, 33.1, 28.5, 25.6, 25.3.

HRMS for $[\text{M}+\text{H}]^+$ Obtained 215.1758, required 215.1760.

FTIR ν_{max} (cm^{-1}) 3360 (N-H), 3271 (N-H), 2930 (C-H), 1681 (C=O amide), 1598 (N-H scissoring), 1515 (N-H amide).

Synthesis of *tert*-butyl-((1*R*,2*R*)-2-(3-(3,5-bis(trifluoromethyl)phenyl)thioureido)cyclohexyl)carbamate **120**



1-isothiocyanato-3,5-bis(trifluoromethyl)benzene **109** (290 mg, 195 μ L, 1.07 mmol) was added *via* microsyringe to a stirred solution of *tert*-butyl-((\pm)-*trans*-2-aminocyclohexyl)-carbamate **119** (230 mg, 1.07 mmol) in dry THF (6 mL) slowly and dropwise at 0°C. This was cooled to ambient temperature and stirred for 27h. After this time, further 1-isothiocyanato-3,5-bis(trifluoromethyl)benzene **109** (89 mg, 60 μ L, 0.33 mmol) was added dropwise at 0°C, heated to 40°C and stirred for 19h. The reaction was cooled to ambient temperature, and the volatile solvents removed under reduced pressure. The crude product was purified (silica) elution 30% EtOAc/ heptane to afford the product as a brown oil. This was dissolved in Et₂O and removed under reduced pressure to give the product (\pm)-**120** as an orange-brown crystalline solid (135 mg, 0.28 mmol, 26%).

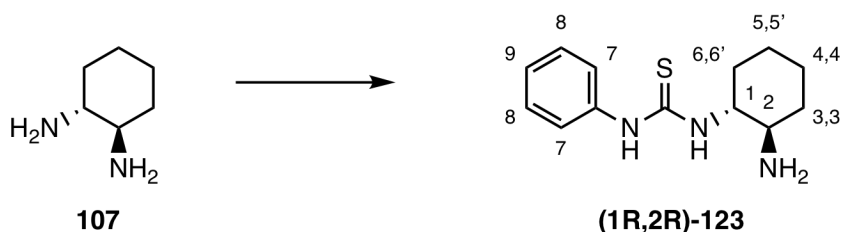
¹H NMR (DMSO-d₆, 400 MHz, δ) 8.22 (s, 2H, **H₈**), 7.89 (br s, 1H, N-**H**), 7.73 (s, 1H, **H₉**), 6.83 (br s, 1H, N-**H**), 4.11 (br s, 1 H, **H₁**), 2.09 (br s, 1H, **H₂**), 1.86-1.76 (m, 2H, **H_{3,3',6,6'}**), 1.69-1.61 (br s, 2H, **H_{3,3',6,6'}**), 1.32 (br s, 9H, **H₇**), 1.21-1.04 (m, 4H, **H_{4,4',5,5'}**).

¹³C NMR (DMSO-d₆, 100 MHz, δ) 180.2, 156.4, 122.5 (q, *J* = 563 Hz), 122.3 (q, *J* = 22 Hz), 78.3, 57.3, 53.5, 32.3, 28.6, 24.5.

HRMS for [**M+H**]⁺ Obtained 485.1598, required 485.1572.

R_f 0.38 (20% EtOAc/hex).

Synthesis of 1-((1*R*,2*R*)-2-aminocyclohexyl)-3-(3,5-bis(trifluoromethyl) phenyl)thiourea **123**



(1*R*,2*R*)-1,2-Diaminocyclohexane **107** (1 eq, 590 mg, 5.17 mmol) was stirred in CH₂Cl₂ at 0°C under N₂. The flask was fitted with a pressure equalising dropping funnel, and a solution of phenyl isothiocyanate **122** (0.67 eq, 468 mg, 3.46 mmol, 0.42 mL) in CH₂Cl₂ (6 mL) was added dropwise over 15 minutes. The mixture was allowed to warm to ambient temperature, and stirred for 22 hours. The solution was acidified to pH 3 using 1M HCl, until a precipitate formed. This was removed *via* vacuum filtration, and dissolved in 1M NaOH until pH 12 was reached. The product was extracted using CH₂Cl₂, dried (MgSO₄) and the volatile solvent removed under reduced pressure to afford the product **123** (799 mg, 3.20 mmol, 93%).

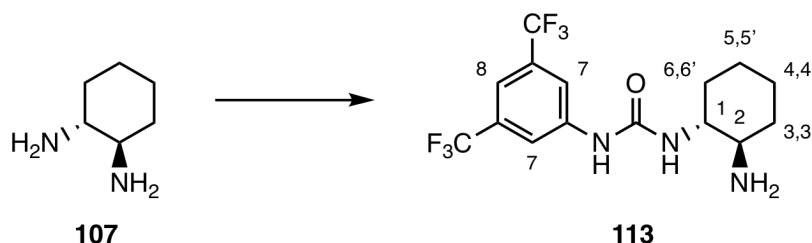
¹H NMR (CDCl₃, 400 MHz, δ) 7.44 – 7.34 (m, 2H, **H**_{7/8}), 7.33 – 7.21 (m, 3H, **H**_{7/8,9}), 6.06 (d, 1H, *J* = 6.6 Hz, N-**H**), 4.19 – 3.89 (m, 1H, **H**₁), 2.59 – 2.37 (m, 1H, **H**₂), 2.21 – 2.10 (m, 1H, **H**_{6/6'}), 1.99 – 1.87 (m, 1H, **H**_{3/3'}), 1.78 – 1.65 (m, 2H, **H**_{3/3'/6/6'}), 1.41 – 1.17 (m, 4H, **H**_{4,4',5,5'}).

¹³C NMR (CDCl₃, 100 MHz, δ) 158.7, 129.7, 129.6, 124.4, 123.6, 62.1, 35.0, 32.1, 29.4, 24.9, 24.0.

HRMS for [**M+H**]⁺ Obtained 250.1421, required 250.1378.

R_f (10% MeOH/CH₂Cl₂)

Synthesis of 1-((1*R*,2*R*)-2-aminocyclohexyl)-3-(3,5-bis(trifluoromethyl)phenyl)urea **113**



(±)-*Trans*-1,2-diaminocyclohexane **107** (1.14 g, 1.20 mL, 10 mmol) was stirred in dry CH₂Cl₂ (135 mL) at 0°C under N₂. A solution of 1-isocyanato-3,5-bis(trifluoromethyl)benzene (1.71 g, 1.16 mL, 6.7 mmol) in dry CH₂Cl₂ (30 mL) was added dropwise to the amine over an hour. This was stirred for a further 30 minutes at 0°C, the ice bath removed, and stirred at ambient temperature for 66 hours. The solution was acidified to pH 3 using 1M HCl, and washed with CH₂Cl₂. The aqueous layer was basified to pH 12, and the desired product extracted using CH₂Cl₂. This was dried (MgSO₄) and the volatile solvents removed under reduced pressure to afford the product **113** (1.08 g, 1.92 mmol, 41%).

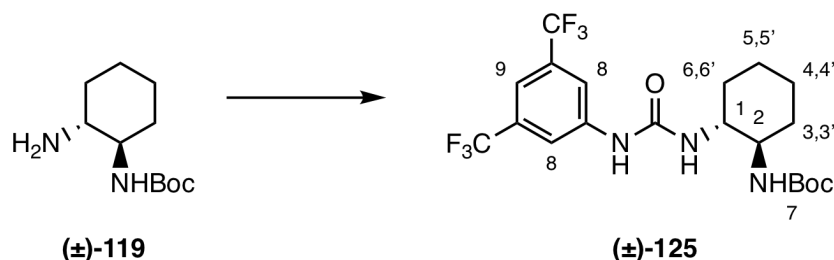
¹H NMR (DMSO-*d*₆, 400 MHz, δ) 9.35 (br s, 1H, N-**H**), 8.08 (s, 2H, **H**₇), 7.54 (s, 1H, **H**₈), 6.57 (d, 1H, *J* = 8.0 Hz, N-**H**), 4.34 (br s, 2H, **NH**₂), 3.30 - 3.22 (m, 1H, **H**₁), 2.62 - 2.52 (m, 1H, **H**₂), 1.94 - 1.78 (m, 2H, **H**_{3/3'/6/6'}), 1.72 - 1.56 (m, 2H, **H**_{3/3'/6/6'}), 1.34 - 1.06 (m, 4H, **H**_{4,4',5,5'}).

¹³C NMR (DMSO-*d*₆, 100 MHz, δ) 154.8, 142.7, 130.6 (*q*, *J* = 32.5 Hz), 123.6 (*q*, *J* = 283.5 Hz), 117.3, 113.4, 54.3, 54.2, 33.1, 31.9, 24.6, 24.1.

HRMS for [**M+H**]⁺ found = 370.1328, required = 370.1354. Data matches the literature [155].

FTIR ν_{max} (cm⁻¹) 3291 2893 (m) 1668 (C=O) 1551

Synthesis of *tert*-butyl-*trans*-((±)-2-(3-(3,5-bis(trifluoromethyl)phenyl)ureido)cyclohexyl) carbamate (±)-125



Tert-butyl-((±)-*trans*-2-aminocyclohexyl)carbamate **119** (1 eq, 1.030 g, 4.81 mmol) was dissolved in dry CH₂Cl₂ (10 mL), put under an N₂ atmosphere and cooled to 0 °C. A solution of 1-isocyanato-3,5-bis(trifluoromethyl)benzene **124** (1 eq, 4.81 mmol, 0.83 mL, 1.23 g) in dry CH₂Cl₂ (1 mL) was added with stirring. The reaction was allowed to warm to ambient temperature and stirred for 20h. The solid was filtered, and washed with dry Et₂O to afford the product (±)-**125** as a white powder (1.839 g, 3.92 mmol, 82%).

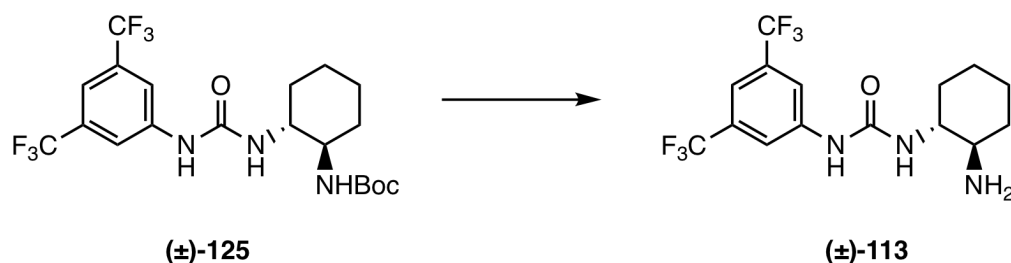
¹H NMR (DMSO-d₆, 400 MHz, δ) 9.26 (br s, 1H, N-H), 8.04 (s, 2H, **H**₈), 7.53 (s, 1H, **H**₉), 6.73 (d, 1H, *J* = 8.8 Hz, N-H), 6.16 (d, 1H, *J* = 8.3 Hz, N-H), 3.44 - 3.34 (m 1H, **H**₁), 3.26 - 3.14 (m, 1H, **H**₂), 1.93 - 1.84 (m, 1H, **H**_{6/6'}), 1.80 - 1.72 (m, 1H, **H**_{3/3'}), 1.68 - 1.58 (m, 2H, **H**_{3/3'/6/6'}), 1.27 (s, 9H, **H**₇), 1.24 - 1.12 (m, 4H, **H**_{4,4',5,5'}).

¹³C NMR (DMSO-d₆, 100 MHz, δ) 155.9, 154.7, 142.8, 130.7 (q, *J* = 32.5 Hz), 123.4 (q, *J* = 272.5 Hz), 117.2, 113.4, 77.6, 53.7, 53.6, 32.6, 32.0, 28.1, 24.6, 24.5.

CHN calculated C 51.17; H 5.37; N 8.95 Obtained C 51.16; 5.40; 8.93

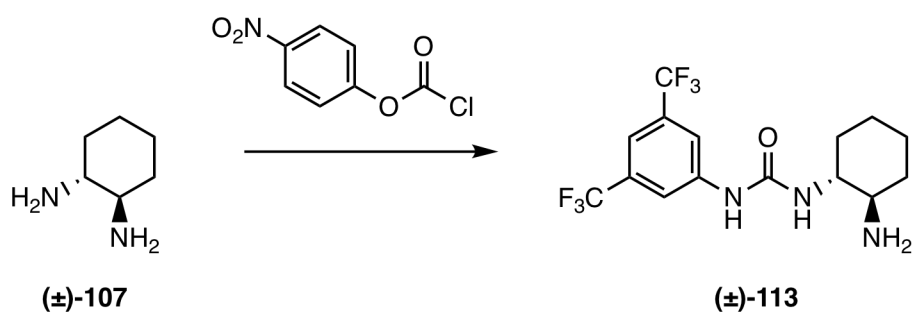
HRMS for [M+H]⁺ calculated = 480.1878, observed = 470.1902. Data matches the literature [152].

Synthesis of 1-((1*R*,2*R*)-2-aminocyclohexyl)-3-(3,5-bis(trifluoromethyl)phenyl)urea **113
via Boc-deprotection of (±)-**125****



tert-Butyl-((±)-*trans*-2-(3-(3,5-bis(trifluoromethyl)phenyl) ureido)cyclohexyl)carbamate **125** (1.83 g, 3.90 mmol) was stirred in a solution of trifluoroacetic acid (5 eq, 19.5 mmol, 15 mL) in dry CH₂Cl₂ (60 mL) at room temperature under an N₂ atmosphere for 18h. The volatile solvents were removed under vacuum, the pH adjusted to pH 10 with 2M NaOH, and the product extracted using CH₂Cl₂. The layer was dried (MgSO₄) and the volatile solvent removed under reduced pressure to afford the product **113** (1.10 g, 2.98 mmol, 76%) as a white powder. Data matches previous synthesis.

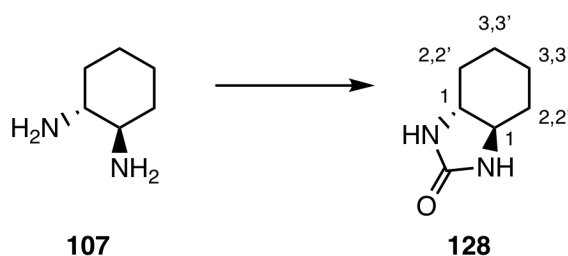
Synthesis of 1-((1*R*,2*R*)-2-aminocyclohexyl)-3-(3,5-bis(trifluoromethyl)phenyl)urea **113
via 4-nitrophenyl chloroformate**



3,5-bis(Trifluoromethyl)aniline (1 eq, 3 mmol, 470 µL) was stirred in CH₂Cl₂ (9.9 mL) at room temperature. Pyridine (1.1 eq, 3.3 mmol, 267 µL) was added, followed by 4-nitrophenyl chloroformate (1 eq, 3 mmol, 605 mg) and the mixture stirred for 5 minutes. A solution

of (\pm)-*trans*-1,2-diaminocyclohexane **107** (3 eq, 9 mmol, 1.08 mL) in CH₂Cl₂ (3.3 mL) was added, followed by DIPEA (3 eq, 9 mmol, 1.57 mL), and stirred for 2h. The mixture was washed with NaHCO₃ (x2), brine (x2) and H₂O (x2). A precipitate formed which was filtered out, and the mother liquor was dried (MgSO₄), and the volatile solvent removed under reduced pressure. The crude product was purified using silica column chromatography (elution 10% MeOH/ CH₂Cl₂) to afford the pure product (\pm)-**113** (213 mg, 0.58 mmol, 19%). NMR matches previous.

Synthesis of (3aR,7aR)-octahydro-2H-benzo[d]imidazol-2-one (*1R,2R*)-**128**



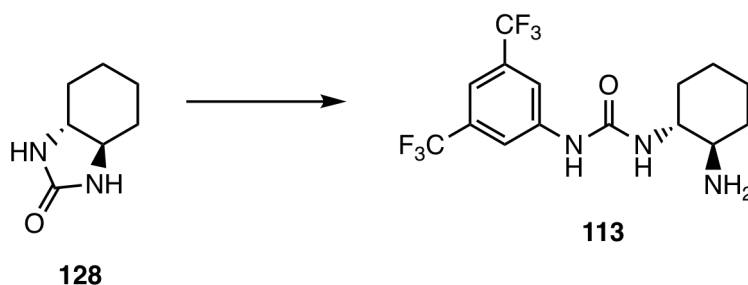
(*1R,2R*)-1,2-diaminocyclohexane (1 eq, 314 mg, 2.75 mmol) was dissolved in *iso*-propanol (3 mL). Diphenyl carbonate (1.1 eq, 648 mg, 3.02 mmol) was added, and the mixture refluxed at 85°C for 18h. The mixture was filtered, the solids washed with MeOH, and the volatile solvents of the filtrate removed under reduced pressure. The crude oil was purified using silica column chromatography (elution 10% MeOH/CH₂Cl₂). The solvent was removed under reduced pressure to afford the product **128** (325 mg, 2.38 mmol, 87%) as a white powder.

¹H NMR (CDCl₃, 400 MHz, δ) 4.86 (br s, 2H, N-H), 3.17 - 3.09 (m, 2H, **H**₁), 1.99 - 1.92 (m, 2H, **H**_{2,2'}), 1.83 - 1.77 (m, 2H, **H**_{2,2'}) (+ small impurity), 1.50 - 1.30 (m, 4H, **H**_{3,3'}).

¹³C NMR (CDCl₃, 100 MHz, δ) 165.6, 61.2, 29.6, 24.1.

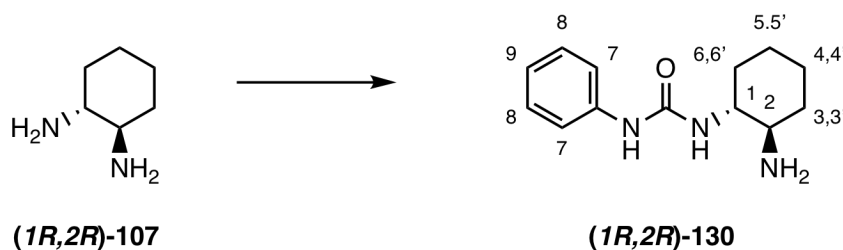
R_f = 0.43 (10% MeOH/CH₂Cl₂). Data is in accordance with the literature [155].

Synthesis of 1-((1*R*,2*R*)-2-aminocyclohexyl)-3-(3,5-bis(trifluoromethyl)phenyl)urea **113
via (3*aR*,7*aR*)-octahydro-2*H*-benzo[*d*]imidazol-2-one (**128**)**



(3*aR*,7*aR*)-octahydro-2*H*-benzo[*d*]imidazol-2-one **128** (1 eq, 280 mg, 2.0 mmol) was dissolved in diglyme (0.5 mL). To this was added 3,5-bis(trifluoromethyl) aniline (1.05 eq, 477 mg, 2.1 mmol, 330 μ L) and methanesulfonic acid (0.14 mL), and the solution heated at 120 $^{\circ}$ C for 40 minutes. The mixture was left to cool, and H₂O (5 mL) was added followed by NaHCO₃ (0.98 g). The product was extracted with EtOAc (x2), dried (MgSO₄), and the volatile solvents removed under reduced pressure. The mixture was dissolved in EtOAc, acidified to pH 3 using 1M HCl, and the aqueous layer basified to pH 12 using 1M NaOH. The product was extracted with EtOAc, dried (MgSO₄), and the volatile solvents removed under reduced pressure to afford the product **113** (91 mg, 12%, 0.25 mmol). The data matches previous.

Synthesis of 1-((1*R*,2*R*)-2-aminocyclohexyl)-3-(3,5-bis(trifluoromethyl)phenyl)urea **130**



(1*R*,2*R*)-1,2-diaminocyclohexane **107** (1 eq, 630 mg, 5.52 mmol) was stirred in CH₂Cl₂ (50 mL) at 0°C under N₂. The flask was fitted with a pressure equalising dropping funnel, and a solution of phenyl isocyanate (0.67 eq, 440 mg, 3.70 mmol, 0.40 mL) in CH₂Cl₂ (10 mL) added dropwise over 15 minutes. The mixture was allowed to warm to ambient temperature, and stirred for 20 hours. A precipitate formed, which was removed *via* filtration. The mother liquor was acidified to pH 3 using 1M HCl, the layers separated, and 1M NaOH added to the aqueous layer until pH 12 was reached. The product was extracted using CH₂Cl₂, dried (MgSO₄) and the volatile solvent removed under reduced pressure to afford the product **130** (186 mg, 0.80 mmol, 22%).

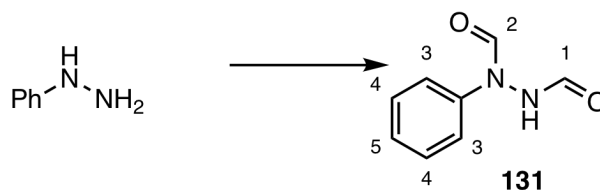
¹H NMR (CD₃OD, 400 MHz, δ) 7.35 (app d, 2H, *J* = 7.7 Hz, **H₈**), 7.24 (app t, 2H, *J* = 7.9 Hz, **H₈**), 6.97 (app t, 1H, *J* = 7.4 Hz, **H₇**), 3.36 (td, 1H, *J* = 4.1, 10.6 Hz, **H₁**), 2.46 (td, 1H, *J* = 3.8, 10.3 Hz, **H₂**), 2.02 - 1.93 (m, 2H, **H_{3/3'/6/6'}**), 1.78 - 1.69 (m, 2H, **H_{3/3'/6/6'}**), 1.40 - 1.21 (m, 4H, **H_{4,4',5,5'}**).

¹³C NMR (CD₃OD, 100 MHz, δ) 158.3, 140.9, 129.8, 123.4, 120.2, 56.8, 56.2, 34.9, 33.9, 26.3, 25.9. Data matches the literature [155].

HRMS for [M+H]⁺ Calculated 234.1606, observed 234.1590.

R_f = (10% MeOH/CH₂Cl₂).

Synthesis of *N,N'*-diformyl-*N*-phenyl hydrazine **132**



Phenylhydrazine (5.0 mL, 50.8 mmol) was cooled to 0°C and stirred. Formic acid (12.0 mL, 318 mmol) was added, turning the solution a crimson colour. This was fitted with a reflux condenser and the reaction was heated under reflux at 80°C for 22h. The solution was allowed to cool to room temperature, and dry Et₂O was added and put in the fridge for 48h

to encourage precipitation. The solid was filtered recrystallised from hot EtOH in 4 batches to give the product **131** (2.51g, 15.3 mmol, 30%) as shiny off-white powder.

^1H NMR (400 MHz, DMSO- d_6 , δ) 10.80 (s, 1H, N-H), 8.93 (s, 0.1H, **H₂**), 8.80 (s, 0.50H, **H₂**), 8.53 (s, 0.05H, **H₁**), 8.39 (s, 0.40H, **H₂**), 8.29 (s, 0.35H, **H₁**), 8.28 (s, 0.50H, **H₁**), 8.13 (s, 0.10H, **H₁**), 7.58 - 7.17 (m, 5H, **H_{3,4,5}**).

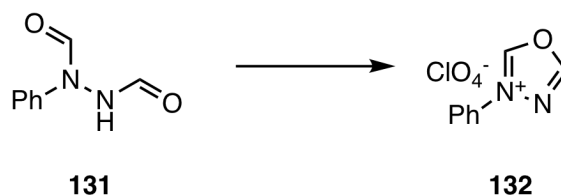
^{13}C NMR (100 MHz, DMSO- d_6 , δ) 163.9, 161.5, 160.0, 159.7, 148.1, 129.6, 129.0, 126.1, 126.0, 121.0, 119.7.

FTIR ν_{max} (cm^{-1}) 3158 (N-H) 2926 (C-H) 1687 (C=O) 1652 (C=O) 1590 (N-H amide)

HRMS for $[\text{M}+\text{Na}]^+$ Calculated 187.0368, observed 187.0368.

CHN found C 58.62, H 4.86, N 16.87, required C 58.53, H 4.91, N 17.06.

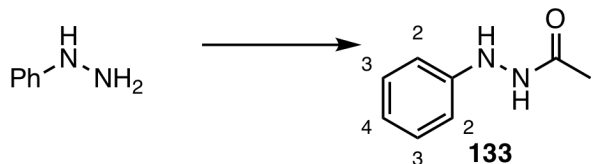
Synthesis of 3-phenyl-1,3,4-oxadiazol-3-ium perchlorate **132**



To a dry round-bottomed flask was added *N,N'*-diformyl-*N*-phenyl hydrazine **131** (492 mg, 3.00 mmol). This was cooled to 0°C under an N_2 atmosphere, and Ac_2 (8.8 eq, 2.50 mL) added. HClO_4 (70%) (0.55 mL, 2.98 mmol) was added dropwise over and stirred for 15 minutes until a solid precipitated. The mixture was vacuum filtered under a stream of N_2 , and the solid washed with dry Et_2O (2 mL). The material **132** was a white powder (609 mg, 2.48 mmol, 83%).

No ^1H NMR or ^{13}C NMR could be obtained due to instability of the compound. The IR spectra was in accordance with the literature [76].

FTIR ν_{max} (cm^{-1}) 3066, 1691, 1328, 1058, 767, 664.

Synthesis of *N*'-phenylacetohydrazide **133**

To an oven-dried round-bottomed flask was added phenylhydrazine (3.0 mL, 30.5 mmol), and placed under an N₂ atmosphere. Dry CH₂Cl₂ (20 mL) was added, stirred and cooled to 0°C. NEt₃ (2.60 mL, 18.3 mmol) was added *via* syringe and stirred for 15 minutes. An oven-dried pressure equalising dropping funnel was fitted, and Ac₂O (1.50 mL, 16.2 mmol) in dry CH₂Cl₂ (35 mL) added dropwise at 0°C over 7h. This was allowed to warm to room temperature and stirred for 62h. The organic layer was washed with 2M NaOH, separated, dried (MgSO₄), and the volatile solvents removed under reduced pressure. The orange solid was washed with EtOAc to afford **133** as an off-white solid (1.26 g, 8.38 mmol, 52%).

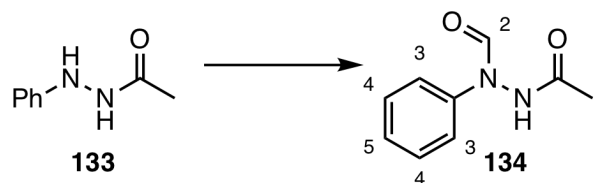
¹H NMR (DMSO-d₆, 400MHz, δ) 9.59 (0.88H, d, *J* = 2.3 Hz, N-H), 8.91 (0.12H, s, N-H) 7.95 (0.12H, s, N-H), 7.63 (0.88H, d, *J* = 2.3 Hz, N-H), 7.21-7.18 (0.24H, app t, H_{2,3,4}), 7.15-7.12 (1.76H, app t), 6.77-6.74 (0.36H, app t, H_{2,3,4}), 6.71 - 6.70 (2.64H, m, H_{2,3,4}), 1.90 (2.64H, s, H₁), 1.86 (0.36H, s, H₁). Ratio of 0.12 : 0.88 rotamers.

¹³C NMR (DMSO-d₆, 100MHz, δ) 175.2, 169.0, 149.4, 148.8, 129.1, 128.7, 118.9, 118.4, 112.1, 111.5, 20.6, 19.2.

CHN Obtained C 63.88; H 6.67; N 18.77. Required C 63.98; H 6.71; N 18.65.

HRMS for [M+H]⁺ Obtained 150.0867, requires 150.0871. Data matches the literature [76].

Synthesis of *N'*-formyl-*N'*-phenylacetohydrazide **134**



N'-phenylacetohydrazide **133** (1 eq, 2.61 g, 17.38 mmol) was added to a round-bottomed flask, and formic acid (2.82 eq, 1.85 mL, 49.01 mmol) was added dropwise at 0°C. This was then heated to 50°C for 24 h. After cooling to room temperature, dry Et₂O was added, and the mixture stored in the fridge overnight to encourage precipitation. The solid was filtered and washed with dry Et₂O. The crude product was recrystallized from hot EtOH to give the product **134** (1.76 g, 57%, 9.88 mmol) as a white powder.

2 rotamers in a ratio 0.40 : 0.60.

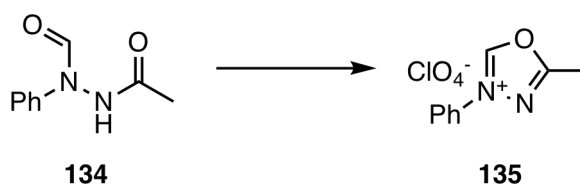
¹H NMR (DMSO-d₆, 400MHz, δ) 10.95 (s, 0.40 H, **H**₂), 10.52 (s, 0.60 H, **H**₂), 8.79 (s, 0.60 H, N-**H**), 8.26 (s, 0.40 H, N-**H**), 7.50 - 7.16 (m, 5 H, **H**_{3,4,5}), 2.03 (s, 1.20 H, **H**₁), 2.00 (s, 1.80 H, **H**₁).

¹³C NMR (DMSO-d₆, 100MHz, δ) 169.8, 168.3, 164.2, 159.7, 140.9, 139.7, 129.4, 128.8, 125.7, 125.6, 120.7, 119.4, 20.4.

HRMS for [M+H]⁺ Obtained 179.0829, required 179.0821. Data matches the literature [76].

R_f = 0.66 (10% MeOH/CH₂Cl₂)

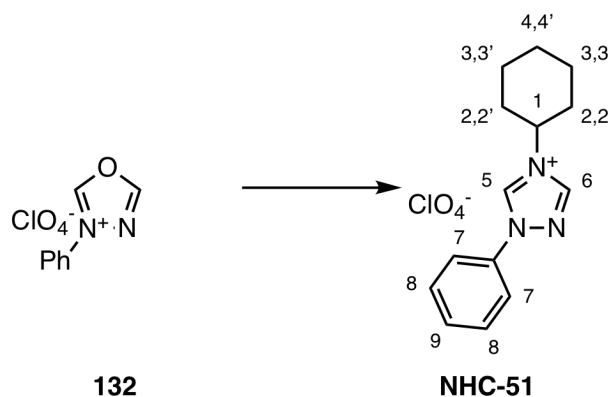
Synthesis of 5-methyl-3-phenyl-1,3,4-oxadiazol-3-ium perchlorate **135**



To a dry round-bottomed flask was added *N*'-formyl-*N*-phenylacetohydrazide **134** (1 eq, 750 mg, 4.20 mmol). This was cooled to 0°C under an N₂ atmosphere, and Ac₂O (8.8 eq, 3.45 mL) was added. HClO₄ (70%) (0.36 mL, 2.40 mmol) was added dropwise and stirred for 15 minutes. The mixture was vacuum filtered under a stream of N₂, and the solid washed with dry Et₂O (1 mL) to afford the product **135** (1 eq, 520 mg, 84%) as a white powder.

Used crude immediately in further steps due to instability.

Synthesis of 4-cyclohexyl-1-phenyl-1*H*-1,2,4-triazol-4-ium perchlorate NHC-51 using MeCN



3-phenyl-1,3,4-oxadiazol-3-ium perchlorate **132** (225 mg, 0.91 mmol) and oven-dried 3Å molecular sieves (270 mg, pellets) were added to an oven dried round bottomed flask. This was sealed with a Suba-Seal and put under an N₂ atmosphere. A solution of dry MeCN (2.2 mL) and cyclohexylamine (90 mg, 0.11 mL, 0.91 mmol) were added *via* syringe. This was stirred for 70 h at room temperature. Dry Et₂O (2.0 mL) was added to encourage precipitation, and the solid filtered under a stream of N₂ to afford 4-cyclohexyl-1-phenyl-4*H*-1,2,4-triazol-1-ium perchlorate **NHC-51** (111 mg, 35%) as a yellow solid. All data was in accordance with the literature [76].

¹H NMR (400 MHz, DMSO-d₆, δ) 10.86 (s, 1H, **H**_{5/6}) 9.54 (s, 1H, **H**_{5/6}) 7.94 (m, 2H, **H**₇) 7.68 (m, 3H, **H**_{8,9}) 4.45 (tt, 1H, *J* = 3.8, 11.7 Hz, **H**₁) 2.25 (d, 2H, *J* = 5.5 Hz, **H**_{2,2'}) 1.96 – 1.62 (m, 5H **H**_{2/2',3/3'/4/4'}) 1.53 – 1.33 (m, 2H, **H**_{3/3'/4/4'}) 1.32 – 1.13 (m, 1H, **H**_{3/3'/4/4'}).

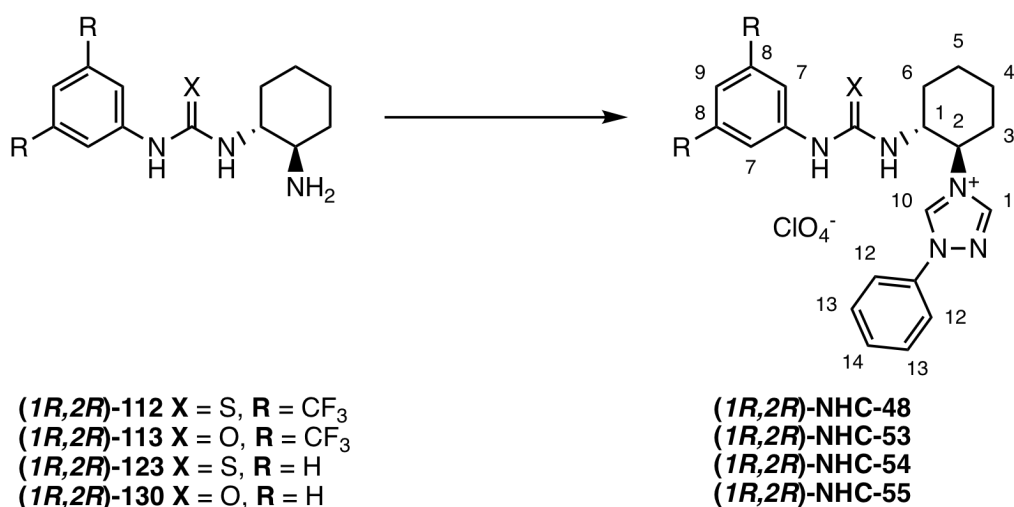
^{13}C NMR (100 MHz, DMSO- d_6 , δ) 144.3, 140.9, 135.6, 130.9, 130.6, 121.1, 58.8, 32.5, 24.8, 24.6.

HRMS for $[\text{M}^+]$ Obtained 228.1635, required 228.1501.

mp 254°C (Lit. 248 – 250°C)

CHN Found: C, 50.2; H = 5.5; N = 12.6. Requires C = 51.3; H = 5.5; N = 12.8).

General synthesis of cyclohexyl-(1,2)-diamine (thio)urea triazolium salts



4-((1*R*,2*R*)-2-(3-(3,5-bis(trifluoromethyl)phenyl)thioureido)cyclohexyl)-1-phenyl-1*H*-1,2,4-triazol-4-ium perchlorate NHC-48

3-Phenyl-1,3,4-oxadiazol-3-ium perchlorate **132** (1 eq, 571 mg, 2.32 mmol) was added to an oven-dried round-bottomed flask, and AcOH (1.86 mL) added. 1-((1*R*,2*R*)-2-aminocyclohexyl)-3-(3,5-bis(trifluoromethyl)phenyl)thiourea (**1*R*,2*R*)-112** (1 eq, 895 mg, 2.32 mmol) was added, and heated to 80°C for 1h. The solvents were removed under reduced pressure, the crude product dissolved in CH₂Cl₂ and washed with 5M HCl (x3) and the aqueous washed with CH₂Cl₂. The organics were combined, dried (MgSO₄), filtered, and the volatile solvents removed under reduced pressure. This was purified by silica column chromatography (elution 10% MeOH/CH₂Cl₂) to afford the product (**1*R*,2*R*)-NHC-48** (182 mg, 0.29 mmol, 13%).

¹H NMR (CDCl₃, 400 MHz, δ) 11.83 (s, 1H, **H**_{10/11}), 10.36 (s, 1H, N-**H**), 9.05 (d, 1H, J = 9.4 Hz, N-**H**), 8.85 (s, 1H, **H**_{10/11}), 7.96 (s, 2H, **H**₇), 7.93 - 7.86 (m, 2H, **H**₁₂), 7.52 - 7.45 (m, 4H, **H**_{9,13,14}), 4.94 (qd, 1H, J = 4.0, 10.8 Hz, **H**₁), 4.80 Hz (td, 1H, J = 4.0 Hz, 11.5 Hz, **H**₂), 2.47-2.39 (m, 1H, **H**_{3/3'/6/6'}), 2.29 - 2.22 (m, 1H, **H**_{3/3'/6/6'}), 2.16 - 2.07 (m, 1H, **H**_{3/3'/6/6'}), 2.04 - 1.99 (m, 1H, **H**_{3/3'/6/6'}), 1.96 - 1.87 (m, 1H, **H**_{4/4'/5/5'}), 1.74 - 1.61 (m, 1H, **H**_{4/4'/5/5'}), 1.61 - 1.47 (m, 2H, **H**_{4/4'/5/5'}).

¹³C NMR (CDCl₃, 100 MHz, δ) 181.7, 142.2, 140.8, 140.7, 134.6, 131.6, 131.4, 131.3, 130.5, 123.0, 120.4, 117.8 (q, J = 4.0 Hz), 64.2, 56.3, 31.9, 30.8, 24.6, 24.5.

HRMS for [**M**]⁺ Obtained 514.1481, required 514.1495.

FTIR ν_{\max} (cm⁻¹) 2921, 1542, 1473, 1382.

R_f 0.35 (10% MeOH/CH₂Cl₂)

4-((1*R*,2*R*)-2-(3-(3,5-bis(trifluoromethyl)phenyl)ureido)cyclohexyl)-1-phenyl-1*H*-1,2,4-triazol-4-ium perchlorate NHC-53

3-phenyl-1,3,4-oxadiazol-3-ium perchlorate **132** (2.5 mmol, 615 mg) was added to an oven-dried round-bottomed flask, and sealed under N₂. AcOH (2.0 mL) was added, followed by 1-((1*R*,2*R*)-2-aminocyclohexyl)-3-(3,5-bis(trifluoromethyl) phenyl)urea (**1*R*,2*R***)-**113** (1 eq, 923 mg, 2.5 mmol). This was heated to 110°C for 2h. The work-up was as previous to obtain the product (**1*R*,2*R***)-**NHC-53** (32 mg, 5%, 0.13 mmol) as a white powder.

¹H NMR (DMSO-d₆, 400 MHz, δ) 11.25 (s, 1H, N-**H**), 9.99 (s, 1H, **H**₁₀), 9.49 (s, 1H, **H**₁₁), 7.88 - 7.38 (m, 2H, **H**₁₂), 7.79 (s, 2H, **H**₇), 7.69 - 7.30 (m, 3H, **H**_{13,14}), 7.47 (s, 1H, **H**₉), 7.23 (d, 1H, J = 8.5 Hz, N-**H**), 4.50 - 4.39 (m, 1H, **H**₁), 4.01 - 3.89 (m, 1H, **H**₂), 2.33 - 2.23 (m, 1H, **H**_{3/3'}), 2.21 - 2.10 (m, 1H, **H**_{3/3'/6/6'}), 2.08 - 2.00 (m, 1H, **H**_{6/6'}), 1.95 - 1.80 (m, 2H, **H**_{4/4'/5/5'}), 1.59 - 1.49 (m, 1H, **H**_{3/3'/6/6'}), 1.47 - 1.38 (m, 2H, **H**_{4/4'/5/5'}).

¹³C NMR (DMSO-d₆, 100 MHz, δ) 154.8, 144.9, 142.0, 141.6, 134.9, 130.7, 130.6, 130.4, 130.1, 123.2 (q, J = 273 Hz), 120.6, 117.1 (m), 63.6, 52.9, 31.4, 30.4, 24.2, 24.0.

HRMS for [**M**+]⁺ Found 498.1745, required 498.1729.

FTIR ν_{\max} (cm⁻¹) 3393 (sm), 3123 (sm), 2957 (C-H), 1661 (m), 1584 (m), 1512 (m).

R_f 0.06 (10% MeOH/CH₂Cl₂)

1-phenyl-4-((1*R*,2*R*)-2-(3-phenylureido)cyclohexyl)-1*H*-1,2,4-triazol-4-ium perchlorate NHC-54

The reaction to form the product was as above from starting material **123**. After turning the reaction off, the volatile solvents were removed and the mixture purified (silica, 10% MeOH/CH₂Cl₂) to afford the pure product (64 mg, 0.14 mmol, 21% yield).

¹H NMR (CDCl₃, 400 MHz, δ) 10.49 (s, 1H, **H**_{10/11}), 8.80 (s, 1H, **H**_{10/11}), 7.68 - 7.61 (m, 2H, **H**_{7/8/12/13}), 7.47 - 7.36 (m, 3H, **H**_{7/8/12/13}), 7.11 (app d, 2H, $J = 7.8$ Hz, **H**_{7/8/12/13}), 7.05 (app t, 2H, $J = 7.8$ Hz, **H**_{9/14}), 6.88 (app t, 1H, $J = 7.2$ Hz, **H**_{9/14}), 6.23 (d, 1H, $J = 9.3$ Hz, N-H), 4.53 (td, 1H, $J = 3.6, 11.4$ Hz, **H**₁), 4.07 (qd, 1H, $J = 3.6, 10.4$ Hz, **H**₂), 2.44 - 2.35 (m, 1H, **H**_{6/6'}), 2.19 - 2.12 (m, 1H, **H**_{3/3'}), 2.10 - 1.97 (m, 2H, **H**_{3/3'/6/6'}), 1.95 - 1.88 (m, 1H, **H**_{4/4'/5/5'}), 1.62 - 1.46 (m, 3H + H₂OH_{4/4'/5/5'}).

¹³C NMR (CDCl₃, 100 MHz, δ) 155.4, 142.6, 139.9, 138.7, 134.6, 131.1, 130.3, 128.7, 122.8, 120.8, 119.3, 65.0, 53.0, 32.3, 31.1, 24.7, 24.6.

HRMS for [M]⁺ Obtained 378.1724, required 378.1752.

FTIR ν_{\max} (cm⁻¹) 3379 (N-H), 2934 (C-H), 1670 (C=O), 1596 (C=C), 1540 (N-H scissoring), 1497 (C=N).

R_f 0.16 (10% MeOH/CH₂Cl₂)

1-phenyl-4-((1*R*,2*R*)-2-(3-phenylthioureido)cyclohexyl)-1*H*-1,2,4-triazol-4-ium perchlorate NHC-55.

The reaction to form the product was as above from starting material **130**. After turning the reaction off, the volatile solvents were removed and the mixture purified (silica, 10% MeOH/CH₂Cl₂) to afford the pure product (51 mg, 0.11 mmol, 15%).

¹H NMR (CDCl₃, 400 MHz, δ) 10.29 (s, 1H, N-H), 8.78 (s, 1H, **H**_{10/11}), 8.28 (br s, 1H, **H**_{10/11}), 7.78 - 7.71 (m, 2H, **H**_{7/8/9/12/13/14}), 7.57 - 7.48 (m, 3H, **H**_{7/8/9/12/13/14}), 7.32 - 7.18

(m, 5H, **H**_{7/8/9/12/13/14}), 7.14 - 7.09 (m, 1H, N-**H**), 4.96 (qd, 1H, *J* = 3.7, 10.4 Hz, **H**₁), 4.68 (td, 1H, *J* = 3.7, 11.5 Hz, **H**₂), 2.51 - 2.43 (m, 1H, **H**_{6/6'}), 2.25 - 2.17 (m, 1H, **H**_{3/3'}), 2.06 - 1.97 (m, 2H, **H**_{3/3'/6/6'}), 1.96 - 1.90 (m, 1H, **H**_{4/4'/5/5'}), 1.71 - 1.48 (m, 3H, + H₂O, **H**_{4/4'/5/5'}).

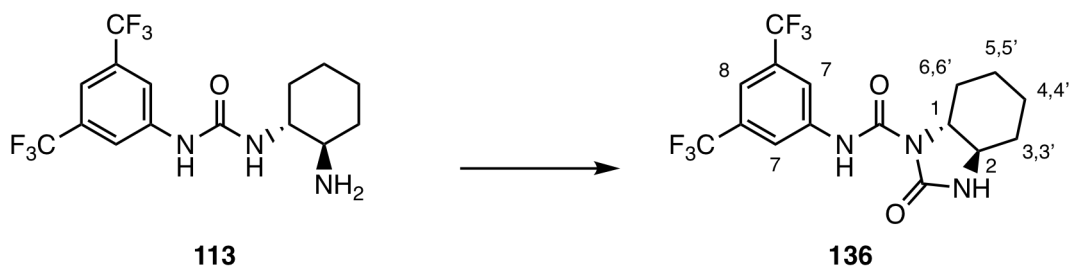
¹³C NMR (CDCl₃, 100 MHz, δ) 182.1, 142.9, 139.8, 138.1, 134.8, 131.3, 130.5, 128.8, 126.1, 124.9, 121.1, 64.1, 56.4, 31.8, 31.3, 24.6, 24.5.

FTIR ν_{\max} (cm⁻¹) 3319, 2938, 1674, 1596, 1568, 1529.

HRMS for [**M**]⁺ obtained 378.1724, req 378.1752.

R_f 0.43 (10% MeOH/CH₂Cl₂)

Synthesis of (3a*R*,7a*R*)-*N*-(3,5-bis(trifluoromethyl)phenyl)-2-oxooctahydro-1*H*-benzo[*d*]-imidazole-1-carboxamide **136**



1-((1*R*,2*R*)-2-aminocyclohexyl)-3-(3,5-bis(trifluoromethyl)phenyl)urea **113** (1.2 mmol, 443 mg, 1 eq) was dissolved in DMSO (0.6 mL), and 20N NaOH (1 eq, 1 mmol, 48 mg, 60 μ L) added. This was cooled to 0 °C, and CS₂ (1 eq, 1 mmol, 91 mg, 76 μ L) added dropwise to give a red solution. The ice bath was removed, the reaction stirred for 10 mins to give a yellow solution with a brown solid. The ice bath returned, 3-chloro-2-butanone (1 eq, 1.2 mmol, 128 mg, 121 μ L) was added dropwise, and stirred at rt for 20h. Distilled H₂O (1.2 mL) was added, the reaction cooled to 0°C and stirred for 15 minutes. The liquid was decanted, the solid dissolved in EtOH (1.2 mL) and HCl (conc, 0.06 mL) added. This was heated to 80°C reflux with a water condenser for 1h. The volatile solvents were removed under reduced pressure, and the crude material purified using silica column chromatography (50%

EtOAc/hexane) to afford (3a*R*,7a*R*)-*N*-(3,5-bis(trifluoromethyl)phenyl)-2-oxooctahydro-1*H*-benzo[*d*]imidazole-1-carboxamide (120 mg, 0.30 mmol, 25%) **136** as the major product.

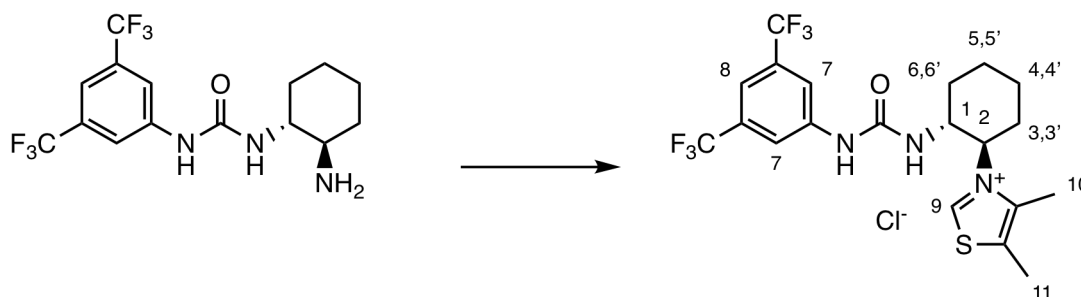
¹H NMR (CDCl₃, 400 MHz, δ) 10.60 (s, 1H, N-**H**), 7.99 (s, 2H, **H**₇), 7.54 (s, 1H, **H**₈), 5.22 (s, 1H, N-**H**), 3.53 (td, 1H, *J* = 3.0, 11.1 Hz, **H**₁), 3.23 (td, 1H, *J* = 3.0, 11.2 Hz, **H**₂), 3.00 - 2.93 (m, 1H **H**_{6/6'}), 2.10 - 2.03 (m, 1H, **H**_{3/3'}), 1.96 - 1.85 (m, 2H, **H**_{3/3'/6/6'}), 1.64 - 1.37 (m, 4H, **H**_{4,4',5,5'}).

¹³C NMR (CDCl₃, 100 MHz, δ) 160.8, 151.9, 139.6, 132.6, 132.2, 123.2 (q, *J* = 276 Hz), 119.5 (m), 116.9, 63.9, 58.3, 30.1, 29.5, 24.3, 24.0.

CHN Calculated C 48.61, H 3.82, N 10.63. Obtained C 48.49, H 3.83, N 10.07.

FTIR ν_{max} (cm⁻¹) 3303, 1722, 1687, 1549, 1450.

Synthesis of 3-((1*R*,2*R*)-2-(3-(3,5-bis(trifluoromethyl)phenyl)ureido)cyclohexyl)-4,5-dimethylthiazol-3-ium chloride NHC-50-Cl



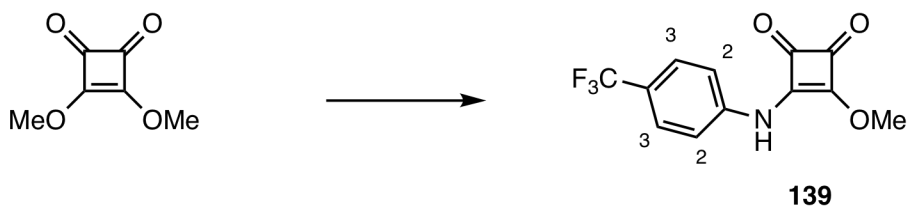
1-((1*R*,2*R*)-2-aminocyclohexyl)-3-(3,5-bis(trifluoromethyl)phenyl)urea **130** (3 mmol, 1.10 g, 1 eq) was dissolved in DMSO (1.5 mL), and 20N NaOH (1 eq, 1 mmol, 120 mg, 150 μ L) added. This was cooled to 0 °C, and CS₂ (1 eq, 1 mmol, 228 mg, 180 μ L) added dropwise. The ice bath was removed, the reaction stirred for 1h. The ice bath was replaced, 3-chloro-2-butanone (1 eq, 3 mmol, 320 mg, 303 μ L) was added dropwise, and the mixture was stirred at ambient temperature for 20h. Distilled H₂O (3 mL) was added, the reaction cooled to 0°C and stirred for 15 minutes. The liquid was decanted, the residue dissolved in EtOH (3 mL) and HCl (conc, 0.15 mL) added. This was heated to 80°C reflux with a water

condenser for 1h. The material was passed through a silica column (100% EtOAc) to afford (1*R*,2*R*)-NHC-50-Cl (60 mg, 0.12 mmol, 4%).

¹H NMR (CDCl₃, 400 MHz, δ) 10.22 (s, 1H, N-H), 9.51 (s, 1H, **H**₉), 8.24 (s, 1H, **H**₈), 7.84 (s, 2H, **H**₇), 7.34 (s, 1H, N-H), 4.81 - 4.70 (m, 1H, **H**₁), 4.44 - 4.32 (m, 1H, **H**₂), 2.71 (s, 3H, **H**_{10/11}), 2.48 (s, 3H, **H**_{10/11}), 2.25 - 2.17 (m 4H, **H**_{3/3'/6/6'}), 1.96 - 1.84 (m, 2H, **H**_{4/4'/5/5'}), 1.60 - 1.49 (m, 2H, **H**_{4/4'/5/5'}).

¹³C NMR (CDCl₃, 100 MHz, δ) 153.29, 141.43, 133.91, 131.96, 131.63, 124.82, 122.11, 118.03, 114.83, 67.79, 52.76, 41.12, 32.95, 24.96, 24.69, 12.74.

Synthesis of 3-methoxy-4-((4-(trifluoromethyl)phenyl)amino)-cyclobut-3-ene-1,2-dione **139**



Dimethyl squarate (3.80 mmol, 540 mg, 1 eq.) and dry MeOH (12 mL) were stirred at room temperature. 4-trifluoromethylaniline (3.80 mmol, 612 mg, 0.48 mL, 1 eq.) was added *via* syringe, and stirred for 42h. The solid was filtered to afford 3-methoxy-4-((4-(trifluoromethyl)phenyl)amino)cyclobut-3-ene-1,2-dione **139** (690 mg, 2.54 mmol, 67%) as a yellow powder.

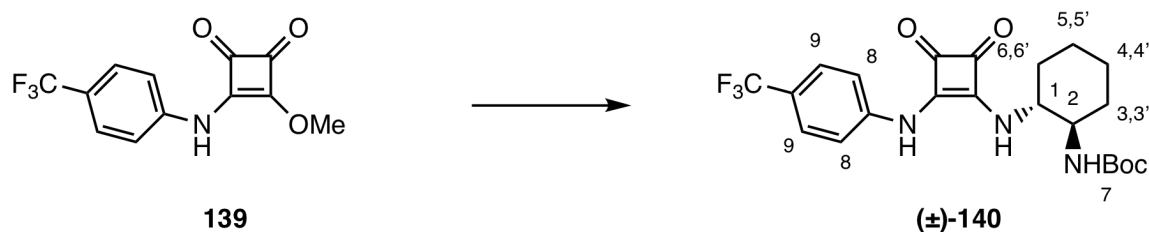
¹H NMR (400 MHz, DMSO-d₆, δ) 11.01 (s, 1H, N-H), 7.71 (d, 2H, *J* = 8.5 Hz, **H**₃), 7.55 (d, 2H, *J* = 8.5 Hz, **H**₂), 4.40 (s, 3H, **H**₁).

¹³C NMR (100 MHz, DMSO-d₆, δ) 187.6, 184.5, 179.6, 169.2, 141.6, 126.4 (q, *J*_{C-F} = 3.8 Hz), 123.8 (q, *J*_{C-F} = 22.2 Hz), 123.0, 119.4, 60.8. Data matches the literature [45].

HRMS for [**M**+**H**]⁺ Found 272.0507, required 272.0535.

FTIR ν_{\max} (cm⁻¹) 3189, 3113, 1800, 1715, 1610, 1566, 1539, 1514. Data matches the literature [198].

Synthesis of *tert*-butyl-(*trans*-(\pm)-2-((3,4-dioxo-2-((4-(trifluoromethyl)phenyl)amino)-cyclobut-1-en-1-yl)amino)cyclohexyl)carbamate (\pm)-140



3-methoxy-4-((4-(trifluoromethyl)phenyl)amino)cyclobut-3-ene-1,2-dione **139** (1 eq, 339 mg, 1.25 mmol) was added to a stirred solution of *tert*-butyl (*trans*-(\pm)-2-aminocyclohexyl)carbamate **119** (1.5 eq, 402 mg, 1.88 mmol) in dry CH_2Cl_2 (5 mL), and stirred at rt for 19h. The volatile solvents were removed under reduced pressure, and impurities washed out of the solid under vacuum using dry Et_2O . This afforded the product (\pm)-**140** as an off-white solid (400 mg, 0.88 mmol, 71%).

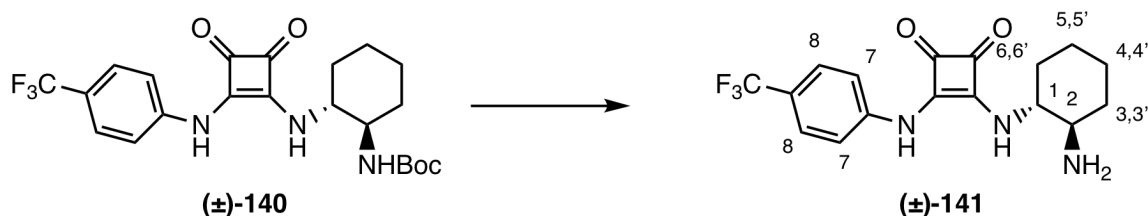
^1H NMR (DMSO- d_6 , 400 MHz, δ) 9.91 (br s, 1H, N-H), 7.67 (d, 3H, $J = 8.6$ Hz, **H**₉, coalesced with 1 x N-H), 7.60 (d, 2H, $J = 8.6$ Hz, **H**₈), 6.81 (d, 1H, $J = 13.3$ Hz, N-H), 3.67 (br s, 1H, **H**₁), 1.99 (d, 1H, $J = 13.3$ Hz, **H**₂), 1.82 - 1.63 (m, 2H, **H**_{3/3'/6/6'}), 1.47 - 1.14 (m, 6H, **H**_{3-6,3'-6'}), 1.25 (s, 9H, **H**₇).

^{13}C NMR (DMSO- d_6 , 100 MHz, δ) 184.2, 180.0, 169.7, 162.6, 155.5, 142.8, 126.7, 124.6 (q, $J_{\text{C-F}} = 271.2$ Hz), 122.2 (q, $J_{\text{C-F}} = 32.6$ Hz), 117.7, 77.7, 58.8, 54.1, 32.9, 31.4, 28.0, 24.5, 24.3.

HRMS for $[\text{M}+\text{H}]^+$ Obtained 454.1962, required 454.1954.

CHN Calculated C 58.27, H 5.78, N 9.27. Obtained C 58.20, H 5.79, N 9.28.

Synthesis of 3-((*trans*-(\pm)-2-aminocyclohexyl)amino)-4-((4-(trifluoromethyl)phenyl)amino)cyclobut-3-ene-1,2-dione (\pm)-141 via Boc-deprotection of (\pm)-140



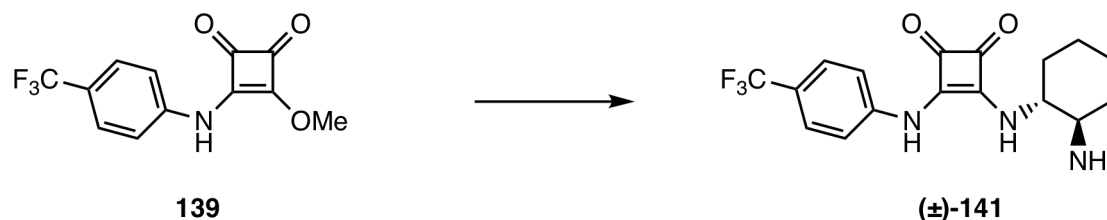
HCl/dioxane (4M, 17 mL) was cooled to 0°C under N₂. *tert*-Butyl-(*trans*-($1\pm$)-2-((3,4-dioxo-2-((4-(trifluoromethyl)phenyl)amino)cyclobut-1-en-1-yl)amino)cyclohexyl)carbamate (\pm)-**140** (390 mg, 0.86 mmol) was added in one portion, the ice bath removed, and the mixture stirred at room temperature for 2h. The volatile solvents were removed under reduced pressure. The crude product was dissolved in a mixture of NaHCO₃ and EtOAc. The EtOAc layer was separated, dried (MgSO₄), and the volatile solvents removed under reduced pressure to afford the product (\pm)-**141** (234 mg, 0.66 mmol, 77%).

¹H NMR (CD₃OD, 400 MHz, δ) 7.67 - 7.58 (m, 4H, **H**_{7,8}), 3.78 - 3.68 (m, 1H, **H**₁), 2.65 - 2.56 (m, 1H, **H**₂), 2.13 - 1.99 (m, 2H, **H**_{3/3'/6/6'}), 1.87 - 1.74 (m, 2H, **H**_{3/3'/6/6'}), 1.50 - 1.24 (m, 4H, **H**_{4,4',5,5'}).

¹³C NMR (CD₃OD, 100 MHz, δ) 182.1, 171.3, 165.1, 143.7, 127.6, 127.2, 125.9, 124.5, 119.4, 61.8, 56.4, 35.0, 34.6, 25.9, 25.8.

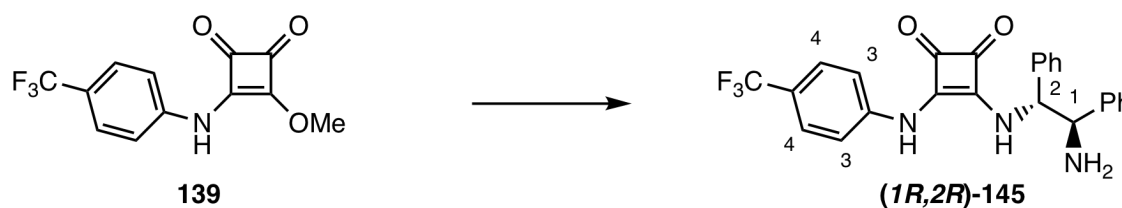
CHN Calculated C 57.59, H 5.13, N 11.89. Obtained C 57.28, H 5.35, N 10.40.

Direct synthesis of 3-((*trans*-(±)-2-aminocyclohexyl)amino)-4-((4-(trifluoromethyl)-phenyl)amino)cyclobut-3-ene-1,2-dione (±)-141



trans-(±)-Cyclohexane-1,2-diamine **139** (1 eq, 268 mg, 2.34 mmol) and dry CH₂Cl₂ (12 mL) were added to a flask, and 3-methoxy-4-((4-(trifluoromethyl)phenyl)amino)cyclobut-3-ene-1,2-dione (1 eq, 636 mg, 2.34 mmol) added. This was stirred at room temperature for 24h. a solid precipitated out, which was then filtered under vacuum to obtain 3-((-*trans*-(±)-2-aminocyclohexyl)amino)-4-((4-(trifluoromethyl)phenyl)amino)cyclobut-3-ene-1,2-dione (±)-**141** (619 mg, 1.75 mmol, 75%).

Synthesis of 3-(((1*R*,2*R*)-2-amino-1,2-diphenylethyl)amino)-4-((4-(trifluoromethyl)-phenyl)amino)cyclobut-3-ene-1,2-dione **145**



(1*R*,2*R*)-Diphenylethane-1,2-diamine (532 mg, 2.50 mmol) was stirred in dry MeOH (35 mL) at room temperature, and 3-methoxy-4-((4-(trifluoromethyl)phenyl)amino)cyclobut-3-ene-1,2-dione **139** (680 mg, 2.50 mmol) added. A precipitate formed, and the mixture stirred at room temperature for 46h. The reaction was filtered to give the product (*1R*,2*R*)-**145** as a yellow powdery solid (774 mg, 69%, 1.71 mmol).

^1H NMR(DMSO- d_6 , 400 MHz, δ) 7.69 (2H, d, J = 8.5 Hz, H_4), 7.61 (2H, d, J = 8.5 Hz, H_3), 7.53 - 7.15 (10H, m, Ar), 5.36 (1H, d, J = 4.4 Hz, H_2), 4.44 (1H, d, J = 4.4 Hz, H_1).

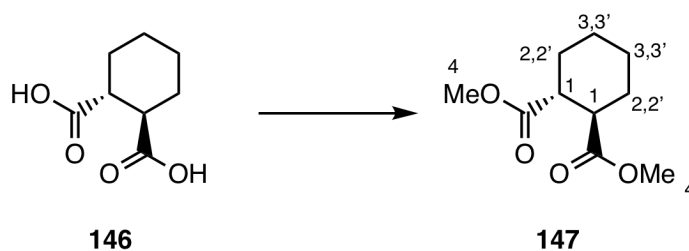
^{13}C NMR(DMSO- d_6 , 100 MHz, δ) 184.3, 180.3, 169.5, 163.0, 142.8 (d, $J_{\text{C-F}}$ = 13.7 Hz), 140.4, 129.0, 128.5, 127.9, 127.4, 127.3, 127.1, 126.7, 126.6, 118.0 (d, $J_{\text{C-F}}$ = 10.1 Hz).

HRMS for $[\text{M}+\text{H}]^+$ 242.1586, observed = 242.1463. Data matches the literature [199].

R_f 0.05 (10% MeOH/ CH_2Cl_2 /textsubscript2)

8.2.3 Chapter 4: 1,4-Diamine-Derived Catalysts

Synthesis of dimethyl (\pm)-*trans*-cyclohexane-1,2-dicarboxylate **147**



(\pm)-*Trans*-cyclohexane-1,2-dicarboxylic acid (\pm)-**146** (5 mmol, 860 mg) and MeOH (10 mL) were stirred under an N_2 atmosphere. An opening vent was added, and SOCl_2 (2 eq, 0.72 mL) added dropwise. This was stirred at room temperature for 8h. The volatile solvent was evaporated under a stream of N_2 to afford the product (\pm)-**147** (1.00g, 5.00 mmol, 100%).

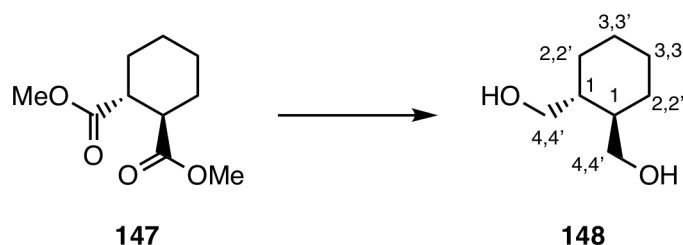
^1H NMR (CDCl_3 , 400 MHz, δ) 3.67 (s, 6H, H_4), 2.71 - 2.50 (m, 2H, H_1), 2.14 - 1.98 (m, 2H, $\text{H}_{2/2'}$), 1.86 - 1.72 (m, 2H, $\text{H}_{2/2'}$), 1.46 - 1.20 (m, 4H, $\text{H}_{3/3'}$).

^{13}C NMR (CDCl_3 , 100 MHz, δ) 175.6, 52.1, 44.8, 29.0, 25.2

FTIR $\nu(\text{cm}^{-1})$ 2943 (CH), 1731 (C=O ester).

HRMS for $[\text{M}+\text{H}]^+$ found 201.1103, required 201.1127. Data matches the literature [200].

Synthesis of ((±)-*trans*-cyclohexane-1,2-diyl)dimethanol **148** via LiAlH_4 reduction



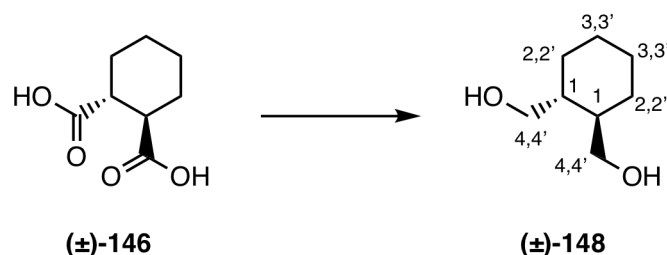
LiAlH_4 in THF (1.0 M, 4.4 eq, 621 mg, 16.3 mmol, 16 mL) was added to an oven-dried round-bottomed flask and stirrer under an N_2 atmosphere. This was cooled to 0°C , and a solution of dimethyl (±)-*trans*-cyclohexane-1,2-dicarboxylate (±)-**147** (1 eq, 745 mg, 3.72 mmol) in dry THF (3.7 mL) was added dropwise. Further THF (7.8 mL) was added, and the reaction stirred at rt for 6h. H_2O (2.60 mL) was added dropwise at 0°C to quench the excess hydride. The solid $\text{Al}(\text{OH})_3$ was filtered out, the product dried over MgSO_4 and the volatile solvents removed to afford the product (±)-**148** as a colourless oil (179 mg, 0.89 mmol, 24%).

^1H NMR (CDCl_3 , 400 MHz, δ) 3.66 - 3.58 (m, 2H, $\text{H}_{4/4'}$), 3.57 - 3.50 (m, 2H, $\text{H}_{4/4'}$), 3.12 (br s, 2H, O-H), 1.79 - 1.67 (m, 2H, $\text{H}_{2/2'}$), 1.65 - 1.58 (m, 2H, $\text{H}_{2/2'}$), 1.36 - 1.28 (m, 2H, $\text{H}_{3/3'}$), 1.27 - 1.19 (m, 2H, $\text{H}_{3/3'}$), 1.12 - 0.96 (m, 2H, H_1).

^{13}C NMR (CDCl_3 , 100 MHz, δ) 68.0, 44.8, 30.0, 26.2.

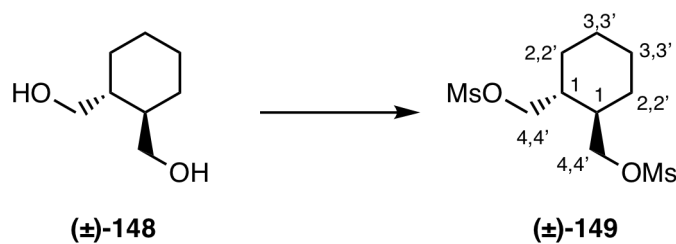
FTIR (ν_{max} cm^{-1}) 3273 (OH), 2900 (C-H). Data matches the literature [161].

Synthesis of ((±)-*trans*-cyclohexane-1,2-diyl)dimethanol **148** from the dicarboxylic acid



$\text{BH}_3 \cdot \text{Me}_2\text{S}$, 2M in THF (2.1 eq, 32.1 mmol, 16.1 mL) was added *via* syringe to a 100 cm³ oven-dried round-bottomed flask and stirrer under N_2 . This was diluted with dry THF (7 mL). (\pm)-*trans*-Cyclohexane-1,2-dicarboxylic acid (\pm)-**146** (1 eq, 15.3 mmol, 6.89 g) added portionwise to the stirred complex at room temperature, with an exotherm and bubbling upon addition. The mixture was heated to reflux (75°C) for 18h. A clear gel formed. The volatile solvent was removed under reduced pressure, and the crude residue quenched with dropwise addition of H_2O until effervescence stopped. The product was extracted with CH_2Cl_2 (x3), the fractions combined, and the organic layer washed with sat. NaHCO_3 . The organic layer was dried (MgSO_4), filtered, and the volatile solvent removed under reduced pressure to give the product (\pm)-**148** (1.69 g, 11.7 mmol, 77%) as a colourless oil which solidified upon standing. Data is as above.

Synthesis of ((\pm)-*trans*-cyclohexane-1,2-diyl)bis(methylene)- dimethanesulfonate **149**



((\pm)-*trans*-Cyclohexane-1,2-diyl)dimethanol (\pm)-**148** (1 eq, 352 mg, 2.48 mmol) was stirred in dry CH_2Cl_2 (14 mL) and NEt_3 (2.1 eq, 527 mg, 5.21 mmol, 0.72 mL) added. This was stirred at -10°C under N_2 , and MsCl (3.25 eq, 852 mg, 7.44 mmol, 576 μL) was added dropwise. This was stirred for a further 15 min, the solution washed with H_2O , 1M HCl , sat. NaHCO_3 and sat. NaCl . The layer was dried (MgSO_4) and filtered. The crude residue was passed through a silica plug, eluting using CH_2Cl_2 . The volatile solvents were removed under reduced pressure to afford the product (\pm)-**149** as an oil, which solidified to colourless crystals upon standing. (210 mg. 0.70 mmol, 28%).

^1H NMR (CDCl_3 , 400 MHz, δ) 4.31 (dd, 2H, $J = 3.7$ Hz, 10.3 Hz, $\text{H}_{4/4'}$), 4.20 (dd, 2H, $J = 3.7$ Hz, 10.3 Hz, $\text{H}_{4/4'}$), 3.05 (s, 6H, CH_3 (OMs)), 1.89 - 1.77 (m, 4H, $\text{H}_{1/2/2'/3/3'}$), 1.76 - 1.69 (m, 2H, $\text{H}_{1/2/2'/3/3'}$), 1.39 - 1.24 (m, 4H, $\text{H}_{1/2/2'/3/3'}$).

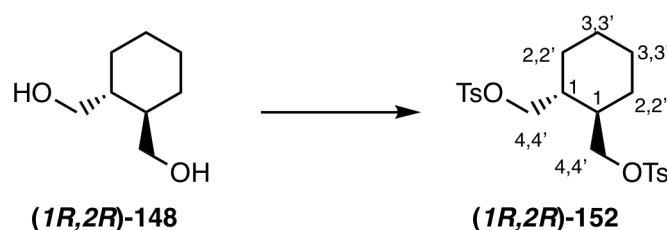
^{13}C NMR (CDCl_3 , 400 MHz, δ) 72.1, 38.7, 37.4, 29.4, 25.4. Data matches the literature [201].

HRMS for $[\text{M}+\text{Na}]^+$ found 323.0532, required 323.0594.

FTIR (ν_{max} cm^{-1}) 1337.

Synthesis of ((1*R*,2*R*)-cyclohexane-1,2-diyl)bis(methylene)- bis(4-methylbenzenesulfonate)

152



((1*R*,2*R*)-cyclohexane-1,2-diyl)dimethanol (**(1*R*,2*R*)-148**) (11.7 mmol, 1.69 g) in dry pyridine (5.6 mL) was added dropwise to a stirred mixture of TsCl (3 eq, 35.2 mmol, 6.71 g), DMAP (0.15 eq, 215 mg, 1.76 mmol) and dry pyridine (7 mL) cooled to 0°C under N_2 . This was stirred at rt for 3h, and H_2O (5.7 mL) added. This was stirred for a further 60 mins at rt. The solid was collected under vacuum filtration, and washed with $\text{H}_2\text{O}/\text{MeOH}$ to obtain the product **(1*R*,2*R*)-152** as a white powder (2.55 g, 48%, 5.63 mmol).

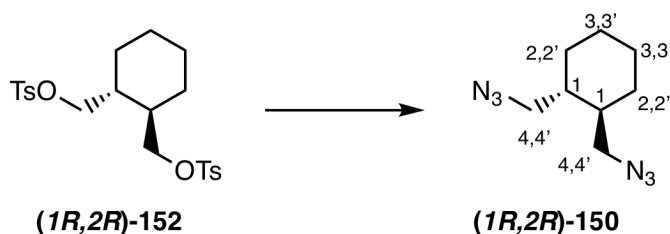
^1H NMR (CDCl_3 , 400 MHz, δ) 7.74 (d, 4H, $J = 8.2$ Hz, Ar (Ots)), 7.35 (d, 4H, $J = 8.2$ Hz, Ar (OTs)), 3.87 (m, 2H ($\text{H}_{4/4'}$)), 2.46 (s, 6H, CH_3 (OTs)), 1.69 - 1.60 (m, 4H, $\text{H}_{1/2/2'/3/3'}$), 1.57 - 1.52 (m, 2H, $\text{H}_{1/2/2'/3/3'}$), 1.20 - 1.13 (m, 4H, $\text{H}_{1/2/2'/3/3'}$).

^{13}C NMR (CDCl_3 , 100 MHz, δ) 145.0, 132.9, 130.1, 128.1, 72.2, 38.0, 29.1, 25.4, 21.8.

HRMS for $[\text{M}+\text{Na}]^+$ found 475.1219, required 475.1220.

FTIR (ν_{max} cm^{-1}) 2938, 2861, 1597, 1350.

Synthesis of (1*R*,2*R*)-1,2-bis(azidomethyl)cyclohexane **150**



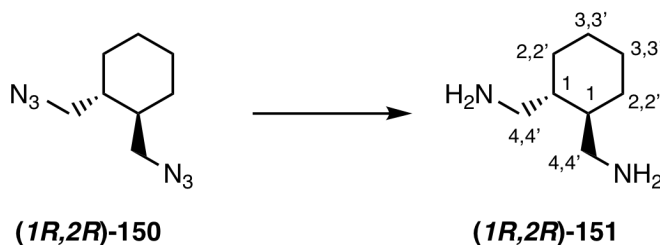
((1*R*,2*R*)-cyclohexane-1,2-diyl)bis(methylene) bis(tosylate) (**152**) (1 eq, 5.63 mmol, 2.55 g) was dissolved in DMF (30 mL). NaN₃ was added, and the mixture heated to 55°C for 22h. This was left to cool and diluted with H₂O (80 mL). The product was extracted with Et₂O (3x80 mL) and washed with further H₂O (80 mL). The organic layer was dried (MgSO₄) and the volatile solvents removed under reduced pressure to give the product (**150**) as a slightly yellow oil (619 mg, 3.19 mmol, 57%).

¹H NMR (CDCl₃, 400 MHz, δ) 3.34 (overlapping q, 4H, *J* = 11.4, 12.0 Hz, **H**_{4/4'}), 1.80 - 1.71 (m, 4H, **H**_{1/2/2'/3/3'}), 1.50 - 1.42 (m, 2H, **H**_{1/2/2'/3/3'}), 1.29 - 1.16 (m, 4H, **H**_{1/2/2'/3/3'}).

¹³C NMR (CDCl₃, 100 MHz, δ) 55.3, 39.9, 30.5, 25.7.

FTIR (cm⁻¹) ν₂₉₂₆, 2856 (C-H), 2086 (N₃), 1448 (CH₂ deformation). Data matches the literature [161].

Synthesis of ((1*R*,2*R*)-cyclohexane-1,2-diyl)dimethanamine **151**



10% Pd/C (62 mg) was added to a 250 cm³ 3-necked round-bottomed flask and put under N₂. Dry MeOH (25 mL) was added and a solution of ((1*R*,2*R*)-cyclohexane-1,2-diyl)diazide

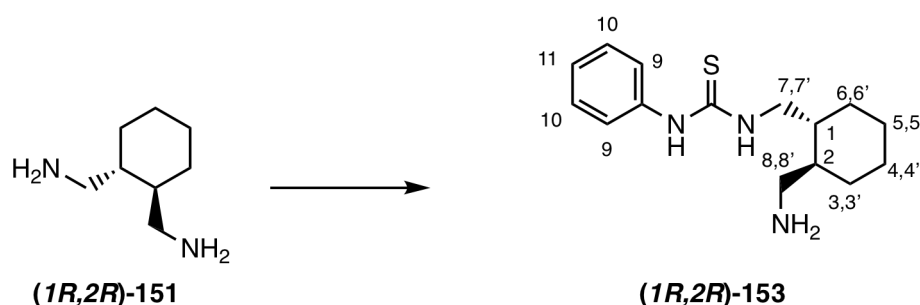
(*1R,2R*)-**150** (1 eq, 619 mg, 3.19 mmol) in MeOH (5 mL) added. This was evacuated/filled with N₂ (x3), and evacuated/filled with H₂ (x3). This was stirred at room temperature for 22h. The reaction was evacuated, filled with N₂ and filtered through Celite under an N₂ atmosphere. The volatile solvents were removed under reduced pressure to afford the product (*1R,2R*)-**151** (444 mg, 3.12 mmol, 99%).

¹H NMR(CDCl₃, 400 MHz, δ) 2.80 (dd, 2H, *J* = 2.6, 12.8 Hz, **H**_{4/4'}), 2.58 (dd, 2H, *J* = 6.1, 12.8 Hz, **H**_{4/4'}), 1.82 - 1.70 (m, 4H, **H**_{2/2'/3/3'}), 1.47 (br s, 4H, N-H), 1.27 - 1.16 (m, 4H, **H**_{2/2'/3/3'}), 1.11 - 1.01 (m, 2H, **H**₁).

¹³C NMR (CDCl₃, 100 MHz, δ) 45.3, 42.4, 29.9, 26.1.

FTIR (cm⁻¹) ν₃₂₈₅ (N-H stretch), 2914, 2849 (C-H stretch), 1602 (N-H scissoring), 1446 (CH₂ deformation). Data matches the literature [161].

Synthesis of 1-(((*1R,2R*)-2-(aminomethyl)cyclohexyl)methyl)-3-phenylthiourea **153**



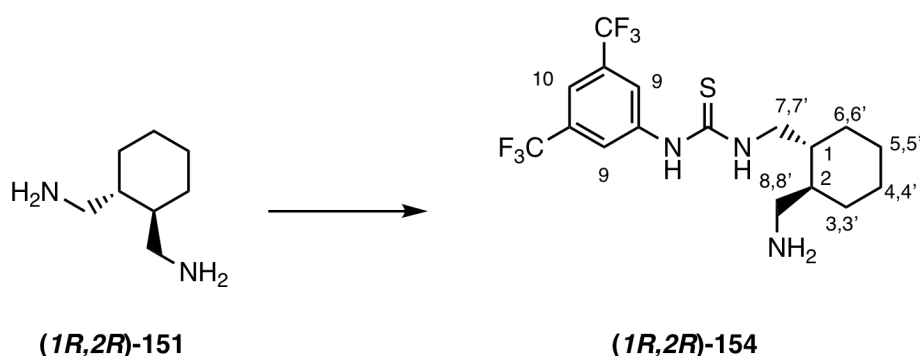
((*1R,2R*)-cyclohexane-1,2-diyl)diamine (*1R,2R*)-**151** (1 eq, 2.19 mmol, 299 mg) was stirred in dry CH₂Cl₂ (21 mL) and put under N₂. This was cooled to 0°C, and a solution of phenyl thiocyanate (0.67 eq, 1.40 mmol, 189 mg, 168 μL) in dry CH₂Cl₂ (4 mL) added dropwise over 30 minutes using a dropping funnel. The mixture was stirred at rt for 24h. The volatile solvents were removed under reduced pressure, and the product purified by silica column chromatography (elution 10% MeOH/CH₂Cl₂, R_f = 0.1) to afford the product (*1R,2R*)-**153** (303 mg, 78%, 1.09 mmol) as a white solid.

^{13}C NMR (CDCl_3 , 100 MHz, δ) 180.69, 132.46, 129.77, 126.24, 119.64, 97.57, 77.48, 77.16, 76.84, 73.86, 31.78, 31.63, 31.39, 31.07, 26.17, 25.99.

HRMS for $[\text{M}+\text{H}]^+$ found 278.1760, req 278.1685.

FTIR (cm^{-1}) ν 3610, 3345, 2979, 2157, 1364.

Synthesis of 1-(((1*R*,2*R*)-2-(aminomethyl)cyclohexyl)methyl)-3-(3,5-bis(trifluoromethyl)-phenyl)thiourea **154**



((1*R*,2*R*)-cyclohexane-1,2-diyl)diamine (**151**) (1 eq, 0.09 mmol, 13 mg) was stirred in dry CH_2Cl_2 (1.2 mL) and put under N_2 . This was cooled to 0°C , and a solution of 3,5-bis(trifluoromethyl)phenylisothiocyanate **109** (0.67 eq, 0.06 mmol, 11 mg, 7 μL) in dry CH_2Cl_2 (0.2 mL) added dropwise over 30 minutes using a dropping funnel. The mixture was stirred at rt for 24h. The volatile solvents were removed under reduced pressure, and the product purified by silica column chromatography (elution 10% $\text{MeOH}/\text{CH}_2\text{Cl}_2$) to afford the product (**154**) (17 mg, 68%, 0.04 mmol).

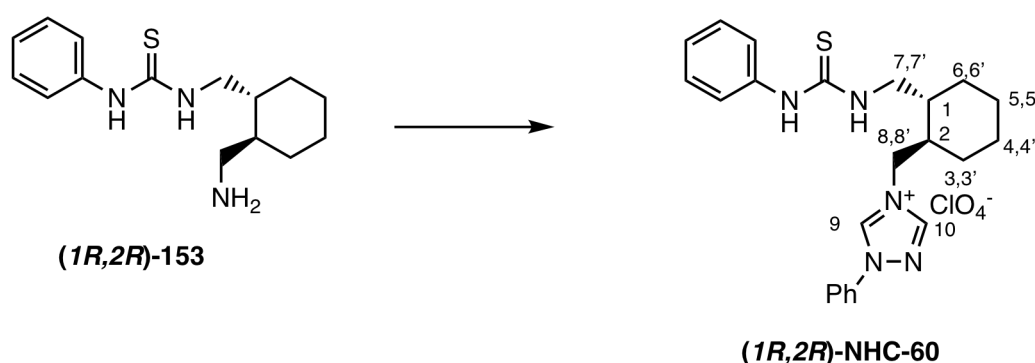
^1H NMR (CDCl_3 , 400 MHz, δ) 7.91 (s, 2H, H_9), 7.63 (s, 1H, H_{10}), 3.78-3.55 (m, 2H, $\text{H}_{7/7'}$), 2.90-2.75 (m, 2H, $\text{H}_{8/8'}$), 1.95-1.51 (m 5H, $\text{H}_{1-6/3'-6'}$), 1.47-1.07 (m, 5H, $\text{H}_{1-6/3'-6'}$).

HRMS for $[\text{M}+\text{H}]^+$ found 414.1479, required 414.1439.

Rf 0.10 (10% $\text{MeOH}/\text{CH}_2\text{Cl}_2$)

Synthesis of 1-phenyl-4-(((1*R*,2*R*)-2-((3-phenylthioureido)methyl)cyclohexyl)methyl)-1*H*-1,2,4-triazol-4-ium perchlorate (1*R*,2*R*)-NHC-60

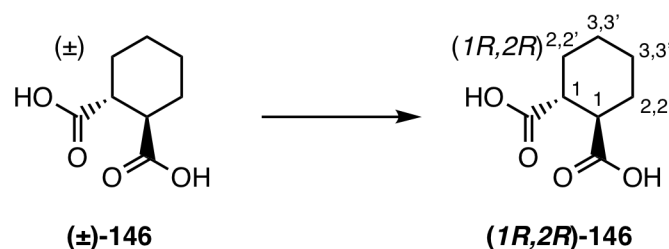
The reaction to form the product was as above in Chapter 3 from starting material **153**. After turning the reaction off after 6h, the volatile solvents were removed and the mixture purified (silica, 10% MeOH/CH₂Cl₂) to afford the product with trace impurities (18 mg, 0.04 mmol, 5% yield).



¹H NMR (CDCl₃, 400 MHz, δ) 10.60 (s, 1H, N-H), 8.93 (s, 1H, **H**_{9/10}), 8.11 (s, 1H, **H**_{9/10}), 7.88 (dd, *J* = 7.6, 2.0 Hz, 2H, **Ar**), 7.63 – 7.51 (m, 3H, **Ar**), 7.37 (d, *J* = 4.4 Hz, 4H, **Ar**), 7.22 (dd, *J* = 8.8, 4.6 Hz, 1H, **Ar**), 6.75 (s, 1H, N-H), 5.02 (dd, *J* = 13.9, 3.9 Hz, 1H, **H**_{7/7'}), 4.42 (dd, *J* = 13.9, 8.5 Hz, 1H, **H**_{7/7'}), 4.04 – 3.92 (m, 1H, **H**_{8/8'}), 3.68 – 3.54 (m, 1H, **H**_{8/8'}), 1.74 (m, 4H, **H**_{1-6/3'-6'}), 1.32 – 1.16 (m, 4H, **H**_{1-6/3'-6'}), 1.16 – 0.99 (m, 2H, **H**_{1-6/3'-6'}).

HRMS for [M+H]⁺ found 406.2068, required = 406.2065.

Chiral resolution to obtain (1*R*,2*R*)-cyclohexane-1,2-dicarboxylic acid **146**



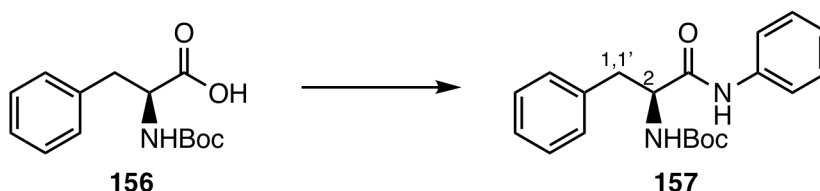
As per prepared by Dwivedi *et al.* [163]. (±)-*Trans*-cyclohexyl-1,2-dicarboxylic acid (1 eq, 50 mmol, 8.61 g), was stirred in EtOH (40 mL). This was heated to 75°C, and (*R*)- α -methylbenzylamine (1 eq, 50 mmol, 6.06 g, 6.36 mL) was added. This was cooled to 35°C, and stirred for 24h. A solid white precipitate, which was filtered and washed with EtOH. A recrystallization from hot EtOH yielded white, shiny crystals of the chiral salt. This was suspended in EtOAc (75 mL) and stirred with 1M HCl (75 mL) for 1h. The aqueous was washed with NaCl, and extracted with more EtOAc. The organic was dried (MgSO₄), filtered, and the volatile solvents removed under reduced pressure to afford the product (2.64 g, 15.3 mmol, 61%).

¹H NMR (DMSO-d₆, 400 MHz, δ) 12.07 (br s, 2H, O-H), 2.40 - 2.29 (m, 2H, **H₁**), 1.98 - 1.89 (m, 2H, **H_{2/2'}**), 1.74 - 1.64 (m, 2H, **H_{2/2'}**), 1.31 - 1.17 (m, 4H, **H_{2/2'}**).

Data matches the literature [202].

8.2.4 Chapter 5: Phenylalanine-Derived Catalysts

Synthesis of *tert*-butyl-(*S*)-(1-oxo-3-phenyl-1-(phenylamino)propan-2-yl)carbamate **157**



(*L*)-Boc-Phe-OH **156** (1.061 g, 4.0 mmol) was dissolved in dry CH₂Cl₂ (20 mL) under N₂ and cooled to 0°C. To the solution was added 1,3-dicyclohexylcarbodiimide (DCC) (1 eq, 825 mg, 4.0 mmol) in small portions followed by stirring in an at this temperature for 15 min. Aniline (1 eq, 364 μ L, 4.0 mmol) was then added to the solution, and the reaction was allowed to warm to room temperature and stir for 24h. The reaction was filtered, and the filtrate was washed twice with H₂O. The organic fractions were combined and dried (MgSO₄). The solution was filtered, and the filtrate was recovered and concentrated under vacuum.

Hexane was added to encourage precipitation, and the precipitate to give the product **157** (854 mg, 2.51 mmol, 63%) as a white powder.

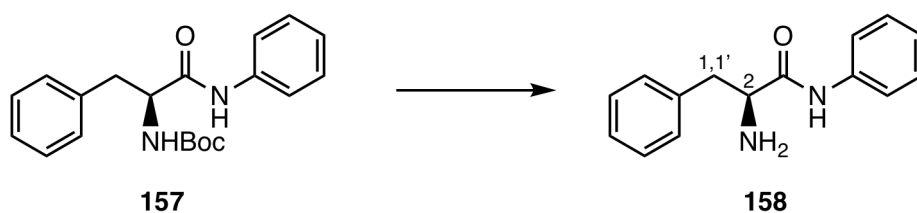
$^1\text{H NMR}$ (CDCl_3 , 400 MHz, δ) 7.75 - 7.64 (br s, 1H, N-H), 7.39 - 7.34 (m, 2H, Ar), 7.34 - 7.21 (m, 7H, Ar), 7.09 (t, 1H, $J = 7.3$ Hz, Ar), 5.14 (br s, 1H, H_2), 4.45 (br s, 1H, $\text{H}_{1/1'}$), 3.15 (d, 2H, $J = 6.9$ Hz, $\text{H}_{1/1'}$), 1.43 (s, 9H, CH_3 (Boc)).

$^{13}\text{C NMR}$ (CDCl_3 , 100 MHz, δ) 169.8, 137.5, 136.8, 129.5, 129.0, 128.9, 127.2, 124.6, 120.2, 56.9, 38.6, 34.1, 28.4. Data matches the literature [203].

$[\text{M}+\text{H}]^+$ Obtained 341.2076, calculated 341.1860.

CHN Obtained C 70.39, H 7.40, N 8.57. Calculated C 70.57, H 7.11, N 8.23.

Synthesis of (S)-2-amino-N,3-diphenylpropanamide **158**



A solution of 4M HCl in dioxane (20 mL) in a round-bottomed flask was cooled to 0°C. *Tert*-butyl (S)-((1-oxo-3-phenyl-1-((phenylamino)propan-2-yl)carbamate **157** (1 eq, 567 mg, 1.66 mmol) was added in one portion, the ice bath removed, and the reaction stirred for 30 minutes until the reaction was complete by TLC. The HCl salt was extracted using H_2O , and the product basified with NaHCO_3 . The product was extracted using CH_2Cl_2 , dried (MgSO_4), and the volatile solvents removed to give the product **158** (461 mg, 100%, 1.66 mmol).

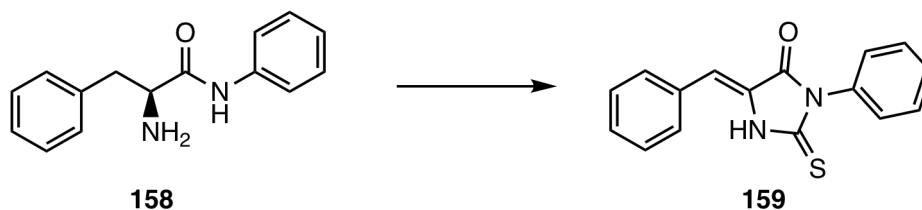
$^1\text{H NMR}$ (CDCl_3 , 400 MHz, δ) 9.44 (s, 1H, N-H), 7.62 (d, 2 H, $J = 7.5$ Hz, Ar), 7.39 - 7.24 (m, 7H, Ar), 7.13 (t, 1 H, $J = 7.5$ Hz, Ar), 3.77 (dd, 1 H, $J = 3.9$ Hz, 9.5 Hz, H_2), 3.41 (dd, 3 H, $J = 3.9$ Hz, 13.9 Hz, $\text{H}_{1/1'}$), 2.82 (dd, 1 H, $J = 9.5$ Hz, 13.9 Hz, $\text{H}_{1/1'}$).

^{13}C NMR (CDCl_3 , 100 MHz, δ) 172.5, 137.9, 137.8, 129.4, 129.1, 129.0, 127.1, 124.3, 119.6, 57.0, 40.9. Data matches the literature [168].

HRMS for $[\text{M}+\text{H}]^+$ found 241.1381, calculated 241.1341.

R_f = 0.51 (10% MeOH/ CH_2Cl_2)

Synthesis of (Z)-5-benzylidene-3-phenyl-2-thioxoimidazolidin-4-one **159**



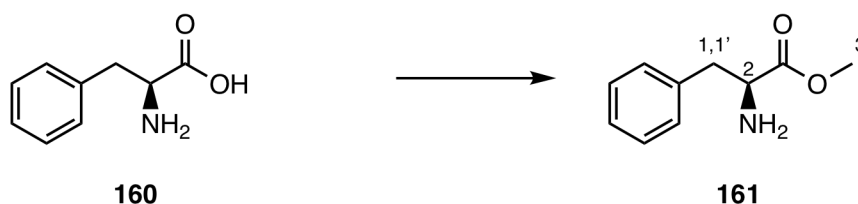
To a mixture of (*S*)-2-amino-*N*,3-diphenylpropanamide **158** (430 mg, 1.79 mmol) in DMSO (0.90 mL) was added 20M NaOH (1 eq, 1.79 mmol, 90 μL). This was stirred, cooled to 0 $^{\circ}\text{C}$, CS_2 (1 eq, 1.79 mmol, 108 μL) added dropwise and the solution stirred for 2 hours. The mixture was cooled to 0 $^{\circ}\text{C}$, and 3-chloro-2-butanone (1 eq, 191 mg, 1.79 mmol, 0.18 mL) added dropwise. The ice bath was removed, and the reaction stirred for 24h. H_2O , deionized (1.80 mL) was added and the mixture stirred at 0 $^{\circ}\text{C}$ for 10 minutes until a solid formed. The surrounding liquid was decanted, and the solid dissolved in abs. EtOH (1.80 mL). Conc HCl (90 μL) was added, and the mixture refluxed at 75 $^{\circ}\text{C}$ for 1h. The mixture was placed in the fridge overnight to encourage precipitation. The solid was filtered and purified using silica column chromatography (elution 20% EtOAc/hexane) to give the product **159** (67 mg, 10%, 0.18 mmol).

^1H NMR (CDCl_3 , 400 MHz, δ) 8.94 (br s, 1H, N-H), 7.67 - 7.30 (m, 10H, Ar), 6.84 (s, 1H, -CH=C-).

^{13}C NMR (CDCl_3 , 100 MHz, δ) 172.4, 167.5, 130.1, 129.8, 129.5, 129.4, 129.2, 128.3, 113.8, 102.6, 92.4.

HRMS for **[M+H]** Obtained 281.0694, required 281.0749. Data matches the literature [204].

Synthesis of methyl *L*-phenylalaninate **161**

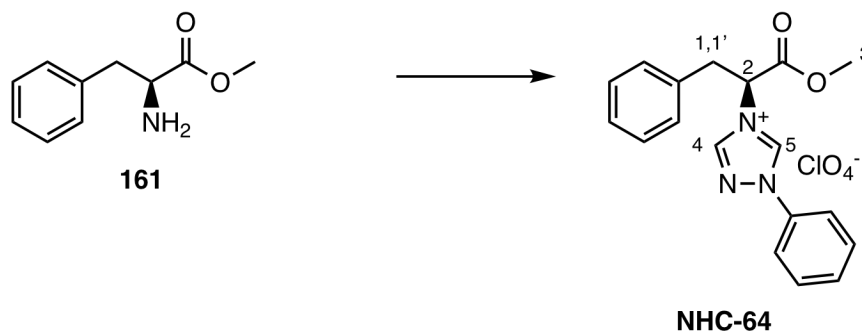


(*L*)-Phenylalanine **160** (1 eq, 10 mmol, 1.69 g) was stirred in dry MeOH (20 mL), put under an N₂ atmosphere and cooled to -10°C. SOCl₂ (1.1 eq, 11 mmol, 1.31 g, 0.80 mL) was added dropwise over 15 minutes. This was stirred at room temperature for a further 19h. The volatile solvents were removed under reduced pressure. The material was dissolved in EtOAc, washed with H₂O, NaHCO₃, and sat. NaCl. The organic layer was dried (MgSO₄), filtered, and the volatile solvent removed under reduced pressure to afford the product **161** (995 mg, 5.55 mmol, 56%).

¹H NMR (400 MHz, CDCl₃, δ) 7.34 - 7.16 (m, 5H, **Ar**), 3.77 - 3.74 (m, 1H, **H₂**), 3.71 (s, 3H, **H₃**), 3.09 (dd, 1H, *J* = 5.0, 13.5 Hz, **H_{1/1'}**), 2.86 (dd, 1H, *J* = 8.0, 13.5 Hz, **H_{1/1'}**).

FTIR (cm⁻¹) 3372 (N-H), 2951 (C-H), 1732 (C=O ester), 1603 (C=C arom).

HRMS for **[M+H]⁺** found = 180.0813 required = 180.1019.

Synthesis of (S)-4-(1-methoxy-1-oxo-3-phenylpropan-2-yl)-1-phenyl-1*H*-1,2,4-triazol-4-ium perchlorate NHC-64

3-phenyl-1,3,4-oxadiazol-3-ium perchlorate **132** (1.366 g, 5.55 mmol) was added to a round-bottomed flask under N₂. AcOH (3 mL) was added. methyl *L*-phenylalaninate **161** (995 mg, 5.55 mmol, 1 eq) was added, and the mixture heated to 110°C for 2h. The precipitate was collected to afford the product **NHC-64** (42 mg, 2%, 0.11 mmol).

¹H NMR (DMSO-d₆, 400 MHz, δ) 11.07 (br s, 1H, **H_{4/5}**), 9.56 (br s, 1H, **H_{4/5}**), 7.92 - 7.88 (m, 2H, **Ar**), 7.75 - 7.63 (m, 3H, **Ar**), 7.37 - 7.23 (m, 5H, **Ar**), 5.89 (app t, 1H, *J* = 7.9 Hz, **H₂**), 3.76 (s, 3H, **H₃**), 3.65 (dd, 1H, *J* = 7.1, 14.0 Hz, **H_{1/1'}**), 3.54 (dd, 1H, *J* = 8.6, 14.0 Hz, **H_{1/1'}**)

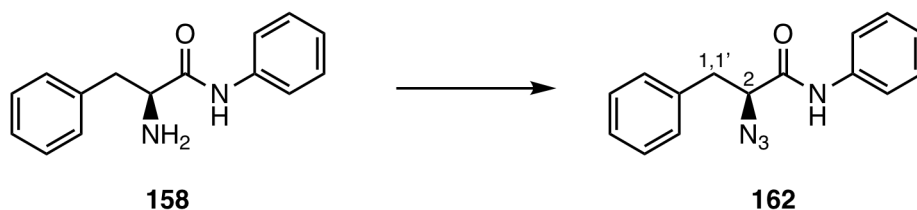
¹³C NMR (DMSO-d₆, 100 MHz, δ) 167.3, 145.0, 141.5, 134.7, 134.3, 130.9, 130.3, 129.1, 128.9, 127.6, 120.8, 61.6, 53.5, 37.3.

CHN calculated C 53.01, H 4.45, N 10.30. Calculated C 52.16, H 4.30, N 10.02.

HRMS for [**M**]⁺ found = 308.1305, required = 308.1394.

FTIR (cm⁻¹) 3138 (sm), 1746 (strong) 1572 (m).

Synthesis of (S)-2-azido-N,3-diphenylpropanamide **162**



(S)-2-amino-N,3-diphenylpropanamide **158** (1 eq, 367 mg, 1.53 mmol) was stirred in MeOH (7.5 mL) and cooled to 0°C. The diazotransfer reagent (1.05 eq, 1.60 mmol, 434 mg) was added, followed by CuSO₄·5H₂O (1 mol%, 4 mg) and K₂CO₃ (2.1 eq, 444 mg, 3.21 mmol). This was allowed to warm to ambient temperature and stirred for 3h. The solution was diluted with H₂O (10 mL) and acidified to pH 2 with 1M HCl. The product was extracted with EtOAc (x3), washed with NaHCO₃, and dried (MgSO₄). The volatile solvents were removed under reduced pressure to afford the product **162** (280 mg, 1.05 mmol, 69%).

¹H NMR (CDCl₃, 400 MHz, δ) 7.92 (br s, 1H, N-H), 7.49 - 7.45 (m, 2H, Ar), 7.37 - 7.28 (m, 7H, Ar), 7.17 - 7.12 (m, 1H, Ar), 4.35 (dd, 1H, *J* = 4.2, 8.1 Hz, H₂), 3.44 (dd, 1H, *J* = 4.2, 14.1 Hz, H_{1/1'}), 3.13 (dd, 1H, 1H, *J* = 8.1, 14.1 Hz, H_{1/1'}).

¹³C NMR (CDCl₃, 100 MHz, δ) 166.8, 136.9, 136.1, 129.7, 129.2, 129.0, 127.6, 125.2, 120.4, 66.1, 39.0.

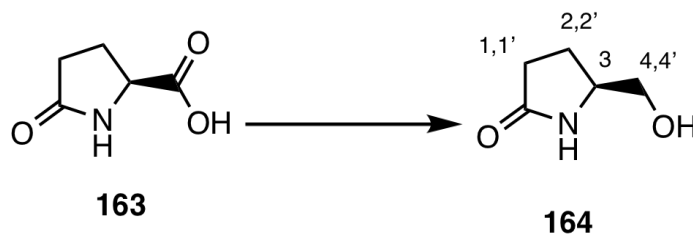
R_f = 0.47 (10% MeOH/CH₂Cl₂)

HRMS for [M]⁺ found = 267.1101, required = 267.1235.

Material decomposed, so no other data was collected.

8.2.5 Chapter 6: Piperidine-Derived Catalyst

Synthesis of (S)-5-(hydroxymethyl)pyrrolidin-2-one **164**



As per Ender's method [205]. *L*-pyroglutamic acid **163** (1 eq, 3.25 g, 25.2 mmol) was added to an oven-dried 100 cm³ rbf, and dry MeOH (15 mL) added. This was cooled to -10°C under N₂, and SOCl₂ (1.5 eq, 4.49 g, 37.8 mmol, 2.75 mL) added slowly dropwise. This was stirred at ambient temperature for a further 3 h, until all precipitate dissolved to give a clear colourless solution. The volatile liquids were removed under reduced pressure to give an oil. This was dissolved in abs. EtOH (15 mL) and cooled to 0°C. NaBH₄ (2.1 eq, 2.00 g, 53.0 mmol) was slurried in abs. EtOH (15 mL) and added portionwise by pipette, giving an exotherm and effervescence. The mixture was left to warm to ambient temperature and stirred for 18h. This was quenched with AcOH (3.5 mL) dropwise, stirring for 1h. The precipitate was removed by passing through Celite® x3, and the crude product dry-loaded onto silica. This was purified by column chromatography on silica gel (20% MeOH in EtOAc, **R_f** 0.27), to give the product **164** (2.52 g, 87 %, 21.9 mmol) as an oil which solidified upon standing.

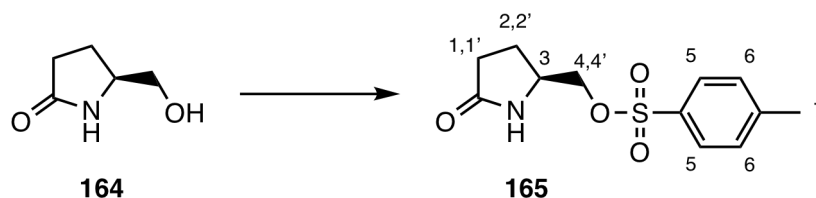
¹H NMR (CD₃OD, 400 MHz, δ) 5.51 (br s, 1H, N-H), 3.79 – 3.71 (m, 1H, **H_{4/4'}**), 3.58 (dd, 1H, *J* = 4.4 Hz, 12.3 Hz, **H_{4/4'}**), 3.49 (dd, 1H, *J* = 5.6 Hz, 11.3 Hz, **H₃**), 2.44 – 1.85 (m, 4H, **H_{1,1',2,2'}**).

¹³C NMR (CD₃OD, 100 MHz, δ) 181.2, 65.9, 57.7, 31.1, 23.9.

CHN theoretical C 52.16 H 7.88 N 12.17. Obtained C 51.70 H 7.95 N 11.84

FTIR (ν_{max} cm⁻¹) 3199 (OH stretch), 2921 (CH stretch), 1652 (C=O lactam stretch) All data is in accordance with the literature [205].

Synthesis of (S)-(5-oxopyrrolidin-2-yl)methyl- 4-methylbenzenesulfonate **165**



L-pyroglutaminol **164** (1 eq, 2.52 g, 21.9 mmol) and TsCl (1.2 eq, 5.00 g, 26.3 mmol) and CH₂Cl₂ (75 mL) were added to a flask and put under an N₂ atmosphere. NEt₃ (1.6 eq, 3.56 g, 35.2 mmol, 4.90 mL) was added, followed by DMAP (0.1 eq, 267 mg, 2.19 mmol). This was stirred at ambient temperature for 72h. The mixture was diluted with CH₂Cl₂ (53 mL), poured into water (120 mL) and acidified with conc. HCl (1.52 mL). The layers were separated, and the aqueous layer washed with CH₂Cl₂ (2 x 35 mL). The organics were dried (MgSO₄). The crude product was dry-loaded onto silica, and purified by column chromatography on silica gel (5% MeOH in EtOAc, *R_f* 0.35), to give the product **165** (4.43 g, 75%, 16.4 mmol) as a white powder.

¹H NMR (CDCl₃, 400 MHz, δ) 7.89 (d, 2H, *J* = 8.2 Hz, **H**₅), 7.37 (d, 2H, *J* = 8.2 Hz, **H**₆), 5.79 (br s, 1H, NH), 4.06 (dd, 1H, *J* = 3.5, 9.7 Hz, **H**_{4/4'}), 3.97 – 3.89 (m, 1H, **H**_{4/4'}), 3.86 (dd, 1H, *J* = 7.5, 9.7 Hz, **H**₃), 2.46 (s, 3H, **H**₇), 2.35 – 2.28 (m, 2H, **H**_{1/1'}), 2.27 – 2.16 (m, 1H, **H**_{2/2'}), 1.81 – 1.71 (m, 1H, **H**_{2/2'}).

¹³C NMR (CDCl₃, 100 MHz, δ) 177.5, 145.6, 132.5, 130.2, 128.1, 72.2, 52.7, 29.2, 22.9, 21.9.

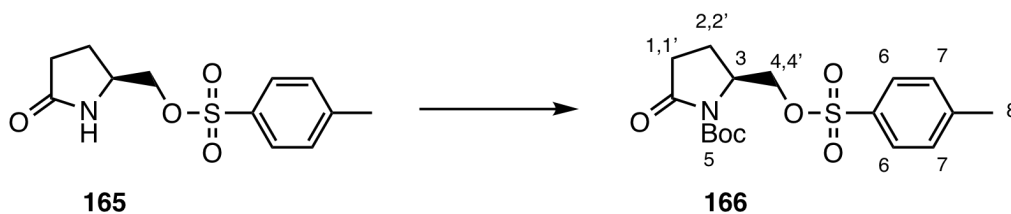
CHN theoretical C 53.52 H 5.61 N 5.20. Obtained C 53.42 H 5.58 N 5.19

FTIR (ν_{max} cm⁻¹) 3921 (NH stretch) 1653 (C=O lactam stretch).

HRMS for [M+Na]⁺ Found = 292.0614, required = 292.0620.

All data is in accordance with the literature [206].

Synthesis of *tert*-butyl-(*S*)-2-oxo-5-((tosyloxy)methyl)pyrrolidine-1-carboxylate **166**



The tosylated material **165** (1 eq, 4.43 g, 16.4 mmol) was dissolved in CH₂Cl₂ (85 mL) and DMAP (1.2 eq, 2.41 g, 19.7 mmol) added. Boc₂O (2 eq, 7.17 g, 32.9 mmol) and NEt₃ (1.6 eq, 2.69 g, 26.5 mmol, 3.7 mL) were added simultaneously. The mixture was left to stir at ambient temperature for 24h, and the solution turned from colourless through yellow to dark brown. H₂O (3.0 mL) was added with vigorous stirring. The mixture was diluted with CHCl₃ (80 mL) and washed sequentially with 0.5 M HCl (3x70 mL), sat. NaHCO₃ (1x70 mL) and brine (1x70 mL). The two layers were combined, dried (MgSO₄) and the volatile solvents removed under reduced pressure. The crude product was purified by column chromatography on silica gel (1% MeOH in CHCl₃) to give the product **166** (5.63 g, 15.2 mmol, 80%) as a yellow powder.

¹H NMR (CDCl₃, 400 MHz, δ) 7.76 (d, 2H, *J* = 8.2 Hz, **H**₆), 7.35 (d, 2H, *J* = 8.2 Hz, **H**₇), 4.33 – 4.28 (m, 1H, **H**₃), 4.24 (dd, 1H, *J* = 4.4 Hz, 10.2 Hz, **H**_{4/4'}), 4.17 (dd, 1H, *J* = 2.7 Hz, 10.2 Hz, **H**_{4/4'}), 2.67 – 2.56 (m, 1H, **H**_{1/1'/2/2'}), 2.44 (s, 3H, **H**₈), 2.39 (ddd, 1H, *J* = 2.6 Hz, 10.1 Hz, 18.0 Hz, **H**_{1/1'/2/2'}), 2.22 – 2.10 (m, 1H, **H**_{1/1'/2/2'}), 2.03 – 1.95 (m, 1H, **H**_{1/1'/2/2'}), 1.44 (s, 9H, **H**₅).

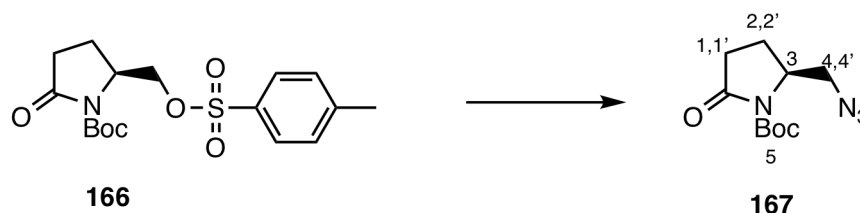
¹³C NMR (CDCl₃, 100 MHz, δ) 173.7, 149.6, 145.4, 132.5, 130.2, 128.0, 83.7, 69.8, 56.1, 31.6, 28.0, 21.8, 20.6.

HRMS for [M+Na]⁺ obtained = 392.1138, required = 392.1144.

NMR data is in accordance with the literature [207].

FTIR (ν_{max} cm⁻¹) 2980 (C-H), 1776 (C=O). Data is in accordance with the literature [208].

Synthesis of *tert*-butyl-(*S*)-2-(azidomethyl)-5-oxopyrrolidine-1-carboxylate **167**



Boc-protected product **166** (1 eq, 5.51 g, 14.9 mmol) was dissolved in DMF (120 mL), put under an N₂ environment, and stirred until the solid dissolved. NaN₃ (1 eq, 969 mg, 14.9 mmol) was added, and the mixture heated to 55 °C for 22h. The mixture was left to cool to ambient temperature, diluted with H₂O (120 mL) and extracted with Et₂O (3x100 mL). The organic layers were combined and washed with H₂O (2x120 mL). The ether was dried (MgSO₄) and the volatile solvent removed under reduced pressure to give the product **167** (2.05 g, 8.53 mmol, 57%) as a yellow oil.

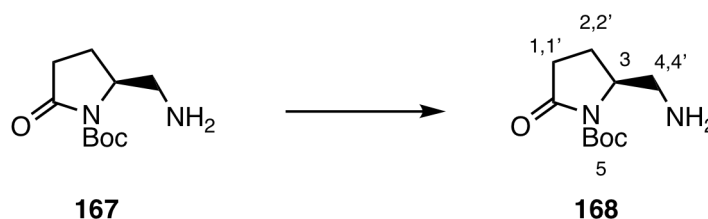
¹H NMR (CDCl₃, 400 MHz, δ) 4.29 – 4.23 (m, 1H, N-H), 3.67 (dd, 1H, *J* = 5.7 Hz, 12.3 Hz, **H**_{4/4'}), 3.54 (dd, 1H, *J* = 2.9 Hz, 12.3 Hz, **H**_{4/4'}), 3.54 (dd, 1H, *J* = 2.9 Hz, 12.3 Hz, **H**₃), 2.75 – 2.63 (m, 1H, **H**_{1/1'/2/2'}), 2.44 (ddd, 1H, *J* = 2.7 Hz, 10.0 Hz, 17.8 Hz, **H**_{1/1'/2/2'}), 2.22 – 2.07 (m, 1H, **H**_{1/1'/2/2'}), 1.96 – 1.88 (m, 1H), **H**_{1/1'/2/2'}, 1.55 (s, 9H, **H**₅).

¹³C NMR (CDCl₃, 100 MHz, δ) 173.9, 150.0, 83.7, 56.7, 53.8, 31.5, 28.2, 21.4. NMR data is in accordance with the literature [209].

HRMS for [M+Na]⁺ Obtained 263.1116, calculated 263.1120.

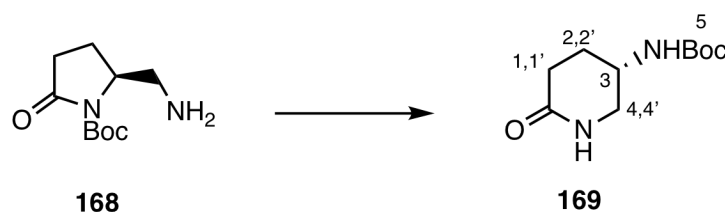
R_f = 0.75 (10% MeOH/CH₂Cl₂)

Synthesis of *tert*-butyl-(*S*)-2-(aminomethyl)-5-oxopyrrolidine-1-carboxylate **168**



10% Pd/C (800 mg) was added to a 3-necked round bottomed flask, under N₂, and dry MeOH (50 mL) was added. To this was added a solution of the Boc-protected material **167** (1 eq, 3.17 g, 13.2 mmol) in dry MeOH (5 mL). This was stirred, the flask evacuated and purged with N₂ x3, and purged with H₂ (x3). This was stirred for 48h, and H₂ replaced periodically. Once complete by TLC, the mixture was purged under N₂, filtered through Celite® under N₂ and the volatile solvents were removed under reduced pressure. This was purified by column chromatography on silica gel (10% MeOH in CH₂Cl₂) to give the product **168** (772 mg, 3.60 mmol, 42%) as a yellow solid. The product was taken through crude to the next step.

Synthesis of *tert*-butyl-(*S*)-(6-oxopiperidin-3-yl)carbamate **169**



The primary amine **168** (2.60 mmol, 558 mg) was dissolved in dry MeOH (10 mL) and heated to 65 °C for 24h. The volatile solvent was removed under reduced pressure to afford the rearranged product **169** as a slightly yellow crystalline solid (555 mg, 100%, 2.60 mmol).

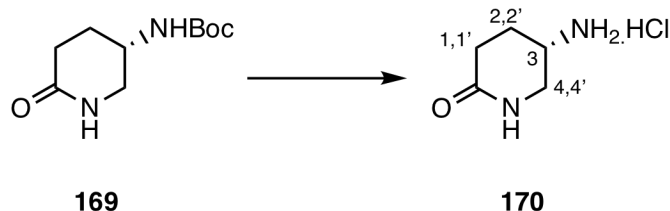
¹H NMR (CDCl₃, 400 MHz, δ) 5.89 (br s, 1H, N-H), 4.69 (br d, 1H, *J* = 6.6 Hz, N-H), 3.97 (br s, 1H, **H**₃), 3.56 (app. br d, 1H, *J* = 12.2 Hz, **H**_{4/4'}), 3.16 (dd, 1H, *J* = 6.9 Hz, 12.2 Hz, **H**_{4/4'}), 2.46 (t, 2H, *J* = 6.9 Hz, **H**_{1,1'}), 2.06 – 1.97 (m, 1H **H**_{2/2'}), 1.91 – 1.81 (m, 1H, **H**_{2/2'}), 1.45 (s, 9H, **H**₅).

¹³C NMR (CDCl₃, 100 MHz, δ) 171.2, 155.2, 77.4, 47.2, 44.4, 28.7, 28.5, 26.7.

HRMS for [M+H]⁺ Obtained 215.1396, required 215.1396.

FTIR (ν_{max} cm⁻¹) 3322, 2966, 1724, 1634. Data matches the literature [209].

Synthesis of (S)-5-aminopiperidin-2-one hydrochloride **170**



The Boc-protected δ -lactam **169** (1 eq, 406 mg, 1.89 mmol) was dissolved in 1,4-dioxane (2.50 mL) and 4M HCl in 1,4-dioxane (5.0 mL) added. This was stirred for 1h at ambient temperature, and a solid precipitated out. The solvent was removed under reduced pressure to afford the hydrochloride salt **170** (286 mg, 1.89 mmol, 100%) as a lightly pink solid.

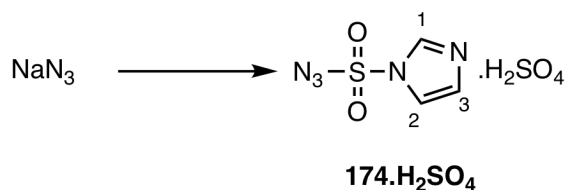
^1H NMR (D_2O , 400 MHz, δ) 3.83 – 3.71 (m, 1H, **H**₃), 2.65 (dd, 1H, $J = 4.6$ Hz, 13.0 Hz, **H**_{4/4'}), 3.39 (dd, 1H, $J = 7.0$ Hz, 13.0 Hz, **H**_{4/4'}), 2.53 – 2.47 (m, 2H, **H**_{1,1'}), 2.28 – 2.19 (m, 1H, **H**_{2/2'}), 2.07 – 1.97 (m, 1H, **H**_{2/2'}).

^{13}C NMR (D_2O , 100 MHz, δ) 173.9, 44.1, 43.3, 26.8, 23.4.

FTIR 3040 (m), 2834 (m), 2597 (s), 1697 (l).

Data matches the literature [210].

Synthesis of 1*H*-imidazole-1-sulfonyl azide. H_2SO_4 **174.H₂SO₄**



NaN_3 (1 eq, 10.0 mmol, 650 mg) was suspended in CH_3CN (5 mL) and cooled to 0°C under N_2 . Sulfuryl chloride (1 eq, 10.0 mmol, 0.81 mL) was added dropwise, the ice bath removed and the mixture stirred at ambient temperature for 21h. Imidazole (1.9 eq, 19.0 mmol, 1.29 g) was added portionwise over 10 minutes at 0°C , with the solution turning dark orange. The

reaction was stirred at 0°C for 3h. The mixture was diluted with EtOAc (20 mL) washed with H₂O (20 mL x2) and basified with NaHCO₃ (sat., 20 mL x2). The organic layer was dried (MgSO₄). H₂SO₄ (1 eq, 10.0 mmol, 981 mg, 0.53 mL) was added dropwise at 0°C, and the mixture stirred at ambient temperature for 16 h. The white solid was filtered to give diazotransfer reagent **174.H₂SO₄** (795 mg, 2.93 mmol, 29%). All sodium azide waste was safely quenched before disposal.

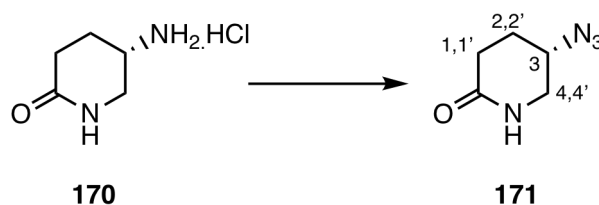
¹H NMR (DMSO-d₆, 400 MHz, δ) 8.59 (s, 1H, **NH**⁺), 7.97 (s, 1H, **HSO₄⁻**), 7.33 (s, 1H, **CH**), 6.77 (br s, 2H, **CH** + H₂O).

¹³C NMR (DMSO-d₆, 100 MHz, δ) 137.7, 130.8, 118.9.

FTIR (ν_{max} cm⁻¹) 2175 (N₃ stretch), 1301 (asymm. S=O stretch), 1126 (symm. S=O stretch).

Data matches the literature [173].

Synthesis of (*S*)-5-azidopiperidin-2-one **171**



The hydrochloride salt **170** (1 eq, 286 mg, 1.89 mmol) was dissolved in MeOH (8.2 mL), and K₂CO₃ (2.8 eq, 731 mg, 5.30 mmol) and CuSO₄·5H₂O (1 mol%, 5 mg) added. This was put under N₂ and **174.H₂SO₄** (1.2 eq, 615 mg, 2.26 mmol) added at ambient temperature. This was stirred for 5h. H₂O (15 mL) was added, and the mixture acidified to pH 3 using 1M HCl. The aqueous layer was extracted (EtOAc x3), the organics washed with brine and dried (MgSO₄). The volatile solvents were removed under reduced pressure. The crude material was purified by column chromatography on silica gel (2% MeOH in EtOAc) to give the azide **171** (65 mg, 24%, 0.46 mmol) as white needles.

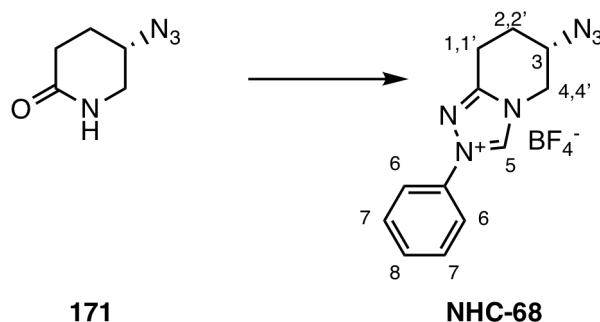
^1H NMR (CDCl_3 , 400 MHz, δ) 7.00 (br s, 1H, N-H), 3.94 – 3.87 (m, 1H, H_3), 3.48 (app dq, 1H, $J = 1.9$ Hz, 12.5 Hz, $\text{H}_{4/4'}$), 3.28 (app ddq, 1H, $J = 1.1$ Hz, 5.7 Hz, 12.6 Hz, $\text{H}_{4/4'}$), 2.53 (ddd, 1H, $J = 6.8$ Hz, 7.8 Hz, 18.1 Hz, $\text{H}_{1/1'}$), 2.38 (app dt, $J = 6.5$ Hz, 18.1 Hz, $\text{H}_{1/1'}$), 2.10 – 1.92 (m, 2H $\text{H}_{2/2'}$).

^{13}C NMR (CDCl_3 , 100 MHz, δ) 171.3, 54.0, 45.7, 27.9, 25.6.

FTIR (ν_{max} cm^{-1}) 3176 (NH stretch) 2945 (CH stretch) 2091 (N_3 stretch), 1656 (C=O stretch).

Rf = 0.23 (2% MeOH/EtOAc)

Synthesis of (*S*)-6-azido-2-phenyl-5,6,7,8-tetrahydro-2*H*-[1,2,4]triazolo[4,3-*a*]pyridin-4-ium tetrafluoroborate NHC-68



Azide **171** (1 eq, 69 mg, 0.46 mmol) was dissolved in dry CH_2Cl_2 (0.5 mL) and added dropwise to a suspension of Me_3OBF_4 (1 eq, 68 mg, 0.46 mmol) in CH_2Cl_2 (2 mL). After stirring for 19h, phenylhydrazine (1.1 eq, 55 mg, 0.51 mmol, 50 μL) was added and stirred for 30h. The solvent was removed under reduced pressure, and the material dissolved in MeOH to transfer to a pressure vial. The material was concentrated under a stream of N_2 to roughly 0.3 mL, and $\text{HC}(\text{OMe})_3$ (0.9 mL) added. This was sealed under air and heated to 80 $^\circ\text{C}$ for 18h. The volatile solvents were removed under reduced pressure and the material purified by column chromatography on silica gel (6-10% MeOH in CH_2Cl_2) to give the product **NHC-68** (69 mg, 0.21 mmol, 46%).

^1H NMR (CD_3CN , 400 MHz, δ) 9.69 (s, 1H, **H**₅), 7.80 – 7.75 (m, 2H, **H**₆), 7.70 – 7.64 (m, 3H, **H**_{7,8}), 4.58 – 4.53 (m, 1H, **H**₃), 4.47 – 4.37 (m, 2H, **H**_{4/4'}), 3.21 – 3.15 (m, 2H, **H**_{1/1'}), 2.39 – 2.30 (m, 1H, **H**_{2/2'}), 2.25 – 2.18 (m, 1H, **H**_{2/2'}).

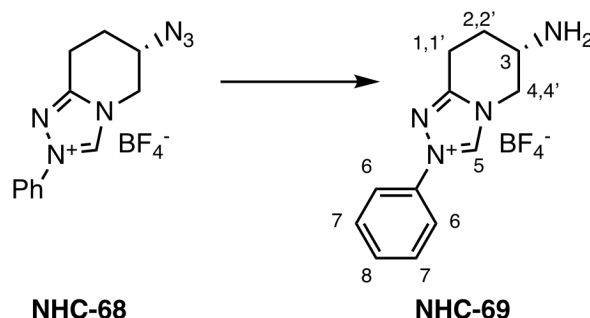
^{13}C NMR (CD_3CN , 100 MHz, δ) 153.7, 140.9, 136.1, 132.0, 131.3, 122.0, 53.5, 50.1, 23.7, 17.9.

HRMS for [**M**+]⁺ Required 241.1202, obtained 241.1206.

FTIR (ν_{max} cm^{-1}) 2113 (N_3), 1583 ($\text{C}=\text{C}$).

Rf 0.39 (10% MeOH/ CH_2Cl_2).

Synthesis of (*S*)-6-amino-2-phenyl-5,6,7,8-tetrahydro-2*H*-[1,2,4]triazolo[4,3-*a*]pyridin-4-ium tetrafluoroborate **NHC-69**



Pd/C (10 mg) was added to a 3-necked round bottomed flask and suspended in MeOH (3.5 mL). This was put under N_2 , and a solution of the azide-protected triazolium **NHC-68** (1 eq, 69 mg, 0.21 mmol) in MeOH (1.5 mL) added. The flask was purged with 1 atm H_2 and stirred for 2.5h. The Pd/C was filtered off through Celite® under a stream of N_2 and the volatile solvents removed under reduced pressure to give the product **NHC-69** (56 mg, 0.19 mmol, 89%) as a yellow solid.

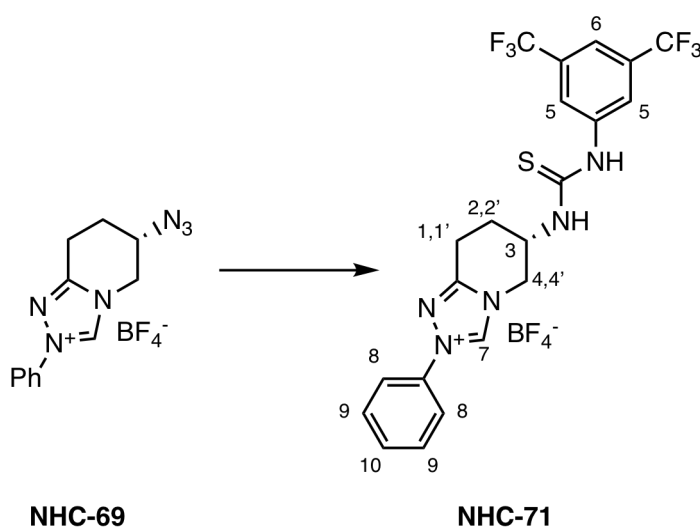
^1H NMR (CD_3CN , 400 MHz, δ) 9.67 (s, 1H, **H**₅), 7.80 – 7.75 (m, 2H, **H**₆), 7.69 – 7.62 (m, 3H, **H**_{7,8}), 4.33 (dd, 1H, $J = 3.9$ Hz, 13.0 Hz, **H**₃), 4.07 (dd, 1H, $J = 5.3$ Hz, 13.0 Hz, **H**_{4/4'}), 3.67 – 3.60 (m, 1H, **H**_{4/4'}), 3.29 – 3.19 (m, 1H, **H**_{1/1'}), 3.07 (dt, 1H, $J = 6.2$ Hz, 18.0 Hz, **H**_{1/1'}), 2.12 – 2.06 (m, 1H, **H**_{2/2'}, obscured by H_2O), 2.05 – 1.97 (m, 1H, **H**_{2/2'}).

^{13}C NMR (CD_3CN , 100 MHz, δ) 154.5, 140.7, 136.2, 131.9, 131.3, 122.0, 52.6, 44.3, 26.8, 18.6.

HRMS for $[\text{M}^+]$ Calculated 215.1297, obtained 215.1303.

Rf 0.02 (10% MeOH/ CH_2Cl_2).

Synthesis of (*S*)-2-phenyl-6-(3-phenylthioureido)-5,6,7,8-tetrahydro-2*H*-[1,2,4]triazolo-[4,3-*a*]pyridin-4-ium tetrafluoroborate **NHC-71**



(*S*)-6-amino-2-phenyl-5,6,7,8-tetrahydro-[1,2,4]triazolo[4,3-*a*]pyridin-2-ium **NHC-69** (1 eq, 45 mg, 0.15 mmol) was suspended in dry CH_2Cl_2 (3 mL) 3,5-bis(trifluoromethyl)phenyl isothiocyanate (1 eq, 41 mg, 0.15 mmol, 28 μL) was added at room temperature. This was stirred for 18h. The mixture was concentrated to 0.5 mL, and passed through a silica plug eluting with 10% MeOH/ CH_2Cl_2 to afford the pure product **NHC-71** (14 mg, 16%, 0.02 mmol).

^1H NMR (CD_3CN , 400 MHz, δ) 9.69 (s, 1H, **H**₇), 8.60 (br s, 1H, N-H), 8.13 (s, 2H, **H**₅), 7.81 - 7.75 (m, 3H, **H**_{6,8}), 7.71 - 7.62 (m, 3H, **H**_{9,10}), 7.19 (d, 1H, J = 6.8 Hz, N-H), 5.12 - 5.03 (m, 1H, **H**₃), 4.72 (dd, 1H, J = 4.9, 13.2 Hz, **H**_{4/4'}), 4.39 (dd, 1H, J = 6.7, 13.2 Hz, **H**_{4/4'}), 3.26 (app t, 2H, J = 6.9 Hz, **H**_{1,1'}), 2.37 - 2.30 (m, 2H, **H**_{2/2'}).

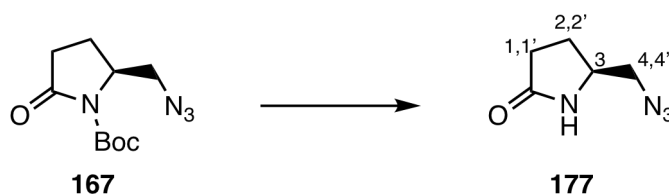
^{13}C NMR (CD_3CN , 100 MHz, δ) 182.9, 154.0, 141.8, 140.8, 136.1, 132.4, 132.1, 131.4, 131.3, 125.0, 122.0, 49.3, 47.9, 24.0, 19.5.

HRMS for $[\text{M}^+]$ Obtained 486.1198, calculated 486.1182.

FTIR (ν_{max} cm^{-1}) 3364, 2172, 1584, 1542, 1474.

Rf = 0.15 ($\text{MeOH}/\text{CH}_2\text{Cl}_2$).

Synthesis of (*S*)-5-(azidomethyl)pyrrolidin-2-one **177**

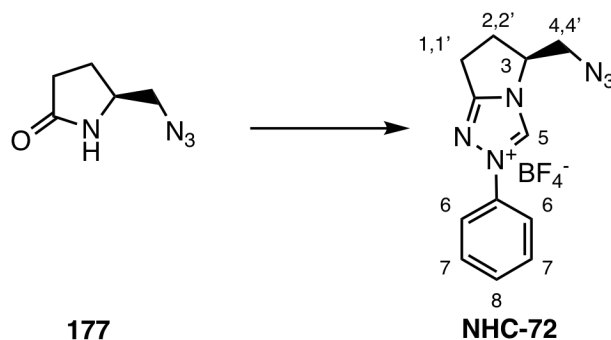


The Boc-azide **167** (1.43 g, 5.96 mmol) was dissolved in 1,4-dioxane (10 mL) and 4M HCl/dioxane (6 mL) added. This was stirred for 18h at rt and full conversion measured by TLC. The volatile solvents were removed, and the product dissolved in CH_2Cl_2 (50 mL) and washed with sat. NaHCO_3 until basic (the amine is H_2O soluble so the smallest quantity was used). The product was extracted with CH_2Cl_2 , dried (MgSO_4) and the volatile solvents removed under reduced pressure to give (*S*)-5-(azidomethyl)pyrrolidin-2-one **177** (750 mg, 90%, 5.33 mmol) as a yellow oil. Data matches the literature [78].

^1H NMR (CDCl_3 , 400 MHz, δ) 6.32 (br s, 1H, N-H) 3.85 – 3.77 (m, 1H, H_3), 3.47 (dd, 1H, $J = 4.3, 12.2$ Hz, $\text{H}_{4/4'}$), 3.30 (dd, 1H, $J = 7.3, 12.2$ Hz, $\text{H}_{4/4'}$), 2.42 - 2.33 (m, 2H, $\text{H}_{1/1'}$), 2.32 – 2.23 (m, 1H, $\text{H}_{2/2'}$), 1.88 – 1.77 (m, 1H, $\text{H}_{2/2'}$).

^{13}C NMR (CDCl_3 , 100 MHz, δ) 178.1, 56.3, 53.5, 29.7, 24.2.

Synthesis of (*S*)-5-(azidomethyl)-2-phenyl-6,7-dihydro-5*H*-pyrrolo[2,1-*c*][1,2,4]triazol-2-ium tetrafluoroborate NHC-72



(*S*)-5-(azidomethyl)pyrrolidin-2-one **177** (1 eq, 750 mg, 5.33 mmol) was dissolved in dry CH₂Cl₂ (4 mL) and added dropwise to a suspension of Me₃OBf₄ (1 eq, 789 mg, 5.33 mmol) in CH₂Cl₂ (25 mL). After stirring for 6h, phenylhydrazine (1.1 eq, 634 mg, 5.87 mmol, 0.58 mL) was added and stirred for 18h (darkens to brown). The solvent was removed under reduced pressure, the crude product dissolved in HC(OMe)₃ (10.5 mL) and MeOH (2.5 mL) and added to a sealed tube under air and heated to 80 °C for 24h. The volatile solvent was removed under reduced pressure and dissolved in chloroform, and a precipitate formed which was filtered and collected. The mixture was added to Et₂O and further precipitate was isolated. All of the precipitate was combined and dried under high vacuum to obtain (*S*)-5-(azidomethyl)-2-phenyl-6,7-dihydro-5*H*-pyrrolo[2,1-*c*][1,2,4]triazol-2-ium tetrafluoroborate **NHC-72** (368 mg, 1.17 mmol, 22%). Data matches the literature [78].

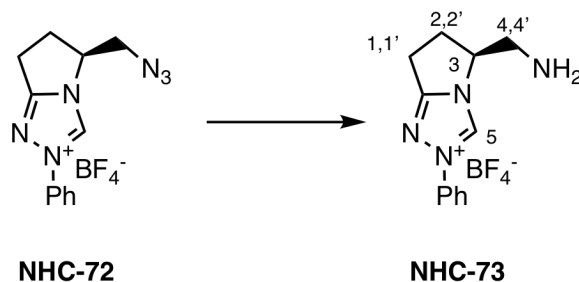
¹H NMR (CD₃CN, 400 MHz, δ) 9.80 (s, 1H, **H**₅), 7.83 – 7.78 (m, 2H, **H**₆), 7.70 – 7.64 (m, 3H, **H**_{7,8}), 4.90 – 4.83 (m 1H, **H**₃), 4.03 (dd, 1H, *J* = 3.8, 13.2 Hz, **H**_{4/4'}), 3.72 (dd, 1H, *J* = 8.5, 13.2 Hz, **H**_{4/4'}), 3.28 – 3.19 (m, 2H, **H**_{1,1'}), 3.02 – 2.91 (m, 1H, **H**_{2/2'}), 2.58 – 2.50 (m, 1H, **H**_{2/2'}).

¹³C NMR (CD₃CN, 100 MHz, δ) 163.8, 138.1, 136.6, 131.9, 131.2, 122.2, 61.0, 53.2, 31.0, 22.2. Matches lit.

[**M**]⁺ Calculated 241.1202, Obtained 241.1201.

FTIR $\nu(\text{cm}^{-1})$ 3123, 2111, 1583, 1518, 1445, 1390, 1288, 1223, 1030.

Synthesis of (S)-5-(aminomethyl)-2-phenyl-6,7-dihydro-5H-pyrrolo[2,1-c][1,2,4]triazol-2-ium tetrafluoroborate NHC-73



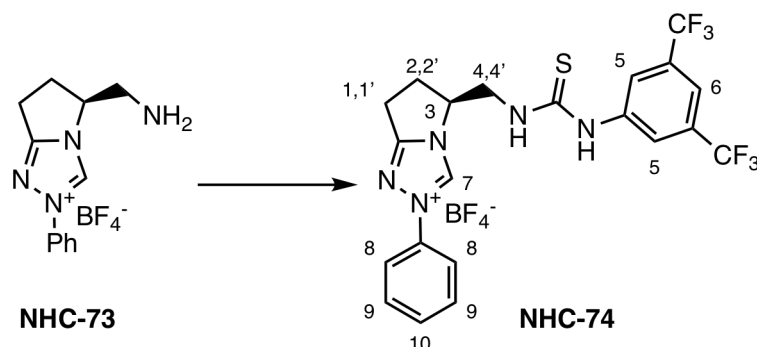
In a modification of Waser and coworkers' procedure, Pd/C (15 mg) was added to a 3-necked round bottomed flask and suspended in MeOH (7 mL). This was put under N_2 , and (S)-5-(azidomethyl)-2-phenyl-6,7-dihydro-5H-pyrrolo[2,1-c][1,2,4]triazol-2-ium (1 eq, 140 mg, 0.43 mmol) in MeOH (3 mL) was added. The flask was purged with 1 atm H_2 and stirred for 2.5h. The Pd/C was filtered off through Celite under a stream of N_2 and the volatile solvents were removed under reduced pressure to give (S)-5-(aminomethyl)-2-phenyl-6,7-dihydro-5H-pyrrolo[2,1-c][1,2,4]triazol-2-ium tetrafluoroborate **NHC-73** (64 mg, 0.21 mmol, 49%) as a yellow oil. Data matches the literature [78].

^1H NMR (CD_3CN , 400 MHz, δ) 9.87 (s, 1H, **H**₅), 7.83 – 7.78 (m, 2H, **H**₆), 7.68 – 7.62 (m, 3H, **H**_{7,8}), 4.72 – 4.64 (m, 1H, **H**₃), 3.25 – 3.10 (m, 4H, **H**_{1,1',4,4'}), 2.93 – 2.84 (m, 1H, **H**_{2/2'}), 2.55 – 2.45 (m, 1H, **H**_{2/2'}).

^{13}C NMR (CD_3CN , 100 MHz, δ) 162.8, 137.2, 135.8, 130.8, 130.2, 121.2, 63.3, 44.0, 30.1, 21.4.

[M]⁺ Calculated 215.1297, obtained 215.1321.

Synthesis of Waser and coworkers catalyst (*S*)-5-((3-(3,5-bis(trifluoromethyl)phenyl)thioureido)methyl)-2-phenyl-6,7-dihydro-5*H*-pyrrolo[2,1-*c*][1,2,4]triazol-2-ium tetrafluoroborate **NHC-74 [78]**



(*S*)-5-(aminomethyl)-2-phenyl-6,7-dihydro-5*H*-pyrrolo[2,1-*c*][1,2,4]triazol-2-ium **NHC-73** (1 eq, 64 mg, 0.21 mmol) was dissolved in dry CH_2Cl_2 (3.5 mL) and to this was added the isothiocyanate **109** (1 eq, 58 mg, 0.21 mmol, 39 μL). This was stirred at rt for 24h. The volatile solvents were removed under reduced pressure. The material was dissolved in Et_2O and a precipitate formed. This was filtered to afford (*S*)-5-((3-(3,5-bis(trifluoromethyl)phenyl)thioureido)methyl)-2-phenyl-6,7-dihydro-5*H*-pyrrolo[2,1-*c*][1,2,4]triazol-2-ium tetrafluoroborate **NHC-74** as a pure product (60 mg, 0.11 mmol, 50%). Data matches the literature [78].

^1H NMR (CD_3CN , 400 MHz, δ) 9.79 (s, 1H, **H**₇), 8.76 (s, 1H, N-**H**), 8.11 (s, 2H, **H**₅), 7.80 - 7.73 (m, 3H, **H**_{6,8}), 7.68 - 7.62 (m, 3H, **H**_{9,10}), 7.30 (t, 1H, NH, $J = 5.5$ Hz), 5.15 (sept, 1H, $J = 4.1$ Hz, **H**₃), 4.22 - 4.15 (m, 1H, **H**_{4/4'}), 4.12 - 4.04 (m, 1H, **H**_{4/4'}), 3.37 - 3.22 (m, 2H, **H**_{1,1'}), 3.06 - 2.94 (m, 1H, **H**_{2/2'}), 2.70 - 2.60 (m, 1H, **H**_{2/2'}).

^{13}C NMR (CD_3CN , 100 MHz, δ) 184.1, 164.0, 141.7, 138.3, 136.6, 132.3, 132.0, 131.3, 125.4 (m), 123.5 (q, $J = 271$ Hz), 122.2, 119.5 (m), 61.3, 47.1, 31.4, 22.1.

[**M**]⁺ Obtained 486.1152, calculated 486.1182.

CHN Obtained C 44.42, H 3.32, N 11.93. Required C 44.00, H 3.17, N 12.22.

References

- [1] L. Pasteur. Memoire sur la relation qui peut exister entre la forme cristalline et la composition chimique, et sur la cause de la polarisation rotatoire. *Comptes rendus l'Académie des Sci.*, 26:535–539, 1848.
- [2] W. T. Kelvin. The molecular tactics of a crystal. (*Book*) Clarendon Press, 1894.
- [3] N. A. McGrath, M. Brichacek, and J. T. Njardarson. A graphical journey of innovative organic architectures that have improved our lives. *J. Chem. Educ.*, 87(12):1348–1349, 2010.
- [4] S. K. Teo, W. A. Colburn, W. G. Tracewell, K. A. Kook, D. I. Stirling, M. S. Jaworsky, M. A. Scheffler, S. D. Thomas, and O. L. Laskin. Clinical pharmacokinetics of thalidomide. *Clin. Pharmacokinet.*, 43(5):311–327, 2004.
- [5] M. Reist, P. A. Carrupt, E. Francotte, and B. Testa. Chiral inversion and hydrolysis of thalidomide: Mechanisms and catalysis by bases and serum albumin, and chiral stability of teratogenic metabolites. *Chem. Res. Toxicol.*, 11(12):1521–1528, 1998.
- [6] C. Tian, P. Xiu, Y. Meng, W. Zhao, Z. Wang, and R. Zhou. Enantiomerization Mechanism of Thalidomide and the Role of Water and Hydroxide Ions. *Chem. Eur. J.*, 18(45):14305–14313, 2012.
- [7] H. Rzepa. Thalidomide. The role of water in the mechanism of its aqueous racemisation. *Chemistry with a Twist (Blog by Imperial College London)*, Nov. 2012.
- [8] X. Chen, K. M. Engle, D. H. Wang, and Y. Jin-Quan. Palladium(II)-catalyzed C-H activation/C-C cross-coupling reactions: Versatility and practicality. *Angew. Chem. Int. Ed.*, 48(28):5094–5115, 2009.
- [9] K. F. Heck and J. P. Nolley. Palladium-Catalyzed Vinylic Hydrogen Substitution Reactions with Aryl, Benzyl, and Styryl Halides. *J. Org. Chem.*, 37(14):2320–2322, 1972.
- [10] E. Negishi, A. O. King, and N. Okukado. Selective Carbon-Carbon Bond Formation via Transition Metal Catalysis. 3. A Highly Selective Synthesis of Unsymmetrical Biaryls and Diarylmethanes by the Nickel- or Palladium-Catalyzed Reaction of Aryl- and Benzylzinc Derivatives with Aryl Halides. *J. Org. Chem.*, 42(10):1821–1823, 1977.
- [11] N. Miyauro and A. Suzuki. Stereoselective Synthesis of Arylated (*E*)-Alkenes by the Reaction of Alk-1-enylboranes with Aryl Halides in the Presence of Palladium Catalyst. *J. C. S. Chem. Comm.*, (0):866–867, 1979.

- [12] I. Arends, R. Sheldon, and U. Hanefeld. Introduction: Green Chemistry and Catalysis. *Green Chem. Catal.*, (0):97–98, 2007.
- [13] L. Bernardi, M. Fochi, M. Comes Franchini, and A. Ricci. Bioinspired organocatalytic asymmetric reactions. *Org. Biomol. Chem.*, 10(15):2911, 2012.
- [14] R. Mahrwald. Organocatalytic methods for CC bond formation. *Drug Discov. Today Technol.*, 10(1):29–36, 2013.
- [15] A. Moyano. Activation Modes In Asymmetric Organocatalysis. (Book) *Stereoselective Organocatalysis: Bond Formation Methodologies and Activation Modes*, (0):11–80, 2013.
- [16] U. Eder, G. Sauer, and R. Wiechert. New type of asymmetric cyclization to optically active steroid CD partial structures. *Angew. Chem. Int. Ed.*, 10(7):496–497, 1971.
- [17] Z. G. Hajos and D. R. Parrish. Asymmetric Synthesis of Bicyclic Intermediates of Natural product chemistry. *J. Org. Chem.*, 39(12):1615–1621, 1974.
- [18] S. Bahmanyar, K. N. Houk, H. J. Martin, and B. List. Quantum mechanical predictions of the stereoselectivities of proline-catalyzed asymmetric intermolecular aldol reactions. *J. Am. Chem. Soc.*, 125(9):2475–2479, 2003.
- [19] M. Nielsen, D. Worgull, T. Zweifel, B. Gschwend, S. Bertelsen, and K. A. Jørgensen. Mechanisms in aminocatalysis. *Chem. Commun.*, 47(2):632–649, 2011.
- [20] M. N. Hopkinson, C. Richter, M. Schedler, and F. Glorius. An overview of N-heterocyclic carbenes. *Nature*, 510(7506):485–496, 2014.
- [21] Z. Li, X. Li, and J. P. Cheng. An Acidity Scale of Triazolium-Based NHC Precursors in DMSO. *J. Org. Chem.*, 82(18):9675–9681, 2017.
- [22] M. Scholl, T. M. Trnka, J. P. Morgan, and R. H. Grubbs. Increased ring closing metathesis activity of ruthenium-based olefin metathesis catalysts coordinated with imidazolin-2-ylidene ligands. *Tetrahedron Lett.*, 40(12):2247–2250, 1999.
- [23] X. Bugaut and F. Glorius. Organocatalytic umpolung: N-heterocyclic carbenes and beyond. *Chem. Soc. Rev.*, 41:3511–3522, 2012.
- [24] J. Seayad and B. List. Asymmetric Organocatalysis. *Org. Biomol. Chem.*, 3:719–724, 2005.
- [25] M. S. Sigman and E. N. Jacobsen. Schiff base catalysts for the asymmetric strecker reaction identified and optimized from parallel synthetic libraries. *J. Am. Chem. Soc.*, 120(19):4901–4902, 1998.
- [26] T. Akiyama, J. Itoh, K. Yokota, and K. Fuchibe. Enantioselective Mannich-Type Reaction Catalyzed by a Chiral Brønsted Acid. *Angew. Chem. Int. Ed.*, 43(12):1566–1568, 2004.
- [27] D. Uraguchi and M. Terada. Chiral Brønsted Acid-Catalyzed Direct Mannich Reactions via Electrophilic Activation. *J. Am. Chem. Soc.*, 126(17):5356–5357, 2004.

- [28] I. D. Gridnev, M. Kouchi, K. Sorimachi, and M. Terada. On the mechanism of stereoselection in direct Mannich reaction catalyzed by BINOL-derived phosphoric acids. *Tetrahedron Lett.*, 48(3):497–500, 2007.
- [29] D. Parmar, E. Sugiono, S. Raja, and M. Rueping. Complete field guide to asymmetric BINOL-phosphate derived Brønsted acid and metal catalysis: History and classification by mode of activation; Brønsted acidity, hydrogen bonding, ion pairing, and metal phosphates. *Chem. Rev.*, 114(18):9047–9153, 2014.
- [30] K. Kaupmees, N. Tolstoluzhsky, S. Raja, M. Rueping, and I. Leito. On the acidity and reactivity of highly effective chiral Brønsted acid catalysts: Establishment of an acidity scale. *Angew. Chem. Int. Ed.*, 52(44):11569–11572, 2013.
- [31] A. Berkessel, P. Christ, N. Leconte, J. M. Neudörfl, and M. Schäfer. Synthesis and structural characterization of a new class of strong chiral Brønsted acids: 1,1-binaphthyl-2,2-bis(sulfonyl)imides (JINGLES). *Eur. J. Org. Chem.*, (27):5165–5170, 2010.
- [32] Y. Huang, A. K. Unni, A. N. Thadani, and V. H. Rawal. Single enantiomers from a chiral-alcohol catalyst. *Nature*, 424(6945):146, 2003.
- [33] B. M. Nugent, R. A. Yoder, and J. N. Johnston. Chiral Proton Catalysis: A Catalytic Enantioselective Direct Aza-Henry Reaction. *J. Am. Chem. Soc.*, 126(11):3418–3419, 2004.
- [34] J. Huang and E. J. Corey. A new chiral catalyst for the enantioselective Strecker synthesis of α -amino acids. *Org. Lett.*, 6(26):5027–5029, 2004.
- [35] T. Akiyama, J. Itoh, and K. Fuchibe. Recent Progress in Chiral Brønsted Acid Catalysis. *Adv. Synth. Catal.*, 348(9):999–1010, 2006.
- [36] T. Akiyama. Stronger Brønsted acids. *Chem. Rev.*, 107(12):5744–5758, 2007.
- [37] J. Merad, C. Lalli, G. Bernadat, J. Maury, and G. Masson. Enantioselective Brønsted Acid Catalysis as a Tool for the Synthesis of Natural Products and Pharmaceuticals. *Chem. Eur. J.*, (24):3925–3943, 2017.
- [38] J. Hine, K. Ahn, J. C. Gallucci, and S. M. Linden. 1,8-Biphenylenediol Forms Two Strong Hydrogen Bonds to the Same Oxygen Atom. *J. Am. Chem. Soc.*, 106(25):7980–7981, 1984.
- [39] M. C. Etter, M. Zia-Ebrahimi, Z. Urbańczyk-Lipkowska, and T. W. Panunto. Hydrogen Bond Directed Cocrystallization and Molecular Recognition Properties of Diarylureas. *J. Am. Chem. Soc.*, 112(23):8415–8426, 1990.
- [40] M. C. Etter and T. W. Panunto. 1,3-Bis(m-nitrophenyl)urea: An exceptionally good complexing agent for proton acceptors. *J. Am. Chem. Soc.*, 110(17):5896–5897, 1988.
- [41] M. C. Etter. Encoding and Decoding Hydrogen-Bond Patterns of Organic Compounds. *Acc. Chem. Res.*, 23(4):120–126, 1990.

- [42] T. Okino, Y. Hoashi, and Y. Takemoto. Enantioselective Michael Reaction of Malonates to Nitroolefins Catalyzed by Bifunctional Organocatalysts. *J. Am. Chem. Soc.*, 125(42):12672–12673, 2003.
- [43] T. Okino, Y. Hoashi, T. Furukawa, X. Xu, and Y. Takemoto. Enantio- and diastereoselective michael reaction of 1,3-dicarbonyl compounds to nitroolefins catalyzed by a bifunctional thiourea. *J. Am. Chem. Soc.*, 127(1):119–125, 2005.
- [44] Y. Takemoto. Recognition and activation by ureas and thioureas: stereoselective reactions using ureas and thioureas as hydrogen-bonding donors. *Org. Biomol. Chem.*, 3(24):4299, 2005.
- [45] W. Yang and D. M. Du. Highly enantioselective michael addition of nitroalkanes to chalcones using chiral squaramides as hydrogen bonding organocatalysts. *Org. Lett.*, 12(23):5450–5453, 2010.
- [46] W. Yang and D.-M. Du. Squaramide-catalysed enantio- and diastereoselective sulfa-Michael addition of thioacetic acid to α,β -disubstituted nitroalkenes. *Org. Biomol. Chem.*, 10(34):6876–6884, 2012.
- [47] H. X. He, W. Yang, and D. M. Du. Enantioselective Aza-Henry Reaction of Imines Bearing a Benzothiazole Moiety Catalyzed by a Cinchona-Based Squaramide. *Adv. Synth. Catal.*, 355(6):1137–1148, 2013.
- [48] H. X. He and D. M. Du. Organocatalytic enantioselective strecker reaction of imines containing a thiazole moiety by using a cinchona-based squaramide catalyst. *Eur. J. Org. Chem.*, 2014(28):6190–6199, 2014.
- [49] H.-X. He and D.-M. Du. Squaramide-catalysed enantioselective Mannich reaction of imines bearing a heterocycle with malonates. *RSC Adv.*, 3(37):16349–16358, 2013.
- [50] B. L. Zhao, J. H. Li, and D. M. Du. Squaramide-Catalyzed Asymmetric Reactions. *Chem. Rec.*, 17(10):994–1018, 2017.
- [51] A. Jeppesen, B. E. Nielsen, D. Larsen, O. M. Akselsen, T. I. Sølling, T. Brock-Nannestad, and M. Pittelkow. Croconamides: a new dual hydrogen bond donating motif for anion recognition and organocatalysis. *Org. Biomol. Chem.*, 15(13):2784–2790, 2017.
- [52] V. E. Zwicker, K. K. Y. Yuen, D. G. Smith, J. Ho, L. Qin, P. Turner, and K. A. Jolliffe. Deltamides and Croconamides: Expanding the Range of Dual H-bond Donors for Selective Anion Recognition. *Chem. Eur. J.*, 24(5):1140–1150, 2018.
- [53] F. Wöhler and J. von Liebig. Untersuchungen über das Radikal der Benzoessäure. *Ann. der Pharm.*, 3(3):249–282, 1832.
- [54] D. T. Ukai T, Tanaka R. A new catalyst for acyloin condensation. *J. Pharm. Soc. Jpn.*, (63):296, 1943.
- [55] B. List. Asymmetric Organocatalysis 1: Lewis Base and Acid Catalysts (Book) Thieme, Science of Synthesis. (1):591– 618, 2012.

- [56] R. Breslow and R. Kim. The thiazolium catalyzed benzoin condensation with mild base does not involve a 'dimer' intermediate. *Tetrahedron Lett.*, 35(5):699–702, 1994.
- [57] R. Breslow. On the Mechanism of Thiamine Action. IV. 1 Evidence from Studies on Model Systems. *J. Am. Chem. Soc.*, 80(14):3719–3726, 1958.
- [58] J. Mahatthananchai and J. W. Bode. Catalyzed Reactions Involving Acyl Azoliums. *Acc. Chem. Res.*, 47(2):696–707, 2014.
- [59] S. Gehrke and O. Hollóczki. Are There Carbenes in N-Heterocyclic Carbene Organocatalysis? *Angew. Chem. Int. Ed.*, (56):16395–16398, 2017.
- [60] J. C. Sheehan and D. H. Hunneman. Homogeneous Asymmetric Catalysis. *J. Am. Chem. Soc.*, 88(15):3666–3667, 1966.
- [61] T. Haral and J. C. Sheehan. Asymmetric Thiazolium Salt Catalysis of the Benzoin Condensation. *J. Org. Chem.*, 39(9):1196–1199, 1974.
- [62] W. Tagaki, Y. Tamura, and Y. Yano. Asymmetric benzoin condensation catalyzed by optically active thiazolium salts in micellar two-phase media. *Bull. Chem. Soc. Jpn.*, 53(2):478–480, 1980.
- [63] R. L. Knight and F. J. Leeper. Synthesis of and asymmetric induction by chiral bicyclic thiazolium salts. *Tetrahedron Lett.*, 38:3611–3614, 1997.
- [64] A. U. Gerhard and F. J. Leeper. Synthesis of and asymmetric induction by chiral polycyclic thiazolium salts. *Tetrahedron Lett.*, 38:3615–3618, 1997.
- [65] C. A. Dvorak and V. H. Rawal. Catalysis of benzoin condensation by conformationally-restricted chiral bicyclic thiazolium salts. *Tetrahedron Lett.*, 39(19):2925–2928, 1998.
- [66] J. Pesch, K. Harms, and T. Bach. Preparation of axially chiral N,N'-diarylimidazolium and N-arylthiazolium salts and evaluation of their catalytic potential in the benzoin and in the intramolecular stetter reactions. *Eur. J. Org. Chem.*, (9):2025–2035, 2004.
- [67] S. Orlandi, M. Caporale, M. Benaglia, and R. Annunziata. Synthesis of new enantiomerically pure C1- and C2-symmetric N-alkyl-benzimidazolium and thiazolium salts. *Tetrahedron Asymmetry*, 14(24):3827–3830, 2003.
- [68] F. López-Calahorra, J. Castells, L. Domingo, J. Marti, and J. M. Bofill. Use of 3,3'-Polymethylene-Bridged Thiazolium Salts Plus Bases as Catalysts of the Benzoin Condensation and its Mechanistic Implications: Proposal of a New Mechanism in Aprotic Conditions. *Heterocycles*, 37(3):1579–1597, 1994.
- [69] A. Miyashita, Y. Suzuki, M. Kobayashi, N. Kuriyama, and T. Higashino. Azolium salts as effective catalysts for benzoin condensation and related reactions. *Heterocycles*, 43(3):509–512, 1996.
- [70] J. H. Teles, J.-P. Melder, K. Ebel, R. Schneider, E. Gehrler, W. Harder, S. Brode, D. Enders, K. Breuer, and G. Raabe. Benzoin-Type Condensations of Formaldehyde Catalyzed by Stable Carbenes. *Helv. Chim. Acta*, 79:61–83, 1996.

- [71] D. Enders, K. Breuer, and J. H. Teles. A Novel Asymmetric Benzoin Reaction Catalyzed by a Chiral Triazolium Salt. *Helv. Chim. Acta*, 79:1217–1221, 1996.
- [72] R. L. Knight and F. J. Leeper. Comparison of chiral thiazolium and triazolium salts as asymmetric catalysts for the benzoin condensation. *J. Chem. Soc. Perkin Trans. 1*, (0): 1891–1894, 1998.
- [73] D. Enders and U. Kallfass. An efficient nucleophilic carbene catalyst for the asymmetric benzoin condensation. *Angew. Chem. Int. Ed.*, 41(10):1743–1745, 2002.
- [74] D. Enders and J. Han. Synthesis of enantiopure triazolium salts from pyroglutamic acid and their evaluation in the benzoin condensation. *Tetrahedron Asymmetry*, 19(11):1367–1371, 2008.
- [75] Y. Ma, S. Wei, J. Wu, F. Yang, B. Liu, J. Lan, S. Yang, and J. You. From mono-triazolium salt to bis-triazolium salt: Improvement of the asymmetric intermolecular benzoin condensation. *Adv. Synth. Catal.*, 350(16):2645–2651, 2008.
- [76] S. E. O'Toole and S. J. Connon. The enantioselective benzoin condensation promoted by chiral triazolium precatalysts: stereochemical control via hydrogen bonding. *Org. Biomol. Chem.*, 7(17):3584–3593, 2009.
- [77] L. Baragwanath, C. A. Rose, K. Zeitler, and S. J. Connon. Highly enantioselective benzoin condensation reactions involving a bifunctional protic pentafluorophenyl-substituted triazolium precatalyst. *J. Org. Chem.*, 74(23):9214–9217, 2009.
- [78] J. P. Brand, J. I. O. Siles, and J. Waser. Synthesis of chiral bifunctional (thio)urea N-heterocyclic carbenes. *Synlett*, (6):881–884, 2010.
- [79] X.-Y. Chen and S. Ye. N-Heterocyclic carbene-catalyzed reactions of C-C unsaturated bonds. *Org. Biomol. Chem.*, 11:7991–7998, 2013.
- [80] S. Dwivedi, S. Gupta, and S. Das. N-Heterocyclic Carbenes (NHCs) in Asymmetric Organocatalysis. *Curr. Organocatalysis*, 1(1):13–39, 2014.
- [81] H. Stetter and G. Dämbkes. Über die präparative Nutzung der Thiazoliumsalz-katalysierten Acyloin- und Benzoin-Bildung. *Synthesis*, (11):733–735, 1976.
- [82] H. Stetter and G. Dämbkes. Über die präparative Nutzung der 1,3-Thiazolium-salz-katalysierten Acyloin- und Benzoin-Bildung. *Synthesis*, 4:309–310, 1980.
- [83] S. E. O'Toole, C. A. Rose, S. Gundala, K. Zeitler, and S. J. Connon. Highly chemoselective direct crossed aliphatic-aromatic acyloin condensations with triazolium-derived carbene catalysts. *J. Org. Chem.*, 76(2):347–357, 2011.
- [84] C. A. Rose, S. Gundala, C.-L. Fagan, J. F. Franz, S. J. Connon, and K. Zeitler. NHC-catalysed, chemoselective crossed-acyloin reactions. *Chem. Sci.*, 3(3):735, 2012.
- [85] I. Piel, M. D. Pawelczyk, K. Hirano, R. Fröhlich, and F. Glorius. A family of thiazolium salt derived N-heterocyclic carbenes (NHCs) for organocatalysis: Synthesis, investigation and application in cross-benzoin condensation. *Eur. J. Org. Chem.*, (0): 5475–5484, 2011.

- [86] C. A. Rose, S. Gundala, S. J. Connon, and K. Zeitler. Chemoselective crossed acyloin condensations: Catalyst and substrate control. *Synthesis*, (2):190–198, 2011.
- [87] N. Malik and P. Erhardt. Synthesis of 6a-hydroxypterocarpanes via intramolecular benzoin condensation. *Tetrahedron Lett.*, 54(31):4121–4124, 2013.
- [88] T. Ema, K. Akihara, R. Obayashi, and T. Sakai. Construction of contiguous tetrasubstituted carbon stereocenters by intramolecular crossed benzoin reactions catalyzed by N-heterocyclic carbene (NHC) organocatalyst. *Adv. Synth. Catal.*, 354(17):3283–3290, 2012.
- [89] M.-q. Jia and S.-l. You. N - Heterocyclic Carbene-Catalyzed Enantioselective Intramolecular N - Tethered Aldehyde Ketone Benzoin Reactions. *ACS Catal.*, 3: 622–624, 2013.
- [90] C. G. Goodman and S. Johnson. Dynamic Kinetic Asymmetric Cross-Benzoin Additions of β - Stereogenic α - Keto Esters. *J. Am. Chem. Soc.*, 136:14698–14701, 2014.
- [91] D. Enders, O. Niemeier, and G. Raabe. Asymmetric synthesis of chromanones via N-heterocyclic carbene catalyzed intramolecular crossed-benzoin reactions. *Synlett*, (15):2431–2434, 2006.
- [92] Z. Rafiński and A. Kozakiewicz. Enantioselective Synthesis of Chromanones Bearing Quaternary Substituted Stereocenters Catalyzed by (1R)-Camphor-Derived N-Heterocyclic Carbenes. *J. Org. Chem.*, 80(15):7468–7476, 2015.
- [93] H. Takikawa and K. Suzuki. Modified chiral triazolium salts for enantioselective benzoin cyclization of enolizable keto-aldehydes: Synthesis of (+)-sappanone B. *Org. Lett.*, 9(14):2713–2716, 2007.
- [94] Y. Hachisu, J. W. Bode, and K. Suzuki. Catalytic intramolecular crossed aldehyde-ketone benzoin reactions: A novel synthesis of functionalized preanthraquinones. *J. Am. Chem. Soc.*, 125(28):8432–8433, 2003.
- [95] L. He, Y. R. Zhang, X. L. Huang, and S. Ye. Chiral bifunctional N-heterocyclic carbenes: Synthesis and application in the aza-Morita-Baylis-Hillman reaction. *Synthesis*, (17):2825–2829, 2008.
- [96] Y. R. Zhang, L. He, X. Wu, P. L. Shao, and S. Ye. Chiral N-heterocyclic carbene catalyzed Staudinger reaction of ketenes with imines: Highly enantioselective synthesis of N-boc β -lactams. *Org. Lett.*, 10(2):277–280, 2008.
- [97] G.-Q. Li, L.-X. Dai, and S.-L. You. Thiazolium-derived N-heterocyclic carbene-catalyzed cross-coupling of aldehydes with unactivated imines. *Chem. Commun.*, (8): 852–854, 2007.
- [98] Z.-H. Gao, X.-Y. Chen, H.-M. Zhang, and S. Ye. N-Heterocyclic carbene-catalyzed [3+3] cyclocondensation of bromoenals with aldimines: highly enantioselective synthesis of dihydropyridinones. *Chem. Commun.*, 51(60):12040–12043, 2015.

- [99] S. Yetra, A. Patra, and A. Biju. Recent Advances in the N-Heterocyclic Carbene (NHC)-Organocatalyzed Stetter Reaction and Related Chemistry. *Synthesis*, 47(10):1357–1378, 2015.
- [100] A. T. Biju, N. Kuhl, and F. Glorius. Extending NHC-catalysis: Coupling aldehydes with unconventional reaction partners. *Acc. Chem. Res.*, 44(11):1182–1195, 2011.
- [101] H. Stetter and M. Schreckenberger. Eine neue Methode zur Addition von Aldehyden an aktivierte Doppelbindungen. *Angew. Chem. Int. Ed.*, (2):7391, 1973.
- [102] D. Enders, K. Breuer, J. Runsink, and J. H. Teles. The First Asymmetric Intramolecular Stetter Reaction. Preliminary Communication. *Helv. Chim. Acta*, 79(7):1899–1902, 1996.
- [103] J. R. De Alaniz and T. Rovis. A highly enantio- and diastereoselective catalytic intramolecular Stetter reaction. *J. Am. Chem. Soc.*, 127(17):6284–6289, 2005.
- [104] Z. Q. Rong, Y. Li, G. Q. Yang, and S. L. You. D-camphor-derived triazolium salts for enantioselective intramolecular Stetter reactions. *Synlett*, (7):1033–1037, 2011.
- [105] Z. Rafiński. Enantioselective benzoin condensation catalyzed by spirocyclic terpene-based N-heterocyclic carbenes. *Tetrahedron*, 72(15):1860–1867, 2016.
- [106] Z. Rafiński. Novel ()- β -Pinene-Derived Triazolium Salts: Synthesis and Application in the Asymmetric Stetter Reaction. *ChemCatChem*, 8(16):2599–2603, 2016.
- [107] J. Ma, Y. Huang, and R. Chen. N-heterocyclic carbene-catalyzed (NHC) three-component domino reactions: highly stereoselective synthesis of functionalized acyclic ϵ -ketoesters. *Org. Biomol. Chem.*, 9(6):1791–1798, 2011.
- [108] D. M. Flanigan, F. Romanov-Michailidis, N. A. White, and T. Rovis. Organocatalytic Reactions Enabled by N-Heterocyclic Carbenes. *Chem. Rev.*, 115(17):9307–9387, 2015.
- [109] Y. Wang, D. Wei, and W. Zhang. Recent Advances on Computational Investigations of N-Heterocyclic Carbene Catalyzed Cycloaddition/Annulation Reactions: Mechanism and Origin of Selectivities. *ChemCatChem*, 10(2):338–360, 2018.
- [110] S. Li, L. Wang, P. Chauhan, A. Peuronen, K. Rissanen, and D. Enders. Asymmetric Synthesis of Five-Membered Spiropyrazolones via N-Heterocyclic Carbene (NHC)-Catalyzed [3+2] Annulations. *Synthesis*, 49(8):1808–1815, 2017.
- [111] Y. Zhang, S. Wu, S. Wang, K. Fang, G. Dong, N. Liu, Z. Miao, J. Yao, J. Li, W. Zhang, C. Sheng, and W. Wang. Divergent cascade construction of skeletally diverse "privileged" pyrazole-derived molecular architectures. *Eur. J. Org. Chem.*, 2015(9):2030–2037, 2015.
- [112] Q. Ni, J. Xiong, X. Song, G. Raabe, and D. Enders. NHC-catalyzed activation of α,β -unsaturated N-acyltriazoles: an easy access to dihydropyranones. *Chem. Commun.*, 51(78):14628–14631, 2015.

- [113] P. J. Fuchs and K. Zeitler. An N-Heterocyclic Carbene-Mediated, Enantioselective and Multicatalytic Strategy to Access Dihydropyranones in a Sequential Three-Component One-Pot Reaction. *Org. Lett.*, 19(22):6076–6079, 2017.
- [114] C. Fang, J. Cao, K. Sun, J. Zhu, T. Lu, and D. Du. Direct and Enantioselective Synthesis of NH-Free 1,5-Benzodiazepin-2-ones by an N-Heterocyclic Carbene Catalyzed [3+4] Annulation Reaction. *Chem. Eur. J.*, (24):2103–2108, 2018.
- [115] D. Gillet, J. Barbier, L. Johannes, B. Stechmann, and S.-K. Bai. Inhibitors of the Shiga toxins trafficking through the retrograde pathway. (*WIPO Int. Patent No. IB 2009 006334*), 2009.
- [116] G. Zhang, W. Xu, J. Liu, D. K. Das, S. Yang, S. Perveen, H. Zhang, X. Li, and X. Fang. Enantioselective intermolecular all-carbon [4+2] annulation *via* N-heterocyclic carbene organocatalysis. *Chem. Commun.*, 53(100):13336–13339, 2017.
- [117] J. Yan, K. Shi, C. Zhao, L. Ding, S. Jiang, L. Yang, and G. Zhong. NHC-catalyzed [4+2] cycloaddition reactions for the synthesis of 3-spirocyclic oxindoles *via* a C–F bond cleavage protocol. *Chem. Commun.*, 54:1567–1570, 2018.
- [118] S. Li, X.-Y. Chen, H. Sheng, C. von Essen, K. Rissanen, and D. Enders. N-Heterocyclic Carbene Catalyzed Asymmetric Synthesis of Dihydropyranothiazoles via Azolium Enolate Intermediates. *Synthesis*, (Table 1):1047–1052, 2017.
- [119] K.-Q. Chen, H.-M. Zhang, D.-L. Wang, D.-Q. Sun, and S. Ye. Enantioselective N-heterocyclic carbene-catalyzed synthesis of indenopyrones. *Org. Biomol. Chem.*, 13(24):6694–6697, 2015.
- [120] K. E. Ozboya and T. Rovis. A late-stage strategy for the functionalization of triazolium-based NHC catalysts. *Synlett*, 25(18):2665–2668, 2014.
- [121] C. Selg, W. Neumann, P. Lönnecke, E. Hey-Hawkins, and K. Zeitler. Carboranes as Aryl Mimetics in Catalysis: A Highly Active Zwitterionic NHC-Precatalyst. *Chem. Eur. J.*, 23(33):7834, 2017.
- [122] M. S. Kerr, J. Read De Alaniz, and T. Rovis. An efficient synthesis of achiral and chiral 1,2,4-triazolium salts: Bench stable precursors for N-heterocyclic carbenes. *J. Org. Chem.*, 70(14):5725–5728, 2005.
- [123] K. N. Houk and P. H. Y. Cheong. Computational prediction of small-molecule catalysts. *Nature*, 455(7211):309–313, 2008.
- [124] P. H. Y. Cheong, H. Zhang, R. Thayumanavan, F. Tanaka, K. N. Houk, and C. F. Barbas. Pipelic acid-catalyzed direct asymmetric Mannich reactions. *Org. Lett.*, 8(5):811–814, 2006.
- [125] T. Dudding and K. N. Houk. Computational predictions of stereochemistry in asymmetric thiazolium- and triazolium-catalyzed benzoin condensations. *Proc. Natl. Acad. Sci. U. S. A.*, 101(16):5770–5775, 2004.

- [126] E. A. Meyer, R. K. Castellano, and F. Diederich. *Interactions with Arenes Interactions with Aromatic Rings in Chemical and Biological Recognition Angewandte*. Number 11. 2003. 1210–1250 pp.
- [127] M. Nic, J. Jirat, and B. Kosata. *IUPAC. Compendium of Chemical Terminology, (the "Gold Book")*. Blackwell Scientific Publications, Oxford, 2nd edition, 2006.
- [128] G. Helmchen. The 50th Anniversary of the Cahn – Ingold – Prelog Specification of Molecular Chirality. *Angew. Chem. Int. Ed.*, 55:6798–6799, 2016.
- [129] R. S. Menon, A. T. Biju, and V. Nair. Recent advances in N-heterocyclic carbene (NHC) -catalysed benzoin reactions. *Beilstein J. Org. Chem.*, (12):444–461, 2016.
- [130] S. M. Mennen, J. D. Gipson, Y. R. Kim, and S. J. Miller. Thiazolylalanine-Derived Catalysts for Enantioselective Intermolecular AldehydeImine Cross-Couplings. *J. Am. Chem. Soc.*, 127(6):1654–1655, 2005.
- [131] D. M. Walden, O. M. Ogba, R. C. Johnston, and P. H.-Y. Cheong. Computational Insights into the Central Role of Nonbonding Interactions in Modern Covalent Organocatalysis. *Acc. Chem. Res.*, 49:1279–1291, 2016.
- [132] R. C. Johnston, D. T. Cohen, C. C. Eichman, K. A. Scheidt, and C. P. Ha-Yeon. Chemical Science Catalytic kinetic resolution of a dynamic racemate : highly stereoselective beta-lactone formation by N - heterocyclic carbene catalysis. *Chem. Sci.*, 5:1974–1982, 2014.
- [133] M. Schumacher and B. Goldfuss. Quantifying N-heterocyclic carbenes as umpolung catalysts in the benzoin reaction : balance between nucleophilicity and electrophilicity. *New J. Chem.*, 39:4508–4518, 2015.
- [134] R. L. Knight. *Synthesis of and Asymmetric Induction by Chiral Azolium Salts*. PhD thesis, University of Cambridge, 1998.
- [135] T. Ascah. Innovations in Chiral Chromatography: Overview of Modern Chiral Stationary Phases. *Report.*, (29.2):18–20, 2011.
- [136] T. R. Hoye, C. S. Jeffrey, and F. Shao. Mosher ester analysis for the determination of absolute configuration of stereogenic (Chiral) carbinol carbons. *Nat. Protoc.*, 2(10): 2451–2458, 2007.
- [137] H. Stetter. Catalyzed Addition of Aldehydes to Activated Double Bonds—A New Synthetic Approach. *Angew. Chem. Int. Ed.*, 15(11):639–647, 1976.
- [138] O. Bortolini, C. Chiappe, M. Fogagnolo, A. Massi, and C. S. Pomelli. Formation, Oxidation, and Fate of the Breslow Intermediate in the N-Heterocyclic Carbene-Catalyzed Aerobic Oxidation of Aldehydes. *J. Org. Chem.*, 82(1):302–312, 2017.
- [139] J. R. De Alaniz, M. S. Kerr, J. L. Moore, and T. Rovis. Scope of the asymmetric intramolecular stetter reaction catalyzed by chiral nucleophilic triazolinyldiene carbenes. *J. Org. Chem.*, 73(6):2033–2040, 2008.

- [140] J. Christoffers, Y. Schulze, and J. Pickardt. Synthesis, resolution, and absolute configuration of trans-1-amino-2-dimethylaminocyclohexane. *Tetrahedron*, 57:1765–1769, 2001.
- [141] M. Kaik and J. Gawroński. Facile monoprotection of trans-1,2-diaminocyclohexane. *Tetrahedron Asymmetry*, 14(11):1559–1563, 2003.
- [142] G. Suez, V. Bloch, G. Nisnevich, and M. Gandelman. Design and development of bioinspired guanine-based organic catalyst for asymmetric catalysis. *Eur. J. Org. Chem.*, (11):2118–2122, 2012.
- [143] A. Berkessel and B. Seelig. A simplified synthesis of Takemoto’s catalyst. *Synthesis*, (12):2113–2115, 2009.
- [144] J. P. Brand, J. Ignacio, O. Siles, and J. Waser. Synthesis of Chiral Bifunctional (Thio)Urea N-Heterocyclic Carbenes. *Synlett*, (6):881–884, 2010.
- [145] R. B. Strand, T. Solvang, C. A. Sperger, and A. Fiksdahl. Preparation of chiral 1,2,4-triazolium salts as new NHC precatalysts. *Tetrahedron Asymmetry*, 23(11-12):838–842, 2012.
- [146] J. F. Larrow and E. N. Jacobsen. (R,R)-N,N’-bis(3,5-di-tert-butylsalicylidene)-1,2-cyclohexanediamino manganese (III) chloride, a highly enantioselective epoxidation catalyst. *Org. Synth.*, 75(September):1, 1998.
- [147] M. Sylla-Iyarreta Veitía, C. Ferroud, M. Joudat, M. Wagner, A. Falguières, and A. Guy. Ready Available Chiral Azapyridinomacrocycles N-Oxides; First Results as Lewis Base Catalysts in Asymmetric Allylation of p-Nitrobenzaldehyde. *Heterocycles*, 83(9):2011, 2011.
- [148] G. E. Tumambac and C. Wolf. Enantioselective analysis of an asymmetric reaction using a chiral fluorosensor. *Org. Lett.*, 7(18):4045–8, 2005.
- [149] F. Yu, Z. Jin, H. Huang, T. Ye, X. Liang, and J. Ye. A highly efficient asymmetric Michael addition of α,α -disubstituted aldehydes to maleimides catalyzed by primary amine thiourea salt. *Org. Biomol. Chem.*, 8(20):4767–4774, 2010.
- [150] S. V. Chankeshwara and A. K. Chakraborti. Catalyst-free chemoselective N - tert-butylloxycarbonylation of amines in water. *Org. Lett.*, (8):1–63, 2006.
- [151] L. H. Uppadine, F. R. Keene, and P. D. Beer. Approaches towards the enantioselective recognition of anionic guest species using chiral receptors based on rhenium(i) and ruthenium(ii) with amide bipyridine ligands. *J. Chem. Soc. Dalt. Trans.*, (14):2188–2198, 2001.
- [152] K. Dudziński, A. M. Pakulska, and P. Kwiatkowski. An efficient organocatalytic method for highly enantioselective michael addition of malonates to enones catalyzed by readily accessible primary amine-thiourea. *Org. Lett.*, 14(16):4222–4225, 2012.
- [153] M. Perillo, A. Di Mola, R. Filosa, L. Palombi, and A. Massa. Cascade reactions of glycine Schiff bases and chiral phase transfer catalysts in the synthesis of α -amino acids 3-substituted phthalides or isoindolinones. *RSC Adv.*, 4(9):4239–4246, 2014.

- [154] Y. Sohtome, A. Tanatani, Y. Hashimoto, and K. Nagasawa. Development of novel chiral urea catalysts for the hetero-Michael reaction. *Chem. Pharm. Bull. (Tokyo)*, 52 (4):477–480, 2004.
- [155] Á. L. Fuentes De Arriba, D. G. Seisdedos, L. Simón, V. Alcázar, C. Raposo, and J. R. Morán. Synthesis of monoacylated derivatives of 1,2- cyclohexanediamine. Evaluation of their catalytic activity in the preparation of Wieland-Miescher ketone. *J. Org. Chem.*, 75(23):8303–8306, 2010.
- [156] I. Piel, M. D. Pawelczyk, K. Hirano, R. Fröhlich, and F. Glorius. A family of thiazolium salt derived N-heterocyclic carbenes (NHCs) for organocatalysis: Synthesis, investigation and application in cross-benzoin condensation. *Eur. J. Org. Chem.*, (0): 5475–5484, 2011.
- [157] W. Yang and D. M. Du. Chiral squaramide-catalyzed highly enantioselective michael addition of 2-hydroxy-1,4-naphthoquinones to nitroalkenes. *Adv. Synth. Catal.*, 353 (8):1241–1246, 2011.
- [158] N. Busschaert, I. L. Kirby, S. Young, S. J. Coles, P. N. Horton, M. E. Light, and P. A. Gale. Squaramides as potent transmembrane anion transporters. *Angew. Chem. Int. Ed.*, 51(18):4426–4430, 2012.
- [159] N. Busschaert, R. B. P. Elmes, D. D. Czech, X. Wu, I. L. Kirby, E. M. Peck, K. D. Hendzel, S. K. Shaw, B. Chan, B. D. Smith, K. A. Jolliffe, and P. A. Gale. Thiosquaramides: pH switchable anion transporters. *Chem. Sci.*, 5(9):3617–3626, 2014.
- [160] M. J. White and F. J. Leeper. Kinetics of the thiazolium ion-catalyzed benzoin condensation. *J. Org. Chem.*, 66(11):5124–5131, 2001.
- [161] M. Gay, Á. M. Montaña, C. Batalla, J. M. Mesas, and M. T. Alegre. Design, synthesis and SAR studies of novel 1,2-bis(aminomethyl)cyclohexane platinum(II) complexes with cytotoxic activity. Studies of interaction with DNA of iodinated seven-membered 1,4-diaminoplatinocycles. *J. Inorg. Biochem.*, 142:15–27, 2015.
- [162] H. Rzepa. Mechanism of the reduction of a carboxylic acid by borane: revisited and revised. *Chemistry with a Twist (Blog by Imperial College London)*, 2011.
- [163] S. P. D. Dwivedi, R. C. Singh, and R. G. Chadva. Process for Preparing Benzoisothiazol-3-yl-piperazine-1-yl- Methyl-cyclohexyl-Methanisoindol-1,3-dione and its Intermediates. (*WIPO Int. Patent No. WO 2013/121440 A1*), 2013.
- [164] E. R. Jarvo and S. J. Miller. Amino acids and peptides as asymmetric organocatalysts. *Tetrahedron*, 58(13):2481–2495, 2002.
- [165] L.-W. Xu and Y. Lu. Primary amino acids: privileged catalysts in enantioselective organocatalysis. *Org. Biomol. Chem.*, 6(12):2047, 2008.
- [166] E. Steeples, A. Kelling, U. Schilde, and D. Esposito. Amino acid-derived N-heterocyclic carbene palladium complexes for aqueous phase Suzuki–Miyaura couplings. *New J. Chem.*, 40(6):4922–4930, 2016.

- [167] S. J. Connon. The design of novel, synthetically useful (thio)urea-based organocatalysts. *Synlett*, (3):354–376, 2009.
- [168] A. B. Enyong and B. Moasser. Ruthenium-catalyzed N-alkylation of amines with alcohols under mild conditions using the borrowing hydrogen methodology. *J. Org. Chem.*, 79(16):7553–7563, 2014.
- [169] D. Lawrence. *Towards the synthesis of a new N-heterocyclic carbene catalyst with a hydrogen bonding moiety*. Masters' project, University of Cambridge, 2017.
- [170] C. J. Cavender and V. J. Shiner. Trifluoromethanesulfonyl Azide. Its Reaction with Alkyl Amines to Form Alkyl Azides. *J. Org. Chem.*, 37(22):3567–3569, 1972.
- [171] P. T. Nyffeler, C. H. Liang, K. M. Koeller, and C. H. Wong. The chemistry of amine-azide interconversion: Catalytic diazotransfer and regioselective azide reduction. *J. Am. Chem. Soc.*, 124(36):10773–10778, 2002.
- [172] E. D. Goddard-Borger and R. V. Stick. An efficient, inexpensive, and shelf-stable diazotransfer reagent: Imidazole-1-sulfonyl azide hydrochloride. *Org. Lett.*, 9(19):3797–3800, 2007.
- [173] G. T. Potter, G. C. Jayson, G. J. Miller, and J. M. Gardiner. An Updated Synthesis of the Diazo-Transfer Reagent Imidazole-1-sulfonyl Azide Hydrogen Sulfate. *J. Org. Chem.*, 81:3443–3446, 2016.
- [174] V. Castro, J. B. Blanco-Canosa, H. Rodriguez, and F. Albericio. Imidazole-1-sulfonyl azide-based diazo-transfer reaction for the preparation of azido solid supports for solid-phase synthesis. *ACS Comb. Sci.*, 15(7):331–334, 2013.
- [175] A. K. Pandiakumar, S. P. Sarma, and A. G. Samuelson. Mechanistic studies on the diazo transfer reaction. *Tetrahedron Lett.*, 55(18):2917–2920, 2014.
- [176] G. Valot, D. Mailhol, C. S. Regens, D. P. O'Malley, E. Godineau, H. Takikawa, P. Philipps, and A. Fürstner. Concise total syntheses of amphidinolides C and F. *Chem. Eur. J.*, 21(6):2398–2408, 2015.
- [177] I. E. Wrona, A. E. Gabarda, G. Evano, and J. S. Panek. Total synthesis of reblastatin. *J. Am. Chem. Soc.*, 127(43):15026–15027, 2005.
- [178] S. Hanessian, S. Giroux, and M. Buffat. Total synthesis and structural confirmation of (+)-longicin. *Org. Lett.*, 7(18):3989–3992, 2005.
- [179] N. Huh and C. M. Thompson. Enantioenriched N-(2-chloroalkyl)-3-acetoxypiperidines as potential cholinotoxic agents. Synthesis and preliminary evidence for spirocyclic aziridinium formation. *Tetrahedron*, 51(21):5935–5950, 1995.
- [180] S. Dey, P. U. Karabal, and A. Sudalai. Concise Enantioselective Synthesis of Naturally Active (S)-3-Hydroxypiperidine. *Synth. Commun.*, 45(13):1559–1565, 2015.
- [181] R. Mohan, J. Nuss, and J. Harris. Heterocyclic compounds for the treatment of disease. (WIPO Int. Patent No. WO 2017083756, (0):1–96, 2017.

- [182] J. Clayden, N. Greeves, S. Warren, and P. Wothers. *Organic Chemistry (Book)*. 2000.
- [183] T. Dudding and K. N. Houk. Computational predictions of stereochemistry in asymmetric thiazolium- and triazolium-catalyzed benzoin condensations. *Proc. Natl. Acad. Sci. U. S. A.*, 101(16):5770–5775, 2004.
- [184] J. P. Malerich, K. Hagihara, and V. H. Rawal. Chiral Squaramide Derivatives are Excellent Hydrogen Bond Donor Catalysts. *J. Am. Chem. Soc.*, (0):14416–14417, 2008.
- [185] J. R. De Alaniz and T. Rovis. A highly enantio- and diastereoselective catalytic intramolecular Stetter reaction. *J. Am. Chem. Soc.*, 127(17):6284–6289, 2005.
- [186] M. He, J. R. Struble, and J. W. Bode. Highly enantioselective azadiene diels-alder reactions catalyzed by chiral N-heterocyclic carbenes. *J. Am. Chem. Soc.*, 128(26): 8418–8420, 2006.
- [187] H. Takikawa and K. Suzuki. Modified chiral triazolium salts for enantioselective benzoin cyclization of enolizable keto-aldehydes: Synthesis of (+)-sappanone B. *Org. Lett.*, 9(14):2713–2716, 2007.
- [188] H. U. Vora and T. Rovis. N-Heterocyclic Carbene Catalyzed Asymmetric Hydration: Direct Synthesis of alpha-Protio and alpha-Deuterio alpha-Chloro and alpha-Fluoro Carboxylic Acids. *J. Am. Chem. Soc.*, 132:2860–2861, 2010.
- [189] B. Cardinal-david, D. E. A. Raup, and K. A. Scheidt. Cooperative N-Heterocyclic Carbene / Lewis Acid Catalysis for Highly Stereoselective Annulation Reactions with Homoenolates. *J. Am. Chem. Soc.*, (IV):5345–5347, 2010.
- [190] D. A. Dirocco, K. M. Oberg, and T. Rovis. Isolable analogues of the Breslow intermediate derived from chiral triazolylidene carbenes. *J. Am. Chem. Soc.*, 134(14): 6143–6145, 2012.
- [191] M. D. Hanwell, D. E. Curtis, D. C. Lonie, T. Vandermeersch, E. Zurek, and G. R. Hutchison. Avogadro: an advanced semantic chemical editor, visualization, and analysis platform. *J. Cheminform.*, 4(17):1–17, 2012.
- [192] M. Miteva, F. Guyon, and P. Tufféry. Frog2: Efficient 3D conformation ensemble generator for small compounds. *Nucleic Acids Res.*, (0):W622–W627., 2010.
- [193] C. F. Macrae, I. J. Bruno, J. A. Chisholm, P. R. Edgington, P. McCabe, E. Pidcock, L. Rodriguez-Monge, R. Taylor, J. van de Streek, and P. A. Wood. Mercury CSD 2.0 - New Features for the Visualization and Investigation of Crystal Structures. *J. Appl. Cryst.*, 41:466–470, 2008.
- [194] H. E. Gottlieb, V. Kotlyar, and A. Nudelman. NMR Chemical Shifts of Common Laboratory Solvents as Trace Impurities. *J. Org. Chem.*, 62(3):7512–7515, 1997.
- [195] N. J. Parmar, B. D. Parmar, T. R. Sutariya, R. Kant, and V. K. Gupta. An efficient synthesis of some thiopyranopyrazole-heterocycles via domino reaction in a Brønsted acidic ionic liquid. *Tetrahedron Lett.*, 55(44):6060–6064, 2014.

- [196] X.-J. Zhang, S.-P. Liu, J.-H. Lao, G.-J. Du, M. Yan, and A. S. C. Chan. Asymmetric conjugate addition of carbonyl compounds to nitroalkenes catalyzed by chiral bifunctional thioureas. *Tetrahedron: Asymmetry*, 20(12):1451–1458, 2009.
- [197] D. W. Lee, H. Ha, and W. K. Lee. Selective Mono-BOC Protection of Diamines. *Synth. Commun.*, 37(5):737–742, 2007.
- [198] W. Yang and D. M. Du. Highly enantioselective michael addition of nitroalkanes to chalcones using chiral squaramides as hydrogen bonding organocatalysts. *Org. Lett.*, 12(23):5450–5453, 2010.
- [199] Y. Liu, A. Lu, K. Hu, Y. Wang, H. Song, Z. Zhou, and C. Tang. Bifunctional primary amine-squaramide catalyzed enantioselective intramolecular Michael addition of keto-enones: A convenient process to the stereocontrolled construction of trans-dihydrobenzofuran skeletons. *Eur. J. Org. Chem.*, (22):4836–4843, 2013.
- [200] W. Chen, X. Tang, W. Dou, B. Wang, L. Guo, Z. Ju, and W. Liu. The Construction of Homochiral Lanthanide Quadruple-Stranded Helicates with Multiresponsive Sensing Properties toward Fluoride Anions. *Chem. Eur. J.*, 23(41):9804–9811, 2017.
- [201] J. de Mier-Vinué, Á. M. Montaña, V. Moreno, and M. J. Prieto. Synthesis and Characterization of [(1,4-diamine)dichloro]platinum(II) Compounds Preliminary Studies on their Biological Activity. *Zeitschrift für Anorg. und Allg. Chemie*, 631(11):2054–2061, 2005.
- [202] T. A. K. Al-Allaf, D. Steinborn, K. Merzweiler, and C. Wagner. Platinum (II) and palladium (II) complexes analogous to oxaliplatin with different cyclohexyldicarboxylate isomeric anions and their *in vitro* antitumour activity. Structural elucidation of [Pt(C₂O₄)(cis-dach)]. *Transition Metal Chemistry*, (28):717–721, 2003.
- [203] F. Fécourt, B. Delpech, O. Melnyk, and D. Crich. Se -(9-fluorenylmethyl) selenoesters; Preparation, reactivity, and use as convenient synthons for selenoacids. *Org. Lett.*, 15(14):3758–3761, 2013.
- [204] M.-W. Ding, Y. Sun, and Z.-J. Liu. An Efficient Synthesis of 2-Alkylthio-5-phenylmethylidene-4H-imidazolin-4-ones. *Synth. Commun.*, 33(8):1267–1274, 2003.
- [205] D. Enders, O. Niemeier, and T. Balensiefer. Asymmetric intramolecular crossed-benzoin reactions by N-heterocyclic carbene catalysis. *Angew. Chem. Int. Ed.*, 45(9):1463–1467, 2006.
- [206] T. Hjelmgaard, I. Sjøtofte, and D. Tanner. Total Synthesis of Pinnamine and Anatoxin-a via a Common Intermediate. A Caveat on the Anatoxin-a Endgame. *J. Org. Chem.*, 70:5688–5697, 2005.
- [207] C. Y. Kawasoko, P. Foletto, O. E. D. Rodrigues, L. Dornelles, R. S. Schwab, and A. L. Braga. Straightforward synthesis of non-natural l-chalcogen and l-diselenide N-Boc-protected- γ -amino acid derivatives. *Org. Biomol. Chem.*, 11(31):5173, 2013.
- [208] J. Ackermann, M. Matthes, and C. Tamm. Approaches to the Synthesis of Cytochalasans. *Helvetica Chimica Acta*, 73:122–132, 1990.

-
- [209] J. Massé and N. Langlois. Synthesis of 5-Amino- and 4-Hydroxy- 2-Phenylsulfonylmethylpiperidines. *Heterocycles*, 77(1):417–432, 2009.
- [210] S. K. Panday and N. Langlois. Enantioselective Synthesis of (S)-5-Aminopiperidin-2-one from (S) -Pyroglutaminol. *Tetrahedron Lett.*, 36(45):8205–8208, 1995.

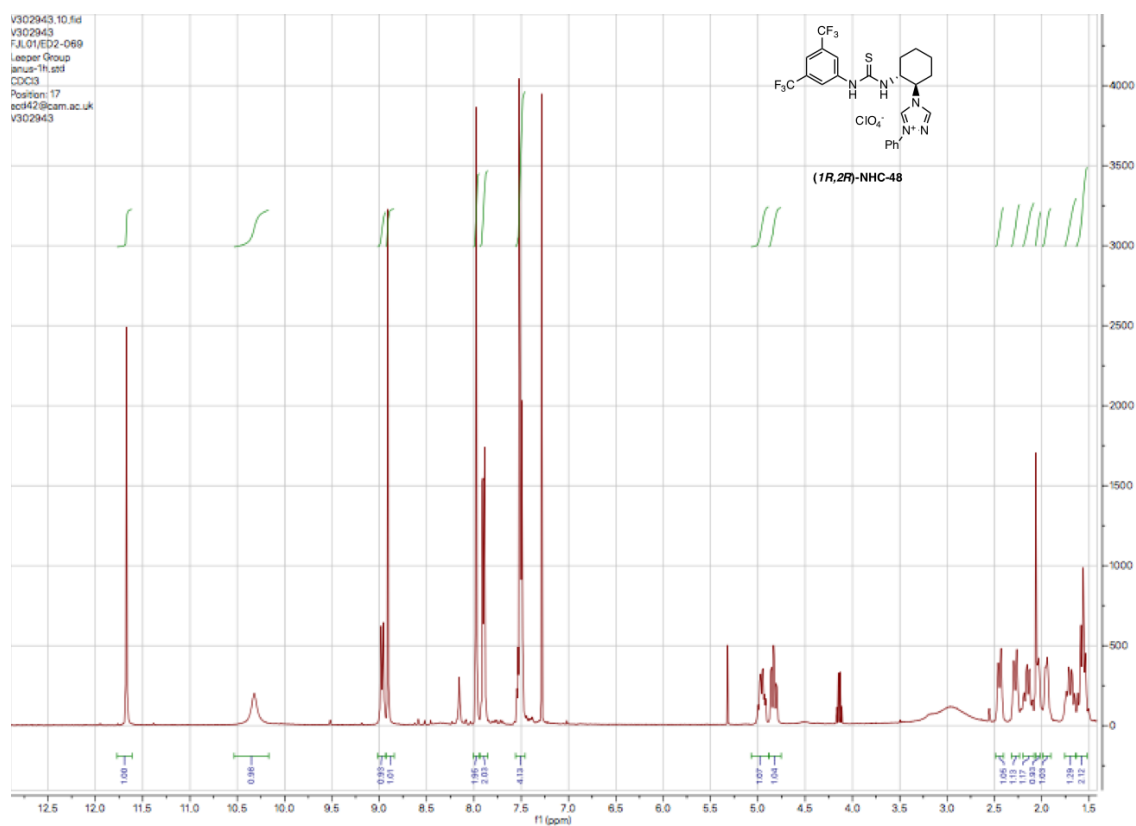
Appendix A

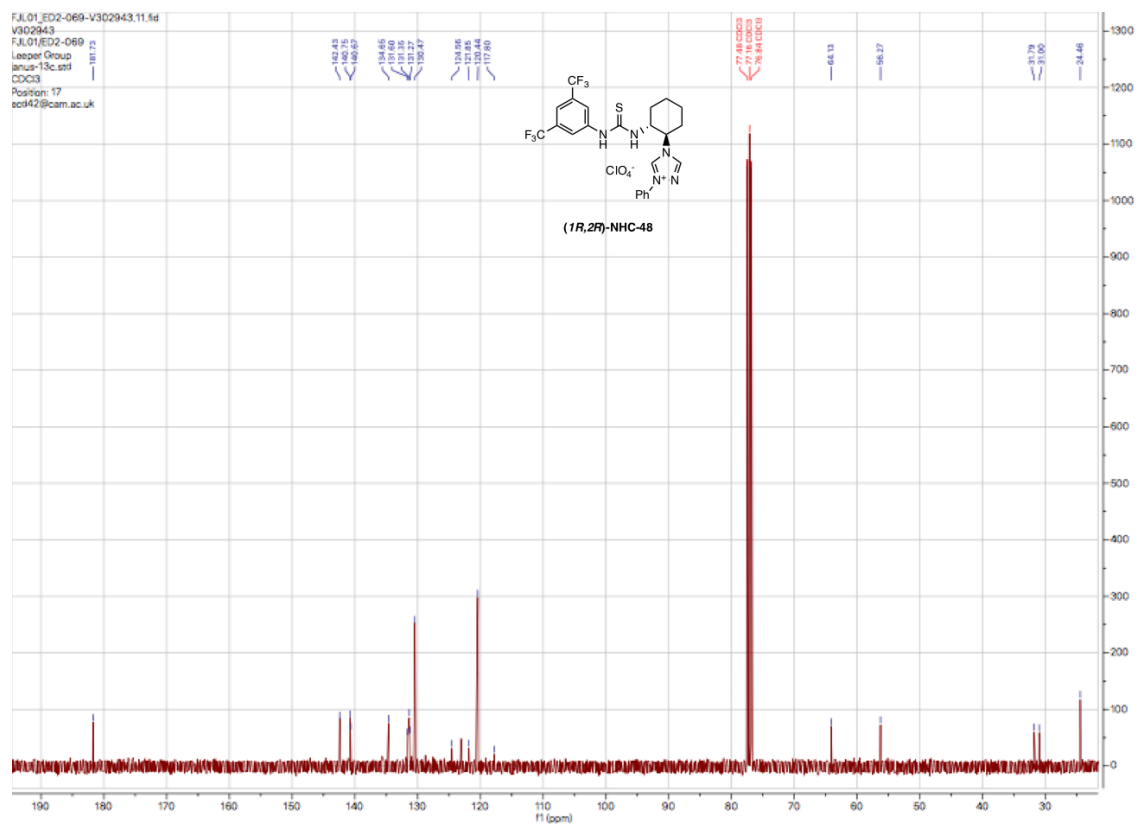
Supporting Information

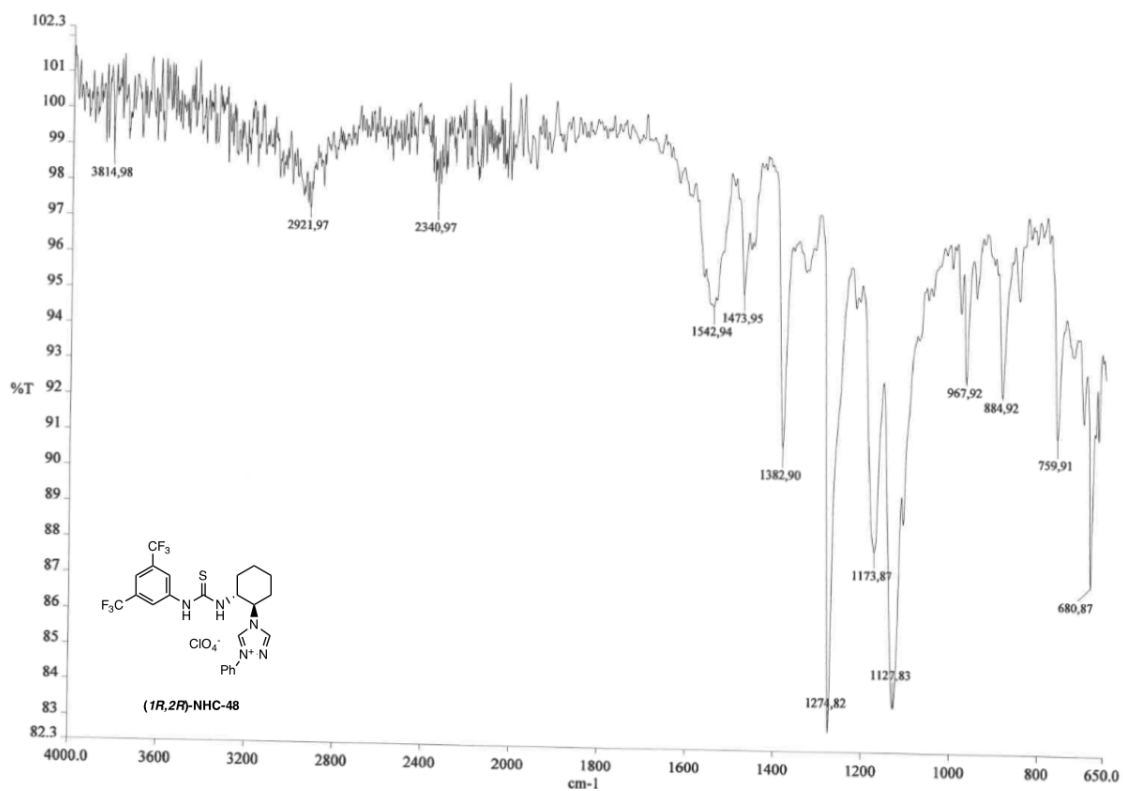
A.1 New Compound Data

A.1.1 Chapter 3 Compounds

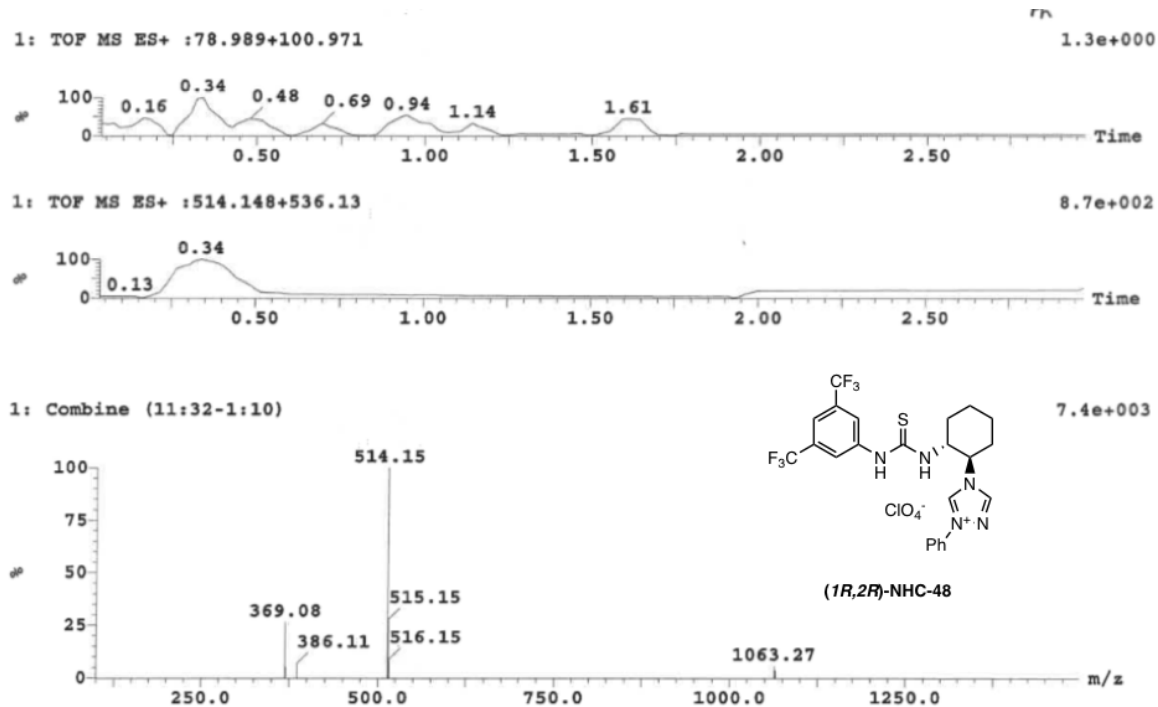
4-((*1R,2R*)-2-(3-(3,5-bis(trifluoromethyl)phenyl)thioureido)cyclohexyl)-1-phenyl-4*H*-1,2,4-triazol-1-ium perchlorate (*1R,2R*)-NHC-48

^1H NMR, 400 MHz

^{13}C NMR, 100 MHz

IR Spectrum (cm⁻¹)

High Resolution Mass Spectrum



Mass	Calc. Mass	mDa	PPM	DBE	Formula	i-FIT
514.1481	514.1495	-1.4	-2.7	20.5	C19 H16 N17 S	1.1
514.1481	514.1498	-1.7	-3.3	16.5	C21 H19 N11 F3 S	1.2
514.1481	514.1500	-1.9	-3.7	12.5	C23 H22 N5 F6 S	1.5
514.1481	514.1501	-2.0	-3.9	5.0	C20 H24 N2 F10 S	20.0
514.1481	514.1498	-1.7	-3.3	9.0	C18 H21 N8 F7 S	20.4
514.1481	514.1496	-1.5	-2.9	13.0	C16 H18 N14 F4 S	20.9
514.1481	514.1493	-1.2	-2.3	17.0	C14 H15 N20 F S	21.5
514.1481	514.1500	-1.9	-3.7	20.0	C26 H20 N8 F2 S	28.8
514.1481	514.1502	-2.1	-4.1	16.0	C28 H23 N2 F5 S	29.7
514.1481	514.1471	1.0	1.9	4.0	C18 H26 N4 F8 S2	60.2
514.1481	514.1471	1.0	1.9	11.5	C21 H24 N7 F4 S2	60.3
514.1481	514.1468	1.3	2.5	15.5	C19 H21 N13 F S2	60.3
514.1481	514.1473	0.8	1.6	7.5	C23 H27 N F7 S2	60.4
514.1481	514.1469	1.2	2.3	8.0	C16 H23 N10 F5 S2	60.9
514.1481	514.1466	1.5	2.9	12.0	C14 H20 N16 F2 S2	61.7
514.1481	514.1464	1.7	3.3	21.5	C24 H15 N11 F3	81.3
514.1481	514.1462	1.9	3.7	25.5	C22 H12 N17	81.3
514.1481	514.1466	1.5	2.9	17.5	C26 H18 N5 F6	81.3
514.1481	514.1466	1.5	2.9	25.0	C29 H16 N8 F2	91.1
514.1481	514.1468	1.3	2.5	21.0	C31 H19 N2 F5	91.7

Elemental Analysis

Name..... Emma Durham

Date..... 05/03/16

No. of Specimen EP2 USG

Analyse for C, H, N

Elements present..... C, H, N, O, F, S, Cl

M. pt. or B. pt.

Method of purification Column

Approx. values % C 52.4, H 7.74, N 2.44

Any remarks: my name is 2,5,6 ClO₄ (cylind)

I J 014849

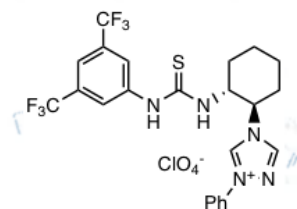
Results

1 3285 → C = 47.64
H = 4.14
N = 11.38

1 2308 → C = 47.57
H = 4.15
N = 11.34

II

Theoretical values and structural formulae

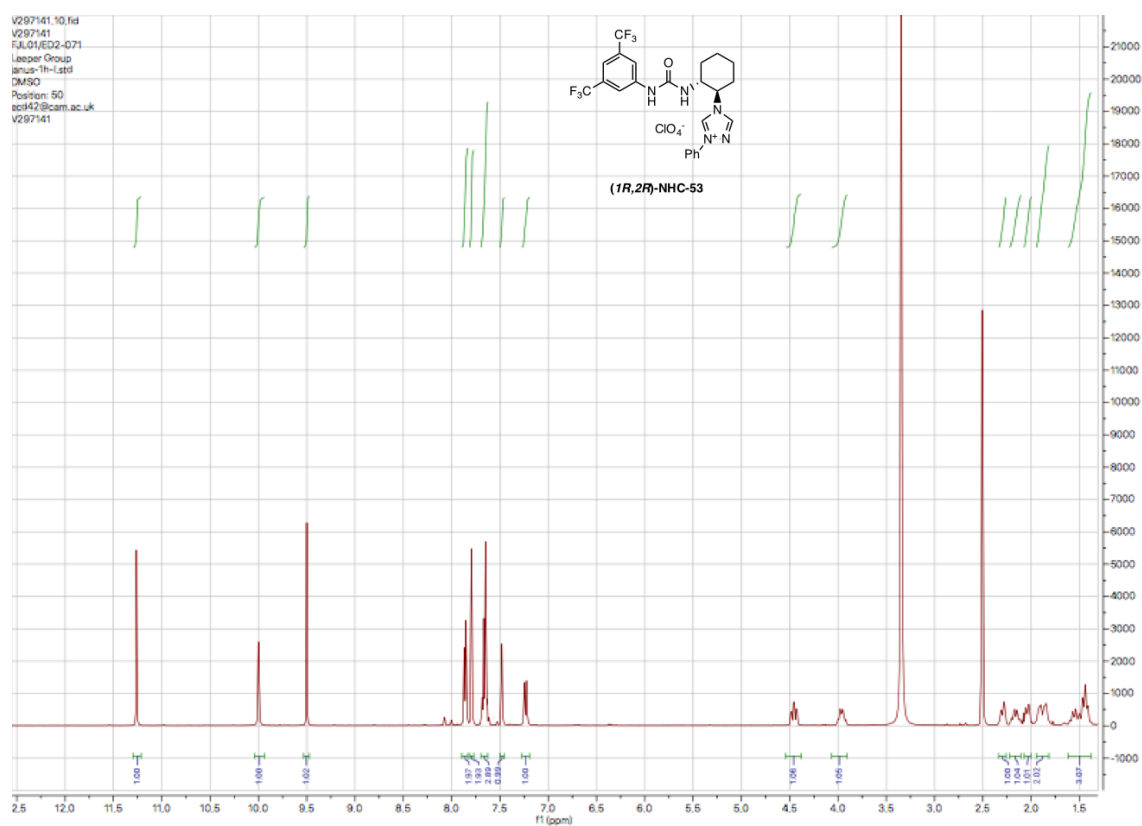


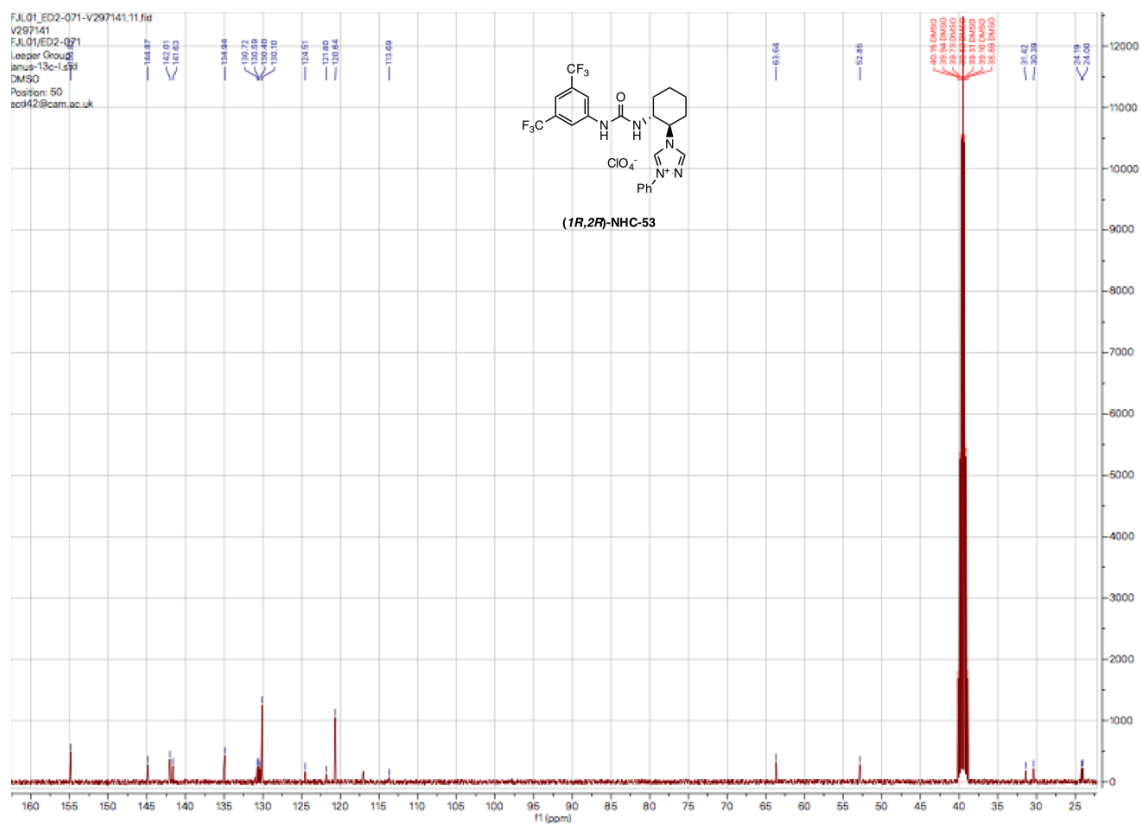
(1R,2R)-NHC-48

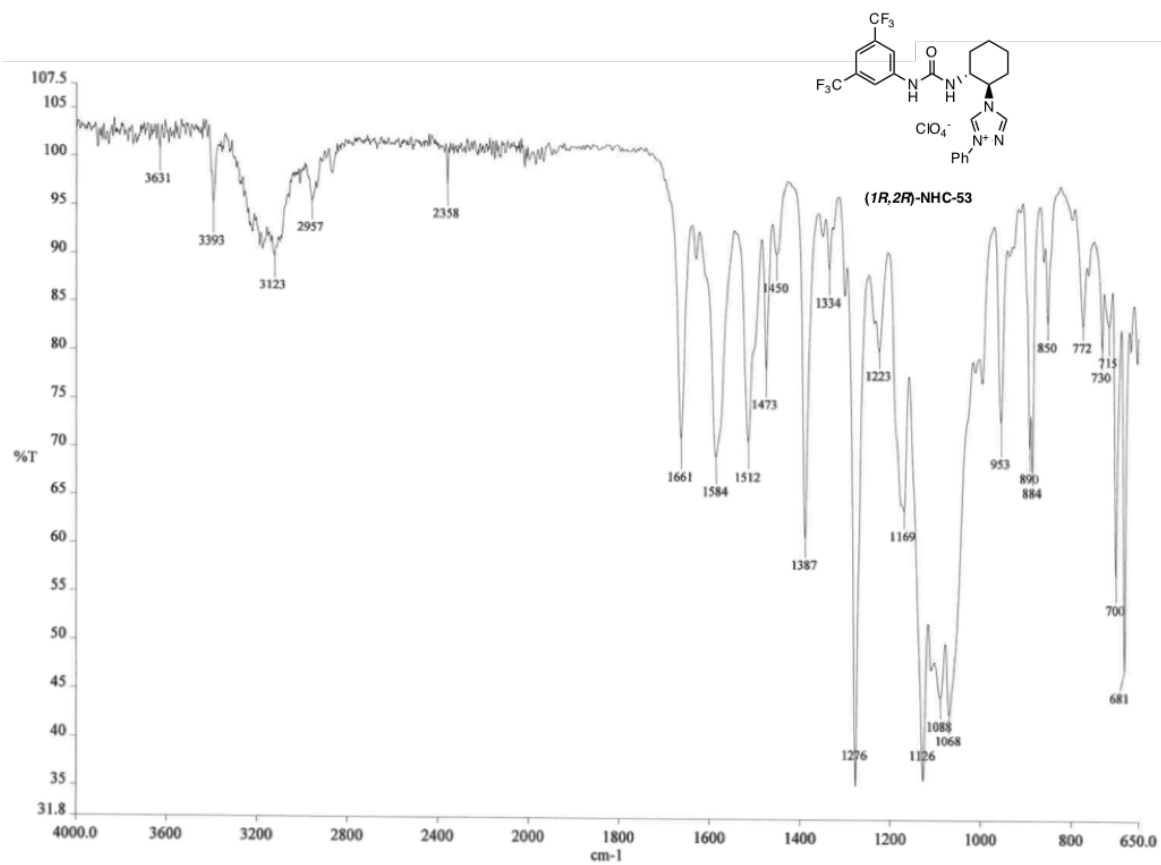
(Section II to be filled in after analysis)

4-((1*R*,2*R*)-2-(3-(3,5-bis(trifluoromethyl)phenyl)ureido)cyclohexyl)-1-phenyl-4*H*-1,2,4-triazol-1-ium perchlorate (1*R*,2*R*)-NHC-53

¹H NMR, 400 MHz



^{13}C NMR, 100 MHz

IR Spectrum (cm^{-1})

High Resolution Mass Spectrum

Openlynx Report - Leeper_FJ

Page 1

Sample: 1
File: Leeper_FJ932-1
Description:

Vial: 1:65
Date: 02-Jun-2016
Method: C:\MassLynx\Acc-mass-5ul.oip

Sample ID: ED2-071
Time: 14:24:36
Group: Leeper_FJ

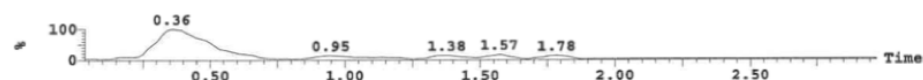
Printed: Thu Jun 02 14:37:17 2016

Sample Report:

Sample 1 Vial 1:65 ID ED2-071 File Leeper_FJ932-1 Date 02-Jun-2016 Time 14:24:36

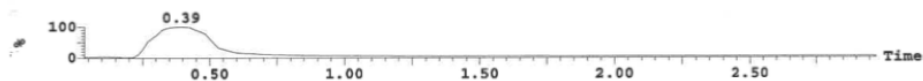
1: TOF MS ES+ : 86.002+107.984

2.2e+001



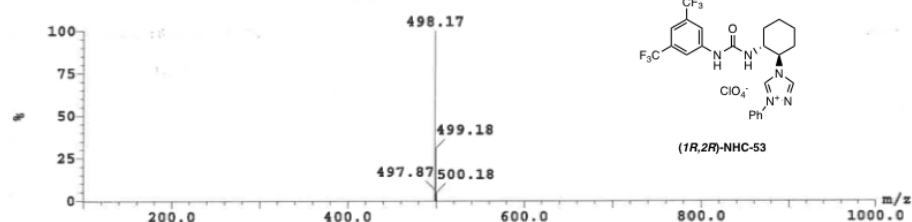
1: TOF MS ES+ : 498.178+520.16

1.5e+004



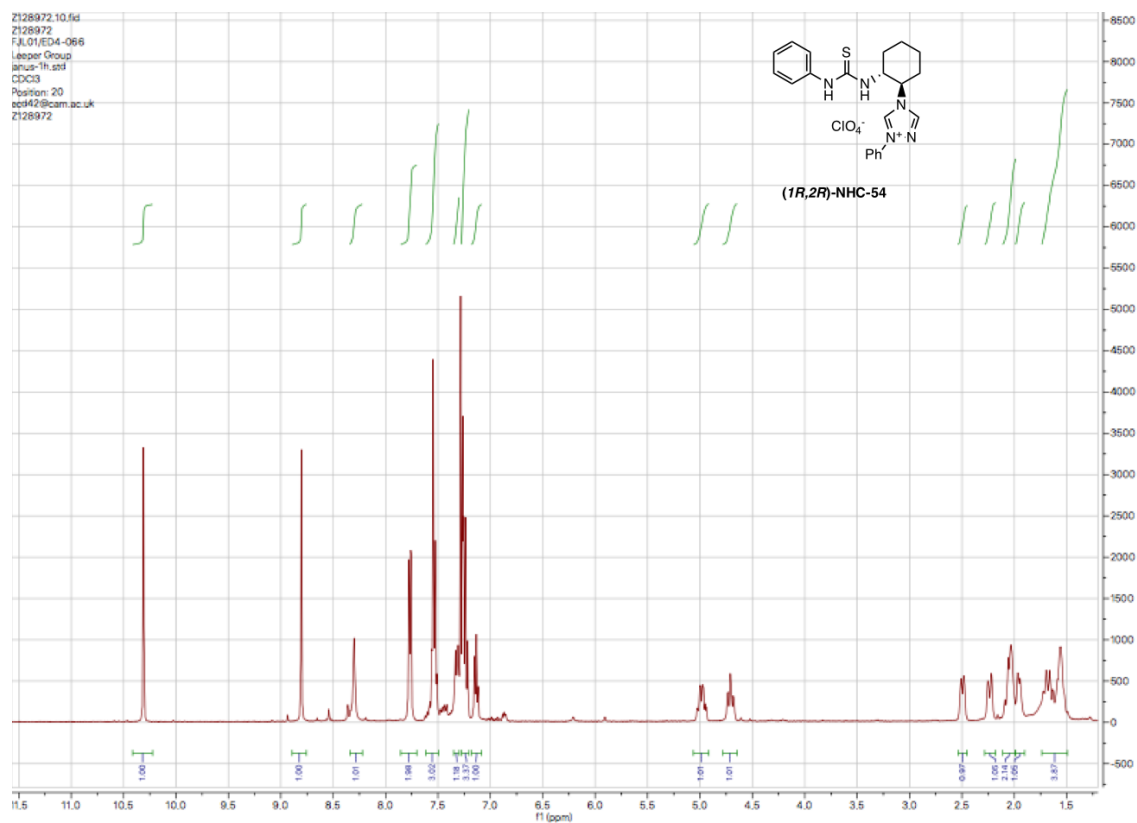
1: Combine (10:32-1:10)

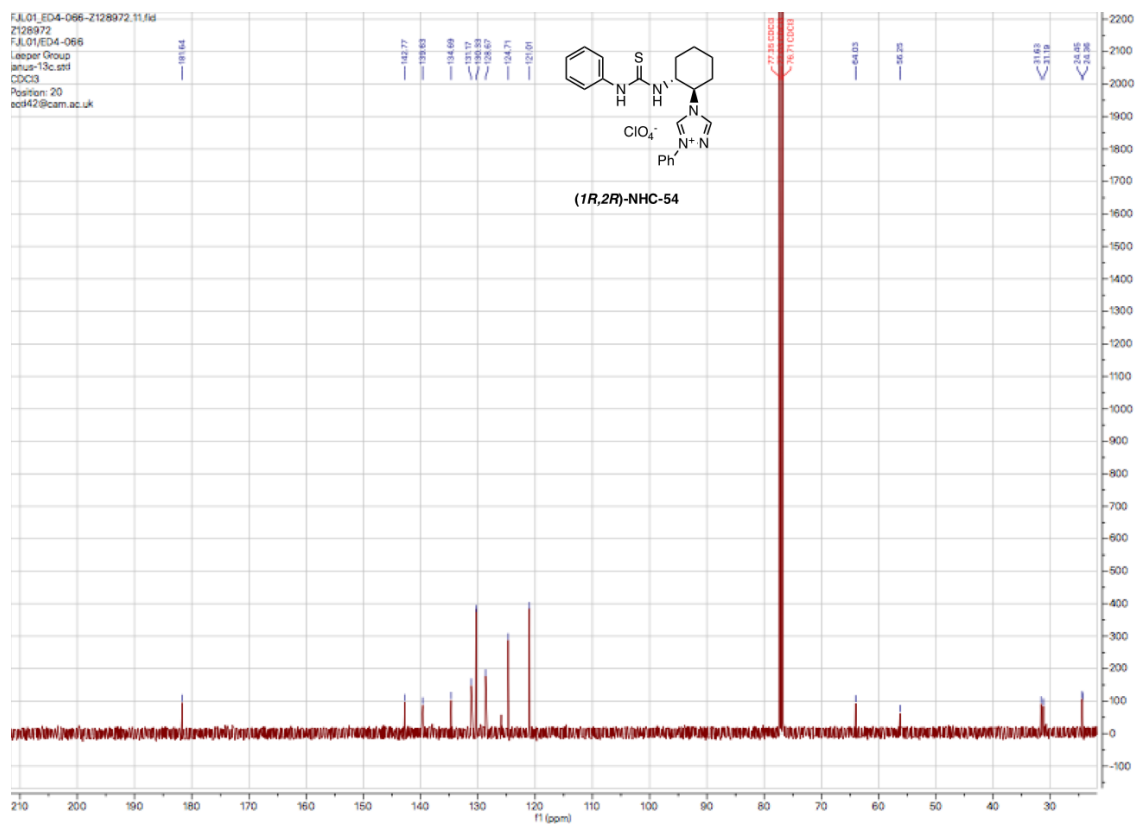
1.4e+005

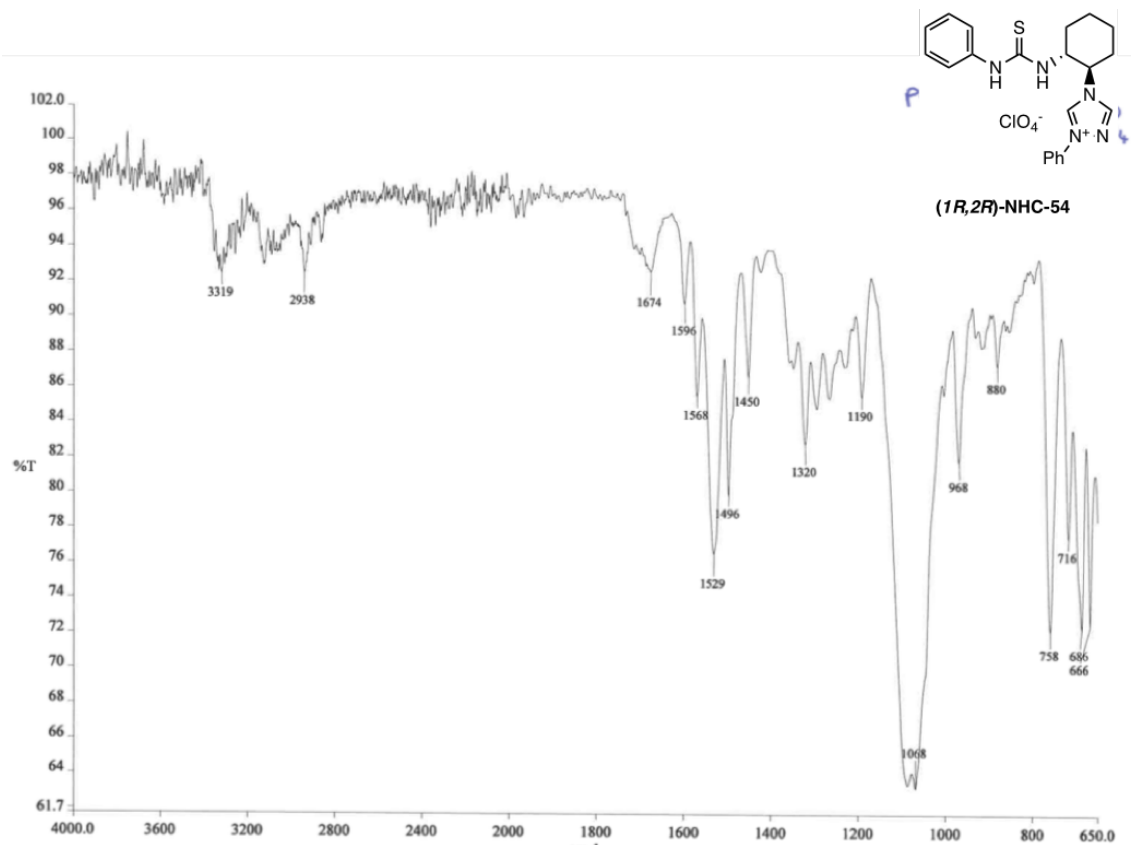


Mass	Calc. Mass	mDa	PPM	DBE	Formula	i-FIT
498.1745	498.1753	-0.8	-1.6	21.0	C24 H19 N12 Na	8.7
498.1745	498.1756	-1.1	-2.2	17.0	C26 H22 N6 F3 Na	13.0
498.1745	498.1758	-1.3	-2.6	13.0	C28 H25 F6 Na	17.9
498.1745	498.1751	-0.6	-1.2	19.5	C23 H20 N11 O3	24.0
498.1745	498.1753	-0.8	-1.6	15.5	C25 H23 N5 O3 F3	25.4
498.1745	498.1728	1.7	3.4	20.0	C26 H20 N8 O F2	53.0
498.1745	498.1731	1.4	2.8	16.0	C28 H23 N2 O F5	56.6
498.1745	498.1742	0.3	0.6	12.0	C25 H26 N2 O4 F3 Na	66.5
498.1745	498.1740	0.5	1.0	16.0	C23 H23 N8 O4 Na	68.7
498.1745	498.1753	-0.8	-1.6	15.5	C25 H25 N5 O5 Na	76.8
498.1745	498.1742	0.3	0.6	12.0	C25 H24 N2 O2 F6	79.8
498.1745	498.1740	0.5	1.0	16.0	C23 H21 N8 O2 F3	83.0
498.1745	498.1737	0.8	1.6	20.0	C21 H18 N14 O2	88.8
498.1745	498.1764	-1.9	-3.8	19.0	C25 H22 N8 O4	90.9
498.1745	498.1766	-2.1	-4.2	15.0	C27 H25 N2 O4 F3	97.8
498.1745	498.1767	-2.2	-4.4	20.5	C26 H21 N9 O Na	97.9
498.1745	498.1769	-2.4	-4.8	16.5	C28 H24 N3 O F3 Na	108.7
498.1745	498.1731	1.4	2.8	16.0	C28 H25 N2 O3 F2 Na	134.1
498.1745	498.1728	1.7	3.4	14.5	C27 H26 N O6 F2	162.8
498.1745	498.1729	1.6	3.2	12.5	C23 H24 N5 O3 F3 Na	183.6

498.1729
required

1-phenyl-4-((1*R*,2*R*)-2-(3-phenylthioureido)cyclohexyl)-4*H*-1,2,4-triazol-1-ium perchlorate (1*R*,2*R*)-NHC-54**¹H NMR, 400 MHz**

^{13}C NMR, 100 MHz

IR Spectrum (cm^{-1})

High Resolution Mass Spectrum

Openlynx Report - Leeper_FJ

Sample: 3

File: Leeper_FJ1028-3

Description:

Vial: 1:46

Date: 06-Apr-2018

Method: C:\MassLynx\Acc-mass-HI-acid-5ul.olp

Sample ID: ED4-066

Time: 14:35:20

Group: Leeper_FJ

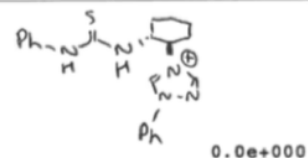
Page 3

Printed: Fri Apr 06 14:47:28 2018

Sample Report (continued):

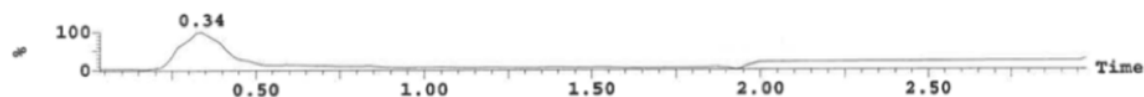
Sample 3 Vial 1:46 ID ED4-066 File Leeper_FJ1028-3 Date 06-Apr-2018 Time 14:35:20

1: TOF MS ES+ : 59.991+81.973



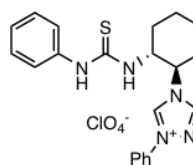
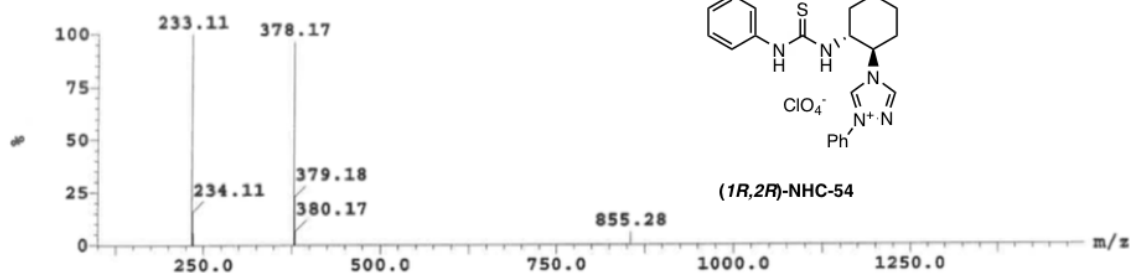
1: TOF MS ES+ : 378.178+400.16

1.1e+002



1: Combine (8:32-1:10)

8.2e+002



(1R,2R)-NHC-54

Mass	Calc. Mass	mDa	PPM	DBE	Formula
378.1724	378.1719	0.5	1.3	17.5	C ₂₄ H ₂₀ N ₅
378.1724	378.1719	0.5	1.3	4.5	C ₉ H ₂₄ N ₁₃ S ₂
378.1724	378.1710	1.4	3.7	11.0	C ₇ H ₁₄ N ₂₀
378.1724	378.1728	-0.4	-1.1	-2.0	C ₁₁ H ₃₄ N ₆ S ₄

i-FIT

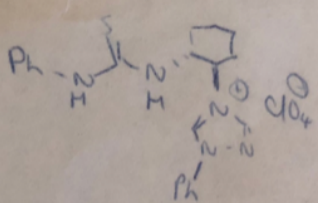
8.2

15.3

28.2

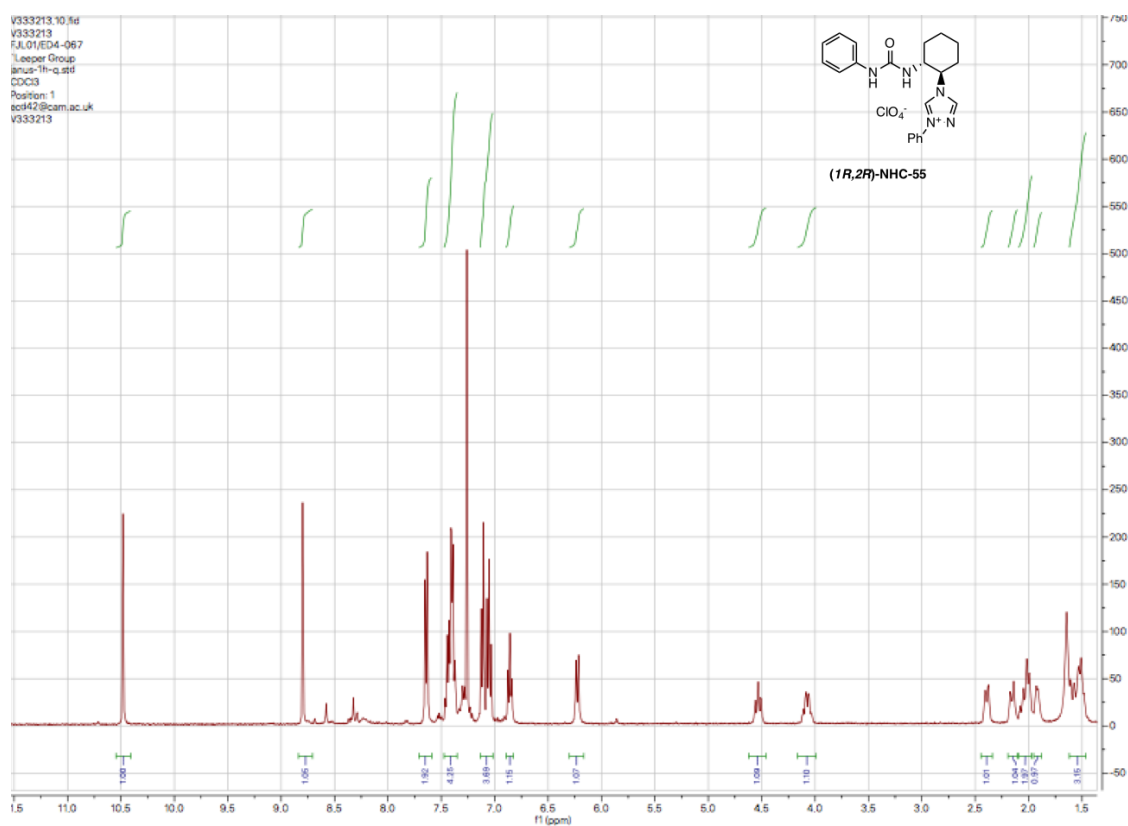
75.3

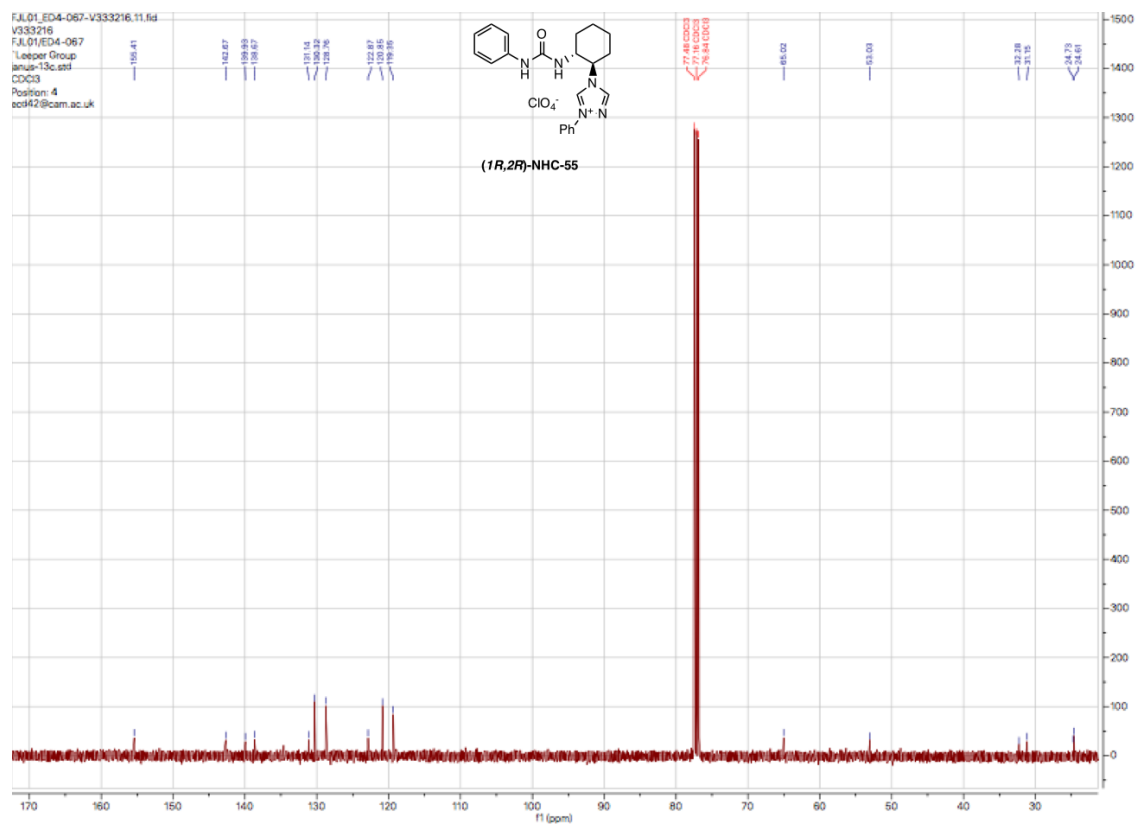
Elemental Analysis

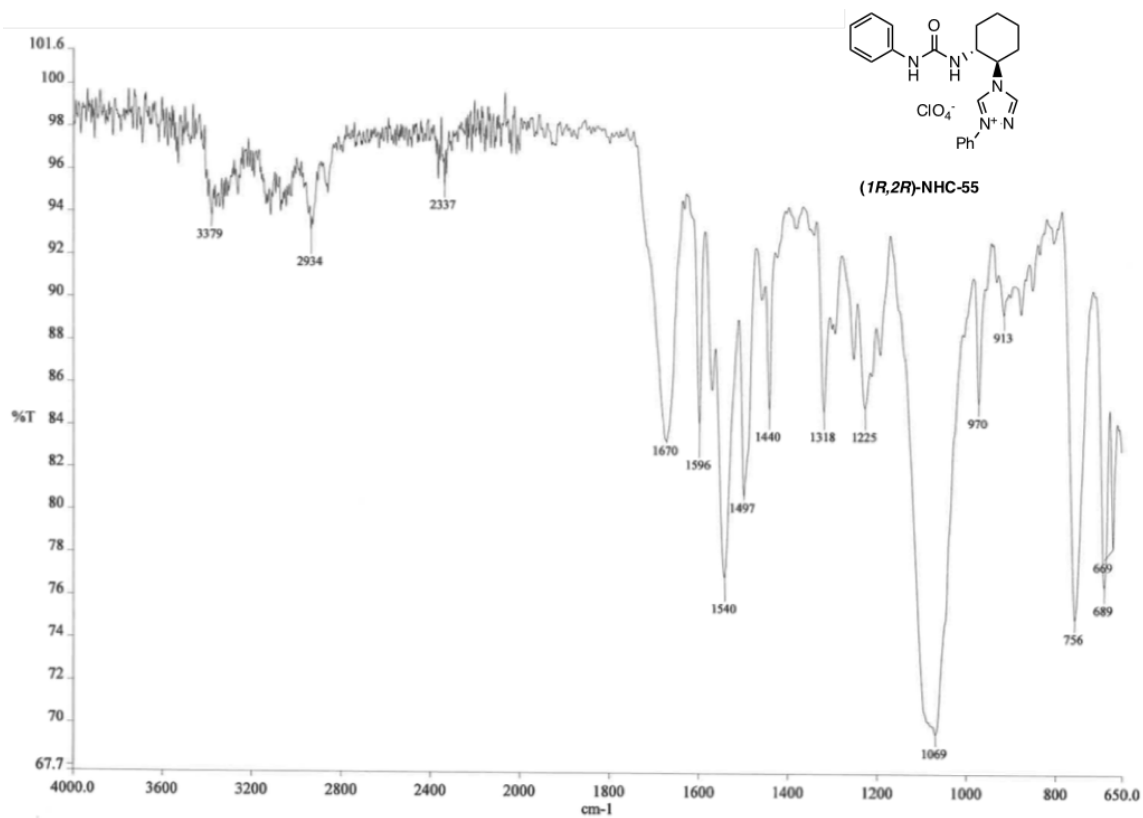
Name..... <u>EMMA DURHAM</u>	I J 014864
Date..... <u>25/04/18</u>	Results
No. of Specimen..... <u>ED4-066</u>	1.4664 → C = 53.22 H = 5.16 N = 14.66
Analyse for..... <u>C, H, N</u>	1.3874 → C = 53.14 H = 5.09 N = 14.68
Elements present..... <u>C, H, N, S, Cl, O</u>	II
M. pt. or B. pt.	Theoretical values and structural formulae
Method of purification..... <u>Column chromatography</u>	
Approx. values %..... <u>C 52.77, H 5.06, N 14.65</u>	(Section II to be filled in after analysis)
Any remarks:	

**1-phenyl-4-((1*R*,2*R*)-2-(3-phenylureido)cyclohexyl)-4*H*-1,2,4-triazol-1-ium perchlorate
(1*R*,2*R*)-NHC-55**

¹H NMR, 400 MHz



^{13}C NMR, 100 MHz

IR Spectrum (cm⁻¹)

High Resolution Mass Spectrum

Openlynx Report - Leeper_FJ

Sample: 2
 File: Leeper_FJ1031-2
 Description:

Vial: 1:75
 Date: 25-Apr-2018
 Method: C:\MassLynx\Acc-mass-HI-acid-5ul.olp

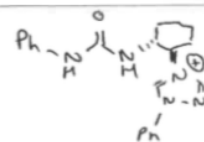
Sample ID: ED4-067
 Time: 11:50:01
 Group: Leeper_FJ

Page 2

Printed: Wed Apr 25 12:06:15 2018

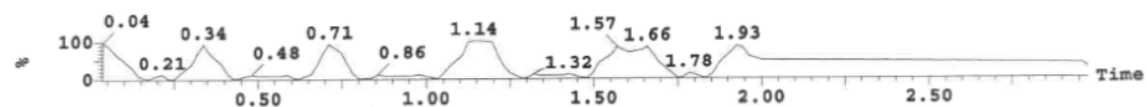
Sample Report (continued):

Sample 2 Vial 1:75 ID ED4-067 File Leeper_FJ1031-2 Date 25-Apr-2018 Time 11:50:01



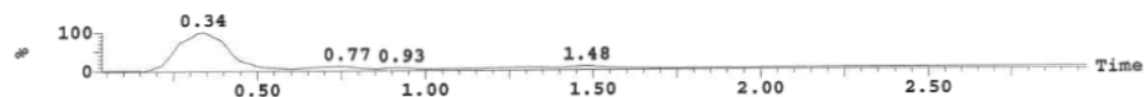
1: TOF MS ES+ :82.981+104.963

4.1e-001



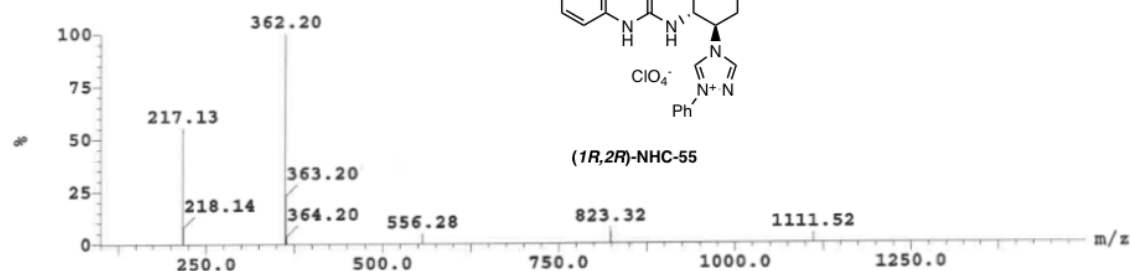
1: TOF MS ES+ :362.198+384.18

3.8e+001



1: Combine (8:32-1:11)

2.5e+002

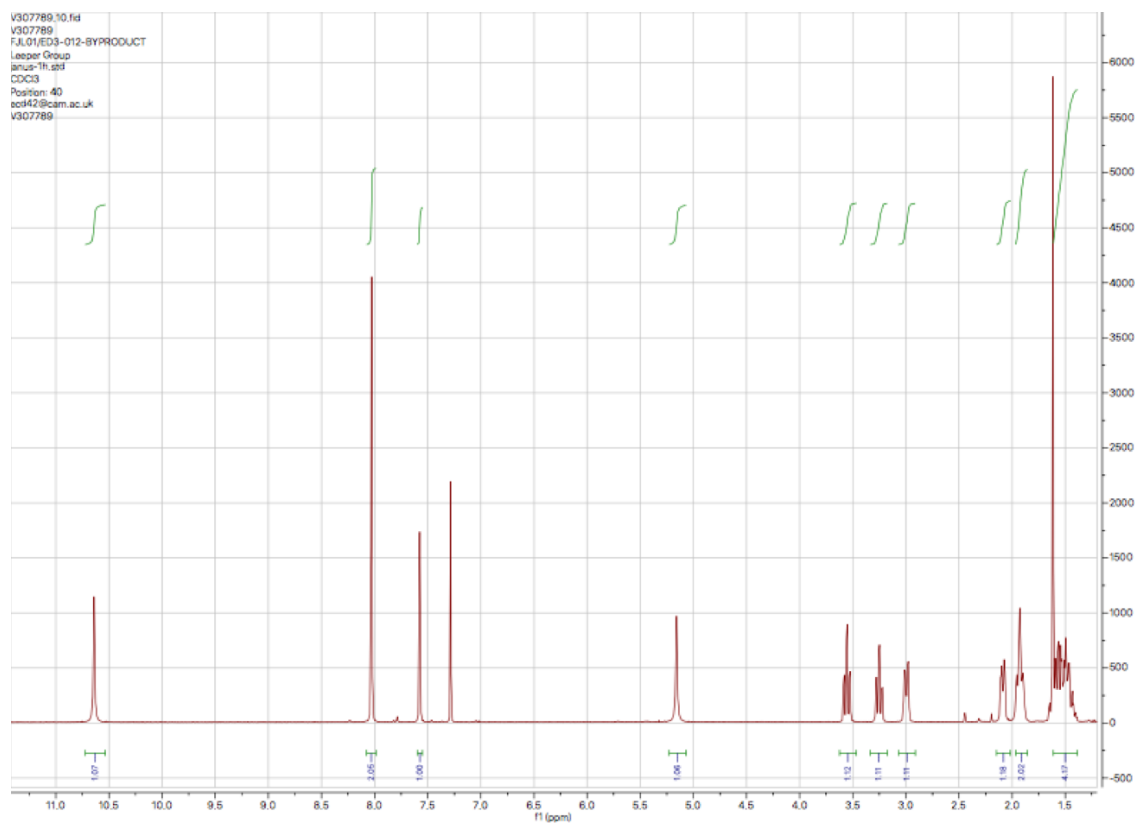


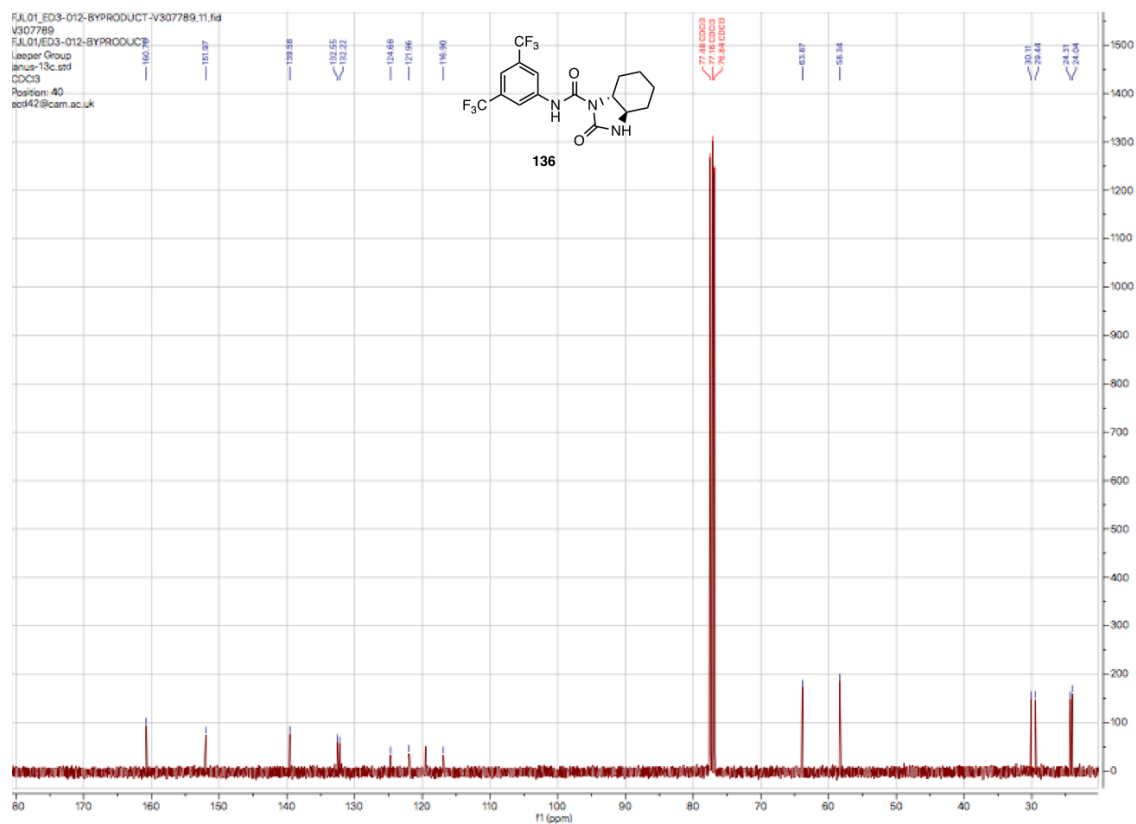
Mass	Calc. Mass	mDa	PPM	DBE	Formula	i-FIT
362.1980	362.1967	1.3	3.6	13.0	C19 H22 N8	0.2
362.1980	362.1977	0.3	0.8	5.0	C14 H27 N8 Na S	3.9
362.1980	362.1968	1.2	3.3	0.0	C4 H26 N16 S2	19.8
362.1980	362.1976	0.4	1.1	6.5	C21 H32 N S2	20.9
362.1980	362.1986	-0.6	-1.7	-1.5	C16 H37 N Na S3	36.6

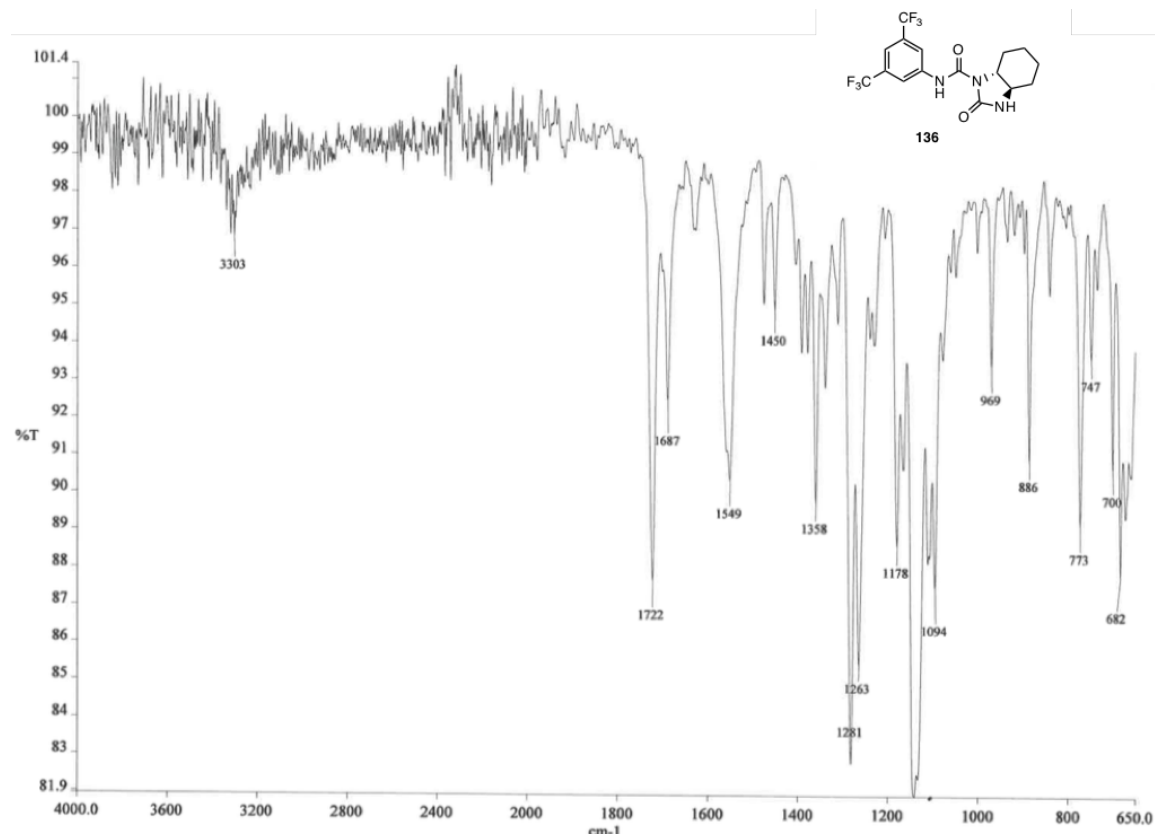
362.1981.

(3*aR*,7*aR*)-*N*-(3,5-bis(trifluoromethyl)phenyl)-2-oxooctahydro-1*H*-benzo[*d*]imidazole-1-carboxamide 136

¹H NMR, 400 MHz



^{13}C NMR, 100 MHz

IR Spectrum (cm^{-1})

Elemental Analysis

Name..... *Ennio Duran*

Date..... *16/12/16*

No. of Specimen..... *ED3-012*

Analyse for..... *C, H, N, S*

Elements present..... *C, H, N, O, F*

M. pt. or B. pt.

Method of purification..... *Column chromatography*
(SiO₂ / hexane)

Approx. values %..... *C 48.61 H 3.32*
N 10.63 S 0.00

Any remarks:..... *Cyclization product would*
predict these but are matches
for this product. Just to check!

I J 014852

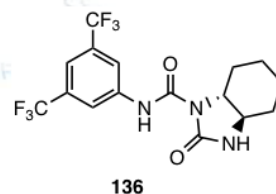
Results

1.5038 mg → *C = 48.49%*
H = 3.83%
N = 10.07%

1.5376 mg → *C = 48.43%*
H = 3.76%
N = 10.01%

II

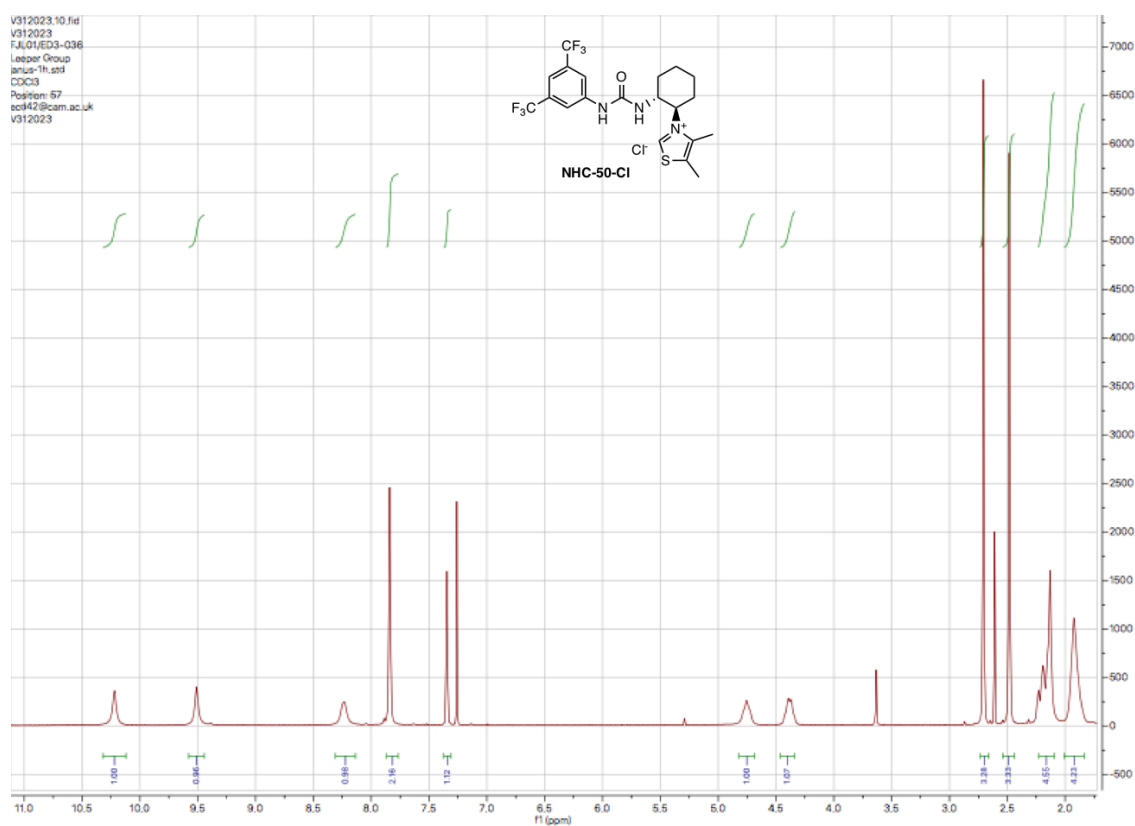
Theoretical values and structural formulae

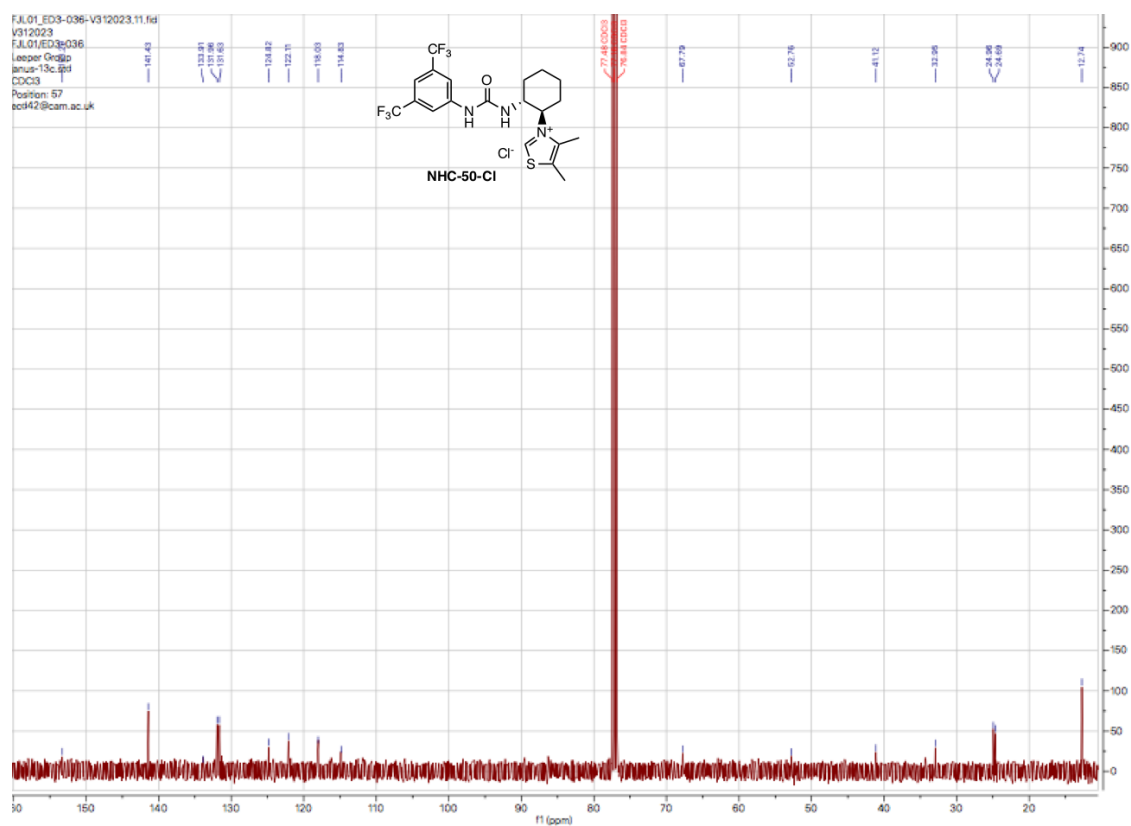


(Section II to be filled in after analysis)

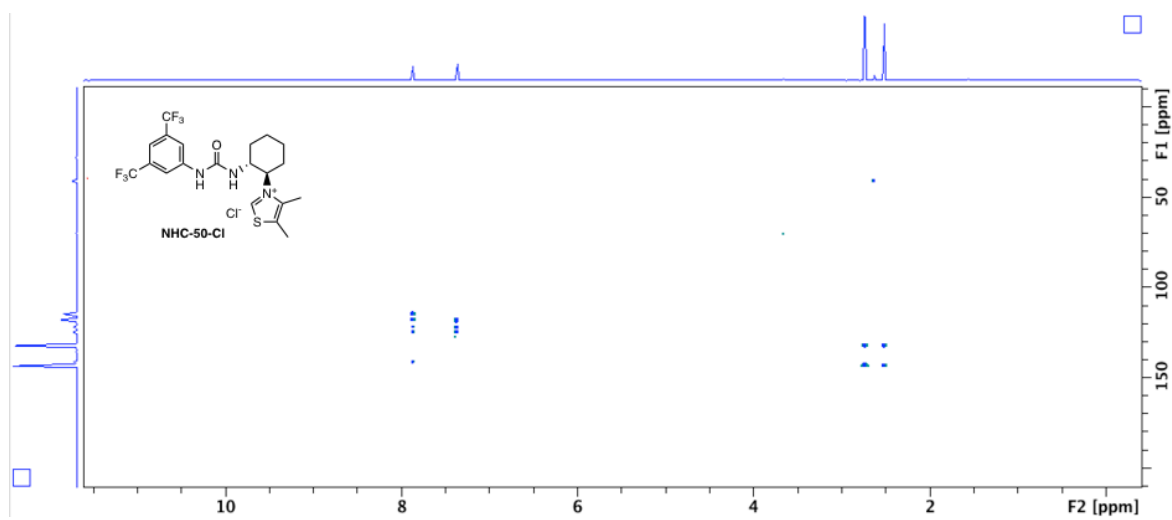
3-((1*R*,2*R*)-2-(3-(3,5-bis(trifluoromethyl)phenyl)ureido)cyclohexyl)-4,5-dimethylthiazol-3-ium chloride (1*R*,2*R*)-NHC-50-Cl

¹H NMR, 400 MHz



^{13}C NMR, 100 MHz

HMBC



High Resolution Mass Spectrum

Openlynx Report - Leeper_FJ

Sample: 1
File: Leeper_FJ967-1
Description:

Vial: 1:21
Date: 17-Feb-2017
Method: C:\MassLynx\Acc-mass-5ul.olp

Sample ID: ED3-036
Time: 09:22:46
Group: Leeper_FJ

Page 1

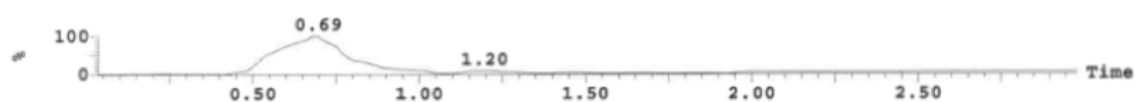
Printed: Fri Feb 17 09:27:03 2017

Sample Report:

Sample 1 Vial 1:21 ID ED3-036 File Leeper_FJ967-1 Date 17-Feb-2017 Time 09:22:46

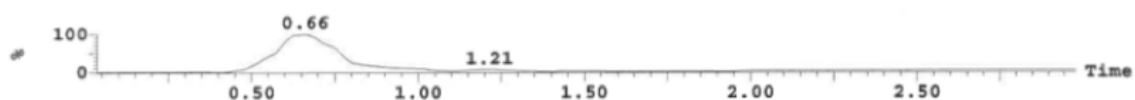
1: TOF MS ES+ :117.974+139.956

1.3e+002



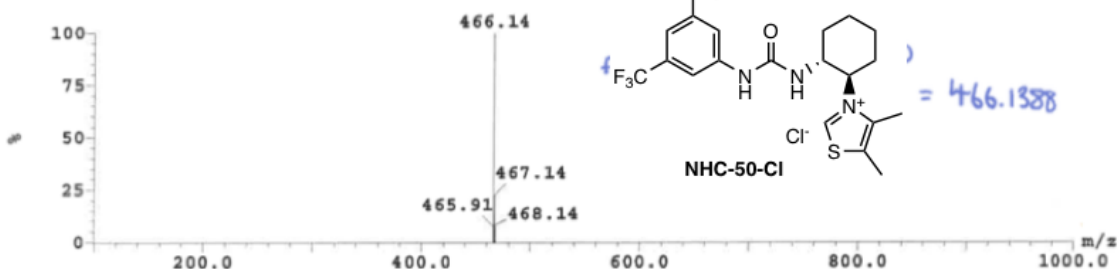
1: TOF MS ES+ :466.138+488.12

2.1e+004



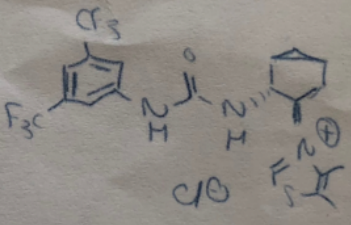
1: Combine (21:32-1:10)

1.2e+005



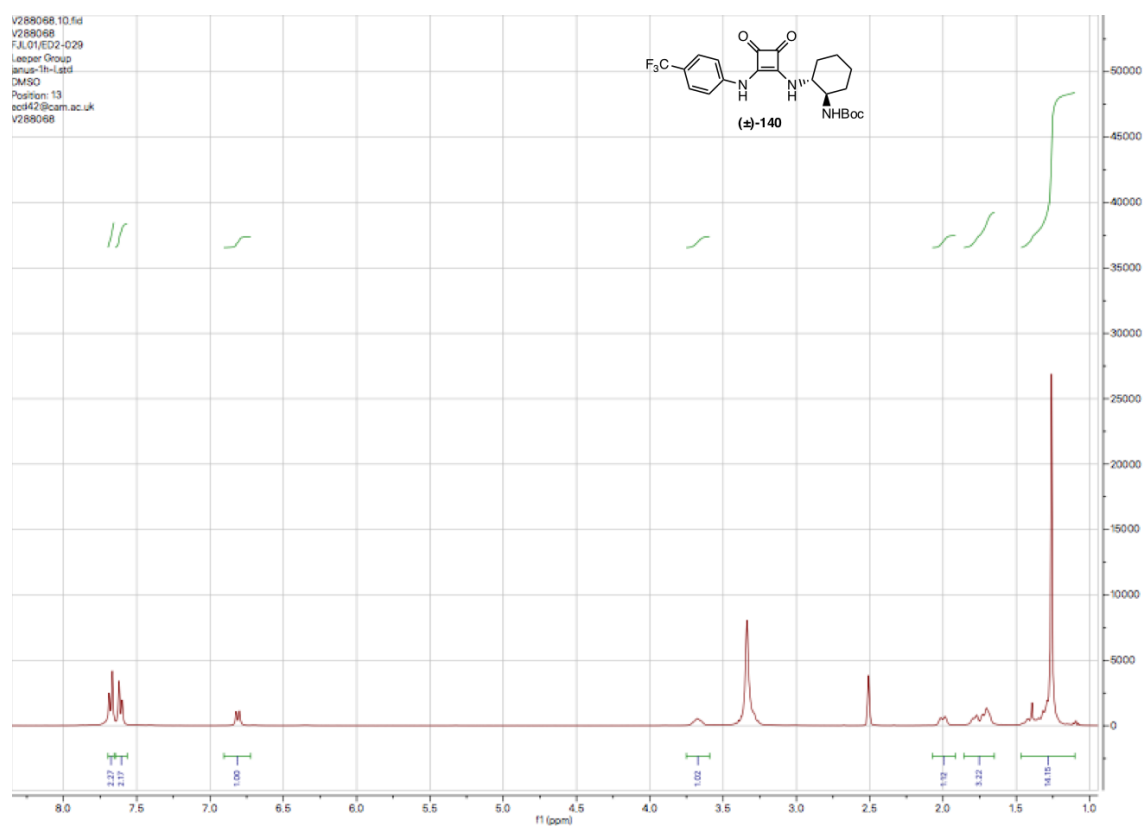
Mass	Calc. Mass	mDa	PPM	DBE	Formula	i-FIT
466.1369	466.1372	-0.3	-0.6	7.5	C17 H25 N5 O7 Na S	7.0
466.1369	466.1372	-0.3	-0.6	7.5	C17 H23 N5 O5 F3 S	13.3
466.1369	466.1383	-1.4	-3.0	11.0	C17 H22 N8 O6 S	13.7
466.1369	466.1385	-1.6	-3.4	7.0	C19 H25 N2 O6 F3 S	15.5
466.1369	466.1370	-0.1	-0.2	11.5	C15 H20 N11 O5 S	17.1
466.1369	466.1347	2.2	4.7	6.5	C19 H26 N O8 F2 S	35.0
466.1369	466.1386	-1.7	-3.6	7.0	C19 H27 N2 O8 Na S	38.0
466.1369	466.1372	-0.3	-0.6	13.0	C16 H19 N12 O2 Na S	49.4
466.1369	466.1375	-0.6	-1.3	9.0	C18 H22 N6 O2 F3 Na S	50.6
466.1369	466.1377	-0.8	-1.7	5.0	C20 H25 O2 F6 Na S	51.7
466.1369	466.1361	0.8	1.7	4.0	C17 H26 N2 O6 F3 Na S	60.8
466.1369	466.1359	1.0	2.1	8.0	C15 H23 N8 O6 Na S	69.4
466.1369	466.1383	-1.4	-3.0	5.5	C18 H28 N O11 S	69.6
466.1369	466.1350	1.9	4.1	8.0	C20 H25 N2 O5 F2 Na S	80.9
466.1369	466.1350	1.9	4.1	8.0	C20 H23 N2 O3 F5 S	81.7
466.1369	466.1347	2.2	4.7	12.0	C18 H20 N8 O3 F2 S	82.7
466.1369	466.1364	0.5	1.1	5.5	C18 H23 N3 O F6 Na S	85.7
466.1369	466.1361	0.8	1.7	9.5	C16 H20 N9 O F3 Na S	89.8
466.1369	466.1370	-0.1	-0.2	6.0	C16 H26 N4 O10 S	92.8
466.1369	466.1386	-1.7	-3.6	12.5	C18 H21 N9 O3 Na S	94.0

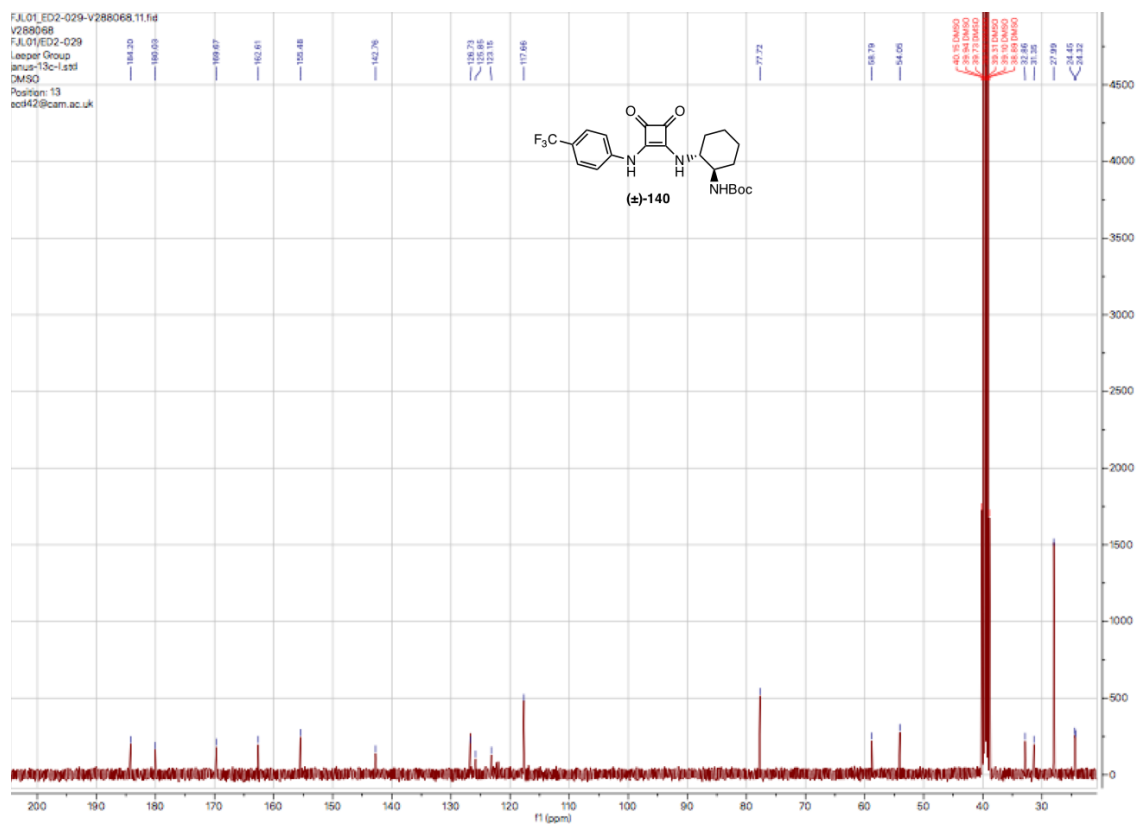
Elemental Analysis

Name.....	EMMA DURHAM	I	J 014865
Date.....	25/04/18		
No. of Specimen	ED3-036		
Analyse for	C, H, N		
Elements present.....	CHNOFSCl		
M. pt. or B. pt		Results	
Method of purification	Precipitation	1.3612	→ C = 46.02 H = 4.37 N = 7.87
Approx. values %	C 47.86 H 4.42 N 8.37	1.4020	→ C = 46.03 H = 4.43 N = 7.91
Any remarks:		II Theoretical values and structural formulæ	
			
		(Section II to be filled in after analysis)	

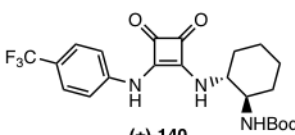
***tert*-Butyl-((±)-*trans*-2-((3,4-dioxo-2-((4-(trifluoromethyl)phenyl)amino)cyclobut-1-en-1-yl)amino)cyclohexyl)carbamate (±)-140**

¹H NMR, 400 MHz



^{13}C NMR, 100 MHz

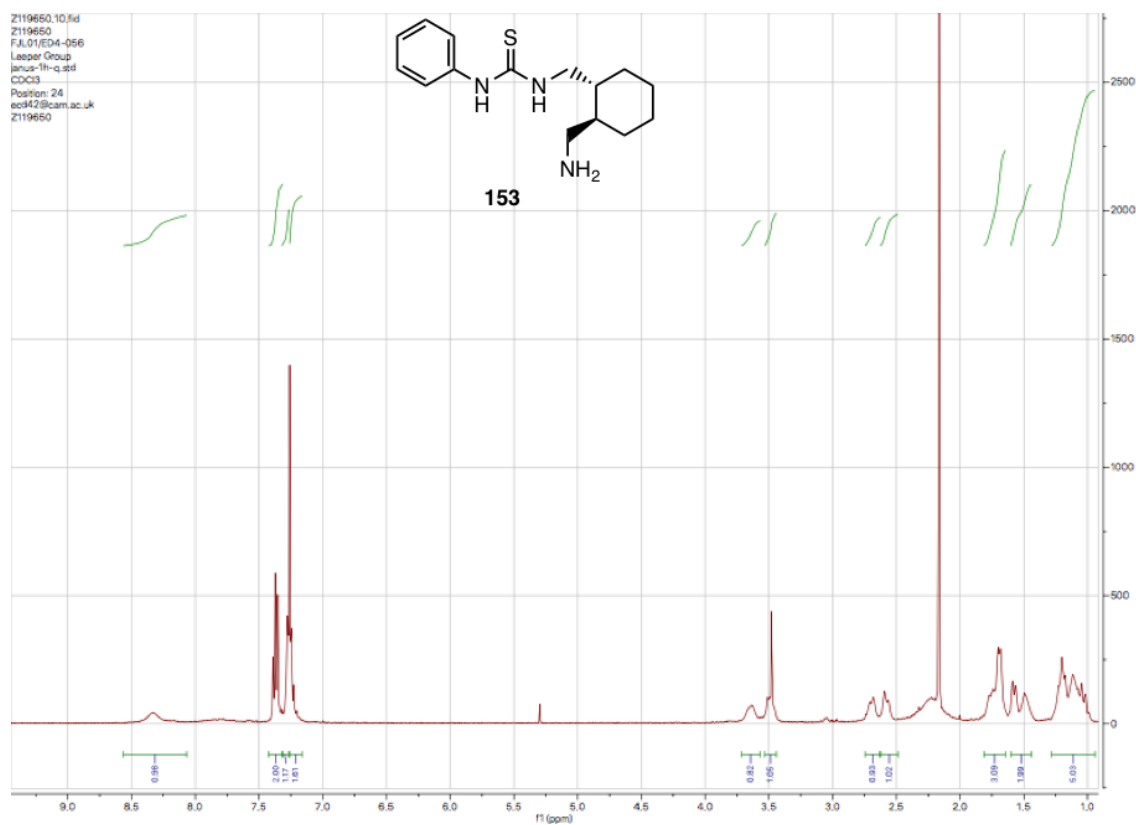
Elemental Analysis

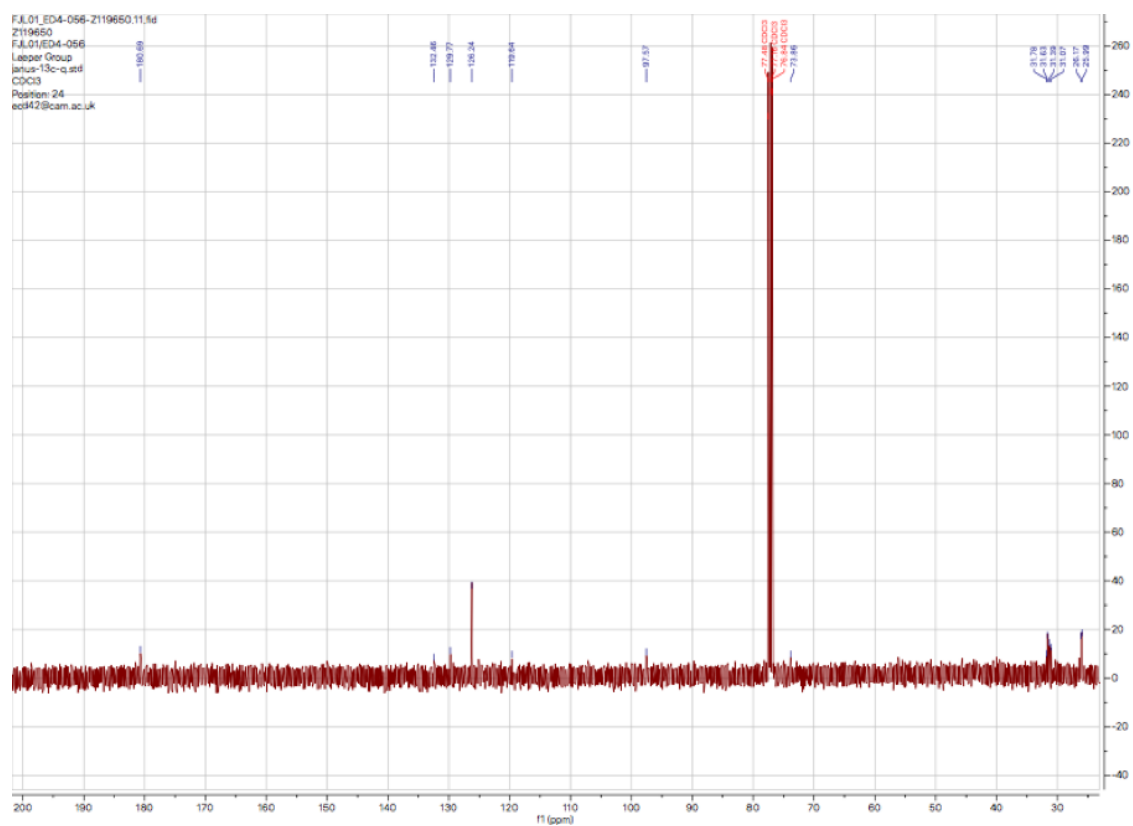
I		J 014840
Name.....	Emma Durham	Results 1.9082 mg. → C=58.20% H= 5.79% N= 9.28% 1.8598 mg. → C=58.11% H= 5.77% N= 9.26%
Date.....	15/01/16	
No. of Specimen	ED2-027	
Analyse for	C, H, N	
Elements present.....	C, H, N, O, F	
M. pt. or B. pt.		II Theoretical values and structural formulae  (±)-140
Method of purification	Recrystallisation	
Approx. values %	C 58.27 H 5.78 N 9.27	
Any remarks:		
(Section II to be filled in after analysis)		

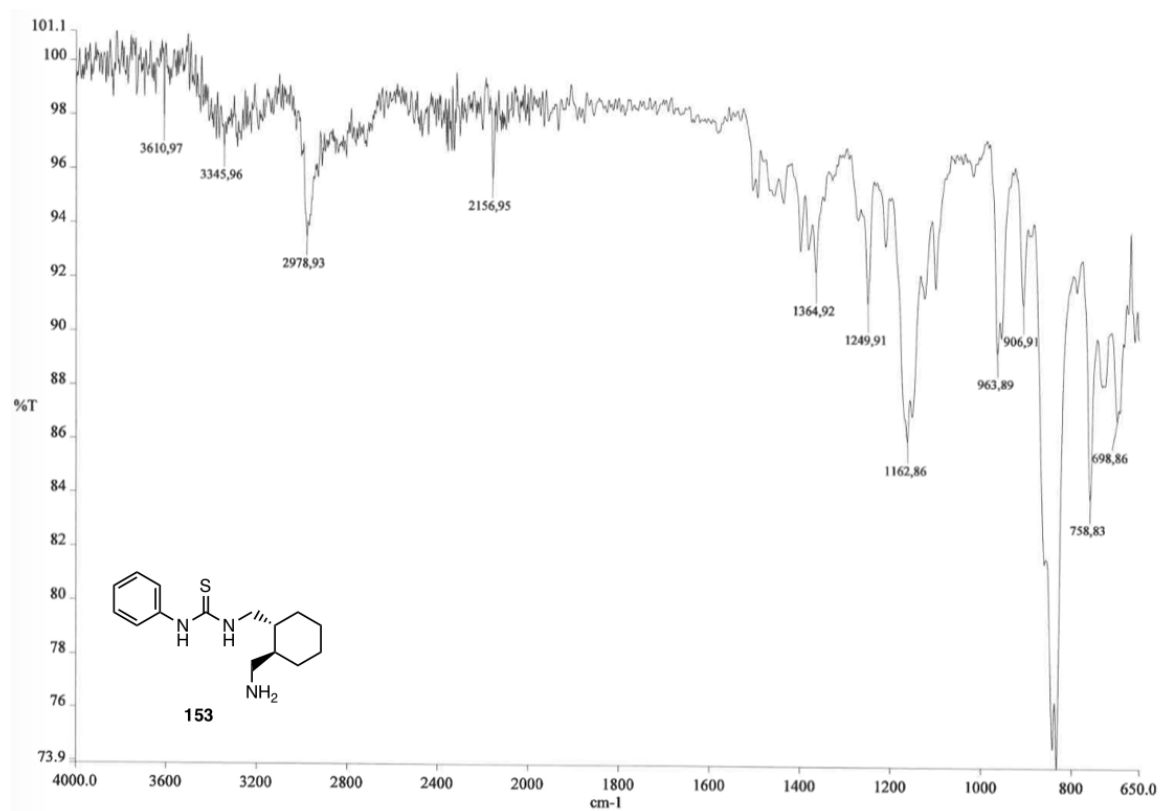
A.1.2 Chapter 4 Compounds

1-(((1*R*,2*R*)-2-(aminomethyl)cyclohexyl)methyl)-3-phenylthiourea **153**

^1H NMR, 400 MHz



^{13}C NMR, 100 MHz

IR Spectrum (cm^{-1})

High Resolution Mass Spectrum

Openlynx Report - Leeper_FJ

Page 1

Sample: 1
File: Leeper_FJ1017-1
Description:

Vial: 1:53
Date: 30-Oct-2017
Method: C:\MassLynx\Acc-mass-5ul.olp

Sample ID: ED4-056
Time: 15:26:48
Group: Leeper_FJ

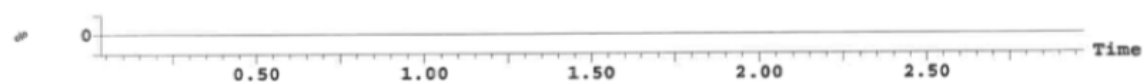
Printed: Mon Oct 30 15:30:53 2017

Sample Report:

Sample 1 Vial 1:53 ID ED4-056 File Leeper_FJ1017-1 Date 30-Oct-2017 Time 15:26:48

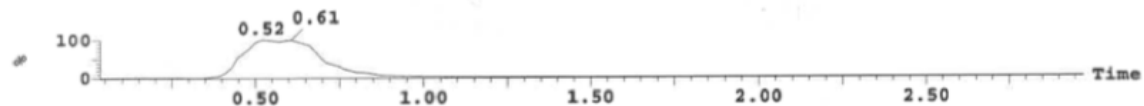
1: TOF MS ES+ : 59.991+81.973

0.0e+000



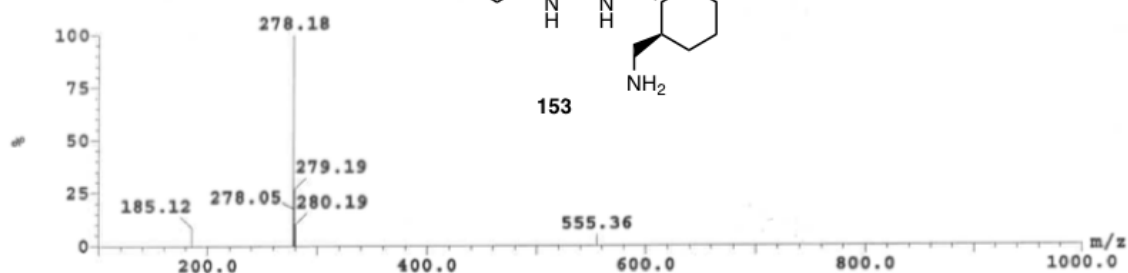
1: TOF MS ES+ : 278.178+300.16

4.2e+004



1: Combine (8:32-1:10)

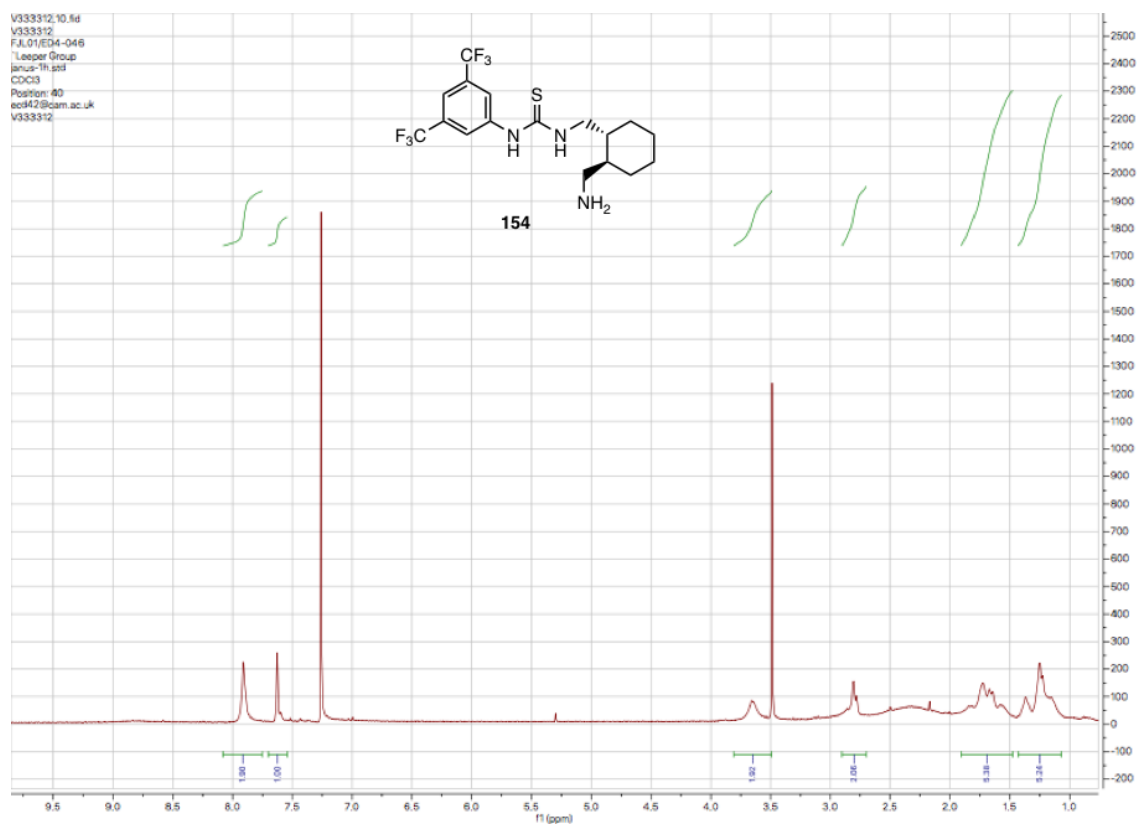
3.4e+005



Mass	Calc. Mass	mDa	PPM	DBE	Formula
278.1760	278.1758	0.2	0.7	-4.5	C ₉ H ₃₂ N ₃ S ₃

I-FIT
13725.5

278.1690 CMJ

1-(((1*R*,2*R*)-2-(aminomethyl)cyclohexyl)methyl)-3-phenylthiourea 154**¹H NMR, 400 MHz**

High Resolution Mass Spectrum

Openlynx Report - Leeper_FJ

Sample: 1
File: Leeper_FJ1015-1
Description:

Vial: 1:37
Date: 16-Oct-2017
Method: C:\MassLynx\Acc-mass-5ul.oip

Sample ID: ED4-046
Time: 11:53:20
Group: Leeper_FJ

Page 1

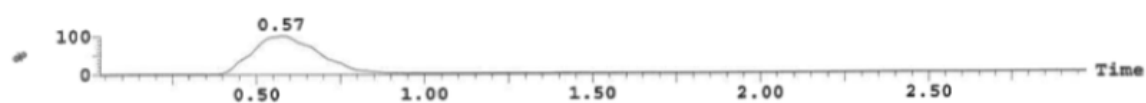
Printed: Mon Oct 16 11:57:25 2017

Sample Report:

Sample 1 Vial 1:37 ID ED4-046 File Leeper_FJ1015-1 Date 16-Oct-2017 Time 11:53:20

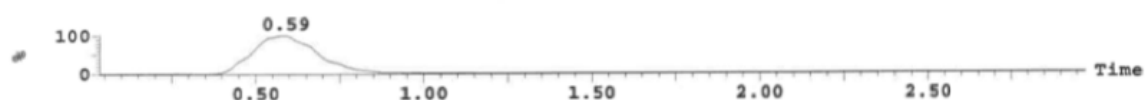
1: TOF MS ES+ :101.979+123.961

1.3e+003



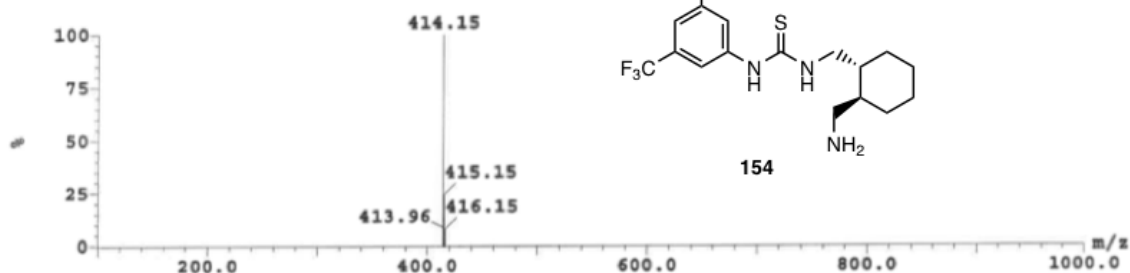
1: TOF MS ES+ :414.148+436.13

3.5e+004



1: Combine (17:32-1:10)

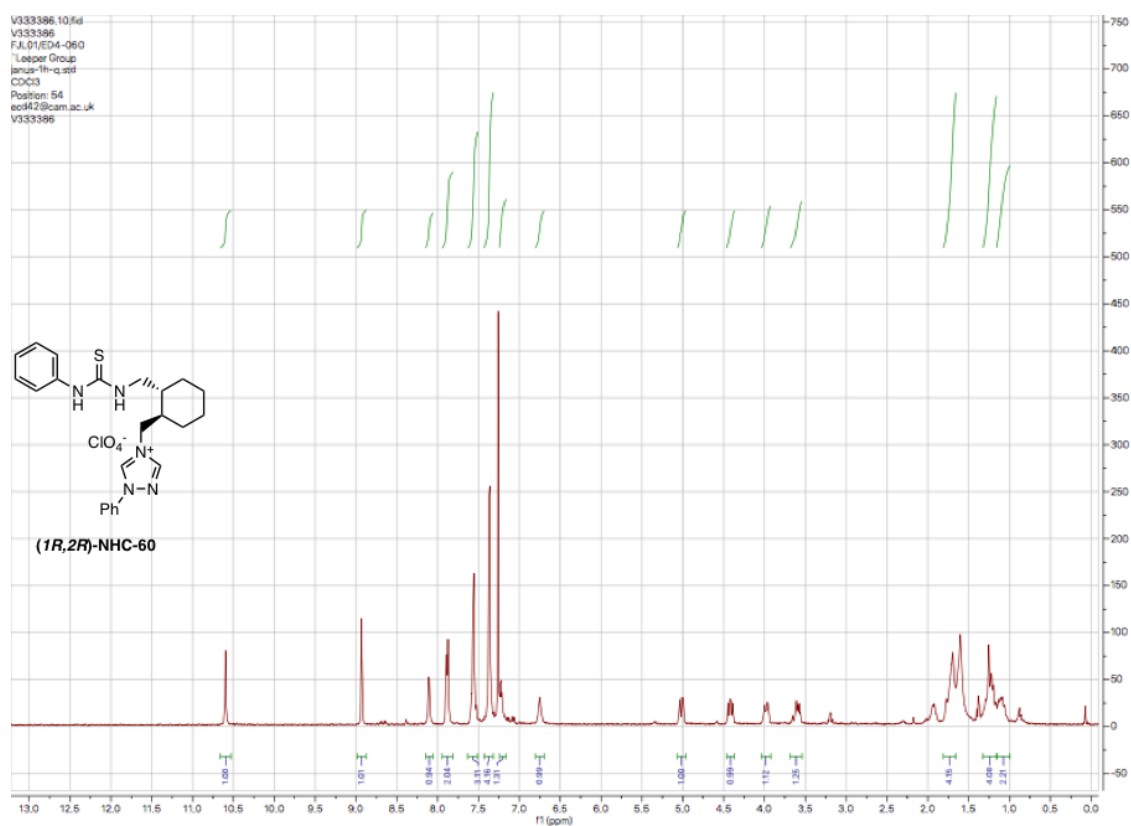
2.5e+005



Mass	Calc. Mass	mDa	PPM	DBE	Formula	I-FIT
414.1479	414.1477	0.2	0.5	13.5	C20 H21 N7 Na S	141.3
414.1479	414.1479	0.0	0.0	9.5	C22 H24 N F3 Na S	143.8
414.1479	414.1497	-1.8	-4.3	9.5	C12 H18 N13 F2 S	1633.8
414.1479	414.1472	0.7	1.7	0.5	C14 H26 N3 F6 S2	2714.0
414.1479	414.1470	0.9	2.2	4.5	C12 H23 N9 F3 S2	2759.2
414.1479	414.1474	0.5	1.2	11.5	C22 H25 N3 F S2	2794.4
414.1479	414.1468	1.1	2.7	8.5	C10 H20 N15 S2	2809.1
414.1479	414.1478	0.1	0.2	-1.5	C14 H25 N F8 Na S	3048.3
414.1479	414.1475	0.4	1.0	2.5	C12 H22 N7 F5 Na S	3108.7
414.1479	414.1473	0.6	1.4	6.5	C10 H19 N13 F2 Na S	3165.1
414.1479	414.1467	1.2	2.9	21.5	C25 H16 N7	3674.5
414.1479	414.1470	0.9	2.2	17.5	C27 H19 N F3	3684.8
414.1479	414.1468	1.1	2.7	6.5	C19 H20 N F8	5458.5
414.1479	414.1466	1.3	3.1	10.5	C17 H17 N7 F5	5488.6
414.1479	414.1463	1.6	3.9	14.5	C15 H14 N13 F2	5523.2
414.1479	414.1484	-0.5	-1.2	3.5	C17 H30 N3 F Na S3	8127.0
414.1479	414.1495	-1.6	-3.9	-1.5	C4 H19 N13 F7 S	11145.4
414.1479	414.1493	-1.4	-3.4	2.5	C2 H16 N19 F4 S	11255.1
414.1479	414.1466	1.3	3.1	-2.5	C2 H21 N15 F5 S2	11475.5
414.1479	414.1480	-0.1	-0.2	-3.5	C7 H28 N9 F3 Na S3	11602.1

1-phenyl-4-(((1*R*,2*R*)-2-((3-phenylthioureido)methyl)cyclohexyl)methyl)-1*H*-1,2,4-triazol-4-ium perchlorate (1*R*,2*R*)-NHC-60

¹H NMR, 400 MHz



High Resolution Mass Spectrum

Openlynx Report - Leeper_FJ

Sample: 4
File: Leeper_FJ1031-4
Description:

Vial: 1:77
Date: 25-Apr-2018
Method: C:\MassLynx\Acc-mass-HI-acid-5ul.olp

Sample ID: ED4-060
Time: 11:58:08
Group: Leeper_FJ

Page 4

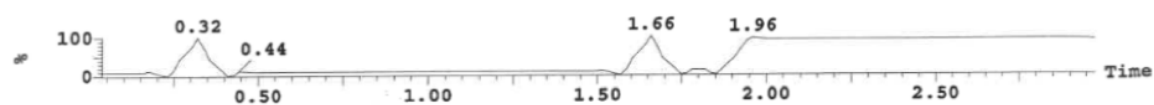
Printed: Wed Apr 25 12:06:15 2018

Sample Report (continued):

Sample 4 Vial 1:77 ID ED4-060 File Leeper_FJ1031-4 Date 25-Apr-2018 Time 11:58:08

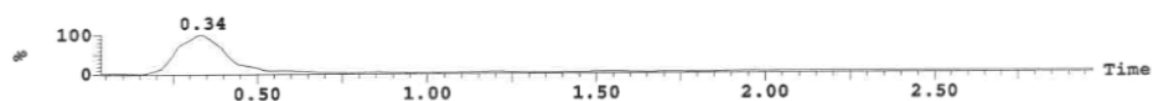
1: TOF MS ES+ : 82.981+104.963

e-001



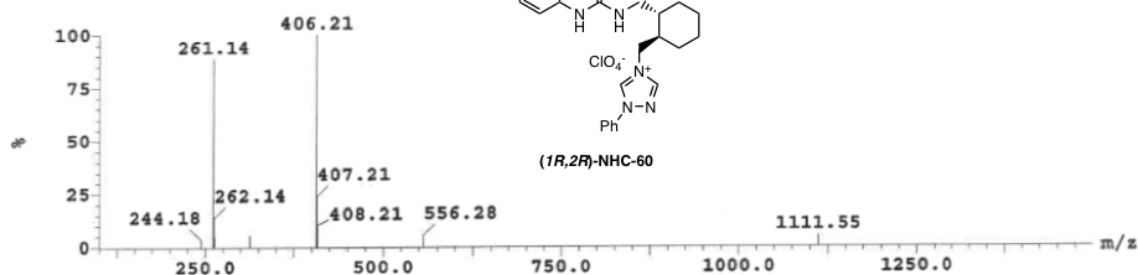
1: TOF MS ES+ : 406.208+428.19

5.0e+001



1: Combine (8:32-1:10)

3.4e+002

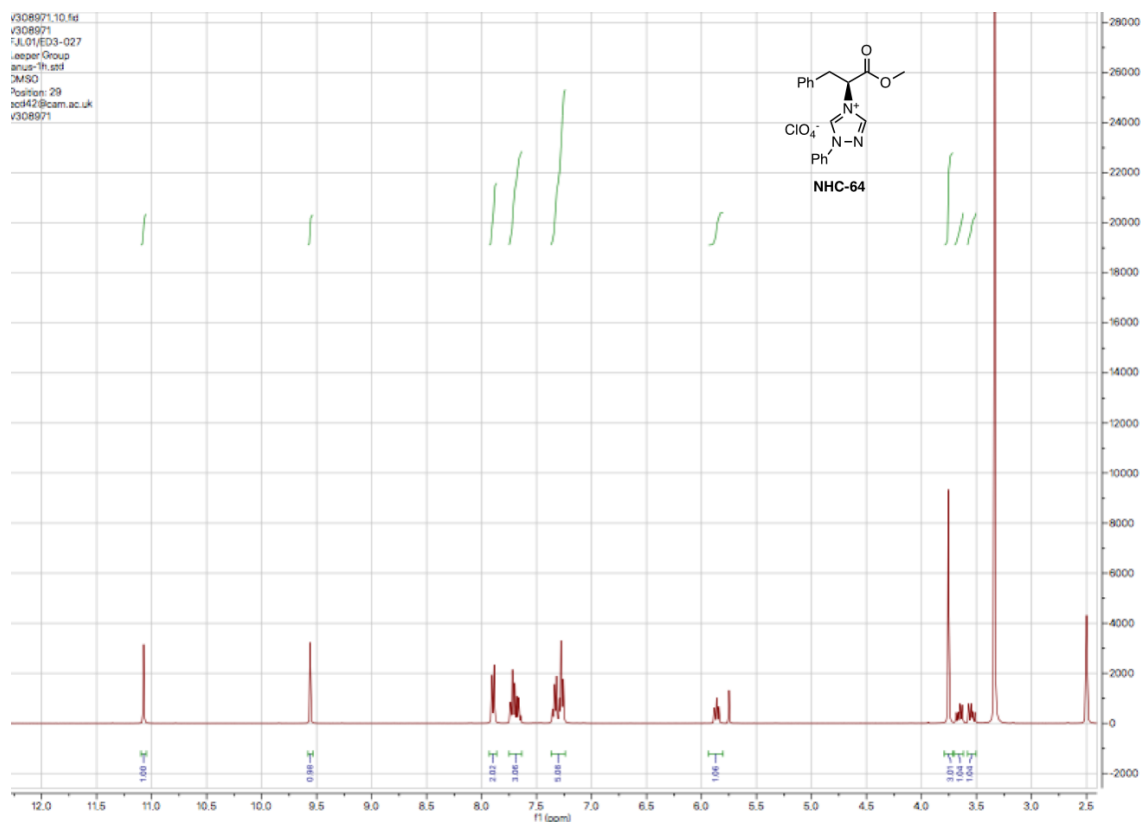


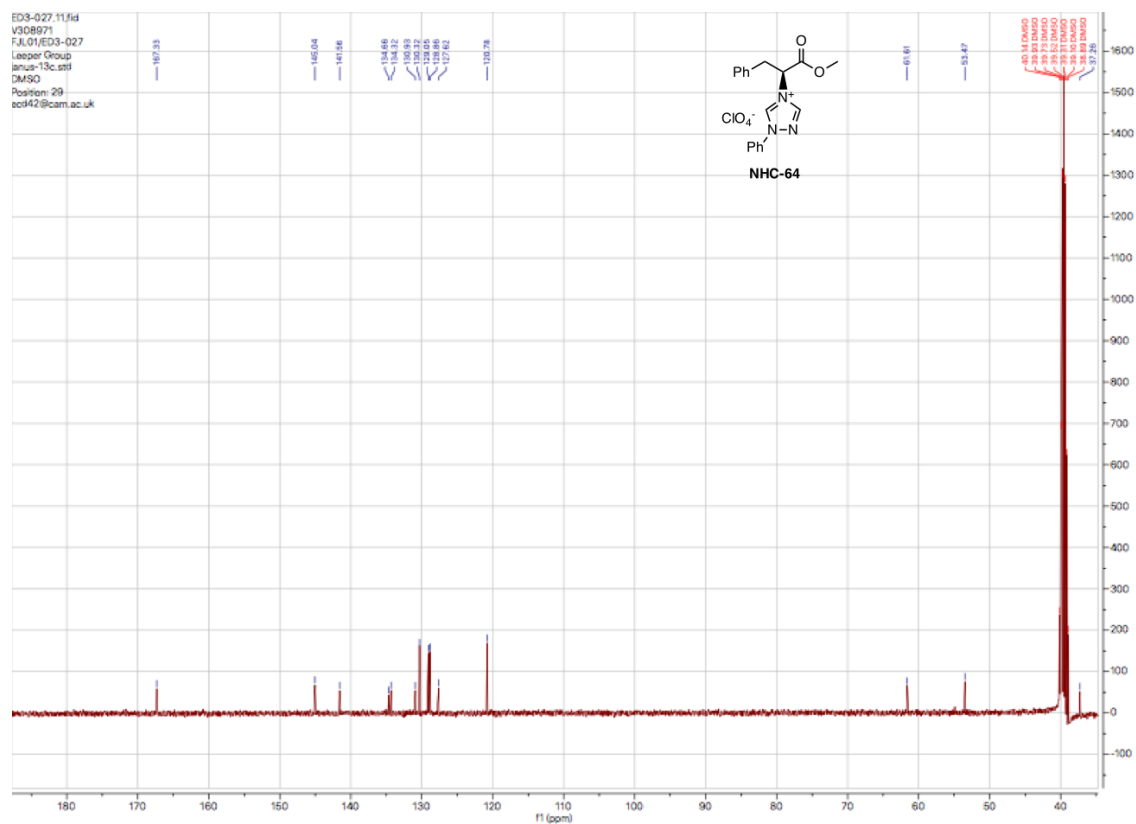
Mass	Calc. Mass	mDa	PPM	DBE	Formula	I-FIT
406.2068	406.2075	-0.7	-1.7	4.5	C18 H33 N5 Na S2	0.4
406.2068	406.2065	0.3	0.7	12.5	C23 H28 N5 S	2.2 ←
406.2068	406.2066	0.2	0.5	-0.5	C8 H32 N13 S3	6.9
406.2068	406.2057	1.1	2.7	6.0	C6 H22 N20 S	7.6
406.2068	406.2066	0.2	0.5	11.0	C16 H23 N12 Na	9.9
406.2068	406.2067	0.1	0.2	-2.0	C H27 N20 Na S2	11.8

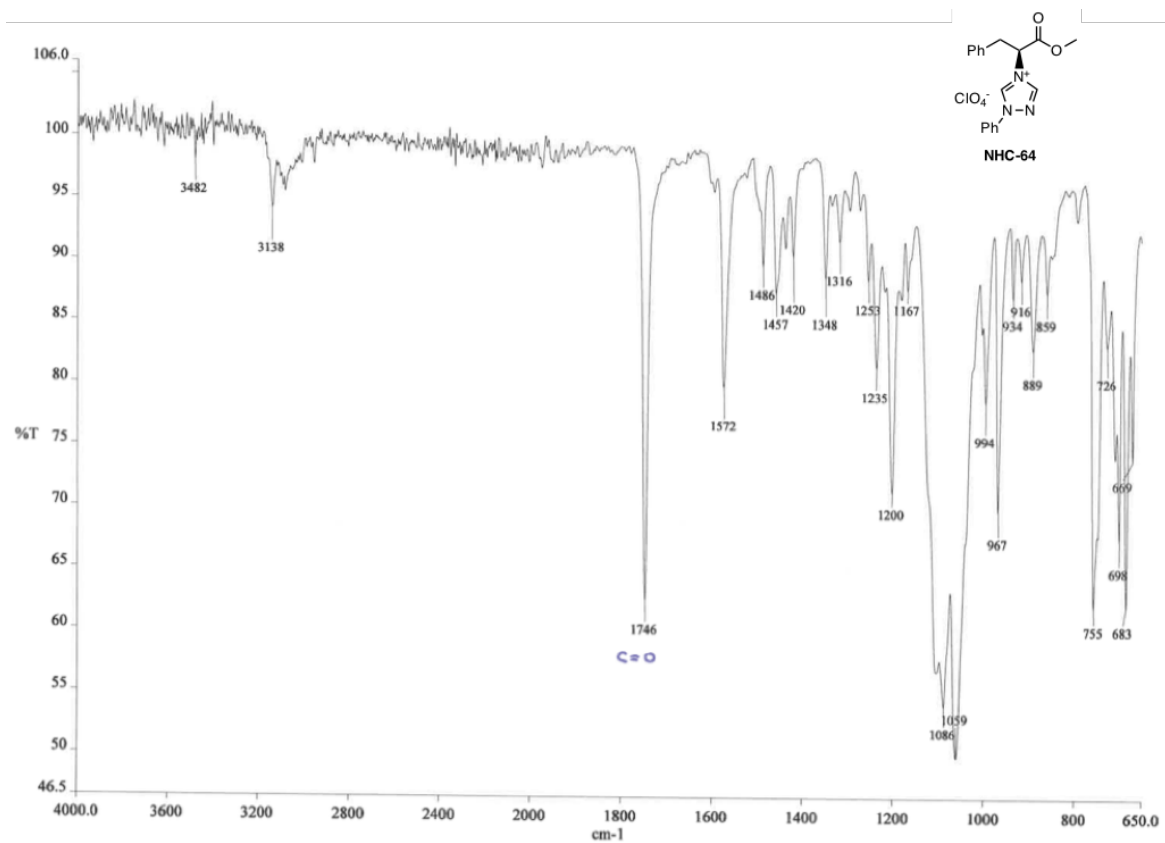
A.1.3 Chapter 5 Compounds

(S)-4-(1-methoxy-1-oxo-3-phenylpropan-2-yl)-1-phenyl-1*H*-1,2,4-triazol-4-ium perchlorate NHC-64

¹H NMR, 400 MHz



^{13}C NMR, 100 MHz

IR Spectrum (cm^{-1})

High Resolution Mass Spectrum

Openlynx Report - Leeper_FJ

Page 1

Sample: 1
File: Leeper_FJ969-1
Description:

Vial: 1:84
Date: 27-Feb-2017
Method: C:\MassLynx\Acc-mass-5ul.olp

Sample ID: ED3-027-2
Time: 11:13:18
Group: Leeper_FJ

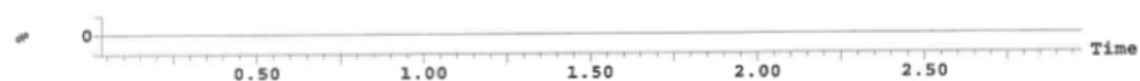
Printed: Mon Feb 27 11:18:19 2017

Sample Report:

Sample 1 Vial 1:84 ID ED3-027-2 File Leeper_FJ969-1 Date 27-Feb-2017 Time 11:13:18

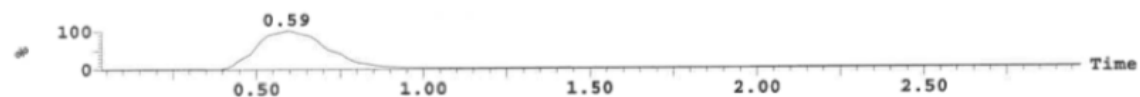
1: TOF MS ES+ : 67.003+88.985

0.0e+000



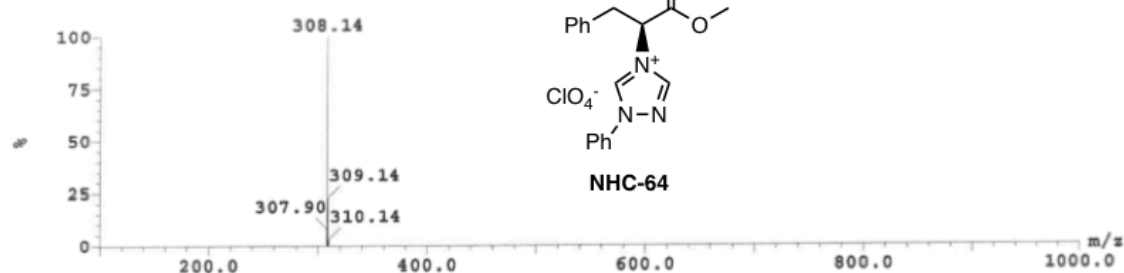
1: TOF MS ES+ : 308.138+330.12

3.9e+003



1: Combine (20:32-1:10)

2.3e+004



Mass	Calc. Mass	mDa	PPM	DBE	Formula	I-FIT
308.1350	308.1362	-1.2	-3.9	9.0	C14 H17 N6 O Na	163.4
308.1350	308.1359	-0.9	-2.9	7.5	C13 H18 N5 O4	199.2
308.1350	308.1348	0.2	0.6	4.0	C13 H21 N2 O5 Na	259.4
308.1350	308.1348	0.2	0.6	9.5	C12 H15 N9 Na	268.4
308.1350	308.1345	0.5	1.6	8.0	C11 H16 N8 O3	307.9
308.1350	308.1345	0.5	1.6	2.5	C12 H22 N O8	341.5

Elemental Analysis

Name.....Emma DUEHAM
 Date.....15/01/17
 No. of Specimen.....ED3-027
 Analyse for.....C, H, N
 Elements present.....C, H, N, O, Cl
 M. pt. or B. pt.
 Method of purification.....Precipitation from
 Acetic Acid/diethyl ether
 Approx. values %.....C 53.01 H 4.45
 N 10.3
 Any remarks:

I J 014853

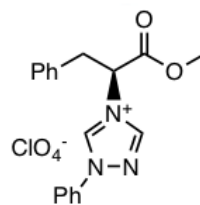
Results

1.5348 mg → C = 52.16 %
 H = 4.30 %
 N = 10.02 %

1.4788 mg → C = 52.20 %
 H = 4.30 %
 N = 9.96 %

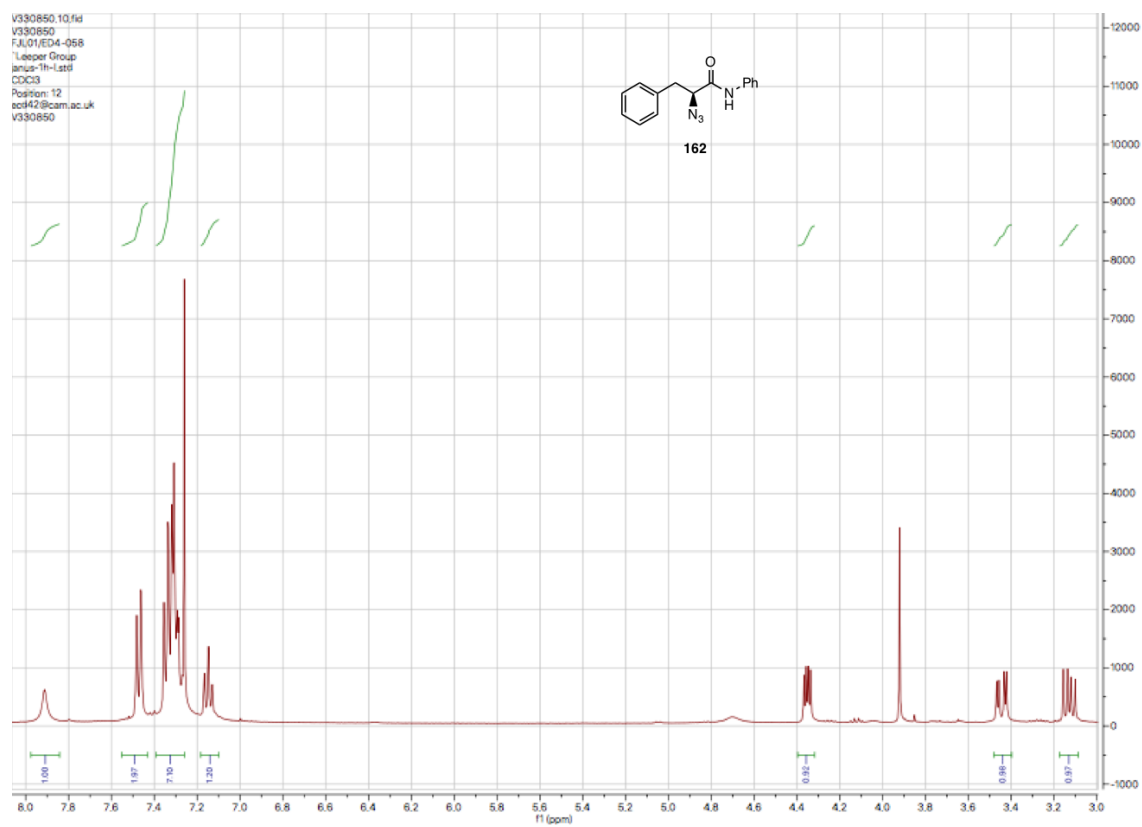
II

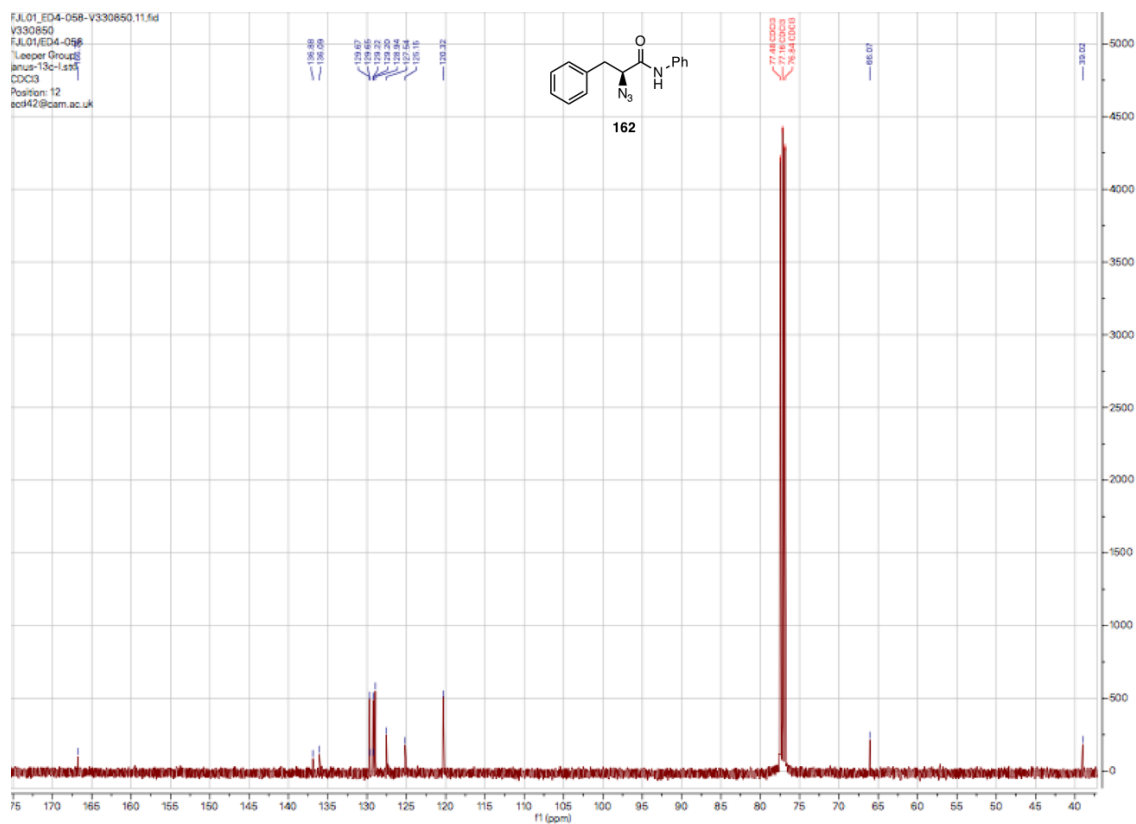
Theoretical values and structural formulae



NHC-64

(Section II to be filled in after analysis)

(S)-2-azido-N,3-diphenylpropanamide 162 **^1H NMR, 400 MHz**

^{13}C NMR, 100 MHz

High Resolution Mass Spectrum

Openlynx Report - Leeper_FJ

Page 1

Sample: 1
File: Leeper_FJ1031-1
Description:

Vial: 174
Date: 25-Apr-2018
Method: C:\MassLynx\Acc-mass-HI-acid-5ul.o1p

Sample ID: ED4-058
Time: 11:45:58
Group: Leeper_FJ

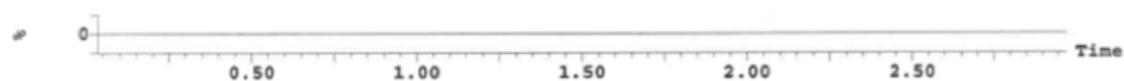
Printed: Wed Apr 25 12:06:15 2018

Sample Report:

Sample 1 Vial 1:74 ID ED4-058 File Leeper_FJ1031-1 Date 25-Apr-2018 Time 11:45:58

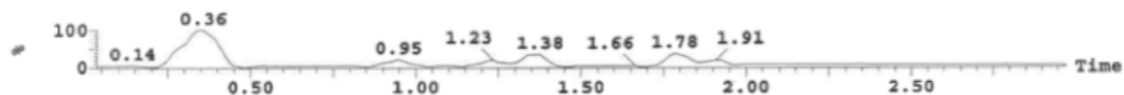
1: TOF MS ES+ : 67.003+88.985

0.0e+000



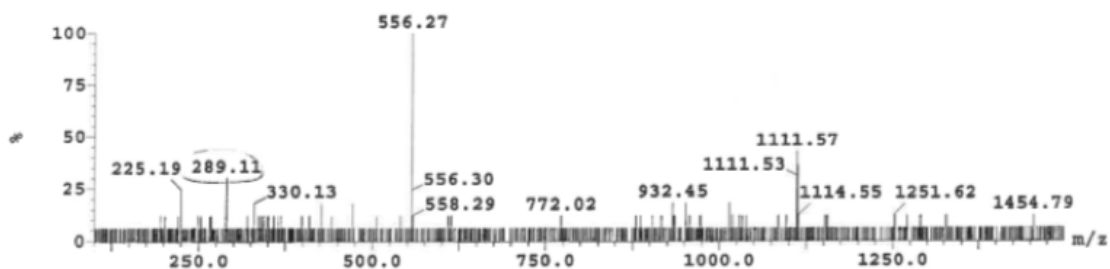
1: TOF MS ES+ : 267.128+289.11

2.0e+000



1: Combine (8:32-1:10)

1.7e+001

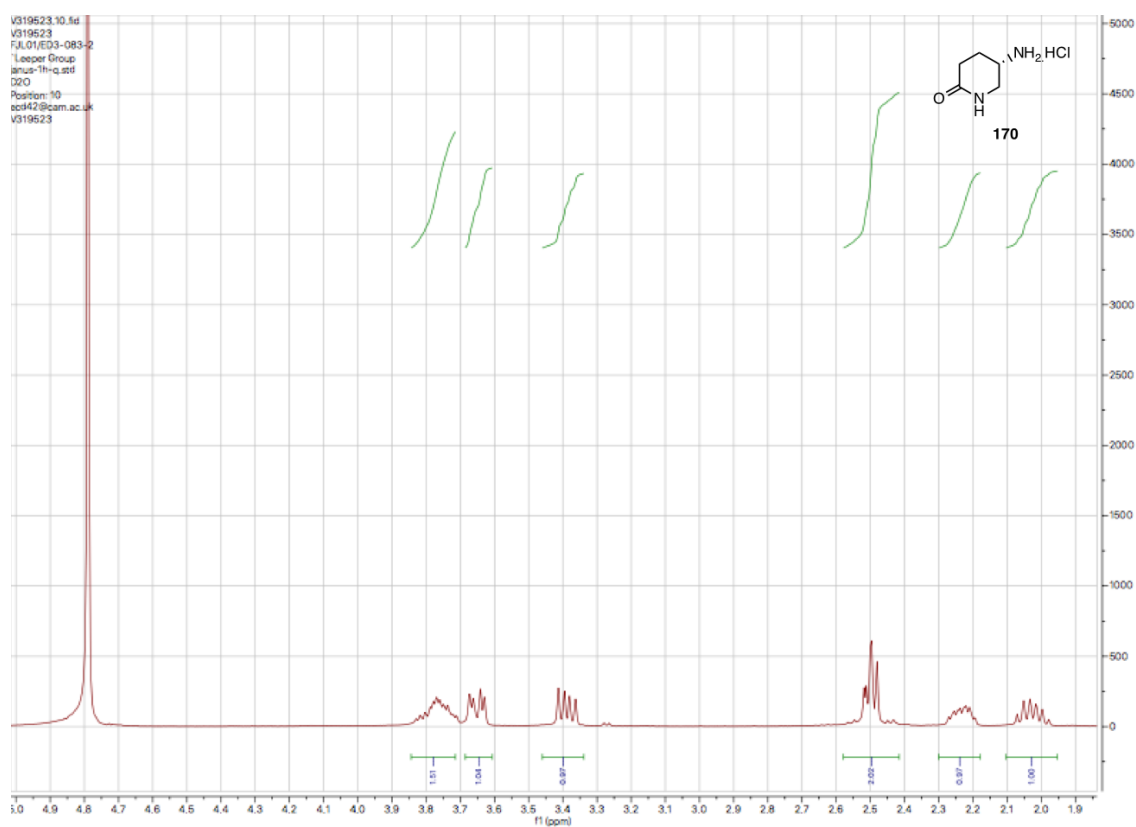


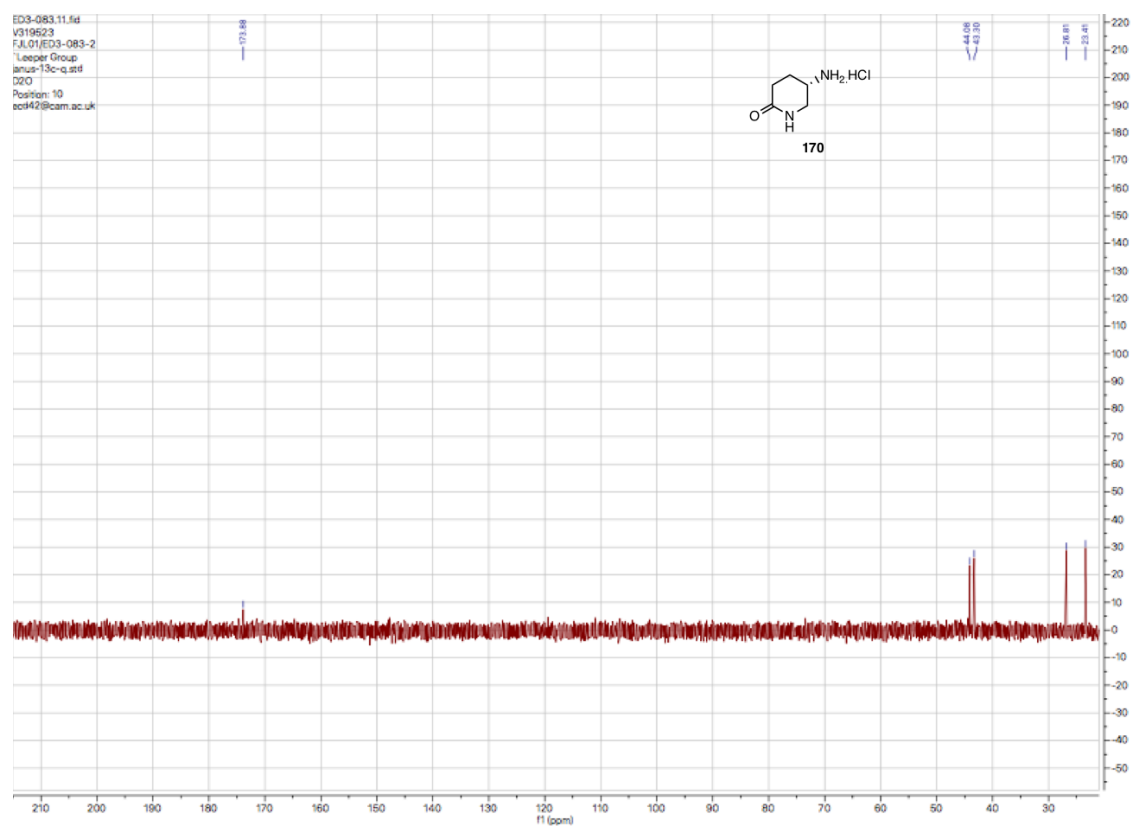
Mass	Calc. Mass	mDa	PPM	DBE	Formula	i-FIT
267.1101	267.1109	-0.8	-3.0	7.5	C14 H16 N2 O2 Na	2773013.3
267.1101	267.1093	0.8	3.0	6.5	C11 H15 N4 O4	2773013.3
267.1101	267.1096	0.5	1.9	8.0	C12 H14 N5 O Na	2773013.3
267.1101	267.1107	-0.6	-2.2	11.5	C12 H11 N8	2773013.3
267.1101	267.1107	-0.6	-2.2	6.0	C13 H17 N O5	2773013.3
289.1129	289.1135	-0.6	-2.1	-0.5	C9 H21 O10	2773013.0
289.1129	289.1137	-0.8	-2.8	1.0	C10 H20 N O7 Na	2773013.0
289.1129	289.1121	0.8	2.8	0.0	C7 H19 N3 O9	2773013.0
289.1129	289.1124	0.5	1.7	1.5	C8 H18 N4 O6 Na	2773013.0
289.1129	289.1135	-0.6	-2.1	5.0	C8 H15 N7 O5	2773013.0
289.1129	289.1137	-0.8	-2.8	6.5	C9 H14 N8 O2 Na	2773013.0
289.1129	289.1121	0.8	2.8	5.5	C6 H13 N10 O4	2773013.0
289.1129	289.1124	0.5	1.7	7.0	C7 H12 N11 O Na	2773013.0
289.1129	289.1135	-0.6	-2.1	10.5	C7 H9 N14	2773013.0

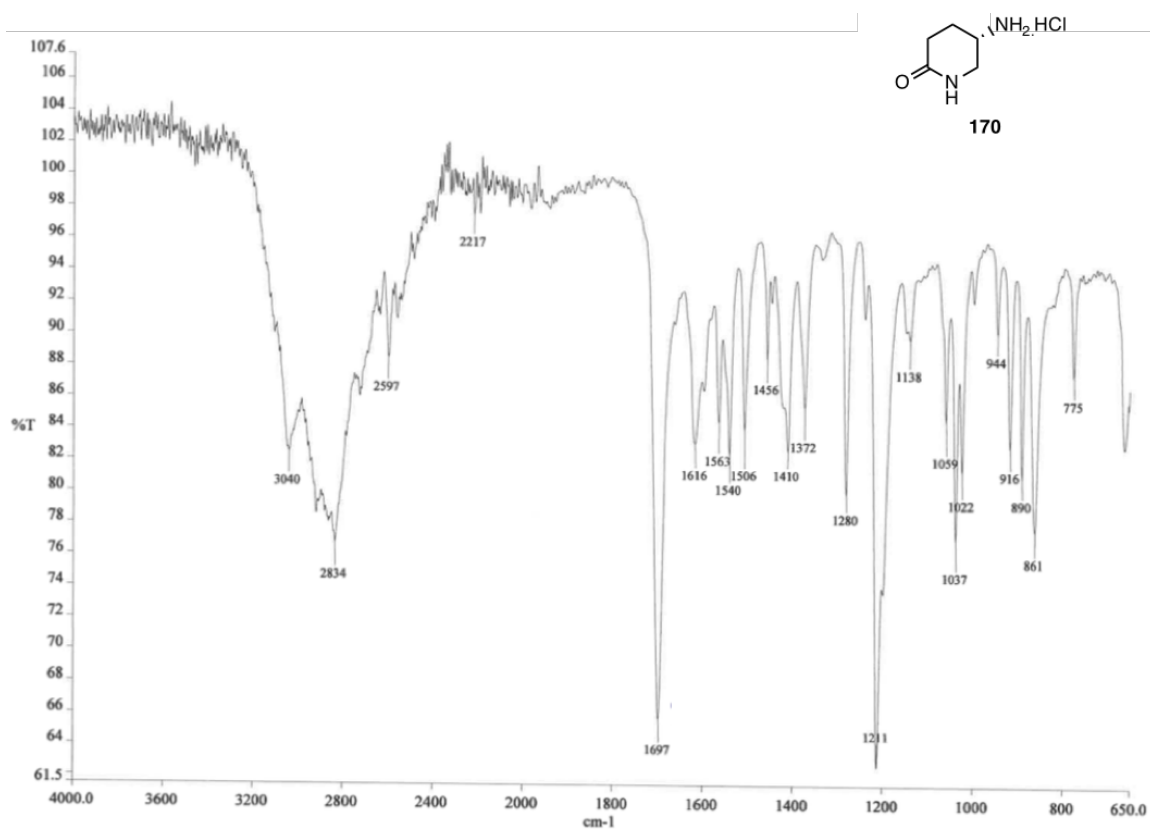
A.1.4 Chapter 6 Compounds

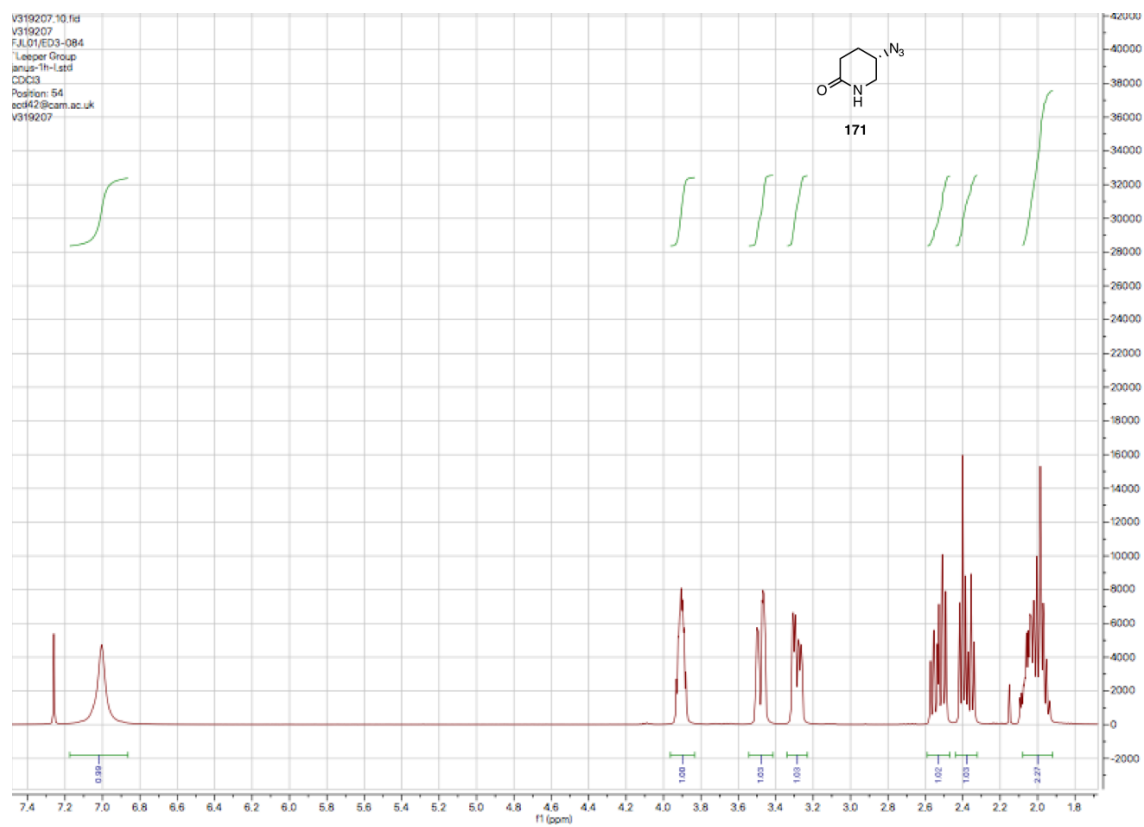
(S)-5-aminopiperidin-2-one hydrochloride 170

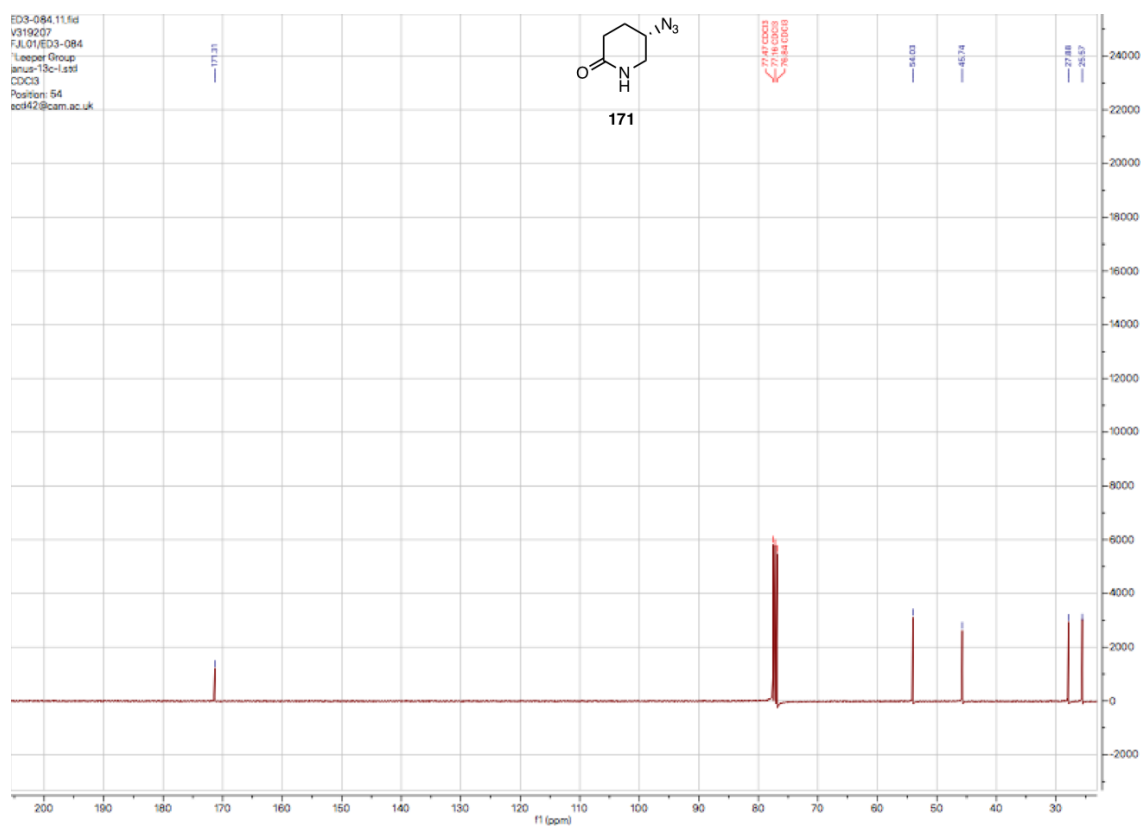
^1H NMR, 400 MHz

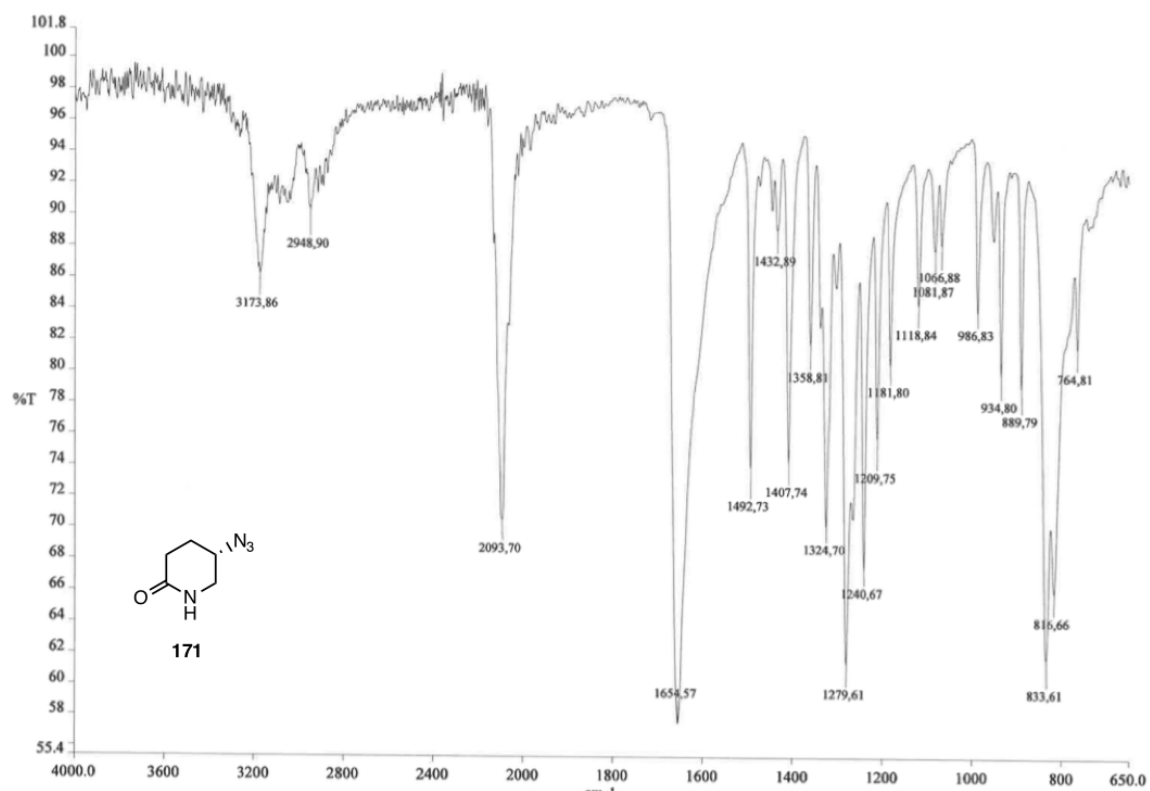


^{13}C NMR, 100 MHz

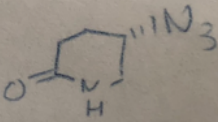
IR Spectrum (cm^{-1})

(S)-5-azidopiperidin-2-one 171 **^1H NMR, 400 MHz**

^{13}C NMR, 100 MHz

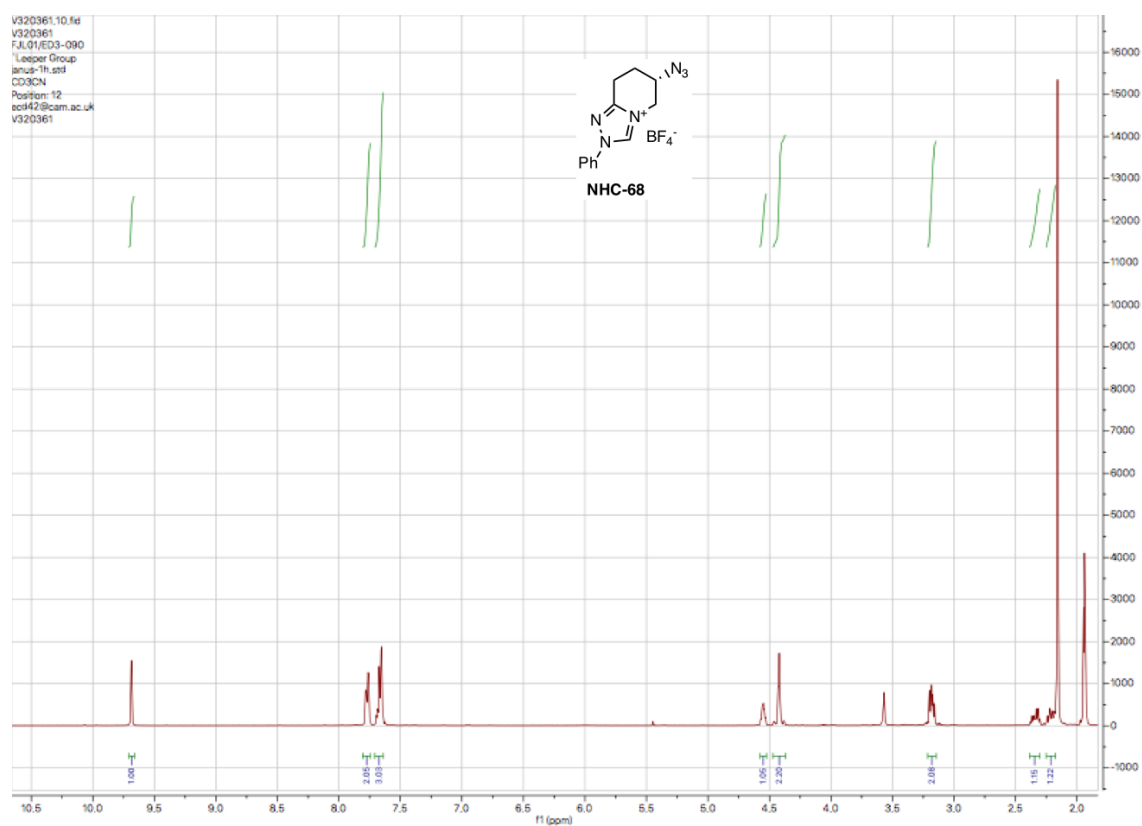
IR Spectrum (cm^{-1})

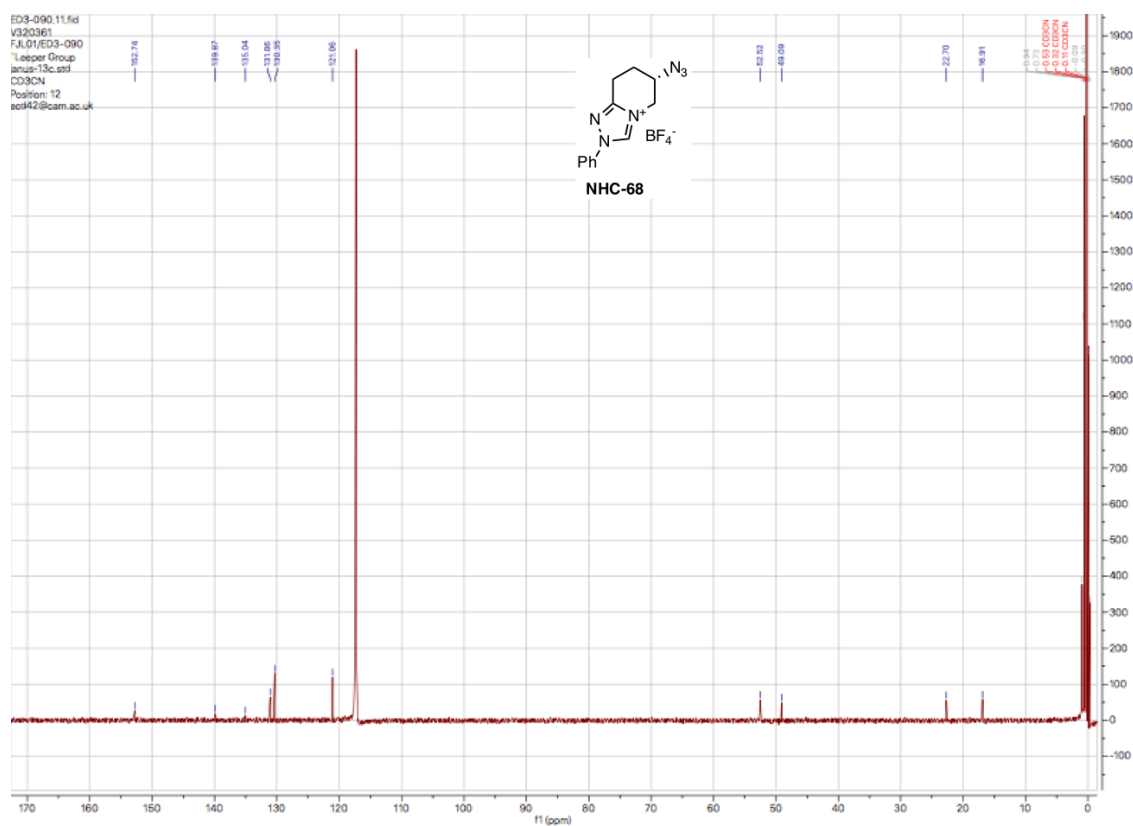
Elemental Analysis

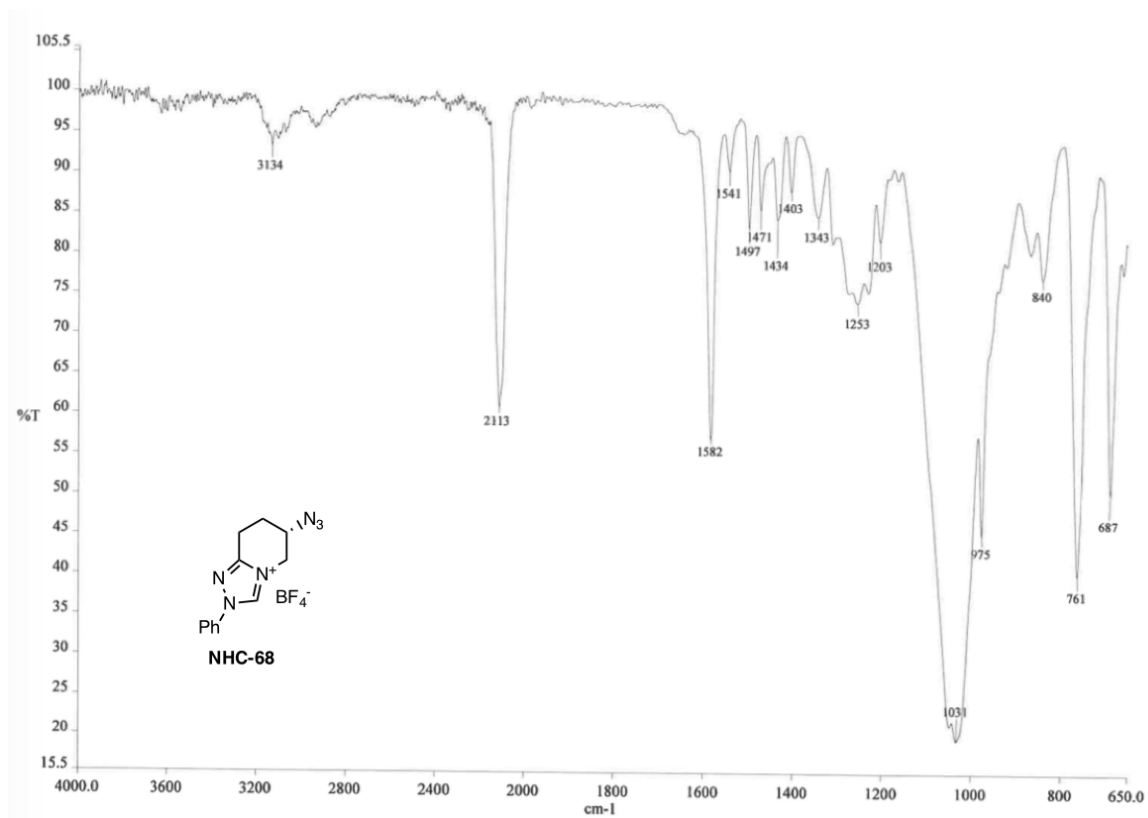
Name..... E. DURHAM		I J 014867	
Date..... 27/04/18		Results	
No. of Specimen..... ED3-084		1.7349 → C = 42.47	
Analyse for..... C, H, N		H = 5.70	
Elements present..... C, H, N, O		N = 38.39	
M. pt. or B. pt.		1.6021 → C = 42.38	
Method of purification..... Column chromatography		H = 5.70	
Approx. values %..... C 42.85 H 5.75		N = 39.52	
N 39.98		II	
		Theoretical values and structural formulae	
			

(S)-5-(azidomethyl)-2-phenyl-6,7-dihydro-5H-pyrrolo[2,1-c][1,2,4]triazol-2-ium tetrafluoroborate (1*R*,2*R*)-NHC-68

¹H NMR, 400 MHz



^{13}C NMR, 100 MHz

IR Spectrum (cm^{-1})

High Resolution Mass Spectrum

Openlynx Report - Leeper_FJ

Page 1

Sample: 1 Vial: 1:56
File: Leeper_FJ998-1 Date: 11-Jul-2017
Description: Method: C:\MassLynx\Acc-mass-5ul.oip

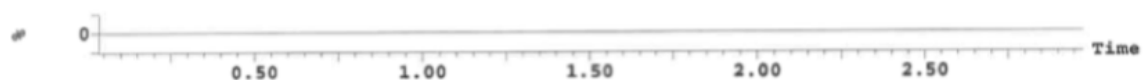
Sample ID: ED3-090
Time: 15:22:14
Group: Leeper_FJ

Printed: Tue Jul 11 15:26:19 2017

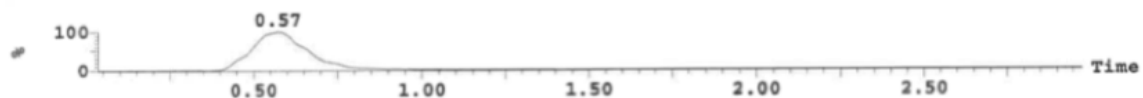
Sample Report:

Sample 1 Vial 1:56 ID ED3-090 File Leeper_FJ998-1 Date 11-Jul-2017 Time 15:22:14

1: TOF MS ES+ : 51.008+72.99 0.0e+000

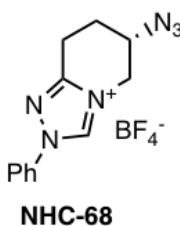
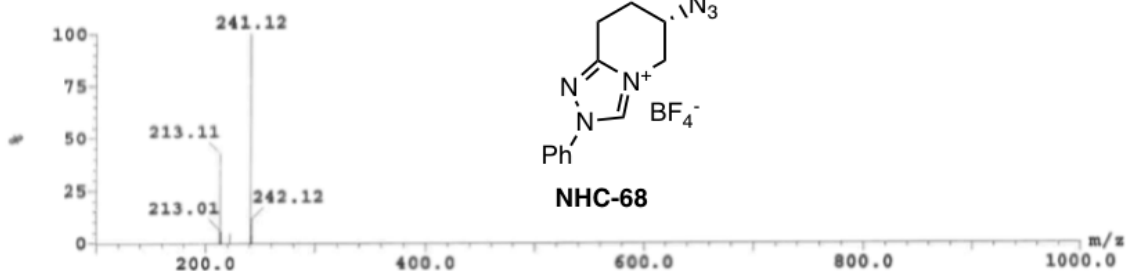


1: TOF MS ES+ : 241.118+263.1 1.3e+004



1: Combine (18:32-1:10)

8.4e+004

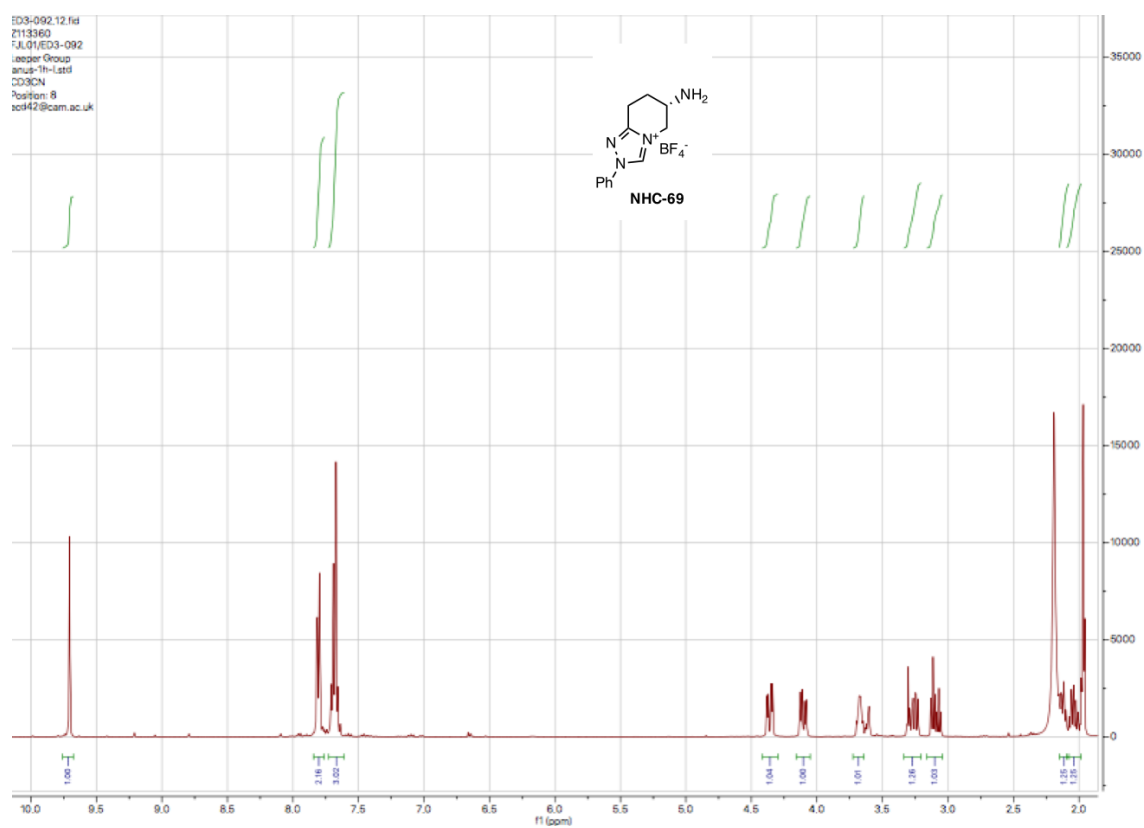


Mass	Calc. Mass	mDa	PPM	DBE	Formula
241.1206	241.1202	0.4	1.7	9.5	C ₁₂ H ₁₃ N ₆

I-FIT
583.7

(S)-5-(aminomethyl)-2-phenyl-6,7-dihydro-5H-pyrrolo[2,1-c][1,2,4]triazol-2-ium tetrafluoroborate NHC-69

^1H NMR, 400 MHz



ED3-092-10.fid
7113360
Fuj.01/ED3-092
Leaper Group
anup-13c-1.asi
COCON
Position: 8
ed442@cam.ac.uk

154.51 148.67 138.17 131.86 131.82 121.93

52.64 44.29 26.80 18.27

1.34 1.35 1.69 COCON 1.70 COCON 1.71 COCON 0.01

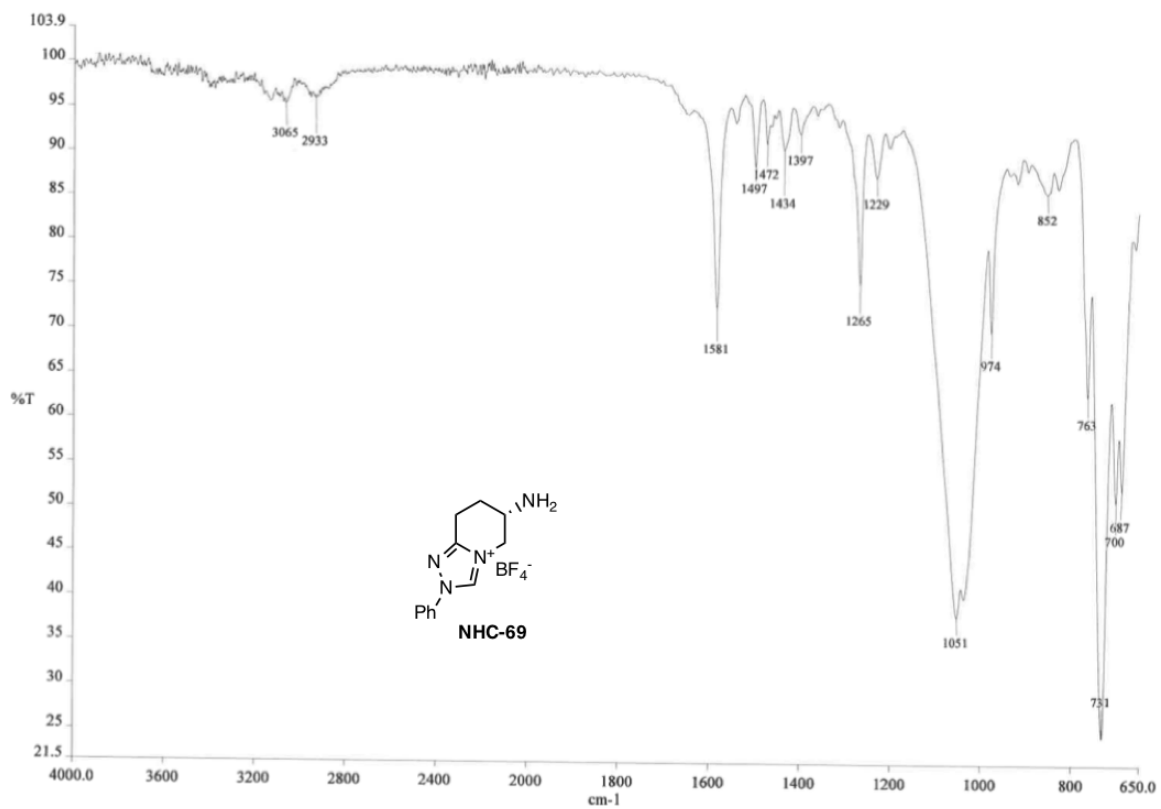
Nc1cc[n+]2c1nc(Nc3ccccc3)n2.[B-](F)(F)F

NHC-69

170 160 150 140 130 120 110 100 90 80 70 60 50 40 30 20 10 0

f1 (ppm)

15000 14000 13000 12000 11000 10000 9000 8000 7000 6000 5000 4000 3000 2000 1000 0 -1000

IR Spectrum (cm^{-1})

High Resolution Mass Spectrum

Openlynx Report - Leeper_FJ

Page 1

Sample: 1
File: Leeper_FJ1000-1
Description:

Vial: 1:60
Date: 11-Jul-2017
Method: C:\MassLynx\Acc-mass-5ul.olp

Sample ID: ED3-092
Time: 17:31:05
Group: Leeper_FJ

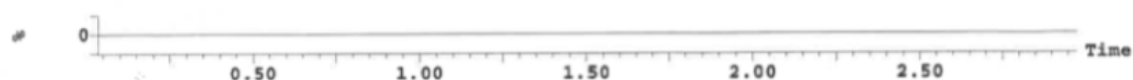
Printed: Tue Jul 11 17:35:17 2017

Sample Report:

Sample 1 Vial 1:60 ID ED3-092 File Leeper_FJ1000-1 Date 11-Jul-2017 Time 17:31:05

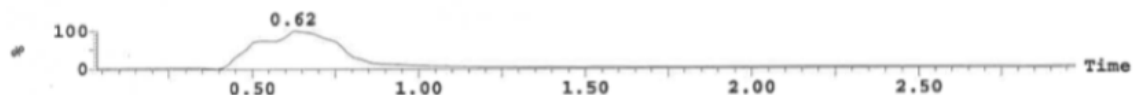
1: TOF MS ES+ : 51.008+72.99

0.0e+000



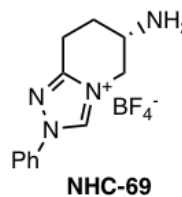
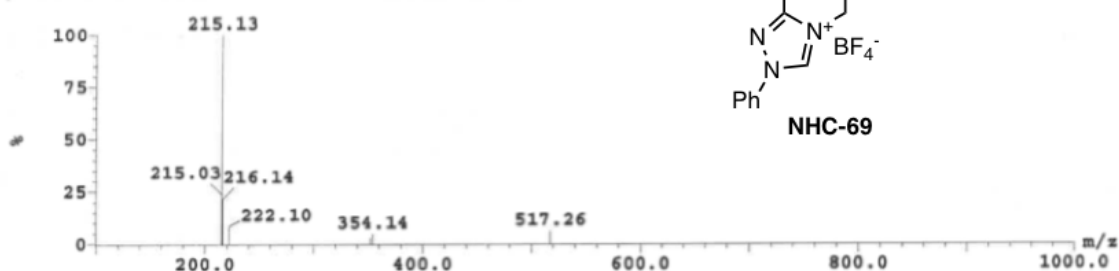
1: TOF MS ES+ : 215.128+237.11

6.6e+003



1: Combine (20:32-1:10)

4.2e+004

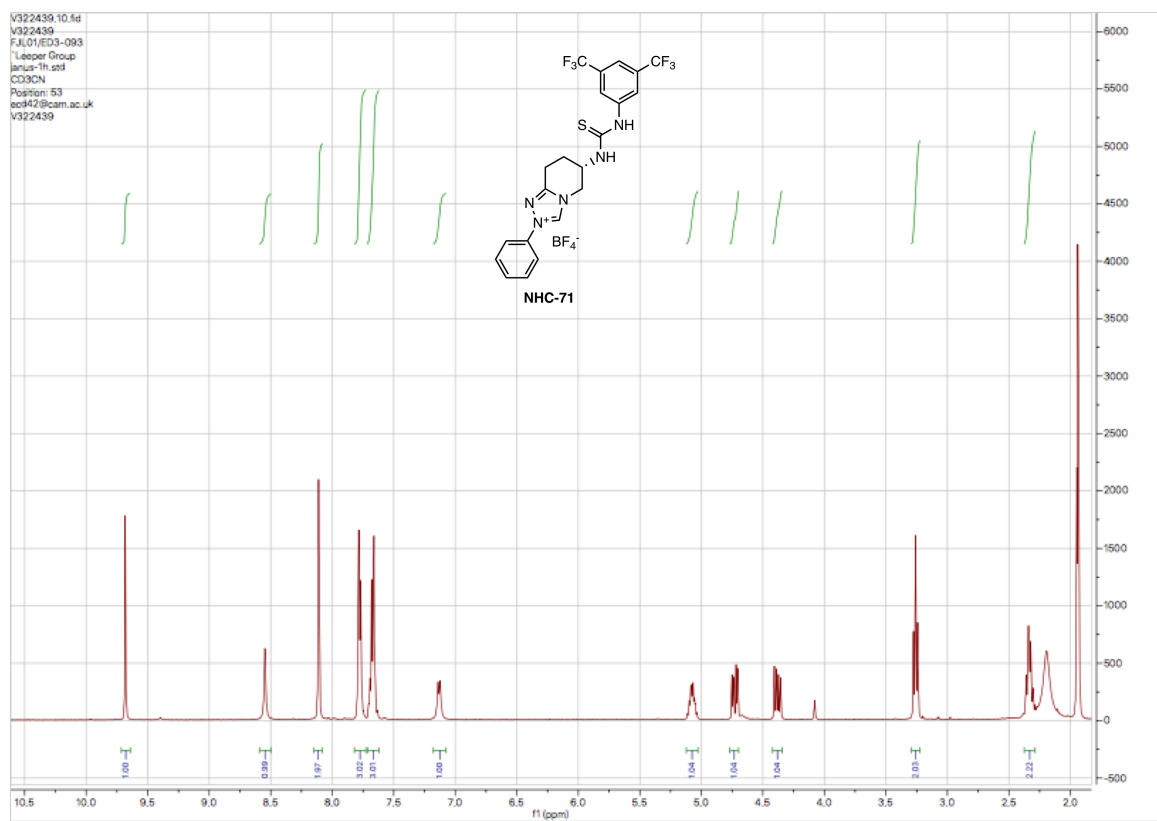


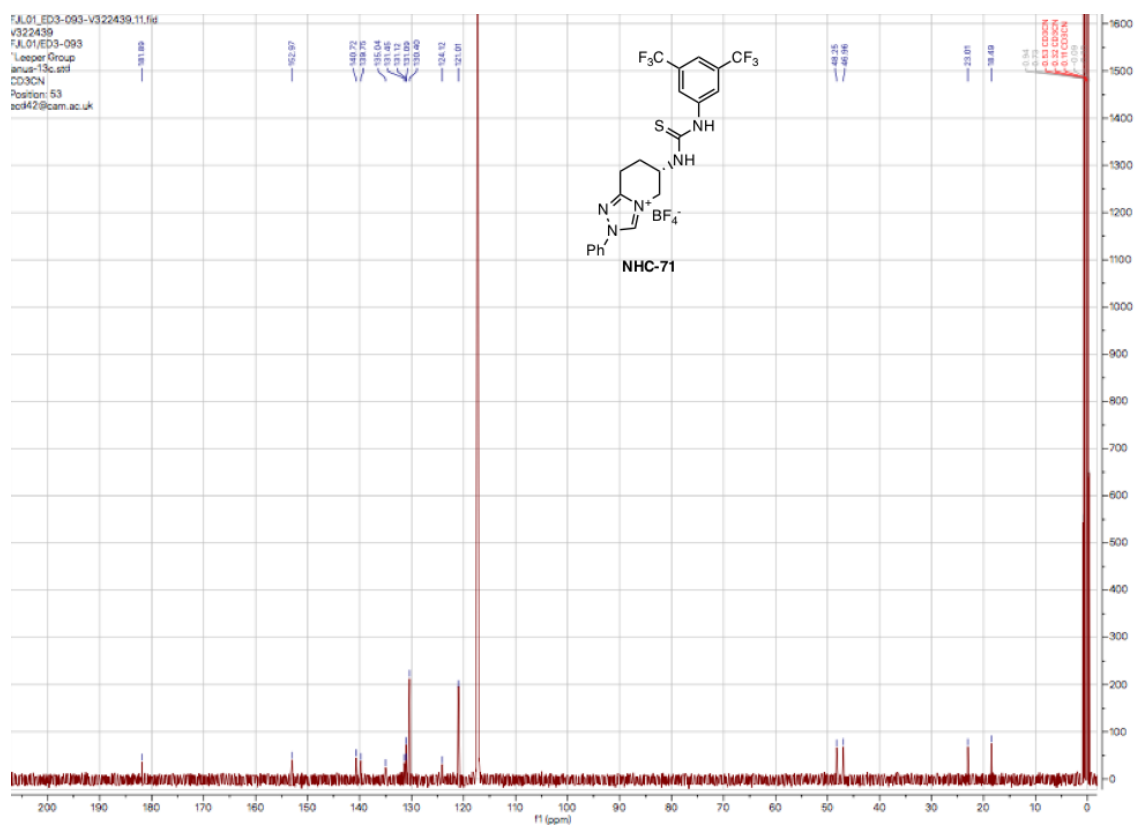
Mass	Calc. Mass	mDa	PPM	DBE	Formula
215.1303	215.1297	0.6	2.8	7.5	C ₁₂ H ₁₅ N ₄

I-FIT
389.8

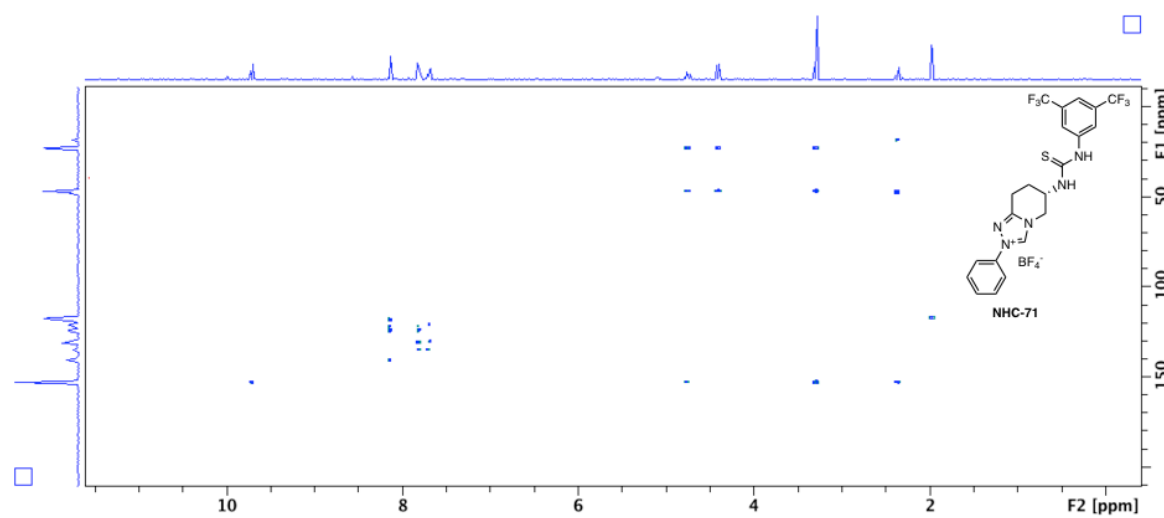
(S)-5-((3-(3,5-bis(trifluoromethyl)phenyl)thioureido)methyl)-2-phenyl-6,7-dihydro-5H-pyrrolo[2,1-c][1,2,4]triazol-2-ium tetrafluoroborate NHC-71

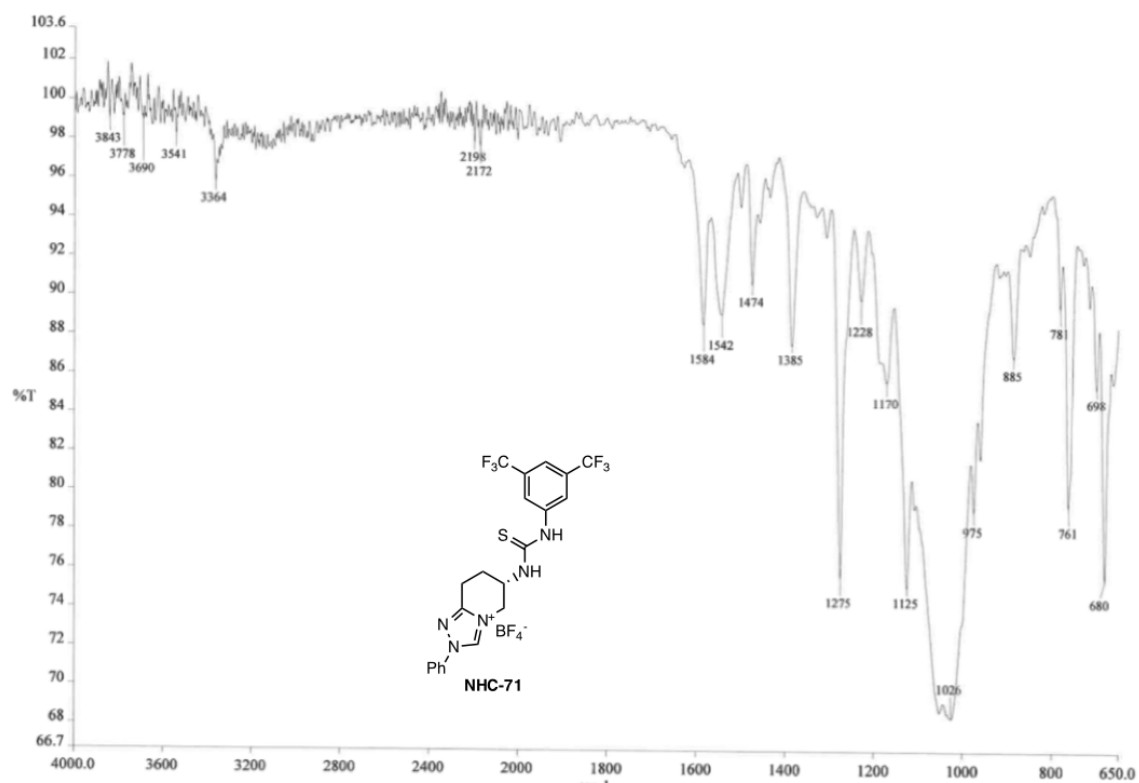
¹H NMR, 400 MHz



^{13}C NMR, 100 MHz

HMBC



IR Spectrum (cm^{-1})

High Resolution Mass Spectrum

Openlynx Report - Leeper_FJ

Sample: 1
File: Leeper_FJ1029-1
Description:

Vial: 1:59
Date: 08-Apr-2018
Method: C:\MassLynx\Acc-mass-HI-acid-5ul.oip

Sample ID: ED3-093
Time: 10:49:58
Group: Leeper_FJ

Page 1

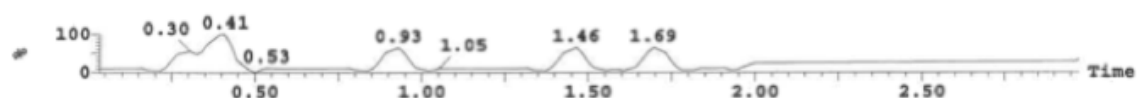
Printed: Sun Apr 08 11:06:03 2018

Sample Report:

Sample 1 Vial 1:59 ID ED3-093 File Leeper_FJ1029-1 Date 08-Apr-2018 Time 10:49:58

1: TOF MS ES+ : 78.989+100.971

6.2e-001



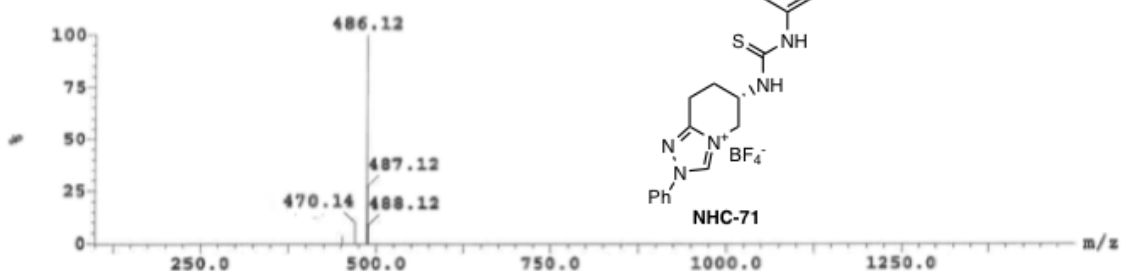
1: TOF MS ES+ : 486.118+508.1

2.6e+002



1: Combine (13:32-1:10)

1.7e+003

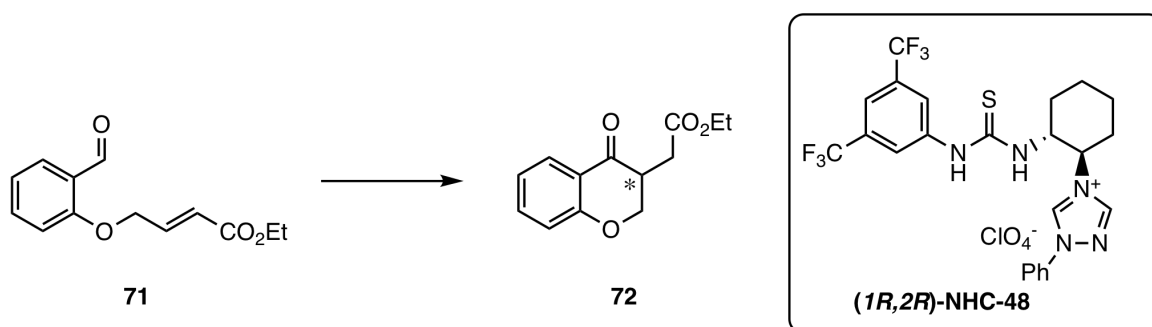


Mass	Calc. Mass	mDa	PPM	DBE	Formula	I-FIT
486.1198	486.1187	1.1	2.3	12.5	C21 H18 N5 F6 S	0.9
486.1198	486.1185	1.3	2.7	16.5	C19 H15 N11 F3 S	1.0
486.1198	486.1182	1.6	3.3	20.5	C17 H12 N17 S	1.1
486.1198	486.1187	1.1	2.3	20.0	C24 H16 N8 F2 S	2.5
486.1198	486.1189	0.9	1.9	16.0	C26 H19 N2 F5 S	2.6
486.1198	486.1188	1.0	2.1	5.0	C18 H20 N2 F10 S	10.5
486.1198	486.1185	1.3	2.7	9.0	C16 H17 N8 F7 S	10.7
486.1198	486.1183	1.5	3.1	13.0	C14 H14 N14 F4 S	10.9
486.1198	486.1180	1.8	3.7	17.0	C12 H11 N20 F S	11.2
486.1198	486.1221	-2.3	-4.7	7.5	C18 H22 N5 F6 S2	12.3
486.1198	486.1218	-2.0	-4.1	11.5	C16 H19 N11 F3 S2	12.4
486.1198	486.1216	-1.8	-3.7	15.5	C14 H16 N17 S2	12.5
486.1198	486.1220	-2.2	-4.5	15.0	C21 H20 N8 F2 S2	13.7
486.1198	486.1189	0.9	1.9	23.5	C29 H17 N5 F S	13.8
486.1198	486.1214	-1.6	-3.3	25.0	C24 H11 N12 F	19.2
486.1198	486.1216	-1.8	-3.7	21.0	C26 H14 N6 F4	19.2
486.1198	486.1218	-2.0	-4.1	17.0	C28 H17 F7	19.4
486.1198	486.1216	-1.8	-3.7	28.5	C29 H12 N9	22.7
486.1198	486.1221	-2.3	-4.7	0.0	C15 H24 N2 F10 S2	22.9
486.1198	486.1218	-2.0	-4.1	24.5	C31 H15 N3 F3	22.9

A.2 HPLC Traces from the Stetter Reaction and Benzoin Condensation

A.2.1 Stetter Reaction

NHC-48



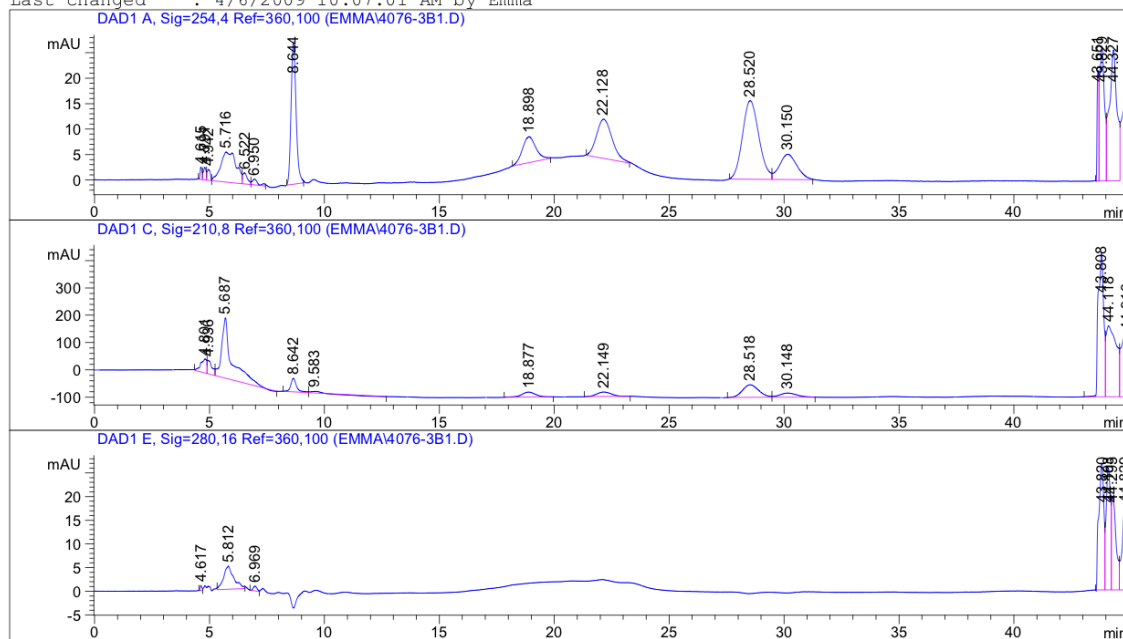
Data File C:\HPCHEM\1\DATA\EMMA\4076-3B1.D

Sample Name: ED4-076-3b

```

=====
Injection Date   : 4/6/2009 2:26:22 PM      Seq. Line :    1
Sample Name     : ED4-076-3b              Location  : Vial 73
Acq. Operator   : Emma                    Inj       :    1
Acq. Instrument : hplc                    Inj Volume: 10 µl
Acq. Method     : C:\HPCHEM\1\METHODS\EMMA.M\STETTER.M
Last changed    : 4/6/2009 2:25:57 PM by Emma
                  (modified after loading)
Analysis Method : C:\HPCHEM\1\METHODS\EMMA.M\STETTER.M
Last changed    : 4/6/2009 10:07:01 AM by Emma
=====

```



Fraction Information

Fraction collection off

No Fractions found.

Area Percent Report

```

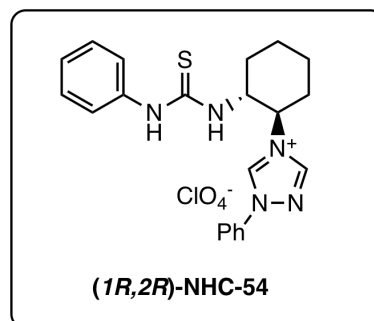
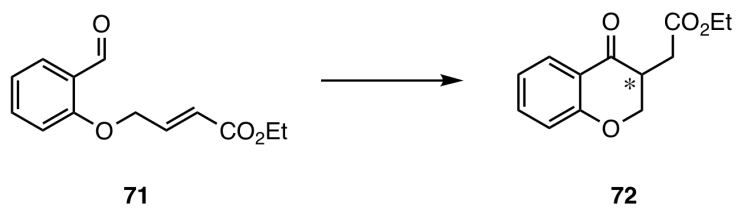
Sorted By      :      Signal
Multiplier     :      1.0000
Dilution       :      1.0000
Use Multiplier & Dilution Factor with ISTDs

```

Signal 1: DAD1 A, Sig=254.4 Ref=360,100

Peak #	RetTime [min]	Type	Width [min]	Area [mAU*s]	Height [mAU]	Area %
1	4.615	BV	0.0931	14.70233	2.41263	0.4156
2	4.791	VV	0.1185	20.68052	2.49926	0.5846
3	4.942	VV	0.1250	20.25747	2.12882	0.5727
4	5.716	VV	0.5841	280.66440	5.93066	7.9341
5	6.522	VV	0.2042	31.33158	2.17354	0.8857
6	6.950	VB	0.2434	21.12983	1.17724	0.5973

NHC-54



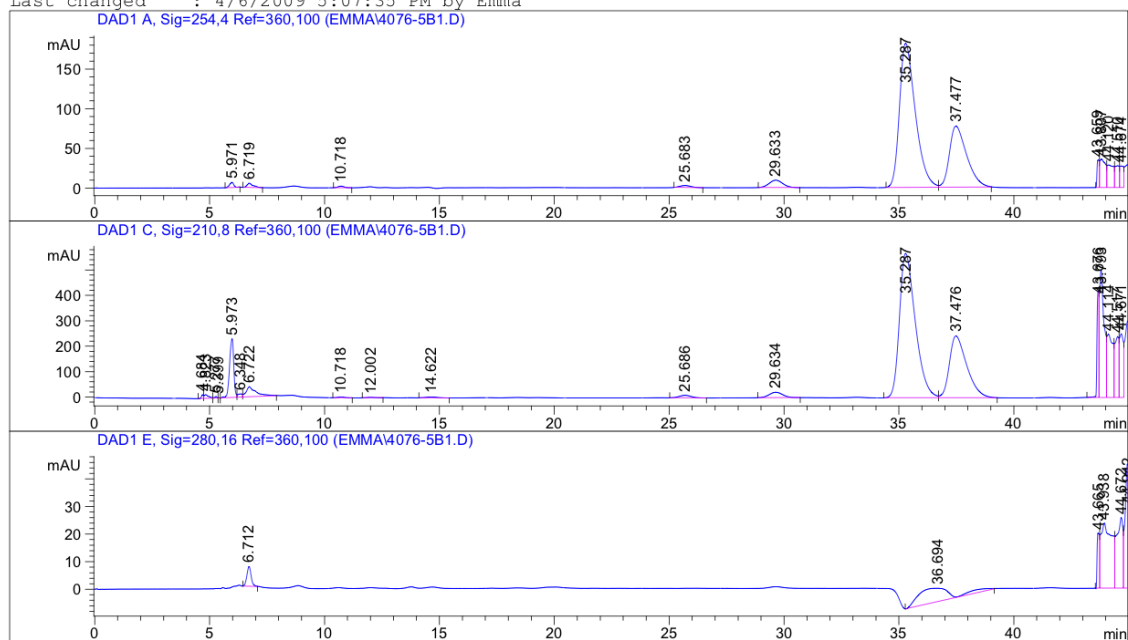
Data File C:\HPCHEM\1\DATA\EMMA\4076-5B1.D

Sample Name: ED4-076-5b

```

=====
Injection Date : 4/6/2009 3:52:04 PM      Seq. Line : 1
Sample Name   : ED4-076-5b              Location  : Vial 74
Acq. Operator : Emma                    Inj       : 1
Acq. Instrument : hplc                  Inj Volume: 10 µl
Acq. Method   : C:\HPCHEM\1\METHODS\EMMA.M\STETTER.M
Last changed  : 4/6/2009 3:50:26 PM by Emma
Analysis Method : C:\HPCHEM\1\METHODS\EMMA.M\STETTER.M
Last changed   : 4/6/2009 5:07:35 PM by Emma
=====

```



Fraction Information

Fraction collection off

No Fractions found.

Area Percent Report

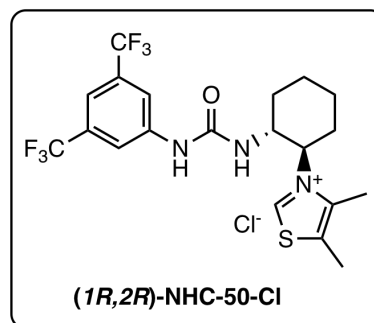
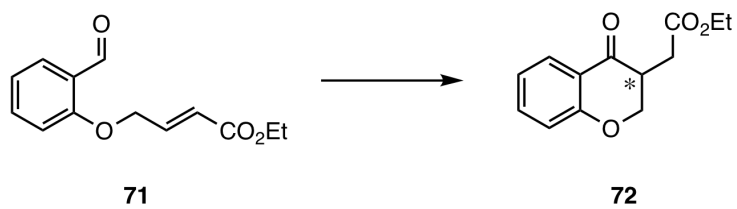
```

=====
Sorted By      : Signal
Multiplier    : 1.0000
Dilution      : 1.0000
Use Multiplier & Dilution Factor with ISTDs
=====

```

Signal 1: DAD1 A, Sig=254,4 Ref=360,100

Peak #	RetTime [min]	Type	Width [min]	Area [mAU*s]	Height [mAU]	Area %
1	5.971	PB	0.2088	87.67876	6.52176	0.5639
2	6.719	PB	0.2620	97.23576	5.30148	0.6254
3	10.718	PP	0.2693	36.50894	1.96030	0.2348
4	25.683	BP	0.4200	84.89311	2.50094	0.5460
5	29.633	BB	0.5912	387.96997	9.29053	2.4953
6	35.287	BB	0.7189	8738.93848	181.77385	56.2053
7	37.477	BB	0.7750	4031.96973	77.23650	25.9320

NHC-50-cl

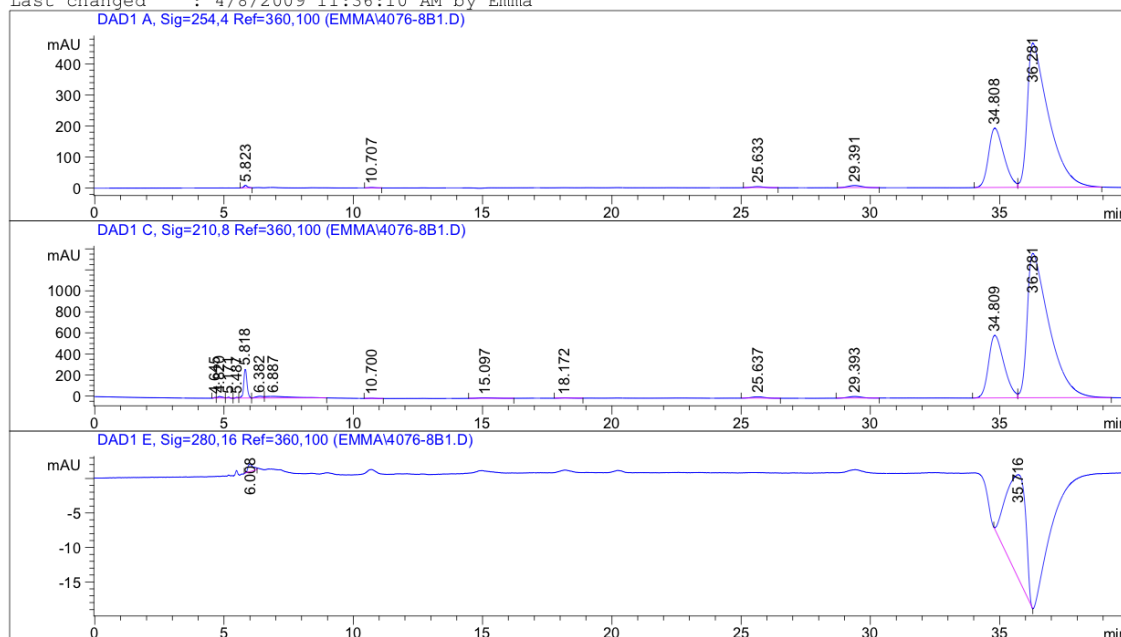
Data File C:\HPCHEM\1\DATA\EMMA\4076-8B1.D

Sample Name: ED4-076-8b

```

=====
Injection Date : 4/8/2009 11:37:52 AM      Seq. Line : 1
Sample Name    : ED4-076-8b                Location  : Vial 83
Acq. Operator  : Emma                      Inj       : 1
Acq. Instrument: hplc                      Inj Volume: 10 µl
Method         : C:\HPCHEM\1\METHODS\EMMA.M\STETTER.M
Last changed   : 4/8/2009 11:36:10 AM by Emma
=====

```



```

=====
Fraction Information
=====

```

```

Fraction collection off
=====

```

```

No Fractions found.
=====

```

```

=====
Area Percent Report
=====

```

```

Sorted By      : Signal
Multiplier     : 1.0000
Dilution       : 1.0000
Use Multiplier & Dilution Factor with ISTDs

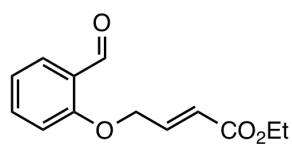
```

Signal 1: DAD1 A, Sig=254,4 Ref=360,100

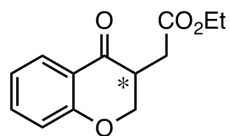
Peak #	RetTime [min]	Type	Width [min]	Area [mAU*s]	Height [mAU]	Area %
1	5.823	BP	0.1477	79.81973	8.05058	0.2284
2	10.707	BB	0.2475	23.39238	1.39586	0.0669
3	25.633	BB	0.4311	114.90322	3.49943	0.3287
4	29.391	BB	0.4902	266.89716	7.00985	0.7636
5	34.808	BV	0.6317	7906.30713	191.48978	22.6192
6	36.281	VB	0.8146	2.65626e4	464.91830	75.9932

```
Totals :                      3.49539e4  676.36380
```

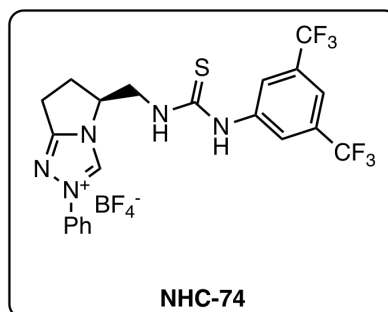
NHC-71



71



72



NHC-74

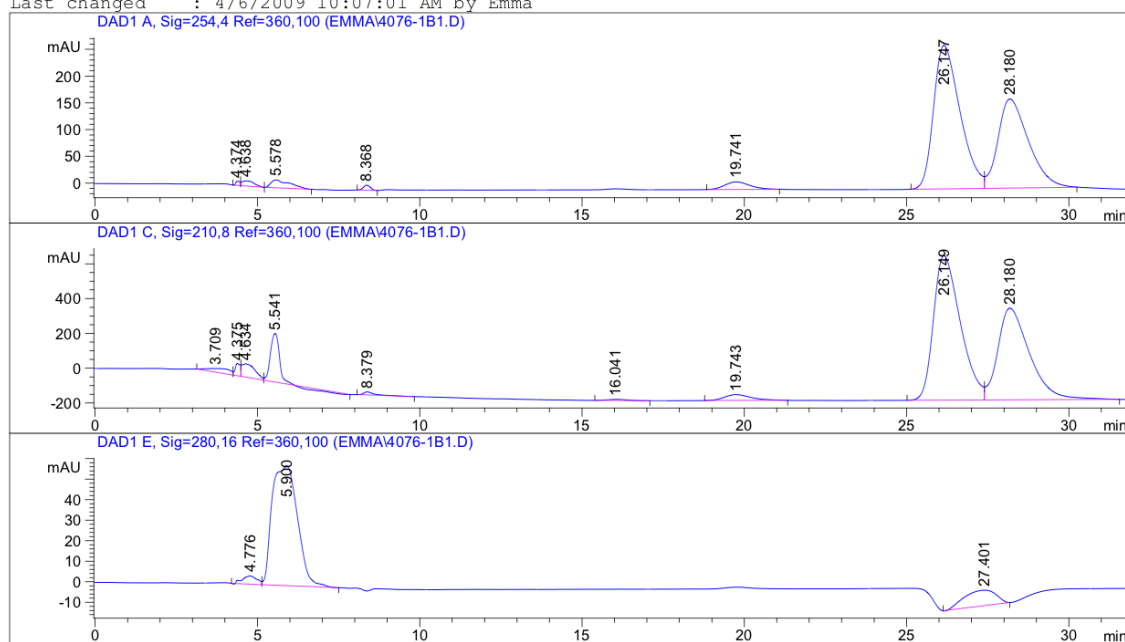
Data File C:\HPCHEM\1\DATA\EMMA\4076-1B1.D

Sample Name: ED4-076-1b

```

=====
Injection Date : 4/6/2009 11:25:15 AM      Seq. Line : 1
Sample Name    : ED4-076-1b                Location  : Vial 71
Acq. Operator  : Emma                      Inj       : 1
Acq. Instrument: hplc                      Inj Volume: 10 µl
Acq. Method    : C:\HPCHEM\1\METHODS\EMMA.M\STETTER.M
Last changed   : 4/6/2009 11:24:14 AM by Emma
                  (modified after loading)
Analysis Method: C:\HPCHEM\1\METHODS\EMMA.M\STETTER.M
Last changed   : 4/6/2009 10:07:01 AM by Emma
=====

```



```

=====
Fraction Information
=====

```

```

Fraction collection off
=====

```

```

No Fractions found.
=====

```

```

=====
Area Percent Report
=====

```

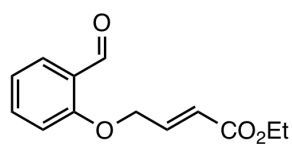
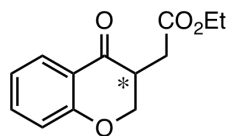
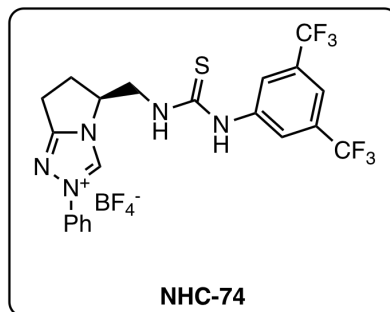
```

Sorted By      : Signal
Multiplier     : 1.0000
Dilution       : 1.0000
Use Multiplier & Dilution Factor with ISTDs

```

Signal 1: DAD1 A, Sig=254,4 Ref=360,100

Peak #	RetTime [min]	Type	Width [min]	Area [mAU*s]	Height [mAU]	Area %
1	4.374	PV	0.1292	71.85613	7.81672	0.2559
2	4.638	VP	0.3316	256.69626	9.73469	0.9141
3	5.578	VB	0.5761	614.95758	14.94471	2.1898
4	8.368	BP	0.2492	146.15094	9.40779	0.5204
5	19.741	BB	0.7906	772.72241	14.11787	2.7516
6	26.147	BV	0.8619	1.52839e4	268.57474	54.4253

NHC-74**71****72****NHC-74**

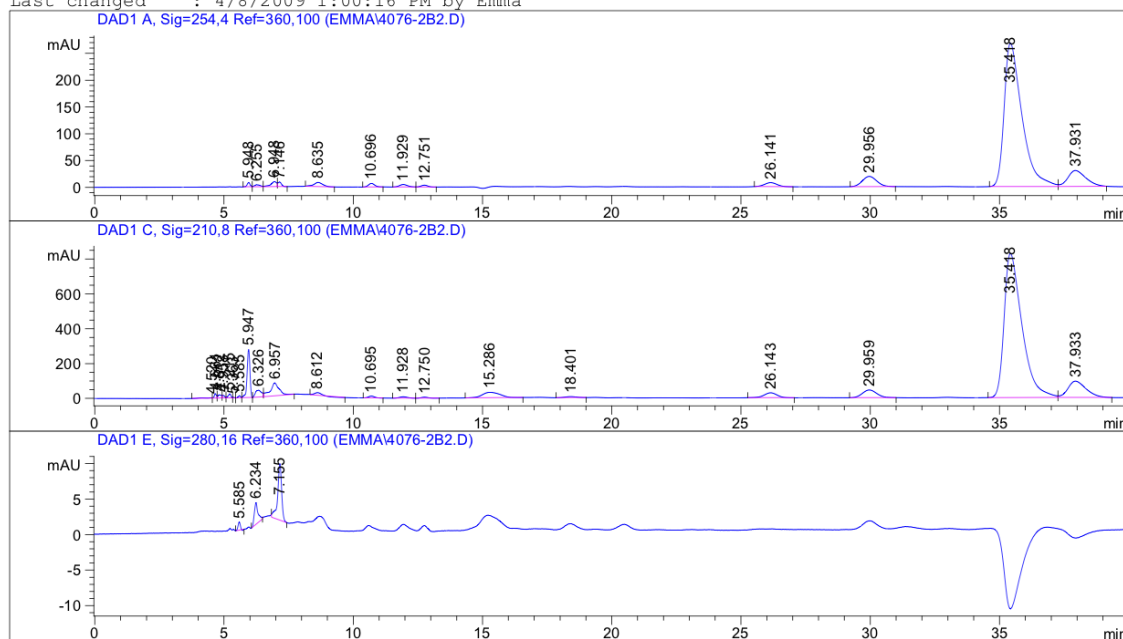
Data File C:\HPCHEM\1\DATA\EMMA\4076-2b2.D

Sample Name: ED4-076-2b

```

=====
Injection Date   : 4/8/2009 1:01:46 PM      Seq. Line :    1
Sample Name     : ED4-076-2b              Location  : Vial 72
Acq. Operator   : Emma                    Inj       :    1
Acq. Instrument : hplc                   Inj Volume: 10 µl
Sequence File   : C:\HPCHEM\1\SEQUENCE\EMMA.S
Method          : C:\HPCHEM\1\METHODS\EMMA.M\STETTER.M
Last changed    : 4/8/2009 1:00:16 PM by Emma
=====

```



Fraction Information

Fraction collection off

No Fractions found.

Area Percent Report

```

Sorted By      : Signal
Multiplier     : 1.0000
Dilution      : 1.0000
Use Multiplier & Dilution Factor with ISTDs

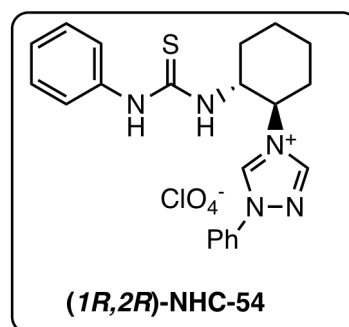
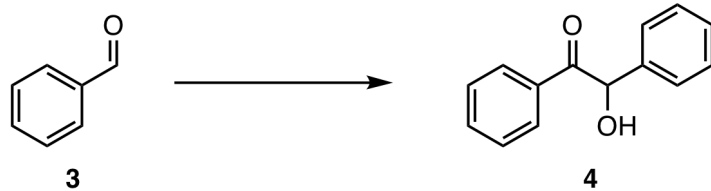
```

Signal 1: DAD1 A, Sig=254,4 Ref=360,100

Peak #	RetTime [min]	Type	Width [min]	Area [mAU*s]	Height [mAU]	Area %
1	5.948	BV	0.1237	63.42466	8.06600	0.3942
2	6.255	VV	0.1902	56.96402	3.77133	0.3541
3	6.948	VV	0.2320	148.23926	9.30050	0.9215
4	7.146	VP	0.1419	81.15688	8.45827	0.5045
5	8.635	BP	0.3683	195.52353	7.80457	1.2154
6	10.696	PB	0.2627	112.20849	6.58813	0.6975
7	11.929	PV	0.3168	100.20448	4.58774	0.6229
8	12.751	VP	0.2772	61.45446	3.42676	0.3820

A.2.2 Benzoin Condensation

NHC-54



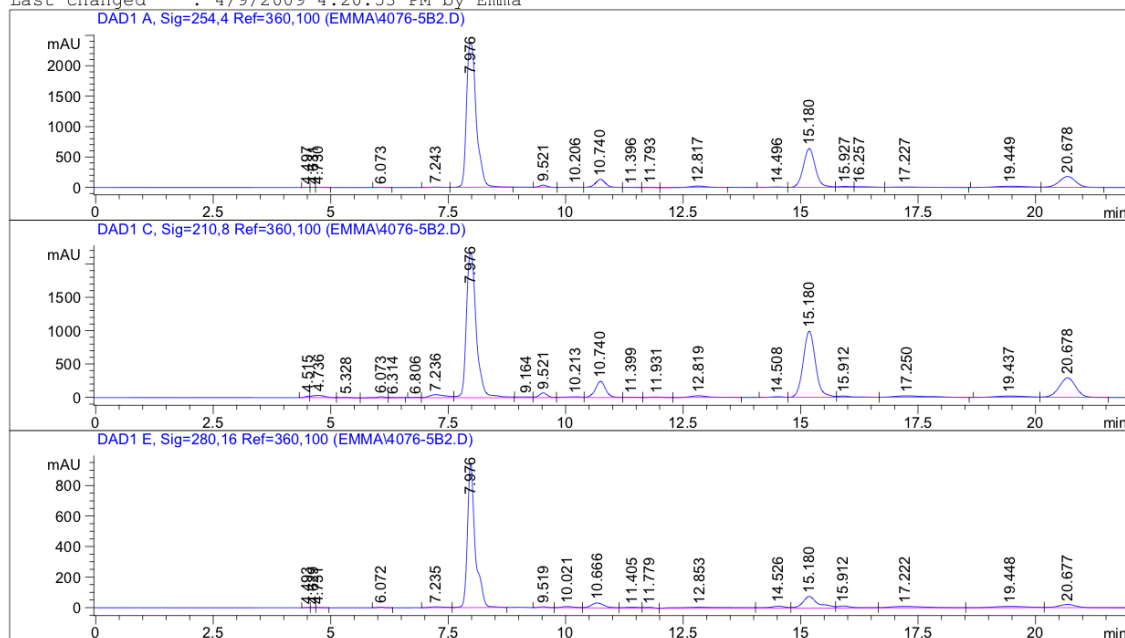
Data File C:\HPCHEM\1\DATA\EMMA\4076-5b2.D

Sample Name: ED4-076-5b

```

=====
Injection Date   : 4/9/2009 4:50:08 PM      Seq. Line   :    2
Sample Name     : ED4-076-5b              Location    : Vial 62
Acq. Operator   : Emma                    Inj         :    1
Acq. Instrument : hplc                     Inj Volume  : 10 µl
Sequence File   : C:\HPCHEM\1\SEQUENCE\EMMA.S
Method          : C:\HPCHEM\1\METHODS\EMMA.M\BENZFIN.M
Last changed    : 4/9/2009 4:20:53 PM by Emma
=====

```



Fraction Information

Fraction collection off

No Fractions found.

Area Percent Report

```

Sorted By      :      Signal
Multiplier     :      1.0000
Dilution       :      1.0000
Use Multiplier & Dilution Factor with ISTDs

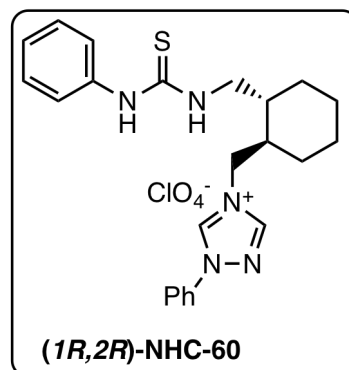
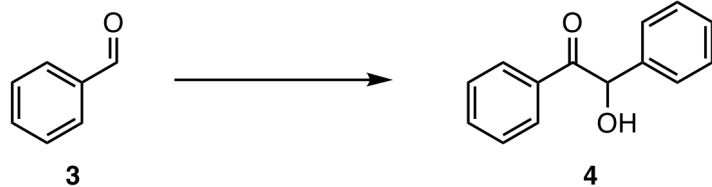
```

Signal 1: DAD1 A, Sig=254,4 Ref=360,100

Peak #	RetTime [min]	Type	Width [min]	Area [mAU*s]	Height [mAU]	Area %
1	4.497	BV	0.0935	17.71148	2.88851	0.0319
2	4.631	VV	0.0921	19.40448	3.05702	0.0349
3	4.730	VP	0.1303	31.06484	3.22592	0.0559
4	6.073	BP	0.1386	22.99557	2.56364	0.0414
5	7.243	VV	0.2883	98.79774	5.18617	0.1779
6	7.976	VP	0.2250	3.41243e4	2383.77441	61.4453
7	9.521	BP	0.1689	378.07556	35.30897	0.6808
8	10.206	BV	0.3007	84.68625	3.76074	0.1525

hplc 4/9/2009 5:12:16 PM Emma

Page 1 of 3

NHC-60

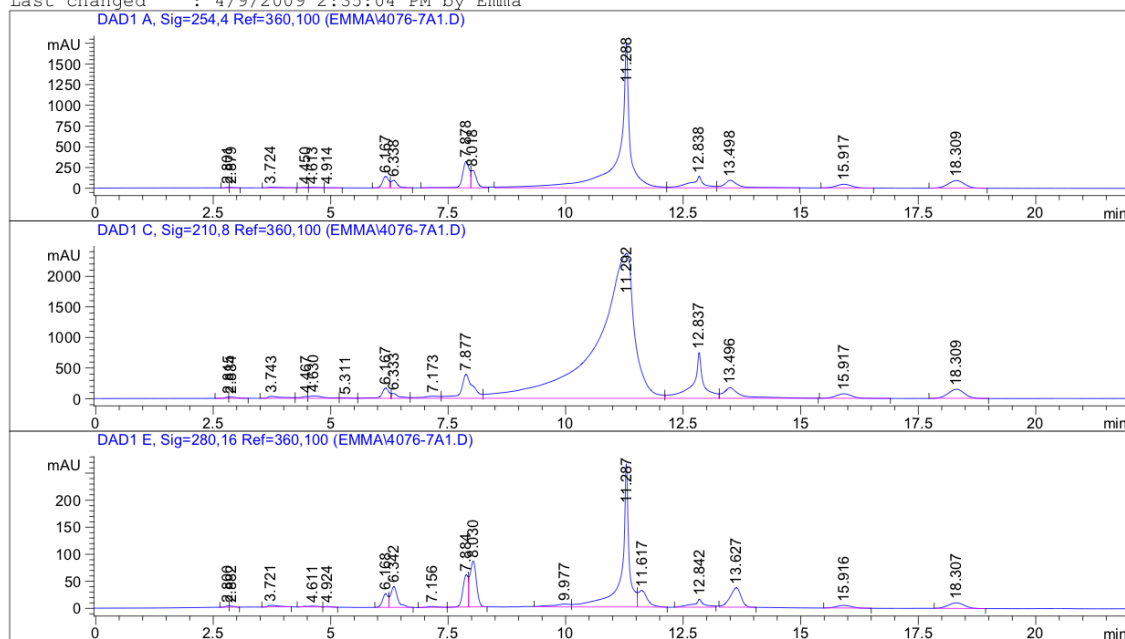
Data File C:\HPCHEM\1\DATA\EMMA\4076-7a1.D

Sample Name: ED4-076-7a

```

=====
Injection Date : 4/9/2009 3:44:38 PM      Seq. Line : 1
Sample Name    : ED4-076-7a              Location  : Vial 63
Acq. Operator  : Emma                    Inj       : 1
Acq. Instrument : hplc                   Inj Volume: 10 µl
Sequence File  : C:\HPCHEM\1\SEQUENCE\EMMA.S
Method         : C:\HPCHEM\1\METHODS\EMMA.M\BENZFIN.M
Last changed   : 4/9/2009 2:35:04 PM by Emma
=====

```



```

=====
Fraction Information
=====

```

```

Fraction collection off
=====

```

```

No Fractions found.
=====

```

```

=====
Area Percent Report
=====

```

```

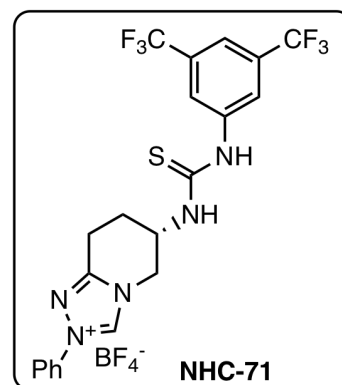
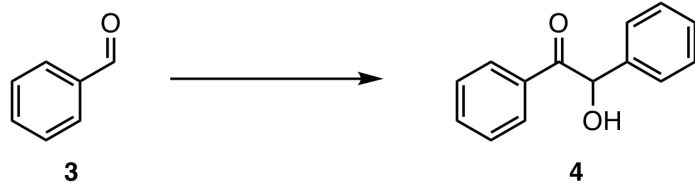
Sorted By      : Signal
Multiplier     : 1.0000
Dilution       : 1.0000
Use Multiplier & Dilution Factor with ISTDs

```

Signal 1: DAD1 A, Sig=254,4 Ref=360,100

Peak #	RetTime [min]	Type	Width [min]	Area [mAU*s]	Height [mAU]	Area %
1	2.801	BV	0.0903	28.34315	4.98655	0.0642
2	2.879	VB	0.0962	34.84482	5.06671	0.0789
3	3.724	PB	0.2763	156.33495	7.72005	0.3540
4	4.450	BV	0.1306	46.78534	5.22043	0.1059
5	4.613	VV	0.1871	82.51295	5.90152	0.1868
6	4.914	VB	0.1361	16.52746	1.60558	0.0374
7	6.167	BV	0.1393	1288.80432	140.08284	2.9184
8	6.338	VB	0.1369	850.68744	91.16984	1.9263

NHC-71



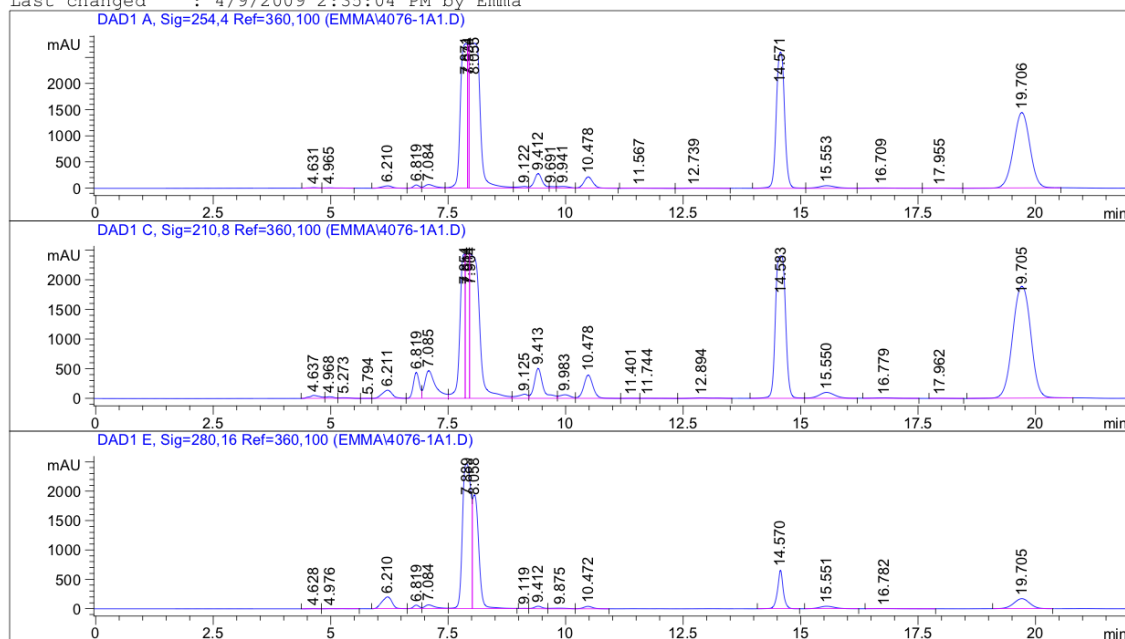
Data File C:\HPCHEM\1\DATA\EMMA\4076-1a1.D

Sample Name: ED4-076-1a

```

=====
Injection Date   : 4/9/2009 2:37:17 PM      Seq. Line   :    1
Sample Name     : ED4-076-1a              Location    : Vial 61
Acq. Operator   : Emma                    Inj         :    1
Acq. Instrument : hplc                     Inj Volume  : 10 µl
Sequence File   : C:\HPCHEM\1\SEQUENCE\EMMA.S
Method          : C:\HPCHEM\1\METHODS\EMMA.M\BENZFIN.M
Last changed    : 4/9/2009 2:35:04 PM by Emma
=====

```



Fraction Information

Fraction collection off

No Fractions found.

Area Percent Report

```

Sorted By      : Signal
Multiplier     : 1.0000
Dilution       : 1.0000
Use Multiplier & Dilution Factor with ISTDs

```

Signal 1: DAD1 A, Sig=254,4 Ref=360,100

Peak #	RetTime [min]	Type	Width [min]	Area [mAU*s]	Height [mAU]	Area %
1	4.631	BV	0.1961	129.56163	9.43981	0.0836
2	4.965	VB	0.2493	128.26329	6.46961	0.0827
3	6.210	PP	0.2498	687.88647	45.12768	0.4438
4	6.819	VV	0.1377	553.53149	62.27352	0.3571
5	7.084	VV	0.2318	1106.60059	70.22770	0.7139
6	7.871	VV	0.1282	2.75538e4	2765.77441	17.7750
7	7.934	VV	0.0272	5455.17773	2748.48486	3.5191
8	8.055	VV	0.2184	4.28610e4	2772.62817	27.6498